U.S. Geological Survey
Toxic Substances Hydrology Program—

Proceedings of the Technical Meeting, Charleston, South Carolina, March 8–12, 1999

Water-Resources Investigations Report 99-4018A
Volume 1 of 3 - Contamination From Hard-Rock Mining

USGS
science for a changing world

U.S. Geological Survey
Toxic Substances Hydrology Program—
Proceedings of the Technical Meeting,
Charleston, South Carolina,
March 8-12, 1999

David W. Morganwalp and Herbert T. Buxton, Editors

U.S. GEOLOGICAL SURVEY

Water-Resources Investigations Report 99-4018A

Volume 1 of 3 - Contamination From Hard-Rock Mining

West Trenton, New Jersey

1999

USGS
science for a changing world

U.S. DEPARTMENT OF THE INTERIOR

BRUCE BABBITT, *Secretary*

U.S. GEOLOGICAL SURVEY

Charles G. Groat, *Director*

For additional information
write to:

Coordinator
Toxic Substances Hydrology Program
U.S. Geological Survey
412 National Center
Reston, Virginia 20192

Copies of this report can be
purchased from:

U.S. Geological Survey
Branch of Information Services
Box 25286
Denver, Colorado 80225-0286

PREFACE

The U.S. Geological Survey (USGS) Toxic Substances Hydrology (Toxics) Program was initiated in 1982. The goal of the Program is to provide earth science information on the behavior of toxic substances in the Nation's hydrologic environments. Contamination of surface water, ground water, soil, sediment, and the atmosphere by toxic substances is among the most significant issues facing the Nation. Contaminants such as excessive nutrients, organic chemicals, metals, and pathogens enter the environment, often inadvertently, via industrial, agricultural, mining, or other human activities. The extent of their migration and their persistence often are difficult to ascertain. Estimates of the costs and time frames for cleanup of contamination and protection of human and environmental health can best be described as astounding, despite continual efforts by governments and industries worldwide to improve environmental technologies.

Contaminant sources and environmental occurrence have a wide range of scales. Some contaminants are released from point sources, such as leaks or discharges from industrial facilities. Some are released from multiple, closely spaced releases, such as domestic septic systems. Still others are released relatively uniformly over broad areas with similar land-use practices, such as agricultural and residential land uses. Contaminants are detected at high concentrations locally in the immediate vicinity of a release, at varied concentrations where multiple releases disperse within watersheds or regional hydrologic systems, and at relatively low (but still potentially toxic) concentrations where they enter systems from broad uniform sources. Common to contamination at all these scales is the need to:

- Measure the contaminants and their transformation products in environmental samples;
- Characterize the physical processes and properties that affect their propagation in the environment;
- Define the chemical and microbial processes that transform or degrade the contaminants;
- Describe contaminant-biota interactions that control their effects on ecosystems, the food chain, and human health;
- Understand the ultimate fate of contaminants with the potential long-term implications for human and environmental health; and
- Develop simulation models that enable prediction of potential exposure and effective design of waste disposal facilities, monitoring networks, and remediation alternatives.

To meet these needs, the Toxics Program provides information and technology to Federal and State resource-management agencies and industry. The Toxics Program: (1) conducts intensive field investigations of representative cases of subsurface contamination at local releases; (2) conducts watershed- and regional-scale investigations of contamination affecting aquatic ecosystems from nonpoint and distributed point sources; and (3) develops methods and models — methods to detect, identify, and measure emerging environmental contaminants; and models to interpret the persistence and fate of contamination and to design waste-disposal and remediation strategies.

Intensive field investigations are established at sites contaminated with predominant types of environmental contamination, in commonly occurring geohydrologic and geochemical settings. Contamination types currently under investigation include chlorinated solvents, sewage effluent, toxic metals, radionuclides, and petroleum products, including fuel oxygenates. These long-term research projects are conducted by interdisciplinary research teams that comprehensively identify and characterize the physical, chemical, and biological processes that affect contaminant transport, transformation, and fate at the site. Through extensive characterization and field experimentation, the sites provide field-laboratory conditions that enhance research opportunities. Results from the sites are generalized by focused field and laboratory experiments at other sites that describe the range of field conditions for the controlling

processes. Knowledge and methods produced at these representative sites improve the effectiveness and reduce the cost of characterization and remediation at similar sites across the Nation.

A unifying theme of these investigations is characterization of the natural response of hydrologic systems to contamination. This, when combined with comprehensive assessment of the processes that affect contaminant transport and fate, make assessing the potential of natural attenuation and remediation-performance monitoring undertakings in which the Toxics Program can excel. The long-term nature of the research provides a unique opportunity to evaluate the potential and limitations of natural-attenuation remediation alternatives.

Watershed- and regional-scale investigations are developed to address contamination problems typical of specific land uses or human activities that may pose a threat to human and environmental health throughout significant parts of the Nation. Current watershed- and regional-scale investigations address contamination from agricultural chemicals in the Midwest corn belt; cotton agriculture across the southern U.S.; human activities in estuarine ecosystems; historic hard-rock mining in watersheds in mountain terrain and southwestern alluvial basins; and mercury emissions on aquatic ecosystems.

In some cases, these investigations involve characterizing contaminant sources and their mechanisms for affecting aquatic ecosystems. This is the case in ongoing investigations of watersheds that may be affected by hundreds of abandoned mine sites. In some cases, watershed- and regional-scale investigations involve widespread detection of mixtures of contaminants or contaminant transformation products at levels near or below existing water-quality standards or advisories. This is the case in investigations of agricultural land uses which have documented that mixtures of pesticides and their metabolites accumulate to significantly higher levels than the individual parent compounds. In still other cases, these investigations identify chemicals in environmental samples for which standards have not yet been developed. In these cases, the Program provides information to resource managers and regulators that is useful for developing new water-quality standards or registering use of new chemicals, such as new pesticides or industrial chemicals.

These investigations complement the National Water-Quality Assessment (NAWQA) Program, which has the goal of assessing the status and trends of the quality of the Nation's ground- and surface-water resources. The Toxics Program watershed- and regional-scale investigations focus rapidly on new issues, emerging contaminants, and understanding the processes that affect whether a chemical may be of widespread concern. This information is used for planning future NAWQA Program activities.

New scientific models and methods are developed as part of both intensive field investigations and watershed- and regional-scale investigations. Simulation models provide tools to predict environmental occurrence and estimate exposure risks, as well as design remediation and monitoring strategies. A strength of models developed by the Toxics Program is that they are developed and applied to explain the complex field conditions at Program field sites. This makes them particularly well suited for application to real problems. New and improved water-quality analytical methods enable (1) detection of new chemicals in environmental samples, such as new pesticides and fuel oxygenates; (2) detection of chemicals at lower levels, which enables our understanding of the processes that control the environmental and human health effects of chemicals, such as mercury; and (3) identification of persistent transformation products of contaminants, such as pesticide metabolites. These methods and models are transferred to public and private practitioners for widespread use across the Nation.

Most scientists involved with Toxics Program activities are from the USGS National Research Program and District (state) Offices. However, as interdisciplinary approaches to solving contamination problems have become more successful, more ecologists, geologists, chemists, hydrologists, geochemists, and digital data-collection experts from across the USGS have become involved in Program activities. In

addition, many scientists from universities, other Federal agencies, and industry are taking advantage of research opportunities afforded by the Program and its field sites, and are active members of the research teams.

Each project is steered by a core group of scientists from the research team. This core group, led by the project coordinator(s), guides the development of a research plan that integrates the multi-disciplinary activities at the site. They facilitate opportunities that become available for a wide range of related research. Although not an emphasis of the Toxics Program, many innovative, engineered-remediation technologies have been tested at the Program field sites because their extensive characterization provides a basis for effective evaluation of technology design and performance. Long-term data sets from the sites have been used by other Federal agencies to test decision-support software for site characterization or to test new hydrologic simulation models. Research plans for each project undergo periodic review by a panel of USGS and non-USGS scientists to improve the research approach and identify opportunities to enhance the research team. Field support for research projects is provided by experienced specialists located in the local USGS District Office.

The Toxics Program is coordinated with the U.S. Environmental Protection Agency, the U.S. Department of Agriculture, the Department of Defense, the Department of Energy, the Nuclear Regulatory Commission, and other U.S. Department of the Interior agencies to ensure that current and future research priorities are being addressed.

The long-term cooperation and assistance offered by the Federal, State, and local agencies, and by private entities that administer or own the Program's research sites has been essential to the success of the Toxics Program. Their continued support is greatly appreciated.

Herb Buxton
Coordinator, Toxic Substances
Hydrology Program

CONTENTS

CONTENTS--Continued

CONTENTS--Continued

Page

CONTENTS OF VOLUME 2 - CONTAMINATION OF HYDROLOGIC SYSTEMS AND RELATED ECOSYSTEMS

SECTION B—Mercury Contamination of Aquatic Ecosystems

SECTION C—Occurrence, Distribution, and Fate of Agricultural Chemicals in the Mississippi River Basin

CONTENTS OF VOLUME 3 - SUBSURFACE CONTAMINATION FROM POINT SOURCES

SECTION G—Research in Characterizing Fractured Rock Aquifers

Modifications to the solute-transport model MOC3D for simple reactions, double porosity, and age, with application at Mirror Lake, New Hampshire, and other sites by D.J. Goode.

Simulation of mass transport using the FracTran98 Module of FracSys2000 by D.M. Diodato.

Borehole packers for *in situ* geophysical and microbial investigations in fractured rock by A.M. Shapiro, J.W. Lane, Jr., and J.R. Olimpio.

INTRODUCTION

This report contains papers presented at the seventh Technical Meeting of the U.S. Geological Survey (USGS), Toxic Substances Hydrology (Toxics) Program. The meeting was held March 8-12, 1999, in Charleston, South Carolina. Toxics Program Technical Meetings are held periodically to provide a forum for presentation and discussion of results of recent research activities.

The objectives of these meetings are to:

- Present recent research results to essential stakeholders,
- Encourage synthesis and integrated interpretations among scientists with different expertise who are working on a contamination issue, and
- Promote exchange of ideas among scientists working on different projects and issues within the Toxics Program.

The Proceedings is published in three volumes. Volume 1 contains papers that report on results of research on contamination from hard-rock mining. Results include research on contamination from hard rock mining in arid southwest alluvial basins, research on hard rock mining in mountainous terrain, and progress from the USGS Abandoned Mine Lands Initiative. This Initiative is designed to develop a watershed-based approach to characterize and remediate contamination from abandoned mine lands and transfer technologies to Federal land management agencies and stakeholders.

Volume 2 contains papers on contamination of hydrologic systems and related ecosystems. The papers discuss research on the response of estuarine ecosystems to contamination from human activities. They include research on San Francisco Bay; mercury contamination of aquatic ecosystems; and investigation of the occurrence, distribution, and fate of agricultural chemicals in the Mississippi River Basin. This volume also contains results on development and reconnaissance testing of new methods to detect emerging contaminants in environmental samples.

Volume 3 contains papers on subsurface contamination from point sources. The papers discuss research on: hydrocarbons and fuel oxygenates at gasoline release sites; ground-water contamination by crude oil; complex contaminant mixtures from treated wastewater discharges; waste disposal and subsurface transport of contaminants in arid environments; ground water and surface water affected by municipal landfill leachate; natural attenuation of chlorinated solvents; and characterizing flow and transport in fractured rock aquifers.

In all, the more than 175 papers contained in this proceedings reflect the contributions of more than 350 scientists who are co-authors. These scientists are from across the USGS, as well as from universities, other Federal and State agencies, and industry.

More information on the Toxic Substances Hydrology Program, including a searchable bibliography of publications and selected on-line publications, is available on the World Wide Web at: **http://toxics.usgs.gov/toxics/**

ACKNOWLEDGMENTS

The editors acknowledge with great appreciation the assistance provided by Kim Crutchfield, Judy Salvo, Nana Snow, Judy Griffin, Patti Greene, and Ray Douglas. Their efforts in the planning, organization, and arrangements made for this seventh Technical Meeting of the Toxics Program made it both successful and enjoyable. Sincere thanks to Bill Ellis for assisting authors with preparation of papers for publication and for preparation and layout of this manuscript. Chet Zenone, Larry Slack, Anthony Buono, and John Flager assisted through review and improvement of the papers in this proceedings. Thanks are extended to the South Carolina District for their warm hospitality. Thanks also to the many scientists whose contributions and accomplishments are reflected in this proceedings; their continued efforts ensure continued success for the USGS Toxic Substances Hydrology Program.

Synthesis of Watershed Characterization for Making Remediation Decisions

By Briant A. Kimball, Kenneth E. Bencala, and John M. Besser

ABSTRACT

The Abandoned Mine Lands Initiative combines expertise from each division of the U.S. Geological Survey. The watershed orientation of the initiative leads to a synthesis of information from many areas of study. Geologic and geochemical studies contribute information about mineral deposits, their role in premining conditions, and their potential for contributing metals to mine drainage. Hydrologic and geochemical studies indicate the transport and transformation of metals from the sources to the streams. Biological studies show the effects of metals on the aquatic organisms and habitats, and help to establish goals for improving the habitats. All of these studies are uni-

INTRODUCTION

Accomplishing the objectives of the Abandoned Mine Lands (AML) Initiative requires the synthesis of information from many disciplines. This paper starts with the "water" view. Often, the water approach to watershed studies has revolved around data collection at the outlet to the watershed (fig. 1a). This view of the watershed serves several important purposes. It provides the integration of solute sources and watershed processes--the results of the watershed "machine." Decisions about remediation, however, require detailed information about specific sources of mine drainage within the watershed, their relative significance, and their effects on the stream ecosystem. The view of the watershed from the outlet does not provide such process-based information, even if the information from the outlet is combined with many individual samples at mine-drainage sources.

Influences of acid mine drainage occur on different scales. An individual mine might affect a single hillside, a small tributary, or the entire watershed downstream. Each site may contribute to the metal load of a watershed. Because of the legal requirements for waste discharge permits, there commonly is documentation of information about the location and chemistry of drainage from individual mining activities in a watershed. However, this leaves us without a context for understanding how individual sources interact and contribute to metal loads on a watershed scale.

Upland watersheds in mining districts generally contain many mines and mining wastes, not just one site that affects the water quality (fig. 1b). Remediation currently must proceed on a site-by-site basis. Estimates of the number of mines in the Rocky Mountains on public and private land are in the tens of thousands. The expense of this remediation would be more than private landowners or the public could bear. Remediation on this scale needs a comprehensive approach; an approach at the watershed scale. If water-quality standards can be achieved in a watershed by remediation of a select, limited number of sites, there could be great savings of money, and limited resources could do the most good. If we have to make expensive choices, then we want to choose those sites that will produce the greatest results for cleaning up the water. This is the approach of the AML Initiative.

The question is how do we identify those principal sources in a watershed? If we can identify a source as being a major contributor, what do we need to know about that source? How do

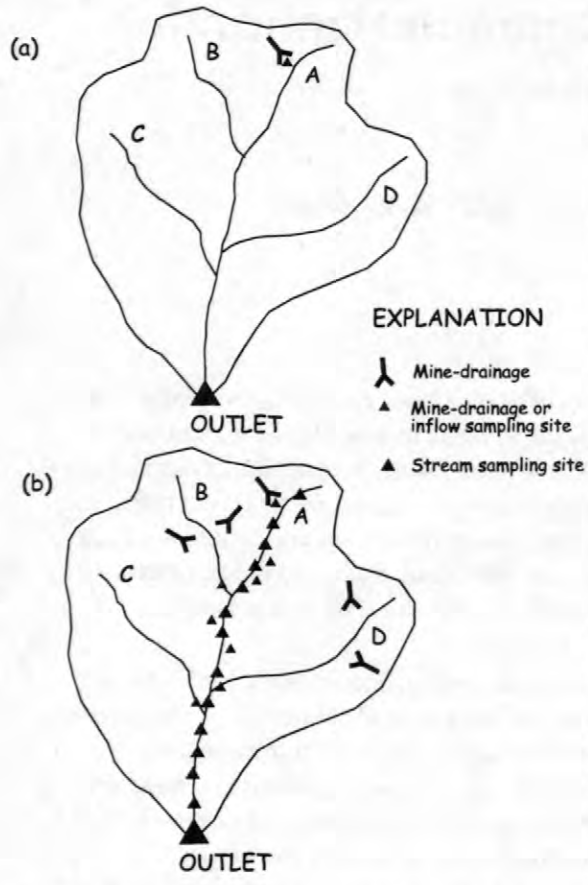

Figure 1. (a) Schematic watershed views showing (a) data collection at the watershed outlet verses (b) the detail of information needed for remediation decisions.

each of the principal sources affect the stream ecosystem? These are not just hydrologic questions, but they are questions that require the combined efforts all the divisions of the U.S. Geological Survey (USGS). The answers require more than the "water" view.

SYNTHESIS FOR THE WATERSHED APPROACH

The depth of the many scientific disciplines within the USGS provides the expertise for a comprehensive understanding of metals from mining (Buxton and others, 1997). The watershed concept brings all the disciplines together to understand premining levels, sources, transport and transformations, and biological effects of metals. When all of this information is synthesized, land management agencies will have a better scientific basis for making decisions and choosing sites for remediation.

Metal Sources and Premining Conditions

Not all mineral deposits were created equally. Differences in mineralogy give rise to different potential contributions of acid water and metals to streams. A classification of mineral deposits and their potential contributions has provided the basis of maps that are helpful for selecting watersheds to be studied in the AML Initiative.

The delivery of acid and metals from a source to a stream greatly depends on the geologic structure around the mineral deposit and the catchment hydrology. Mineral deposits that are associated with faults and fractures may have a direct route to a stream through ground-water inflows. Deposits that are more or less sealed from the stream may contribute to streams only through surface drainage from an adit. The amount of surface drainage that enters the ground and then affects the stream by diffuse seepage is also a geologic and hydrologic question. The geologic structure of a site might make remediation very difficult or might actually contribute to successful remediation.

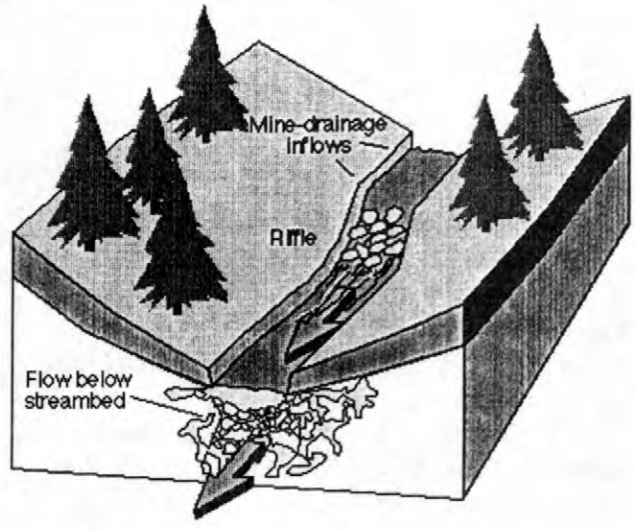

Figure 2. Schematic pattern of streamflow in upland watersheds. Much of the flow occurs below the streambed in the hyporheic zone.

The nature of premining conditions always is an important consideration for mine-drainage issues. Did mining cause current conditions, or were these conditions present naturally before mining occurred? In mineralized belts, the potential for natural acidic, metal-rich drainage is great. Establishing estimates of likely premining conditions can help establish reasonable remediation goals.

The question of premining conditions is being approached through several disciplines. The geomorphology of a stream reveals much about past sedimentation and changes that could have occurred with the onset of mining. Isotope geochemistry of sediment cores reveals changing sources of lead and the chronology of sedimentation. Aqueous isotope geochemistry also may hold keys to distinguishing sulfate contributed by mining from natural weathering of sulfide minerals. Another promising avenue to past environmental conditions may be through paleobotany. Studying pollen, plants, and insects from cores may reveal the health of past habitats.

Transport and Transformation of Metals

A watershed is more than a pipe transporting solutes downstream (Bencala and others, 1993). Streamflow in a mountain watershed generally is down a steep gradient and through pools and riffles in cobble-bottomed streams. These physical conditions lead to streamflow through the hyporheic zone—formally defined as that part of the alluvium that contains at least 10 percent stream water (fig. 2). This hydrologic condition complicates the measurement of loads for planning remediation because actual loads of metals include both surface and hyporheic flow. When flow from a tributary enters the stream, the total load is more than the measureable surface flow entering the stream. The actual effect of a given metal source in a watershed is tied to the total load that enters the stream, not the total amount that leaves the source.

The geochemical consequences of the hyporheic zone are important to the transformation of solutes (Harvey and Fuller, 1998). Hyporheic conditions can cause extensive interaction with minerals, bacteria, and even chemically reducing conditions. These interactions may improve water-quality conditions by removing solutes or changing the dominant chemical species of a toxic metal. The opposite also could occur; the interactions may create conditions that are more toxic. Because both outcomes are possible, it is very important to understand what is occurring in the stream. The full understanding comes from synthesis of hydrology, geochemistry, and biology.

Many transformations of solutes occur in the water column during transport. These transformations are very evident in streams affected by mine drainage because you can see the results of chemical reactions by distinctive zones of color on the streambed. Mixing of metal-rich, acidic water from mine drainage with higher-pH water results in the rapid formation of iron and aluminum colloids in the water column. These submicron solids quickly aggregate and provide extensive surface area for the sorption of copper, lead, zinc, and other metals (Kimball and others, 1995). As the aggregated colloids are transported downstream they become trapped by algae growing on streambed cobbles and settle out of the stream in pooled areas. As this occurs, mine drainage gets its characteristic ochre color. Seasonal removal of the cobble coatings by snowmelt runoff also can release high metal concentrations at a critical time of year (Church and others, 1997).

Biological Implications of Transformations

Transformations of metals that occur in surface and hyporheic flow of streams can influence both the severity and mechanisms of adverse effects on stream ecosystems. Acute toxicity due to metals, or effects that occur as a result of relatively short-term exposure, is typically related to the concentration of the dissolved species of a metal. Acute toxicity in a stream may occur as a result of an episodic event such as a spill of mining wastes or increased concentrations during high flow. Acutely toxic conditions, if frequent or persistent, can eliminate virtually all macroscopic life in severely contaminated streams. However, sensitivity to metals differs widely among different species of aquatic organisms, so episodic acute toxicity evènts may eliminate only the most sensi-

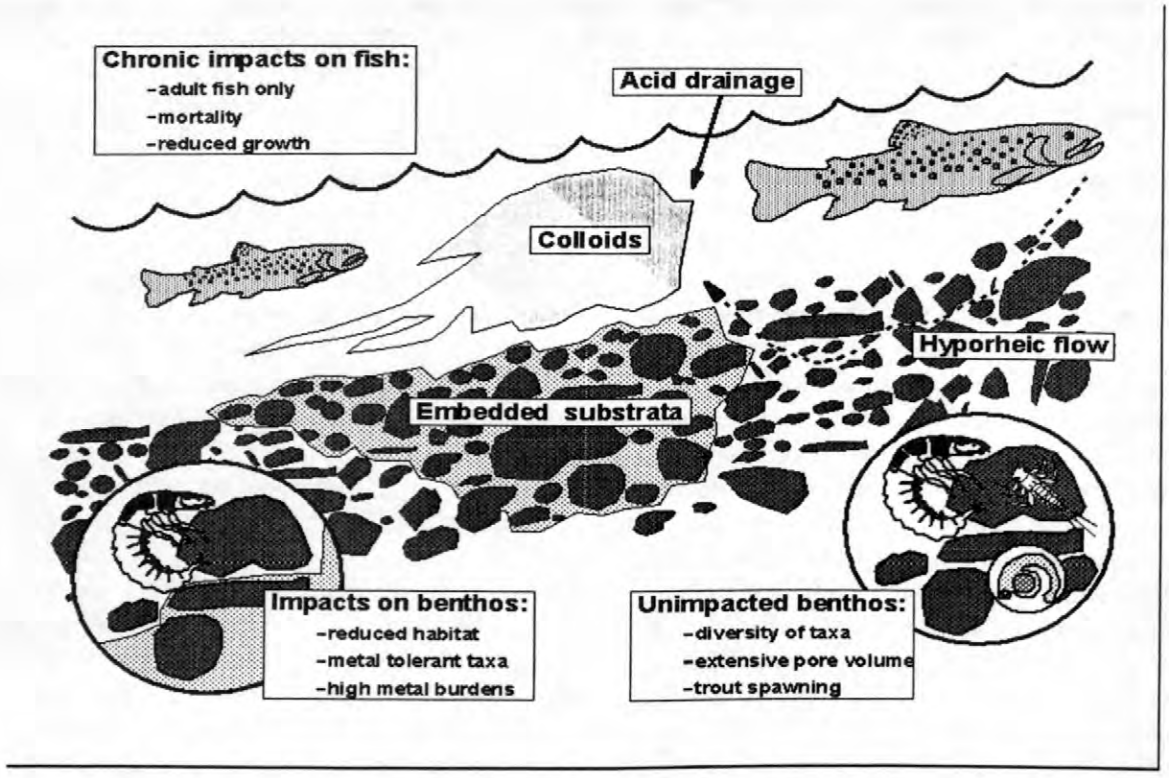

Figure 3. Schematic diagram showing relation of colloids to aquatic health and habitat.

tive species of algae, invertebrates, and fish, leaving a community consisting of relatively tolerant species. In contrast to the rapid loss of species typical of acute toxicity, chronic or long-term metal toxicity can lead to a communty that contains fewer individuals, which grow more slowly and fail to reproduce. Such communities may be sustained by only by constant immigration of organisms from less contaminated locations. Chronic toxicity results from long-term exposure to lower concentrations of metals, including exposure via diet as well as from water.

The sorption of dissolved metals to colloidal iron and aluminum reduces the threat of acute metal toxicity but does not make these metals completely unavailable to stream biota. When colloids become incorporated into streambed coatings (known as periphyton or biofilm), which are the primary habitat for stream algae, they can be ingested and accumulated into the tissues of benthic invertebrates that graze on the algae. Metals associated with these grazers can become available to fish, such as trout, which rely on benthic invertebrates for much of their diet in mountain streams. When grazers (or the larger invertebrates that prey on them) are eaten by fish, metals in colloids and in invertebrate tissues can dissolve in the acidic digestive tract of the fish. Mayer and others (1996) and Chen and Mayer (1998) have shown this to be a mechanism of metal delivery to fish. Metals absorbed via the gut can accumulate in internal organs such as the liver and kidney, which are the primary sites of chronic metaltoxicity.

The incorporation of aggregated iron- and aluminum-rich colloids into stream gravels can adversely affect stream biota both by toxicity and by degrading benthic habitats. Aggregated colloids can also fill (embed) pore spaces in stream gravels, reducing or eliminating habitat that is inhabited by benthic invertebrates and required by stream fish as spawning habitat. Accumulation of metal-rich colloids in stream sediments may result in metal concentrations in sediment pore water or in hyporheic flow that are greater than those in stream water. These elevated metal concentrations may be toxic to benthic invertebrates or, for example, newly hatched trout. All of these processes can adversely affect fish populations by reducing sur-

vival, food availability (i.e. growth), and reproduction.

SYNTHESIS FOR WATERSHED DECISIONS

The experience of the AML Initiative shows that significant spatial detail is necessary to make meaningful decisions about sources of mine drainage, transport and transformation of metals, and effects on aquatic organisms. Integration of the watershed by data collected at the outlet does not provide the detail needed. Integration of data from small sections of the watershed, however, carries the integration concept to the appropriate scale. This can be accomplished with tracer-injection studies and synoptic sampling of streams and inflows (Kimball, 1997).

Focusing on spatial detail in the watershed leads to a synthesis of geologic, geochemical, hydrologic, and biological information. The synthesis is aided by analysis using GIS presentation and investigation. Often, exploring the data in their spatial context makes relations clear and solutions apparent. Another meaningful tool to evaluate the instream effects of alternate remediation choices is through solute-transport simulation. Simulations incorporate the best understanding of sources to the stream and instream processes and evaluate the extent to which remediation options can decrease concentrations of metals and colloids in streams.

REFERENCES

Bencala, K.E., Duff, J.H., Harvey, J.W., Jackman, A.P., and Triska, F.J., 1993, Modelling within the stream-catchment continuum, *in* Jakeman, A. J., Beck, M. B., and McAlleer, M. J., eds. Modeling Change in the Environmental Systems: New York, Wiley, p. 163-187.

Buxton, H.T., Nimick, D.A., von Guerard, P., Church, S.E., Frazier, A., Gray, J.R., Limpin, B.R., Marsh, S.P., Woodward, D. Kimball, B. Finger, S. Ischinger, L. Fordham, J.C. Power, M.S., Bunck, C., and Jones, J.W., 1997, A science-based, watershed strategy to support effective remediation of abandoned mine lands: Proceedings of the Fourth International Conference on Acid Rock Drainage, Vancouver, B.C., May 31-June 6, 1997, p. 1869-1880.

Chen, Z. and Mayer, L.M., 1998, Mechanisms of Cu Solubilization during Deposit Feeding: Environmental Science & Technology, v. 32, p. 770-775.

Church, S.E., Kimball, B.A., Fey, D.L., Ferderer, D.A., Yager, T.J., and Vaughn, R.B., 1997, Source, transport and partitioning of metals between water, colloids, and bed sediments of the Animas River, Colorado: U.S. Geological Survey Open-File Report 97-151, 135 p.

Harvey, J.W. and Fuller, C.C., 1998, Effect of enhanced manganese oxidation in the hyporheic zone on basin-scale geochemical mass balance: Water Resources Research, v. 34, p. 623-636.

Mayer, L.M., Chen, C.W., Findlay, R.H., Fang, J., Sampson, S., Self, R.F.L., Jumars, P.A., Quetel, C., and Donard, O.F.X., 1996, Bioavailability of sedimentary contaminants subject to deposit-feeder digestion: Environmental Science & Technology, v. 30, p. 2641-2645.

Kimball, B.A., 1997, Use of tracer injections and synoptic sampling to measure metal loading from acid mine drainage: U.S. Geological Survey Fact Sheet FS-245-96.

Kimball, B.A., Callender, E., and Axtmann, E.V., 1995, Effects of colloids on metal transport in a river receiving acid mine drainage, upper Arkansas River, Colorado, U.S.A.: Applied Geochemistry, v. 10, p. 285-306.

AUTHOR INFORMATION

Briant A. Kimball, U.S. Geological Survey, Salt Lake City, Utah (bkimball@usgs.gov)

Kenneth E. Bencala, U.S. Geological Survey, Menlo Park, California (kbencala@usgs.gov)

John M. Besser, U.S. Geological Survey, Columbia, Missouri (john_besser@nbs.gov)

A Watershed Approach to Contamination from Abandoned Mine Lands: The USGS Abandoned Mine Lands Initiative

Thousands of abandoned hard-rock mines located throughout the western United States reflect the historic development of the west, yet at the same time, represent a potential threat to human and environmental health. Abandoned mine lands are areas adjacent to or affected by abandoned mines. Abandoned mine lands often contain mineral deposits, mine wastes (the rock removed to get to the ore deposits), and tailings (the crushed rock left over from the ore processing) that contaminate the surrounding watershed and its associated ecosystem.

Many abandoned mines are located on or adjacent to public lands administered by federal land management agencies. Initiation of cleanup activities at some sites has brought the realization that, in watersheds that may have many hundreds of abandoned mine sites, effective and cost-efficient cleanup requires characterization at a broader scale than the individual sites. It requires a watershed-based approach.

The USGS Abandoned Mine Lands (AML) Initiative is part of a larger strategy of the U.S. Department of the Interior and the U.S. Department of Agriculture to clean up federal lands contaminated by abandoned mines. The USGS AML Initiative was implemented in 1997. It is being conducted in two pilot watersheds - the Boulder River in Montana, and the Upper Animas River in Colorado (figure 1).

The goal of the Initiative is to develop a watershed-based approach for gathering the scientific information needed to effectively characterize and remediate contamination from abandoned mine lands. USGS has formed a multi-disciplined team comprised of ecologists, geologists, water-quality experts, hydrologists, geochemists, and digital data collection and mapping experts from many program areas. The team is providing the scientific knowledge needed by land managers and other stakeholders to mitigate the adverse environmental effects of abandoned mine lands.

The objectives of this interdisciplinary, watershed-based strategy are to:

- Determine the physical, chemical, and biological processes that control the environmental effects of abandoned mine lands.
- Define the extent of contamination and of adverse effects on the aquatic ecosystem.
- Define pre-mining background conditions to establish realistic targets for cleanup activities. Some areas, mined because of their mineral abundance, had affected water quality before mining activities.
- Identify sites that most substantially affect watershed quality and public safety, enabling resources to be invested where they will provide the greatest good.
- Develop scientific information and methods to characterize contamination, evaluate human and environmental health risk, and design and monitor remediation.
- Transfer these methods and information to federal land management agencies and industry to enable efficient clean up of abandoned mine lands nationwide.

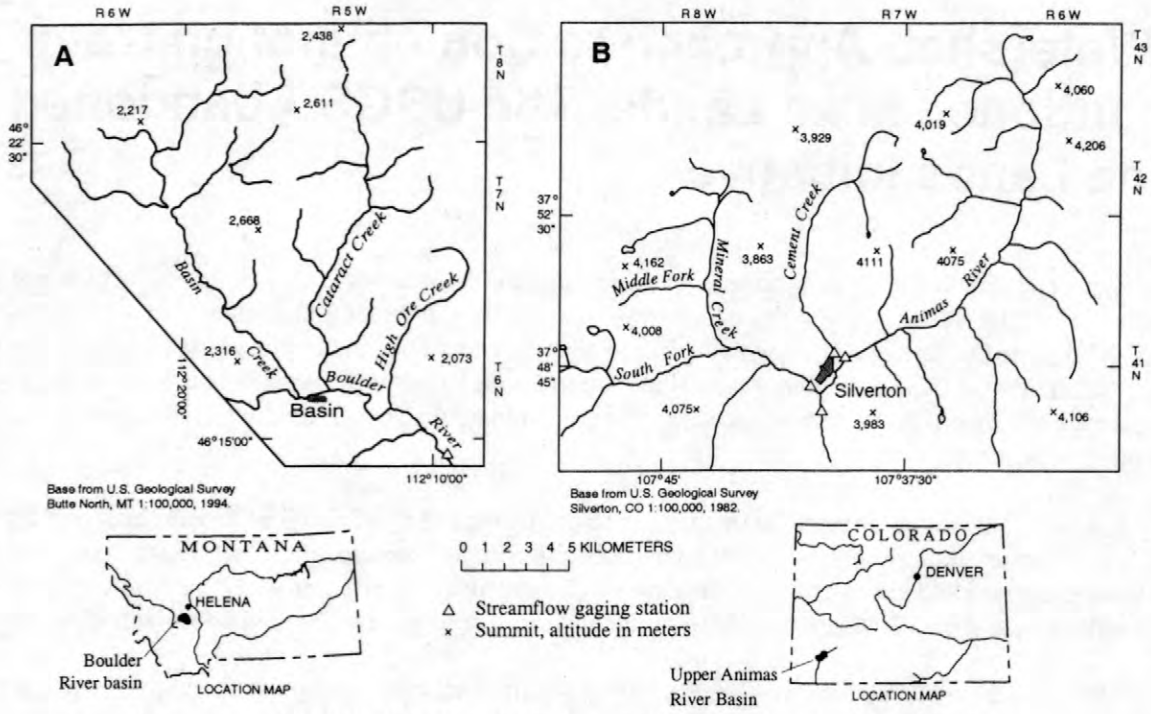

Figure 1. Location of USGS Abandoned Mine Lands Initiative Watershed Investigations. A. Boulder River Montana. B. Upper Animas River, Colorado.

The papers in the following section describe the broad range of scientific methods being developed and applied to characterize contamination from abandoned mine lands in the Boulder River and Upper Animas River watersheds. Today, these scientists are bringing together their diverse expertise to explain the interconnection of physical, chemical, and biological processes that affect the dispersal, and effects of that contamination within a watershed. USGS AML Initiative activities will conclude in the year 2001. Lessons learned regarding successful implementation of a watershed approach to characterize contamination from abandoned mine lands will be presented. However, the investigators already are assured that close collaboration among an interdisciplinary team of scientists is an essential ingredient for success.

More information on the USGS AML Initiative is available on the World Wide Web at: **http://amli.usgs.gov/amli/**.

For additional information contact:

Herbert T. Buxton, USGS, W. Trenton,
New Jersey, (email: hbuxton@usgs.gov)

Characterization of Metals in Water and Bed Sediment in Two Watersheds Affected by Historical Mining in Montana and Colorado

By David A. Nimick, Stanley E. Church, Tom E. Cleasby, David L. Fey, Briant A. Kimball, Kenneth J. Leib, M. Alisa Mast, and Winfield G. Wright

ABSTRACT

Characterization of metals in water and bed sediment is essential for planning effective and cost-efficient remediation in watersheds affected by historical mining. To aid cleanup efforts on Federal land, pilot investigations that are part of the USGS Abandoned Mine Lands Initiative are being conducted in two watersheds in Colorado and Montana. Assessment of ore-related metals and other trace elements in water and sediment in these watersheds provides information to delineate stream reaches having elevated metal concentrations, determine sources of contaminated material, understand the transport of dissolved and particulate metals, and evaluate the potential for metal toxicity to biota.

INTRODUCTION

Metals from mineralized areas and abandoned mine lands affect water quality and biota in many watersheds of the United States. As part of a cooperative effort with Federal land-management agencies, the USGS implemented an Abandoned Mine Lands Initiative in 1997. The goal of the initiative is to develop a strategy for gathering and communicating the scientific information needed to formulate effective and cost-efficient characterization and remediation of the effects of historical mining using a watershed approach (Buxton and others, 1997). The overall scientific strategy is based on understanding the fundamental geologic, hydrologic, geochemical, and biologic processes that cause the environmental degradation often observed downstream from historical mining districts. The watershed approach is intended to identify and characterize those contaminated sites that have the most profound effect on water and ecosystem quality within the watershed. Land-management agencies then can utilize the scientific information to prioritize and develop effective remediation plans. The pilot studies are being conducted in two watersheds: the Boulder River watershed near Helena, Montana (fig. 1), and the upper Animas River watershed upstream from Silverton, Colorado (fig. 2).

In characterizing the occurrence of metals in a watershed, key objectives include determining the

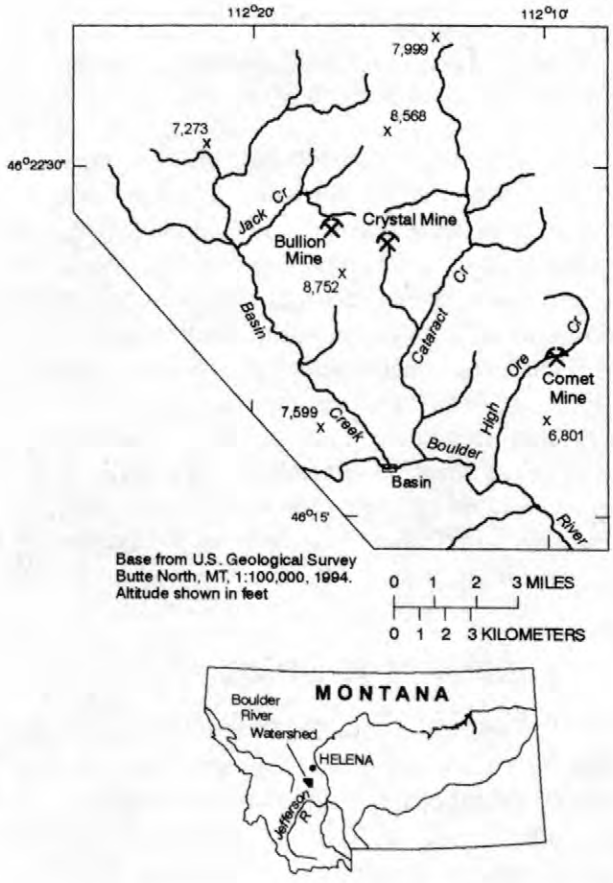

Figure 1. Location of the Boulder River watershed, southwestern Montana.

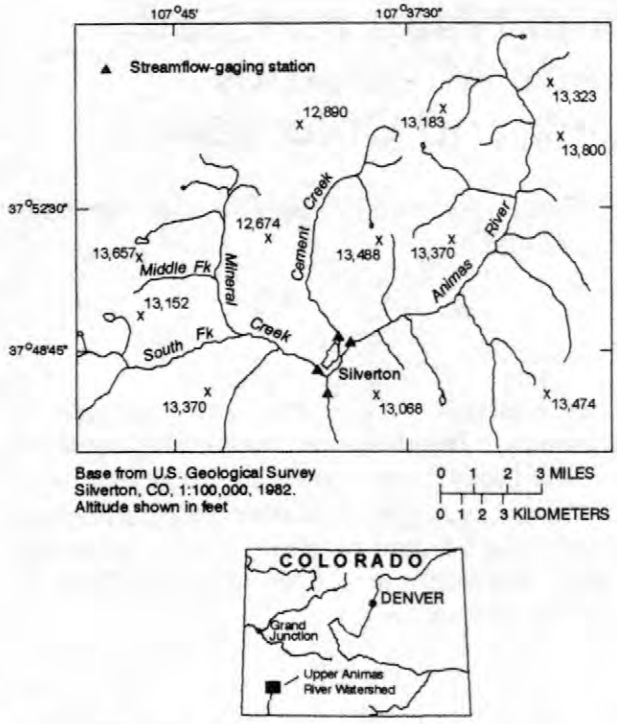

Figure 2. Location of the upper Animas River watershed, southwestern Colorado.

seasonal and spatial distribution of ore-related metal concentrations in water and bed sediment throughout the watershed, and then identifying the significant natural and mining-related source(s) of those contaminants. Sources of these metals can be determined from downstream changes in ore-related metal concentrations in water and bed sediment and from metal-loading studies using tracer-injection techniques. Natural and mining-related sources of metals in mineralized watersheds can be distinguished by comparing water-quality and isotope data in relation to the location of mined areas and geologic units.

DESCRIPTION OF STUDY AREAS

Historical metal-mining activity began in the late 1870s in the Boulder River and upper Animas River watersheds. Principal metals produced include silver, gold, lead, zinc, and copper. Ore bodies are sulfidic, and acidic drainage occurs in both areas. The mining districts in the Boulder River watershed are located primarily in three tributaries to the river (fig. 1), whereas the mining districts in the upper Animas River watershed are located in the headwaters (fig. 2). There are about 120 inactive mines and prospects in the Boulder River watershed and over 1,000 in the upper Animas River watershed. Mineralization in the Boulder River watershed occurs in quartz veins, and hydrothermal alteration is confined to narrow halos around the mineral deposits. In the upper Animas River watershed, mineralization is in vein and breccia-pipe deposits, but alteration occurs on a regional scale. The primary environmental effect of mining in both watersheds is degraded water quality and aquatic habitat, both of which adversely affect aquatic and fishery resources. Some streams are devoid of fish and others have impaired fisheries. Inactive mines can affect streams through direct discharge of acid drainage from adits, seepage from waste rock and tailings piles, and erosion of mining waste and tailings by storm or snowmelt runoff.

METALS IN WATER

Degradation of water quality can be one of the most negative effects of historical mining activity on aquatic biota. Water quality was characterized by systematic sampling of streams throughout the watersheds, comparing metal concentrations to aquatic-life standards, and estimating annual loading of metals to the main streams in the watershed. Water-quality measurements also were made in reference streams draining unmineralized subbasins underlain by the same or similar lithologic units.

Boulder River Watershed

In streams of the Boulder River watershed, pH values are near-neutral to slightly alkaline except in isolated circumstances where acid discharge from inactive mines affects small streams with limited dilution or acid-neutralization capacity. In comparison to five reference streams, ore-related metal concentrations in many stream reaches draining mined areas are elevated. For example, cadmium, copper, lead, and zinc concentrations commonly exceed chronic aquatic-life criteria (U.S. Environmental Protection Agency, 1986). Downstream concentration profiles in streams of the Boulder River watershed indicate that the primary sources of ore-related metals are three large inactive mines: the Comet Mine in High Ore Creek, the Bullion Mine in a

tributary to Jack Creek, and the Crystal Mine in a tributary to Cataract Creek. Downstream from these three mines, chronic aquatic-life criteria for at least one ore-related metal were exceeded at all sampling sites, including sites in the Boulder River between Basin Creek and the Jefferson River. Arsenic is pervasive in both mined and unmined areas; concentrations are elevated throughout the watershed, but are typically much lower than the chronic aquatic-life criterion [190 micrograms per liter (µg/L)].

During snowmelt runoff, cadmium (fig. 3) and zinc concentrations decrease, whereas lead (fig. 3) concentrations increase. Cadmium and zinc are predominantly dissolved [using 0.001-micrometer (µm) filtration] and presumably are diluted during high flow. Lead is primarily in the particulate phase (>0.45 µm in size), and its concentration increases as higher flows transport more sediment. Copper is partitioned more equally into both the dissolved and particulate phases. Partitioning and seasonality are important factors affecting the severity and timing of aquatic toxicity.

The occurrence of cadmium and zinc in the dissolved phase indicates that ore-related metals are introduced to streams by inflow of surface and ground water rather than by entrainment of tailings by runoff. At the Bullion and Crystal Mines, adit discharge is likely the primary source of metals. At the Comet Mine, leachate from tailings appears to be the primary source.

The annual loads of ore-related metals from Basin, Cataract, and High Ore Creeks, and at two sites on the Boulder River upstream and downstream of these tributary streams, were estimated by applying metal-transport regression relations developed from water-quality data for 12 sample sets to daily mean flow estimates derived from the continuous streamflow record for a nearby stream gage on the Boulder River. Although the three tributaries combined contributed only 33 percent of the annual streamflow at the downstream sampling site on the Boulder River, they contributed 41 to 89 percent of the cadmium, copper, lead, and zinc loads. Cataract Creek contributed the largest metals loads to the Boulder River.

Upper Animas River Watershed

During low flow in the upper Animas River watershed (fig. 2), Cement Creek has the lowest pH (3.9) and transports most of its metal load in the

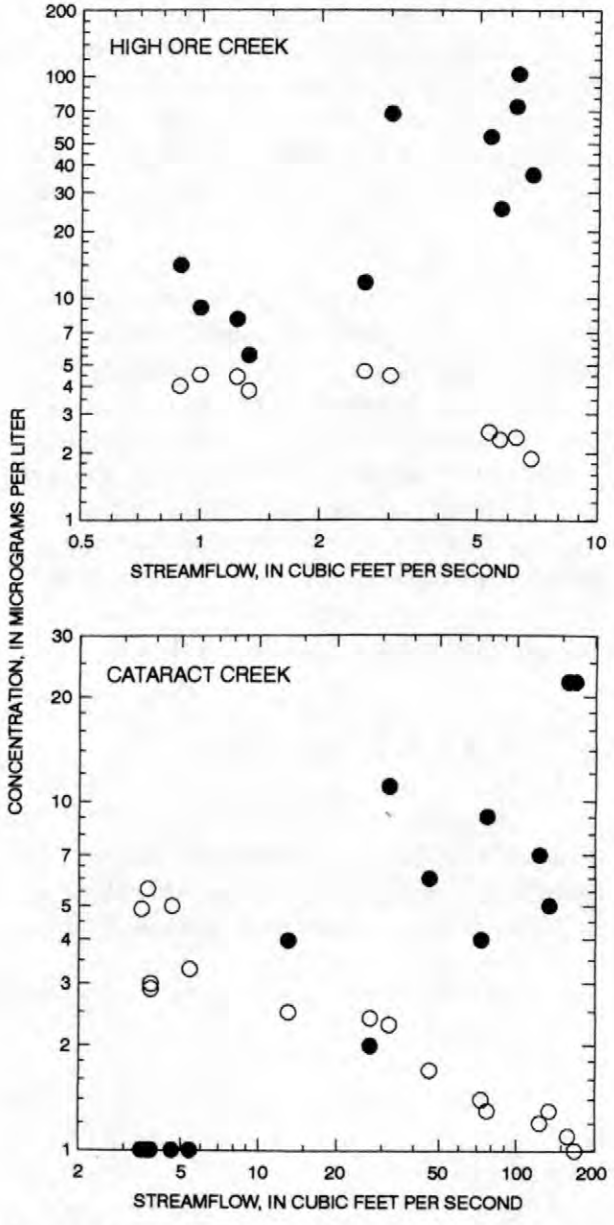

Figure 3. Relation of streamflow to concentrations of dissolved cadmium (open circles) and total-recoverable lead (solid circles) in water from High Ore and Cataract Creeks, Boulder River watershed, Montana, 1996-98.

dissolved (0.001-µm filtration) phase. Mineral Creek has a pH of 4.5 to 6.5 at low flow and transports most of its metal load in the colloidal phase (>0.45 µm). Similarly, most of the metal load in the Animas River upstream of Cement Creek is colloidal. Downstream from Cement Creek, the dissolved metal load from Cement Creek is largely partitioned to the colloidal phase in the higher-pH water of the Animas River (Church and others, 1997). After forming, colloids aggregate, settle, and become an integral component of the bed sediment,

where they are stored until subsequent high flow transports the metal-rich sediment downstream. Zinc and aluminum concentrations commonly exceed aquatic-life criteria in the upper Animas River watershed; copper may also impact aquatic health (Besser and others, 1998; Nimmo and others, 1998).

Preliminary data suggest that during low flow Mineral Creek and Cement Creek contribute 80 to 90 percent of the dissolved (using 0.45-μm filtration) sulfate, iron, and copper loads to the upper Animas River watershed. During high flow, the contribution of sulfate, iron, and copper from Cement and Mineral Creeks decreases to about 50 to 60 percent because of the increases in metal loading from mainstem sources upstream of the tributaries. Contributions of dissolved zinc from the two tributaries are approximately the same (30 percent) during high flow and low flow.

METALS IN BED SEDIMENT

Ore-related metals derived from mine wastes and acidic drainage typically accumulate in the bed sediment of streams downstream from inactive, historical mines. Concentration profiles for bed sediment can be used to delineate stream reaches having elevated ore-related metal concentrations, help locate sources of contaminated material, and help define the transport of dissolved and particulate metals. In addition, biologists can use concentration data to evaluate the potential metal toxicity of bed sediment to biota.

Total and leachable metal concentrations were determined in bed sediment from both watersheds. Most of the total metal content in the sediment occurred in the operationally-defined leachable, or colloidal, fraction, which is reasonable because ore-related metals typically are associated with iron oxyhydroxide (for example, ferrihydrite) and oxyhydroxysulfate (for example, schwertmannite) mineral coatings. The total extraction used a mixture of strong acids, whereas the leachable extraction used warm (50° C) 2M HCl-1%H_2O_2 (Church and others, 1993). Downstream profiles of total zinc concentrations in bed sediment (figs. 4 and 5) are shown as examples of the downstream trends in metal concentrations in both watersheds.

Boulder River Watershed

Profiles of ore-related metal concentrations in bed sediment in the Boulder River watershed

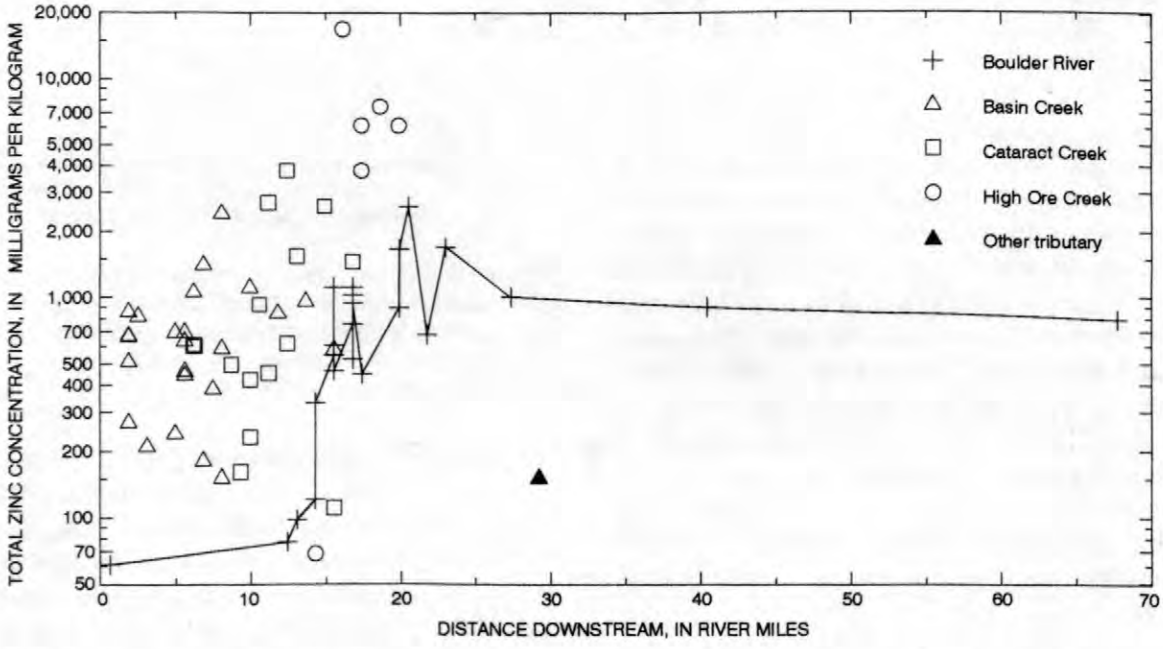

Figure 4. Total zinc concentration in bed sediment from the Boulder River and its tributaries. Boulder River data are plotted by distance downstream from an arbitrary starting point upstream of Basin Creek. Data for tributaries are plotted in river miles along the tributary; the confluences with the Boulder River are at 15.5 miles for Basin Creek, 17 miles for Cataract Creek, and 20 miles for High Ore Creek.

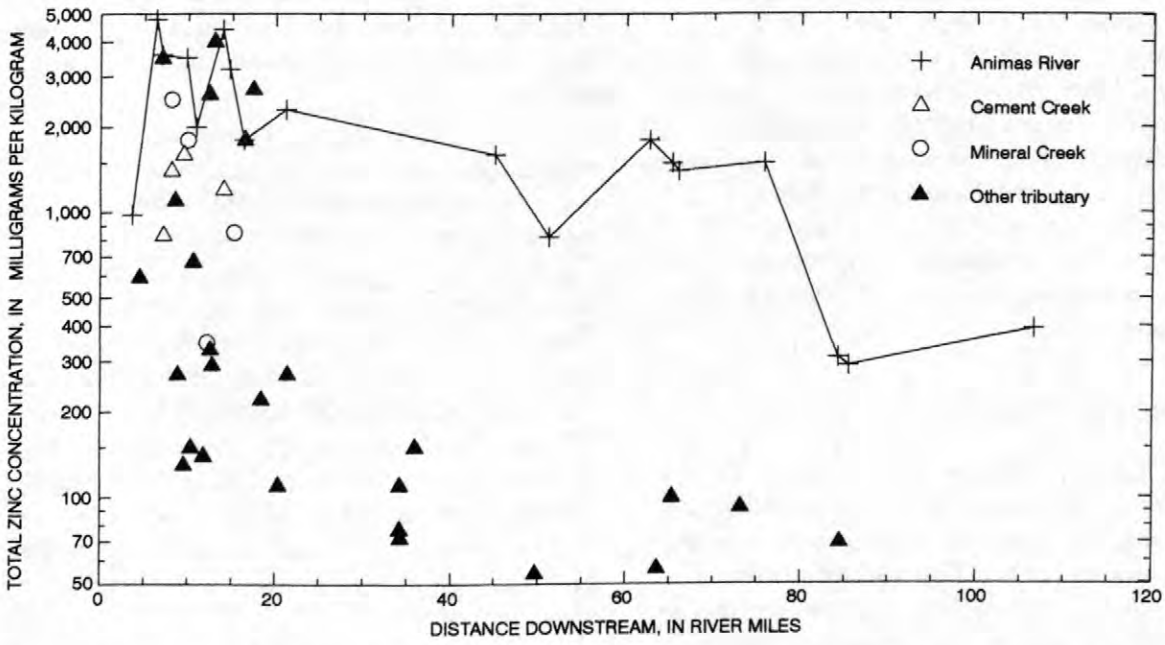

Figure 5. Total zinc concentrations in bed sediment from the Animas River and its tributaries. Animas River data are plotted by distance downstream from an arbitrary starting point. Data for Cement Creek and Mineral Creek are in river miles along the tributary; the confluences with the Animas River are at 15 miles for Cement Creek and 16 miles for Mineral Creek. Data for tributaries of Cement Creek, Mineral Creek, and the Animas River are for samples taken at the mouth of each tributary.

were similar to the concentration profiles observed for water. The highest concentrations of leachable and total ore-related metals in bed sediment occur immediately downstream from the three large mines cited previously; however, concentrations of these metals in unmineralized subbasins are near average concentrations in the Earth's crust. Arsenic, antimony, copper, lead, and zinc are concentrated in the leachable phase, indicating sorption to the bed sediment. Concentrations of trace elements not associated with the mineral deposits (for example, barium, cobalt, strontium, and titanium) are similar in mineralized and unmineralized subbasins.

The downstream concentration profile for each element is determined by the rate at which the dissolved element sorbs to colloids and the rate of downstream transport of the colloidal phase of the bed sediment. Total and leachable concentrations of arsenic, copper, lead, and zinc (fig. 4) in bed sediment of the Boulder River are elevated above crustal values for more than 60 miles downstream of the study area. Downstream concentration profiles indicate that arsenic and lead are removed from solution within a short distance from their sources. Copper and zinc are transported farther downstream and sorbed to colloids as the pH of the stream increases downstream from the source of acidity.

Upper Animas River Watershed

Downstream profiles of metal concentrations in bed sediment in the upper Animas River watershed are similar to the patterns observed in the Boulder River watershed. Copper, lead, arsenic, and zinc are concentrated in the colloidal (leachable) phase of the sediment, with the highest concentrations occurring immediately downstream from historical mining areas. Arsenic and copper concentrations in bed sediment of the Animas River approach crustal values about 60 miles downstream, whereas lead and zinc (fig. 5) concentrations do not approach crustal values for more than 100 miles downstream. Unlike the Boulder River watershed, there were numerous mill sites in the upper Animas River watershed. Prior to

1935, tailings at these mill sites were impounded behind earthen dams. Many of these dams eventually failed, and large masses of tailings were transported downstream and deposited on the flood plains of the Animas River and its tributaries. These deposits now provide a large, diffuse source of mining-related metals to the watershed. In addition, weathering of the extensively altered rocks in the watershed provides a substantial natural load of ore-related metals and other trace elements to the streams.

SOURCES OF METALS

Characterizing sources of metals to streams in mined watersheds involves not only identifying and quantifying point and nonpoint sources along stream reaches but also distinguishing between sources that are related to mining and those that are not. Refining methods to address these issues has been an important part of the pilot watershed investigations.

Quantification of Metal Sources to Streams

Detailed metal-loading studies (or tracer-injection studies) have been an important tool for identifying and quantifying individual surface and subsurface sources of metal loading to specific stream reaches from both mining-related and natural geologic sources. These studies utilize tracer-injections to accurately determine streamflow in coarse-substrate stream channels and synoptic water-quality sampling to determine metal concentrations (Kimball, 1997).

Three studies have been conducted in the Boulder River watershed. One study helped characterize metal loading from the many mines along an 8-mile reach of Cataract Creek in 1997 (Cleasby and others, 1998). Two tracer studies conducted in 1998 were designed to characterize metal sources at specific mine sites scheduled for remediation. These two studies were conducted along 1- to 2-mile reaches of the small streams directly affected by surface and subsurface inflow from the Bullion and Crystal Mines.

Seven tracer studies have been conducted in the upper Animas River watershed. Four of these were used to characterize loading to Cement Creek and the Animas River from mining-related and natural geologic sources. Two studies focused on loading in smaller subbasins, and one specifically examined geochemical reactions in the mixing zone below the confluence of an acidic and a neutral-pH stream.

In analyzing results of tracer studies, four calculations integrate all the metal sources and processes of the watershed: (1) the instream load is calculated for each stream site as the product of sample concentration and discharge, (2) the cumulative total load to the stream is calculated by summing all positive changes of instream load between stream sites, (3) the cumulative load from visible surface inflows is calculated by summing the products of inflow sample concentrations and the flows as estimated by the change in discharge between stream sites bracketing the inflow, and (4) the load derived from nonpoint sources is estimated by subtracting surface inflow loads from total instream load.

Comparison of the load calculations for a tracer-injection study in Cement Creek indicates that 65 percent of the dissolved zinc load at low flow was from nonpoint sources in contrast to point sources such as adit discharge. Presumably, these nonpoint sources include, but are not limited to, the ground-water metals load derived from the weathering of altered rock within the watershed and from diffuse flow of subsurface waters through alluvial fans beneath the inflowing tributary streams. Sixty-nine percent of the zinc load in Cement Creek was transported to the Animas River as dissolved (<0.001 μm filtration) zinc; the other 31 percent of the zinc load was transferred to colloidal iron and was either transported as colloidal load or settled and was temporarily stored in the streambed. Most of the colloidal bed-sediment load is flushed annually by snowmelt or rainfall runoff and contributes to large zinc loads in the Animas River during high flow.

Distinguishing Natural Geologic and Mining Related Sources of Metals

Watersheds that experienced historical mining activity also contain undisturbed mineralized rocks that may weather and contribute acidity and metals to streams. Differentiating between metals loads derived from undisturbed natural geologic sources and mining-related sources is essential to put the anthropogenic contribution in perspective. Information on the

relative contributions of metals from natural geologic sources and mining-related sources in a watershed is useful for prioritizing subbasins for remediation and for establishing post-mining water-quality goals.

In the Boulder River watershed, natural sources of metals appear to be minimal because metal concentrations in water and sediment upstream of mining activities are not elevated. This conclusion is reasonable because the mineralized veins only crop out in small areas and hydrothermal alteration is not extensive.

Both natural and mining-related sources contribute acid and metals to the upper Animas River watershed. Metal loads from these two sources were distinguished by areal water-quality sampling, by comparing water-quality data to the geology of specific stream reaches, and by examining isotopes of oxygen in sulfate extracted from these waters.

More than 70 streams, springs, and adits were sampled during summer 1997 in the Cement Creek basin. Although prospect pits, historical mines, and abandoned mill sites are scattered throughout this area, much of the watershed, particularly at higher elevations, is relatively undisturbed. Water from springs draining altered volcanic rock upstream of any past mining activity can have pH values as low as 3 or as high as 8, depending upon the degree of alteration and the mineralogy of the alteration suite within the area of the subbasin sampled (Bove and others, 1998). Mining-affected and unmined areas produce acidic to neutral surface waters; however, concentrations of major ions and dissolved trace elements generally are higher at the affected sites than at unmined sites. The median pH of water samples collected at the mining-affected sites was 4.3 (range of 2.8 to 7.3) compared to the median value of 6.6 (range of 3.0 to 8.0) at the unmined sites. Sulfate concentrations at all sites ranged from 1 to 450 µg/L and were generally higher at the mining-affected sites (median of 138 µg/L) than at the unmined sites (median of 56 µg/L). Dissolved zinc concentrations were highly variable among the sample sites, ranging from <10 to 14,600 µg/L. Results from springs and streams in unmined areas revealed a geographic pattern in surface-water chemistry that appears to be related to the degree of bedrock alteration. The eastern part of the Cement Creek basin is underlain primarily by propylitically altered lavas, which produce neutral surface water (pH values of 6.4 to 8.0) with relatively low concentrations of dissolved metals except zinc (as high as 230 µg/L). The western part of the Cement Creek basin is more intensely altered than the eastern part and includes pervasive argillic alteration in the northwest quadrant and quartz-sericite-pyrite alteration localized along structures (Luedke and Burbank, 1996). Water draining from this part of the Cement Creek basin is generally more acidic (pH ranging from 3.2 to 4.6) and has elevated concentrations of dissolved metals.

The oxygen isotopes of dissolved sulfate are a useful diagnostic tool for distinguishing natural and mining-related sources of dissolved constituents. The kinetics of sulfide-oxidation reactions differ in natural and mining-related geochemical systems; hence, oxygen-isotope ratios are larger in natural springs draining unmined areas and smaller in mine-drainage water. Dissolved-constituent concentrations also are higher in mine drainage. Given these differences, the proportion of dissolved constituents derived from natural and mining-related sources can be determined using the isotope and concentration data in mass-balance calculations. This method has been applied in two subbasins using data collected during low flow. In the Middle Fork Mineral Creek subbasin, 71 percent of the dissolved sulfate is estimated to originate from natural sources. In the Cement Creek subbasin, 75 percent of the dissolved zinc comes from natural sources.

CONCLUSIONS

The watershed approach is designed to identify the contaminant sources that have the most profound effect on water quality. In the Boulder River watershed, a few large mines appear to be the most important sources of ore-related metals, and loading from natural geologic sources is minimal. In contrast, ore-related metals in the upper Animas River watershed are derived from both mining-related and natural sources. In some drainages, the proportion of metals derived from undisturbed natural geologic sources may be so large that complete cleanup of mining-related sources may not decrease metal concentrations in streams to a level that is suitable for aquatic organisms. In addition, no single mine can be considered the primary source of metals. Instead, significant loads are contributed by small subbasins where the

combined load from numerous mines and natural sources constitute a large source to one of the major streams in the watershed. Consequently, remediation planning in the Boulder River watershed targets individual mines whereas entire subbasins may be targeted in the upper Animas River watershed.

REFERENCES

Besser, J.M., Brumbaugh, William, Church, S.E., and Kimball, B.A., 1998, Metal uptake, transfer, and hazards in the stream food web of the upper Animas River watershed, Colorado *in* Nimick, D.A., and von Guerard, Paul, eds., Science for watershed decisions on abandoned mine lands--Review of preliminary results, Denver, Colorado, February 4-5, 1998: U.S. Geological Survey Open-File Report 98-297, p. 20.

Bove, D.J., Wright, W.G., Mast, M.A., and Yager, D.B., 1998, Natural contributions of acidity and metals to surface waters of the upper Animas River watershed, Colorado *in* Nimick, D.A., and von Guerard, Paul, eds., Science for watershed decisions on abandoned mine lands--Review of preliminary results, Denver, Colorado, February 4-5, 1998: U.S. Geological Survey Open-File Report 98-297, p. 37.

Buxton, H.T., Nimick, D.A., von Guerard, Paul, Church, S.E., Frazier, Ann, Gray, J.R., Lipin, B.R., Marsh, S.P., Woodward, Daniel, Kimball, Briant, Finger, Susan, Ischinger, Lee, Fordham, J.C., Power, M.S., Bunck, Christine, and Jones, J.W., 1997, A science-based, watershed strategy to support effective remediation of abandoned mine lands: Proceedings of the Fourth International Conference on Acid Rock Drainage, Vancouver, B.C., May 31-June 6, 1997, p. 1869-1880.

Church, S.E., Holmes, C.W., Briggs, P.H., Vaughn, R.B., Cathcart, James, and Marot, Margaret, 1993, Geochemical and lead-isotope data from stream and lake sediments, and cores from the upper Arkansas River drainage--Effects of mining at Leadville, Colorado, on heavy-metal concentrations in the Arkansas River: U.S. Geological Survey Open-File Report 93-534, 61 p.

Church, S.E., Kimball, B.A., Fey, D.L., Ferderer, D.A., Yager, T.J., and Vaughn, R.B., 1997, Source, transport and partitioning of metals between water, colloids, and bed sediments of the Animas River, Colorado: U.S. Geological Survey Open-File Report 97-151, 135 p.

Cleasby, T.E., Nimick, D.A., and Kimball, B.A., 1998, Quantification of metal loading by tracer injection methods in Cataract Creek, Boulder River watershed, Montana--Study design *in* Nimick, D.A., and von Guerard, Paul, eds., Science for watershed decisions on abandoned mine lands--Review of preliminary results, Denver, Colorado, February 4-5, 1998: U.S. Geological Survey Open-File Report 98-297, p. 36.

Kimball, B.A., 1997, Use of tracer injections and synoptic sampling to measure metal loading from acid mine drainage: U.S. Geological Survey Fact Sheet FS-245-96, 4 p.

Luedke, R.G., and Burbank, W.S., 1996, Preliminary geologic map of the Silverton 7.5-minute quadrangle, San Juan County, Colorado: U.S. Geological Survey Open-File Report 96-275, 15 p., 1 pl., scale 1:24,000.

Nimmo, D.W.R., Castle, C.J., and Besser, J.M., 1998, A toxicological reconnaissance of the upper Animas River watershed near Silverton, Colorado *in* Nimick, D.A., and von Guerard, Paul, eds., Science for watershed decisions on abandoned mine lands--Review of preliminary results, Denver, Colorado, February 4-5, 1998: U.S. Geological Survey Open-File Report 98-297, p. 19.

U.S. Environmental Protection Agency, 1986, Quality criteria for water 1986: Washington, D.C., Office of Water Regulations and Standards, EPA 440/5/86-001, variously paged.

AUTHOR INFORMATION

David Nimick and Tom Cleasby, U.S. Geological Survey, Helena, Montana

David Fey, Alisa Mast, and Stan Church, U.S. Geological Survey, Denver, Colorado

Ken Leib and Winfield Wright, U.S. Geological Survey, Durango, Colorado

Briant Kimball, U.S. Geological Survey, Salt Lake City, Utah

Determination of Pre-mining Geochemical Conditions and Paleoecology in the Animas River Watershed, Colorado

By S.E. Church, D.L. Fey, E.M. Brouwers, C.W. Holmes, and Robert Blair

ABSTRACT

Determination of the pre-mining geochemical baseline in bed sediments and the paleoecology in a watershed impacted by historical mining activity is of utmost importance in establishing watershed restoration goals. We have approached this problem in the Animas River watershed using geomorphologic mapping methods to identify old pre-mining sediments. A systematic evaluation of possible sites resulted in collection of a large number of samples of pre-mining sediments, overbank sediments, and fluvial tailings deposits from more than 50 sites throughout the watershed. Chemical analysis of individual stratigraphic layers has resulted in a chemical stratigraphy that can be tied to the historical record through geochronological and dendochronological studies at these sites.

Preliminary analysis of geochemical data from more than 500 samples from this study, when coupled with both the historical and geochronological record, clearly show that there has been a major impact by historical mining activities on the geochemical record preserved in these fluvial bed sediments. Historical mining activity has resulted in a substantial increase in metals in the very fine sand to clay sized component of the bed sediment of the upper Animas River, and Cement and Mineral Creeks. Enrichment factors for metals in modern bed sediments, relative to the pre-mining sediments, range from a factor of 2 to 6 for arsenic, 4 to more than 10 for cadmium, 2 to more than 10 for lead, 2 to 5 for silver, and 2 to more than 15 for zinc. However, the pre-mining bed sediment geochemical baseline is high relative to crustal abundance levels of many ore-related metals and the watershed would readily be identified as a highly mineralized area suitable for mineral exploration if it had not been disturbed by historical mining activity. We infer from these data that the water chemistry in the streams was less acidic prior to historical mining activity in the watershed.

Paleoentologic evidence does not indicate a healthy aquatic habitat in any of the stream reaches investigated above the confluence of the Animas River with Mineral Creek (fig. 1) prior to the impact of historical mining activity. The absence of paleoentologic remains is interpreted to reflect the poor preservation regime of the bed sediment materials sampled. The fluvial sediments sampled in this study represent higher energy environments than are conducive to the preservation of most aquatic organisms including fish remains. We interpret the sedimentological data to indicate that there has been substantial loss of riparian habitat in the upper Animas River above Howardsville as a result of historical mining activity.

INTRODUCTION

Determination of the metal concentrations present in stream reaches in watersheds affected by historical, inactive mines is necessary to help define remediation and restoration goals facing federal land-management agencies (FLMA). We estimate that more than forty percent of the headwaters in watersheds in or west of the Rocky Mountains have been impacted by past mining

activities (Church and others, 1998b). The determination of water quality, stream habitat, and aquatic community structure that existed prior to mining are needed to define pre-mining conditions and guide watershed restoration. There are no direct measures of water quality prior to historical mining activities; an alternative approach must be found to evaluate pre-mining water-quality conditions.

Historical mining activity has also profoundly changed the ground-water flow regime in most watersheds where mining has occurred. Waters flowing from adits represent the focusing of this modified ground-water flow regime. However, this increased artificial porosity within the ground-water system has resulted in an accelerated rate of oxidation of sulfide minerals in the near-surface environment, which increases the metal loads contributed by these anthropogenic features. Partitioning metal loads between the pre-mining component caused by chemical weathering processes, and that caused by the increased rate of oxidation as a result on the increased porosity caused by mining is not generally possible.

Determination of the pre-mining geochemical baseline in watersheds affected by historical mining activities is a difficult task if one is limited to the water-quality measurements that can be made today. Metals and acidity are released from the chemical weathering of mine waste dumps as well as from the hydrothermally altered rocks that occur within the watershed. One approach to determining what the pre-mining conditions were is to determine the anthropogenic contribution of metals from mine adits and waste dumps, and subtract these measured loads from the geochemical baseline measured today. This approach is a difficult one to apply in watersheds, and is limited by the completeness of data from anthropogenic point sources of metals, transport rates of metals from these point sources to streams, and pathways of metals from these point sources to the streams. This approach is also severely limited by the assumption that the ground-water baseflow has not been significantly changed by mining activity, an assumption we challenge.

An alternative approach to determining the pre-mining background conditions has been developed and tested in the Animas River watershed. The fluvial sedimentological record provides an indirect measure of pre-mining water quality through the analysis of the trace metal concentrations in the iron oxy/hydroxide and oxy/sulfate minerals that precipitated out of stream waters as colloidal fractions (Church and others, 1997). We have applied geomorphologic mapping methods to determine the relative ages of various river-terrace gravel deposits preserved within the stream reaches. These river-terrace deposits are generally erosional remnants of earlier fluvial gravel deposits, although a few overbank deposits representing high water flooding events and representative fluvial tailings deposits have also been sampled. We sampled fluvial gravels in terraces preserved above the maximum flood-stage level, as determined by overbank deposits left by the 1911 Gladstone flood, and determined trace metal concentrations in these bed sediments using the same sampling, processing, and analytical methods used to determine trace metal concentrations in the bed sediments today (Church and others, 1997). In some cases where the sedimentary samples represented sedimentary sites where the deposition rate was slow, we also initiated ^{210}Pb (lead), ^{14}C (carbon), and ^{137}Cs (cesium) geochronological studies to provide an absolute age of the deposits. Dendochronology has been used to determine minimum ages of the terraces. These pre-mining terrace sediment sites have proven to be relatively easy to identify in the watershed, although they are not readily available everywhere within the watershed. Preliminary results of our investigation of the trace metal concentrations in pre-mining fluvial sediments were reported in Church and others (1998a).

We also sampled and dated pre-mining sediments from a trench dug across a braided section of the upper Animas River between Eureka and Howardsville (site 3, fig. 1). Details of this investigation are reported in Vincent and others (1999). In this report, we will document the field methods and summarize the analytical results available from these samples.

Paleoentological analyses was conducted on a subset of these samples that represented low-energy sites of deposition. Analysis of the biotic material from the watershed habitats, as preserved

in the fluvial sedimentological record, also can provide valuable information on both terrestrial and aquatic community structure. Analysis of trace element chemistry of the various organisms preserved in the various core materials could be used to provide another indirect measure of water chemistry. Results from these investigations provide permissive data if organisms are preserved, but not definitive data if the results are negative. Our studies to date do not provide any indication of a healthy aquatic community in the study area prior to mining.

Geology of the Study Area

The Animas River drainage basin (fig. 1) has its headwaters in the mountainous terrain above Silverton, Colo. and drains south into the San Juan River in northern New Mexico. Elevations range from more than 13,000 ft. (4,000 m) at the headwaters to less than 6,000 ft. (1,800 m) at the confluence with the San Juan River south of Aztec, New Mexico. The major population center in the basin is the city of Durango, Colo. The geology exposed at the surface and underlying the basin is varied. Precambrian rocks crop out in the eastern part of the drainage basin in the Animas Canyon area south of Silverton forming the high rugged mountainous area of the Animas Canyon. Paleozoic and Mesozoic sedimentary rocks crop out in the southern part of the drainage basin. The headwaters of the Animas River watershed are underlain by Tertiary igneous intrusive and volcanic rocks that formed as a result of a late Tertiary age episode of andesitic to dacitic volcanism followed by a later episode of ash-flows, lava flows and intrusions of dacitic to rhyolitic composition (Lipman and others, 1976). During this later episode of volcanism, the Silverton caldera formed. Pervasive and intense hydrothermal alteration and mineralization events postdate the formation of the Silverton caldera by several million years (Casadevall and Ohmoto, 1977). This area of the Animas River watershed above Silverton has been extensively fractured, hydrothermally altered, and mineralized by Miocene hydrothermal activity.

Placer gold was discovered in 1871 on Arrastra Creek above Silverton by soldiers exploring the Bakers Park area. Following the signing of a treaty with the Ute Indians in 1873, between 1,000 and 1,500 mining claims were staked in the Animas River watershed upstream from Silverton. Mining activity spread rapidly throughout the area. The chimney deposits associated with Red Mountain located in the headwaters of Mineral Creek were discovered in 1881. The railroad was brought up from Durango in 1882 providing cheap transportation for ore concentrates from the many mills in and above Silverton to the smelters in Durango (Sloan and Skowronski, 1975). Mining continued in the Animas River watershed at various levels of activity until 1991 when the Sunnyside Mine closed. The Sunnyside Gold Corp. initiated restoration activities in the watershed in 1994.

Geomorphology of Fluvial Deposits

Many of the sediment samples in this study come from fluvial deposits associated with stream terraces. An understanding of the geomorphic evolution of the stream valleys and these terraces is necessary to properly evaluate the meaning of the geochemical data. Surficial deposits of the Animas River watershed were mapped using color aerial photographs (Blair, 1998) resulting in a surficial geologic strip map of the major tributaries representing an area of about one kilometer in width and extending about 125 m above the active flood plain.

The upper Animas River and Mineral Creek follow the concentric fracture system created during the formation of the Silverton caldera (fig. 1). These fractures predisposed the volcanic rocks to accelerated weathering and erosion by allowing water seepage both from hydrothermal as well as meteoric sources. Today, surficial deposits in the stream valleys are dominantly glacial, fluvial, and colluvial. Although there have been multiple glacial episodes over the past 2 million years (Atwood and Mather, 1932; Gillam, 1998) only vestiges of the most recent glaciation (maximum extent about 18,000 years BP) are present today. For example, Mineral Creek and the upper Animas River have classic U-shaped valleys and both contain morainal deposits (Blair, 1998).

Fluvial deposits, representing both overbank deposits left by flood waters and erosional remnants, are found in stream terraces on the valley floors along with alluvial fan deposits, glacial deposits, colluvial deposits, and modern flood plain sediments. Stream terraces indicate that some change has taken place in the fluvial energy of the stream. Changes in energy are caused by changes in discharge, stream gradient, and sediment load. These changes can come about from long-term climatic change, short-term weather phenomena, temporary channel blockage, and human impact. All of the stream terraces in the Animas River watershed north of Durango, with one possible exception near Bakers Bridge, are post glacial. Terraces with elevations greater than 2 meters above the modern channel are probably the result of long-term climatic changes associated with neoglacial events, such as the "Little Ice Age" which spanned from about 1350 to 1750 AD. Terraces less than 2 meters above the modern stream channel are more likely associated with short-term weather phenomena, such as rare intense thunderstorms, or from human impact such as damming or altering discharge. This interpretation has been confirmed by the detailed trenching study of the upper Animas River between Howardsville and Eureka where human activity has induced braided stream channel conditions causing aggradation. These studies have shown that old sediments, that is greater than 2,000 years BP by ^{14}C geochronological methods, are buried beneath the gravels that are present in the upper Animas River below Eureka (Vincent and others, 1999).

Field investigations indicate that fluvial gravel deposits preserved in terraces at greater than 2 meters above the active stream level are probably older than 1860. The fluvial sediments in these terraces were laid down prior to mining activity and reflect the pre-mining geochemical background for the representative drainage, assuming no post-depositional human impact has occurred. These older terraces are relatively rare in narrow canyons less than 100 m wide, such as between Howardsville and Silverton, and just north of Eureka (fig. 1). These narrow canyons act as high energy funnels during major storm events which flush out and redistribute previously deposited sediment. Where valleys widen to several 100 meters, older gravel terraces are usually preserved above the modern stream level; for example, at Bakers Park where the town of Silverton is located, along upper Mineral Creek (sites 13-15, fig. 1), and along selected reaches of the Animas Canyon between Silverton and Durango. Historical evidence of the age of these elevated remnant terrace deposits can also be deduced from in a study of the overbank deposits resulting from the 1911 Gladstone storm. On October 5, 1911, the largest historic flood on record occurred in the upper Animas River watershed. This flood, called the Gladstone storm, reworked existing alluvial channel sediment and deposited overbank sediments on midstream bars and new flood plain deposits at elevations less than 2 meters above the active flood plain in several localities in the upper Animas River watershed (Pruess, 1996).

Human impact on the floodplain in the Animas River watershed has been significant, particularly in the modern active flood plains. It is estimated from the geomorphic mapping studies (Blair, 1998) that forty percent of the entire channel length within the Upper Animas watershed has been altered in some way (Blair, 1998). The flood plain between Howardsville and Eureka has been totally impacted directly or indirectly by human activity as shown by the dramatic change in channel morphology at the trench site (Vincent and others, 1999). A great deal of sediment movement has occurred here over the past 130 years to establish the now defunct town of Eureka (fig. 1), stabilization of the channel to maintain the old bridge crossing, road construction, gravel mining, and mineral processing. Another example of human impact on the active flood plain occurred when aggressive stoping beneath an alpine lake in 1978. This activity resulted in collapse of the mine roof and lake floor into the mine, draining the water from Lake Emma into the Sunnyside Mine. The associated flush of sediment-laden waters from the Gladstone portal down Cement Creek coated the entire active flood plain with muddy sediment.

METHODS

Field Sampling Methods

Using the geomorphological maps, we walked the segments of the river channels where pre-mining sediments might be preserved in old terrace deposits. Terraces were sampled a number of sites in the watershed above the confluence of the Animas River with Mineral Creek. These localities are shown schematically on fig. 1. Terrace deposits were also sampled at several sites in the Animas Canyon between Silverton and Bakers Bridge about 25 km upstream from Durango Colo. These terrace deposits were sampled, whenever possible, beneath old large Engelmann Spruce which were cored if live or sampled where dead for dendochronological determination of the minimum age of the terrace deposits. These terrace deposits were generally composed of poorly sorted fluvial gravels containing lithic clasts ranging from 10 to 30 cm in diameter. These sections generally had no discernable stratigraphy, so the sections were sampled in lifts taken on 15 to 30 cm intervals throughout the exposed section. The gravels were sieved to pass a 2 mm stainless steel screen, and sent to the laboratory for further processing. In the laboratory the samples were dry-sieved to pass 100 mesh in the same manner as the stream sediments (Church and others, 1997). The sample material analyzed (that is, <150 micrometers) constitutes the very fine sand, silt, and clay sized fraction of the pre-mining fluvial sediments.

Below Bakers Bridge, the Animas River is a mature, meandering river with numerous oxbow lakes. We sampled the fluvial deposits in these oxbow lakes, one of which was active circa 1896 (see the historical photographs by Whitman Cross, in Atwood and Mather, 1932, plate 25; U.S. Geological Survey, 1898) just above the town of Durango in what was known at the turn of the century as the town of Animas City. Five-cm diameter cores of fluvial sediments up to depths of 3 meters were taken from these oxbow lakes and the core intervals divided along stratigraphic boundaries for sampling. Sandy layers were sieved as described above prior to chemical analysis. Stratigraphic intervals from this youngest meander contain deposits that have elevated concentrations of Ag, As, Cd, Cu, Pb, and Zn resulting from the transport and deposition of fluvial tailings in the Animas River whereas the stratigraphic intervals sampled in the older oxbow lakes at this site contain metal concentrations at or near crustal abundance levels.

Analytical Methods

Samples from the cores and lift sequences of the fluvial sediments were analyzed using two different analytical procedures: a mixed-acid total digestion, and a weak partial-dissolution extraction, both followed by ICP-AES (inductively-coupled plasma atomic emission spectroscopy) analysis.

The total digestion procedure utilizes a mixed acid digestion of 0.2g of sample (Briggs, 1996). The resulting solution is analyzed for 40 major and trace elements. This procedure is very effective in dissolving most minerals, including silicates, oxides and sulfides. Some refractory minerals such as zircon, chromite and tin oxides are only partially attacked. However, these minerals and the elements associated with them are not of concern to this study. To monitor the quality of the analyses, laboratory duplicates were analyzed to assess precision, and three standard reference materials (SRM's) were analyzed with each set of samples to assess accuracy. The reference materials were NIST-2704, NIST-2709 and NIST-2711, available from the National Institute of Standards and Technology (NIST, 1993a, 1993b, and 1993c).

Whereas the mixed-acid procedure releases all of the metals contained in a sample, the application of a partial-digestion technique releases metals bound within different mineral phases. These data can be quite informative in the study of metal enrichment in bed sediments due to the coating of grain surfaces by iron- and manganese-oxide minerals with metals released during weathering (Chao, 1984). We used a weak, warm-acid leach (50°C 2M hydrochloric acid-1 percent hydrogen peroxide) to dissolve hydrous amorphous iron- and manganese-oxide colloids or sediment-coatings which contain sorbed metals of interest (appendix II and III;

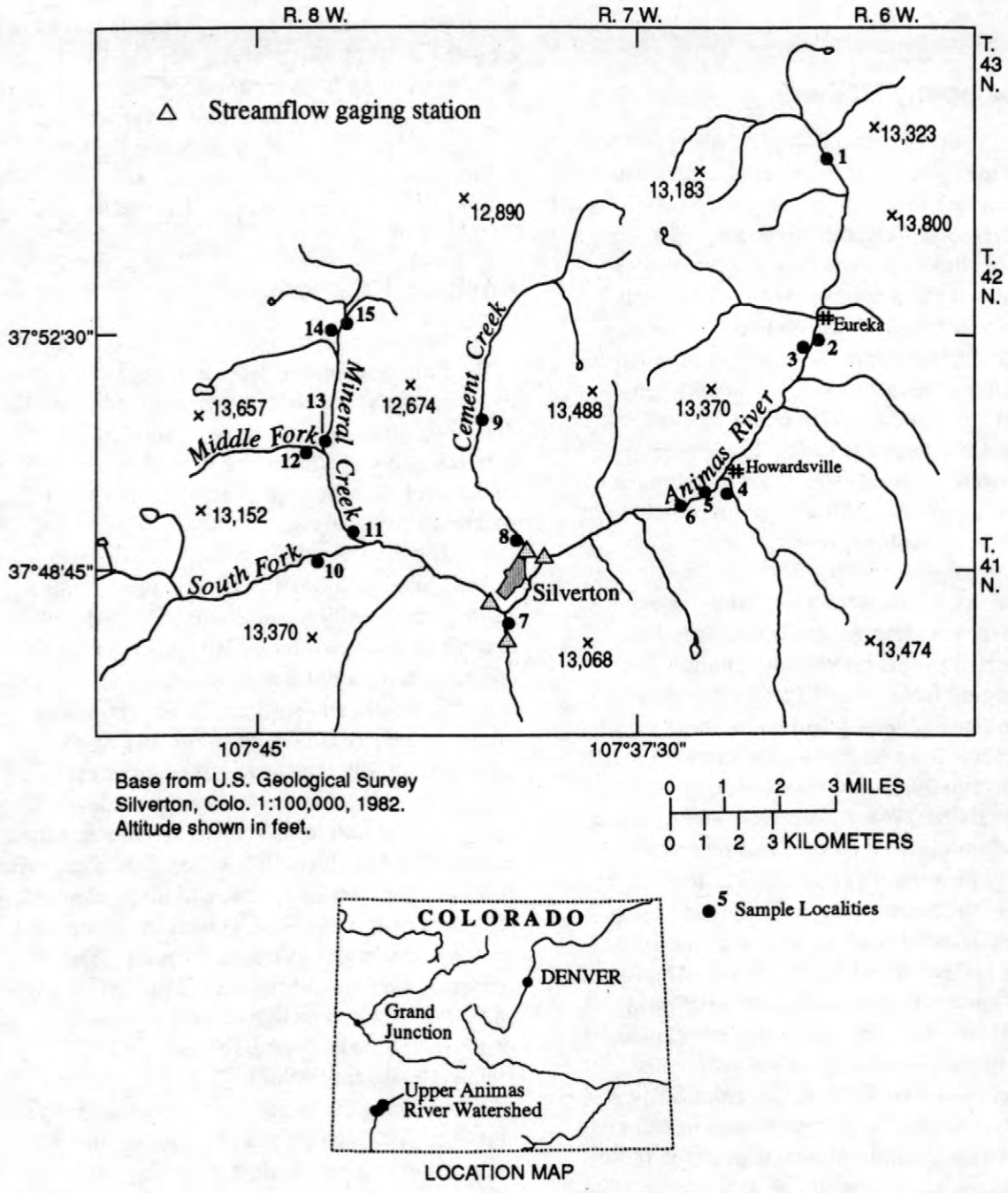

Figure 1. Map of the upper Animas River watershed showing localities of samples taken to determinine pre-mining background. The map area shows only the upper Animas River watershed which is the focal area of the current study. Additional samples are discussed in the text from localities as far downstream as Durango, about 75 river kilometers south of Silverton, Colo. on the Animas River. Bakers Bridge is located at the base of the Animas River Canyon section about 50 river kilometers south of Silverton, Colo.

Church and others, 1993). In this procedure, a 2-g sample is leached with 15 mL of the solution for three hours, centrifuged and analyzed for 35 major and trace elements by ICP-AES. Replicates and the same reference materials were also analyzed with each sample set to access analytical quality and reproducibility.

Geochronology

Where the data on pre-mining sediment quality needed to construct a strategy for restoration is absent, other means of determining environmental changes may be obtained by examining the changes in fauna and flora coupled to chronological scales defined by the distribution of radioactive isotopes. This method of establishing chronologies is based on a known property of radioactive material, ***the half-life***. A half-life of an isotope is the amount of time it takes for half a given number of parent atoms to decay to an isotope of another daughter element. The age of sediment containing a radioactive isotope with a known half-life is calculated by knowing the original concentration and measuring the percent of the remaining radioactive material. The requirements for a radioisotope to be a candidate for dating are that: 1) the chemistry of the parent isotope is known; 2) the half-life is known; 3) the initial amount of the isotope per unit substrate is known or can be accurately estimated; 4) once the isotope is encapsulated within the substrate, the only change in concentration is due to radioactive decay, that is the sample has remained a closed system; 5) the abundance of the daughter isotope must be relatively easy to measure if the technique is to be useful, and 6) the effective age range must be applicable to the time span required to solve the problem (about 8 half lives). In the Animas River watershed, there are four radioisotopes that satisfy these criteria and provide useful data: ^{7}Be, ^{14}C, ^{137}Cs, and ^{210}Pb.

Berylium-7

^{7}Be is formed in the atmosphere by the interaction of cosmic rays and nitrogen. This isotope has a short half-life of about 54 days. Since ^{7}Be is a very reactive, it readily sorbs to soils and sediment upon being swept from the atmosphere by rainfall. The presence of ^{7}Be in the sediment is a useful indication that the sediment was in contact with the atmosphere within a few months of the time of collection of the sample. Furthermore, if the ^{7}Be activity is relatively uniform between different samples sites within the same watershed, the uniformity of the ^{7}Be activity is very useful in establishing that the parent isotope activity of longer-lived isotopes are also in equilibrium with atmospheric processes producing the parent isotope, and that the assumptions necessary for ^{210}Pb dating are reasonable assumptions for the ^{210}Pb flux.

Lead-210

^{210}Pb, with a half-life of 22.8 years, is ideal for environmental studies. A member of the ^{238}U series, the disequilibrium between ^{210}Pb and ^{226}Ra is caused by the physio-chemical activity of the intermediate gaseous progenitor, ^{222}Rn. This isotope, in turn, rapidly decays to form ^{210}Pb. The highly reactive lead is rapidly sorbed to or incorporated in the depositing sediment. This flux produces a concentration of unsupported or excess ^{210}Pb activity, which is the lead that has an activity higher than that of the ambient ^{210}Pb which is in equilibrium with ^{226}Ra. Ages of deposition of individual layers of sediment are calculated by determining the decrease in ^{210}Pb activity at consecutive intervals. If the initial concentration of ^{210}Pb is known, or can be estimated using ^{7}Be activity data, then the "age" (T_{age})of a horizon is calculated by the following:

$$T_{age} = \ln(A\,^{210}Pb_0 / A\,^{210}Pb_h) \times 1/\lambda \quad (1)$$

or substituting the constants,

$$T_{age} = \ln(A\,^{210}Pb_0 / A\,^{210}Pb_h) \times 1/0.03114; \quad (2)$$

where

$A^{210}Pb_0$ is the unsupported or "excess" ^{210}Pb activity in disintegrations per minute at time zero (the present),

$A\ ^{210}Pb_h$ is the activity in disintegrations per minute at depth h, and

λ is the decay constant, or half-life of ^{210}Pb.

Carbon-14

^{14}C is also produced in the Earth's atmosphere by the interaction of cosmic-ray particles with nitrogen (N), oxygen (O), and carbon (C). Of these, nitrogen (N) is the most important in terms of the amount of ^{14}C produced. An additional source of ^{14}C was thermonuclear activity in the late 1950's and early 1960's. This additional contribution reached its peak between 1963 (northern hemisphere) and 1964 (southern hemisphere). From whatever source, the ^{14}C atoms produced are rapidly oxidized to CO_2 and are assimilated into the carbon cycle. ^{14}C has a half-life of 5,568 years producing an effective range of applicability of 100 to 70,000 years. The dates are reported as radiocarbon years before present, where present is, by international convention, 1950. The modern reference standard is 95 percent of the ^{14}C content of the National Bureau of Standards Oxalic Acid and calculated using the Libby ^{14}C half life (5,568 years). The bomb produce carbon is determined by comparing the 1950 carbon activity to the present carbon activity and is represented by the symbol -Δ. Prior to 1950 the atmospheric $\Delta^{14}C$ value was about -50 ‰, as a result of the thermonuclear activity the $\Delta^{14}C$ increased to 200 ‰ in 1964-1965. This value has been slowly decreasing as the "bomb" carbon is removed from the atmosphere. The "bomb" carbon signature provides a valuable reference marker against which other "dating" methods can be calibrated.

Cesium –137

^{137}Cs, with a half-life of 30.3 years, is a thermonuclear byproduct. Its presence is directly related to the atmospheric testing of nuclear devices during the latter half of the 1950's and early 1960's. Under ideal conditions, ^{137}Cs activity in the sediments deposited should mirror the ^{137}Cs production curve. With the exception of the Chernobyl failure, there has been no ^{137}Cs released to the atmosphere since the cessation of atmospheric nuclear testing. ^{137}Cs activity is now below the limit of detection in modern sediments. In the acidic bogs and wetlands sediments, ^{137}Cs has been demonstrated to be mobile and thus not a reliable isotope for "dating" purposes. However, since it is a group one element like sodium and potassium, it should behave conservatively in aqueous mediums.

All measurements of continuous variables are made with a degree of uncertainty (error). There are random errors, systematic errors, or observational errors, which all combine to introduce a degree of measurement uncertainty. Random errors arise from radioactive decay processes, or from the statistical uncertainty of measurements of parent and daughter isotope radioactivity. Systematic errors occur if there is a miscalibration of the instrumentation. Observational errors arise from unrecognized "contamination or disturbance" of the sample which violates the closed system behavior required for geochronological applications. In isotopic dating of sediment, it is assumed that the "law of superposition" is applicable. If sedimentary mixing, either natural or anthropogenic is unrecognized, the parent/daughter systematics have been destroyed and the results will be erroneous. In addition to the sources of error enumerated, there is a problem inherent in measurements of radioactivity. The ^{210}Pb procedure requires the precise measurement of the activity ^{210}Pb and its parent ^{226}Ra. Each of these measurements have an inherent degree of statistical uncertainty. As the differences in these two activities become small, it becomes impossible to differentiate between the two. For this reason, the lower limit of age measurements for the ^{210}Pb procedure is approximately 150 years. However, as most of the historical mining activity in the western U. S. has occurred following the Civil War, the ^{210}Pb geochronometer is ideally suited to study the environmental impacts caused by historical mining activity in fluvial systems.

As defined, the age of a layer of material is determined by the ratio of activity between T_0 and the activity at the horizon investigated. In determining the ages of a horizon, there are two levels of precision possible. The first is a crude

estimated based solely on the determination of presence or absence of "excess" ^{210}Pb over the ambient parent ^{226}Ra. If "excess" ^{210}Pb activity exists, then the sediment is less than 150 years old. The second level of precision is necessary to provide the high degree of time resolution required in most environmental investigations. In these studies, the high age precision is determined by measuring the "excess" ^{210}Pb activity of sequential samples in homogenous sediment. In this procedure, each measurement validates the previous and succeeding one resulting in a smooth curve of decreasing "excess" ^{210}Pb activity with depth. As a result, the age measurements are internally consistent. This type of curve is the norm in lake environments where one can reasonably expect a uniform rate of sedimentation, but this behavior can not be expected in fluvial systems.

In fluvial sediments where sedimentary sequences are not deposited at a uniform rate, the use of radioisotopes to "date" stratigraphic horizons is more complex. In such situations, there are a number of parameters, which must be determined to refine a date beyond the simple interpretation that the sample is less than 150 years old. These parameters are: 1) the flux of the parent and daughter isotopes to the system and 2) the adsorption coefficient of the isotopes in the sediment as they were deposited. A series of sites were sampled within the Animas River watershed to determine these parameters. To date, the top portions of eight cores have been examined to determine the flux of ^{210}Pb to the Animas River watershed and have yielded data consistent with the ^{210}Pb flux rate that has been determined in cores taken throughout the country. From our preliminary data, the incident ^{210}Pb flux is about 1.0 ± 0.3 dpm/cm^2/year in the Animas River study area. The measurements needed to determine the adsorption factors for ^{210}Pb have not yet been completed.

Paleoentologic Studies

Fine-grained sediments from cores taken along the Animas River watershed were examined for the remains of terrestrial and aquatic flora and fauna that might be preserved in the historical sedimentological record. Aquatic and terrestrial invertebrates, vertebrates, and plant megafossils would represent a qualitative proxy for the variety of habitats sampled along the Animas River, including active river and stream channels, abandoned oxbows, riparian habitats, and ponded systems such as beaver dammed ponds. Each of these habitats can be characterized by a distinct group of organisms, many of which have hard body parts, such as chitinized or scleritinized exoskeletons, cellulose or woody stems, or silicified or calcified skeletal components, that are preserved in the sediments. In some skeletal systems, particularly those with calcified body parts, trace elements are incorporated into the lattice structure and provide an additional quantitative proxy for water composition (De Deckker and Forester, 1988; Timmermans, 1993).

Samples examined for this study represent fine-grain sands, silts, and clays taken from cored localities. Lift samples and terrace gravels represent environments that are not conducive either to organism survival or to preservation of microscopic-sized remains, and so these lithologies were generally not examination. Samples from sites 2, 3, 7, 9, and 14 (fig. 1) were examined as were two sites in the Animas Canyon reach and many of the samples from the fluvial sediments in the oxbow lakes sampled near Durango. All samples were processed using methods that avoid agitation, chemicals, or high temperatures; in this manner, very delicate remains such as insect wings are recovered. Additionally, any analyses for trace elements, stable isotopes, or amino acids can be conducted on the organic remains without concern for thermal or chemical alteration of samples recovered. Samples were wet-weighed, placed in warm water with sodium bicarbonate and Calgon (sodium hexametaphosphate), and frozen. Subsequent thawing allows physical disaggregation of the clays. Sediment was washed through a 230 mesh-sieve (63 micrometers,) and all material larger than 150 micrometers was examined under a binocular microscope. Sample residues were examined and characterized for all organic remains of fauna and flora, preservation, and associated grain-size and lithology of the microscopic minerals and rock fragments.

RESULTS AND SUMMARY

Geomorphologic mapping of the fluvial deposits in the study area has identified numerous sites where pre-mining bed sediments may be preserved. We have examined many of these sites and collected fluvial sediments from fifty-two sites plus the trench site (site 3, fig. 1). Fluvial materials from these sites represent pre-mining bed sediments, old historical bed sediments, overbank flood deposits, both pre-mining and historical, fluvial tailings deposits representing different milling processes, pre-mining riparian habitat, and historical and modern beaver ponds. More than 500 samples from these sites have been analyzed for their total metal concentrations. Preliminary analysis of the geochemical data, when coupled with both the historical and geochronological record, clearly show that there has been a major impact by historical mining activities on the geochemistry of the fluvial bed sediments. The impact of historical mining activity is clearly recorded in the sedimentological record as shown in the study of sediments from the trench section (Vincent and others, 1999). Historical mining activity has resulted in a substantial increase in metals in the very fine sand to clay sized component of the bed sediments of the upper Animas River, and Cement and Mineral Creeks. Enrichment factors for metals in modern bed sediments, relative to those sediments that are clearly pre-mining in age, range from a factor of 2 to 6 for arsenic, 4 to more than 10 for cadmium, 2 to more than 10 for lead, 2 to 5 for silver, and 2 to more than 15 for zinc.

Preliminary geochronological results from the silt layer exposed in the trench from the braided reach under a gravel bed in the upper Animas River between Howardsville and Eureka (site 3, fig 1) indicate that this layer was deposited just prior to the start up of mining. The data from samples from the top portion of the silt layer exhibit ^{210}Pb disequilibrium. This suggests that the top of the silt deposit is less than 100-to-150 years BP. Preliminary geochronological results from sediments from the oxbow lakes in the lower Animus River flood plain near Animas City indicate that these cores do show ^{210}Pb disequilibrium and one core, 98ABB270B, has been dated. The age profile from this core indicates episodic sedimentation. The top 8 cm of sediment in this core appears to have accumulated slowly over the past 40 years. The flat nature of the ^{210}Pb distribution between 8 and 20 cm is indicative of very rapid sedimentation. The ^{210}Pb and concurrent ^{137}Cs data suggest that this layer was deposited about 50 years ago. The bottom most stratigraphic interval from this core indicates another period of rapid sediment deposition and has a calculated ^{210}Pb age of about 70 years. The lack of equilibrium in these samples means that the core did not reach older sediment.

Nearly all of the samples examined for paleoentologic evidence included some vegetative material, ranging from fine matted material characteristic of subaquatic plants from ponds, quiet streams, or overbank water accumulations, to concentrated fecal pellets laden with plant material, most probably representing sediments deposited in beaver ponds, to woody material characteristic of terrestrial upright plants growing in established riparian soils some distance from the main river channel. Cores that have been dated as pre-mining, especially those with significantly older sediments from the trench (site 3, fig. 1), show significant peatification of the woody plant remains, ranging from recognizable but altered stems to clumps of highly altered material. These intervals have been dated using ^{14}C methods. Most of the associated mineral grains consist of fine sand and silty material; occasional samples contain angular, fresh, uncoated sulfide mineral grains with essentially no fine-grained sediment or organic remains. This depositional environment clearly represents a rapid influx of mill tailings from an upstream source related to mining. In general, upstream samples from overbank habitats contain only floral remains; aquatic invertebrates and vertebrates are conspicuous by their absence. These are interpreted to represent riparian habitat.

Crustaceans were recovered from two cores, from a modern beaver pond along an old channel of the Animas River near Needleton abandoned in 1927 (Osterwald, 1995) and from an old abandoned oxbow near Durango. The modern beaver pond, which is fed by groundwater, included a number of calcified

valves of a freshwater crustacean, with the valves coated with iron oxides. The abandoned oxbow occurrence included a single daphniid ephippia (a chitinized egg case). The abundance and excellent state of preservation of ostracods from the beaver pond core indicate that neutral to alkaline pH waters without elevated trace element concentrations existed for a period of months. The daphniid occurrence in the oxbow sediments represents a nektonic or swimming crustacean with a short life cycle and is probably indicative of a flush of clean water probably from snowmelt; associated mineral grains with small amounts of vegetative debris further support a rapid influx of sediment from upstream sources.

Paleoentologic evidence does not indicate a healthy aquatic habitat in any of the stream reaches investigated above the confluence of the Animas River with Mineral Creek (fig. 1) prior to the impact of mining activity. The absence of paleoentologic remains is interpreted to reflect the poor preservation regime of the bed sediment materials sampled. The fluvial sediments sampled in this study were deposited in higher energy environments than are conducive to the preservation of most aquatic organisms including fish remains. In comparison with water quality observed today in the streams (Church and others, 1997), the bed sediment chemistry of the sediments today would suggest that pre-mining water was less acidic prior to mining and carried a smaller colloidal sediment load than is found in these stream reaches today.

Restoration goals and objectives for the upper Animas River watershed must take into account the evidence from the pre-mining fluvial record which indicates that metal loads and acidity in the water column were substantially lower than they are today. However, the profound changes in the ground-water flow system caused by mining activity and the substantial dispersed metal source in the fluvial sediments caused by the industry practice of discharging mill tailings into mountain streams throughout the west prior to 1935 are environmental impacts that may have prolonged influence on the overall restoration plan for the upper Animas River watershed. Additional studies that focus on the impact of removal of know point sources within the upper Animas River watershed are required before it is feasible to determine the extent to which watershed restoration can approach the original pre-mining bed sediment geochemical baseline.

AUTHOR INFORMATION

Stanley E. Church, U.S. Geological Survey, Denver, Colo., (303) 236-1900, schurch@usgs.gov,
David L. Fey, U.S. Geological Survey, Denver, Colo., (303) 236-8923, dfey@usgs.gov
Elisabeth M. Brouwers, U.S. Geological Survey, Denver, Colo., (303) 236-5440, brouwers@usgs.gov
Charles W. Holmes, U.S. Geological Survey, St. Petersburg, Florida, (813) 893-3100x3056, cholmes@usgs.gov, and
Robert Blair, Dept. of Geology, Fort Lewis College, Durango, Colo., (970) 247-7263, BLAIR_R@fortlewis.edu.

REFERENCES

Atwood, W.W., and Mather, K.F., 1932, Physiography and Quaternary Geology of the San Juan Mountains, Colorado: U.S. Geological Survey Professional Paper, 166, 207 p.

Blair, Robert, 1998, Progress report on surficial deposits and geomorphology of major drainages of the upper Animas River watershed, Colorado, *in* Nimick, D.A., and von Guerard, Paul, eds., Science for watershed decisions on abandoned mine lands: review of preliminary results, Denver, Colorado, February 4-5, 1998: U.S. Geological Survey Open-File report 98-297, p. 28.

Briggs, P.H., 1996, Forty elements by inductively coupled-plasma atomic emission spectrometry, *in* Arbogast, B.F., ed., Analytical methods manual for the Mineral Resources Program, U.S. Geological Survey Open-File Report 96-525, p. 77-94.

Casadevall, Tom, and Omoto, H., 1977, Sunnyside mine, Eureka mining district, San Juan County, Colorado: Geochemistry of gold and base metal ore deposition in a volcanic

environment: Economic Geology, v. 92, p. 1285-1320.

Chao, T.T., 1984, Use of partial dissolution techniques in geochemical exploration: Journal of Geochemical Exploration, v. 20, p. 101-135.

Church, S.E., Holmes, C.E., Briggs, P.H., Vaughn, R.B., Cathcart, James and Marot, Margaret, 1993, Geochemical and lead-isotope data from stream and lake sediments, and cores from the upper Arkansas River drainage: Effects of mining at Leadville Colorado on heavy-metal concentrations in the Arkansas River: U.S. Geological Survey Open-File Report 93-534, 61 p.

Church, S.E., Kimball, B.A., Fey, D.L., Ferderer, D.A., Yager, T.J. and Vaughn, R.B., 1997, Source, transport and partitioning of metals between water, colloids, and bed sediments of the Animas River, Colorado: U.S. Geological Survey Open-File Report 97-151, 135 p.

Church, S.E., Fey, D.L. and Brouwers, E.M., 1998a, Determination of pre-mining background using sediment cores from old terraces in the upper Animas River watershed, Colorado, *in* Nimick, D.A. and von Guerard, Paul, eds., Science for Watershed Decisions on Abandoned Mine Lands: A Review of Preliminary Results, Denver, Colorado, February 4-5, 1998: U.S. Geological Survey Open-File Report 98-296, p. 40.

Church, S.E., Sole, T.C., Yager, D.B., and McCafferty, A.M., 1998b, The role of geoenvironmental maps and statewide assessments in prioritizing watersheds for remediation of abandoned mine lands, *in* Nimick, D.A., and von Guerard, Paul, eds., Science for watershed decisions on abandoned mine lands: review of preliminary results, Denver, Colorado, February 4-5, 1998: U.S. Geological Survey Open-File report 98-297, p. 4.

De Deckker, P. and Forester, R.M., 1988, The use of ostracods to reconstruct continental palaeoenvironmental records, *in* De Deckker, P., Colin, J.-P., and Peypouquet, J.-P., eds., Ostracoda in the Earth Sciences: Elsevier, p. 175-200.

Gillam, Mary, 1998, Late Cenozoic geology and soils of the lower Animas River Valley, Colorado and New Mexico: University of Colorado, Ph.D. Dissertation, 477 p.

Lipman, P.W., Fisher, F.S., Mehnert, H.H., Naeser, C.W., Luedke, R.G., and Steven, T.A., 1976, Multiple ages of mid-Tertiary mineralization and alteration in the western San Juan Mountains, Colorado: Economic Geology, v. 71, p. 571-588.

National Institute of Standards and Technology (NIST), 1993a, Certificate of Analysis Standard Reference Material 2704, Buffalo River Sediment.

_____, 1993b, Certificate of Analysis Standard Reference Material 2709, San Joaquin Soil.

_____, 1993c, Certificate of Analysis Standard Reference Material 2711, Montana Soil.

Osterwald, D.B., 1995, Cinders & Smoke: Western Guideways, Ltd., Lakewood, Colo. 166 p.

Pruess, Jonathan, 1996, Paleoflood reconstructions within the Animas River Basin upstream from Durango, Colorado: Colorado State University, M.S. Thesis, 192 p.

Sloan, R.E., and Skowronski, C.A., 1975, The Rainbow Route, An Illustrated History of the Silverton Railroad, the Northern Silverton Railroad, and the Silverton, Gladstone, & Northerly Railroad, Denver, Colo.: Sundance Publications Limited, 416 p.

Timmermans, Klaas R., 1993, Accumulation and effects of trace metals in freshwater invertebrates, *in* Dallinger, R. and Rainbow, P.S., eds., Ecotoxicology of metals in invertebrates: Lewis Publishers, p. 133-148.

Vincent, K.R., Church, S.E., and Fey, D.L., 1999, Geomorphological context of metals-laden sediments the Animas River flood plain, Colorado: this volume.

U.S. Geological Survey, 1898, Topographic map of the Durango quadrangle, Colo., scale 1:62,500.

Use of Tracer-Injection and Synoptic-Sampling Studies to Quantify Effects of Metal Loading from Mine Drainage

By Briant A. Kimball, Robert L. Runkel, Kenneth E. Bencala, and Katherine Walton-Day

ABSTRACT

Thousands of abandoned and inactive mines are located in environmentally sensitive mountain watersheds. Cost-effective remediation of the effects of metals from mining in these watersheds requires knowledge of the most significant sources of metals. The significance of a given source not only depends on the concentration of a toxic metal, but also on the total mass of metal added to streams. To determine loads, we combined tracer-injection methods, to provide reliable discharge measurements on a watershed scale, with synoptic sampling, to provide spatially detailed concentration data. The resulting load profiles indicate which sources have the greatest impact on streams, where the streambed will receive metal precipitates, and where ground-water inflows are the greatest. This information is an important part of planning for remediation.

INTRODUCTION

Thousands of abandoned and inactive mines are located in environmentally sensitive mountain watersheds. Cost-effective remediation of the effects of metals from mining in these watersheds requires science-based knowledge of metal sources, transport, and effects. Regulatory and land management agencies need the answers to some basic questions to plan cost-effective remediation. First, which sources of mine drainage in a watershed have the greatest effect on the stream? Second, what natural processes or instream chemical reactions move metals from the water column to the streambed where the metals can affect aquatic organisms? Finally, does a remediation plan for an individual site need to account for the complexity of surface- and ground-water sources of metals?

The purpose of this discussion is to present an approach that represents a practical application of the research methods and models that have been developed as part of the Upper Arkansas Surface-Water Toxics Project as part of the Toxic Substances Hydrology Program. A recent study in Cement Creek, Colorado, a tributary of the Animas River, illustrates the approach used to provide preremediation information as part of the Abandoned Mine Lands Initiative. Because Cement Creek receives mine drainage from many sources in the watershed it is a good watershed to demonstrate the complexity of mine-drainage inflows and the availability of solutions (fig. 1).

AN APPROACH FOR MOUNTAIN STREAMS

Because of the work of many local, State, and Federal agencies, much is known about the location and chemical character of mine drainage in the Western United States. Information about individual mines can indicate potentially toxic sources of metals to streams but does not necessarily provide the complete picture for making decisions about remediation on a watershed scale. The complete picture of the effects of metals on a stream is not just the metal concentration, which directly relates to acute toxicity, but also the metal load, which relates to chronic toxicity. Calculating load

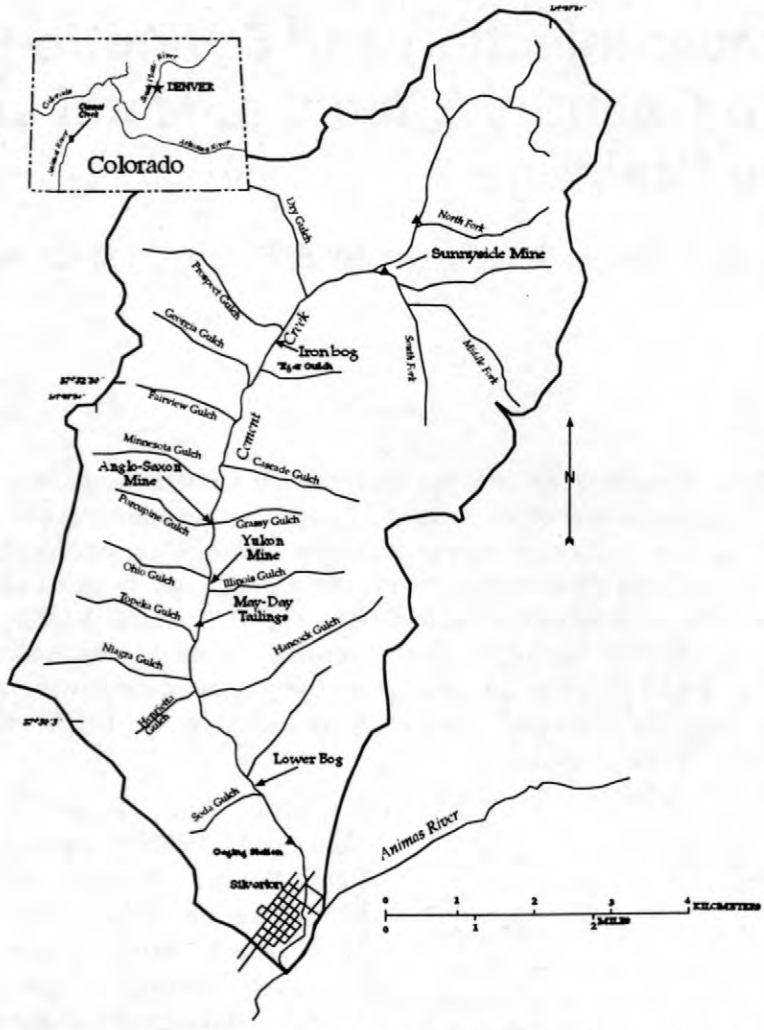

Figure 1. (a) Schematic watershed views showing (a) data collection at the watershed outlet verses (b) the detail of information needed for remediation decisions.

requires both chemical concentrations and discharge. Discharge measurements in mountain streams, however, are difficult, even under the best of conditions, because much of the flow in mountain streams is among the streambed cobbles. The Cement Creek study illustrates the combination of a tracer-dilution study for discharge determinations, with synoptic sampling for detailed chemical composition of stream and inflow sites. Synoptic samples are provide a "snapshot" of the changes along a stream at a given point in time.

Adding a tracer: Discharge by dilution

Discharge in mountain streams can be measured with good precision by adding a conservative dye or salt tracer to a stream and calculating discharge from the amount of dilution as the tracer moves downstream (Bencala and others, 1990; Kimball, 1997). Because we know the concentration of the injected tracer and the rate at which it is added to the stream, we know the mass added to the stream (Zellweger and others, 1988). By using the conservation of mass, we can calculate the discharge by measuring the concentration of the tracer upstream and downstream from the injection point. A 12-kilometer reach of Cement Creek was separated into two separate injection reaches because there was active remediation at the Sunnyside Mine. A sodium chloride tracer was added upstream from the mine and a lithium chloride tracer was added

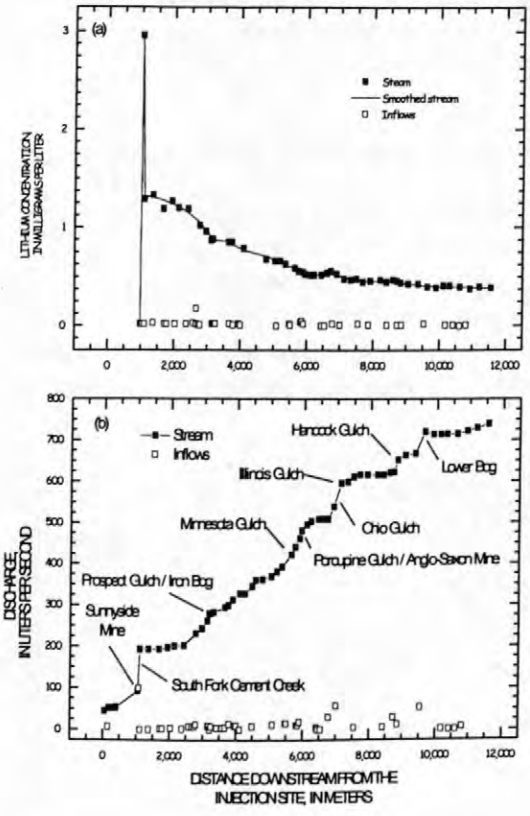

Figure 2. (a) Variation of lithium concentration with distance downstream from the injection site. The relatively low concentration of lithium in inflow samples indicates that lithium was an effective tracer.

downstream from the mine. After the tracers had reached a steady state along the stream reaches, synoptic samples were collected at sites downstream from the injection points to document the incrementaldecrease of tracer concentration due to water entering the stream (fig. 2a). The profile of lithium concentration allows the calculation of discharge at the synoptic sites (fig. 2b). With the tracer measurement, a change in discharge between two stream sites represents the total amount of water entering the stream from surface- and groundwater sources in that stream segment.

Synoptic sampling

Synoptic sampling includes both stream and inflow sites. Before the injection study, every visible inflow is identified for sampling. Stream sites for sampling are chosen upstream and downstream from each inflow, giving three points to make a mass-balance calculation for each inflow (points A, B, and I, fig. 3). Additional stream sites are chosen along the study reach to quantify ground-water inflows where there are no visible inflows (point C, fig. 3). Chemical analyses of synoptic samples provide a detailed profile of metal concentrations along the study reach.

Adding a tracer: Discharge by dilution

Discharge in mountain streams can be measured precisely by adding a conservative dye or salt tracer to a stream and calculating discharge from the amount of dilution as the tracer moves downstream (Bencala and others, 1990; Kimball, 1997). Because we know the concentration of the injected tracer and the rate at which it is added to the stream, we know the mass added to the stream (Zellweger and others, 1988). By using the conservation of mass, we can calculate the discharge by measuring the concentration of the tracer upstream and downstream from the injection point. A 12-kilometer reach of Cement Creek was separated into two separate injection reaches because there was active remediation at the Sunnyside Mine. A sodium chloride tracer was added upstream from the mine and a lithium chloride tracer was added downstream from the mine. After the tracers had reached a steady state along the stream reaches, synoptic samples were collected at sites downstream from the injection points to document the incrementaldecrease of tracer concentration due to water entering the stream (fig. 2a[1]). The profile of lithium concentration allows the calculation of discharge at the synoptic sites (fig. 2b). With the tracer measurement, a change in discharge between two stream sites represents the total amount of water entering the stream from surface- and groundwater sources in that stream segment.

LOAD PROFILES: A "SNAPSHOT" IN TIME

Zinc concentrations of stream and inflow samples illustrate the spatial detail along the 12-

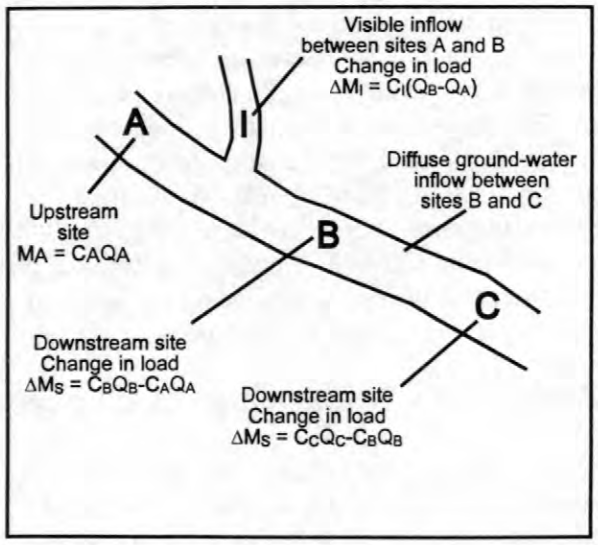

Figure 3. Schematic diagram showing mass-balance calculations around an inflow to a stream.

kilometer stream reach (fig. 4a). The instream concentration of zinc did not vary greatly, despite the large range of zinc concentration among the inflows. The profile of sampled instream load was calculated from the concentrations and the discharge values (fig. 4b). The profiles of concentration and load help answer the basic questions about the sources of metals and the effectiveness of remediation. First, although there are many sources of mine drainage, the principal sources are indicated by the sharp increases in the sampled instream load (fig. 4b).

Identifying important sources of metals

To rank the relative importance of the load from a particular stream segment or a group of stream segments requires another view of the load information. The net change in load between any two stream sampling sites can be positive, indicating an increase of load, or negative, indicating a loss through physical or chemical processes (fig. 3). The net change is:

Zinc concentrations of stream and inflow samples illustrate the spatial detail along the 12-kilometers stream reach (fig. 4a). The profile of sampled instream load was calculated from the concentrations and the discharge values (fig. 4b). The profiles of concentration and load help answer the basic questions about the sources of metals and the effectiveness of remediation. First, although there are many sources of mine drainage, the principal sources are indicated by the sharp increases in the sampled instream load (fig. 4b).

Identifying important sources of metals

To rank the relative importance of the load from a particular stream segment or a group of stream segments requires another view of the load information. The net change in load between any two stream sampling sites can be positive, indicating an increase of load, or negative, indicating a

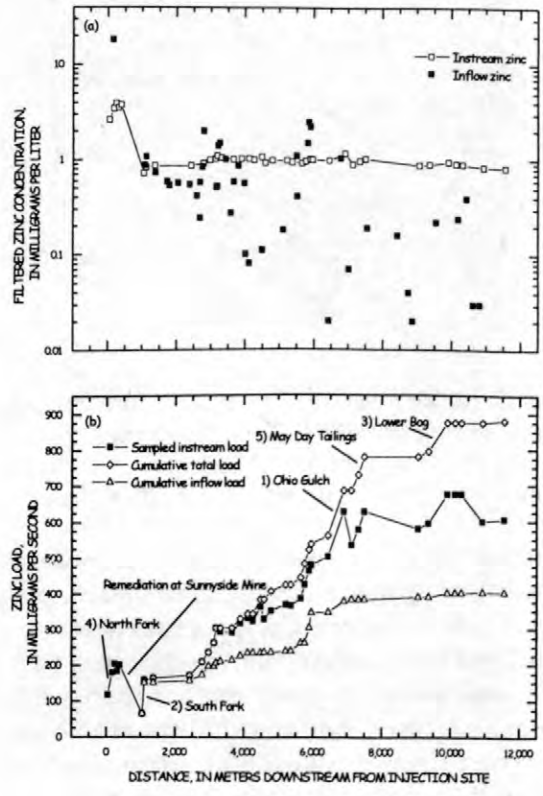

Figure 4. Variation of (a) zinc concentration and (b) zinc load with distance in samples from Cement Creek, Colorado. The five largest inflows are indicated by name and a number for its rank. The sampled instream load represents the calculated load at each stream site. The cumulative total load represents a summation of the entire load entering the stream. The cumulative inflow load represents the part of the total load that can be attributed to sampled inflows.

loss through physical or chemical processes (fig. 3). The net change is:

$$\Delta M_s = C_B Q_B - C_A Q_A \quad (1)$$

where

ΔM_s is the net change in load for a stream segment, in milligrams per second,
C_B is the solute concentration at the downstream site, in milligrams per liter,
Q_B is the stream discharge at the downstream site, in liters per second,
C_A is the solute concentration at the upstream site, in milligrams per liter,
Q_A is the stream discharge at the upstream site, in liters per second.

Calculation of the minimum total load entering the stream along a study reach is the cumulative sum of all the positive values of for individual stream segments. The percentage of the cumulative total load that is contributed by any one segment is found by dividing the value of for that segment by the cumulative sum (fig. 4b). For example, the contribution from Ohio Gulch between 6,447 meters and 6,907 meters is about 14 percent of the cumulative total load. This calculation points out the five largest loads to Cement Creek (fig. 4b).

The sampled instream load also indicates the effectiveness of remediation at the Sunnyside Mine (fig. 4b). Almost all the zinc load that was present upstream from the mine was removed. The remediation decreased the zinc load that Cement Creek contributes to the Animas River, but substantial loads downstream from the Sunnyside Mine add a large zinc load.

The profile of sampled instream load indicates that there were many small sources of zinc load all along the study reach. All these relatively small sources add up to a substantial percentage of the cumulative total load. This "dispersed" loading complicates plans for remediation because even if the major sources can be controlled, the many small sources may still contribute too much zinc to allow adequate stream recovery. So a remediation plan for this stream would be immense. The load profile indicates that there may be some cost-effective targets for remediation that may decrease the input of zinc to the Animas River. This may be a more reasonable objective than trying to lower zinc concentrations to aquatic standards in Cement Creek itself.

Identifying effects on the stream

The difference between the sampled instream load and the cumulative total load indicates how much zinc was removed from the stream through chemical and physical processes (fig. 4b). If there were no instream losses of load, then the sampled instream load and the cumulative total load would be exactly the same. The two accounts of load only differ if there are stream segments with negative values of . Where the net change in load decreased, zinc was removed from the stream and added to the streambed. In those stream segments, metals should be more available to benthic invertebrates and the likelihood that metals enter the food chain is great. For example, between 6,907 meters and 7,131 meters downstream, a large amount of zinc was removed and there was visual evidence of the precipitate on the streambed. Stream segments where metals are added to the streambed will be the most affected parts of the stream.

Identifying ground-water inflow

A second way to view the net change in zinc load is possible if there is a sampled inflow in a stream segment. The change in mass can be expressed as:

$$\Delta M_I = C_I(Q_B - Q_A) \quad (2)$$

where

ΔM_I is the net change in load for a stream segment, assuming that the inflow concentration represents the average concentration of water entering the stream in that stream segment,
C_I is the solute concentration in the inflow sample, in milligrams per liter, and

Q_B and Q_B are as defined previously. The cumulative sum of values is the cumulative inflow load

and represents that part of the cumulative total load that can be attributed to sampled inflows (fig. 4b).

If C_I is an accurate representation of the concentration for all the water entering the stream in that segment, then ΔM_I will equal ΔM_S. If ΔM_S. is greater than ΔM_I, the difference between them may be due to the diffuse seepage of ground-water inflow. This could result from an average concentration of water entering the stream that is greater than the concentration sampled in the inflow. Although this is not proof of ground-water inflow, it indicates a likely source of ground water with a higher concentration entering the stream in that segment. Thus, differences between the cumulative total load and the cumulative inflow load could indicate zones of ground-water inflow. For the Cement Creek data in the stream reach around Ohio Gulch, from 6,447 meters to 6,907 meters downstream, meters shows a substantial difference between the two calculations. Although there was loading from the visible inflow of Ohio Gulch, the total load was greater, so there must have been zinc load from ground-water input.

This information is important for evaluating specific sites for remediation. A remediation plan must account for visible and dispersed sources of metal load, and this likely is the easiest way to identify the presence of dispersed ground-water inflow. It assumes that the average concentration of water entering the stream is the same as the sampled inflow concentration. If the sampled inflows completely accounted for the entire load entering the stream, then the cumulative total and the cumulative inflow loads would be the same.

The load profile answers important questions about sources of mine drainage, where the streambed is affected, and inputs of ground water. The load profile summarizes the effects of particular sources on the stream. These are important answers needed for effective remediation planning.

REFERENCES CITED

Bencala, K.E., McKnight, D.M., and Zellweger, G.W., 1990, Characterization of transport in an acidic and metal-rich mountain stream based on a lithium tracer injection and simulations of transient storage: Water Resources Research, v. 26, no. 5, p. 989-1000.

Kimball, B.A., 1997, Use of tracer injections and synoptic sampling to measure metal loading from acid mine drainage: U.S. Geological Survey Fact Sheet FS-245-96.

Zellweger, G.W., Bencala, K.E., McKnight, D.M., Hirsch, R.M., and Kimball, B.A., 1988, Practical aspects of tracer experiments in acidic, metal enriched streams, *in* Mallard, G.E., ed., U.S. Geological Survey Toxic Substances Hydrology Program—Surface-Water Contamination, Open-File Report 87-764, p. 125-130.

AUTHOR INFORMATION

Briant A. Kimball, U.S. Geological Survey, Salt Lake City, Utah (bkimball@usgs.gov)

Robert L. Runkel, U.S. Geological Survey, Denver, Colorado (runkel@usgs.gov)

Kenneth E. Bencala, U.S. Geological Survey, Menlo Park, California (kbencala@usgs.gov)

Katherine Walton-Day, U.S. Geological Survey, Denver, Colorado (kwaltond@usgs.gov)

Application of the Solute-Transport Models OTIS and OTEQ and Implications for Remediation in a Watershed Affected by Acid Mine Drainage, Cement Creek, Animas River Basin, Colorado

By Katherine Walton-Day, Robert L. Runkel, Briant A. Kimball, and Kenneth E. Bencala

ABSTRACT

The solute-transport model OTIS and the reactive solute-transport model OTEQ were used to simulate geochemical conditions in Cement Creek, a tributary to the Animas River in southwestern Colorado. Results with OTIS indicated that removal of iron and zinc is required to simulate observed stream conditions on September 20, 1996. Two remediation scenarios that depicted remediation of lesser and greater amounts of zinc from Prospect and Ohio Gulches and the May Day Dump indicated that these actions would reduce zinc concentrations at the mouth of Cement Creek by 7 percent and 13 percent, respectively. OTIS simulations do not account for the effects of changing stream pH on metal concentrations. OTEQ is used to quantify these effects. Preliminary OTEQ simulations indicated that precipitation of ferrihydrite improved the agreement between simulated and observed pH in the mixing zone of Illinois Gulch and Cement Creek. However, observed zinc removal in this zone was not successfully simulated due to the spatial nature of the mixing process and lack of data about the identity and thermodynamic properties of precipitates forming in the mixing zone. Use of OTEQ to simulate remediation requires a better understanding of the processes that occur in streams affected by acid mine drainage.

INTRODUCTION

The solute-transport model OTIS and the reactive solute-transport model OTEQ can be used to help understand the dominant hydrologic and geochemical processes controlling water quality in streams. OTIS (One-dimensional-Transport with Inflow and Storage; Runkel, 1998) has been used to describe the hydrologic processes controlling solute transport in streams. In particular, OTIS is useful to quantify the effects of storage zones on solute transport. OTIS also can account for two types of chemical reactions: kinetic sorption and first-order decay. OTIS has been used to quantify hydrologic processes in a mountain stream (Broshears and others, 1993). Harvey and Fuller (1998) have used OTIS to quantify the combined effects of hydrologic and geochemical processes on manganese transport. Additional applications of OTIS are discussed by Runkel and others (1999).

In streams affected by acid mine drainage, OTEQ (OTis with EQuilibrium calculations; [Runkel and others, 1996a] in which MINTEQ [Allison and others, 1991] is linked with OTIS to perform the equilibrium calculations) has been used to help understand geochemical changes that occurred in streams due to experimental modification of instream pH (Broshears and others, 1996; Runkel and others, 1996b). For example, when instream pH was raised by injection of sodium carbonate in a stream in central Colorado, simulations with OTEQ indicated that carbonate chemistry, the formation of microcrystalline gibbsite and ferrihydrite, and buffering interactions with the streambed were important factors explaining aluminum, iron, and pH behavior. In addition, the simulations revealed some of the limitations of applying the equilibrium assumption to the results of the experiment and that iron chemistry, in particular, was subject to kinetic

restraints (Broshears and others, 1996). In an instream experiment in which ambient stream pH was lowered by injection of sulfuric acid, simulations with OTEQ supported conclusions that increases in dissolved iron concentrations were due to dissolution of hydrous iron oxides and photoreduction of ferric iron (Runkel and others, 1996b). Both of these applications of OTEQ indicated that the model can be used as a tool to help quantify geochemical effects of pH-dependent processes within the context of hydrologic transport.

OTIS and OTEQ have been developed, in part, to guide remediation decisions in watersheds affected by acid mine drainage (Broshears and others, 1996). Both models can be used to explore potential changes in water chemistry that may occur as a result of remedial actions. The objective of this paper is to present examples where both models are used to help understand stream hydrology and geochemistry and to simulate effects of remediation in a stream affected by acid mine drainage. Situations appropriate for application of each model are discussed.

Site Description

Cement Creek is a headwater stream draining an area of approximately 52 square kilometers (km^2) and is a tributary to the Animas River in southwestern Colorado (fig. 1). The main source of streamwater is assumed to be snowmelt runoff. The highest flows occur during May and June. Numerous tributaries to Cement Creek exhibit a wide range of water-quality characteristics; some are acidic from natural weathering of sulfide minerals, others are acidic from mining activities, and others are not acidic. Most of the streambed of Cement Creek is coated with orange-colored iron-rich mineral precipitates. On September 20, 1996, zinc concentrations varied from about 0.7 to 1.2 milligrams per liter (mg/L), which greatly exceeds aquatic-life standards (U.S. Environmental Protection Agency, 1986). Bedrock in the basin consists of altered volcanic and volcaniclastic rocks related to formation of the Silverton Caldera. Rocks on the eastern side of the basin are propylitically altered. On the western side of the basin, rocks have been more intensely altered, and quartz-sericite-pyrite (QSP) alteration is pervasive (Luedke and Burbank, 1996). Propylitically altered rocks commonly contain calcite and have some capacity to buffer low-pH water. Rocks that have been more intensely altered, however, lack alkalinity-generating minerals, such as carbonates, that would help buffer low-pH water. The chemistry of Cement Creek seems to be dominated by inflows of natural and mining-related low-pH water and intensely altered rocks because the pH of the stream is less than 4.0 over much of its length.

METHODS

In September 1996, a synoptic sampling was done in conjunction with injection of a conservative tracer in Cement Creek. Data collected were used to help quantify the effects of metal loading from acid mine drainage according to methods described by Kimball (1997). In addition, the data were used as input for the OTIS and OTEQ simulations.

Tracer-Injection Experiment

Beginning on September 19, 1996, a solution of concentrated lithium chloride was pumped into the South Fork of Cement Creek at the injection site (992 meters [m] downstream from an arbitrary stream datum; fig. 1). The injection continued for approximately 48 hours. Injecting a conservative solute in this manner allows steady-state concentrations of lithium to be reached at all downstream sites because the duration of the injection is much longer than travel time for a conservative solute. After steady-state concentrations have been achieved, streamflow discharge can be calculated at sites downstream from the injection location by measuring the dilution of lithium concentration.

During the second day of the injection (September 20, 1996), water samples were collected from 33 stream sites and 45 inflow sites over a 10.5 km reach of river downstream from the injection site. The concentration of lithium at each site was used to calculate the streamflow discharge. The amount of ground-water and surface-water inflow between stream sites was determined from the difference between the calculated

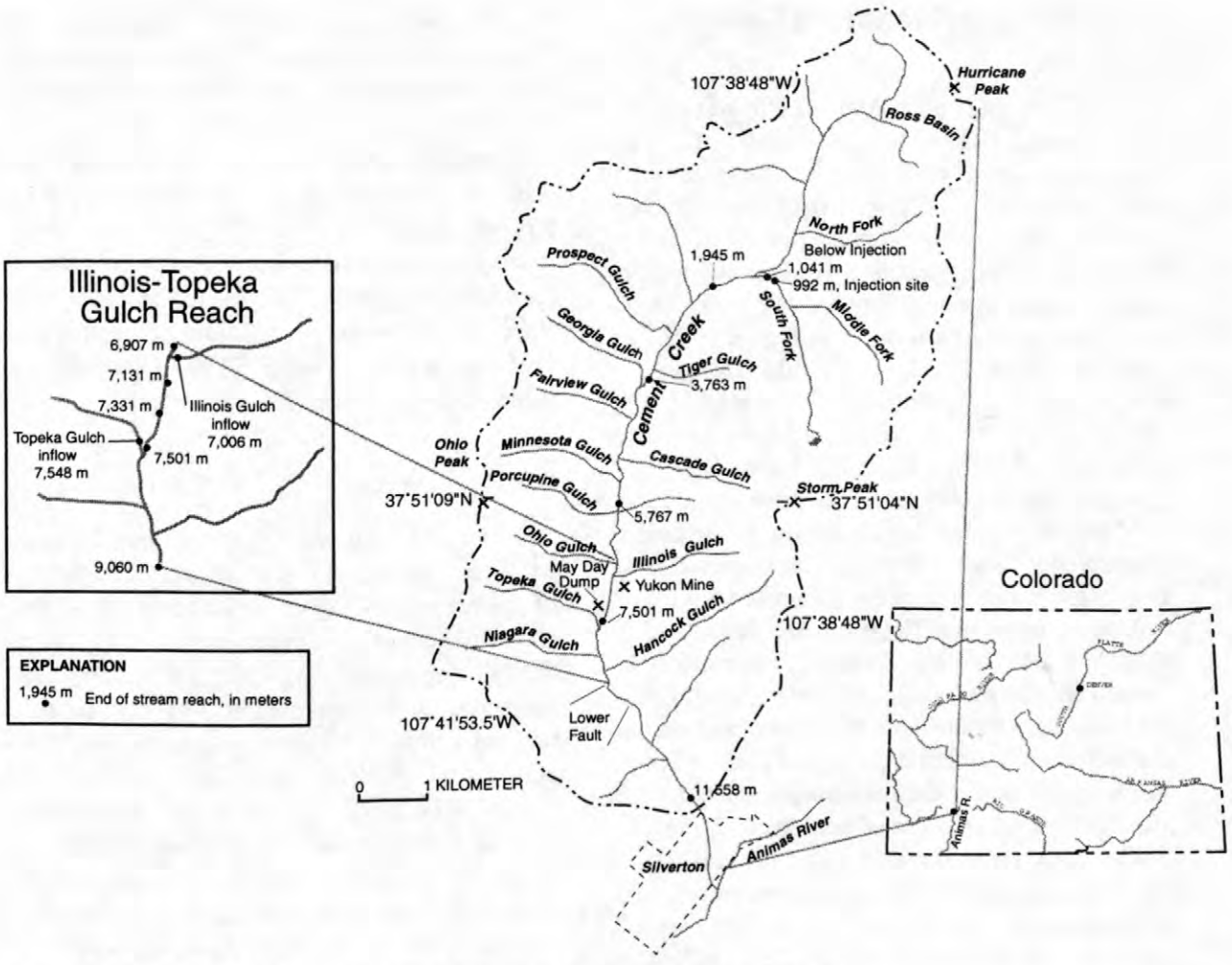

Figure 1. Study area location map, Cement Creek, Animas River Basin, Colorado.

discharge at each site. The instantaneous load of a solute at any site is calculated as the product of streamflow discharge and solute concentration. For conservative solutes, the average inflow solute concentration within a stream reach was determined by dividing the increase of instantaneous load between sites by the inflow discharge. For nonconservative solutes such as zinc and iron, a different procedure was used. The minimum total loading to the stream was calculated by summing all positive changes of instream load between stream sites (Kimball and others, 1998). These calculated loads are greater than actual stream loads. The average inflow solute concentration between sites was determined by dividing the increase of minimum total load by the inflow discharge.

Laboratory Analysis

Water samples were filtered through 0.1-micrometer (μm) membrane filters in the field to determine operationally-defined dissolved metals. Samples were acidified with concentrated nitric acid and were analyzed for metals by use of inductively coupled plasma-atomic emission spectrometry (ICP-AES) (Garbarino and Taylor, 1979). Values of pH were measured the day of sample collection from an unfiltered, untreated aliquot of each sample. Lithium concentrations were determined on filtered, unacidified samples by use of flame atomic absorption spectrometry. An aliquot of filtered, unacidified sample was analyzed for ferrous and total iron concentrations by use of a colorimetric technique (Skougstad and others, 1979). Ferric iron concentration was the difference between total and ferrous iron concentrations.

Collection and Analysis of Sediment Samples

To determine the significance of mixing zones on stream chemistry, two samples of streambed material were collected upstream from and within the mixing zone of Illinois Gulch and Cement Creek (fig. 1) in August 1998. On the day of sample collection, hydrologic conditions were similar to those on September 20, 1996: mean daily discharge at the stream gage at the mouth of Cement Creek was 19 cubic feet per second (ft^3/s) on September 20, 1996, and 21 ft^3/s on August 18, 1998, the day of sediment collection (Crowfoot and others, 1996; J.B. Evans, U.S. Geological Survey, oral commun., 1999). Samples of flocculent material from the streambed were collected by agitating flocculent-coated sand and cobble material from the streambed with ambient streamwater. The water and suspended flocculent material were decanted, and more streambed material was added and agitated with the flocculent/streamwater mixture to increase the concentration of flocculent material in the mixture. The resulting flocculent/streamwater slurries were dried and digested by use of both weak (2 molar hydrochloric acid combined with 1 percent hydrogen peroxide) and strong (mixed nitric, hydrochloric, perchloric, and hydrofluoric) acid solutions. The slurries were analyzed by ICP-AES according to procedures in Church and others (1993) and Briggs (1996).

Modeling

OTIS

Transient simulations of the lithium chloride injection featured six reaches of the river ending at 1,041 m; 1,945 m; 3,763 m; 5,767 m; 7,501 m; and 11,558 m (fig. 1). Samples were collected at the end of each reach from September 19 to 21, 1996. Hydraulic and transient storage parameters for these reaches were estimated using OTIS and OTIS-P. (OTIS-P is a modified version of OTIS in which a nonlinear regression package automates parameter estimation [Runkel, 1998]).

After the transient simulation, the steady-state profile of lithium concentrations was simulated. The stream was subdivided into 29 reaches. Values for lateral inflow (q_{LATIN}) were calculated to coincide with the stream-reach lengths. The instream lithium concentration resulting from the injection (2.96 mg/L) defined the upper boundary condition.

Steady-state, nonreactive simulations of iron and zinc concentrations used the hydraulic parameters determined from the OTIS simulations and reach-specific estimates of inflow concentrations for each solute as described in the "Tracer Injection Experiment" section. Simulations of reactive transport were performed using OTIS-P to estimate the value of the first-order decay coefficient.

OTEQ

OTEQ is a reactive transport model whose inputs include nearly complete chemical analyses of upstream boundary conditions and inflow samples and the hydraulic parameters from OTIS. Initial calculations with MINTEQ are used to determine the minimum number of constituents necessary to reproduce equilibrium aqueous speciation for the upstream boundary condition. In addition, MINTEQ calculations are used to determine the total hydrogen ion concentration necessary to simulate observed pH values for the upstream boundary condition and all inflows. Reach-specific values of inflow concentrations of iron and zinc were calculated as described previously. For the stream reach simulated by OTEQ, only two inflows modified the stream pH: Illinois and Topeka Gulches.

OTEQ simulations used all constituents for the upstream boundary condition except for chloride and copper. These two solutes were not important for aqueous speciation. Constituent concentrations at the upstream site were (in mg/L): calcium, 141; magnesium, 8.3; sodium, 3.8; sulfate, 496; fluoride, 1.3; aluminum, 5.98; manganese, 3.04; ferrous iron, 9.48; ferric iron, 0.49; zinc, 1.17; total carbon, 0.15; and pH (in standard units), 3.88.

A formation constant for ferrihydrite ($K_f = 10^{-3.92}$) was determined from the ion activity product for ferrihydrite at the upstream site (6,907 m). This value is similar to the value of $10^{-3.65}$ used by Broshears and others (1996) for their OTEQ simulations and to values reported in the literature that range from 10^{-3} to 10^{-5} (Broshears and others, 1996).

STEADY-STATE OTIS SIMULATIONS

Simulation of Baseline Stream Conditions

Steady-state observed and simulated lithium concentrations show the decreasing profile characteristic of a gaining stream (fig. 2). Profiles of iron and zinc concentrations (figs. 3 and 4) indicate that simulations require first-order removal coefficients to mimic measured data. For both solutes, first-order removal coefficients are required within several reaches of the stream and generally are greater downstream from inflows having elevated pH values (table 1). Reactive removal of iron, and sometimes zinc, apparently is most active in the mixing zones downstream from inflows having near-neutral pH values or elevated iron concentrations. The reaction/removal mechanism for iron is most likely formation of iron oxyhydroxide minerals. Zinc probably sorbs to, or coprecipitates with, the iron minerals. Comparison of the first-order removal coefficients in table 1 indicates that the confluence with Illinois Gulch is an important zone for iron and zinc removal.

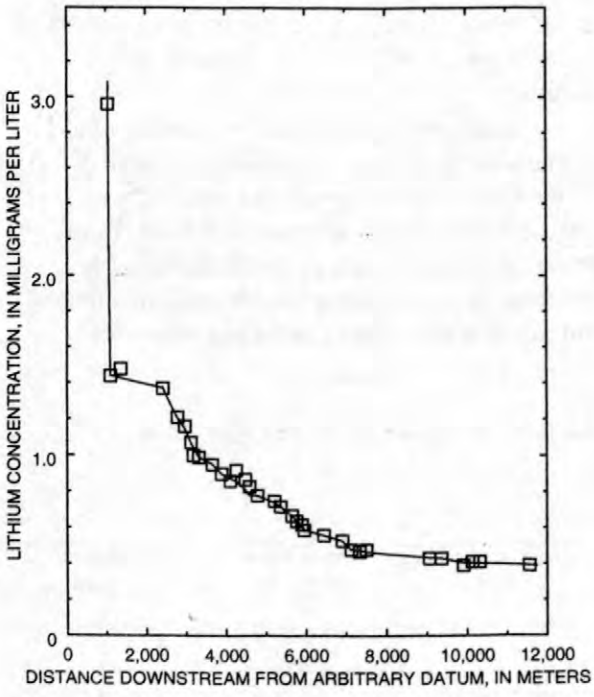

Figure 2. Steady-state lithium profile. Solid line represents simulation. Open squares are lithium concentrations in synoptic samples collected September 20, 1996.

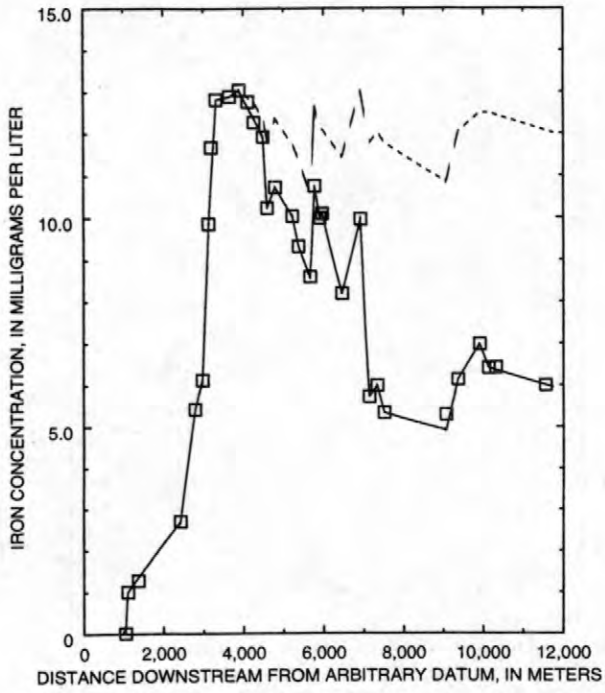

Figure 3. Profiles of simulated and observed dissolved iron concentrations for September 20, 1996, synoptic sampling. Dashed line represents conservative simulation. Solid line represents simulation with first-order decay. Open squares are iron concentrations measured in synoptic samples.

Simulation of Remediation of Selected Zinc Sources and Implications

Two different remediation scenarios for zinc were simulated. In scenario 1, relatively modest reductions in loads from some of the largest mining-related zinc sources on Federal lands included the following:

- Reduction of zinc loads from Prospect Gulch by 16 percent (this amount approximates the load that occurs from federally owned lands in the gulch).
- Reduction of zinc loads from Ohio Gulch by 20 percent (this is the maximum load resulting from mining-related sources. The other 80 percent of the load results from natural-background sources [W.G. Wright, U.S. Geological Survey, oral commun., 1998]).
- Reduction of zinc loads from the May Day Dump by 50 percent (this mine dump is on Federal lands).

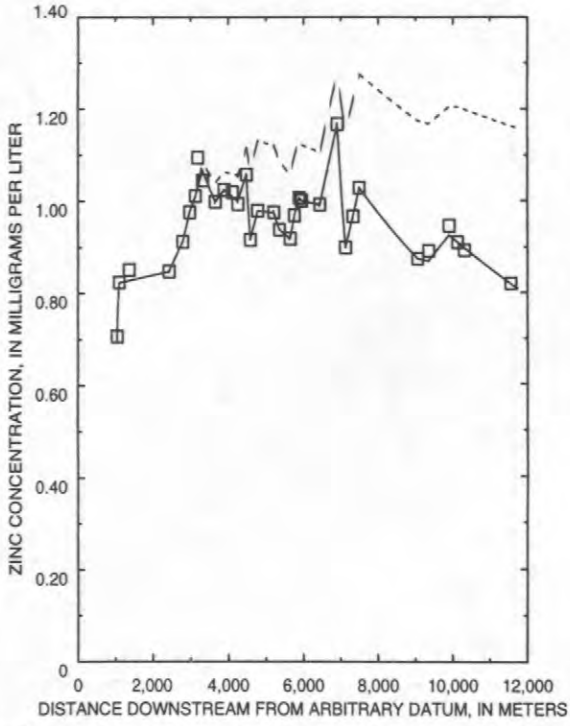

Figure 4. Profiles of simulated and observed zinc concentrations for September 20, 1996, synoptic sampling. Dashed line represents conservative simulation. Solid line represents simulation with first-order decay. Open squares are zinc concentrations measured in synoptic samples.

Remediation scenario 2 simulates more complete removal of zinc from sources that are considered some of the largest zinc sources in the basin:

- Reduction of zinc loads from Prospect Gulch by 80 percent (this amount approximates the load that occurs from all mining sources in the gulch).
- Reduction of zinc loads from Ohio Gulch by 20 percent (no change from scenario 1).
- Reduction of zinc loads from the May Day Dump by 100 percent.

Simulation results (fig. 5) indicate that remediation scenario 1 reduces zinc concentrations at the mouth of Cement Creek (11,558 m) by only 7 percent, and scenario 2 reduces zinc concentrations by 13 percent. The small effect of the remediation occurs because large loads of zinc remain in unremediated surface-water and ground-water sources. Some of these sources are natural; some are mining related. Remediation of additional surface-water sources of zinc is not possible without large fiscal expenditure. Remediation of ground-water sources of acidic, metal-rich water is not feasible using current technologies.

We expect that simulations underestimate the effects of remediation for two reasons. First, the simulations do not consider the effects that remediation would have on instream pH. Remediation of sources of zinc to the stream likely would result in pH increases in those inflows and, thus, some amount of pH increase in Cement Creek. Increased stream pH would cause formation of more iron minerals in the main channel. Additional loss of zinc would occur due to sorption or coprecipitation with the iron minerals. Second, the simulations do not consider the effects of the increased pH in mixing zones. Increased stream pH would also cause larger areas of elevated pH within mixing zones of tributary streams. Increased pH in these zones would likely cause greater amounts of mineral precipitation, coprecipitation, and zinc sorption.

Another simplification in these simulations is that reactions with iron are not considered. Remediation of sources of zinc to the stream probably also would decrease iron loads from those sources to the creek and thereby lower instream iron concentrations. Iron is instrumental in removing dissolved metals from the water

Table 1. Stream reaches (shown in fig. 1) requiring first-order removal coefficients greater than 1×10^{-4} s^{-1}, Cement Creek, Animas River Basin, Colorado

[Distances are meters downstream from arbitrary datum]

Bottom of stream reach	Iron removal coefficient, s^{-1}	Zinc removal coefficient, s^{-1}
4,586 meters (downstream from adit having pH = 7.3)	4.6×10^{-4}	4.2×10^{-4}
5,365 meters (downstream from Cascade Gulch—pH = 7.1)	1.4×10^{-4}	--
6,447 meters (downstream from inflow having pH = 6.8)	1.5×10^{-4}	--
7,131 meters (downstream from Illinois Gulch—pH = 7.6)	1.1×10^{-4}	3.8×10^{-4}
7,501 meters (downstream from several inflows having elevated iron concentrations)	3.2×10^{-4}	--
10,130 meters (downstream from inflows having elevated iron concentrations)	2.1×10^{-4}	--

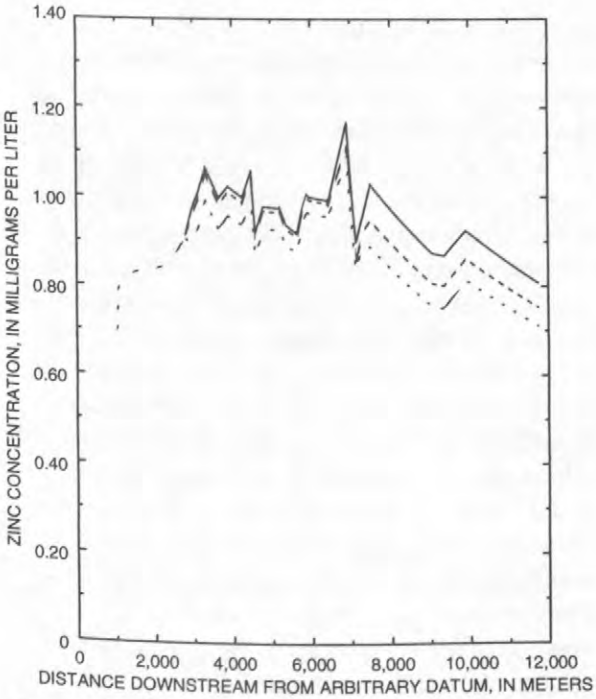

Figure 5. OTIS simulations of no remediation compared to two different remediation scenarios. Solid line represents simulation with first-order decay and no remediation as in figure 4. Dashed line represents simulation of remediation scenario 1. Dotted line represents simulation of remediation scenario 2.

column through coprecipitation and sorption. When considering remediation, it is therefore important also to consider the effects of low iron concentrations in the stream and mixing zone on dissolved concentrations of other metals.

OTEQ SIMULATIONS—ILLINOIS-TOPEKA GULCH REACH

The OTIS simulations are helpful in beginning to compare the effects of different remediation strategies and identifying locations where chemical reactions are occurring. The chemical reactions included in OTIS are simplified, however, and cannot simulate pH-dependent changes. OTEQ is used to improve the understanding of the effects of increased stream pH resulting from remediation. The OTEQ simulations include a limited reach of Cement Creek (6,907 m to 9,060 m) that includes inflows from Illinois Gulch, the Yukon Mine, May Day Dump, and Topeka Gulch (fig. 1). Discrete inflows downstream from Topeka Gulch are not included in this modeling exercise.

Effect of Ferrihydrite Precipitation on pH Profile

The first OTEQ simulation used the stream pH and iron and zinc concentrations measured at 6,907 m as the boundary condition and allowed no mineral precipitation. The only inflows that modify stream pH in this reach are Illinois and Topeka Gulches. In this conservative simulation (fig. 6, dashed line), simulated pH values are greater than observed pH values. Clearly, the inflow of high-pH water from Illinois Gulch is subject to instream reactions that decrease the pH. A second simulation allowing ferrihydrite precipitation and maintaining a fixed ratio of ferrous to total iron more closely approximates stream pH, particularly in the Illinois Gulch subreach (ending at 7,131 m) (fig. 6, solid line). In this simulation, the ferrous to total iron ratio was fixed at 0.95 (based on analyses of iron species in the reach from 6,907 to 9,060 m). Simulation results indicate that ferrihydrite precipitation and redox control of dissolved iron species may be occurring in this reach. The precipitation of ferrihydrite produces hydrogen ions and thus negates the pH increase that could occur in the stream at the Illinois Gulch confluence.

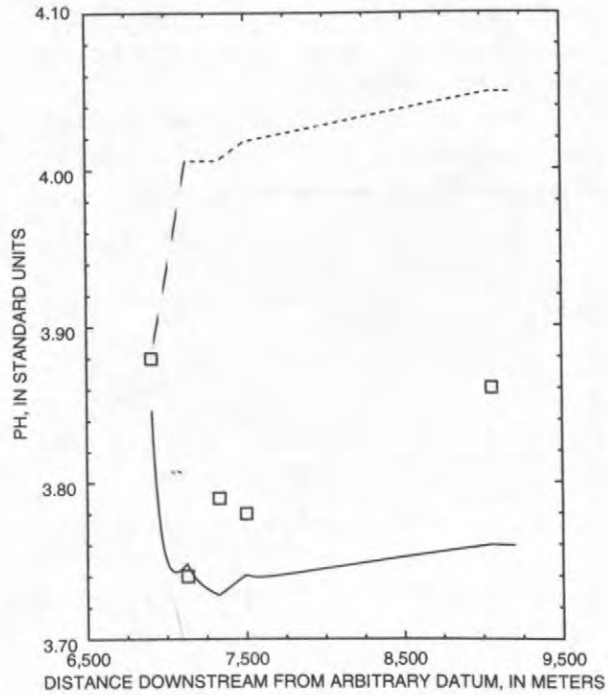

Figure 6. OTEQ simulations of pH allowing no reactions (dashed line) and allowing precipitation of ferrihydrite and redox control of iron speciation (solid line) in Illinois-Topeka Gulch reach from 6,907 to 9,060 meters. Open squares represent stream pH's.

Zinc Simulations

Similar to the OTIS simulations, OTEQ simulations of nonreactive zinc transport through the Illinois-Topeka Gulch reach overestimate the instream zinc concentrations (fig. 7). Identifying the actual mechanism causing zinc removal in the Illinois Gulch mixing zone is problematic because thermodynamic data do not support the precipitation of a zinc solid phase. Without a clear understanding of the mechanism, it is difficult to simulate conditions existing during the synoptic sampling; much less changes that might occur with remediation. However, several potential reactions that might remove zinc from the water column must be considered.

Formation of iron and aluminum minerals in the Illinois Gulch mixing zone might cause the coprecipitation or sorption of zinc, thus removing zinc from the water column. Coprecipitation can involve (a) the adsorption of zinc onto freshly formed hydrous oxide colloids, (b) solid solution formation by zinc incorporation into the hydrous oxide lattice, or (c) a combination of these processes (Karthikeyan and others, 1997). The question from a modeling standpoint is how to represent one or more of these processes within the framework of an equilibrium-based model. What are the stoichiometry and thermodynamic properties for the solid or solids? What are the sorption characteristics of the solids?

The identity, stoichiometry, and thermodynamic properties of the iron mineral or minerals forming in the mixing zone are problematic. In the previous section, simulations of pH that incorporated ferrihydrite precipitation improved the fit with observed data; however, other iron minerals including schwertmannite, goethite, and possibly jarosite also may be precipitating. The thermodynamic properties of schwertmannite are not well-defined, although a conditional log $K_{sp} = 18$ was suggested by Bigham and others (1996). These authors concluded that the dominant iron-hydroxysulfate minerals precipitating from acid mine waters vary with pH. In waters having pH less than 2.6, jarosite may be present; in waters having pH from 2.8 to 4.5, schwertmannite dominates over other forms of iron; and in waters having pH greater than 6.5, ferrihydrite and goethite are the dominant precipitates. Based on these results, it seems that the dominant mineral precipitating in Cement Creek probably is schwertmannite, whereas in the Illinois Gulch mixing zone, ferrihydrite and goethite also might be forming. Although ranges of K_{sp} values are known for these minerals, sorption characteristics for schwertmannite are not quantified.

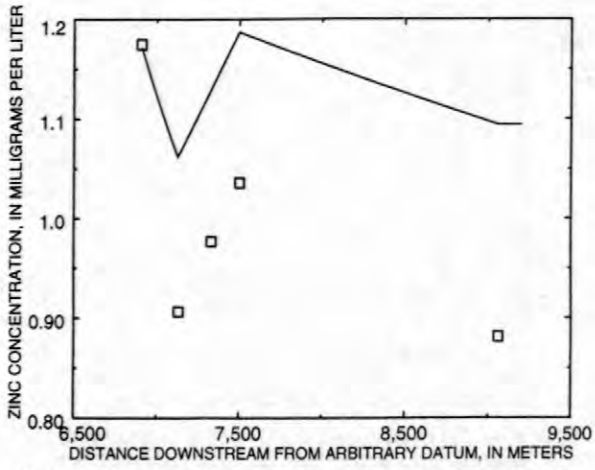

Figure 7. OTEQ zinc simulations in Illinois-Topeka Gulch reach. Solid line is nonreactive simulation; open squares are stream data.

Aluminum minerals forming in the mixing zone of Illinois Gulch may influence zinc concentration. Cross-stream profiles of pH collected at the same time as the stream-sediment samples indicated that pH values in the mixing zone ranged from 4.0 to 7.6. This pH range is sufficient to precipitate aluminum minerals. Nordstrom and Alpers (in press) indicate that in waters having a pH greater than 5.0, solubility of microcrystalline to amorphous $Al(OH)_3$ controls concentrations of dissolved aluminum. In addition, both the weak and strong acid digestions of streambed sediments showed greater amounts of aluminum and lesser amounts of iron in the sediment collected from the mixing zone compared with that collected upstream from the mixing zone (table 2). The elevated aluminum content of the sediment collected from the mixing zone indicates that precipitation of an aluminum phase is occurring and dominating precipitation of the iron phase (the molar ratio of aluminum to iron is 2.2 in the mixing zone sediment and 0.02 in the upstream sediment). This 2 order-of-magnitude shift in the molar aluminum to iron ratio is associated with a 2 order-of-magnitude shift in the zinc content of the sediments (table 2). Although this evidence is not sufficient to conclude that an aluminum-zinc phase is forming, it is sufficient to conclude that local mixing

increases pH enough to remove aluminum and zinc from the water column in the mixing zone. Without additional characterization of the streambed precipitates, it is difficult to model this process.

Table 2. Concentrations (in percent dry weight) of selected metals in weak-acid extractions of stream sediments collected from upstream and directly within the Illinois Gulch mixing zone, Animas River Basin, Colorado

Metal	Concentration in sediment from mixing zone	Concentration in sediment upstream from mixing zone
Aluminum	16	0.27
Iron	15	34
Zinc	0.175	0.0022

It is likely that a precipitating iron phase controls zinc behavior in the Illinois Gulch mixing zone. Sorption of zinc onto ferrihydrite requires a pH in the range of 5.0 to 7.0 to occur (Dzombak and Morel, 1990). The pH in the Illinois Gulch mixing reach is less than 4.1 in both the reactive and nonreactive simulations (fig. 6), indicating that sorption of zinc to ferrihydrite will not occur in OTEQ simulations. Within OTEQ simulations, the addition of the elevated pH water from Illinois Gulch is discretized over 224 m. In reality, Illinois Gulch enters Cement Creek at a discrete location approximately 1 m wide. Profiles of pH measured within the mixing zone immediately downstream from Illinois Gulch in August 1998 indicate that the pH increases enough for existing and newly precipitating iron minerals to sorb zinc in some areas of the mixing zone. However, modeling pH profiles and geochemical processes occurring across the width of the stream requires a two-dimensional model.

Simulating the removal of zinc using OTEQ in areas such as the Illinois Gulch mixing zone presents challenges. More information is needed on the identity, thermodynamic, and sorptive properties of minerals precipitating in the mixing zone. In addition, high-pH inflows such as Illinois Gulch probably should be simulated at the physical scale of the actual mixing. Because mixing is a small-scale, two-dimensional process, mixing zones may require more detailed field work and finer spatial discretization to characterize the hydrologic and geochemical processes.

SUMMARY

Simulating conditions present in Cement Creek on September 20, 1996, using OTIS and OTEQ produced mixed results. Simulation with OTIS presents the advantage of being relatively simple and fast. From a geochemical standpoint, the OTIS simulations helped pinpoint areas where the most significant geochemical activity was occurring. The OTIS simulations also helped illustrate the possible effects of two different remediation scenarios. However, the disadvantage of OTIS is that chemical reactions are greatly simplified, and the simulations do not account for effects of increasing stream pH on metal concentrations. Simulating conditions using OTEQ has the advantage that it can quantify pH-related changes and changes related to sorption and mineral precipitation. However, this type of modeling takes more time and data to be successful. To date, simulation of preremediation conditions using OTEQ is incomplete; thus far, simulations are unable to account for the reactive loss of zinc that occurs in the Illinois Gulch mixing zone. Simulations are complicated by the fact that mixing is a two-dimensional process and OTEQ is a one-dimensional model. In addition, some of the processes occurring in streams affected by acid mine drainage are poorly understood and are difficult to quantify in an equilibrium-based model. More information about chemical reactions and mineral precipitates in mixing zones must be acquired in order to accurately model mixing zones.

The OTIS package with applications and documentation is available at

http://webserver.cr.usgs.gov/otis/.

REFERENCES

Allison, J.D., Brown, D.S., Novo-Gradec, K.J., 1991, MINTEQA2/PRODEFA2, a geochemical assessment model for environmental systems—Version 3.0 User's manual: U.S. Environmental Protection Agency Report EPA/600/3-91/021, Washington, D.C., 106 p.

Bigham., J.M., Schwertmann, U., Traina, S.J., Winland, R.L., and Wolf, M., 1996, Schwertmannite and the chemical modeling of iron in acid sulfate waters: Geochimica et Cosmochimica Acta, v. 60, no. 12, p. 2111–2121.

Briggs, P.H., 1996, Forty elements by inductively coupled-plasma atomic emission spectrometry, *in* Arbogast, B.F., ed., Analytical methods manual for the Mineral Resources Program:

U.S. Geological Survey Open-File Report 96–525, p. 77–94.

Broshears, R.E., Bencala, K.E., Kimball, B.A., and McKnight, D.M., 1993, Tracer-dilution experiments and solute-transport simulations for a mountain stream, Saint Kevin Gulch, Colorado: U.S. Geological Survey Water-Resources Investigations Report 92–4081, 18 p.

Broshears, R.E., Runkel, R.L., Kimball, B.A., McKnight, D.M., and Bencala, K.E., 1996, Reactive solute transport in an acidic stream—Experimental pH increase and simulation of controls on pH, aluminum, and iron: Environmental Science and Technology, v. 30, no. 10, p. 3016–3024.

Church, S.E., Holmes, C.W., Briggs, P.H., Vaughn, R.B., Cathcart, James, and Marot, Margaret, 1993, Geochemical and lead-isotope data from stream and lake sediments, and cores from the upper Arkansas River drainage—Effects of mining at Leadville Colorado on heavy-metal concentrations in the Arkansas River: U.S. Geological Survey Open-File Report 93–534, 61 p.

Crowfoot, R.M., Paillet, A.V., Ritz, G.F., Smith, M.E., Jenkins, R.A., and O'Neill, G.B., 1996, Water resources data, Colorado, water year 1996, volume 2. Colorado River Basin: U.S. Geological Survey Water-Data Report CO–96–2, p. 428.

Dzombak, D.A., and Morel, F.M.M., 1990, Surface complexation modeling—Hydrous ferric oxide: New York, John Wiley, 393 p.

Garbarino, J.R., and Taylor, H.E., 1979, An inductively-coupled plasma atomic-emission spectrometer method for routine water quality testing: Applied Spectroscopy, v. 33, p. 220–226.

Harvey, J.W., and Fuller, C.C., 1998, Effect of enhanced manganese oxidation in the hyporheic zone on basin-scale geochemical mass balance: Water Resources Research, v. 34, no. 4, p. 623–636.

Karthikeyan, K.G., Elliott, H.A., and Cannon, F.S., 1997, Adsorption and coprecipitation of copper with the hydrous oxides of iron and aluminum: Environmental Science and Technology, v. 31, no. 10, p. 2721–2725.

Kimball, B.A., 1997, Use of tracer injections and synoptic sampling to measure metal loading from acid mine drainage: U.S. Geological Survey Fact Sheet 245–96, 4 p.

Kimball, B.A., Runkel, R.L., Walton-Day, Katherine, and Bencala, K.E., 1998, Integration of mine-drainage effects in watersheds using tracer injections and synoptic sampling [abs.]: EOS, v. 79, no. 17, p. S127.

Luedke, R.G., and Burbank, W.S., 1996, Preliminary geologic map of the Silverton 7.5-minute quadrangle, San Juan County, Colorado: U.S. Geological Survey Open-File Report 96–275, 15 p., 1 pl.

Nordstrom, D.K., and Alpers, C.N., in press, Geochemistry of acid mine waters, *in* Plumlee, G.S., and Logsdon, M.J., The environmental geochemistry of mineral deposits, part A—Processes, techniques, and health issues: Reviews in Economic Geology, v.7A, Society of Economic Geologists.

Runkel, R.L., 1998, One-dimensional transport with inflow and storage (OTIS)—A solute transport model for streams and rivers: U.S. Geological Survey Water-Resources Investigations Report 98-4018, 73 p.

Runkel, R.L., Bencala, K.E., Broshears, R.E., and Chapra, S.C., 1996a, Reactive solute transport in streams, 1. Development of an equilibrium-based model: Water Resources Research, v. 32, no. 2, p. 409–418.

Runkel, R.L, McKnight, D.M., Bencala, K.E., and Chapra, S.C., 1996b, Reactive solute transport in streams, 2. Simulation of a pH modification experiment: Water Resources Research, v. 32, no. 2, p. 419–430.

Runkel, R.L., Bencala, K.E., and Kimball, B.A.,1999, Modeling solute transport and geochemistry in streams and rivers, Morganwalp, D.W., and Buxton, H.T., eds., U.S. Geological Survey Toxic Substances Hydrology Program--Preceedings of the Technical Meeting, Charleston, South Carolina, March 8-12, 1999--Volume 1--Contamination from Hardrock Mining: U.S. Geological Survey Water-Resources Investigations Report 99-4018A, this volume.

Skougstad, M.W., Fishman, M.J., Friedman, L.C., Erdmann, D.E., and Duncan, S.S., 1979, Methods for the determination of inorganic substances in water and fluvial sediments: U.S. Geological Survey Techniques of Water-Resources Investigations, book 5, chap. A1, 626 p.

U.S. Environmental Protection Agency, 1986, Quality criteria for water, 1986: Office of Water Regulations and Standards, U.S. Environmental Protection Agency, Washington, D.C., EPA 440/5-86-001, 440 p.

AUTHOR INFORMATION

Katherine Walton-Day and Robert L. Runkel, U.S. Geological Survey, Denver, Colorado (kwaltond@usgs.gov)

Briant A. Kimball, U.S. Geological Survey, Salt Lake City, Utah

Kenneth E. Bencala, U.S. Geological Survey, Menlo Park, California

Aquatic Physical Habitat and Hydrology in Abandoned Mined Land Studies

By Robert T. Milhous

ABSTRACT

Abiotic and non-chemical factors may limit the ability of a stream to respond to improvements in traditional water quality parameters because physical habitat and sediment characteristics may also limit the populations of aquatic animals. A reach of the Upper Animas River in southwestern Colorado is analyzed to show possible limits caused by physical habitat and sediment. Habitat for trout in the Animas River near Howardsville may be limited by high streamflows (because of high velocities) and by winter conditions (by velocities too high for winter habitat needs and low depths). The characteristics of the substrate (bed material) may offset the impacts of high velocities in the spring and the depths and velocities in the winter. The characteristics of the sediment in the river limit the winter habitat. In the river below Howardsville, large rocks provide shelter to trout during winter and spring runoff; fewer velocity shelters are available above Howardsville. Spawning gravels are available in the river below Howardsville but these gravels occur above the water surface of the fall spawning flows, but would be covered by spring spawning flows. Taken as a whole, it is expected the numbers and sizes of the fish would be larger below Howardsville than above if the number and size of velocity shelters is the only factor limiting fish populations. If the location of the spawning gravels is also a limiting factor, then the river spawning fish would be spring spawners, such as cutthroat trout. There are beaver ponds upstream of Howardsville that may provide fall spawning habitat for brook trout. An informal goal for the Upper Animas River is to establish a brown trout fishery. This is not a desirable goal because: (1) brown trout require that 50–70% of the river be pools and that the river must be shaded, however, there are few pools in the subject reach; and (2) brown trout spawn in the fall but the spawning gravels are high in the cross section where they can only be used by spring spawners. The existing Animas River requires a trout that can use the substrate in the main channel as habitat during most of the year. The trout most adapted to a river with few pools and gravel/cobble/rubble substrate is the brook trout. Cutthroat trout could also use the river because spawning gravels are available during spring runoff.

INTRODUCTION

As part of the Abandoned Mined Lands Initiative (AMLI) in the Upper Animas River Basin, Colorado, a reconnaissance study was done to determine if physical habitat may be a limiting factor for populations of aquatic animals. Toxicity is almost certainly the primary limiting factor on the populations of fish and other aquatic animals in the Upper Animas River ecosystem (Besser and others, 1998). However, physical habitat and hydrologic factors may restrict the ability of a recovery program to reach the species and fish biomass goals that may be established for the program. The program may then be considered ineffective because the goals were not reached. Consideration of physical habitat and hydrological limitations, in addition to toxicology, will result in improved fishery goals for recovery of the aquatic ecosystem.

Formal goals of a recovery program have not been established for the Upper Animas. The informal goal, apparently, is to establish a brown trout fishery in the reach of the Animas River downstream of Silverton. At this time, there are two third-order streams in the Upper Animas Basin supporting a fishery, the South Fork of Mineral Creek and the Animas River between Eureka and Silverton. There has been little mining-related impact on the South Fork of Mineral Creek, however, mining and milling

activities have had considerable impact on the Animas River between Eureka and Silverton. Although there have been no formal recovery goals established for the Eureka to Silverton Reach, this paper assumes a reasonable goal would be to improve the trout fishery in the Eureka to Silverton Reach and explore the possibility that physical habitat, along with the characteristics of the streamflow, may influence the fishery. Because of the informal brown trout fishery goal, comments will be made on factors that may limit a brown trout fishery and not limit a fishery for other trout. Physical habitat factors will be described first, then hydrologic factors will be integrated with the physical habitat to show the abiotic considerations that should be included in an AMLI aquatic restoration project. The hydrologic considerations are: (1) the magnitude and variation of the streamflows, and (2) the sediment in the stream bed (substrate).

In this paper, the biotic limitations caused by metals in the water and the impacts that past mining and milling have had on the physical characteristics of the river are ignored. Altering the physical habitat by: (1) changing the sediment load in the river through construction of a modified channel; or (2) causing a change in the riparian vegetation, are also ignored. A comprehensive study should include both of these elements. This paper concentrates on the existing river and its ability to produce habitat for fish. A comprehensive study would also include other aquatic animals, especially aquatic invertebrates. To reiterate, this paper is incomplete because direct toxicity, interrelations among toxicity, physical habitat, and sediment, and the effects of physical habitat modifications have not been considered. Another assumption is that the fishery restoration goal should include natural reproduction. Other alternatives include a 'put-and-take' fishery or a 'put-and-grow' fishery (stock fingerlings and let them grow to a catchable size).

The Upper Animas River is located in Southwestern Colorado where a number of studies are underway to understand the hydrology, toxicology, and physical aquatic habitat of the basin. The studies have an overlapping goal of demonstrating the importance of considering physical habitat factors when linking water quality, toxicity, and fish populations. The hydrology of the basin is described by Milhous (1998a). Background information on the Upper Animas Basin and the aquatic biology of the basin has been given by Besser and others (1998) and by Besser and others (1998). A toxicity study was described by Nimmo and others (1998). The reach of the Animas River between Eureka and Silverton has two characteristics: (1) a relatively low gradient section above Howardsville with beaver ponds and gravel substrate, and (2) a steeper reach downstream of Howardsville with cobble and rubble substrate and no beaver ponds. About midway between Howardsville and Silverton is a short section with rock walls, pools, and some gravel in backwater areas of the size needed by trout for spawning. There are some short sections with undercut banks in the reach above Howardsville. There is little shading of the Animas River between Eureka and Silverton.

PHYSICAL HABITAT FOR TROUT

A relationship between discharge and one representation of physical habitat in rivers was determined for the Animas River near Howardsville using the Physical Habitat Simulation System (Milhous and others, 1989). Specifics of the actual simulation used for the Animas River are given in Milhous (1998b). The function developed and the daily streamflows for a typical water year (1994), are given in Figure 1. The

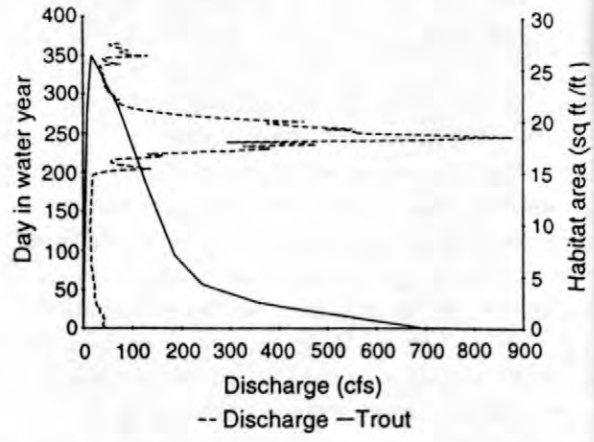

Figure 1. The 1994 daily streamflows and the relation between habitat and discharge for trout in the Animas River near Howardsville.

annual discharge for 1994 was 97 cfs, which is equal to or exceeded 60% of the years; the maximum daily discharge was 879 cfs which is exceeded 27% of the years. In other words, the maximum discharge was relatively large in 1994, but the total volume was on the low side. The physical habitat function shown in Figure 1 is applicable to adult trout (rainbow, brown, brook, and cutthroat). The function is of reconnaissance quality, meaning there may be a small amount of habitat at the higher flows and as the flows approach zero because pools are not adequately represented in the model.

Comparing the trout habitat function to the streamflow indicates that both high and streamflows may limit trout habitat. The low flows shown in Figure 1 are representative of the flows in the winter. The minimum 7-day winter streamflow was 14.3 cfs in 1994 (exceeded by about 40% of the years) compared to a range for the 61 years of record of 10–21 cfs, with about two-thirds of the years having winter streamflows in the range of 11–17 cfs.

TROUT POPULATIONS AND HABITAT NEEDS

Brook trout are found in the reach of the Animas River upstream of Howardsville. Below Howardsville, brook trout, rainbow trout, and cutthroat trout have been collected (State of Colorado, 1992). The rainbow trout are probably a result of stocking in the early 1990's. The number of trout collected in October 1992 along the reach between Silverton and Eureka is given in Table 1. There were no trout found in the Animas River above Eureka. The trout biomass densities given in Figure 2 are from the same locations as in Table 1. The first three locations (A40a, A45, and A53) are above Howardsville and the last three (A53a, A55a, and A68) are below Howardsville. Residents of Silverton have reported catching trout in the reach near A55a. The biomass of brook trout is reduced at the two locations where other trout species are found, possibly caused by competition with the other trout species. Some of the habitat needs for each of the trout species considered in this paper are summarized in Table 2.

Trout use pools and undercut banks as resting places and as velocity shelters which allow the fish to conserve energy. When the pools are close to fast water, trout can rest in the pools and feed in the fast water. Trout will also use the gravel, cobble, and rubble in the river channel as resting places and velocity shelters (substrate shelters). If the number of pools and undercut banks are limited, the numbers and size of the trout will be limited to those using the channel. The sources used for Table 2 suggest that the size of the fish and the ability of the fish to use the substrate shelters and, therefore, the stream channel, is related to the percent of the substrate in the 100 to 400 mm size range.

The information in this section will be used in the discussion that follows.

HIGH STREAMFLOW LIMITS ON PHYSICAL HABITAT

The velocities in the Animas River are too high for optimal adult trout habitat when the streamflows are high. When the velocities are high, the fish must seek shelters and other ways of reducing their expenditure of energy. In such situations, the fish are considered to be under stress caused by a lack of appropriate physical habitat. An index to habitat stress has been developed and is described in detail by Milhous (1998b). The index is a measure of the stress on the fish that may be caused by higher velocities. As the velocities increase with an increase in streamflows, they will pass a threshold above which the habitat is not desirable but below which the index is zero. The index is analogous to the effects of floods for humans (and other terrestrial animals. Streamflows that are within the bank cause little or no stress on humans (a human habitat index would be zero). As the water over-tops the bank, the index would be greater than zero, but not large (analogous to human stress that might occur and may be of slight concern but usually not a significant concern). As the habitat stress index increases, the impact of the high flows on the fish and invertebrate populations could be significant (the same as the impact of major floods on human populations). A duration

Table 1. Numbers of trout collected in October 1992 in the Animas River between Eureka and Silverton. Data from the State of Colorado (1992).

Site ID	Brook	Rainbow	Cutthroat	Location
	(number of fish/1,000 ft of stream)			
A40a	46.7			above Maggie Gulch
A45	136.7			above P&G tailings
A53	63.6			below P&G tailings
A53a	61.4			below Cunningham Gulch
A55a	21.0[a]	1.0	1.0	above Arrastra Gulch
A68	34.2	36.8		above 14th Street Bridge

[a]The brook trout sample at A55a included fry.

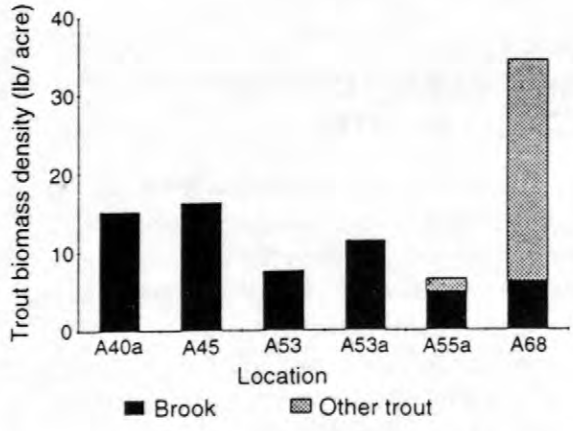

Figure 2. Density of trout measured in October 1992 in the Animas River between Eureka and Silverton. Data from the State of Colorado (1992).

curve for the habitat stress index for the Animas River near Howardsville is given in Figure 3.

Application of the habitat stress index to the Animas River demonstrated that in slightly more than 50% of the years, there was no real habitat stress on the trout populations caused by high streamflows; however, during about 20% of the years, the habitat stress could be important. For the remaining 30% of the years, some habitat stress occurs.

This suggests that there could be variation in the trout population caused by variation in the streamflows alone. This has been demonstrated for the Gunnison River, which is just north of the Animas Basin (Nehring and Miller, 1987). In the Gunnison River, higher streamflows caused a significant loss of young-of-year trout which reduced the population of adult trout in subsequent years.

Trout adjust to higher velocities by using velocity shelters where the velocity is significantly lower than in the surrounding water. Velocity shelters are important for allowing fish to escape habitat stress caused by high streamflows. In many rivers the most important velocity shelters are pools, root wads, and undercut banks on the sides of the stream, and large bed elements such as cobbles and boulders on the stream bed (Raleigh, 1982). There are few pools and undercut banks along the Animas River between Eureka and Silverton. Small pools are found in the vicinity of Arrastra Creek and some undercut banks above Howardsville. Most, but not all, of the velocity shelters in the reach are cobbles and boulders. The size of fish that can be sheltered by boulders and cobbles is related to the size of the armour on the bed surface. In the section on habitat needs (above) the percent of the bed surface with sizes in the range of 100 to 400 mm was the amount of the stream bed that can be used as velocity shelters. The size of material on the bed surface in the range of 100 to 400 mm is given in Table 3.

Table 3 shows there are good velocity shelters within the river channel below Howardsville but not above, also the velocity shelters are large. The fish would be expected to be larger below Howardsville than above. The population and biomass data suggests, but does not prove, that this may be the case.

Table 2. Habitat characteristics and size of three trout species found in the Upper Animas River watershed and for brown trout. Source: Scott and Crossman (1973); Raleigh (1982); Hickman and Raleigh (1982); Raleigh and others (1984).

Trout species	Spawning period	Average length (inches)	% pools	Shading requirements
Cutthroat	spring	12–15	50	
Brook	fall	10–12	50	intermediate
Brown	fall	16	50–70	needed
Rainbow	spring	12–18	40–60	less important

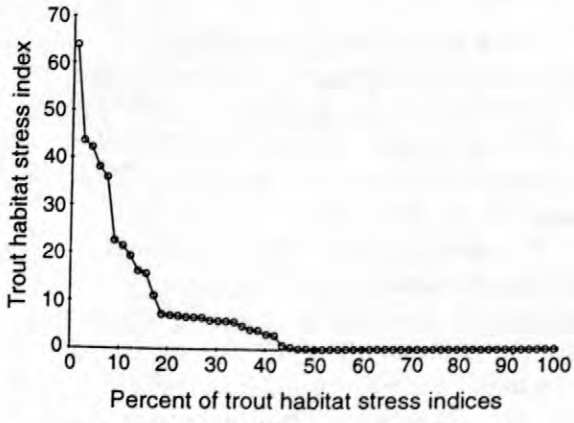

Figure 3. Duration diagram for an annual index to the habitat stress introduced to the trout in the Animas River, Colorado, by high velocities during high flow periods.

There are beaver ponds along the river above Howardsville but none below. The beaver ponds have water flowing through them during high flows, thus providing velocity shelters for the brook trout present above Howardsville.

WINTER STREAMFLOW LIMITS ON HABITAT

The winter streamflows are very low and little physical habitat is available in the Animas River. Any trout in the river would be expected to be under stress caused by the winter conditions. The location of winter habitat is similar to the velocity shelters during spring runoff with two exceptions: (1) the river has essentially no edge (root wads and undercut banks) either because of ice and snow, or the edge of the water is away from the banks, and (2) the substrate (bed material) can be a shelter during the winter. The details of the winter use of the stream bed are described by Meyer and Griffith (1997).

The best winter physical habitat occurs when the streamflows are reasonably stable (Raleigh, 1982). The variation in streamflows during the winter in Animas River is not large because the precipitation is almost all snow during the winter. Between 16 November and 31 March, the median value of the 7-day minimum streamflow is 14 cfs with a median ratio between the 7-day maximum and 7-day minimum streamflow of 1.8. The maximum ratio is 3.9, but two-thirds of the years have a ratio of less than 2.0 (90% less than 2.4). Raleigh (1982) reports the base flow (in this case, winter flows) that are at least 50% of mean annual discharge provide excellent trout habitat, between 25% and 50% fair habitat, and less than 25% poor habitat. The median winter flow in the Animas River at Howardsville is 17% of the median annual discharge.

Voids in the substrate are used by wintering trout as resting locations to avoid expending energy. The specific weight and porosity for a sample collected upstream of Howardsville was determined and compared to the samples from two other rivers in Table 4. Fines (sediment less than 3 mm) are considered to be undesirable in the bed material used as trout habitat. The percent of fines in the bed material is also given in Table 4. The data show the Animas River has less voids than the other two unregulated rivers, but the percent of fines is similar to Soda Butte Creek. The habitat value of the substrate in the Animas

Table 3. The percent of velocity shelters and the maximum size of the surface layer at four locations in the Animas River between Eureka and Silverton. The percent shelters is the difference between the percent of the surface less than 400 mm and more than 100 mm. D/S is downstream of Howardsville and U/S is upstream.

Location	% shelters	Median size of shelters (mm)	Maximum size (mm)
U/S 1	34	123	145
U/S 2	0	---	95
D/S 1	60	142	220
D/S 2	78	171	430

River is probably lower than in the other rivers because the mixture of low porosity and a relatively high percentage of fines means the bed material is firmer than the other two rivers. (In relative terms, Oak Creek is loose, the Animas River is firm, and Soda Butte Creek is intermediate.) The relatively firm substrate and high percentage of fines indicate that the bed material in this reach of the Animas River is probably poor winter trout habitat.

During winter, the streamflows are lower than in the fall. The informal target species is brown trout, which spawn in the fall (October) and the fry leave the redds just before spring runoff. An analysis of the change in width between October and the minimum width during the winter showed that, if the redds were uniformly distributed in the cross section, between 71 and 94% of the redds created in October would survive the winter. The problem is that spawning gravels are not uniformly distributed in the cross section. In fact, no bars or spawning gravels have been found in the subject reach of the Animas River that would be available in October. Spawning gravels have been found near the junction of the Animas River with Arrastra Creek, but these were located above the elevation of the October flows. This means that reproductive success of brown trout would not be likely in the reach between Silverton and Eureka. The spawning gravels are in a location where they could be used by spring spawners, such as rainbow and cutthroat trout. Brook trout are also fall spawners but they probably use the small pockets of gravel that can be found among the beaver ponds.

DISCUSSION

The fish biomass is larger above Howardsville probably because of the existence of beaver ponds and some undercut banks. The data suggest, somewhat unclearly, that the fish are smaller above Howardsville than below, possibly because of the size of the velocity shelters.

The question posed at the beginning of this paper was the desirability of attempting to design a recovery program that had a goal of establishing a brown trout fishery. The goal of establishing a brown trout fishery as part of the aquatic ecosystem restoration effort recovery is rejected for the two reasons given below.

1. Brown trout require that 50–70% of the river are pools and the river must be shaded. There are few pools and the river has little shade.
2. Brown trout spawn in the fall but the spawning gravels are high in the cross section where they can be used by spring spawners but would be unavailable for fall spawners. There probably are some spawning gravels near the beaver ponds, but the environment near the beaver ponds is probably not usable by brown trout (small size of substrate and few to no pools).

The present Animas River requires a trout that can use the substrate in the main channel as habitat during most of the year. The trout most adapted to a river with few pools and gravel/cobble/rubble substrate is brook trout (Raleigh, 1982). Cutthroat trout could also use the river because spawning gravels are available during spring runoff.

Table 4. Specific weight and gravity, porosity, and percent less than 3 mm of the bed material of three unregulated rivers.

Stream	Specific weight (lb/ft3)	Specific gravity	Porosity	% ≤3 mm
Oak Creek, Oregon	105	2.85	0.41	13
Soda Butte Creek, WY-MT				
Upstream	108	2.65	0.35	16
Downstream	104		0.37	23
Animas River, Colorado				
above Howardsville	135	2.80	0.22	20

The objective of this paper was to demonstrate that physical habitat must be considered in the formulation of fishery goals for AMLI and other aquatic restoration efforts. Physical habitat considerations alone could limit or eliminate some species of aquatic animals as is probably the case for the brown trout in the Animas River. The velocity shelters are mostly associated with the gravel/cobble/rubble substrate which means smaller trout, such as brook and cutthroat, should be selected as the target species for habitat restoration.

REFERENCES

Besser, J.M., Brumbaugh, W., Church, S.E., and Kimball, B.A., 1998, Metal uptake, transfer, and hazards in the stream food web of the upper Animas River watershed, Colorado, in Nimick, D.A., and von Guerard, P., eds, Science for watershed decisions on abandoned mine lands: Review of preliminary results, Denver, Colorado, February 4–5, 1998, Open File Report 98–297, U.S. Geological Survey Denver, Colorado, p. 20.

Besser, J.M., Nimmo, D., Milhous, R., and Simon, B., 1998, Impacts of abandoned mine lands on stream ecosystems of the Upper Animas River watershed, Colorado, in Nimick, D.A, and von Guerard, P., eds, Science for watershed decisions on abandoned mine lands: Review of preliminary results, Denver, Colorado, February 4–5, 1998, Open File Report 98–297, U.S. Geological Survey Denver, Colorado, p. 15.

Hickman, T., and Raleigh, R.F., 1982, Habitat suitability index models: cutthroat trout, U.S. Department of the Interior, Fish and Wildlife Service, FWS/OBS-82/10.5, 38 pp.

Meyer, K.A., and Griffith, J.S., 1997. Effects of cobble-boulder substrate on winter residency of juvenile rainbow trout, North American Journal of Fisheries Management 17:77–84.

Milhous, R.T., 1998a, Streamflows and sediment transport capacity in the upper Animas Basin, Colorado, in Morel-Seytoux, H.J., ed., Proceedings of the Eighteenth Annual American Geophysical Union Hydrology Days, Hydrology Days Publications, Atherton, California, pp 177–188.

Milhous, R.T., 1998b, On sediment and habitat in the Upper Animas River watershed, Colorado, in Abt, S.R., Young-Pezeshk, J., and Watson, C.C., eds., Water Resources Engineering '98, American Society of Civil Engineers, Reston, Virginia, pp. 678–683.

Milhous, R.T., Updike, M.A.,and Schneider, D.M., 1989, Physical habitat simulation system reference manual - version II, U.S. Fish and Wildlife Service Biological Report 89(16), Washington, D.C, v.p.

Nehring, R.B., and Miller. D.D., 1987, The influence of spring discharge levels on rainbow and brown trout recruitment and survival, Black Canyon of the Gunnison

River, Colorado, Proceedings of the annual conference of Western Associations of Fish and Wildlife Agencies, July 13–15, 1987, Salt Lake City, Utah.

Nimmo, D., Castle, C.J., and Besser, J.M., 1998, Toxicological reconnaissance of the Upper Animas River watershed near Silverton, Colorado, in Nimick, D.A., and von Guerard, P., eds., Science for watershed decisions on abandoned mine lands: Review of preliminary results, Denver, Colorado, February 4–5, 1998, Open File Report 98–297, U.S. Geological Survey Denver, Colorado, p. 19.

Nimmo, D., and Castle, C.J, 1998, Toxicological evaluation of surface and interstitial waters from headwater streams in the Animas river basin, Data presented at the meeting "Results of AML field studies in the Upper Animas and Boulder River pilot watersheds", Lakewood, Colorado.

Raleigh, R.F., 1982, Habitat suitability index models: Brook trout, U.S. Department of the Interior, Fish and Wildlife Service, FWS/OBS-82/10.24, 42 pp.

Raleigh, R.F., Zuckerman, L.D., and Nelson, P.C, 1984, Habitat suitability index models and instream flow suitability curves: Brown trout, U.S. Department of the Interior, Fish and Wildlife Service, FWS/OBS-82/10.71, 71 pp.

Raleigh, R.F., Hickman, T., Solomon, R.C, and Nelson, P.C, 1984, Habitat suitability index models and instream flow suitability curves: Rainbow trout, U.S. Department of the Interior, Fish and Wildlife Service, FWS/OBS-82/10.60, 64 pp.

Scott, W.B., and Crossman, E.J., 1973, Freshwater fishes of Canada, Bulletin 184, Fisheries Research Board of Canada, Ottawa, Canada, 966 pp.

State of Colorado, 1992, Unpublished records of a biological survey of the Animas River made in 1992.

AUTHOR INFORMATION
Robert T. Milhous
Research Hydraulic Engineer
Midcontinent Ecological Research Center
U.S. Geological Survey
4512 McMurry Avenue
Fort Collins, CO 80525-3400
email: robert_milhous@usgs.gov

Characterizing the Aquatic Health in the Boulder River Watershed, Montana

By Aïda M. Farag, Daniel F. Woodward, Don Skaar, and William G. Brumbaugh.

ABSTRACT

The Boulder River and some of its tributaries receive direct effluent from abandoned mine adits and runoff from old tailings piles located in the basin. This biological assessment identified a pathway of metals exposure in the Boulder River Watershed as measured by concentrations of metals in biofilm (abiotic and biotic material on rock surfaces), invertebrates, and fish collected from the Boulder River and a select number of its tributaries. These data along with data from fishery population surveys are being used to assess the ecological health of the Boulder River and its tributaries. Preliminary data suggest that concentrations of arsenic, copper, cadmium, lead, and zinc are elevated to varying degrees in biological tissues collected from the Boulder River and its tributaries. Tissue damage in fish livers, as measured by an increase of products of lipid peroxidation, along with reductions in fish sizes and populations in lower Cataract Creek were also noted. Thus, exposure to metals may have resulted in a deterioration of fish health and a quantitative loss in fish populations in Cataract Creek. We also documented 100% mortality of fish placed in live containers in the upper sections of the Basin Creek and Cataract Creek and lower High Ore Creek.

INTRODUCTION

The Boulder River Watershed, located in southwest Montana, encompasses lands managed by the Bureau of Land Management and the U.S. Forest Service. Managers from these agencies plan to remediate the effects of past mining activities in the watershed. As part of the Abandoned Mine Lands Initiative, personnel from the U.S. Geological Survey are assisting managers in their attempts to characterize the effects of mining activities in this watershed.

The Boulder River and some of its tributaries receive direct effluent from abandoned mine adits and runoff from old tailings piles. There are three tributaries of concern in this watershed (Figure 1): Basin Creek, Cataract Creek, and High Ore Creek. Wastes from the Bullion Mine are discharged into Jack Creek, which flows into Basin Creek. Basin Creek then flows into the Boulder River below Sullivan Gulch. Uncle Sam Gulch and Morning Glory Mine provide inputs into Cataract Creek which flows into the Boulder River downstream of Basin Creek. The Comet Mine is located along High Ore Creek which flows into the Boulder River upstream of Galena Gulch.

Interest in the effects of mining on aquautic life in the Boulder River began in 1976. Nelson (1976) studied three sections of the Boulder River: below Red Rock Creek, below Cataract Creek, and below High Ore Creek. Reductions in the survival of fish eggs during an egg bioassay and reductions in fish population estimates were noted below Cataract Creek and High Ore Creek. Although metals were not analyzed in sediments, water, or biological tissues, Nelson attributed this population reduction to mining activities in the Boulder River Watershed.

It was not until 1990 that another investigation of the Boulder River was initiated. Gless (1990) designated Basin Creek a "stream of concern," Cataract Creek as "degraded" and High Ore Creek as "extremely degraded." These classifications were based on elevated

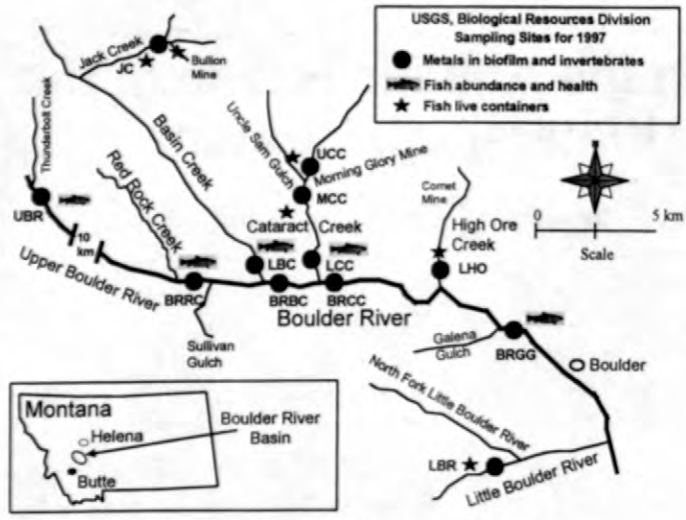

Figure 1. Map of the Boulder River, Montana

concentrations of arsenic (As) observed in the water column and the reduced presence of aquatic life in some creek sections. Gless (1990) observed metals stains and dead vegetation as high as five feet above the stream banks of Cataract Creek.

One goal of the present biological assessment was to identify the biological pathway of metals in the Boulder River Watershed. The concentrations of metals in aquatic biota present in the Boulder River and its tributaries have not been previously documented. Pathways were determined from measured concentrations of metals in biofilm (abiotic and biotic material on rock surfaces), invertebrates, and fish collected from the Boulder River and a select number of its tributaries.

A second goal of this study was to determine the current health status (quality) and population status (quantity) of aquatic life in the Boulder River Watershed. Metal exposures can affect the quantity and quality of the aquatic biota present and deteriorate the overall ecological health of a river system (Farag et al. 1995). No assessments of individual fish health had been previously performed in the Boulder River. Measures of physiological function and tissue residues were used along with fishery population surveys to assess the ecological health of the Boulder River and its tributaries.

Measurements of lipid peroxidation and metallothineins were used to assess the physiological status of fish exposed to metals. Lipid peroxidation results in damage to polyunsaturated fatty acids located in the cell membrane. This damage can decrease fluidity, increase leakiness, and inactivate membrane-bound enzymes. An ultimate result may be cell death and tissue damage (Halliwell and Gutterirdge, 1985; Wills, 1985). These measurements have been associated with reduced growth in laboratory experiments (Woodward et al. 1995). Additionally, metallothioneins are proteins that are induced following metal exposures. While induction of these proteins is often associated with acclimation of fish to metals, the metabolic costs of metallothionein induction have been associated with reduced growth in laboratory experiments (Dixon and Sprague 1981, Roch and McCarter 1984, Marr 1995).

Lipid peroxidation and metallothinein data can then be related to the specific tissue dose of metals accumulated in fish (Farag et al. 1995). Therefore, data that define the physiological status of fish can provide managers with an explanation of the cause-effect relationship between metals present and reductions in fish health and fish populations.

Our third goal was to determine the survivability of trout in sections of creeks that lack fish. Some reaches in tributaries to the Boulder River are devoid of fish. These sections of fishless stream coincide with extreme concentrations of metals in the water. We also sought to determine if the lack of fish presence is due to the water quality in these tributaries.

EXPERIMENTAL PROCEDURES

Biological Pathway Determinations

Four samples each of biofilm and benthic macroinvertebrates were collected from 12 sites (Figure 1). Reference sites on the upper Boulder River, the Boulder River (near Red Rock Creek), and the Little Boulder River were chosen to estimate the pre-mining conditions of the nine experimental sites. The upper Boulder River and the Little Boulder River sites were used as references for tributary sites. A site on the Boulder River near Red Rock Creek was used as a reference for the mainstem sites. Arsenic, cadmium (Cd), copper (Cu), lead (Pb), and zinc (Zn) were measured by inductively coupled plasma-mass spectrometry (ICPMS).

Fish Health and Population Assessment

Sample collections for fish health and population assessments were performed simultaneously at five sites (Figure 1). A site on the upper Boulder River was used as a reference for the lower Cataract Creek and the lower Basin Creek sites. A site on the Boulder River near Red Rock Creek was used as a reference for the site on the Boulder River near Galena Gulch.

Necropsy assessments were performed in the field to define any obvious, gross abnormalities of the resident fish collected for fish health measurements. Gill, liver, and whole body concentrations of As, Cd, Cu, Pb, and Zn were measured by ICPMS. Lipid peroxidation and metallothionein were measured on gill and liver tissues according to Dillard and Tappel (1984) and Hogstrand and Haux (1990) respectively. The metallothionein data are not yet available. Multiple pass depletion was used to estimate fish populations in the tributaries of concern and the mark/recapture method was used to estimate populations in the Boulder River. Lengths and weights were recorded and scales were collected to determine the ages of the resident fish.

Survivability of Fish in Tributaries

Live containers of juvenile westslope cutthroat trout were placed at six sites located in the upper reaches of Basin and Cataract creeks and in lower High Ore Creek. A site on the Little Boulder River was designated as the reference site. Fish were acclimated to Little Boulder River water before the initiation of the experiment. Twenty fish, five in each of four containers, were placed at each site (Figure 1). YSI automatic water quality monitors were deployed in Jack Creek, High Ore Creek, and the Little Boulder River to monitor dissolved oxygen, conductivity, pH, and temperature hourly during the 96-hr study. These measurements were also manually recorded daily at each site. Alkalinity and hardness were measured daily on water samples collected from each site.

RESULTS AND INTERPRETATION

Concentrations of all metals were elevated in biota from most of the tributary sites. The concentrations of metals were generally twice as great in biofilm compared to invertebrates. Concentrations of metals in biofilm and invertebrates decreased at sites furthest downstream from mining sites. The greatest concentrations of Cu and Cd were observed in biofilm from Jack Creek (2060 and >60 µg/g respectively). And concentrations of As, Pb, and Zn were greatest in biofilm from lower High Ore Creek (1910, >100, and 1670 respectively). Additionally, metals accumulated in the biota in the mainstem of the Boulder River. This was most notable at Galena Gulch where > 250 µg/g As, Cu, and Pb were observed in biofilm.

The concentrations of metals in gills and livers collected from resident fish were elevated at lower Basin Creek, lower Cataract Creek, and Boulder River at Galena Gulch, downstream from impacted tributaries. The concentrations were the greatest at lower Cataract Creek where gills and livers from this site had as much Cd (> 60 µg/g) as benthic-macroinvertebrates collected from the same site. Products of lipid peroxidation were elevated in livers but not gills of fish collected from lower Cataract Creek. Furthermore, the size range and number of trout per acre were less in lower Cataract Creek than the reference site (2.7 - 12.4 inches compared to 2.8 - 8.3 and 443±75 trout per acre compared to 63±22).

Survival of westslope cutthroat trout was 0% at all experimental sites by 96 h compared to 95% in the little Boulder River. Much of the

mortality was observed during the first 72 h. For example, survival was 0% in fish held in Bullion Creek and Uncle Sam within 24 h; in lower High Ore, within 48 h; and in middle Cataract Creek, at 72 h. Measurements performed by the USGS - Water Resources Division (personal communication, David Nimick) suggest that this mortality may have been due to elevated concentrations of metals, especially Zn, in the water column. However, additional investigations of survivability are planned because preliminary laboratory assays with site waters did not confirm the results of the live-container study.

The preliminary data suggest that metals are accumulating in biofilm, invertebrates, and fish in all three tributaries of concern and in the mainstem of the Boulder River. Fish health may be affected in lower Cataract Creek as demonstrated by lipid peroxidation, reduced size, reduced number of fish per acre and increased tissue metal concentrations. It is unlikely that fish would survive in the upper reaches of Basin and Cataract creeks or in lower High Ore Creek, where fish are currently not present, regardless of habitat restrictions in these tributaries. The concentrations of metals in the water, especially Zn, may be responsible for the acute mortalities of fish. However, habitat restrictions would likely affect fish movement in these tributaries, especially in sections of Cataract Creek.

Additional data are being compiled to assist with the final determinations of the effects of metals in the Boulder River Watershed. The pathway of metals through the foodchain will be compared to concentrations of metals measured in the water and sediment. Metallothionein data will be incorporated into the final determination of fish health. Also, habitat assessments performed during 1998 will be used to correct for any habitat variability between sites and finalize the population estimates. Finally, the survivability experiment will be repeated during 1999.

REFERENCES

Dillard, C.J., and A.L. Tappel. 1984. Fluorescent damage products of lipid peoxidation. Methods of Enxymology 105:337-341.

Dixon, D.G., and J.B. Sprague. 1981. Copper bioaccumulation and hepatoprotein synthesis during acclimation to copper by juvenile rainbow trout. Aquatic Toxicology 1:69-81.

Farag, A.M., Stansbury, M.A., Hogstrand, C., MacConnell, E., and Bergman, H.L. 1995. The physiological impairment of free ranging brown trout exposed to metals in the Clark Fork River, Montana. Canadian Journal of Fisheries and Aquatic Sciences 52:2038-2050.

Gless, E.E., 1990. Biological and chemical baseline studies along the Bolder River and its tributaries in Jefferson County, Montana. A report to the Jefferson County Commissioners, January 1990.

Halliwell, B. and Gutteridge, J.M.C.. (Editors). 1985. Free radials in biology and medicine. Clarendon Press, Oxford. pp. 139-170.

Hogstrand, C., and C. haux. 1990. A radioimmunoassay for perch (*Perca fluviatilis*) metallothionein. Toxicology and Applied Pharmacology 103:56-65.

Marr, J.C.A., H.L. Bergman, J. Lipton, and C. Hogstrand. 1995. Differences in relative sensitivity of naive and metals-acclimated brwon and arainbow trout exposed to metals respresentative of the Clark Fork River, Montana. Candadian Journal of fisheries and Aquatic Sciences 52:2016-2030.

Nelson, F.A. 1976. The effects of metals on trout populations in the upper Boulder River, Montana. M.S. Thesis, Monatana State University, Bozeman, Montana, 60 pp.

Roch, M., and J.A. McCarter. 1984. Metallothionein induction, growth, and survival of chinook salmon exposed to zinc, copper, and cadmium. Bulletin of Environmental Contamination and Toxicology 32:478-485.

Wills, E.D. 1985. The role of dietary components in oxidative stress in tissue. In: Oxidative Stress in tissues. Edited by H.Sies, Academic Press, New York

Woodward, D.F., A.M. Farag, W.G. Brumbaugh, C.E. Smith, and H.L. Bergman. 1995. Metals-contaminated benthic invertebrates in the Clark Fork River, Montana: effects on age-0 brown trout and rainbow trout. Canadian Journal of Fisheries and Aquatic Sciences 52:1994-2004.

Colloid Formation and the Transport of Aluminum and Iron in the Animas River near Silverton, Colorado

By Laurence E. Schemel, Briant A. Kimball and Kenneth E. Bencala

ABSTRACT

Flows and concentrations of dissolved and colloidal aluminum (Al) and iron (Fe) were measured in the upper Animas River to identify sources of colloids and quantify their transport. Colloidal Al and Fe are important in this reach of the river near Silverton, Colorado, because of effects on river bed habitat, macroinvertebrates, and fish. The largest sources of Al and Fe to the river were Cement Creek (42 percent of the total load) and Mineral Creek (56 percent of the total load). Acidic inflow from Cement Creek (pH 3.8) supplied dissolved Al that formed colloids as it was neutralized upon mixing in the Animas River. The Al supplied by Mineral Creek was colloidal, and nearly all of the Al in the Animas River was colloidal. Both creeks supplied Fe in dissolved and colloidal form. Some colloidal Fe formed in the mixing zone downstream of Cement Creek, and colloidal Fe continued to form downstream in the river as dissolved Fe was oxidized. Although colloidal Al and Fe accumulated on the river bed, transports measured in this 2.5 km reach of the river showed that losses of Al and Fe from the water column as a result of colloid formation were less than 10 percent of the total transport.

INTRODUCTION

Tributaries of the upper Animas River in the San Juan Mountains of Colorado drain a caldera that is rich in sulfide mineral deposits and contains numerous structures and debris from mining activities over the last century (Wright, 1997). Cement and Mineral creeks join the Animas River near Silverton, contributing substantial loads of dissolved and colloidal metals (Church and others, 1997). Colloidal aluminum (Al) and iron (Fe) are of particular concern because they cement the river bed and affect plant and animal life in the river downstream of the confluences (Owen, 1997). The purpose of this study was to quantify the transport of Al and Fe in this reach of the river and identify the sources colloidal Al and Fe.

METHODS

Streamflows (discharges), pH and concentrations of total and dissolved Al and Fe were measured during September 1996 in Cement and Mineral creeks and at four sites in the Animas River (fig. 1). Streamflows were measured at the

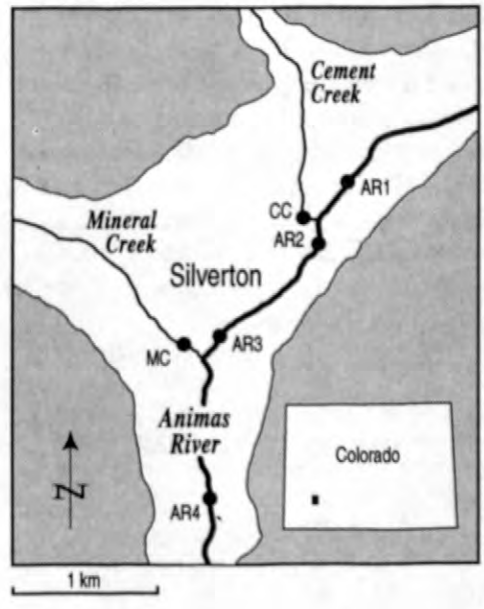

Figure 1. The upper Animas River near Silverton, Colorado.

sites or estimated from gages on the two creeks and at AR1 and AR4. Samples were collected using the equal-discharge-interval method. Filtrates for dissolved metal analysis were collected from a tangential-flow filtration apparatus using 10k Dalton filters (approx. 0.001 micron pore size). Filtered and unfiltered samples for metal analysis were adicified with nitric acid (1 percent final concentration) and digested in polyethylene bottles for two months before analysis. Al and Fe concentrations were measured using an inductively coupled argon plasma atomic emission spectrometer. Mean particle sizes at all sites were within the colloidal range. Concentrations of colloidal Al and Fe reported here are the differences between total (unfiltered) and dissolved concentrations.

RESULTS

Concentrations in Cement Creek (CC) of dissolved Al and Fe and colloidal Fe were the highest observed in this study, and the pH in Cement Creek was the lowest (Table 1.). Upstream in the Animas River at AR1, Al and Fe concentrations were low, and pH was the highest observed in this study. Discharge from Cement Creek into the Animas River created large gradients in chemical concentrations across the channel in the mixing zone (AR2) because of the large differences in pH (>3 units) and in concentrations of Al and Fe between the two streams. The formation of colloidal particles was visibly apparent in the water column, and precipitates also coated bank and bed materials downstream. The Animas River was well mixed farther downstream at AR3, where colloids accounted for nearly all of the Al and more than half of the total Fe in the water column (Table 1.).

Table 1. Concentrations of dissolved (Dis.) and colloidal (Coll.) Al and Fe in micromoles per liter and pH at sites in Cement Creek (CC), Mineral Creek (MC) and the Animas River (AR1-AR4).

Site	pH	Dis. Al	Coll. Al	Dis. Fe	Coll. Fe
AR1	7.54	1	1	0	2
CC	3.84	192	5	71	64
AR3	6.79	1	40	12	17
MC	6.60	1	71	19	30
AR4	6.72	1	49	10	23

Details of reactions that occurred in the Animas River downstream of Cement Creek were examined in a laboratory experiment, in which unflitered samples from the Animas River (at AR1) and Cement Creek were mixed in varying proportions. The mixtures were processed within a few minutes of their preparation. The mixing plot showed that Al, which was dissolved in the low pH water of Cement Creek, formed colloidal particles as pH increased from about 4.5 to 6.5 (fig. 2). This is illustrated by the large departure in dissolved Al from the conservative mixing line and the value for colloidal Al intersecting the line near pH 6.5. Cement Creek supplied both dissolved and colloidal Fe to the Animas River, but the mixing plot indicated that additional colloidal Fe formed as pH was increased to about pH 5.3 (fig. 3). Major differences between Al and

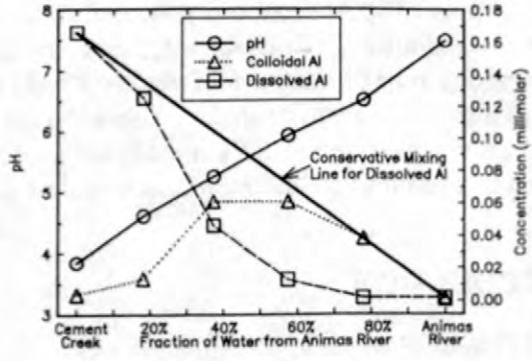

Figure 2. Diagram showing pH and concentrations of dissolved and colloidal Al during mixing of Cement Creek and Animas River (AR1) waters.

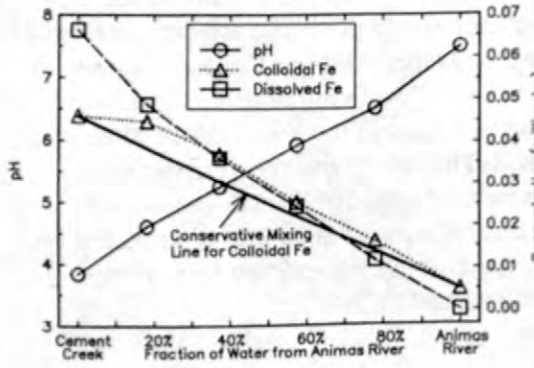

Figure 3. Diagram showing pH and concentrations of dissolved and colloidal Fe during mixing of Cement Creek and Animas River (AR1) waters.

Fe were that colloidal Al had formed at a higher pH, and only about 17 percent of the dissolved Fe had precipitated during mixing.

Nearly all of the Al and about 61 percent of the Fe supplied to the Animas River from Mineral Creek was colloidal (Table 1.). The pH of Mineral Creek was similar to the pH upstream in the Animas River (AR3), and mixing resulted in a small change in pH and no change in the partitioning of Al between colloidal and dissolved forms downstream at AR4. However, a larger fraction of the total Fe was colloidal at AR4 compared to MC and AR3, indicating the formation of additional colloidal Fe downstream of the confluence.

Table 2. Flow in cubic feet per second and transport of total Al and Fe in kilograms per day at sites in Cement Creek (CC), Mineral Creek (MC), and the Animas River (AR1-AR4). Total inputs to the confluences (Sum) are compared to measurements downstream.

Site	Flow	Al transport	Fe transport
AR1	63	10	19
CC	17	221	313
Sum	80	231	332
AR2	80	239	345
AR3	82	224	328
MC	61	291	408
Sum	143	515	736
AR4	147	483	686

Cement and Mineral Creeks were the dominant sources of Al and Fe to the Animas River (Table 2.). Mineral Creek was the larger source, accounting for about 56 percent of the transport of total Al and total Fe in the water column of the Animas River at AR4, compared to about 42 percent for Cement Creek. Transports of total Al and total Fe showed small losses (<10 percent) over the approximately 2.5 km reach of the Animas River. Even though coatings and accumulations of Al- and Fe-rich precipitates were visible in the Animas River between AR2 and AR4, our results show that losses were a small fraction of the total transport under low flow conditions.

DISCUSSION

The formation of colloidal Al and Fe hydroxides or hydrous oxides as acid mine waters are neutralized has been shown in numerous field and laboratory studies (see Nordstom and Ball, 1986; Stumm and Morgan, 1996, and references therein). Nearly half of the colloidal Al in this study reach of the Animas River was formed in the mixing zone near AR2. The formation of colloids in the river might be detrimental to fish and other organisms. Colloidal Al that is freshly formed in the water column can be particularly toxic to fish (Witters and others, 1996). In addition, the Al and Fe colloids contain zinc and copper, which could contribute to the toxic effects observed near AR4 (Nimmo and others, 1998). Aggregates of these colloids accumulate on the stream bed and enter the food chain through benthic invertebrates that are consumed by fish (Woodward and others, 1995).

Transformations of Al and Fe between dissolved and colloidal forms were not apparent within the mixing zone of Mineral Creek with the Animas River, which might be expected by the similar pH values in these two streams. Nearly all of the Al already was in colloidal form in both streams before they mixed, but both the transport and the concentration of colloidal Al were increased in the Animas River downstream of the confluence. Iron was present in dissolved and colloidal forms in both Mineral Creek and at AR3. The formation of additional colloidal Fe downstream from the confluence appeared to result from oxidation of dissolved Fe(II) to Fe(III), which probably was occurring in both streams before they mixed.

Our results showed that more than 90 percent of the input of total Al and Fe was transported past AR4. All of the Al and 70 percent of the Fe was colloidal at AR4, and the dissolved iron would eventually form additional colloidal Fe downstream. Other studies have shown that the colloids supplied by or formed from the Al and Fe discharged by Cement and Mineral creeks affect the riverbed for at least 60 km downstream of AR4 (Owen, 1997).

REFERENCES CITED

Church, S.E., Kimball, B.A., Fey, D.L., Ferderer, D.A., Yager, T.J., and Vaugn, R.B., 1997, Source, transport and partitioning of metals between water, colloids, and bed sediments of the Animas River, Colorado: U.S. Geological Survey Open-file Report 97-151, 135 p.

Nimmo, D.W.R., Castle, C.J., and Besser, J.M., 1998, A toxicological reconnaissance of the Upper Animas River watershed near Silverton, Colorado, Nimick, D.A. and von Guerard, P. eds: U.S. Geological Survey Open-file Report 98-297, p. 19.

Nordstrom, D.K., and Ball, J.W., 1986, The Geochemical Behavior of Aluminum in Acidified Surface Waters: Science, p. 54-56.

Owen, R.J., 1997, Water Quality and Sources of Metal Loading to the Upper Animas River Basin: Colorado Department of Public Health and Environment, Water Quality Division, 31 p.

Stumm, W., and Morgan, J.J., 1996, Aquatic Chemistry, Third Edition: John Wiley and Sons, Inc., New York, 1022 p.

Witters ,H.E., Van Puymbroeck, S., Stouthart, A.J.H.X., and Bonga, S.E.W., 1996, Physicochemical changes of aluminum in mixing zones: mortality and physiological disturbances in brown trout: Environmental Toxicology and Chemistry v. 15, p. 989-996.

Woodward, D.F., Farag, A.M., Bergman, H.L., DeLonay, A.J., Little, E.E., Smith, C.E., and Barrows, F.T., 1995, Metals-contaminated benthic invertebrates in the Clark Fork River, Montana: effects on age-0 brown trout and rainbow trout: Canadian Journal of Fisheries and Aquatic Science, v. 52, p. 1994-2004.

Wright, W.G., 1997, Natural and Mining-Related Sources of Dissolved Minerals During Low Flow in the Upper Animas River Basin, Southwest Colorado: U.S. Geological Survey Fact Sheet FS-148-97.

AUTHOR INFORMATION

Laurence E. Schemel and Kenneth E. Bencala, U.S. Geological Survey, Menlo Park, California (lschemel@usgs.gov, kbencala@usgs.gov,)

Briant A. Kimball, U.S. Geological Survey, Salt Lake City, Utah (bkimball@usgs.gov)

Partitioning of Zinc between Dissolved and Colloidal Phases in the Animas River near Silverton, Colorado

By Laurence E. Schemel, Marisa H. Cox, Briant A. Kimball, and Kenneth E. Bencala

ABSTRACT

Partitioning of zinc (Zn) between dissolved and colloidal phases was studied in the upper Animas River. Most of the Zn was dissolved in the water column, but a variable fraction of the total Zn was associated with aluminum (Al)- and iron (Fe)-rich colloidal particles. Colloids were supplied to the river by tributary creeks that drain areas with natural sulfide mineral deposits and debris from abandoned mines. The fraction of the total Zn that was in the colloidal phase increased with pH in the river, indicating the possibility of adsorption by colloidal Al and Fe. The influence of pH was confirmed in laboratory experiments in which larger fractions of the total Zn were associated with the colloids when pH was increased in samples from the river. The effect of increasing pH was greatest in the sample with the highest concentration of colloidal Al and Fe. The total concentration of colloidal Al and Fe appeared to be a factor limiting the adsorption of Zn during the late summers when the samples were collected. Our results indicate adsorption of Zn would be greater downstream where the pH increases in the river and perhaps during spring when concentrations of colloidal Al and Fe are higher.

INTRODUCTION

Colloidal particles in the water column of the Animas River near Silverton, Colorado, are primarily composed of aluminum (Al) and iron (Fe) precipitates, but also contain zinc (Zn) and other metals (Church and others, 1997). The association of a small, variable fraction of the total Zn with the Al- and Fe-rich colloids possibly indicates adsorption or coprecipitation in the water column (Jenne, 1998). The purpose of this study is to examine factors that influence the partitioning of Zn between dissolved and colloidal phases in the Animas River. Zn is of particular interest in this river system because of its many natural and mining-related sources and its impact on aquatic life (Wright, 1997; Nimmo and others, 1998).

METHODS

Concentrations of total and dissolved Al, Fe, and Zn and pH were measured in Cement Creek (CC) and Mineral Creek (MC) and at sites in the Animas River (fig. 1). Filtrates for dissolved metal analysis were collected from a tangential-flow filtration apparatus using 10k Dalton filters (approx. 0.001 micron pore size). All samples were acidified with nitric acid (1 percent final concentration) and digested at room temperature in polyethylene bottles for two months before analysis. Al, Fe, and Zn were measured by an inductively coupled argon plasma atomic emission spectrometer. Mean particle sizes at all sites were within the colloidal range. Colloid concentrations reported here are the differences between total (unfiltered) and dissolved concentrations.

RESULTS

Zinc was dissolved in the acidic (pH 3.8) waters of Cement Creek, but a fraction of the total Zn was colloidal in the near-neutral-pH waters of the Animas River and Mineral Creek (Table 1.). Little colloidal Al or Fe was present in the Animas River at AR1, but concentrations increased downstream from the Cement Creek

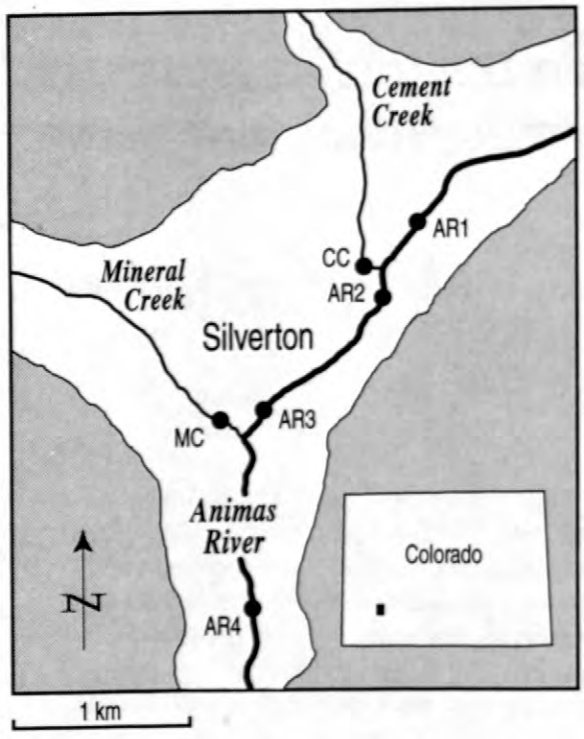

Figure 1. The upper Animas River near Silverton, Colorado.

Table 1. Average concentrations (micromoles per liter) of dissolved (Dis.) Zn and colloidal (Coll.) Zn, Al, and Fe in Cement Creek (CC), Mineral Creek (MC), and the Animas River (AR1-AR4) during September 1996.

Site	Dis. Zn	Coll. Zn	Coll. Al	Coll. Fe
AR1	5.6	0.7	1	2
CC	12	0	5	64
AR3	6.5	1.5	43	28
MC	3.4	0.3	71	21
AR4	5.2	0.7	49	24

confluence. Sources of colloidal Al and Fe were 1) reactions when inflow from Cement Creek mixed with the Animas River, 2) inflow from Mineral Creek, and 3) oxidation in the water column of the Animas River (see Schemel and others, this volume). Aluminum dissolved in Cement Creek formed colloidal Al upon mixing with the Animas River near AR2. Nearly all of the Al in the river downstream of AR2 and in Mineral Creek was in the colloidal phase. Both creeks supplied dissolved and colloidal Fe to the river, and colloidal Fe continued to form in the river as dissolved Fe was oxidized.

The total concentration of Zn was greater than the concentrations of colloidal Al and Fe at AR1. Up to 11 percent of the Zn was colloidal at this site where the concentrations of colloidal Al and Fe were low and pH was high relative to other sites in the river (fig. 2). In the Animas river between AR2 and AR3 downstream of inflow from Cement Creek, the mole ratio of colloidal Al plus Fe to total Zn averaged 9. Up to 22 percent of the total Zn was in the colloidal phase, and an increase in the percent of Zn in the colloidal phase was observed as pH increased. In the mixing zone near AR2, reactions that formed most of the colloidal Al and Fe were largely completed by pH 6.5, although some colloidal Fe continued to form downstream as Fe(II) was oxidized to Fe(III) (see Schemel and others, this volume). The fraction of Zn associated with the colloids between AR2 and AR3 increased most rapidly above pH 6.8, indicating that Zn had adsorbed onto previously formed colloidal Al and Fe. However, coprecipitation or adsorption onto colloidal Fe that was forming in the river might also account for some of the Zn associated with the colloidal phase.

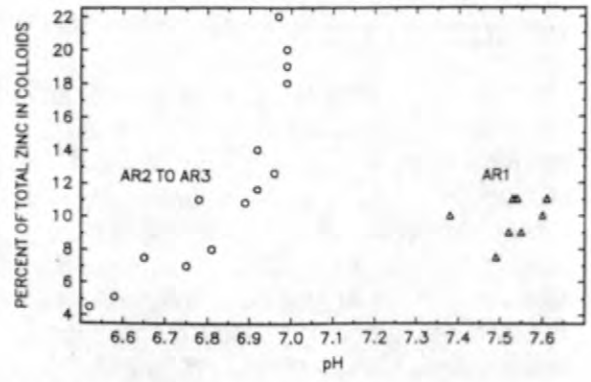

Figure 2. Percentage of total Zn in the colloidal phase versus pH in the water column of the Animas River. Data are from September 1996 and 1997.

The potential for rapid adsorption of Zn by colloidal Al and Fe was tested in the laboratory by increasing the pH of samples collected at MC and AR4 with sodium hydroxide. Samples were removed from the batch reactor when pH became stable, and they were processed within a few minutes. Most of the Al and Fe in these samples was colloidal. As expected, the fraction of Zn associated with the colloids increased with

increasing pH in both cases, but a greater fraction of the Zn was associated with the colloids in the sample from MC (fig. 3). The mole ratio of colloidal Al plus Fe to total Zn in the sample from AR4 was 13, whereas that for MC was 32. Therefore, with increasing pH a larger fraction of the total Zn was colloidal in the sample with higher concentrations of Al and Fe colloids and presumably a greater abundance or density of adsorption sites.

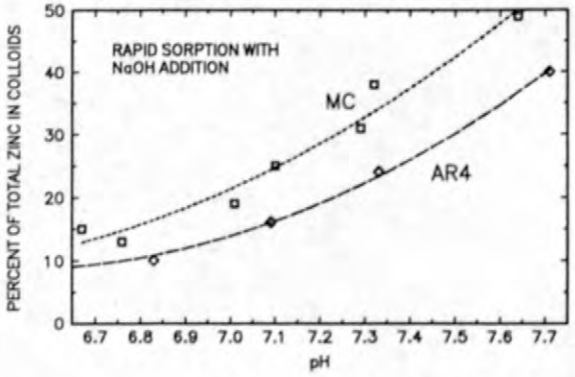

Figure 3. Results of laboratory experiments with samples from Mineral Creek (MC) and the Animas River (AR4) showing the increase in the percentage of total Zn in the colloidal phase with pH increased by the addition of NaOH. Lines are second-order fits to the data.

DISCUSSION

Partitioning of Zn between dissolved and colloidal phases in the water column of the Animas River downstream of AR2 was most likely dependent on two major factors, pH and the abundance of colloidal Al and Fe relative to the concentration of Zn. Most studies that show significant adsorption of Zn over a narrow range of about one pH unit near pH 7 have a large excess of adsorbent, usually Fe or Al hydroxides, relative to the total concentration of Zn (for examples see Duker and others, 1995, and Webster and others, 1998). At the low mole ratios observed in the water column of the Animas River between AR2 and AR4 available sites for adsorption might be limited, and only a small fraction of the total Zn could be adsorbed over the pH range observed in this reach of the river (pH< 7.1).

Results of our laboratory experiment with the sample from AR4 indicated that greater adsorption of Zn might occur downstream of AR4, where pH increases of nearly one-half unit have been measured. Field observations, although limited in number, indicate that one-third or more of the Zn can be associated with the colloidal phase when the pH is higher at AR4 and at locations downstream (Church and others, 1997, and our unpublished data).

Greater adsorption observed in the sample from MC relative to the sample from AR4 indicated that a greater fraction of the total Zn might be colloidal when concentrations of colloidal Al and Fe are higher in the river during spring runoff. This was supported by measurements during the mid- and late-spring runoff period of 1996, when colloidal Zn was a large fraction of the total Zn transport (Church and others, 1997). The very low concentrations of colloidal Al and Fe at AR1 indicated that relatively little Zn could be adsorbed even at the high pH. Consequently, some of the Zn associated with the colloidal fraction at AR1 might not be adsorbed.

REFERENCES CITED

Church, S.E., Kimball, B.A., Fey, D.L., Ferderer, D.A., Yager, T.J., and Vaughn, R.B., 1997, Source, transport, and partitioning of metals between water, colloids, and bed sediments of the Animas River, Colorado: U.S. Geological Survey Open-File Report 97-151, 135 p.

Duker, A., Ledin, A., Karlsson, S. and Allard, B., 1995, Adsorption of zinc on colloidal (hdr)oxides of Si, Al and Fe in the presence of fulvic acid: Applied Geochemistry, v. 10, p. 197-205.

Jenne, E.A., 1998, Adsorption of metals by geomedia: data analysis, modeling , controlling factors, and related issues, Jenne, E.A. ed., Adsorption of Metals by Geomedia: Academic Press, New York, p. 2-73.

Nimmo, D.W.R., Castle, C.J., and Besser, J.M., 1998, A toxicological reconnaissance of the upper Animas River watershed near Silverton, Colorado, Nimick, D.S. and von Guerard, P. eds: U.S. Geological Survey Open-File Report 98-297, p. 19.

Schemel, L.E., Kimball, B.A., and Bencala, K.E., this volume, Colloid formation and the transport of Al and Fe in the Animas River near Silverton, Colorado.

Webster, J.G., Swedlund, P.J., and Webster, K.S., 1998, Trace metal adsorption onto an acid mine drainage iron (III) oxyhydroxy sulfate: Environmental Science and Technology, v. 32, p. 1361-1368.

Wright, W.G., 1997, Natural and mining-related sources of dissolved minerals during low flow in the upper Animas River basin, southwest Colorado: U.S. Geological Survey Fact Sheet FS-148-97.

AUTHOR INFORMATION

Laurence E. Schemel, Marisa H. Cox, and Kenneth E. Bencala, U.S. Geological Survey, Menlo Park, California (lschemel@usgs.gov, mhcox@usgs.gov, kbencala@usgs.gov,

Briant A. Kimball, U.S. Geological Survey, Salt Lake City, Utah (bkimball@usgs.gov,)

Oxygen Isotopes of Dissolved Sulfate as a Tool to Distinguish Natural and Mining-Related Dissolved Constituents

By Winfield G. Wright and D. Kirk Nordstrom

ABSTRACT

Natural and mining-related dissolved-constituent concentrations need to be distinguished in a watershed affected by abandoned mines to prioritize subbasins for remediation and to assist with the establishment of water-quality standards. The oxygen isotopes of dissolved sulfate can be used to distinguish between natural and mining-related sources of dissolved constituents. Several methods employing the oxygen isotopes of dissolved sulfate can be used to determine the relative amounts of natural and mining-related dissolved constituents in water: (1) the isotope-dilution equation for simple mixing zones (two sources and one receiving stream); (2) the isotope mass-balance equation for streams receiving dissolved sulfate from multiple geologic sources; and (3) graphical relations and the mathematical solution of simultaneous equations in a watershed approach. Using the different methods for data collected during low flow, about 71 to 75 percent of the dissolved-constituent concentrations are from natural sources in selected subbasins of the upper Animas watershed.

NATURAL AND MINING-RELATED CONCENTRATIONS OF DISSOLVED CONSTITUENTS

Natural and mining-related concentrations of dissolved constituents need to be distinguished in watersheds affected by abandoned mines in order to prioritize subbasins for remediation and to assist with the establishment of water-quality standards. The typical method for distinguishing between natural and mining-related sources of dissolved constituents is a mass-balance approach, in which all mines and natural streams are sampled synoptically (a snapshot in time), and a mass balance is obtained for a conservative constituent (such as dissolved sulfate or zinc). However, in the mountainous Upper Animas Watershed (fig. 1), this can be a monumental task subject to errors, and theoretically conservative constituents might not be truly conservative. Oxygen isotopes of dissolved sulfate can be used to distinguish natural and mining-related sources on a watershed basis, and the results can be used to verify mass-balance calculations of natural and mining-related dissolved constituents. When used in mass-balance calculations, oxygen isotopes of dissolved sulfate can provide very accurate estimates of natural and mining-related dissolved constituents.

THEORETICAL DESCRIPTION OF THE OXYGEN ISOTOPES OF DISSOLVED SULFATE

Data for the oxygen isotopes of dissolved sulfate (symbol $\delta^{18}O_{SO_4^{2-}}$) can provide insight into the processes that formed the sulfate. In some geologic settings, $\delta^{18}O_{SO_4^{2-}}$ data can reflect the mineralogy of the dissolved-sulfate source. The $\delta^{18}O_{SO_4^{2-}}$ data also can determine whether sulfate reduction has occurred in the water. The analytical measurement of $\delta^{18}O_{SO_4^{2-}}$ is more precise than other hydrologic parameters (such as discharge and analytical determination of inorganic constituents), and could be useful for quantitative calculations.

In sulfide-mineralized geologic regions that have been mined, such as the Upper Animas Watershed (fig. 1), the oxidation of sulfide minerals produces dissolved sulfate (symbol SO_4^{2-}) in natural springs and in mine drainage. These oxidation pro-

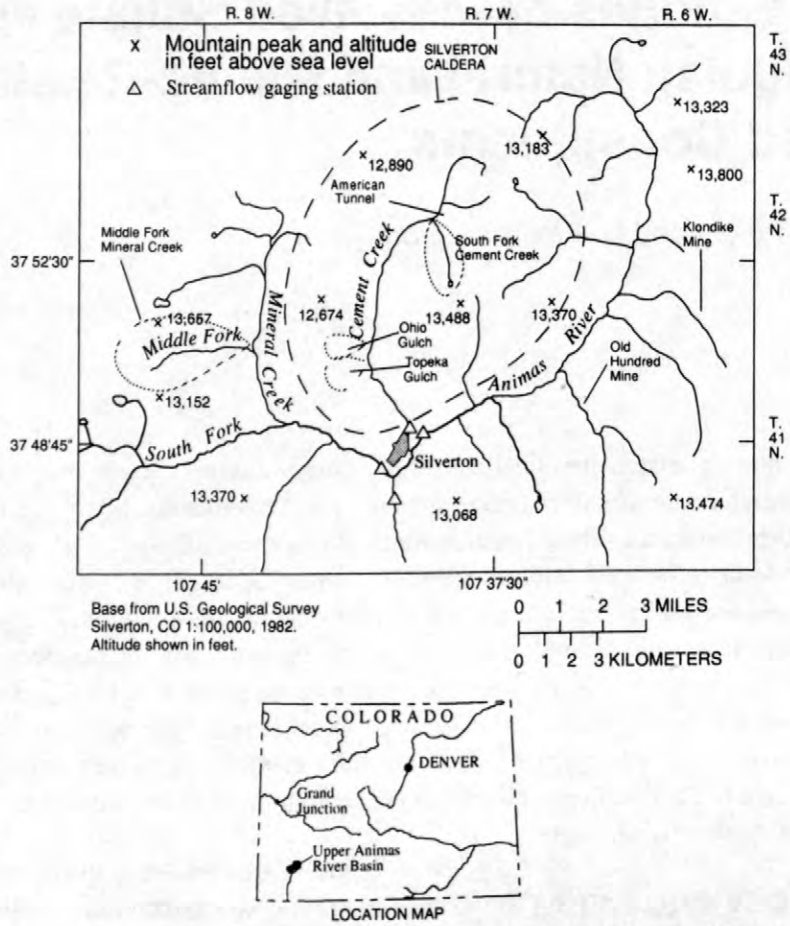

Figure 1. Upper Animas Watershed and locations of study areas.

cesses involve oxygen that has an isotope composition indicative of the reaction mechanism. Oxygen in the dissolved sulfate has two possible sources--dissolved oxygen (symbol $O_{2(aq)}$ for oxygen in the aqueous phase) and oxygen in the water molecule (symbol H_2O). Oxygen isotopes of dissolved sulfate are expressed in per mil (or parts per thousand) relative to the Vienna Standard Mean Ocean Water (VSMOW) on a scale that is normalized such that the $\delta^{18}O$ of the Standard Light Arctic Precipitation (SLAP) water is -55.5 per mil exactly. Precision of $\delta^{18}O_{SO_4^{2-}}$ measurements is ± 0.1 per mil.

Numerous studies of sulfide-mineral oxidation have been conducted in the last two decades. Of particular interest are those studies conducted under conditions similar to environments producing acid mine drainage. The following reactions commonly are used to represent the overall oxidation processes of pyrite (symbol FeS_2):

$$FeS_2 + 7/2\,O_{2(aq)} + H_2O \rightarrow Fe^{2+} + 2SO_4^{2-} + 2H^+ \quad (1)$$

$$FeS_2 + 14Fe^{3+} + 8H_2O \rightarrow 15Fe^{2+} + 2SO_4^{2-} + 16H^+ \quad (2)$$

Reaction (1) is limited by the availability of dissolved oxygen and reaction (2) is limited by the oxidation rate of Fe^{2+} to Fe^{3+}. The ferrous iron (Fe^{2+}) produced from reactions 1 and 2 is subsequently oxidized further to produce ferric iron (symbol Fe^{3+}), which can precipitate as iron oxyhydroxide:

$$Fe^{2+} + 1/4\,O_{2(aq)} + H^+ \rightarrow Fe^{3+}{}_{(solid)} + 1/2\,H_2O \quad (3)$$

Sulfur oxyanions, such as thiosulfate ($S_2O_3^{2-}$), polythionate ($S_nO_6^{2-}$), and sulfite (SO_3^{2-}) are sulfur compounds intermediate to the oxidation pathway of FeS_2 to SO_4^{2-}. The oxidation of sulfur oxyanions can occur quickly, and the

resulting SO_4^{2-} may acquire oxygen via exchange with H_2O (Van Stempvoort and Krouse, 1994). Oxidation of sulfur and sulfur oxyanions may proceed as follows:

$$S_{2\ \text{in pyrite}}^{2-} + OH^- \rightarrow S_2O_3^{2-} \quad (4)$$
(Moses and others, 1987)

$$S_2O_3^{2-} + OH^- \rightarrow S_4O_6^{2-} \rightarrow SO_4^{2-} \quad (5)$$
(Xu and Schoonen, 1995)

$$S_2O_3^{2-} + OH^- \rightarrow SO_4^{2-} \quad (6)$$
(Xu and Schoonen, 1995)

The oxygen molecules (whether in $O_{2(aq)}$ or in H_2O) that are involved in reactions (1)-(6) can, except during sulfate reduction, retain the original isotopic composition of the source of the oxygen. The oxygen isotope composition of H_2O (symbol $\delta^{18}O_{H_2O}$) varies with the altitude of the precipitation that deposited the water on the Earth's surface and with other processes such as evaporation, transpiration, and latitude. For the Upper Animas Watershed, $\delta^{18}O_{H_2O}$ averages about -15.9 per mil. The oxygen-isotope composition of atmospheric oxygen that dissolves in water (symbol $\delta^{18}O_{O_{2(aq)}}$) has the value of +23 per mil (Horibe and others, 1973). Graphically relating $\delta^{18}O_{SO_4^{2-}}$ data to dissolved SO_4^{2-} data can indicate the geochemical mechanisms involved with the formation of the dissolved SO_4^{2-}.

The isotopic composition of $\delta^{18}O_{SO_4^{2-}}$ that results from the reactions can indicate whether the dissolved sulfate is from natural or mining-related sources. If reaction (1) is the predominant reaction pathway, the resulting $\delta^{18}O_{SO_4^{2-}}$ might consist of a greater percentage of the $\delta^{18}O_{O_{2(aq)}}$ composition, as compared with the $\delta^{18}O_{H_2O}$ composition. If reaction (2) is the predominant oxidation pathway, aqueous ferric iron ($Fe^{3+}_{(aq)}$), rather than $O_{2(aq)}$, is the primary agent responsible for oxidation of pyrite in acid conditions. All of the reactions (1)-(6) are mediated by bacteria in the environment; however, mining accelerates the weathering processes through both exposure of fresh minerals to oxygen and increased populations of sulfide-mineral oxidizing bacteria (Taylor and others, 1984). In accelerated weathering environments, reactions (4), (5), and (6) might occur very quickly; consequently, the resulting $\delta^{18}O_{SO_4^{2-}}$ might consist of a greater percentage of the $\delta^{18}O_{H_2O}$ composition, as compared to the $\delta^{18}O_{O_{2(aq)}}$ composition, because of oxygen exchange between H_2O and SO_4^{2-}.

Effects on $\delta^{18}O_{SO_4^{2-}}$ values might be caused by the relative distribution of different sulfur minerals in different rock types. The dissolution of anhydrite, gypsum, barite, and alunite affect the $\delta^{18}O_{SO_4^{2-}}$ compositions. Two samples of vein gypsum collected from a mine dump pile in the Cement Creek subbasin of the Upper Animas Watershed had $\delta^{18}O_{SO_4^{2-}}$ values of +9 and +10 per mil. In a geochemical environment dominated by pyrite oxidation, dissolution of gypsum imparts a mixture of the two processes on the resulting $\delta^{18}O_{SO_4^{2-}}$ compositions.

Microbially-mediated reduction of SO_4^{2-} to sulfide (symbol H_2S, which can be present in the dissolved or gaseous phases) can result in substantial enrichments of sulfur isotopes (symbol $\delta^{34}S_{SO_4^{2-}}$) and $\delta^{18}O_{SO_4^{2-}}$ in residual SO_4^{2-}. The lighter ^{32}S molecule in SO_4^{2-} is preferentially utilized over the ^{34}S molecule by microbes, which enriches (or makes more positive) the $\delta^{34}S_{SO_4^{2-}}$ composition of the remaining SO_4^{2-}. Likewise, the lighter ^{16}O molecule is preferentially utilized over the ^{18}O molecule by microbes, which enriches (or makes more positive) the resulting $\delta^{18}O_{SO_4^{2-}}$. In addition, in geochemically-reducing conditions, the oxygen molecule in $O_{2(aq)}$ and in H_2O become parallel electron acceptors during dissimilatory reduction of SO_4^{2-}; hence both $\delta^{18}O_{O_{2(aq)}}$ and $\delta^{18}O_{H_2O}$ may become enriched isotopically, whereby further FeS_2 oxidation by these isotopically-enriched oxygen molecules produces isotopically enriched $\delta^{18}O_{SO_4^{2-}}$ (C. Kendall, U.S. Geological Survey, written commun., 1997). Several collapsed mines in the Upper Animas Watershed show indications of SO_4^{2-} reduction: zero $O_{2(aq)}$, smell of H_2S gas, and isotopically heavy $\delta^{34}S_{SO_4^{2-}}$ and $\delta^{18}O_{SO_4^{2-}}$ compositions. There is, however, some debate concerning the electron donors available for SO_4^{2-} reduction. Mold on wood timbers in the abandoned mines may provide sufficiently labile organic matter for SO_4^{2-} reduction; however, this hypothesis has not been tested.

OXYGEN ISOTOPES OF DISSOLVED-SULFATE DATA FROM THE UPPER ANIMAS WATERSHED, SOUTHWESTERN COLORADO

The Upper Animas Watershed has complex geology related to the approximately 28 million-year-old Silverton Caldera (fig. 1) and placement of intracaldera lavas. Regional propylitic alteration introduced sulfur as sulfide minerals which are present in veins and disseminated throughout the rocks in varying proportions. Late-stage hydrothermal mineralization is typified by quartz vein filling accompanied by chalcopyrite, pyrite, galena, gold, rhodonite, silver, and sphalerite. Vein gypsum and barite also were introduced by late-stage hydrothermal venting. Copper-molybdenum porphyry complexes and acid-sulfate hydrothermal alteration systems also are present in the region.

Water-quality samples were collected during low flow from natural springs, draining mines, and streams in the Middle Fork Mineral Creek, South Fork Cement Creek, Ohio Gulch, and Topeka Gulch subbasins (fig. 1), as well as from the Klondike Mine, the Old Hundred Mine, and the American Tunnel (fig. 1). Graphically relating $\delta^{18}O_{SO_4^{2-}}$ to $\delta^{34}S_{SO_4^{2-}}$ indicates water from natural springs and mine drainage plot parallel (fig. 2). When comparing natural springs to mine drainage in figure 2, there is an isotopic shift to the left (decrease in oxygen isotope values) from natural springs to mine drainage. This might be explained by the incorporation of a greater percentage of $\delta^{18}O_{H_2O}$ in $\delta^{18}O_{SO_4^{2-}}$ possibly because of bacterially-mediated sulfide oxidation. For the purposes of this report, this isotopic shift is called the kinetic shift. Also shown on figure 2 are the solid- and aqueous-phase endmembers that are incorporated into the oxygen and sulfur isotopic compositions (Casadevall and Ohmoto, 1977; Horibe and others, 1973). When relating all $\delta^{18}O_{SO_4^{2-}}$ data to dissolved SO_4^{2-} and dissolved-calcium concentrations, the importance of gypsum to $\delta^{18}O_{SO_4^{2-}}$ compositions is evident (fig. 3). Data points that have lower dissolved-calcium concentrations and lighter $\delta^{18}O_{SO_4^{2-}}$ compositions represent the sulfide-oxidation region (fig. 3); data points that have lower dissolved-calcium concentrations and heavier $\delta^{18}O_{SO_4^{2-}}$ compositions represent the sulfate-reduction region (sulfate reduction that occurs in collapsed, anoxic mines) (fig. 3); and data points that have higher dissolved-calcium concentrations represent a mixture of sulfide oxidation and gypsum dissolution (fig. 3).

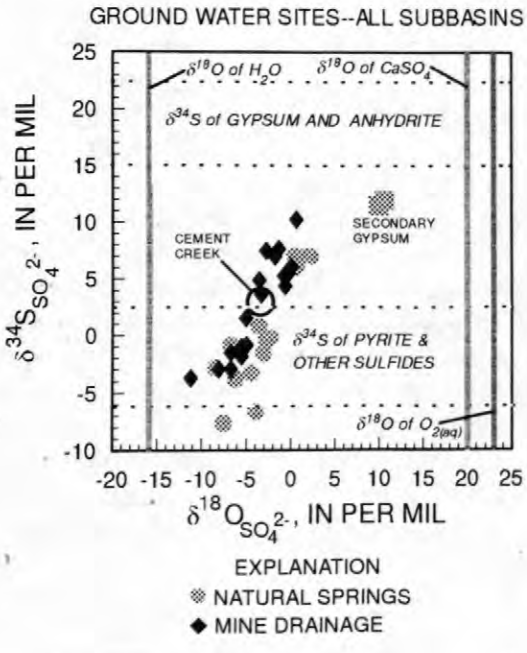

Figure 2. Oxygen isotopes of sulfate related to sulfur isotopes of sulfate in water from springs and mines in the upper Animas watershed during low flow.

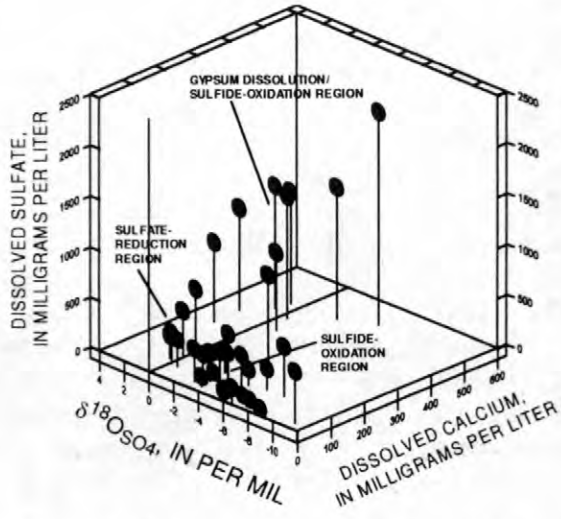

Figure 3. Oxygen isotopes of sulfate related to dissolved sulfate and dissolved calcium in water from ground-water sites (springs and mines) during low-flow.

Graphically relating $\delta^{18}O_{SO_4^{2-}}$ to SO_4^{2-} can help distinguish natural from mining-related dissolved sulfate. Figure 4 shows data from ground-water samples collected during low flow in the Cement Creek subbasin (rock types from the center of the caldera). The isotopically heavier $\delta^{18}O_{SO_4^{2-}}$ compositions probably are affected by gypsum dissolution or SO_4^{2-} reduction, or both. When compar-

ing natural springs to mine drainage in figure 4, the isotopic shift is evident in the data. To illustrate the kinetic shift, three pairs of spring/mine combinations (a-a', b-b', and c-c') are shown on figure 4 where the springs and mines are situated in similar rock types. There is a shift to the left and up on figure 4 from the springs to the mines. A t-test of the paired data indicated that the kinetic shift is significant ($p \leq 0.3$, $r^2=0.78$). The kinetic shift is a result of the mining-related acceleration of weathering processes. The data point for Cement Creek at the mouth of the subbasin, an amalgamation of all water types in the Cement Creek subbasin, plots in the middle of all data points.

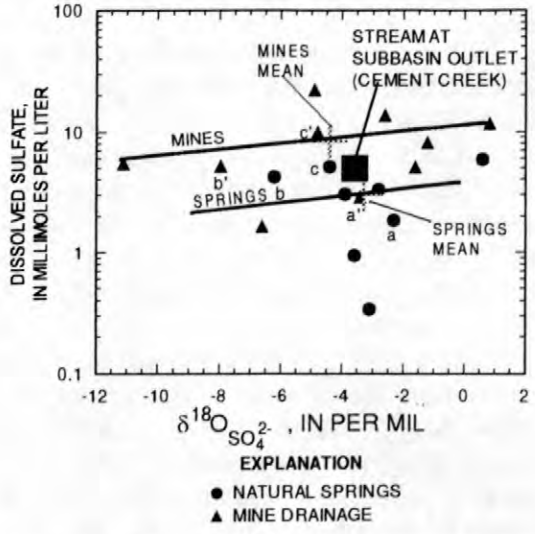

Figure 4. Oxygen isotopes of sulfate related to dissolved sulfate in water from springs and mines in the Cement Creek subbasin during low-flow.

Total-dissolved metals concentrations (Cd, Cu, Co, Fe, Ni, Pb, and Zn) are related to oxygen and sulfur isotopes of sulfate in figure 5. Increased dissolved-metal concentrations in mine drainage are shown in figure 5, which are caused by (1) location of mines along mineralized ore deposits, and (2) acceleration of sulfide-metal oxidation in mines, which creates higher dissolved-metal concentrations in mine drainage compared to natural springs. The kinetic shift (lighter oxygen-isotope compositions in mine drainage) also is evident in the data (fig. 5). This may be caused by the incorporation of a greater proportion of $\delta^{18}O_{H_2O}$ in $\delta^{18}O_{SO_4^{2-}}$ during oxidation of sulfur oxyanions. Some of the mine-drainage samples that plot among the spring samples have similar water-quality characteristics as natural springs.

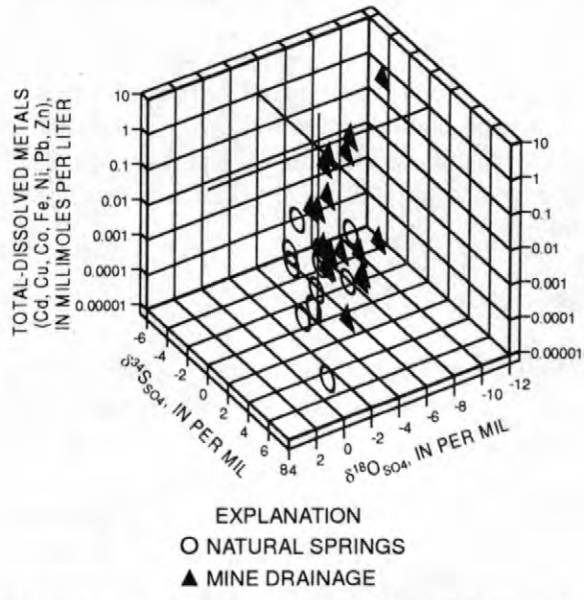

Figure 5. Oxygen isotopes of sulfate related to sulfur isotopes of sulfate and total-dissolved metals in water from springs and mines in the upper Animas watershed during low flow.

USES OF THE OXYGEN ISOTOPES OF DISSOLVED SULFATE

A typical method for distinguishing between natural and mining-related dissolved constituents in a subbasin is to collect water-quality samples, measure discharges, and perform loading mass-balance calculations, in which all mines and natural sources are accounted for. This effort can be a monumental task. The method described in this paper uses the oxygen isotopes of dissolved sulfate in a watershed approach so that all water sources (natural and mining-related) do not need to be sampled, only a representative sampling of the different site types is needed. Current work in the Upper Animas Watershed is, however, using the traditional mass-balance approach to distinguish natural and mining-related dissolved constituents, and the isotope method will be used to verify the mass-balance approach.

The oxygen isotopes of dissolved sulfate also can be used to perform mass-balance calculations. The error associated with analysis of water samples for the $\delta^{18}O_{SO_4^{2-}}$ isotopes is ± 0.1 per mil; therefore, the mass-balance calculations will have great

accuracy using isotopes. Also, in a geologically heterogeneous subbasin, it is possible to determine the source of the dissolved sulfate using $\delta^{18}O_{SO_4^{2-}}$ data.

The following example describes the use of oxygen isotopes of dissolved sulfate in a simple mixing problem to determine how much sulfate came from a particular mine. The sites and conditions of a location in Topeka Gulch are described as follows:

Topeka Gulch (fig. 1):

TOPEKA8=Natural alpine stream upstream from mine; $\delta^{18}O_{SO_4^{2-}}$ = -6.8 per mil.
TOPEKA9=Large draining mine; $\delta^{18}O_{SO_4^{2-}}$ = 0.83 per mil.
TOPEKA10=Mining-affected stream downstream from mine; $\delta^{18}O_{SO_4^{2-}}$ = 0.3 per mil.

To determine the percent of dissolved sulfate that comes from the TOPEKA9 mine, the isotope-dilution equation can be used (Shearer & Kohl 1993):

Isotope-dilution equation:

$$\text{Percent TOPEKA9} = \frac{(\delta^{18}O_{TOPEKA8} - \delta^{18}O_{TOPEKA10})}{(\delta^{18}O_{TOPEKA8} - \delta^{18}O_{TOPEKA9})} \times 100 \quad (7)$$

$$= [(-6.8) - (0.3)/(-6.8) - (0.83)] \times 100$$

= 93 percent of the dissolved sulfate came from the mine.

In this simple example, the isotope-dilution equation calculated that 93 percent of the dissolved sulfate came from the mine at TOPEKA9. The discharge of the stream and the mine are needed to perform a typical sulfate mass balance, and errors are inherent in the discharge and sulfate measurements. When the isotope-dilution equation was used, discharges were not needed, which eliminated the errors in streamflow-discharge measurements and in sulfate analyses.

An example using oxygen isotopes of dissolved sulfate in multiple geologic settings can be applied in the Middle Fork Mineral Creek subbasin (fig. 1). About one-half of the subbasin consists of chlorite-epidote-calcite dominated intracaldera lavas, and one-half of the subbasin consists of rocks altered by a copper-molybdenum porphyry complex. An isotope mass balance is obtained so that natural and mining-related sources balance at the mouth of the subbasin.

Isotope mass-balance equation:

$$\delta QC_{natural} + \delta QC_{mining\text{-}related} = \delta QC_{Middle\ Fork\ at\ mouth} \quad (8)$$

where

- δ is $\delta^{18}O_{SO_4^{2-}}$, in per mil,
- Q is discharge at the site, in cubic feet per second, and
- C is dissolved-sulfate concentration, in mg/L.

The known value is $\delta QC_{Middle\ Fork\ at\ mouth}$, and $\delta_{Middle\ Fork\ at\ mouth}$ = 0.0 per mil.

All of the mines in the Middle Fork Mineral Creek subbasin were sampled during low-flow conditions. Values of $\delta^{18}O_{SO_4^{2-}}$ for the mines ranged from -5.8 to +0.2. Using isotope mass balance, the flow-weighted average $\delta^{18}O_{SO_4^{2-}}$ composition for the mining-related water in the subbasin was calculated as: $\delta_{mining\text{-}related}$ = -0.76 per mil, which is an amalgamation of $\delta^{18}O_{SO_4^{2-}}$ compositions from mining-related sources.

Because two of the three values in equation (8) are known, the remaining unknown can be calculated: $\delta_{natural}$ = +0.32 per mil, which is an amalgamation of $\delta^{18}O_{SO_4^{2-}}$ compositions from natural sources in the subbasin. Because this composition is weighted towards the positive side, and there is gypsum and barite in the copper-molybdenum porphyry complex (contributing heavy $\delta^{18}O_{SO_4^{2-}}$ compositions), much of the SO_4^{2-} concentration at the mouth of the Middle Fork Mineral Creek subbasin probably comes from the porphyry complex. The isotope-dilution equation now can be used to determine the percent of mining-related dissolved sulfate that discharges from the mouth of the Middle Fork Mineral Creek: Mining-related sulfate = 29 percent; therefore, natural sulfate = 71 percent.

The percent of natural and mining-related dissolved zinc also can be determined using the $\delta^{18}O_{SO_4^{2-}}$ data and the solution of simultaneous equations. By determining the geometric means of the natural and mining-related data, the result is two end members and a receiving stream, and the proportion of the two end members in the Cement Creek sample can be solved using simultaneous equations. Solution of the simultaneous equations for the Cement Creek data indicate 75 percent of the

dissolved zinc in Cement Creek comes from natural springs and 25 percent of the dissolved zinc comes from mine drainage during low-flow. This estimate might vary during snowmelt-runoff periods.

A t-test of the $\delta^{18}O_{SO_4^{2-}}$ means for the simultaneous equations solution indicates the differences in the natural and mining-related means are significant to the $p \leq 0.4$ level. A t-test of the dissolved-zinc means indicates the natural and mining-related means are significant to the $p \leq 0.3$ level. Hence, there is a 60 to 70 percent confidence that the means are significantly different, and this confidence must be considered in the interpretation of the simultaneous equations results.

SUMMARY AND CONCLUSIONS

The oxygen isotopes of dissolved sulfate ($\delta^{18}O_{SO_4^{2-}}$) are a useful diagnostic tool to describe the geochemical processes that incorporate dissolved sulfate into water from sulfide-mineral oxidation and from gypsum dissolution. The percentage of natural and mining-related sources of dissolved constituents can be determined using $\delta^{18}O_{SO_4^{2-}}$ data in a watershed approach. Using the isotope dilution equation in simple mixing zones near a mine site, accurate estimates of the percentage of natural and mining-related dissolved sulfate can be determined, and discharge measurements are not needed for the calculation. Using the isotope mass-balance method in a heterogeneous geologic setting, $\delta^{18}O_{SO_4^{2-}}$ data indicated that 71 percent of the dissolved sulfate in the Middle Fork Mineral Creek subbasin came from natural sources and 29 percent came from mining-related sources. Using the graphical method and solution of simultaneous equations in a watershed approach, $\delta^{18}O_{SO_4^{2-}}$ data indicated that 75 percent of the dissolved zinc in the Cement Creek subbasin came from natural sources.

REFERENCES

Casadevall, T.J., and Ohmoto, H., 1977, Sunnyside Mine, Eureka Mining District, San Juan County, Colorado-- Geochemistry of gold and base metal ore deposition in a volcanic environment: Economic Geology, v. 72, p. 1285-1320.

Horibe, Y., Shigehara, K., and Takakuwa, Y., 1973, Isotope separation factor of carbon dioxide-water system and isotopic composition of atmospheric oxygen: J. Geophys. Res., v. 78 n. 15, p. 2625-2629.

Moses, C.O., Nordstrom, D.K., Herman, J.S., and Mills, A.L., 1987, Aqueous pyrite oxidation by dissolved oxygen and by ferric iron: Geochim. et Cosmochim. Acta, v. 51, p. 1561-1571.

Shearer, G., and Kohl, D.H., 1993, Natural abundance of nitrogen-15 isotopes--Fractional contribution of two sources to a common sink and use of isotope discrimination, in Knowles, R., and T.H. Blackburn, eds., Nitrogen isotope techniques: San Diego, Calif., Academic Press, Inc., p. 89-125.

Taylor, B.E., Wheeler, M.C., and Nordstrom, D.K., 1984, Stable isotope geochemistry of acid mine drainage--Experimental oxidation of pyrite: Geochim. et Cosmochim. Acta. v. 48, p. 2669-2678.

Van Stempvoort, D.R., and Krouse, H.R., 1994, Controls of $\delta^{18}O$ in sulfate--Review of experimental data and application to specific environments, in Alpers, C.N., and Blowes, D.W., eds., Environmental geochemistry of sulfide oxidation: Washington, D.C., American Chemical Society, Symposium Series 550, p. 446-480.

Xu, Y., and Schoonen, M.A.A., 1995, The stability of thiosulfate in the presence of pyrite in low-temperature aqueous solutions: Geochim. et Cosmochim. Acta, v. 59, p. 4605-4623.

AUTHOR INFORMATION

Winfield G. Wright
U.S. Geological Survey
Water Resources Division
Durango, Colorado 81301
(wgwright@usgs.gov)

D. Kirk Nordstrom
U.S. Geological Survey
Water Resources Division
National Research Program
Boulder, Colorado 80303
(dkn@usgs.gov)

Modeling Frequency of Occurrence of Toxic Concentrations of Zinc and Copper in the Upper Animas River

By John M. Besser and Kenneth J. Leib

ABSTRACT

Scientists participating in the USGS Abandoned Minelands Initiative have quantified metal concentrations and loadings from mining-related and natural background sources in the upper Animas River of southwestern Colorado, with the goal of guiding remediation decisions by federal land-management agencies. We have compared site-specific toxicity thresholds with frequencies of dissolved metal concentrations in stream water to evaluate the contributions of zinc and copper to toxic effects in fish and aquatic invertebrates in the upper Animas. Median lethal concentrations (LC50s) of zinc and copper were determined for fathead minnows, *Pimephales promelas*, and amphipods, *Hyalella azteca*, from seven-day toxicity tests under water quality conditions typical of the upper Animas. Frequency analysis based on hysteresis models was used to predict seasonal occurrence and daily probabilities of dissolved zinc and copper concentrations at two gaging stations near Silverton, Colorado. Results of these analyses indicate that dissolved zinc concentrations at both locations frequently exceed 7-day LC50s for amphipods, and occasionally exceed zinc LC50s for fathead minnows. In contrast, copper concentrations rarely approach lethal levels for either species. Model results are consistent with recent on-site toxicity tests with these two species. Comparison of modeled zinc and copper concentrations with published toxicity thresholds for brook trout, *Salvelinus fontinalis*, suggest that both zinc and copper contribute to chronic toxicity in resident trout in the upper Animas.

INTRODUCTION

The streams of the upper Animas River watershed receive loadings of heavy metals in water, colloids and sediment from numerous mines and associated waste deposits, as well as from natural sources in highly-mineralized portions of the watershed (Church et al. 1997). Elevated metal concentrations and other impacts associated with mining have resulted in reduction or elimination of stream fish and invertebrate communities.

The USGS Abandoned Mineland Initiative (AMLI) designated the upper Animas watershed as one of two study areas for development of scientific approaches to guide remediation of the impacts of historic mining activities (Nimick and von Guerard 1998). Studies conducted as part of the AMLI have characterized metal concentrations and loadings from mining and from natural background sources; tranformations of metals in stream ecosystems; and the bioavailability, toxicity, and habitat impacts of metals in the upper Animas.

The goal of the AMLI is to assist efforts by federal land management agencies and local stakeholders to plan and evaluate remediation efforts. Remediation with the goal of recovery of stream ecosystems requires an understanding of the mechanisms by which metals adversely affect stream biota. Zinc and copper can affect aquatic biota by a variety of mechanisms, including both acute (short-term) and chronic toxic effects of aqueous metals (USEPA 1985, 1987). Chronic toxicity can also result from exposure to metals in sediment (Kemble et al. 1994), and diet (Woodward et al. 1994). Establishing realistic thresholds for acute and chronic toxicity is

necessary to determine the extent of remediation required for improvement of aquatic communities.

The flow regime of the upper Animas watershed is typical of montane stream systems, with high runoff volumes in the spring and considerably lower discharge in winter. This annual pattern of stream discharge drives trace metal concentrations in the water column. Concentrations of dissolved zinc and copper in the upper Animas River follow a hysteritic pattern that complicates modeling, as solute concentrations at a particular discharge differ between the rising and falling limbs of the hydrograph. A hysteresis model such as that suggested by Aulenbach and Hooper (1994) can use seasonality to account for similar volumes of water that contain differing concentrations of dissolved metals.

We modeled the frequency of toxic concentrations of zinc and copper in the Animas River at USGS gaging stations upstream and downstream of two tributaries, Cement and Mineral Creeks, which drain highly-mineralized watersheds with many abandoned mines (Figure 1). The extensive record of discharge and dissolved metal concentrations at these sites has been used to develop reliable models of recurrence frequency, probability of exceedance, and duration of dissolved metal concentrations at these sites (Leib et al. 1998). Toxic concentrations of zinc and copper were determined in test waters with hardness and other ionic constituents similar to water in the upper Animas. Matching the ionic composition of test waters with site water is important for developing accurate estimates of toxicity thresholds, because metal toxicity can be strongly affected by site-specific water quality factors, such as pH, hardness, and other dissolved constituents (Diamond et al. 1997).

Figure 1. Location of USGS gaging stations on the upper Animas River near Silverton, CO.

METHODS

Modeling Dissolved Metal Concentrations

Water quality samples were in 1997-98 at two streamflow gages on the upper Animas River (Figure 1). Gage A68, Animas River at Silverton Colorado, is located upstream of the confluence of Cement Creek. Gage A72, Animas River Below Silverton Colorado, is located downstream from the confluences of both Cement and Mineral Creeks. Samples were collected monthly during low-flow and bi-weekly or weekly during spring runoff in order to characterize variation of trace metal concentrations throughout the annual hydrographs at the current level of remediation activity in the watershed.

Zinc and copper concentrations were estimated from this record using histeritic multiple linear regression models (Aulenbach and Hooper 1994). These models were based on discharge and date because a continuous record of each is available at the sampling sites. Although other variables might improve model predictions, a continuous record is needed for frequency analysis.

The frequency analysis used in this report is similar to that of traditional flood frequency analysis. Mean daily discharge records (1992-1993, 1995-1997) were grouped into annual data sets, each representing a seasonal cycle. Each year was distributed using a log Pearson type III technique, which helps to account for differences in water volumes during average, wet and dry

years (Interagency Advisory Commitee on Water Data 1992). Metal concentrations corresponding to these normalized discharge values were estimated using the hysterisis models. These results were averaged to estimate the daily probability that a given concentration of dissolved zinc or copper would be equaled or exceeded. Seasonality of dissolved zinc and copper was illustrated using averages of daily discharge records. This average hydrograph was converted to zinc and copper concentrations using the hysteresis models.

Toxicity Testing

The toxicity of copper and zinc to two sensitive laboratory test organisms was determined in a reconstituted water that simulated the water quality conditions in the Animas River. The reconstituted formula recommended by ASTM (1996) was modified to achieve a mixture of major ions representative of conditions in the Animas River (sulfate=100 g/L, chloride 10 mg/L, total hardness 114 mg/L, total alkalinity 16 mg/L, conductivity 255 umhos/cm). Exposure solutions containing zinc ($ZnSO_4.7H_2O$) and copper ($CuSO_4.5H_2O$) were prepared daily from stock solutions, with a series of exposure concentrations prepared by 50% serial dilutions. Metal concentrations in exposure solutions were verified by ICP-mass spectroscopy.

Toxicity tests were conducted with newly-hatched (<48 hour posthatch) fathead minnows, *Pimephales promelas*, and 7-14 day old amphipods, *Hyalella azteca,* following standard methods for testing of effuents and receiving waters (USEPA 1994). Groups of 10 minnows were tested in 500-mL test water in one-liter beakers, with two replicate beakers per concentration. Groups of 10 amphipods were tested in 250-mL test water in 300-mL beakers, with three replicate beakers per concentration. The number of surviving animals in each beaker was recorded after seven days. Median lethal concentrations for each species and each metal were determined by the moving average method (USEPA 1994).

Toxicity data derived from literature sources were used to evaluate sensitivity of several trout species to zinc and copper. Brook trout, *Salvelinus fontinalis*, have been introduced into the upper Animas watershed and are the the most widespread fish species in the watershed. Cutthroat trout, *Onchorhynchus clarki*, are native

Table 1. Median lethal concentrations (LC50) for copper and zinc to fathead minnows *(Pimephales promelas)* and amphipods (*Hyalella azteca*) in 7-day exposures in 'Animas' reconstituted water.

Species	7-d LC50, ug/L, and (95% confidence interval)	
	Zn	Cu
Amphipod	159 (125-200)	58 (48-76)
Fathead minnow	699 (550-890)	33 (25-45)

Table 2. Acute LC50s and chronic toxicity values (in parentheses) for copper and zinc toxicity to three species of trout. Values were calculated for moderately hard water (120 mg/L), based on from USEPA (1985, 1987), except (*) from Nehring and Goettl (1974).

Species	Acute and (Chronic) toxicity values, ug/L	
	Zn	Cu
Brook trout, *S. fontinalis*	4791 (855)	251 (17.4)
Cutthroat trout, *O. clarki*	1529 (--)	151 (--)
Rainbow trout, *O. mykiss*	1572 (603)	98 (11.4)

to the watershed and occur mainly in tributaries that are less affected by mining. The closely-related rainbow trout, *Onchorhynchus mykiss*, has been stocked in portions of the watershed, although it has not been found in recent surveys. Acute LC50s and thresholds for chronic toxicity of zinc and copper to brook trout and rainbow trout were obtained from water quality criteria documents (USEPA 1985, 1987). Acute LC50 values for cutthroat trout were obtained from Nehring and Goettl (1974). Acute toxicity values were adjusted for a water hardness typical of the Animas (120 mg/L as CaCO3) using exponential regression equations (USEPA 1985, 1987).

RESULTS AND DISCUSSION

Toxicity of Zinc and Copper

The toxicity of zinc and copper differed widely between the species tested (Table 1). Amphipods were about four times more sensitive to zinc than were fathead minnows. The relative sensitivity of the two species to copper was reversed, with fathead minnows more sensitive than amphipods. The responses of these species serve as useful benchmarks relative to toxicity thresholds for fish and benthic invertebrates that occur in the Animas watershed, or that may be restored to the watershed after remediation. Mortality of *H. azteca*, determined from seven-day exposures, is a more sensitive response to zinc than chronic toxicity to trout, determined from early life-stage or full life-cycle exposures (Table 2). The high sensitivity of amphipods to zinc is comparable to that of other sensitive taxa of invertebrates, which can be eliminated by even moderate metal pollution (USEPA 1987). The lethal concentration of zinc for fathead minnows in seven-day tests was similar to the chronic toxicity threshold for rainbow trout, which are highly sensitive to metal toxicity. Lethal concentrations of copper for fathead minnows were intermediate between acute and chronic toxicity values for all three trout species.

Frequency of Toxic Concentrations of Zinc and Copper

Hysteresis models based on discharge and season were developed for dissolved zinc at both A68 and A72 and for dissolved copper at A72. Coefficients of determination (r^2) indicated that these models accounted for 82% to 90% of the variation in dissolved metal concentrations. The model for copper at A68 was not used because of its low predictive ability ($r^2<0.4$). Predicted concentrations of dissolved zinc and copper at

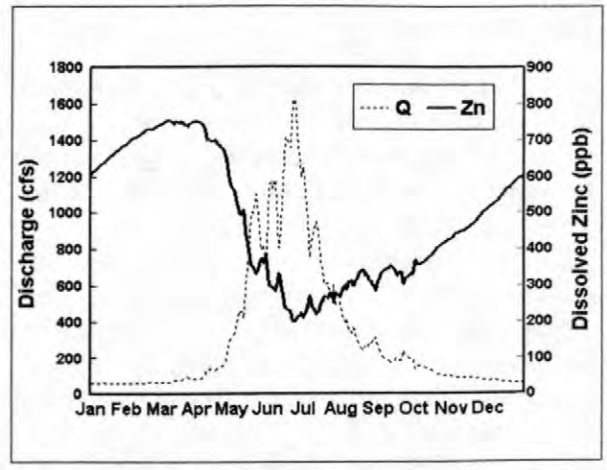

Figure 2. Relationship between stream discharge (Q) and dissolved zinc concentration at gage A72, below Silverton, CO.

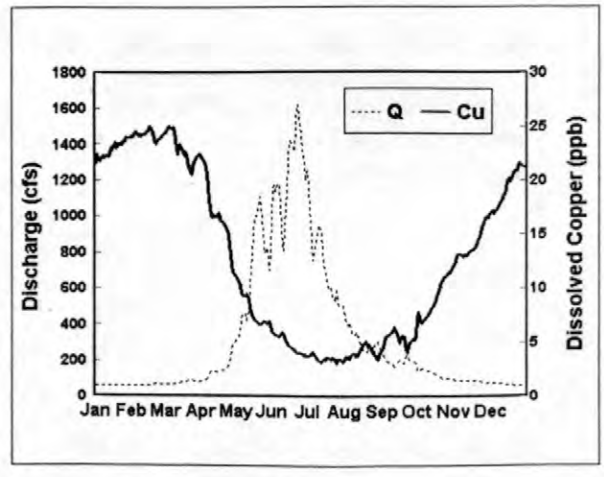

Figure 3. Relationship between stream discharge (Q) and dissolved copper concentration at gage A72, below Silverton, CO.

A72 are plotted vs. 1997 discharge in Figures 2 and 3. Although concentrations of dissolved zinc averaged nearly ten times greater than dissolved copper, concentrations of both metals followed similar patterns of variation with stream discharge and season. Concentrations increased gradually to maxima during the winter low-flow period (November-March). Lowest concentrations occurred during the peak snowmelt period in early summer, and low concentrations persisted during the low-flow period of late summer.

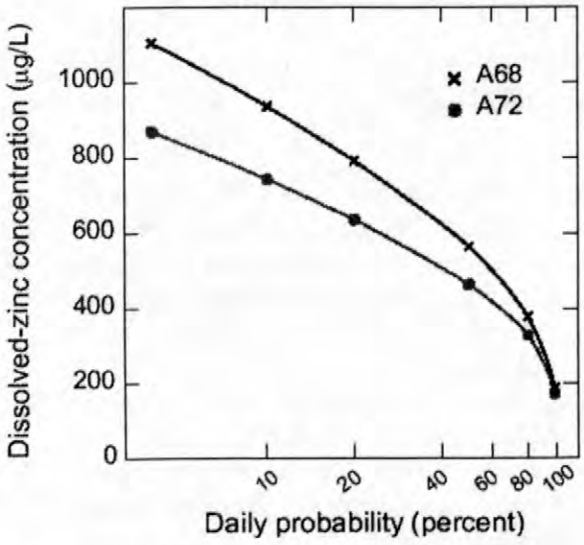

Figure 4. Daily probability of exceeding dissolved zinc concentrations at gaging stations above (A68) and below (A72) Silverton, CO.

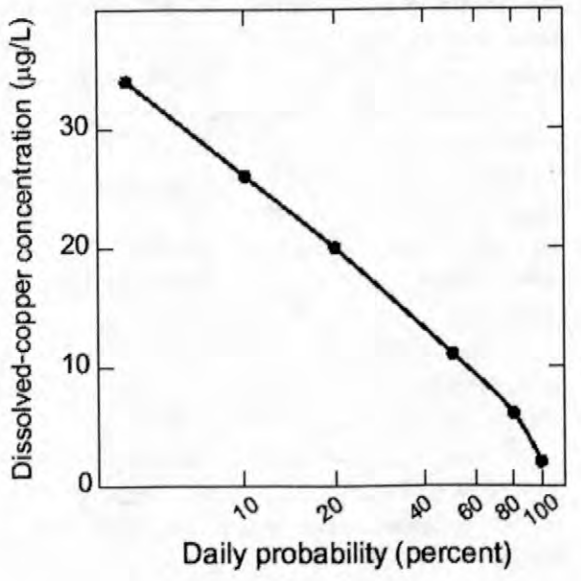

Figure 5. Daily probability of exceeding dissolved copper concentrations at gaging stations below Silverton, CO (A72)

Dissolved metal concentrations predicted over five water years were used to estimate the daily probability of exceeding toxic concentrations of dissolved zinc and copper (Figs. 4 and 5). Elevated concentrations of dissolved zinc represented a greater hazard of toxicity to amphipods and fathead minnows than did dissolved copper. Probabilities of exceeding zinc concentrations lethal to amphipods approached 100% at both A68 and A72 and probabilities of exceeding zinc concentrations toxic to the fathead minnows were approximately 40% at A68 and 15% at A72 (Fig. 4). In contrast, the probability of exceeding copper concentrations lethal to either species at A72 was close to zero (Fig. 5). Although no model of dissolved copper frequency was produced for A68, the risk of copper toxicity is even less at this site, which is located upstream of significant copper loadings from Cement and Mineral Creeks (Fig. 1).

Results of on-site toxicity tests conducted with the same two species in late summer of 1998 are consistent with modeled probabilities of toxicity. Mortality of amphipods approached 100% during 14-day exposures to stream water from A68, A72 and three other sites in the Animas watershed. Little or no mortality of fathead minnows was observed during 7-d exposures to water from either A68 or A72 (unpublished data; J. Besser). These results correspond closely to typical dissolved metal concentrations at A72 during late summer (Figs. 2 and 3)

Limits on Stream Biota of the Animas Watershed

Our results indicate that zinc toxicity is an important factor limiting biological communities in the Animas River near Silverton. High frequencies of dissolved zinc concentrations, which are toxic to invertebrates such as *H. azteca,* are consistent with observations of reduced abundance and low taxonomic diversity of invertebrates at the two study sites and elsewhere in the watershed. The occurrence of adult brook trout at A68 and in upstream reaches of the

Animas during the 1990s (unpublished data, Colorado Division of Wildlife) is also consistent with a low probability (about 10%) of zinc concentrations associated with chronic toxicity in this species. However, periods of chronic zinc toxicity during winter low-flow periods may explain the low densities and poor reproductive success of this population. The greater sensitivity of cutthroat trout to zinc (Table 1) is consistent with the distribution of this species, which occurs in less-contaminated tributaries, but is found only rarely at A68 or elsewhere in the Animas. Station A72 supported a depauperate biological community (no fish and few invertebrates) during the study period, although dissolved zinc concentrations were less at this site than at A68. This contrast suggests that factors in addition to dissolved zinc concentrations influence stream biotic communities in the study reach. Dissolved copper concentrations are greater at A72 than at A68, due to inputs from Cement and Mineral Creeks, and exceed chronic toxicity thresholds for trout for significant portions of the year (approx. 25% probability of exceeding the brook trout chronic level of 17 ug/L).

Trout may be absent from A72 and other reaches of the Animas due to mechanisms other than the direct lethality of zinc or copper that is represented by our models. Trout can detect and avoid sublethal concentrations of metals (Woodward et al. 1995). Trout may also avoid sites with very low densities of benthic invertebrates. Kiffney and Clements (1996) demonstrated that mixtures of metals (zinc, copper, and cadmium) at concentrations less than those typically occurring at A72 can result in substantial mortality of sensitive taxa and life stages of benthic invertebrates. This high sensitivity to toxic effects of metal mixtures can reflect additive or synergistic (greater than additive) toxicity of metals (Kraak et al. 1994). Additional impacts on benthic communities at A72 (and elsewhere in the watershed) can result from loadings of iron and aluminum colloids formed during neutralization of inputs from acidic tributaries. Precipitation of colloids downstream of Cement and Mineral Creeks contributes to degradation of benthic habitats at A72, due to embeddedness of stream gravels, and may also contribute to toxic effects on fish and invertebrates (Kimball et al., this document).

Our predictions of the toxicity of dissolved zinc and copper to aquatic biota are consistent with on-site toxicity evaluations and with observations of impacts on resident stream communities. We hope that this approach will prove to be useful for planning and evaluation of efforts to remediate abandoned minelands in the Animas watershed and elsewhere.

REFERENCES

ASTM (American Society for Testing and Materials), 1997, Standard guide for conducting acute toxicity tests with fishes, macro-invertebrates, and amphibians, E729-96: Annual Book of ASTM standards, v. 11.05, p. 220-240.

Aulenbach, B. T., and Hooper, R. P. 1994. Adjusting solute fluxes for climatic influences: Eos, Transactions, American Geophysical Union, v. 75 (no. 44, Suppl.), p. 233.

Church, S.E., Kimball, B.A., Fey, D.L., Ferderer, D.A., Yager, T.J., and Vaughn, R.B., 1997, Source, transport, and partitioning of metals between water, colloids, and bed sediments of the Animas River, Colorado: U.S. Geological Survey Open-File Report 97-151.

Diamond, J. M., Koplish, D. E., McMahon, J., and Rost, R., 1997, Evaluation of the water-effect ratio procedure for metals in a riverine system: Environmental Toxicology and Chemistry, v.16, p. 509-520.

Interagency Advisory Commitee on Water Data, 1992, Guidelines for determining flood flow frequency: Bulletin 17B of th hydrology commitee, USGS, Office of Water Data Coordination, Reston Virginia.

Kemble, N. E.; Brumbaugh, W. G.; Brunson, E. L.; Dwyer, F. J.; Ingersoll, C. G.; Monda, D. P., and Woodward, D. F., 1994, Toxicity of metal-contaminated sediment from the upper Clark Fork River, Montana, to aquatic invertebrates and fish in laboratory exposures: Environmental Toxicology and Chemistry, v. 13, p. 1985-1997.

Kiffney, P. M. and Clements, W.H., 1996, Size-dependent response of macroinvertebrates to metals in experimental streams: Environmental Toxicology and Chemistry. V.15, p. 1352-1356.

Kraak, M. H. S.; Lavy, D.; Schoon, H.; Toussaint, M.; Peeters, W. H. M., and van Straalen, N. M., 1994, Ecotoxicity of mixtures of metals to the zebra mussel *Dreissena polymorpha*: Environmental Toxicology and Chemistry, v. 13, p. 109-114.

Leib, K.J., Wright, W.G. and Mast, M.A., 1998, Using flood-analysis techniques to estimate dissolved zinc concentrations: Conference on tailings and mine waste.

Nimick, D.A., and von Guerard, P.. 1997, Science for Watershed Decisions on Abandoned Mine Lands: Review of Preliminary Results, Denver, Colorado, February 4-5, 1998: U.S. Geological Survey, Open-File Report 98-297.

Nehring, B.R., and Goettl, J.P., Jr., 1974, Acute toxicity of a zinc-polluted stream to four species of salmonids: Bull. Environ. Contam. Toxicol., v. 12, p. 464-469.

USEPA (U.S. Environmental Protection Agency), 1985, Ambient water quality criteria for copper – 1984: EPA 440/5-84-031, Washington, D.C.

------ 1987, Ambient water quality criteria for zinc – 1987: EPA 440/5-87-002, Washington, D.C.

------ 1994, Short-term methods for assessing the chronic toxicity of effluents and receiving wtaer to freshwater organisms: EPA-600-4-91-002. Washington, D.C.

Woodward, D. F.; Brumbaugh, W. G.; DeLonay, A. J.; Little, E. E., and Smith, C. E., 1994, Effects on rainbow trout fry of a metals-contaminated diet of benthic invertebrates from the Clark Fork River, Montana: Transactions of the American Fisheries Society, v. 123, p. 51-62.

-----, Hansen, J.A., Bergman, H.L., Little, E.E., DeLonay, A.J., 1995, Brown trout avoidance of metals in water characteristic of the Clark Fork River, Montana: Canadian Journal of Fisheries and Aquatic Sciences, v. 52, p. 2031-2037.

AUTHOR INFORMATION

John M. Besser, USGS-Biological Resource Division, Columbia Environmental Research Center, 4200 New Haven Road, Columbia, MO 65201 (john_besser@usgs.gov)

Kenneth J. Leib, USGS-Water Resources Division, P.O. Box 3367, Durango CO 81302 (kjleib@usgs.gov)

Overview of Rare Earth Element Investigations in Acid Waters of U. S. Geological Survey Abandoned Mine Lands Watersheds

By Philip L. Verplanck, D. Kirk Nordstrom, and Howard E. Taylor

ABSTRACT

The geochemistry of rare earth element (REE) variations in acid waters is being studied as part of the U. S. Geological Survey Abandoned Mine Lands Initiative in two pilot watersheds, upper Animas, Colorado and Boulder, Montana. The following objectives are under investigation: (1) comparison of acid mine waters and naturally acidic springs, (2) determination of whether the dominant control on REEs in acid waters is source-related or post-dissolution process-related, (3) determination of the role of iron and aluminum colloid formation on the REE patterns, (4) address the utility of REE geochemistry in acid waters as an analogue for the actinides, and (5) produce a Standard Reference Water Sample for REEs. Results demonstrate that the REE concentrations in acid waters increase with decreasing pH but tend to be two to three orders of magnitude lower than ore elements such as Cu and Zn. REE patterns are generally convex-up for waters in the upper Animas, and they are nearly flat with a negative europium anomalies for waters in the Boulder basin. These results reflect predominantly source-related signatures. Natural acid springs are frequently, but not consistently, characterized by a negative Ce anomaly that may be process-related. Field and laboratory experiments indicate that dissolved REEs are affected by iron and aluminum colloid formation but sorption or coprecipitation with aluminum at pH values greater than 4.5 is stronger than with iron. Uranium and thorium, however, show a tendency to be removed from solution more strongly at lower pH (3-4) values, consistent with expected differences in oxidation state and a stronger affinity for iron precipitation.

INTRODUCTION

Rare earth element (REE) geochemistry is a powerful tool for identifying geochemical processes (Brookins, 1989). This has been demonstrated in many petrologic studies but is just beginning to be applied to aqueous systems. REEs have been used as geochemical tracers because of their unique, coherent chemical behavior. The REEs are a suite of fourteen metals from atomic number 57 (La) to 71 (Lu) that have similar chemical and physical properties. There are, however, small differences in geochemical behavior because with increasing atomic number there is a systematic decrease in ionic radius. The REEs are trivalent with the exception of Ce (also 4+) and Eu (also 2+); therefore, the behavior of Ce and Eu relative to the other REEs can potentially be used as a probe of redox conditions of an environmental system (Loveland, 1989).

Elucidation of the geochemical behavior of REEs in a weathering environment has been hindered by the very low aqueous concentrations, which generally are less than one microgram per liter (μg/L) in surface and ground waters. With the advent of inductively coupled plasma-mass spectrometry (ICP-MS) the determination of REE concentrations in waters has become more routine. Concentrations of REEs are usually normalized to a reference standard, such as chondrite or North American Shale Composite (NASC), or to a sample of interest. By normalizing the REE concentrations, the characteristic zigzag pattern due to the increased stability of the even masses is eliminated, and

subtle variations in the REE pattern can be recognized.

Recent studies have demonstrated the use of REE geochemistry in the interpretation of water-rock interactions (Smedley, 1991; Fee and others, 1992; Johannesson and others, 1997). Relatively few studies have investigated the behavior of REEs in an acidic weathering environment (Auque and others, 1993, 1994; Johannesson and others, 1994; Johannesson and Lyons, 1995; Gimeno and others, 1996; Johannesson and others, 1996), and none of these studies have sampled mined areas. Previous investigations have revealed a general decrease in REE concentrations with pH increase, a characteristic convex-up NASC-normalized pattern, and no consistency with respect to Ce anomalies. Interpretations focus on whether these features are source-related (Smedley, 1991; Sholkovitz, 1995) or process-related (Sholkovitz, 1995; Johannesson and others, 1996; Byrne and Sholkovitz, 1996). One of the main interests has been the effect of iron and aluminum colloids on REEs in rivers, estuaries, and seawater, but there has been no direct study of the effect of colloid formation on REE fractionation between aqueous phase and colloidal phase.

As with most elements, the REE concentrations of stream waters may be controlled by water-rock processes along the subsurface flow path as well as the in-stream environment. These processes include dissolution and precipitation of minerals, oxidation and reduction reactions, and adsorption and desorption reactions with secondary minerals or colloidal particles. In most igneous rocks, the dominant rock type in the study areas, the REEs primarily occur within accessory phases, including apatite, zircon, monazite, allanite, titanite, and epidote. Release of the REEs from these minerals is complex owing to the occurrence of accessory phases as inclusions in major mineral phases. Also, some accessory phases are extremely resistant to weathering. Once released from the primary mineral phase, REEs may be sequestered by secondary mineral phases. Detailed mineralogical data including mineral occurrences, compositions, and morphology are needed to unravel this aspect of acidic weathering environments. This part of the study is in progress and will not be discussed in this overview.

The U. S. Geological Survey (USGS) Abandoned Mine Lands (AML) watersheds are well-suited to investigate the many processes that potentially control the REE geochemistry of acid waters because of the numerous acid water sources and the interdisciplinary approach to watershed characterization. REE geochemistry is being used to try to differentiate between natural and anthropogenic sources of acid waters and metals, as well as to determine processes controlling the fate and transport of metals entering the fluvial system.

This paper is an overview of our investigations into the REE geochemistry of the acidic weathering environment, including water-rock interaction and in-stream processes. Results from field and laboratory investigations are reported. In addition, two new Standard Reference Water Samples were produced to evaluate and control analytical measurements. Such a reference sample has not previously been available.

METHODS

Spring, stream and mine water samples were collected during low flow in the AML pilot watersheds, the upper Animas River basin, Colo. and the Boulder basin, Mont. Water temperature, pH, specific conductance, and Eh were determined on site. The Eh and pH were measured by placing electrodes in a flow-through-cell through which the sample was pumped with a portable peristaltic pump (Ball and others, 1976). The pH electrode was calibrated on site with pH buffers, 1.68, 4.01, 7.00, and 10.00, that bracketed the sample pH value and were equilibrated to the sample temperature. Water samples were filtered through a 142-millimeter (mm)-diameter, 0.1-micrometer (μm)-pore-size filter for major, minor, and trace element analyses. At the USGS Boulder, Colo. facility concentrations of REEs, Zn, U, and Th were determined by ICP-MS (Garbarino and Taylor, 1995) and concentrations of SO_4 were determined by ion chromatography.

At a subset of sampling sites, 2- to 4-liters of unfiltered, unacidified water were collected for

the iron oxidation experiments. These samples were stored at room temperature, and after 6 months, precipitates were concentrated and filtrates were collected using tangential-flow ultrafilters with a nominal cut-off of 10,000 molecular-weight. Filtrates were analyzed by ICP-MS for selected major and trace elements. Precipitates were digested following procedures outlined by Hayes (1993) and analyzed for major and trace elements by ICP-MS. Mineral identification was determined at Ohio State University with X-ray diffraction.

Two well-characterized, acid mine water samples were selected for new Standard Reference Water Samples. Sample PPREE1 is from the Paradise portal, upper Animas River basin, Colorado, and sample SCREE1 is from Spring Creek in the West Shasta mining district of northern California. Fifty liters of each sample were collected and filtration began within three hours of collection in a USGS mobile laboratory truck. Two parallel, 0.1-µm, acid-cleaned, all-plastic plate filters with 293-mm and 142-mm diameters were used, and filtrates were composited into a 50-L acid-washed carboy. Filtration was completed within 1 hour, and the pH of the reference waters was adjusted to less than 2 with concentrated HNO_3.

At the USGS laboratory in Boulder, Colorado, each reference water was split into 250-milliliter aliquots using a ten position, Teflon cone splitter. The aliquots were capped, sealed with parafilm, and numbered sequentially. Seventeen participating laboratories were sent two aliquots of each reference water with no laboratory receiving sequential numbers. Samples spanning the entire range of numbers were analyzed to allow for recognition of sampling biases.

RESULTS AND DISCUSSSION

Standard Reference Water Samples

Seventeen international laboratories, including four USGS facilities, participated in a "round-robin" analysis to determine the "most probable values" (MPVs) for the REEs (table 1). MPVs were determined using a robust statistical treatment that is insensitive to outliers (Peart and others, 1998).

Table 1. Most probable values (MPV) with median absolute deviation (MAD) for two Standard Reference Water Samples. All values in micrograms per liter.

	PPREE1		SCREE1	
Element	MPV	MAD	MPV	MAD
La	80.4	5.9	9.85	0.73
Ce	161.2	7.7	24.6	2.2
Pr	21.2	1.3	4.29	0.28
Nd	92.3	5.7	22.1	0.9
Sm	20.3	1.5	6.71	0.31
Eu	5.95	0.48	1.47	0.07
Gd	23.8	1.7	8.21	0.65
Tb	3.65	0.33	1.34	0.07
Dy	22.0	0.7	8.10	0.34
Ho	4.43	0.09	1.61	0.06
Er	11.9	0.4	4.35	0.21
Tm	1.48	0.05	0.582	0.023
Yb	8.20	0.13	3.39	0.17
Lu	1.12	0.03	0.452	0.014

In general, there was good agreement in the REE determinations among the participating laboratories. For PPREE1 and SCREE1, 87 and 83 percent, respectively, of the individual laboratories' results overlap the MPVs. The percent uncertainty for the individual REE concentrations varies from 2 to 9 percent. The REE reference waters are available upon request.

Identifying Source-Water Signatures

Within the upper Animas River watershed in Colorado numerous naturally-occurring acid springs and acid mine waters contribute metals to the streams. One goal of the AML initiative is to define the current baseline conditions in the watersheds and differentiate between natural and mining contributions of metals to the streams. A number of different techniques are being assessed to reach this goal, including identifing source-water signatures using REE geochemistry.

Two subbasins in the Animas basin with different geological characteristics, including bedrock composition and types of alteration and mineralization, were chosen to investigate techniques for identifying source-water signatures. Prospect Gulch (fig. 1) lies within the Silverton Caldera, and the bedrock consists

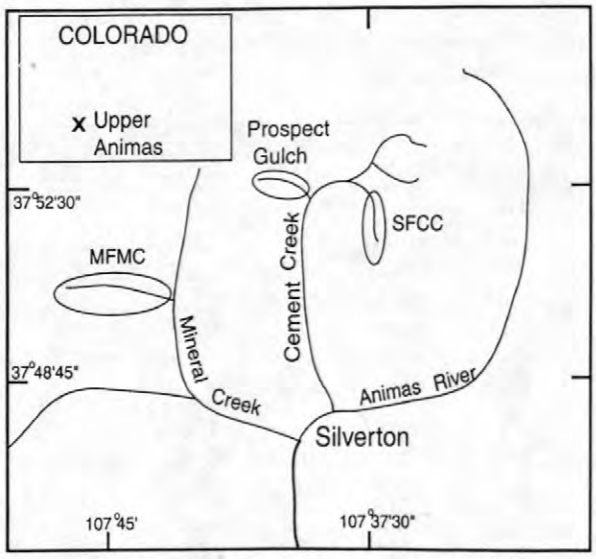

Figure 1. Map of upper Animas River basin. MFMC = Middle Fork Mineral Creek, SFCC = South Fork Cement Creek.

primarily of the Burns Formation, a volcanic unit of rhyodactitic flows and tuffs. Alteration ranges from propylitic in the southern part of the basin to quartz-sericite-pyrite and quartz-alunite in the northern part (Bove and others, 1998). The second subbasin, Middle Fork Mineral Creek (MFMC), is located west of the Silverton Caldera and is underlain by the San Juan Formation, thickly-bedded, reworked volcaniclastic deposits that have been intruded by quartz monzonite porphyries. The volcanic rocks surrounding the largest porphyry are altered to varying degrees from quartz-sericite pyrite to propylitic (Ringrose and others, 1986).

In Prospect Gulch, five mine waters (pH 2.4 to 3.6) and four springs (pH 3.3 to 5.7) were sampled during August and September 1997. The REE patterns (fig. 2) display a middle REE enrichment with a maximum at Eu or Gd. Overall, the springs and the mines have similar patterns with the exception of one spring sample, which has a negative Ce anomaly.

During September 1995 five mine waters (pH 3.1 to 5.7) and five springs (pH 3.1 to 6.8) were sampled in the MFMC. The REE patterns display a greater range in shape than the samples from Prospect Gulch. The mine waters have two types of patterns (fig. 3), two samples display a more sinusoidal pattern and three display a

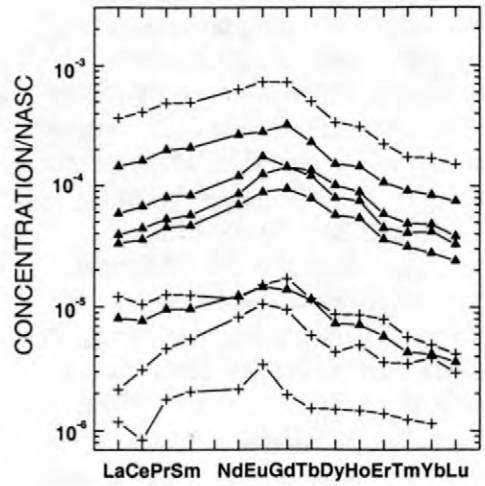

Figure 2. Rare earth element diagram of waters from Prospect Gulch. Concentrations normalized to NASC (Haskin and others, 1968; Gromet and others, 1984). Triangles-mine waters, crosses-natural springs.

middle REE enriched pattern. The two samples with the sinusoidal pattern are from draining adits on the north side of the basin, which is predominantly underlain by propylitically altered volcanic rocks, and the three middle REE

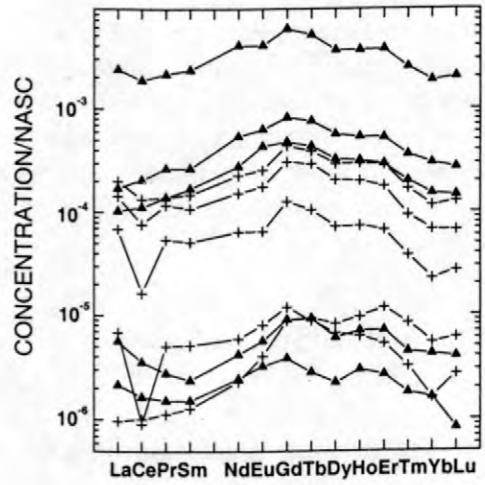

Figure 3. Rare earth element diagram of waters from Middle Fork Mineral Creek. Triangles-mine waters, crosses-natural springs.

enriched mine waters are from the south side of the basin, within or near the quartz monzonite porphyries. The REE patterns of the spring waters display middle REE enrichment with four of the five samples having negative Ce anomalies.

The presence of a negative Ce anomaly most likely reflects differing redox conditions in some of the spring environments as compared with the mine settings. Cerium anomalies have been observed in shallow groundwater samples from the Carnmenellis district, England and are believed to be a result of the oxidation of Ce (III) to insoluble Ce (IV), with subsequent removal (Smedley, 1991). The loss of Ce relative to its neighboring REEs, La and Pr, produces a negative Ce anomaly in the REE patterns. Because Ce anomalies were only observed in some of the spring samples, Ce anomalies may not prove to be a usable source signature. Determinations of whole rock REE compositions of the major geologic units within the subbasins are underway. Preliminary data indicate that the REE patterns of the waters, with the exception of the negative Ce anomaly, reflect the REE compositions of the lithologies along the flow paths.

In the Boulder watershed (Montana) acid mine waters from Crystal Mine and Bullion Mine were analyzed to compare the REE patterns of the Animas water samples with waters derived from different geologic terrains. The two mines occur along a mineralized structure within the Butte Quartz Monzonite of the Boulder batholith (Ruppel, 1963). The REE patterns (fig. 4) are nearly flat with negative Eu anomalies. The host monzonite is characterized by a relatively flat REE pattern with a negative Eu anomaly (Lambe, 1981).

Because the REE patterns of the acid waters seem to reflect the REE patterns of the host rocks, a contrast in the REE composition of the host rock is needed to enable use the REE patterns of acid waters as a source signature. In the Animas basin studies, the mineralization does not appear to significantly affect the REE concentration of the acid waters, such that comparing the REE concentrations to other metals enriched in the mineralized zones may distinguish mine waters from natural springs. In the suite of samples from MFMC and Prospect Gulch, for a given La

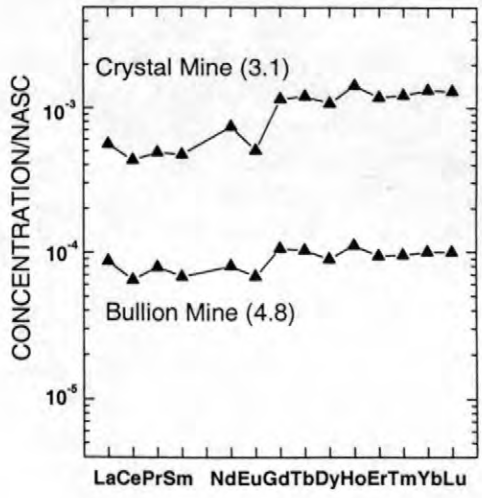

Figure 4. Rare earth element diagram of two mine waters, Boulder basin, Mont. Value of pH in parentheses. Crystal Mine sampled at adit, Bullion Mine sampled in creek below dump pile.

concentration, the mine waters have distinctly higher Zn concentrations compared to background spring samples (fig. 5). Other elements that are not enriched in the mineralized areas may act similarly to La. This observation may prove useful for differentiating between mining and natural sources in areas where the origin (natural or mining-influenced) of acid seeps is uncertain.

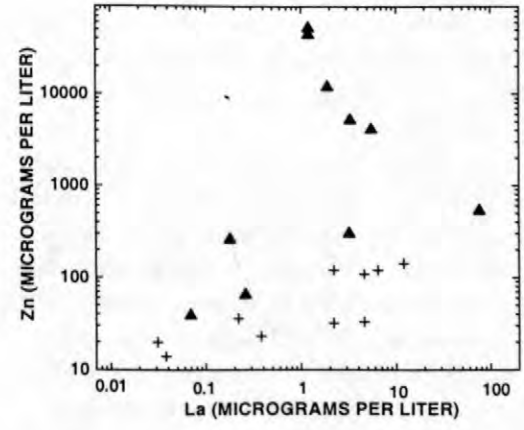

Figure 5. Relation of dissolved La to Zn for mine (triangles) and spring (crosses) waters in Prospect Gulch and Middle Fork Mineral Creek.

In-Stream Processes

The fate and transport of REEs entering the stream environment were investigated using field and laboratory studies. A 2-km stream reach of the South Fork Cement Creek (SFCC), Colo. was sampled during low flow in October 1996. Downstream the pH decreases from 7.1 to 5.1, and loading of REEs and major and trace elements increase due to the addition of acid mine drainage and acid springs. Comparing the measured load at the lowermost sampling site to the sum of the input loads accounts for 77 to 93 percent of the REEs. In contrast, measured loads of Ca, Sr, SO_4, Zn, and Co averaged 117 ± 3 percent of the summed input loads. Values less than 100 percent suggest that REEs are probably being removed in this acidic, alpine stream. Loss of REEs may be related to iron and aluminum colloids that are actively precipitating in the stream channel.

To investigate fate and transport of REEs in a stream reach where pH increases, a suite of samples was collected from Uncle Sam Gulch in the Boulder watershed, Mont. during July 1997. In contrast to SFCC where a number of acid water sources contribute metals to the creek, Uncle Sam Gulch has only one dominant acid water source. Acid mine water from the Crystal Mine (pH=3.1) enters the stream, lowering the pH from 7.2 to 3.6. Within 2 km, the stream pH increases to 6.9, apparently due to dilution or neutralization by circumneutral waters. The streambed is coated with iron precipitates throughout this reach. Upstream of the lower most sampling site, the iron stained stream bed is a lighter color than below the mine site, suggesting that aluminum is precipitating as well.

The total REE concentrations of the stream water along this reach decrease from 31.2 µg/L to 0.5 µg/L. To evaluate if the reduction in the REE concentrations is due to REE removal or due to dilution, we compare the REE variation with a conservative solute, SO_4. Downstream from the mine, the $\Sigma REE/SO_4$ ratio remains relatively constant until the pH of the stream is above a value of 4.3 (fig. 6) indicating that the REEs behave conservatively through this pH range. Compared to SO_4, the REEs are removed from solution before the next sample site, which has a pH value of 6.9. A similar pattern is

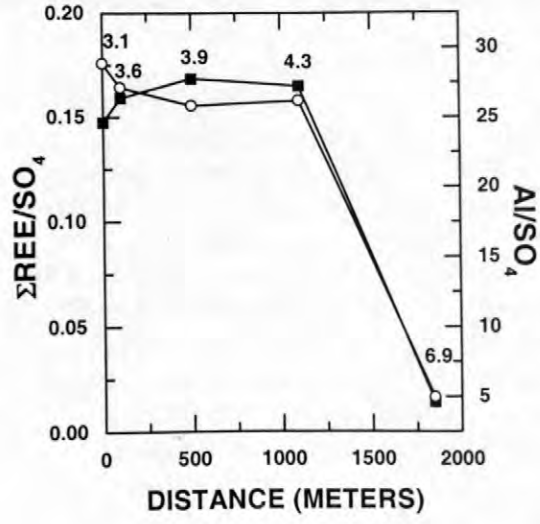

Figure 6. Dissolved $\Sigma REE/SO_4$ (squares) and Al/SO_4 (circles) for stream water samples, Uncle Sam Gulch, Mont. Distance downstream from Crystal Mine adit. Numbers above symbol = pH value of sample.

observed with Al, suggesting that the REEs may have coprecipitated or adsorbed onto aluminum colloids. With this limited data set, we are not able to differentiate between the relative importance of the increase in pH on the extent of adsorption and the role colloid composition plays on the removal of REEs and other metals.

During the August 1998, a tracer experiment was carried out in Uncle Sam Gulch. A subset of samples are being analyzed for REEs and trace metals to better determine the roles of colloid formation and pH variation on the attenuation of REEs and other metals and to quantify the mass transfer from solution to colloid during transport.

REE Partitioning during Laboratory Iron Oxidation Experiment

A laboratory experiment was undertaken to study the partitioning of the REEs between iron colloids and aqueous solutions. These laboratory results will provide a geochemical framework for interpreting field data on fate and transport of REEs and other metals in acidic streams. Unfiltered, unacidified mine water samples were

collected, and the Fe (II) allowed to oxidize at room temperature for six months. The set of waters had initial pH values ranging from 1.7 to 6.2, specific conductance from 775 to 17,000 microsiemens per centimeter, dissolved Fe concentrations from 50 to 675,000 µg/L, and La concentrations from 1 to 210 µg/L. The dissolved iron oxidized and precipitated during the 6-month interval, and at the conclusion, water and precipitates were separated and analyzed for major and trace elements.

The precipitates are enriched in REEs relative to their respective waters, with the enrichment strongly dependent on pH (fig. 7). The REE patterns of the filtrates and precipitates are convex-up with enrichment in the middle REEs relative to the light and heavy REEs. For a given sample, the filtrates and their original waters have similar REE patterns and concentrations because less than 5 percent of the REEs were removed from solution during the experiment. These results indicate that during iron colloid formation, the REEs may be removed from solution without altering the REE pattern of the solution and at pH values less than approximately 4.5, most of the REEs stay in solution.

REEs as Chemical Analogues for Actinides

Rare earth elements have been used as chemical analogues for actinides in a number of biological and geological studies because of their similarity to the actinides in ionic charge and ionic radius (Weimer and others, 1980). We have investigated the role of water composition and colloids in the attenuation of U, Th, and REEs in an acidic weathering environment, and the extent to which the natural analogue concept is appropriate. Within the upper Animas River basin, naturally-occurring acid springs (pH 2.7-6.8) and acid mine drainage (pH 2.3-6.4) dissolve minerals in the country rock, releasing U, Th, and REEs, which are predominantly derived from apatite, monazite, and epidote. Upon entering the stream system, concentrations of trace elements can be attenuated by adsorption to colloids or

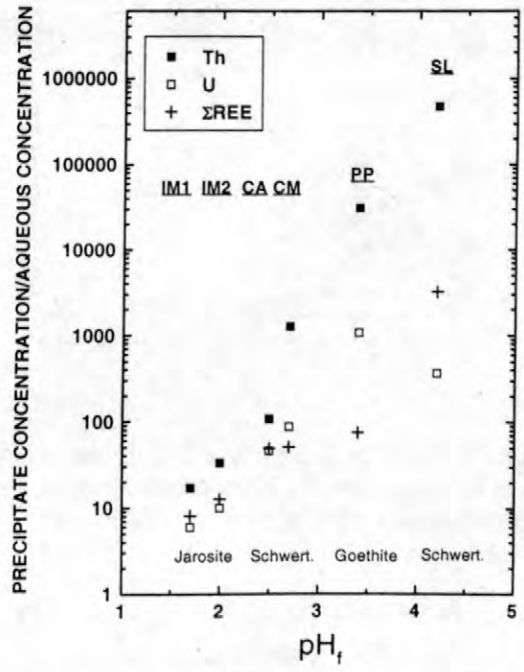

Figure 7. Relation of solid phase enrichment to pH. Concentration in precipitate (µg/g) relative to aqueous phase (µg/g) from iron oxidation experiments. Sample designation: IM1 - Iron Mountain site, Calif. (pH_i = 1.6, pH_f = 1.7), IM2 - Iron Mountain site, Calif. (pH_i = unknown, pH_f = 2.0), CA - Chandler adit, Colo. (pH_i = 2.6, pH_f = 2.5), CM - Crystal Mine, Mont. (pH_i = 3.1, pH_f = 2.7), PP - Paradise portal, Colo. (pH_i = 5.3, pH_f = 3.4), and SL - Silver Ledge Mine, Colo. (pH_i = 6.1, pH_f = 4.2). pH_i = pH initial, pH_f = pH final. Dominant mineral phase of precipitate shown below sample. Schwert. = schwertmannite.

coprecipitating. Laboratory iron oxidation experiments on mine waters, described above, were run to determine the partitioning of the U, Th, and REEs over a range of pH conditions.

In the Animas water samples U, Th, and the REE concentrations are inversely correlated with pH (fig. 8); however, the slopes are strikingly different. The ΣREE show a gradual decrease in concentrations with increasing pH, where as U and Th concentrations have large decreases between pH 3 and 4, then remain relatively low and constant above a pH of 4. Results from the laboratory experiments show that the precipitates become increasingly enriched in U, Th, and REEs compared to the aqueous phase with increasing

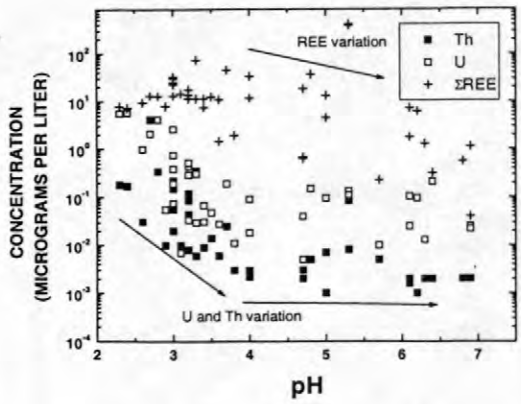

Figure 8. Relation of dissolved U, Th, and ΣREE vs. pH for upper Animas River basin samples, including natural springs, mine effluents, and stream waters.

pH (fig. 7). With the exception of the $pH_i = 5.3$ sample that was predominately goethite, compositions of the solid phases vary from dominantly jarosite in the low-pH samples to dominantly schwertmannite in the high-pH samples. Aluminum-rich phases were not observed in any of the precipitates.

The field and laboratory results suggest that U and Th are primarily adsorbed by hydrated ferric oxides at pH values of 3 to 4. In contrast, REEs tend to remain dissolved until higher pH values are reached, in a manner similar to Al. Aluminum remains in solution until the pH reaches about 5, then hydrolyzes and precipitates as a hydroxysulfate mineral (Nordstrom and Ball, 1986). REEs will likely coprecipitate or adsorb with aluminum-rich solids.

CONCLUSIONS

The AML pilot watersheds are well-suited for investigating the REE geochemistry of acid waters because of the numerous acid water sources and the interdisciplinary approach to watershed characterization. Using REE patterns as a tool to identify source signatures of acid waters is valuable when the REE patterns of the lithologies along the flow path have different REE patterns. To differentiate between natural springs and mine waters using only the REE patterns, either the mineral deposits must have a REE signature distinct from the surrounding lithologies, or secondary processes in the mining or spring environment must lead to REE fractionations. Within the subbasins of the upper Animas watershed, using REE patterns to differentiate between acid springs and mine waters may not be conclusive. Although many acid springs have REE patterns with negative Ce anomalies and the mine waters do not, not all the springs sampled have such patterns.

Within the Animas River basin, the mine environment does not appear to enrich the acid drainage in REEs; thus, comparing the REE concentrations to other metals enriched in the mine waters, such as Zn, may provide a means to discriminate between mining and natural acid water sources. This differential enrichment should provide a useful tool, in conjunction with other geochemical indicators, for determining if seeps in areas impacted by mining are natural or mining-related.

Formation of Fe and Al colloids plays a role in the attenuation of REEs and other metals in streams that receive acid waters. Field and laboratory experiments demonstrate that REEs are removed from solution at pH values greater than 4.5 and that only minor fractionations occur.

ACKNOWLEDGEMENTS

The work by Philip Verplanck was funded by the National Research Council's post-doctoral research program and the USGS AML initiative. B. McCleskey, T. Brinton, D. Roth, and R. Antweiler provided analytical support. Numerous scientists working in the two watersheds provided the framework for this study. Reviews by J. Ball and A. Mast greatly improved the manuscript.

REFERENCES

Auque, L.F., Tena, J.M., Gimeno, M.J., Mandado, Juan, Zamura, Alfredo, and Lopez, P.L., 1993, Distribucion de tierras raras en soluciones y coloides de un sistema natural de acidas (Arroyo Del Val, Zaragoza): Estudios Geologicos, v. 49, no. 1-2, p. 179-188.

———, Tena, J.M., Gimeno, M.J., Lopez, P.L., and Zamura, Alfredo, 1994, Especion de

tierras raras en las soluciones acidas y neutras del sistema de drenaje del Arroyo Del Val, Zaragoza: Estudios Geologicos, v. 50, no. 3-4, p. 179-188.

Ball, J.W., Jenne, E.A., and Burchard, J.M., 1976, Sampling and preservation techniques for waters in geysers and hot springs, *with a section* on gas collection by A.H. Truesdell, *in* Proceedings from Workshop on Sampling Geothermal Effluents, 1st: Environmental Protection Agency 600/9-76-011, p. 218-234.

Bove, D.J., Wright, W.G., Mast, M.A., and Yager, D.B., 1998, Natural contributions of acidity and metals to surface waters of the upper Animas River watershed, Colorado, *in* Nimick, D.A., and von Guerard, Paul, eds., Science for watershed decisions on abandoned mine lands, Denver, Colorado, February 4-5, 1998: U. S. Geological Survey Open-File Report 98-297, p. 37.

Brookins, D.G., 1989, Aqueous geochemistry of rare earth elements, *in* Lipin, B.R. and McKay, G.A., eds., Geochemistry and mineralogy of rare earth elements: Washington, D.C., Mineralogical Society of America, p. 201-225.

Byrne, R.H., and Sholkovitz, E.R., 1996, Marine chemistry of the lanthanides, *in* Gschneidner, K.A., Jr. and Eyring, L.R., eds., Handbook on the Physics and Chemistry of Rare Earths, v. 23: Amsterdam, North-Holland, p. 497-593.

Fee, J.A., Gaudette, H.E., Lyons, W.B., and Long, D.T., 1992, Rare-earth element distribution in Lake Tyrrell groundwaters, Victoria, Australia: Chemical Geology, v. 96, no. 1-2, p. 67-93.

Garbarino, J.R., and Taylor, H.E., 1995, Inductively coupled plasma-mass spectrometric methods for the determination of dissolved trace elements in natural waters: U. S. Geological Survey Open-File Report 94-358, 88 p.

Gimeno, M.J., Auque, L.F., Lopez, P.L., Gomez, J., and Mandado, Juan, 1996, Pautas de distribucion de especies de las tierras raras en las soluciones acidas naturales: Estudios Geologicos, v. 52, no. 1, p. 11-22.

Gromet, L.P., Dymek, R.F., Haskin, L.A., and Korotev, R. L., 1984, The "North American shale composite"; its compilation, major and trace element characteristics: Geochimica et Cosmochimica Acta, v. 48, p. 2469-2482.

Haskin, L.A., Haskin, M.A., Frey, F.A., and Wildman, T.R., 1968, Relative and absolute terrestrial abundances of the rare earths. *in* Ahrens L.H., ed., Origin and distribution of the elements: New York, Pergamon, p. 889-912.

———, and Paster, T.P., 1979, Geochemistry and mineralogy of the rare earths, *in* Gschneidner, K. A., Jr. and Eyring, L. R. eds., Handbook on the Physics and Chemistry of Rare Earths, v. 3: Amsterdam, North-Holland, p. 1-80.

Hayes, H.C., 1993, Metal associations in suspended sediments and bed sediments from the Mississippi River: Golden, Colorado School of Mines, Department of Chemistry and Geochemistry, Master of Science thesis, 131 p.

Johannesson, K.H., Lyons, W.B., Fee, J.H., Gaudette, H.E., and McArthur, J.M., 1994, Geochemical processes affecting the acidic groundwaters of Lake Gilmore, Yilgarn Block, Western Australia; a preliminary study using neodymium, samarium, and dysprosium: Journal of Hydrology, v. 154, no. 1, p. 271-289.

———, and Lyons, W.B., 1995, Rare-earth element geochemistry of Colour Lake, an acidic freshwater lake on Axel Heiberg Island, Northwest Territories, Canada: Chemical Geology, v. 119, no. 1-4, p. 209-223.

———, Lyons, W.B., Yelken, M.A., Gaudette, H.E., and Stetzenbach, K.J., 1996, Geochemical of rare earth elements in hypersaline and dilute acidic waters: Complexation behavior and middle rare-earth enrichments: Chemical Geology, v. 133, no. 1-4, p. 125-144.

———, Stetzenbach, K.J., and Hodge, V.F., 1997, Rare earth elements as geochemical tracers of regional groundwater mixing: Geochimica et Cosmochimica Acta, v. 61, no. 17, p. 3605-3618.

Lambe, R.N., 1981, Crystallization and petrogenesis of the southern portion of the Boulder batholith, Montana: Berkeley, University of California, Ph.D. Thesis, 171 p.

Loveland, Walter, 1989, Environmental sciences, *in* Bunzli, J.-C.G. and Choppin, G.R., eds., Lanthanide Probes in Life, Chemical, and Earth Sciences: New York, Elsevier, p. 391-411.

Nordstrom, D.K., and Ball, J,W., 1986, The geochemical behavior of aluminum in acidified surface waters: Science, v. 232, p. 54-56.

Peart, D.B., Antweiller, R. C., Taylor, H.E., Roth, D.A., and Brinton, T.I., 1998, Re-evaluation and extension of the scope of elements in the U. S. Geological Survey Standard Reference Water Samples: Analyst, v. 123, p. 455-476.

Ringrose, C.R., Harmon, R.S., Jackson, S.E., and Rice, C.M., 1986, Stable isotope geochemistry of a porphyry-style hydrothermal system, West Silverton District, San Juan Mountains, Colorado: Applied Geochemistry, v. 1, no. 3, p. 357-373.

Ruppel, E.T., 1963, Geology of the Basin quadrangle, Montana: U. S. Geological Survey Bulletin 1151, 121 p.

Sholkovitz, E.R., 1995, The aquatic chemistry of rare earth elements in rivers and estuaries: Aquatic Geochemistry, v. 1, no. 1, p. 1-34.

Smedley, P.L., 1991, The geochemistry of rare earth elements in groundwater from the Carnmenellis area, southwest England: Geochimica et Cosmochimica Acta, v. 55, p. 2767-2779.

Weimer, W.C., Laul, J.C., and Kutt, J.C., 1980, Prediction of the ultimate biological availability of transuranium elements in the environment, *in* Baker R.A., ed., Contaminants and Sediments: Ann Arbor, Ann Arbor Science Publisher, p. 465-484.

AUTHOR INFORMATION

Philip L. Verplanck, D. Kirk Nordstrom, and Howard E. Taylor, U.S. Geological Survey, Boulder, Colorado

Development of a Passive Integrative Sampler for Labile Metals in Water

By William G. Brumbaugh, Jimmie D. Petty, James N. Huckins, and Stanley E. Manahan

ABSTRACT

A Stabilized Liquid Membrane Device (SLMD) is described for potential use as an in-situ passive integrative sampler for Cd, Cu, Ni, Pb, and Zn in natural waters. The SLMD (patent pending) consists of a 15 cm long strip of low-density polyethylene (LDPE) layflat tubing containing 1 mL of an equal mixture (v/v) of oleic acid (cis-9-octadecenoic acid) and Kelex-100® (7-[4-ethyl-1-methyloctyl]-8-quinolinol]). The reagent mixture diffuses in a controlled manner to the exterior surface of the LDPE membrane, which results in a relatively constant sequestration rate of several divalent metals for at least four weeks. Concentration factors of several thousand can be realized after just a few days allowing for extraction and quantitation of extremely low levels of these metals by common spectroscopic methods. Data is presented for field deployment of SLMDs at two sites impacted by hard rock mining. Effects of pH and flow-rate on the SLMD sampling rate is discussed.

INTRODUCTION

It has long been recognized in industrial hygiene that the integrated dose is the most important consideration when determining potential chronic hazards to those individuals exposed to a toxicant. Likewise, in the aquatic environment the ability to measure a toxicant dose over an extended period of time can be more meaningful than periodic grab samples which only provide brief "snapshots" of the long-term dose. The U.S. Environmental Protection Agency (USEPA) regulations for discharge wastes presently include limits for one-day maximum and 30-day average concentrations for various pollutants (U. S. Code of Federal Regulations, 1985). Thus, a sampler capable of providing a time-integrated measure of a water contaminant would be very useful for resource managers and regulatory agencies.

An integrated sampling approach has recently been developed for organic contaminants in aquatic ecosystems with the advent of the semipermeable membrane device or SPMD (Huckins and others, 1993; Petty and others, 1995). A similar sampling device suitable for toxic trace elements would also be useful, however, the considerations for passive sampling of trace metals are more complex than for organic contaminants because most dissolved metals and metalloids may simultaneously exist in any one of several ionic, complex-ion, and organically-bound states (Stumm and Morgan, 1981). For most toxic metals, bioavailability and potential toxicity to aquatic organisms is generally thought to be greatest when the metal is in the ionic or "free" dissolved state (Luoma, 1983). However, other labile forms of metals, e.g., those weakly complexed with suspended or dissolved organic matter, or those present as fine colloids may also be somewhat bioavailable to aquatic organisms (Erickson and others, 1996). Therefore, an in-situ passive sampler capable of sequestering only labile forms of aqueous metals would be highly desirable for meaningful environmental hazard assessment. Although passive sampling for trace metals has been briefly investigated by a few researchers (Benes and Steinnes, 1974; Borg and Andersson, 1984; Morrison, 1987; Zhang and

Davison, 1995; Zhang and others, 1995) long-term (days to weeks) integrative sampling for low concentrations of labile metals in water has yet to be demonstrated. For long-term sampling, analyte uptake may become unpredictable due to saturation, fouling, degradation, or other difficulties. In this paper, a passive integrative sampler based on a Stabilized Liquid Membrane Device (SLMD) is described that is suitable for long-term, low-level monitoring of labile forms of selected toxic trace metals.

MATERIALS AND METHODS

The SLMD (patent pending) consists of a heat-sealed 15-cm long strip of low-density polyethylene (LDPE) layflat tubing containing 1 mL of an equal mixture of oleic acid (cis-9-octadecenoic acid) and Kelex-100® (7-[4-ethyl-1-methyloctyl]-8-quinolinol]). Each sampler was fabricated with a small loop on one end of the LDPE tubing for attachment of a tether cord. Prepared SLMDs were stored in zip-lock LDPE bags containing high-purity water. Laboratory exposure experiments were conducted with on-site well water in 2-L glass Mason jars equipped with Teflon-coated lids. Field-deployed samplers were tethered with 10-cm nylon cords attached to bricks placed on the stream bottom in pools about 1 m deep. Some SLMDs were inserted into cellulose dialysis tubing (1,000 MWCO) that was pre-filled with high-purity water. Filtered (0.4 μm pore-size polycarbonate membrane) and unfiltered grab water samples (100 mL) were collected periodically during field deployments. Water samples were acidified to 1% (v/v) HNO3. Exposed SLMDs were rinsed with high-purity water and stored individually in polyethylene bottles. At the laboratory, SLMDs were extracted twice with 20% nitric acid and diluted to a final volume of 100 mL. Analysis of the SLMD extracts and water samples was by inductively coupled plasma-mass spectrometry (ICP-MS).

RESULTS AND DISCUSSION

The basis for sampling by the SLMD is the controlled release of water-insoluble liquid complexing reagent mixture and the formation of stabilized metal complexes on the outer membrane surface. Continual formation of highly insoluble metal-oleates (primarily calcium and magnesium) on the surface of the membrane results in a wax-like, hydrophobic media in which the primary chelating agent (alkylated 8-quinolinol) is highly mobile. In general, the stability constants for oleates of Ca and Mg are several orders of magnitude greater than for the target metals while the reverse is true for stability constants with the alkylated 8-quinolinol. The sequestration process is depicted in Figure 1.

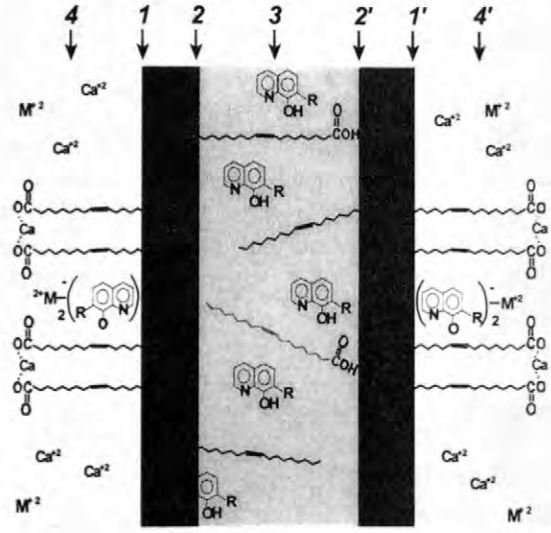

Figure 1. Conceptualized diagram of metal ion sequestration by SLMD. 1 and 1' are outer surfaces of polymeric membrane. 2 and 2' are inner surfaces of membrane. 3 is the hydrophobic reagent mixture sealed inside the membrane. 4 and 4' are the aqueous sampling media. R = alkyl group with 8 to 12 carbons, Ca^{+2} = calcium ion, M^{+2} = metal ion.

Movement of the liquid reagents (based on extraction and gravimetric measure) from the inside to the outside of the membrane and the stability of reagent on the surface (no overall loss of reagent) is illustrated in Figure 2 for freshwater pond exposures up to 56 days. Also illustrated in this figure is a linear uptake of calcium by the SLMD over this time interval. In Figure 3, it is shown that sequestration of metal ions from water was constant for the SLMD for at least 28 days in laboratory static-renewal exposures (2-L exposure water containing 20 ppb each of 5 metals renewed

twice weekly). Typical water concentrations for a 28-d static (non-renewed) exposure are also shown.

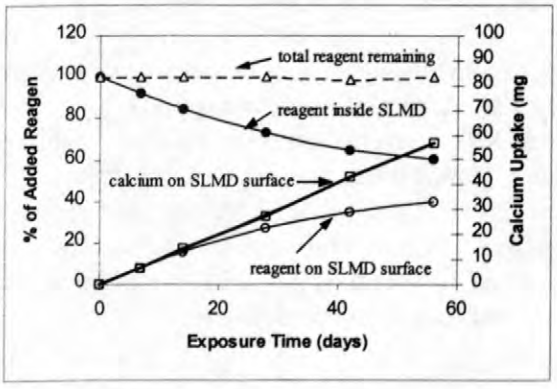

Figure 2. Movement of SLMD reagent mixture from interior to membrane surface and uptake of calcium over a 56-d pond exposure.

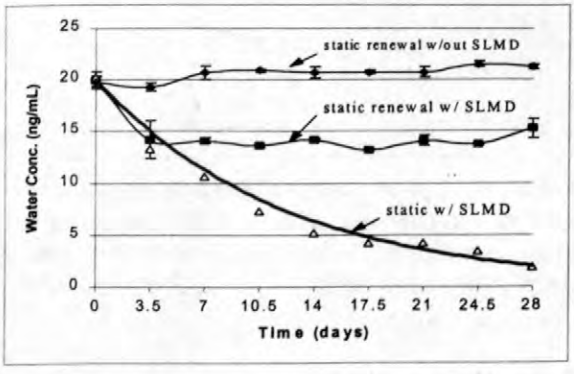

Figure 3. Typical concentration of metal ion in water as a function of time for 28-d static and static-renewal (every 3.5 d) exposures with SLMD (2-L volume; data for nickel shown).

For any passive sampler to be useful beyond screening applications, a predictable sampling rate, i.e., the volume from which the analyte is completely recovered per unit time (liter-equivalents/day) is necessary for back-calculation of the average water concentration. Ideally, the sampling rate for the SLMD sampler should be independent of water characteristics such as pH, ionic strength, temperature, and flow-rate. In addition, sampling rates observed for metal complexes might be dependent on the lability of the metal complex and if so, the SLMD could be very useful in defining the bioavailability of metals when employed as a complementary sampler. Experiments are currently under way to evaluate the sampling rates for various metal complexes.

The effects of pH on the sequestration of Cu, Cd, Ni, Pb, and Zn by the SLMD reagent mixture are depicted in Figure 4. These results indicate that sampling for Cu and Ni will be highly effective over a wide pH range whereas the sampling for Pb, Zn, and in particular Cd, may be limited in unusually acidic waters.

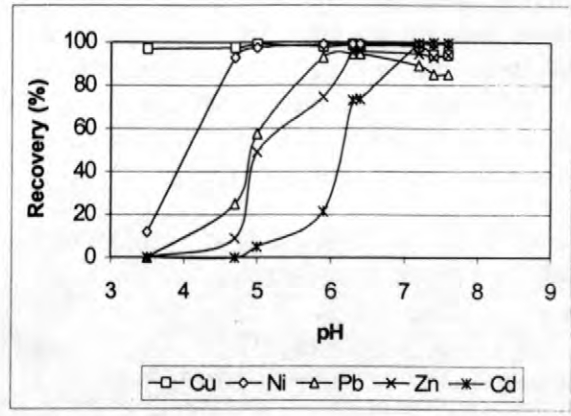

Figure 4. Recovery of metals from water by liquid-liquid extraction with SLMD mixed reagent as a function of pH.

If the transport of analytes to the sampler is dependent on solution flow and mixing, the sampling rate will be difficult to model. The effect of hydrodynamics on the sampling rate is illustrated in Figure 5 in which the metal uptake (removal) rate for a rapidly mixed water is shown.

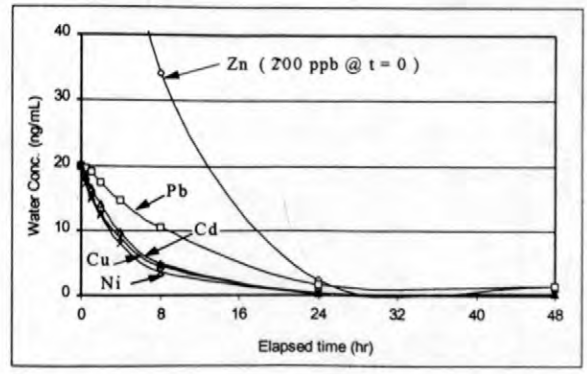

Figure 5. Concentration of metal ions in mixed water containing SLMD as a function of time. (2-L lume, pH 7.6, hard water; zinc = 200 ppb, all others = 20 ppb at time zero).

The stirred-water sampling rate is much greater than for the static exposure (Figure 3). Note that the sampling rate is independent of concentration, i.e., the time to sample >95% of the analyte is the same for Zn at 200 ppb as it is for Cu and Ni at 20 ppb. The SLMD sampling rates for these 5 metals (based on extrapolation of the initial linear portion of each static and stirred-water curve) is summarized in Table 1. This range of sampling rates reflects potential extremes for sampling from quiescent versus fast-flowing waters. In quiescent waters, the sampling rate may be limited by the diffusion rate of analyte ions at the membrane/water boundary whereas in moving waters the metal/reagent reaction kinetics probably controls the sampling rate.

Table 1. Sampling rates (L-eq/d) for SLMD in static and stirred water (pH=7.6, T=20°C).

Water	Cu	Ni	Zn	Cd	Pb
Static	0.15	0.15	0.15	0.15	0.15
Stirred	10.8	10.8	10.8	6.2	3.0

For flowing waters, high SLMD sampling rates can result in large pre-concentration factors ($[metal]_{SLMD}/[metal]_{water}$) that could be very useful for screening applications. This is illustrated in Figure 6 where absolute concentration factors of up to 35,000 were measured for Pb after 4-day SLMD field exposures at five sites on the Coeur d'Alene River (an EPA superfund site). The Pb recovered from the SLMDs correlated well with that measured for grab filtered water samples when averaged over the 4-d sampling interval.

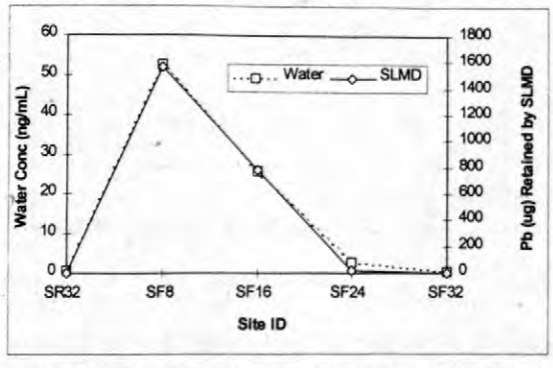

Figure 6. Concentration of Pb in filtered water plotted with mass of Pb recovered from SLMDs deployed for four days at five sites on the Coeur d'Alene River, ID, 1996.

Despite large pre-concentration factors for flowing waters, variable flow dynamics could limit the accuracy of estimating time-averaged water concentrations. One method to control the effects of hydrodynamics for flowing waters is to utilize a diffusion-limiting barrier (e.g., an outer membrane) for controlling uptake of analytes. For the SLMD, conventional cellulose dialysis tubing (1,000 MWCO) was applied for this purpose. A nine-day field test of the SLMD on the Animas River in Colorado, both with and without an outer sheath of dialysis tubing yielded nearly linear sampling over this period (Figure 7).

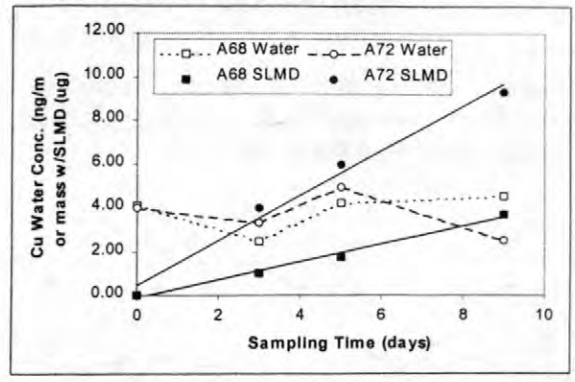

Figure 7. Concentration of Cu in filtered water plotted with Cu recovered from SLMDs sheathed in dialysis tubing. Deployment was for 3, 5, and 9 days at two sites on the upper Animas R., 1997.

Table 2. Sampling rates (L-eq/d) estimated for sheathed and unsheathed SLMDs deployed for 9 days at site A68 in the upper Animas R., 1997.

SLMD	Cu	Ni	Zn	Cd	Pb
Sheathed	0.11	0.17	0.34	0.26	0.12
Unsheathed	1.8	0.40	0.76	0.18	15.6

Sampling rates estimated from these field data (based on filtered grab samples) are summarized in Table 2. In most cases, the sampling rates for sheathed SLMDs were close to the diffusion-limiting rate of 0.15 L-eq/d measured for static laboratory experiments (Table 1). In contrast, sampling rates for unsheathed SLMDs, were generally much higher and more variable among elements due to flow effects and potential sampling of colloidal metals. Thus, it is plausible that the dialysis membrane sheath not only eliminated the uptake of the colloidal and particulate-associated metals, but it may have

served to reduce variation in the sampling rates caused by flow dynamics. Use of sheaths of varying MWCO ranges in combination with the SLMD could allow for the convenient and reliable size characterization of low concentrations of metal species with in-situ passive integrative sampling.

CONCLUSIONS

The stabilized liquid membrane device (SLMD) shows promise for in-situ passive integrative water sampling of toxicologically important divalent metal ions. Field deployment was successfully demonstrated for at least 9 days (longer times were not attempted). Based on laboratory experiments, sampling intervals of up to several weeks are possible. The observed sampling rate will depend greatly on the flow dynamics of the surrounding water, ranging from about 0.15 L-eq/d for quiescent waters to about 10 L-eq/d for fast-flowing waters. Encasement of the SLMD in a sheath of dialysis tubing may minimize effects of flow and also allow for convenient in-situ preconcentrative sampling of specific size classes of metal ion species. Presumably, sampling rates observed for metal complexes are dependent on the lability of the metal and if so, the SLMD could be useful in defining the bioavailability of metals when used as a complementary sampler. Due to possible pH effects for acidic waters, the SLMD will be most widely applicable for Cu and Ni. However, for most natural waters and especially seawater, sampling for Cd, Pb, and Zn will also be effective.

ACKOWLEDGMENTS

We gratefully acknowledge the technical assistance of our colleagues Tom May, Ray Wiedmeyer, Jesse Arms, and Mike Walther.

REFERENCES

Benes, P., and Steinnes, E., 1974, In Situ Dialysis for the Determination of the State of Trace Elements in Natural Waters: Water Research, v.8, p.947-953.

Borg, H., and Andersson, P., 1984, Fractionation of Trace Metals in Acidified Fresh Waters by In Situ Dialysis: Verh. Internat. Verein. Limnol., v. 22, p. 725-729.

Erickson, R.J., Benoit, D.A., Mattson, V.R., Nelson, H.P., and Leonard, E.N., 1996, The Effects of Water Chemistry on the Toxicity of Copper to Fathead Minnows: Environmental Toxicology and Chemistry, v.15, p.181-193.

Huckins, J. N., Manuweera, G. K., Petty, J.D., Mackay, D., and Lebo, J. A., 1993, Lipid-containing semi-permeable membrane devices for monitoring organic contaminants in water: Environmental Science and Technology, v. 27, p. 2489-2496.

Luoma, S.N., 1983, Bioavailability of Trace Metals to Aquatic Organisms - A Review: Science of the Total Environment, v. 28, p.1-22.

Morrison, G.M.P., 1987, Bioavailable Metal Uptake Rate Determination in Polluted Waters by Dialysis with Receiving Resins: Environmental Technology Letters, v. 8, p.393-402.

Petty, J.D., Huckins, J.N., Orazio, C.E., Lebo, J.A., Poulton, B.C., Gale, R.W., Charbonneau, C.S., and Kaiser, E.M., 1995, Determination of Waterborne Bioavailable Organochlorine Pesticide Residues in the Lower Missouri River: Environmental Science and Technology, v. 29, p.2561-2566.

Stumm, W., and Morgan, J.J., 1981, Aquatic Chemistry, An Introduction Emphasizing Chemical Equilibria in Natural Waters: John Wiley and Sons, Inc., New York, NY. pp 434-435.

U. S. Code of Federal Regulations, 1985, Title 40-- Protection of the Environment; Chapter 1--Environmental Protection Agency; Part 125-- Criteria and Standards for the National Pollution Discharge Elimination System.

Zhang, H., and Davison, W., 1995, Performance Characteristics of Diffusion Gradients in Thin Films for the in Situ Measurement of Trace Metals in Aqueous Solution: Analytical Chemistry, v. 67, p.3391-3400.

Zhang, H., Davison, W., Miller, S., and Tych, W., 1995, In Situ High Resolution Measurements of Fluxes of Ni, Cu, Fe, and Mn and Concentrations of Zn and Cd in Porewaters by DGT: Geochimica et Cosmochimica Acta, v. 59, p. 4181-4192.

AUTHOR INFORMATION

William Brumbaugh, Jimmie Petty, and James Huckins, U.S. Geological Survey, Columbia Environmental Research Center, Columbia, Missouri

Stanley Manahan, Department of Chemistry, University of Missouri-Columbia, Columbia, Missouri

Geomorphological Context of Metal-Laden Sediments in the Animas River Floodplain, Colorado

By Kirk R. Vincent, Stanley E. Church, and David L. Fey

ABSTRACT

The watershed of the upper Animas River in the San Juan Mountains of Colorado was the site of extensive mining and ore milling during the late 19th and early 20th centuries. Using geologic mapping, stratigraphic and sedimentological studies of floodplain sediments, geochronology, historical records, and geochemical analysis of sediments, we conclude the following. Prior to mining, the river valley below the town and ore mill site of Eureka was composed of small, multi-thread, gravel bedded channels. These were located within a silty floodplain consisting of willow thickets and possibly intermittent and localized beaver ponds. A radical change in the stream and floodplain environment started sometime around the turn of the century and concluded with aggradation and burial of older sediments with sheets of gravel. This was caused by ore milling, not mining or other activities. Mills in and near Eureka supplied huge quantities of tailings to the river, at rates 50 to 4,700 times greater than the natural (pre-mining) production of sediment from hillslopes. Floodplain sediments have naturally high zinc concentrations of about 1000 parts per million, but ore milling resulted in an increase of zinc concentrations by as much as an order of magnitude. Using vanadium as a lithologic tracer for sediment derived from natural erosion of the watershed, we estimate that the fine fraction of streambed and floodplain sediments deposited after 1900 A.D. contain, in general, two-thirds tailings and one-third natural sediments.

INTRODUCTION

The geomorphological context, depositional setting, and age of sediments used for chemical analysis and delineation of metals added to the environment by historical mining activities, can add insight into the cause and the disposition of those contaminants. Geologic mapping, stratigraphic and sedimentological studies, geochronology, and historical records were used to delineate the depositional timing and stratigraphic distribution of metal-laden sediments in the upper Animas River floodplain. This study illustrates the utility of multidisciplinary approaches in environmental studies, by establishing the pre-mining level of metals in upper Animas River streambed and floodplain sediments, and by demonstrating that the increase in concentration of certain metals in streambed and floodplain sediments coincided with the onset of ore milling activities upstream.

Beginning in the 1870's, the San Juan Mountains of southwestern Colorado was the site of extensive mining and milling of ores containing gold, silver, lead, copper, and zinc (Bird, 1986). The mine and mill sites numbered in the hundreds, but most were short lived. Early mills were constructed exclusively along streams, in part so that tailings would be dispersed downstream, rather than accumulate at the mill sites. By 1920, ore processing mills had become centralized and slurries of mill tailings were discharged or impounded on the floodplains of major streams. During major floods, the mill tailings were transported downstream, dispersing ore-related metals and contaminating downstream floodplains. The present location and extent of tailings in floodplain sediments is largely undocumented. Furthermore, the concentrations of metals in pre-mining streambed and floodplain sediments is unknown. The objective of this study is to address the pre-mining environment of the now braided section of the upper Animas River, determine the pre-mining concentrations of ore-related metals, and provide a chronology that can be tied to historical records of milling activity at Eureka, Colorado.

A trench was excavated across the floodplain of the upper Animas River in order to expose sediments, stratigraphic relationships, and datable material. The site is located upstream of Silverton, and is 1.4 km downstream of the now-defunct mill and town-site of Eureka. This is a subalpine setting at altitude of 2,970 m (meters). The site is

identified as locality 3 on the regional location map of Church and others (their fig. 1, 1999). The floodplain surface consists of multiple braided channels, gravel bars nearly devoid of vegetation, and stream-deposited tailings. The trench spanned 360 m, nearly the full width of the floodplain, and averaged 2.0 m in depth.

METHODS

The geomorphology of the site was studied by mapping geomorphic surfaces, investigating the stratigraphy exposed in the trench, and determining the numerical age, or constraining age, of the various sedimentary deposits. The purpose of the stratigraphic investigation was to decipher the environment of deposition of the sediments, to determine whether any sediments were mill tailings, and to establish the relative, or stratigraphic, ages of the deposits. This involved observation of cross-cutting stratigraphic relationships, sedimentological textures and structures, sedimentary provenance, and biological indicators of environment or age. Sedimentary contacts and structures, sample locations and other information, were documented on a log of the trench wall (unpub. data, 1998).

The numerical age of sedimentary deposits was determined using a variety of tools that provide either an age, or a maximum- or minimum-age constraint. Aerial photographs, taken on known dates, were inspected for the presence or absence of surficial deposits and other identifiable features. Numerous historical artifacts were discovered in the trench wall, constraining the age of the host deposits to be post-1870. These artifacts include iron objects: cans, pots, barrel hoops, and a stove leg; cloth fabric; porcelain; and a brick. A post-1870 age was also established for deposits that consisted of early mining stamp-mill tailings or were stratigraphically above tailings deposits. The annual growth rings of willow stems were used to constrain the age of deposits in which the plants were rooted, and were used to estimate the age of subsequent deposits that partially buried the willow plants (Scott and others, 1997; Sigafoos, 1964). Radiocarbon ages were obtained for twigs and peat found in sedimentary deposits.

Samples for chemical analysis were extracted from the trench wall, or obtained from cores of tailings and silt beds. The trench wall samples were generally about one liter in volume. Four 5 cm (centimeter)-diameter cores, about 1-m long, were taken along the trench. The cores were subsequently divided into 4 to 12 subsamples, with typical volumes of 50 cm^3 (cubic centimeters), based on stratigraphy (that is, visual differences of mineralogy or sedimentology).

Sample preparation and geochemical analysis follows the methods used by Church and others (1997) in their study of the geochemistry of modern streambed sediments of the upper Animas River and its tributaries. All samples containing gravel were passed through a stainless steel sieve with 2 mm (millimeter) mesh opening, and the gravel clasts were discarded. All samples were air dried, and sieved to -100 mesh (< 0.15mm), and then crushed to -150 mesh (< 0.1mm), except for the early stamp-mill tailings, which were crushed to -150 mesh without sieving. The chemistry was determined for very fine sand, silt, and clay-sized particles in the samples of silt-beds, fine-grained tailings, and sandy gravel. For the stamp-mill tailings samples only, the chemistry of the coarse sand and finer particles were determined. The analytical results are therefore representative of the entire samples of silt-bed and tailings deposits, but representative of only the fine-fraction (< 0.15mm) of the sandy gravel samples. The fine-grained particles, in the sandy gravel samples, generally occupied <5% of the original sample mass.

After grinding, all samples were digested using a mixed-acid procedure (Briggs, 1996), by which near complete dissolution of the samples was accomplished. This procedure is very effective in dissolving most minerals, including silicates, oxides and sulfides. Some refractory minerals such as zircon, chromite, and tin oxides are only partially attacked; however, elements contained in these minerals were not of concern in this study. The resulting solutions were analyzed by inductively coupled plasma-atomic absorption emission spectroscopy for major elements and trace elements. We discuss here results for zinc and vanadium. To monitor the quality of analyses, laboratory duplicates were analyzed to assess precision, and three standard reference materials were analyzed with the sample sets to assess analytical accuracy. The reference materials were NIST-2704, NIST-2709, and NIST-2711, available from the National Institute of Standards and Technology (NIST, 1993a, 1993b, and 1993c).

RESULTS

Production of ore-mill tailings

The history of mining and ore milling (fig. 1) upstream of the trench site is presented in order to identify the sources and ages of metal-laden sediments exposed in the trench. The history focuses on a succession of mills at Eureka (1.4 km upstream of the trench), various mines and mills near the Animas Forks town-site, which is also on the Animas River (8 km upstream of the trench), the Midway Mill about 3 km up Eureka Gulch from its confluence with the Animas River at the Eureka town-site, and the Sunnyside Mine on the shores of Lake Emma and its early mill (in upper Eureka Gulch, about 5.5 km upstream from the Eureka town site).

The first prospectors explored the area in 1860 and found a small amount of gold near the eventual site of Eureka, but the Civil War brought those types expeditions to a halt (Bird, 1986). In 1871 expeditions resumed and the prospectors learned that placer mining would not be viable, but that money could be made mining hard rock. Mining did not begin in earnest until after the September 13, 1873, Brunot Treaty which ceded land from the Ute Indian tribe. Through the 1870's mining produced valuable metals, but the quantity of ore (hand sorted and "high-graded" by miners and shipped from the area on mules and burros for processing) was relatively small. Mines around Animas Forks, for example, "were worked in the 1870's and produced 800 tons of ore" (Marshall, 1996, p. 140). During the 1880's and 1890's mining (and eventually ore milling) occurred at a limited scale and was intermittently disrupted by mechanical failures, natural disasters, and economic setbacks. In 1888 the first mill was constructed close to the Sunnyside Mine (a "ten-stamp" mill), and late in 1889 the Midway Mill began operation and processed 15 tons per day (Bird, 1986). Stamps were added to the Midway Mill in 1897, increasing capacity to 50 tons per day, and the first mill in Eureka, designed for a capacity of 125 tons per day, was constructed in 1899 and began production in 1900 (Marshall, 1996).

These stamp mills were generally in full production from 1900 to 1918, but were inefficient. A "stamp" was a piston device used to crush ore to sand-size, and economical minerals were then concentrated using various means, generally mechanical, for railroad shipment to smelters. The remaining material was discharged from a mill's tail-race into the Animas River or its tributaries, and these tailings contained metals. The Eureka Mill, for example, recovered less than 50 percent of the metals contained in lead-zinc ores (Bird, 1986, p. 68). Late in 1904 the Silverton Northern Railroad began service to the town of Animas Forks and the new Gold Prince Mill located there. The Gold Prince Mill was huge, with a reported capacity of 500 tons per day (Marshall, 1996), but production from the mill (and others in the area) was probably small. It was dismantled in 1910, and railroad service to Animas Forks was abandoned in 1916 (Sloan and Skowronski, 1975). Uniquely, the Sunnyside Mine remained profitable, because its ores were rich in gold, and in 1910 the Eureka Mill was processing 3,500 tons of ore per month (Bird, 1986, p. 114). In 1912 an electrostatic zinc recovery plant was added to the Eureka Mill (presumably reducing zinc concentrations in the mill tailings) and that and rising zinc prices probably saved that mine (unlike the others) during World War I.

A new era began in 1918. A new mill was completed in Eureka, capable of processing up to 600 tons of ore per day using a revolutionary selective flotation process that increased mill efficiency and profitability (Bird, 1986). Ore crushing techniques were also significantly improved at this time, resulting in fine-grained tailings composed of silt-sized and finer (<300 mesh) particles. The old stamp mills were abandoned. Full scale production was hampered, however, because of various disasters, until the end of 1919, and then the mine was forced to close late in 1920 because metal prices plunged. The boom years began when the mine reopened in the fall of 1921. The mine was producing 16,000 tons of ore per month by 1923, 20,000 tons per month by 1925, and broke all records by producing 1,100 tons of ore per day by 1929 (Bird, 1986). After the October stock market crash, however, the Sunnyside Mine and Eureka Mill struggled and then closed in September 1930. The mine was reopened again in 1937, faltered, and closed in August 1939. At the time of closing, a total of 2,500,000 tons of ore had been mined and milled, producing $50,000,000 in metals, and Eureka was officially a ghost town (Bird, 1986).

Figure 1 illustrates the rates at which ore was milled, in U.S. short tons per day. About 80 to 90% of the processed ore was released as tailings (King and Allsman, 1950). Using the 80% value and the ore processing rates on figure 1, mill tailings production rates were calculated and converted to metric tonnes. Most coarse-grained stamp mill tailings were produced between 1900 and 1918, at rates in excess of 35,000 tonnes per year. Most fine-

grained tailings were produced after 1921 and before 1930, at rates between 150,000 and 330,000 tonnes per year.

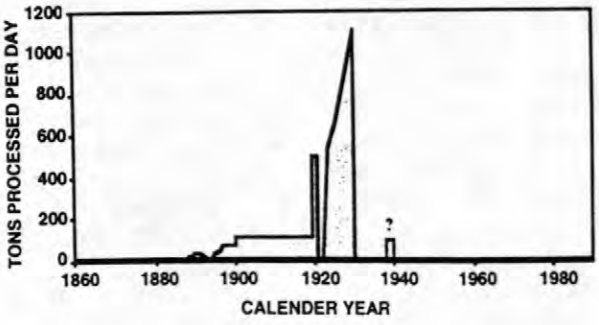

Figure 1. Combined ore processing rates for the succession of mills in the town of Eureka, Colorado, and in Eureka Gulch. These rates (from Bird, 1986; Marshall, 1996; and Sloan and Skowronski, 1975) were quoted in "tons", which presumably means U.S. short tons. One short ton equals 1.016 metric tonnes. Between 80 to 90% of the processed ore was discharged from the mills as tailings (King and Allsman, 1950).

Other sources of sediment

The rates of sediment supply from other sources are estimated for comparison with that from ore milling. Known rates of hillslope sediment yield span 6 orders of magnitude, from 0.004 to 500 tonnes/hectare/year. These two numbers are for primeval forests and for some croplands and construction sites, respectively (Dunne and Leopold, 1978). The prehistorical sediment production rates for the upper Animas River setting were probably at the low end of that spectrum, around 0.01 or perhaps 0.1 tonnes/hectare/year, resulting in total yield from the 73.6 km^2 watershed of 74 to 740 tonnes per year, respectively.

Logging probably did not increase sediment yields significantly because only 12% of the watershed is forested, and only a fraction of that was logged. The area was grazed, and grazing can increase sediment yields by an order of magnitude (Dunne and Leopold, 1978), but only about half of the upper Animas watershed is soil mantled and thus susceptible to increased erosion by grazing. Grazing and to a lesser extent logging, therefore, may have increased the watershed sediment yield by hundreds to a few thousand tonnes per year.

Erosion of mine-waste dumps also supplied sediment to streams. There are 24 mine shafts, 209 mine portals, and 679 prospect pits in the watershed above the trench site, based on the mining symbols on the USGS topographic maps. Each of these excavations has a pile of waste rock, and each waste dump contains about 200 tonnes of material covering an area of about 50 m^2, on average (T. Nash, oral commun., 1999). Together, the waste dumps cover an area of approximately 4.5 hectares. An erosion rate of 100 tonnes/hectare/year is typical for disturbed land in general (Dunne and Leopold, 1978). If this is appropriate for mine dumps, all of the dumps in the watershed lost 450 tonnes of sediment per year, but only a fraction of the sediment mobilized from dumps reached streams because most mine sites are located high on hillslopes many kilometers from streams.

Geomorphological findings

Sediments exposed in the trench generally consist of sandy gravel deposits (83%), silt beds (12.6%), lenses and tabular beds of sand-sized tailings (1.2%), and tabular beds of fine-grained tailings (3.2%). The percentages refer to the area of each deposit type relative to the total 607 m^2 area of the trench wall. The trench was excavated perpendicular to stream flow. The base of the section consists of massive sandy gravel locally containing (1) discontinuous parallel bedding usually inclined <5°, (2) medium, curved, parallel, trough cross-bedding, and (3) 16 thin-to-medium, lenticular (two are tabular) beds of brown sandy-silt <3 m in length.

Eight thick to very-thick beds of brown sandy silt are found in the middle of the section. The silt beds range in length from 4 to 25 m and span ≈30% of the trench length. The bases of the silt beds are generally in planar-horizontal contact with underlying gravel, but lenticular- or wedge-shaped silts also interfinger with underlying gravel. Twigs and peat found near the base of the silt beds have ages of 1,080 ±120 and 2,130 ±145 ^{14}C years before present. At one location, a facies of gravel interfingers with coarse-grained tailings which in turn interfingers with the base of a thick silt bed. From this we infer that the silts were deposited in an impounded channel and are historical (post-1900 A.D.) in age. The silt beds contain (1) lenses of gravel, (2) a few lenses of peat (up to 5 cm thick and <3 m long), (3) 14 peat lamina (1 cm thick and 1 to 10 m long), (4) leaves and root casts possibly left by grasses, and (5) abundant twigs (presumably willow), some of which are in growth position. One twig was obviously chewed by a large mammal,

possibly a beaver. Aside from those features, the silt beds appear massive. Close inspection, however, indicates that the silts beds also contain very thin lenses of fine sand, irregular shaped bands of climbing ripples composed of coarse silt, and 10-cm-deep indentation markings left by large mammal hooves. The silt beds are either overlain conformably, or are truncated by wavy or irregular erosional surfaces. Twigs and peat found near the top of silt beds yielded two "modern" C^{14} ages, which means they are <300 years in age.

Channel-fill deposits truncate the lateral extent of thick silt beds at several locations. These channel-fill deposits consist of sandy gravel that contain (1) discontinuous parallel bedding, (2) medium, curved, parallel, trough cross-bedding, (3) and thin, lenticular or irregular-shaped deposits of coarse sand. Nine of the sand lenses are dominated by very angular grains of ore body minerals (sphalerite, rhodenite, and pyrite), and two lenses contain historical iron objects. We infer that these are deposits of stamp-mill tailings. The upper meter of the section consists of sheets of sandy gravel that are either horizontally bedded or trough cross-bedded. These gravels contain lenses and two beds (3 to 11 m long) of stamp-mill tailings, and historical objects. The following ages are based on growth rings of willows buried by the gravels (M. Scott, USGS, BRD, written commun., 1999). The sheet gravels were deposited during floods that occurred before 1915 A.D. and about 1920 A.D., and the depositional age of the top of these sheet gravels was determined to be 1930 A.D. (± 3 years). This depositional surface extends over 45% of the length of the trench, although it is locally covered by beds of fine-grained tailings. Elsewhere it has been remobilized by flow within braided channels.

The beds of fine-grained tailings are generally massive and are thin to medium in thickness. Willow growth rings indicate the tailings beds were deposited by floods that occurred about 1940 A.D. and about 1970 A.D. (M. Scott, written commun., 1999).

Geochemical results

The stratigraphic investigation provided the basis for ranking the deposits by relative age (fig. 2A and 2B), and allowed us to establish the trends in element-concentrations in the streambed and floodplain sediments. The C^{14} ages allowed identification of those sediments which were definitely deposited before the mining era (fig. 2C). The age constraints provided by the presence of tailings and historical artifacts, and the growth rings of willows, allowed identification of those sediments which were definitely deposited after milling began (fig. 2C). The geochemical data are presented using symbols for 4 deposit types, but in general the sedimentary deposit type does not influence concentrations.

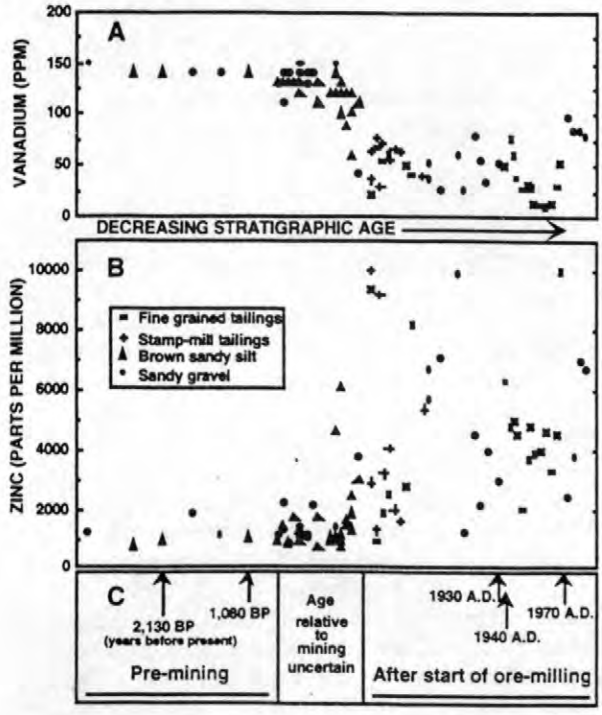

Figure 2. The concentrations of (A) vanadium and (B) zinc in the fine-fraction of sediments of various types, plotted against stratigraphic (relative) age. Numerical ages, based on radiocarbon and tree-ring analysis, are tied to the relative age scale in fig. 2C, and the presence of tailings beds and cultural artifacts identify sediments deposited after the onset of ore milling. All samples were obtained from the trench excavated into Animas River floodplain 1.4 km downstream of the town-site of Eureka, Colorado.

The concentrations of vanadium in sediments (fig. 2A) deposited prior to mining average 140 ppm (parts per million), which is near the 160 ppm crustal abundance of vanadium (Emsley, 1991), and are typical of bedrock in the study area. The concentrations of vanadium in historical (post-1900) deposits average 50 ppm. The vanadium concentrations in some of the fine-grained tailings samples are close to 20 ppm. Thus, the relative loading of natural sediments and mill tailings can be calculated from the dilution of vanadium in historical sediments.

The concentrations of zinc in sediments (fig. 2B) deposited prior to the mining era are uniform and close to 1000 ppm, which is an order of magnitude greater than the 75 ppm crustal abundance of zinc (Emsley, 1991). Compared to this pre-mining background, the concentrations of zinc in most (38 out of 46 samples) of the sediments known to have been deposited after mining began are elevated by as much as ten times. The zinc concentration data do not show patterns of association with sedimentary deposit types.

DISCUSSION AND CONCLUSIONS

We conclude that most metal-laden sediment at the trench site originated from ore-processing mills in and near Eureka. Most of the coarse-grained stamp mill tailings were produced between 1900 and 1918, at rates in excess of 35,000 tonnes per year. That supply rate is 50 to 500 times the natural (pre-mining) production of sediment by erosion from hillslopes in the watershed which is estimated to have been in the range of 70-700 tonnes per year. Most fine-grained tailings were produced after 1921 and before 1930, at rates between 150,000 and 330,000 tonnes per year. Those rates are 200 to 4,700 times greater than the natural production rate of sediment eroded from hillslopes. Accelerated erosion caused by logging and grazing and erosion of mine waste dumps may have contributed a few thousand tonnes of sediment a year, but those sediments contain much lower concentrations of zinc, for example, compared to tailings as discussed below.

The following late-Holocene geological history of the Animas River floodplain is deduced from the results of the trench study discussed above. Prior to 2,000 years ago the fluvial system was dominated by fully braided streams with little silt-bed deposition, or at least little silt-bed preservation. Later, the valley bottom became composed of small, multi-thread, gravel bedded channels coexisting with floodplains consisting of willow carrs and possibly intermittent and localized beaver ponds. The willow thickets (and beaver ponds if and where present) were the terrestrial riparian habitat alongside the multi-thread streams, and were the depositional sites of silt beds. This stream and floodplain condition persisted for some 2,000 years, including an unknown number of decades after mining began in the 1870's.

A radical change in the stream and floodplain environment occurred sometime around the turn of the century, apparently starting with channel incision and widening, followed by aggradation and burial of older sediments with sheets of gravel. Because the aggradational gravel deposits contain lenses of coarse stamp-mill tailings, we interpret that most or all of the gravel aggradation occurred coincident with the major production period of mill tailings, after 1900. Gravel aggradation included deposition during numerous floods including one around 1930, after which gravel aggregation ceased. The Eureka Mill also closed in 1930. We infer that the aggradational episode was caused by the unnatural supply of huge quantities of tailings to the Animas River. Since 1930, the stream has been fully braided with no deposition of silt beds, and the gravel bars are nearly devoid of plant life. During floods in recent decades, however, fine-grained tailings remobilized from near the Eureka mill site were deposited on the braided plain and on remnant willow-covered floodplains downstream of the trench site.

The stratigraphic investigation provided the basis for ranking the deposits by relative age (fig. 2), allowing us to establish trends in element-concentrations in the streambed and floodplain sediments. The C^{14} ages allowed identification of those sediments which were definitely deposited before the mining era. The age constraints provided by the presence of tailings and historical artifacts, and willows growth rings, allowed identification of those sediments which were definitely deposited after ore-milling began. Using this information together, we identify the effect of ore milling on sediment chemistry (fig. 2).

The trend in zinc concentration shows a dramatic increase, by as much as an order of magnitude (fig. 2B). This increase occurred both in sediments deposited in streambeds and bars, and in sediments deposited on brush-covered floodplains. The concentrations of zinc in sediments known to have been deposited prior to the mining era are uniform and close to 1000 ppm. The range is from 750 to 1800 ppm. These sediments were the result of natural erosion of hillslopes in the watershed. The concentrations of zinc are also close to 1000 ppm in most of the samples that have depositional-ages which are uncertain relative to the beginning of mining and milling. Zinc concentrations for all but 5 of the youngest samples range between 650 and 2200 ppm. The concentrations of zinc are elevated, however, in most of the sediments known to have been deposited after mining began, and more specifically after mill-processing of ores

began in earnest. Zinc concentrations for all but 8 of the 41 samples exceed 2200 ppm. We infer, therefore, that the increase in zinc concentrations in streambed and floodplain sediments was caused by the release of huge quantities of tailings from ore mills.

The trend in vanadium concentration is opposite to that for zinc (fig. 2A). The vanadium concentrations in pre-mining sediments are similar to that for typical bedrock in the area. They are also, in general, about three times higher than the concentrations in historical deposits. The vanadium concentrations in some of the fine-grained tailings samples are close to 20 ppm, and thus may represent pure tailings undiluted by natural sediment. Mining did not cause an increase in the release of vanadium to the environment, rather it diluted the natural vanadium concentration with mill tailings. We conclude that vanadium can be used as a lithologic tracer for sediment derived from natural erosion of the watershed. In this case, we conclude that the fine-grained fraction of historical sediments at the trench site are, in general, composed of two-thirds mill tailings and one-third natural sediments unrelated to mining or milling.

REFERENCES

Bird, A.G., 1986, Silverton gold: the story of Colorado's largest gold mine: published by author (ISBN 0-9619382-2-6), 152 p.

Briggs, P.H., 1996, Forty elements by inductively coupled-plasma atomic emission spectrometry, *in* Arbogast, B.F., ed., Analytical methods manual for the Mineral Resources Program: U.S. Geological Survey Open-File Report 96-525, p. 77-94.

Church, S.E., Kimball, B.A., Fey, D.L., Ferderer, D.A., Yager, T.J. and Vaughn, R.B., 1997, Source, transport and partitioning of metals between water, colloids, and bed sediments of the Animas River, Colorado: U.S. Geological Survey Open-File Report 97-151, 135 p.

Church, S.E., Fey, D.L., Brouwers, E.M., Holmes, C.W., and Blair, Robert, 1999, Determination of pre-mining geochemical conditions and paleoecology in the Animas River watershed, Colorado, Morganwalp, D.W., and Buxton, H.T., eds., U.S. Geological Survey Toxic Substances Hydrology Program--Proceedings of the Technical Meeting, Charleston, South Carolina, March 8-12, 1999--Volume 1--Contamination from Hardrock Mining: U.S. Geological Survey Water-Resources Investigations Report 99-4018A, this volume.

Dunne, T., and Leopold, L. B., 1978, Water in environmental planning: San Francisco, W. H. Freeman and Co., 818 p.

Emsley, John, 1991, The elements: Oxford, Clarendon Press, 251 p.

King, W. H., and Allsman, P. T., 1950, Reconnaissance of metal mining in the San Juan region, Ouray, San Juan, and San Miguel Counties, Colorado: U.S. Bureau of Mines Information Circular 7554, 109 p.

Marshall, John, 1996, Mining the hard rock in the Silverton San Juans: Silverton, Simpler Way Book Company, 216 p.

National Institute of Standards and Technology (NIST), 1993a, Certificate of Analysis Standard Reference Material 2704, Buffalo River Sediment.

_____, 1993b, Certificate of Analysis Standard Reference Material 2709, San Joaquin Soil.

_____, 1993c, Certificate of Analysis Standard Reference Material 2711, Montana Soil.

Scott, M.L., G.T. Auble, and J.M. Friedman, 1997, Flood dependency of cottonwood establishment along the Missouri River, Montana, USA: Ecological Applications v. 7, p. 677-690.

Sigafoos, R.S. 1964. Botanical evidence of floods and floodplain deposition: U.S. Geological Survey Professional Paper 485A, 35 p.

Sloan, R.E., and Skowronski, C.A., 1975, The rainbow route: Denver, Sundance Publications Limited, 416 p.

AUTHOR INFORMATION

Kirk R. Vincent, National Research Council Associate with the U.S. Geological Survey, Boulder, Colorado (kvincent@usgs.gov)

Stanley E. Church and David L. Fey, U.S. Geological Survey, Denver, Colorado

Research on Hard-Rock Mining in Mountainous Terrain

The Toxics Program research efforts on hard-rock mining in mountainous terrain has had a change in emphasis in the last several years. The major change has been a concerted effort to work in the pilot watersheds of the USGS Abandoned Mine Lands (AML) Initiative -- the Animas River in Colorado and the Boulder River in Montana. These are mountainous watersheds, with pool-and-riffle streams that receive natural and mine-drainage inflows of surface and ground water. Our role in the AML Initiative has been to adapt and transfer technology developed through field experimentation in St. Kevin Gulch, the Upper Arkansas River watershed, Colorado. This entails adaptation of research methods to the watershed-scale problems faced by Federal land managers in practical field situations.

CHANGING SCALE TO THE WATERSHED

Tracer-injection and synoptic sampling studies in St. Kevin Gulch were on the scale of 2 kilometers (km) or less and at streamflows of less than 1 cubic foot per second (cfs). In this setting, changes in streamflow along the study reach generally were less than an order of magnitude. For the AML Initiative, we have had to adapt methods to a scale of up to 12 km, and streamflow up to 200 cfs, resulting in more than an order of magnitude change in streamflow. This has not meant simply doing a "big" St. Kevin Gulch test by mixing more tracer and injecting it at a greater rate. Transitions from small to large order streams within the basins have required careful evaluation to break the study reach into workable segments. This keeps the tracer concentrations within a reasonable analytical range for each reach, and enables effective interpretation of the tracer-test results.

New sites and different scales have required new thinking and new logistics; each stream has provided new insights. Despite the change in scale, we have found the need to maintain spatially intensive sampling to adequately describe mass balance for inflows to streams. This enables unique identification of various contamination sources and linkage to distinct stream segments within a watershed, information essential for remediation design and monitoring.

UNDERSTANDING INFLOWS

Characterization of the water chemistry of stream inflows has always been an important goal of synoptic sampling. We are able to identify net water-quality changes for stream reaches and to quantify the average concentrations of metals in inflows to these reaches. Characterization of inflows has enabled linkage of the impacts observed in the stream with specific sources of mine drainage. Thus, the goal to understand inflows becomes a goal to understand the pathway of contaminants from a source to the stream. The pathway depends on catchment hydrology as it is influenced by geologic structure. We are expanding our inflow sampling to observe both surface- and ground-water pathways, to make the link between contaminant sources and the streams.

SIMULATING REMEDIATION OPTIONS

Reactive solute-transport models (OTEQ) have been applied to explain the changes in water chemistry downstream, revealing an ability to design and evaluate remediation options. The removal of a mine drainage source is not simply removal of a source term in a contaminant mass-balance exercise. Contaminants are affected by complex reactive processes that occur within the stream. Removal of a metal load can change pH conditions, and in turn, change the overall reaction processes within the stream. Thus, simulation of a remediation option might consider its effect on overall stream chemistry and natural attenuation of metals occurring in the stream. As many options are evaluated with models, we will gain needed understanding of how the many efforts to characterize the watershed fit together to help guide remediation and monitoring efforts.

The papers of this session and two in the session on the USGS Abandoned Mine Lands Initiative reflect progress on these issues.

For additional information contact:

Briant A. Kimball, USGS, Salt Lake City,
Utah, (email: bkimball@usgs.gov)

Modeling Solute Transport and Geochemistry in Streams and Rivers Using OTIS and OTEQ

By Robert L. Runkel, Kenneth E. Bencala, and Briant A. Kimball

ABSTRACT

Solute transport in streams is governed by a suite of hydrologic and geochemical processes. Interactions between hydrologic processes and chemical reactions may be quantified through a combination of field-scale experimentation and simulation modeling. Two mathematical models that are used to simulate solute transport in streams are presented here. A model that considers One-dimensional Transport with Inflow and Storage (OTIS) may be used in conjunction with tracer-dilution methods to quantify hydrologic transport processes (advection, dispersion, and transient storage). Additional applications of OTIS include analyses of nonconservative solutes that are subject to sorption processes and (or) first-order decay. A second model, OTEQ (One-dimensional Transport with EQulibrium chemistry), combines the transport mechanisms in OTIS with a chemical equilibrium submodel that considers complexation, precipitation/dissolution, and sorption. OTEQ may be used to quantify the geochemical processes affecting trace metals.

INTRODUCTION

Many investigators are currently studying streams and the effect of basin loading on stream-water quality. Studies of streams share two common goals: (1) to quantify the hydrologic transport processes controlling solute concentrations, and (2) to quantify the dominant chemical reactions. Both goals may be addressed through a combination of field-scale experimentation and simulation modeling. Tracer-dilution methods, for example, are frequently used to quantify hydrologic transport. During a tracer-dilution experiment, a conservative tracer is injected at the upstream end of a stream reach. Tracer concentrations measured at several downstream locations are used to determine the volumetric flow rate and the additional inflow entering the stream from surface runoff and ground water. Other hydrologic properties, such as traveltime and mixing, are then determined by applying a conservative solute transport model.

Geochemical processes may be identified by analyzing field data that describe the spatial and (or) temporal distribution of solute concentration. A key step in process identification is interpretation of the complex interactions between hydrologic transport and chemical reactions. Given a description of hydrologic transport, reactive transport models may be used to investigate the underlying geochemical processes.

This paper presents two models that are used to simulate the fate and transport of solutes in streams and rivers. Several applications illustrate how the models may be used with field data to identify the dominant processes affecting solute concentrations.

SOLUTE TRANSPORT MODELS

One-Dimensional Transport with Inflow and Storage (OTIS)

The OTIS solute transport model was developed to simulate the transport of solutes in streams and rivers in which one-dimensional transport may be assumed. Although the model is used primarily for conservative solutes, nonconservative solutes that are subject to sorption processes and (or) first-order decay may also be simulated. Several hydrologic processes that govern the downstream transport of solutes are considered in the model. These processes include advection, dispersion, lateral

inflow, and transient storage. Advection, the downstream transport of solute mass at a mean velocity, and dispersion, the spreading of solute mass due to shear stress and molecular diffusion, are considered in most mechanistic models of streamwater quality and solute transport. Consideration of these important mechanisms leads to the familiar advection-dispersion equation (see Runkel and Bencala, 1995, p. 144). Within the OTIS model, additional terms are added to the advection-dispersion equation to account for the effects of transient storage and lateral inflow.

Transient storage has been noted in many streams, where solutes may be temporarily detained in small eddies and stagnant pools of water that are stationary relative to the faster moving water near the center of the channel. In addition, significant portions of the flow may move through the coarse gravel of the streambed and the porous areas within the streambank. The traveltime for solutes carried through these porous areas may be significantly longer than that for solutes traveling within the water column. Lateral inflow is any water that is added to the stream due to ground-water inflow, overland flow, interflow, or small springs. These flows act to dilute (or concentrate) solutes in the stream channel if they carry solute concentrations that are lower (or higher) than the stream-solute concentration.

The OTIS model is formed by writing mass balance equations for two conceptual areas: the main channel and the storage zone. The main channel is defined as that portion of the stream in which advection and dispersion are the dominant transport mechanisms. The storage zone is defined as the portion of the stream that contributes to transient storage; that is, stagnant pools of water and porous areas of the streambed. Water in the storage zone is considered immobile relative to water in the stream channel. The exchange of solute mass between the main channel and the storage zone is modeled as a first-order mass transfer process. Consideration of the hydrologic processes discussed above gives rise to mass conservation equations for the main channel and the storage zone (Bencala and Walters, 1983; Runkel, 1998)[1]:

$$\frac{\partial C}{\partial t} = -\frac{Q}{A}\frac{\partial C}{\partial x} + \frac{1}{A}\frac{\partial}{\partial x}\left\langle AD\frac{\partial C}{\partial x}\right\rangle + \frac{q_{LIN}}{A}(C_L - C) + \alpha(C_S - C) \quad (1)$$

$$\frac{dC_S}{dt} = \alpha\frac{A}{A_S}(C - C_S) \quad (2)$$

where

A	main channel cross-sectional area (L^2),
A_S	storage zone cross-sectional area (L^2),
C	main channel solute concentration (M L^{-3}),
C_L	lateral inflow solute concentration (M L^{-3}),
C_S	storage zone solute concentration (M L^{-3}),
D	dispersion coefficient ($L^2\ T^{-1}$),
Q	volumetric flow rate ($L^3\ T^{-1}$),
q_{LIN}	lateral inflow rate ($L^3\ T^{-1}\ L^{-1}$),
t	time (T),
x	distance (L), and
α	storage zone exchange coefficient (T^{-1}).

These equations describe the hydrologic processes affecting solutes and are therefore applicable to conservative (nonreactive) solutes such as tracers. Nonconservative (reactive) solutes are considered by adding terms to equations (1) and (2). OTIS includes two types of chemical reactions: kinetic sorption and first-order decay. Sorption may take place directly on the streambed or within the storage zone. Addition of terms representing sorption and decay yields:

$$\frac{\partial C}{\partial t} = L(C) + \rho\hat{\lambda}(C_{sed} - K_d C) - \lambda C \quad (3)$$

$$\frac{dC_S}{dt} = S(C_S) + \hat{\lambda}_S(\hat{C}_S - C_S) - \lambda_S C_S \quad (4)$$

where

$\hat{C}_S$	background storage zone solute concentration (M L^{-3})
C_{sed}	sorbate concentration on the streambed sediment (M M^{-1})
K_d	distribution coefficient ($L^3\ M^{-1}$)

[1]The fundamental units of Mass (M), Length (L), and Time (T) are used throughout this paper.

λ main channel first-order decay coefficient (T^{-1})

λ_S storage zone first-order decay coefficient (T^{-1})

$\hat{\lambda}$ main channel sorption rate coefficient (T^{-1})

$\hat{\lambda}_S$ storage zone sorption rate coefficient (T^{-1})

ρ mass of accessible sediment/volume water ($M\,L^{-3}$)

and $L(C)$ and $S(C_S)$ represent the hydrologic processes in the main channel and storage zone, respectively (the right-hand sides of equations (1) and (2)). The sorption parameters introduced here ($\hat{C}_S$, K_d, $\hat{\lambda}$, $\hat{\lambda}_S$ and ρ) are discussed in detail by Bencala (1983). Equation (3) introduces, C_{sed}, a third concentration variable for which a mass balance is required. The streambed sediment concentration (sorbate concentration on the streambed sediment) is governed by:

$$\frac{dC_{sed}}{dt} = \hat{\lambda}(K_d C - C_{sed}) \qquad (5)$$

Equations (3)-(5) describe the spatial and temporal variation in solute concentration as a function of several hydrologic and geochemical parameters. As discussed by Runkel (1998), parameter estimates may be obtained by nonlinear regression using a modified version of OTIS known as OTIS-P.

One-Dimensional Transport with Equilibrium Chemistry (OTEQ)

The OTIS solute transport model provides a framework for the analysis of conservative solutes and nonconservative solutes that are subject to relatively simple chemical reactions. Many cases arise, however, in which solutes are affected by chemical processes that are not considered in such a simple model. Trace metals, for example, may be affected by pH-dependent processes such as precipitation/dissolution and sorption. The OTEQ model described in this section considers these complex reactions within the context of hydrologic transport.

OTEQ is formed by coupling the OTIS solute transport model with a chemical equilibrium submodel. The chemical equilibrium submodel is based on MINTEQ (Allison and others, 1991), a model that computes the distribution of chemical species that exist within a batch reactor at equilibrium. The coupled model considers a variety of processes including advection, dispersion, transient storage, transport and deposition of water-borne solid phases, acid/base reactions, complexation, precipitation/dissolution, and sorption.

Governing equations for OTEQ are formulated in terms of chemical components. The total component concentration (T) consists of dissolved (C), mobile precipitate (P_w), immobile precipitate (P_b), mobile sorbed (S_w), and immobile sorbed (S_b) phases. Processes considered for each phase are depicted in figure 1, where the system is represented as two compartments. The water column compartment contains the three mobile phases, C, P_w and S_w. Immobile substrate (that is, the streambed or debris) constitutes the second compartment, containing the two immobile phases, P_b and S_b. The three mobile phases are subject to hydrologic transport, as represented by the transport operator, L. The dissolved phase, C, takes part in precipitation/dissolution and sorption/desorption reactions that occur within the water column (interactions with P_w and S_w). The dissolved phase is also affected by dissolution of precipitate from the immobile substrate and by sorption/desorption from immobile sorbents (interactions with P_b and S_b). Finally, C may increase or decrease due to external sources and sinks, as denoted by s_{ext}. The precipitated and sorbed phases in the water column settle in accordance with settling velocity ν ($L\,T^{-1}$).

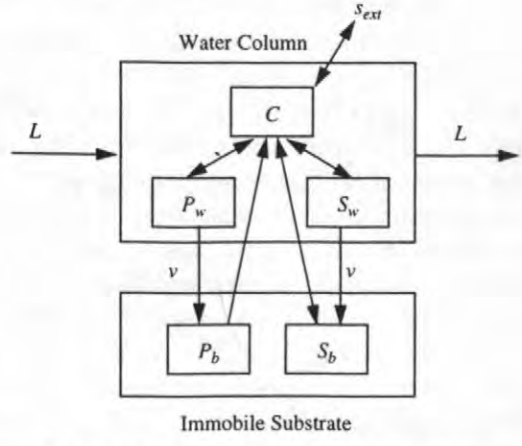

Figure 1. Conceptual surface-water system used to develop the governing differential equations. The total component concentration consists of dissolved (C), mobile precipitate (P_w), immobile precipitate (P_b), mobile sorbed (S_w) and immobile sorbed (S_b) phases. The dissolved and mobile phases are subject to transport, as denoted by L.

Runkel and others (1996a) developed a general mass balance equation for each component by considering the mass associated with each of the five component phases. The mass balance equation for the total component concentration is given by:

$$\frac{\partial T}{\partial t} = L(T) - L(S_b + P_b) + s_{ext} \qquad (6)$$

where the transport operator is as defined in equation (3). Inspection of (6) reveals that T is a function of P_b and S_b. The immobile precipitated and sorbed concentrations are governed by:

$$\frac{\partial P_b}{\partial t} = \frac{v}{d}(P - P_b) - f_b \qquad (7)$$

$$\frac{\partial S_b}{\partial t} = \frac{v}{d}(S - S_b) - g_b \qquad (8)$$

where

- f_b source/sink term for dissolution from the immobile substrate (M $L^{-3}T^{-1}$),
- g_b source/sink term for sorption/desorption from the immobile substrate (M $L^{-3}T^{-1}$),
- d settling depth (L),
- P total precipitate component concentration (= $P_w + P_b$; M L^{-3}), and
- S total sorbed component concentration (= $S_w + S_b$; M L^{-3}).

The governing equation set consists of three differential equations for each component (for T, P_b, and S_b) and the set of algebraic equations representing chemical equilibria. This equation set is solved using a Crank-Nicolson approximation of the differential equations and the sequential iteration approach (Runkel and others, 1996a).

MODEL APPLICATIONS

Several OTIS and OTEQ applications are presented below. Additional OTIS applications are described by Broshears and others (1993), Morrice and others (1997), Harvey and Fuller (1998), and Runkel and others (1998); additional OTEQ applications are described by Broshears and others (1995, 1996), Runkel and others (1996b), and Ball and others (this volume).

Mixing and Traveltime (OTIS)

Data from tracer-injection studies are frequently used to quantify mixing and traveltime in streams and rivers. These hydrologic characteristics are of importance to water-resource managers who are responsible for protecting water supplies from contamination. Given data from tracer-injection studies, stream transport models may be used to estimate the timing, magnitude, and duration of a pollutant cloud that enters a stream due to an accidental spill.

In addition to providing management information, hydrologic parameters derived from tracer-injection data provide insight into the physical characteristics of streams. Values of the transient storage parameters (A_s, α), for example, indicate the degree of mixing due to stagnant pools and flow through porous areas of the streambed. Further, model-derived estimates of traveltime indicate the relevant time scales over which chemical reactions can potentially affect solute concentrations.

In this section we illustrate the use of OTIS to quantify hydrologic processes using tracer-injection data. Our first example uses data from Uvas Creek, a small pool-and-riffle stream in northern California. Bencala and Walters (1983) described a continuous, constant-rate injection of chloride into Uvas Creek. Concentrations were monitored at several downstream locations and streamflow was estimated by tracer dilution.

Application of OTIS to the Uvas Creek chloride injection requires estimates of stream cross-sectional area (A), transient storage (A_s, α) and dispersion (D) for each stream reach. Estimates of stream cross-sectional area are related to traveltime as they control the timing of the chloride profile, whereas estimates of the transient storage parameters represent instream mixing as reflected by the shape of the chloride profile. During a series of simulations, Bencala and Walters (1983) varied A, A_s, α, and D to obtain a match between observed and simulated concentrations. Final simulation results at two sampling locations are shown in figure 2.

Reach-specific parameter estimates developed from tracer-injection data represent integrated or average conditions for a given length of stream.

As noted by Bencala and Walters (1983), physical stream characteristics such as cross-sectional area vary substantially over short spatial scales. As such, estimates of A based on tracer-injection data are preferable to estimates based on surveyed transects that may not be representative of the reach under study.

Estimates of A and A_s developed from the tracer data are consistent with the pool-and-riffle description of Uvas Creek given by Bencala and Walters (1983). The pools act to produce transient storage by temporarily detaining some of the chloride. A dimensionless measure of this storage effect is obtained by calculating the ratio of storage zone cross-sectional area to main channel cross-sectional area (A_s/A). Values of A_s/A for various reaches of Uvas Creek range from 1.0 to 3.0. These values indicate that the pool areas are large relative to the main channel.

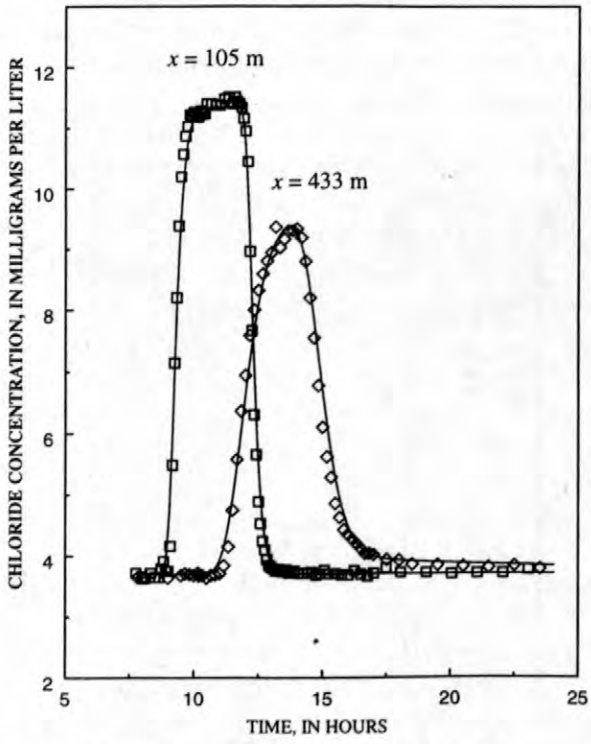

Figure 2. Simulated (solid lines) and observed (symbols) chloride concentrations in Uvas Creek, California (Data and parameter values from Bencala and Walters, 1983).

Analysis of Uvas Creek data relied on a trial-and-error approach wherein parameter estimates were manually adjusted to produce an acceptable match between simulated and observed tracer concentrations. In the following example, parameter estimates are obtained by nonlinear regression using OTIS-P. Laenen and Risley (1997) described several studies in Oregon streams where rhodamine WT was used to determine traveltime. In July 1992, a slug of rhodamine WT was added to the Clackamas River at river mile 13.3 (RM 13.3). Water samples were collected at river miles 11.0, 9.5 and 8.0. Because rhodamine WT was introduced as a slug (as opposed to a continuous injection), data at the first sampling location (RM 11.0) are used to define the upstream boundary condition (fig. 3). Given the boundary condition, the traveltimes (as given by A) and mixing characteristics (as given by A_S, α, D) for the two reaches ending at river miles 9.5 and 8.0 may be determined.

Use of OTIS-P requires a set of initial estimates for the parameters of interest. Here we set A and D for both reaches equal to 50 m^2 and 10 m^2/s, respectively. The exchange coefficient, α, is initially set to 0.0 such that transient storage is not considered. Preliminary OTIS results based on these initial parameter estimates are shown as dashed lines in figure 3. These preliminary profiles indicate that our initial estimates of stream cross-sectional area are too large; the simulated traveltime is overestimated at both RM 9.5 and RM 8.0. In addition, the symmetric simulation profile at RM 8.0 is in contrast to the asymmetry of the observed data. This observation suggests that transient storage may be an important mixing mechanism. Both of these discrepancies may be addressed by developing parameter estimates using OTIS-P. As expected, application of OTIS-P results in an improved simulation (solid lines, fig. 3) and a revised set of parameter estimates (for example, A= 30.4 and 48.1 m^2 for the two reaches).

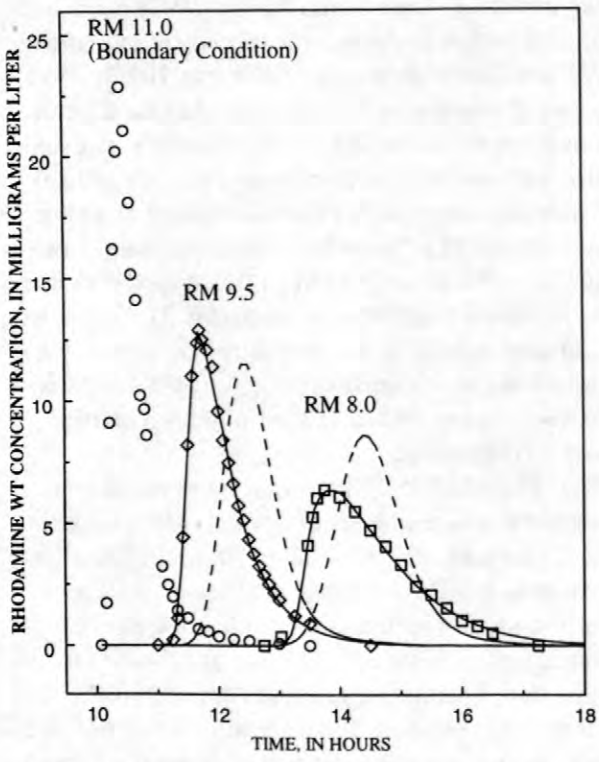

Figure 3. Upstream boundary condition (RM 11.0), observed concentrations (symbols), simulated concentrations based on initial parameter estimates (dashed lines), and simulated concentrations based on final parameter estimates (solid lines) for the Clackamas River, Oregon.

Nutrient Uptake (OTIS)

The examples above illustrate the use of OTIS to quantify hydrologic processes. In this example we show how OTIS may be used to identify chemical reactions. McKnight and Duff (1995) described an experimental addition of lithium chloride (LiCl), phosphate, and nitrate into Green Creek, a glacial meltwater stream in Antarctica. The objective of the study was to quantify stream hydrology and to study nutrient uptake by algal mats that cover the bed of Green Creek. As in the previous examples, a conservative tracer (LiCl) is used to define the hydrologic system. Hydrologic parameters based on the analysis of LiCl transport are then used to evaluate the conservative transport of nitrate and phosphate. A conservative simulation of nitrate is shown as a dashed line in figure 4. As shown in the figure, observed nitrate concentrations are substantially lower than simulated concentrations based on conservative transport. This discrepancy indicates that nitrate concentrations are attenuated by geochemical processes.

Under the assumption that nutrient uptake is a first-order process, the first-order decay coefficients (λ, λ_s) in OTIS are used to quantify the loss of nitrate. Given the hydrologic characterization, OTIS-P is used to estimate uptake in the main channel (λ) and in the storage zone (λ_s). Reach-specific estimates of λ range from $4x10^{-5}$ to $4x10^{-4}$ /s; estimates of λ_s range from $3x10^{-6}$ to $2x10^{-3}$ /s. Simulation results based on these parameter estimates are shown as a solid line in figure 4. Additional mass balance calculations based on λ and λ_s indicate that 84-93 percent of the nitrate loss occurs in the main channel where algal uptake is the likely mechanism of nitrate loss. The remaining loss occurs in the storage zone where possible mechanisms include microbial uptake and nitrate reduction. In contrast, similar analyses indicate that phosphate loss occurs only in the main channel ($\lambda_s = 0$). OTIS thus provides a framework for quantifying the processes that control nutrient concentrations in Green Creek.

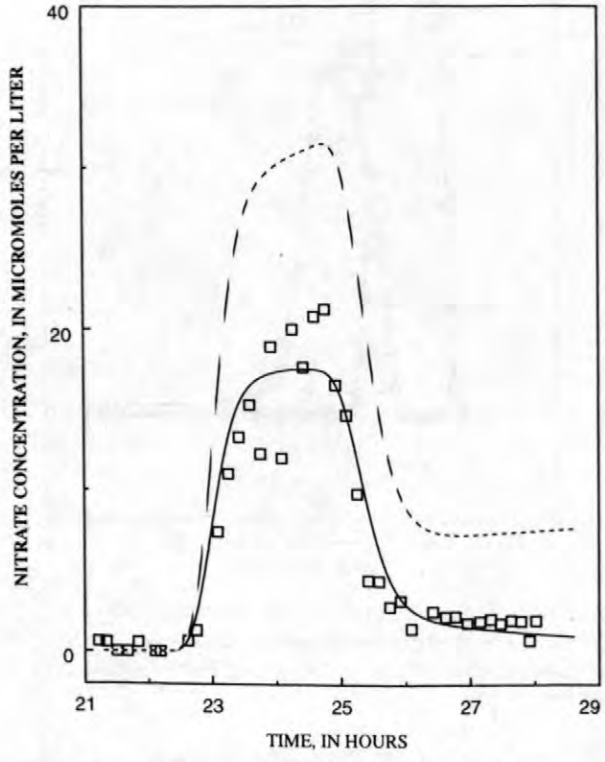

Figure 4. Observed (symbols) and simulated nitrate concentrations in Green Creek, Antarctica, 226 m from the injection point. Simulation results are shown for conservative transport (dashed line) and first-order loss (solid line).

Trace Metal Removal (OTIS and OTEQ)

In addition to the time-variable simulations shown in the previous examples, OTIS may be used to determine the steady-state solute concentrations that result from a constant loading scenario. In this application, we consider the spatial concentration profile of dissolved iron in a small stream. The stream is Saint Kevin Gulch, a headwater stream in the Rocky Mountains of Colorado. Saint Kevin Gulch receives acidic, metal-rich waters from a series of springs that emanate from the toe of a large mine dump. Instream metal concentrations increase and pH levels decrease in the vicinity of the dump. Kimball and others (1991) described a synoptic study conducted in August 1986. During the study, water samples were collected at numerous instream locations and the metal-rich springs. Figure 5 depicts the observed profile of dissolved iron concentration. Two features of the spatial profile are of interest. First, a large increase in dissolved iron occurs at about 400 m; a second feature is the abrupt decrease in dissolved iron concentration below 500 m. The purpose of this application is to quantify the processes responsible for the changes in dissolved iron concentration.

The first step in the analysis is to define the hydrology of the system. Broshears and others (1993) describe the addition of a conservative tracer that coincided with the synoptic study. Data from the tracer addition is used to determine the flow rates and the hydrologic parameters. Observed data from the springs are used to set the lateral inflow concentrations, C_L. OTIS is then used to develop a spatial profile under the assumption that dissolved iron is conservative (nonreactive). Results from this simulation are shown in figure 5 (thick solid line). The close correspondence between observed and simulated iron concentrations in the upper portions of Saint Kevin Gulch (0-500 m) indicates that the initial increase in iron is due to strictly hydrologic factors; that is, iron loading from the metal-rich springs. Simulated iron concentrations decrease downstream after 500 m due to the addition of water from a relatively dilute tributary, but do not match the decrease in the observed data. This discrepancy indicates that chemical reactions affect dissolved iron concentrations below 500 m.

A simple approach to quantifying the chemical reactions is to determine the first-order rate at which iron is lost from the system. Here we use OTIS-P to estimate a first-order decay coefficient for the main channel (λ). A first-order decay rate of 1×10^{-4} /s results in the simulated profile shown in figure 5 (thin solid line). Although the decay-rate approach yields an excellent fit to the data, it provides little insight into the mechanisms responsible for the iron loss. Inspection of the spatial pH profile indicates an increase in pH after 500 m that could result in the precipitation of hydrous iron oxides (pH= 3.3 and 4.0 at 464 and 526 m, respectively). To investigate this possibility, a steady-state OTEQ simulation was conducted. Because OTEQ uses the geochemical data base of MINTEQ, precipitation of ferrihydrite [$Fe(OH)_3$] may be explicitly modeled. OTEQ results reflecting ferrihydrite precipitation are shown as a dashed line in figure 5. These results support the hypothesis that iron is precipitating below 500 m.

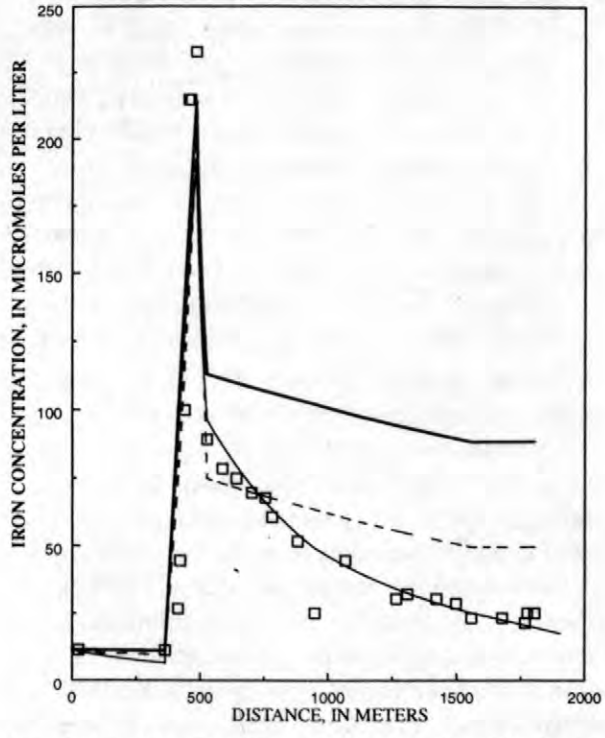

Figure 5. Observed (symbols) and simulated iron concentrations in Saint Kevin Gulch, Colorado. Simulation results are shown for conservative transport (thick solid line), first-order loss (thin solid line) and ferrihydrite precipitation (dashed line).

pH-Dependent Sorption (OTEQ)

OTEQ may also be used to simulate the time-variable behavior of trace metals and pH. As

described by Broshears and others (1996), a pH-modification experiment was conducted at Saint Kevin Gulch to determine the effects of pH variation on trace-metal chemistry. During the experiment, a concentrated solution of sodium carbonate was injected to increase instream pH. Instream pH increased to 4.0-4.2 during the initial step of the injection and 5.0-5.8 during the second step. This increase in pH resulted in decreased concentrations of dissolved iron, aluminum, and copper. Model simulations by Broshears and others (1996) indicate that changes in dissolved iron and aluminum are attributable to the precipitation and dissolution of hydrous metal oxides. In this section we extend the work of Broshears and others (1996) to consider the effects of the pH modification on dissolved copper.

As shown in figure 6, dissolved copper concentrations decreased during the second step of the pH modification experiment. Several characteristics of the data point to specific mechanisms responsible for the loss of dissolved copper. First, formation of copper precipitates is unlikely given the observed pH. Second, total water-borne copper concentrations exceed dissolved concentrations, indicating the presence of particulate copper in the water column. The concurrent presence of particulate iron indicates the possibility of sorption to iron oxides. Finally, the decrease in total copper indicates sorption by the iron-oxide coated streambed.

Given these observations, OTEQ was used to simulate the sorption of copper onto freshly precipitated hydrous ferric oxide (HFO) in the water column and aged HFO on the streambed. In the simulation, sorption reactions between dissolved copper and HFO were governed by the generalized two layer model (Dzombak and Morel, 1990) as implemented within the equilibrium submodel. Simulation of copper sorption requires the specification of several parameters to characterize the sorptive surfaces and sorption reactions. Except where noted below, parameters were set to the recommended values given by Dzombak and Morel (1990). Exceptions included the site density associated with freshly precipitated HFO (set at the maximum value reported by Dzombak and Morel, 1990), the surface complexation constant for copper sorption onto fresh HFO (set at the reported maximum), and the surface complexation constant for sorption onto aged HFO (set below the reported minimum). These deviations from the recommended values were made so that copper was preferentially sorbed to freshly precipitated HFO.

Simulation results are shown in figure 6. Simulated and observed concentrations of dissolved copper are in close agreement immediately following the second pH step. Simulated values generally exceed observed concentrations during the latter part of the pH modification. As the pH modification was discontinued, desorption of copper produced a spike that was in excess of pre-injection copper levels. This spike is accurately reproduced by the simulation. The simulation's failure to reproduce the copper loss during the latter part of the pH modification is attributable to errors in modeling pH. As noted by Broshears and others (1996), a number of issues make concurrent simulation of iron and aluminum precipitation and pH a difficult task. In the work presented here we have made no attempt to improve the simulations of Broshears and others (1996). Simulation of pH therefore underestimates observed pH by 0.1-0.4 units. Given this increment in pH, closer agreement between observed and simulated copper would be obtained. Despite this shortcoming, the OTEQ simulation reproduces the general features of the observed data. OTEQ's ability to consider pH-dependent processes such as precipitation and sorption provides a process-based approach for the study of trace metal fate and transport.

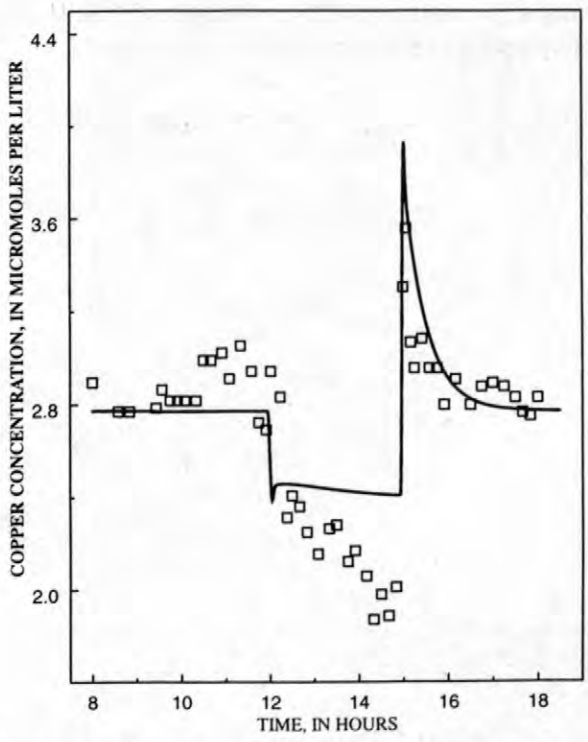

Figure 6. Observed (symbols) and simulated (solid line) copper concentrations in Saint Kevin Gulch, Colorado, 24 m from the injection point.

SOFTWARE AVAILABILITY

The OTIS solute transport model has been documented by Runkel (1998) and is available for public use. Executable versions of the model, source code and sample input files are available at `http://webserver.cr.usgs.gov/otis`. A similar software package for OTEQ will be made available after development of user documentation.

REFERENCES

Allison, J.D., Brown, D.S., and Novo-Gradac, K.J., 1991, MINTEQA2/PRODEFA2, a geochemical assessment model for environmental systems—Version 3.0 User's manual: Washington, D.C., U. S. Environmental Protection Agency, 106 p.

Ball, J.W., Runkel, R.L., and Nordstrom, D.K., 1999, Reactive transport modeling of iron and aluminum from Summitville, Colorado: Preliminary results from the application of OTIS/OTEQ to the Wightman Fork/Alamosa River system, Morganwalp, D.W., and Buxton, H.T., eds., U.S. Geological Survey Toxic Substances Hydrology Program--Proceedings of the Technical Meeting, Charleston, South Carolina, March 8-12, 1999--Volume 1--Contamination from Hardrock Mining: U.S. Geological Survey Water-Resources Investigations Report 99-4018A, this volume.

Bencala, K.E., 1983, Simulation of solute transport in a mountain pool-and-riffle stream with a kinetic mass transfer model for sorption: Water Resources Research, v. 19, no. 3, p. 732-738.

Bencala, K.E., and Walters, R.A., 1983, Simulation of solute transport in a mountain pool-and-riffle stream—A transient storage model: Water Resources Research, v. 19, no. 3, p. 718-724.

Broshears, R.E., Bencala, K.E., Kimball, B.A., and McKnight, D.M., 1993, Tracer-dilution experiments and solute-transport simulations for a mountain stream, Saint Kevin Gulch, Colorado - U.S. Geological Survey Water-Resource Investigations Report 92-4081, 18 p.

Broshears, R.E., Runkel, R.L., and Kimball, B.A., 1995, Interpreting spatial profiles of concentration in acid mine drainage streams, *in* Hotchkiss, W.R., Downey, J.S., Gutentag, E.D., and Moore, J.E., eds., Water resources at risk, Denver, Colo.: Minneapolis, Minn., American Institute of Hydrology, p. LL-10-21.

Broshears, R.E., Runkel, R.L., Kimball, B.A., McKnight, D.M., and Bencala, K.E., 1996, Reactive solute transport in an acidic stream: Experimental pH increase and simulation of controls on pH, aluminum and iron: Environmental Science and Technology, v. 30, no. 10, p. 3016-3024.

Dzombak, D.A., and Morel, F.M.M., 1990, Surface complexation modeling, Hydrous ferric oxide: New York, John Wiley, 393 p.

Harvey, J.W., and Fuller, C.C., 1998, Effect of enhanced manganese oxidation in the hyporheic zone on basin-scale geochemical mass balance: Water Resources Research, v. 34, no. 4, p. 623-636.

Kimball, B.A., Broshears, R.E., Bencala, K.E., and McKnight, D.M., 1991, Comparison of rates of hydrologic and chemical processes in a stream affected by acid mine drainage, *in* Mallard, G.E., and Aronson, D.A., eds., U.S. Geological Survey Toxic Substances Hydrology Program—Proceedings of the technical meeting,

Monterey, California, March 11-15, 1991: U.S. Geological Survey Water-Resources Investigations Report 91-4034, p. 407-412.

Laenen, Antonius, and Risley, J.C., 1997, Precipitation-runoff and streamflow-routing model for the Willamette River Basin, Oregon: U.S. Geological Survey Water-Resources Investigations Report 95-4284, 252 p.

McKnight, D.M., and Duff, J., 1995, Hyporheic zone interactions controlling nutrient uptake by algal mats in an Antarctic stream, 1995 Fall Meeting of the American Geophysical Union, San Francisco, Calif., December 11-15, 1995: Eos Transactions, AGU Fall Meeting Supplement, v. 76, no. 46, p. 226.

Morrice, J.A., Valett, H.M., Dahm, C.N., and Campana, M.E., 1997, Alluvial characteristics, groundwater-surface water exchange and hydrological retention in headwater streams: Hydrological Processes, v. 11, p. 253 - 267.

Runkel, R.L., 1998, One-dimensional transport with inflow and storage (OTIS) - A solute transport model for streams and rivers: U.S. Geological Survey Water-Resources Investigations Report 98-4018, 73 p.

Runkel, R.L., and Bencala, K.E., 1995, Transport of reacting solutes in rivers and streams, *in* Singh, V.P., ed., Environmental Hydrology: Dordrecht, The Netherlands, Kluwer Academic Publishers, p. 137-164.

Runkel, R.L., Bencala, K.E., Broshears, R.E., and Chapra, S.C., 1996a, Reactive solute transport in streams, 1. Development of an equilibrium-based model: Water Resources Research, v. 32, no. 2, p. 409-418.

Runkel, R.L., McKnight, D.M., and Andrews, E.D., 1998, Analysis of transient storage subject to unsteady flow - Diel flow variation in an Antarctic stream: Journal of North American Benthological Society, v. 17, no. 2, p. 143-154.

Runkel, R.L., McKnight, D.M., Bencala, K.E., and Chapra, S.C., 1996b, Reactive solute transport in streams, 2. Simulation of a pH modification experiment: Water Resources Research, v. 32, no. 2, p. 419-430.

AUTHOR INFORMATION

Robert L. Runkel, U.S. Geological Survey, Denver, Colorado (runkel@usgs.gov)

Kenneth E. Bencala, U.S. Geological Survey, Menlo Park, California

Briant A. Kimball, U.S. Geological Survey, Salt Lake City, Utah

Theory and(or) Reality: Analysis of Sulfate Mass-Balance at Summitville, Colorado, Poses Process Questions About the Estimation of Metal Loadings

By Kenneth E. Bencala and Roderick F. Ortiz

ABSTRACT

Characterization of in-stream metal loading from acid mine drainage includes identification of location, discharge, and solute concentrations of inflows to the stream. In using the tracer injection and synoptic sampling method we recognize that drainage from a mine site enters a stream through distributed, dispersed, and ill-defined inflows. The veracity of the method relies upon implicit assumptions related to catchment hydrology, stream hydraulics, and chemical reactivity. As a practical examination of methodology, we analyzed the ambient sulfate data collected during a metal loading characterization of the inactive mine site at Summitville, Colorado. This analysis may be thought of as a 'successive mass-balance comparison.' The results lead us to pose the following issues which can be addressed in further study at acid mine drainage sites:

1. Catchment hydrology: Will extensive chemical sampling in the near-stream zone of the catchment characterize the connections between the stream and its catchment?
2. Stream hydraulics: Will the in-stream water be 'well-mixed' in the complex physical and chemical environments typical of acid mine drainage?
3. Chemical reactivity: Will the amount of sulfate removal be sufficiently slight for this constituent to be useful as an operational ambient tracer?

Although each issue is framed as a methodological issue, resolving each requires study at the process scale. Resolving each of these issues would enhance the degree of process interpretation in the characterization of metal loading using the tracer injection and synoptic sampling method.

INTRODUCTION

A set of quantitative factors influencing the impact of drainage into a stream from a mine site includes the location, discharge, and solute concentrations of inflows to the stream. Conceptually identifying these factors appears to be trivial. One might envision walking along the stream, observing the inflows, noting their location, measuring their discharge and obtaining samples for chemical analysis. In practice drainage from a mine site enters a stream through visible inflows as well as, distributed, dispersed, and ill-defined subsurface flows.

We have been using a combination of tracer injections and synoptic sampling (Kimball, 1997) as a methodology for this quantitative identification of inflow factors. Analysis of the steady tracer injection yields estimates of in-stream discharge along the stream reach of interest. Synoptic sampling of water both in the stream and in areas of visible drainage are then used, with the discharge data, to estimate mass-flow of chemical constituents in the streams and the identified inflows. Typically, the injected tracer will be one or more of the salts of chloride, bromide, sodium, or lithium (Bencala and others, 1990). Also, the ambient constituents of interest will be trace metals (Kimball, 1997) of environmental interest and the metals iron, aluminum, and manganese (Kimball and others, 1994), whose solid precipitates influence the transport of other constituents.

In this paper we analyze the ambient concentration data for sulfate. Sulfate likely is incorporated to some degree into the precipitates coating a mine drainage streambed (Kimball and others, 1994; Bigham and others, 1990, 1996). However, concentration of sulfate typically is high and relative loss in precipitates is low. Thus, while not ideally conservative, sulfate may act as a useful ambient tracer (Bencala and others, 1987 and 1990). The analysis presented is a succession (that is, moving downstream) of mass-balance comparisons in which the mass-balance of in-stream sulfate is recomputed at each sampled site. This analysis is part of an ongoing effort to assess the veracity of the field methods, specifically as the methods rely upon implicit assumptions related to catchment hydrology, stream hydraulics, and chemical reactivity. The results of the analysis lead us to pose process questions about the estimation of metal loadings.

SUCCESSIVE MASS-BALANCE COMPARISON

Kimball (1997) gives an application-oriented discussion of the 'Tracer injection and synoptic sampling method for metal loading characterization.' Underlying the development of the methodology, research investigations in two acidic and metal-enriched streams have been described in Bencala and others (1987 and 1990) and Kimball and others (1994). Following the approach discussed by Kimball(1997), we estimate in-stream discharge and constituent mass-flow (discharge times concentration) at several sites along a stream study-reach. Further, by sampling areas of visible drainage into the stream, we estimate the concentration of constituents to the stream. Thus, progressing successively from one sampled, in-stream site to the next, we can sum the mass-flow at the upstream site with the inflow between the two sites to do a mass-balance comparison with the mass-flow at the downstream site.

Sulfate Data

In this paper, we do the successive mass-balance comparison on the sulfate data collected during a metal loading characterization in Wightman Fork adjacent to the inactive mine site at Summitville, Colorado. The in-stream discharges were estimated from injected chloride tracer data. The study reach for analysis in this paper was 1,748 meters in length, with discharge increasing from 4.6 L/s to 28.0 L/s along this reach and ten sampled, in-stream sites. Nine areas of visible drainage into the stream also were sampled, which correspond to the nine subreach intervals bracketed by the in-stream sites. The estimated discharges from these effective inflows ranged from a slight seepage of 0.1 L/s up to a well-defined tributary with a discharge of 9.9 L/s. Sulfate concentrations in the stream ranged between 48 mg/L and 341 mg/L. Sulfate concentrations in the inflows ranged between 5 mg/L and 2,428 mg/L; a range that is clearly reflective of an upland catchment environment impacted by the mine site.

Summation of Inflow Mass-Flow

Within each of the nine subreaches (delineated by up- and downstream, in-stream samples and an interspersed inflow sample) the downstream sulfate mass-flow was compared to the sum of the upstream and inflow sulfate mass-flows. The maximum in-stream sulfate mass-flow was in excess of 9 g/s. Six of the mass-balance comparisons agreed to within 0.2 g/s. A major disagreement was along a 100m subreach in which sulfate mass-flow increased significantly from approximately 0.9 g/s to in excess of 7 g/s at the downstream sampling site. The in-stream discharge increased 5.1L/s within the subreach. The measured sulfate concentration of the identified inflow within the subreach was almost 2,200 mg/L. Thus the sulfate mass-flow for the inflow within the subreach was approximately 11 g/s. The summation of the upstream sulfate mass-flow in this subreach with the inflow sulfate mass-flow was approximately 12 g/s; that is, almost double the observed downstream value.

DISSCUSSION AND ISSUES FOR FURTHER STUDY

Several of the successive sulfate mass-balance comparisons agreed within 10 percent of

the maximum in-stream sulfate mass-flow. This agreement is a verification of internal consistency of the field methodology using the tracer injection and synoptic sampling to identify the inflows into the stream. These results are by no means an independent test. There were subreaches in which the mass-balance comparisons were in substantial disagreement. Such disagreements are not, in themselves, indicative of quantitative errors in estimation of in-stream discharge or the in-stream mass-flow of any constituent. Such disagreements are instructive in that they indicate issues in the field methodology for which further process study might enhance overall the estimation of metal loadings. The mass-balance computations include information about both the mass-flow of a constituent through inflows to stream and the mass-flow of a constituent within the stream channel. The interpretation of the mass-balance computations is further based on information about the conservative nature of the constituent. Below we pose, as questions, three distinct issues.

Catchment Hydrology

Will extensive chemical sampling in the near-stream zone of the catchment characterize the connections between the stream and its catchment? Much of the water in an upland stream did not enter the stream as discrete inflows. Hydrometric study of the flow of water within the catchment might include detailed mapping of the subsurface water table in selected areas. Alternatively, topographic analyses might be used to identify the likely contributing catchment source areas. Chemical sampling in the near-stream zone might most effectively be viewed as providing additional mass-balance constraints on the bounds of hydrometric interpretations.

Stream Hydraulics

Will the in-stream water be 'well-mixed' in the complex physical and chemical environments typical of acid mine drainage? Within a subreach (demarcated by an upstream and a downstream in-stream water sample) there actually will be multiple inflows and sources of solutes. In effect, an upland stream is always gaining water from the catchment (or at least exchanging water with the catchment through the hyporheic zone). Any sample of stream water might be capturing a flux of inflow water and constituents. Hydrometric and topographic study of the streambed might be used to identify sections of stream with minimal hydrologic connection to the catchment.

Chemical Reactivity

Will the amount of sulfate removal be sufficiently slight for this constituent to be useful as an operational ambient tracer? The analysis of the internal consistency presented in this paper could be extended to include analysis based on geochemical equilibrium to identify both potential over saturation of mineral phases or likely sorption reactions. The practical focus of studies in acid mine drainage has been on metal loadings. Possibly analyses of other major ions might be used in mass-balance comparisons complementing the use of sulfate.

SUMMARY

The analysis of sulfate mass-balance at Summitville, Colorado was internally consistent in several subreachs of Wightman Fork. Substantial disagreements also were shown. From these disagreements we pose issues in the field methodology for which further study might enhance the overall method. The mass-balance computations are based on information about sulfate mass-flow through inflows, sulfate mass-flow within the stream and sulfate geochemistry. Thus, issues arise in catchment hydrology, stream hydraulics, and chemical reactivity. Although each issue is framed as a methodological issue, resolving each requires study at the process scale. Resolving each of the issues would enhance the degree of process interpretation in the characterization of metal loading using the tracer injection and synoptic sampling method.

REFERENCES

Bencala, K.E., McKnight, D.M., and Zellweger, G.W., 1987, Evaluation of natural tracers in

an acidic and metal-rich mountain stream: Water Resources Research, v. 23, no. 5, p. 827-836.

Bencala, K.E., McKnight, D.M., and Zellweger, G.W., 1990, Characterization of transport in an acidic and metal-rich mountain stream based on a lithium tracer injection and simulations of transient storage: Water Resources Research, v. 26, no. 5, p. 989-1000.

Bigham, J.M., Schwertmann, U., Carlson, L., and Murad, E., 1990, A poorly crystallized oxyhydroxysulfate of iron formed by bacterial oxidation of Fe(II) in acid mine waters: Geochimica et Cosmochimica Acta, v. 54, p. 2743-2758.

Bigham, J.M., Schwertmann, U., Traina, S.J., Winland, R.L., and Wolf, M., 1996, Schwertmannite and the chemical modeling of iron in acid sulfate waters: Geochimica et Cosmochimica Acta, v. 60, p. 2111-2121.

Kimball, B.A., 1997, Use of tracer injections and synoptic sampling to measure loadings from acid mine drainage: U.S. Geological Survey Fact Sheet 245-97, 4 p.

Kimball, B.A., Broshears, R.E., Bencala, K.E., and McKnight, D.M., 1994, Coupling of hydrologic transport and chemical reactions in a stream affected be acid mine drainage: Environmental Science and Technology, v. 28, p.2065-2073.

AUTHOR INFORMATION

Kenneth E. Bencala, U.S. Geological Survey, Menlo Park, California (kbencala@usgs.gov , http://nrp.usgs.gov/nrp/proj.bib/bencala.html)

Roderick F. Ortiz, U.S. Geological Survey, Pueblo, Colorado (rfortiz@usgs.gov)

Experimental Diversion of Acid Mine Drainage and the Effects on a Headwater Stream

By Dev K. Niyogi, Diane M. McKnight, William M. Lewis, Jr., and Briant A. Kimball

ABSTRACT

An experimental diversion of acid mine drainage was set up near an abandoned mine in Saint Kevin Gulch, Colorado. A mass-balance approach using natural tracers was used to estimate flows into Saint Kevin Gulch. The diversion system collected about 85 percent of the mine water during its first year of operation (1994). In the first 2 months after the diversion, benthic algae in an experimental reach (stream reach around which mine drainage was diverted) became more abundant as water quality improved (increase in pH, decrease in zinc concentrations) and substrate quality changed (decrease in rate of metal hydroxide deposition). Further increases in pH to levels above 4.6, however, led to lower algal biomass in subsequent years (1995-97). An increase in deposition of aluminum precipitates at pH greater than 4.6 may account for the suppression of algal biomass. The pH in the experimental reach was lower in 1998 and algal biomass increased. Mine drainage presents a complex, interactive set of stresses on stream ecosystems. These interactions need to be considered in remediation goals and plans.

INTRODUCTION

Acid mine drainage has created water-quality concerns worldwide for many years. Remediation activities are currently being implemented at many sources of mine drainage with the goal of improving water quality and promoting ecological recovery in receiving streams. This report describes a study of Saint Kevin Gulch, a headwater stream near Leadville, Colorado, where mine drainage was experimentally diverted from the stream to simulate conditions that might develop following remediation of the site. The characteristics of Saint Kevin Gulch are similar to other streams that are part of the U.S. Geological Survey (USGS) Abandoned Mine Lands Initiative. The studies at Saint Kevin Gulch can be used in selecting well-informed options for remediation at many of these sites. This report describes two data sets: (1) use of a natural tracer to estimate flows associated with the diversion system, and (2) analysis of algal biomass to assess the degree of stream recovery after the diversion.

A natural tracer can be used to quantify flows that are difficult to measure directly. This method uses changes in concentrations of chemicals across inflows to estimate flow rates. Two main requirements are needed for a natural tracer approach to be effective (Bencala and others, 1987). First, the tracer chemical must behave conservatively within the stream reach of interest. Second, there must be a difference in concentration of the tracer between the stream and the inflow. The greater the difference in the concentration, the better is the resolution of the estimates of flow. Bencala and others (1987) used a natural tracer to study flows and solute transport at the confluence of an acidic and a neutral stream in Colorado. Bencala and Ortiz (1999) describe results from a natural (ambient) tracer study in Wightman Fork, a stream in south-central Colorado.

Acid mine drainage affects the aquatic biota by three main mechanisms (McKnight and Feder, 1984; Kelly, 1988): (1) acidity, (2) toxic concentrations of dissolved metals, and (3) precipitation of metal hydroxides (mainly iron and aluminum hydroxides). While many studies have described the effects of mine drainage on aquatic biota (reviewed in Kelly, 1988), information on the recovery of streams from mine drainage is

limited (Chadwick and others, 1986; Nelson and Roline, 1996).

Saint Kevin Gulch currently receives acid mine drainage from several abandoned mines in the watershed. During the summer of 1994, the USGS set up an experimental diversion at one abandoned mine site to evaluate the potential effects of remediation on water quality and biota in the stream. Metal concentrations in the stream were measured to monitor changes in water quality and to quantify inflows by use of a natural-tracer approach. Algal biomass was quantified in the experimental reach, the stream reach around which mine drainage was diverted, as an indicator of ecological recovery. Niyogi and others (in press) reported data on algal biomass from the first 3 years of this experiment. This report summarizes data for an additional 2 years.

SITE DESCRIPTION

Saint Kevin Gulch is a headwater stream in Lake County, Colorado, near the town of Leadville (fig. 1). The stream starts near the Continental Divide and flows into Tennessee Creek, which then flows into the upper Arkansas River. The stream currently receives acid drainage from two abandoned mines and several smaller seeps. This study focused on the lower mine, the Lower Griffin Tunnel, which is the main source of acidity and dissolved metals to the stream.

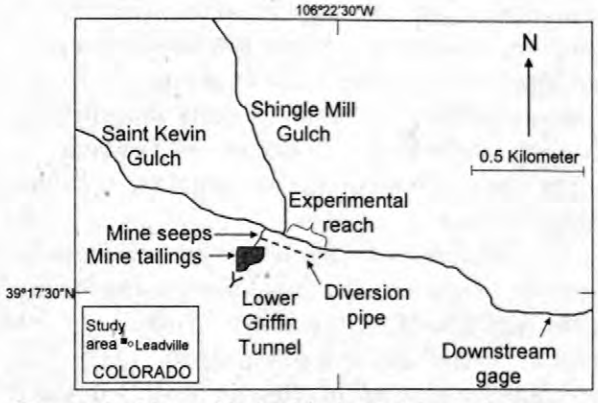

Figure 1. Map of Saint Kevin Gulch study area.

Several small seeps of acid mine drainage emanate from the base of a tailings pile at the lower Griffin mine and flow into Saint Kevin Gulch. Shingle Mill Gulch, a minimally affected tributary, joins Saint Kevin Gulch just downstream from the mine. On July 27, 1994, mine drainage from these seeps was collected into a plastic pipe and diverted to a point about 100 meters downstream from the original inflows (fig. 1). The reach between the Shingle Mill Gulch confluence and the end of the diversion pipe is referred to as the "experimental reach."

The chemistry and biology of Saint Kevin Gulch has been studied previously. Kimball and others (1994) quantified hydrologic and chemical reaction rates in the stream by use of a tracer injection experiment. Broshears and others (1996) performed an experimental addition of sodium carbonate to study chemical reactions under increased pH. McKnight (1988) and Tate and others (1995) have studied the algal communities in Saint Kevin Gulch and their interactions with phosphate.

METHODS

The natural tracer approach used in this study is based on a simple chemical mass balance. Assuming that a given solute behaves conservatively, solute mass balance is

$$C_1 Q_1 + C_t Q_t = C_2 Q_2 \qquad (1)$$

where

C_1 and Q_1 are the concentration and flow for the upstream site (upstream from tributary),

C_t and Q_t are the concentration and flow for a tributary that enters the stream, and

C_2 and Q_2 are the concentration and flow for the downstream site (downstream from tributary).

The downstream flow (Q_2) equals the two input flows (Q_1 and Q_t), assuming that there is no net loss or gain of water within the reach. Therefore,

$$C_1 (Q_2 - Q_t) + C_t Q_t = C_2 Q_2 \qquad (2)$$

Equation 2 can be used to calculate the flow of the tributary given the three concentrations of the tracer and the downstream flow. In 1994, a

gage was operated at a downstream site in Saint Kevin Gulch, about 1.2 kilometers downstream from the mine. With this measured flow and measured solute concentrations (for both stream and tributary sites), flows for tributaries into Saint Kevin Gulch were calculated successively, progressing upstream from the gage site to the mine site.

Upstream from the downstream site (and gage location), flows were calculated for the following inflows (fig. 2): (1) metal-free ground water between the end of diversion pipe and the downstream gage, (2) the flow from the diversion pipe, (3) metal-rich ground water between Shingle Mill Gulch and the diversion pipe, (4) Shingle Mill Gulch, and (5) mine drainage from the seeps (before and after setup of the collection system). The main goal was to compare the flows from the diversion pipe with the remaining ground-water inflow from the mine drainage seeps.

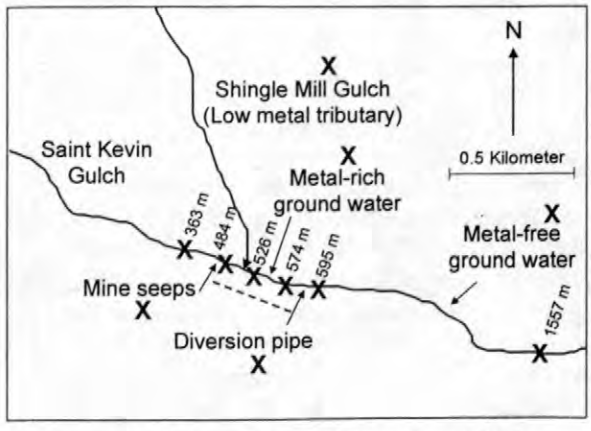

Figure 2. Sampling sites in Saint Kevin Gulch, Colo., for natural-tracer estimation of tributary flows. Arrows indicate inflows to Saint Kevin Gulch. X indicates sites used in natural-tracer estimation of flows. Saint Kevin Gulch sites are labeled as distance (in meters) from an upstream reference point.

A variety of dissolved ions were considered for use as the conservative solute in the flow calculations. Based on a review of the data and previous studies (Bencala and others, 1987; Kimball and others, 1994), dissolved manganese and zinc were selected as conservative tracers for this study. These ions are predicted to behave conservatively in the stream; that is, the ions are not subject to reactions that alter their concentrations. Some ions, such as iron and aluminum, undergo precipitation reactions in the stream and were not used for this reason. Chemical equilibrium models predict that both manganese and zinc should be present as dissolved species in the low pH waters of Saint Kevin Gulch. Moreover, other studies (Smith and others, 1991; Webster and others, 1998) have predicted that manganese and zinc ions (Mn^{2+} and Zn^{2+}) are not readily adsorbed onto suspended solids in the stream (primarily iron and aluminum hydroxides) in the low-pH waters of Saint Kevin Gulch.

Water samples were collected from sites along Saint Kevin Gulch throughout 1994 during ice-free periods (May through October). Both raw (unfiltered) and filtered (0.1 micrometer) samples were collected, acidified, and analyzed for metals by inductively coupled argon plasma atomic emission spectroscopy (Kimball and others, 1994). Samples were collected from six locations along Saint Kevin Gulch (fig. 2), from Shingle Mill Gulch, and from the outlet of the diversion pipe. Mine drainage from the seeps was assumed to have the same manganese and zinc concentration as the diversion pipe water. For the metal-rich ground water downstream from Shingle Mill Gulch, a ground-water chemistry sample was used from a previous study (B.A. Kimball, USGS, unpub. data). Finally, ground water entering Saint Kevin Gulch between the diversion pipe and the downstream gage was assumed to contain neither manganese nor zinc.

Tracer concentrations from raw and filtered samples were usually similar (within 5 percent), as expected from the chemical model predictions indicating little reactivity, as mentioned previously. For most samples, concentrations of manganese and zinc from filtered samples were used in the analyses for flow calculations. In some cases concentrations from raw samples were used because of discrepancies with the data for filtered samples resulting from possible sampling or analytical error. Flow estimates from manganese and zinc concentrations were averaged to determine the final estimate. During each sampling, flow at the end of the diversion pipe also was measured directly with a bucket and stopwatch.

The diversion was maintained during base-flow conditions from 1994 to 1998. In addition to water-quality measurements (pH, dissolved metals), the deposition rate of metal hydroxides and amount of benthic algae growing in the experimental reach were also monitored. The rate of metal hydroxide deposition was measured by placing rocks in the stream and determining the ash mass of deposited material on the rock after several weeks (see Niyogi and others [in press] for more details). Rocks were placed in riffles but not in the few pools along the stream reach. Results are presented as ash mass of material per unit area of streambed per time. Algal biomass in the experimental reach was measured during late summer base flow (early September). Detailed methods for algal sampling are presented in Niyogi and others (in press). Rocks from the stream were collected and algae were scraped off and filtered onto a glass-fiber filter. Filters and algae were extracted by use of a hot ethanol extraction, and chlorophyll-*a* content was determined (Lewis and others, 1984). Results are presented as milligrams of chlorophyll *a* per square meter of streambed.

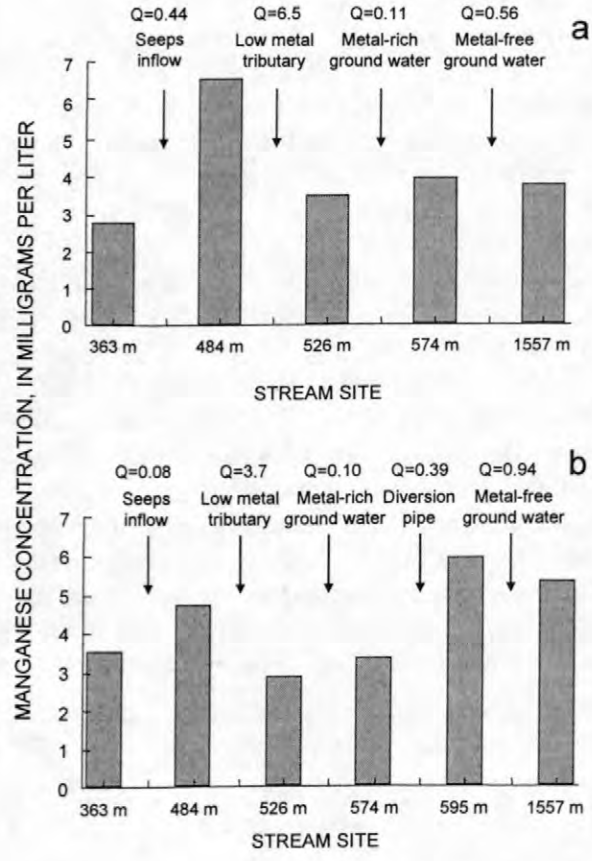

Figure 3. Downstream profile of dissolved manganese concentrations along Saint Kevin Gulch, Colo., before (a) and after (b) diversion system was established. Sites along Saint Kevin Gulch are labeled as distances, in meters, from an upstream reference point. Inflows are listed between stream sites. Estimated flows (Q) are presented in liters per second.

RESULTS

Natural Tracer Estimation of Mine Drainage Flows

Concentrations of manganese and zinc proved reliable for use as natural tracers in Saint Kevin Gulch. As an example, figure 3a shows the downstream gradient in manganese concentrations for samples collected on July 20, 1994, before the mine-drainage diversion was set up. Manganese was present at less than 3 milligrams per liter (mg/L) at a site (363 m) located just upstream from the mine tailings. The main seeps at the mine caused the stream manganese concentration to increase to more than 6 mg/L. Shingle Mill, a relatively uncontaminated tributary of similar flow to Saint Kevin Gulch, joined the stream and caused a decrease in manganese concentration to less than 4 mg/L. Metal-rich ground water then caused a slight increase in manganese concentration in the stream upstream of the diversion outflow. Finally, inflow of relatively uncontaminated ground water over the next kilometer of stream decreased the manganese concentration to 3.8 mg/L at site 1557 m.

Figure 3b shows a similar downstream gradient in manganese concentrations on September 4, 1994, after the diversion system was established. There were still some acidic inflows, through ground water, into the stream from the mine, which caused an increase in manganese concentration. The diversion pipe released the acid mine drainage between the 574 m and 595 m sites, where the manganese concentration increased from 3.3 mg/L to 5.9 mg/L. As before, ground-water inflows diluted the manganese

concentration in the stream at the downstream site (1557 m).

The estimated flows for the mine drainage seeps and diversion pipe are shown in figure 4. The earliest sampling date (May 21, 1994) had the highest flow of the mine drainage seeps, as expected, with snowmelt. Calculated flows from the diversion pipe were validated with direct measurements; estimates and direct measurements were always within 10 percent of each other. The mean percentage of mine drainage collected by the system in 1994 was 85 percent (standard deviation = 4 percent; n = 6 sampling dates).

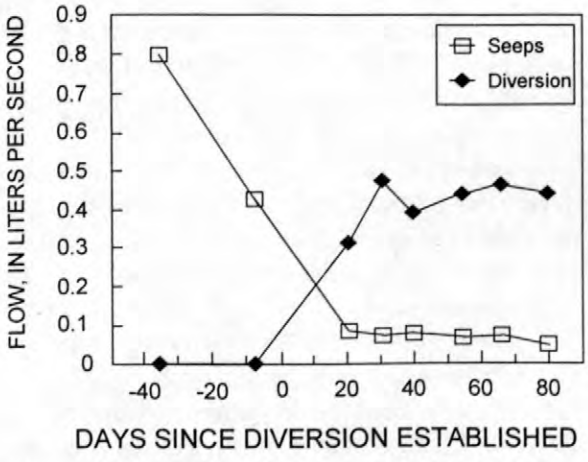

Figure 4. Estimated flows of acid mine drainage from seeps at mine and from diversion pipe. Day 0 is when the diversion system was established, July 27, 1994.

Effects of Diversion on Experimental Reach

Water quality improved substantially in the experimental reach after operation of the diversion system began. The pH and dissolved zinc concentrations for base-flow conditions (early September) from 1993 to 1998 are presented in figure 5. The pH increased from 3.7 during base flow in 1993 (prior to diversion) to 4.5 in 1994. In 1995, the pH increased to 5.4, due partly to increased flow in the stream from a large snowpack that year. The pH was about 4.9 in 1996 and 1997 and was lower (4.4) in 1998. Dissolved zinc concentrations showed a related trend. Lower concentrations of zinc were

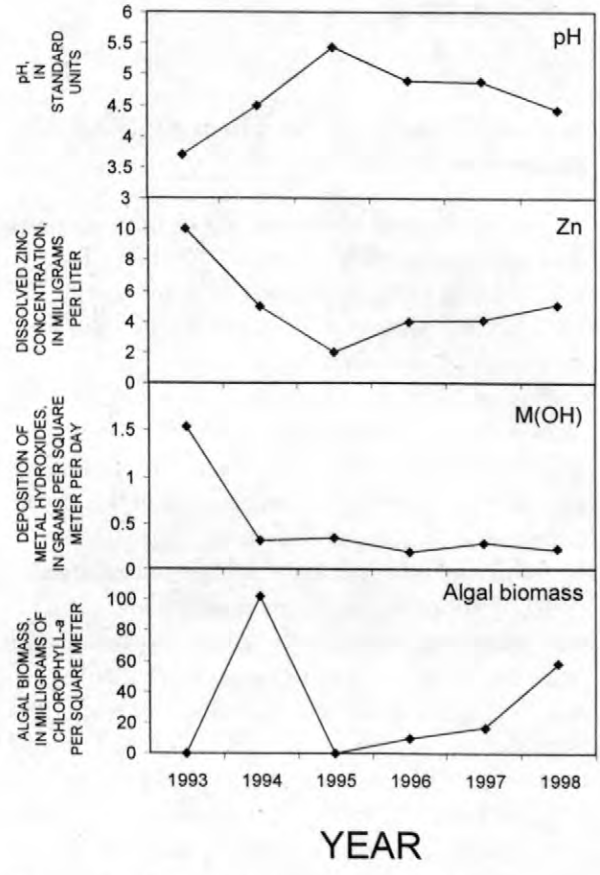

Figure 5. Characteristics of the experimental reach in the year before (1993) and the 5 years after the diversion (established in 1994). Reported values are from samples collected during late summer (early September) base flow. M(OH) refers to deposition rate of metal hydroxides.

measured after the diversion was constructed, and the lowest measured concentration was in 1995.

The deposition rate of metal hydroxides in the experimental reach decreased substantially after the diversion (fig. 5). Differences among the years after the diversion (1994 to 1998) were slight. Algae attained high biomass in 1994, more than 100 milligrams chlorophyll-*a* per square meter (mg chl *a*/m^2) just after the diversion was set up (fig. 5). During the following 3 years, however, algal biomass in the experimental reach was lower and never exceeded 20 mg chl *a*/m^2. Algal biomass was higher (62 mg chl *a*/m^2) in 1998.

DISCUSSION

Natural Tracer Estimation of Mine Drainage Flows

The natural tracer method using manganese and zinc concentrations proved feasible for determining rates for inflows to Saint Kevin Gulch. This simple mass-balance approach for estimates of flow from the diversion pipe compared well with direct measurements. However, there are two main problems in this approach as presented here. First, manganese and zinc may be reactive to some extent in the streams as opposed to being strictly conservative. Kimball and others (1994) modeled manganese concentrations in Saint Kevin Gulch and found that manganese was lost from the streamwater in one small reach. Zinc may also be slightly reactive, as the pH in the experimental reach was approaching values where zinc will sorb to metal hydroxides (Webster and others, 1998).

The second limitation of our natural tracer approach is in estimating ground-water fluxes in the downstream reach of Saint Kevin Gulch. It was assumed that this ground water contained no manganese or zinc. In reality, however, there are some seeps with significant concentrations of metals (Kimball and others, 1994). The complex spatial distribution of ground water with varying chemistry makes the resolution of these ground-water flows difficult, and estimates for these flows would be less reliable than other estimates from more discrete sources. Kimball and others (1994) reported a more intensive sampling effort designed to quantify inflows and instream reactions along Saint Kevin Gulch during a tracer injection experiment. Kimball and others (1994) overcame the limitation of a natural tracer approach by adding lithium, which is not present in significant concentrations in the stream or ground water, and by measuring dilution to calculate inflows.

The tracer aspect of the study was used to determine the percentage of mine drainage collected using a simple system of pipes and trenches. Based on six flow estimates from late summer of 1994, it is estimated that approximately 85 percent of the mine drainage from the abandoned mine was collected by the diversion system. The remaining 15 percent of the mine drainage enters the stream near the mine as subsurface flow and leaks in the diversion system.

Effects of Diversion on Experimental Reach

Before the diversion, in 1993, the reach downstream from Shingle Mill Gulch had a pH of 3.7, a zinc concentration of 10 mg/L, and a deposition rate of metal hydroxides of 1.5 grams per square meter per day ($g\ m^{-2}\ d^{-1}$). Very little algae accumulated during the summer in this reach of Saint Kevin Gulch. As expected, the diversion created an experimental reach with increased pH and lower concentrations of dissolved zinc. The experimental reach also had lower rates of metal hydroxide deposition onto the streambed (fig. 5).

Differences in the water quality of the experimental reach during the 5 years following the diversion (1994 to 1998) were observed. These differences could be due to changes in streamflow, altered water chemistry from upstream because of a treatment system at another mine in the watershed, and changes in the mine-drainage flows and collection system at the lower Griffin mine. Thus, a high flow in 1995 from a large snowpack likely caused a higher pH (5.4) and a lower concentration of dissolved zinc (2 mg/L) in the experimental reach. In 1998, low flow in the stream and an increase in uncollected flows of mine drainage likely caused a low pH (4.4) in the experimental reach.

The response of algal communities to the diversion was complex and varied from year to year. Algae attained high biomass in the experimental reach in 1994 and 1998. There was much less algal biomass in 1995, 1996, and 1997. The pH in the experimental reach was highest and zinc concentrations were lowest during 1995-97, the years with lowest algal biomass. Changes in the rate of metal hydroxide deposition during 1995-97 were modest. The rate of metal hydroxide deposition in the experimental reach was similar to that in a downstream, reference reach, which had high biomass of algae throughout the study (Niyogi and others, in press).

The main difference between the years of high accumulation of algal biomass and low accumulation was a change in the composition of metal hydroxides that were deposited onto the streambed. During 1995-97, the pH in the experimental reach increased to the point at which aluminum hydroxides or other aluminum compounds (Broshears and others, 1996) precipitated out of solution and were deposited onto the streambed (Niyogi and others, in press). Aluminum compounds, including hydroxides and other more complex compounds, typically precipitate at a pH above 4.6 (Nordstrom and Ball, 1986). In 1994 and 1998, the pH remained less than 4.6, and iron hydroxides were the predominant metal compounds deposited. During 1994-98, there were no differences in other factors that might control algal abundance, such as concentrations of nutrients or densities of grazing invertebrates (unpub. data).

It is unclear why algae in the stream (predominantly *Ulothrix* sp.) did not grow as well in areas where aluminum hydroxides were deposited (Niyogi and others, in press). Other ecological indicators, such as invertebrate communities and rates of leaf decomposition, had similar responses in the experimental reach (unpub. data). Despite the higher pH and lower zinc concentrations in the experimental reach, ecological recovery was limited by metal hydroxide deposition, including a change from iron to aluminum compounds in the deposited material. With mine drainage, improved water quality may thus lead to changes in the physical habitat that control ecological responses. Similar patterns have been seen in other streams in Colorado, such as the Snake River (McKnight and Feder, 1984), Wightman Fork, Gamble Gulch, and the Animas River (unpub. data). Other studies also have documented the physical effects of metal hydroxide deposition (Sode, 1983; Robbins and others, 1997).

The interactions between water quality and substrate quality highlight the complex effects of acid mine drainage. Metal hydroxides and other metal compounds remain soluble at low pH but precipitate at higher pH and can coat streambeds. As highly acidic waters increase in pH through buffering or dilution, a stage of precipitation and deposition of iron and then aluminum hydroxides will occur before the waters reach neutral pH. Although low pH and high concentrations of dissolved metals affect aquatic life, the deposition of metal hydroxides can result in more pronounced effects on the biomass of stream biota and ecological processes. Failure to consider the role of precipitation of metal hydroxides can prevent successful prediction of ecological recovery in streams undergoing remediation.

REFERENCES

Bencala, K.E., McKnight, D.M., and Zellweger, G.W., 1987, Evaluation of natural tracers in an acidic and metal-rich stream: Water Resources Research, v. 23, no. 5, p. 827-836.

Bencala, K.E., and Ortiz, R.F., 1999, Theory and(or) reality--Analysis of sulfate mass-balance at Summitville, Colorado, poses process questions about the estimation of metal loadings, *in* Morganwalp, D.W., and Buxton, H.T., eds., U.S. Geological Survey Toxic Substances Hydrology Program--Proceedings of the Technical Meeting, Charleston, South Carolina, March 8-12, 1999--Volume 1--Contamination from Hardrock Mining: U.S. Geological Survey Water-Resources Investigations Report 99-4018A, this volume.

Broshears, R.E., Runkel, R.L., Kimball, B.A., McKnight, D.M., and Bencala, K.A., 1996, Reactive solute transport in an acidic stream--experimental pH increase and simulation of controls on pH, aluminum, and iron: Environmental Science and Technology, v. 30, p. 3016-3024.

Chadwick, J.W., Canton, S.P., and Dent, R.L., 1986, Recovery of benthic invertebrate communities in Silver Bow Creek, Montana, following improved metal mine wastewater treatment: Water, Air, and Soil Pollution, v. 28, p. 427-438.

Kelly, M., 1988, Mining and the freshwater environment: New York, Elsevier Science Publishers, 231 p.

Kimball, B.A., Broshears, R.E., Bencala, K.E., and McKnight, D.M., 1994, Coupling of hydrologic transport and chemical reactions in a stream affected by acid mine drainage:

Environmental Science and Technology, v. 28, p. 2065-2073.
Lewis, Jr., W.M., Saunders III, J.F., Crumpacker, Sr., D.W., and Brendecke, C.M., 1984, Eutrophication and land use: New York, Springer-Verlag, 202 p.
McKnight, D.M., 1988, Metal-tolerant algae in Saint Kevin Gulch, Colorado, U.S. Geological Survey Open-File Report 87-764, p. 113-117.
McKnight, D.M., and Feder, G.L., 1984, The ecological effect of acid conditions and precipitation of hydrous metal oxides in a Rocky Mountain stream: Hydrobiologia, v. 199, p.129-138.
Nelson, S.M., and Roline, R.A., 1996, Recovery of a stream macroinvertebrate community from mine drainage disturbance: Hydrobiologia, v. 339, p. 73-84.
Niyogi, D.K., McKnight, D.M., and Lewis, Jr., W.M., in press, Influences of water and substrate quality for periphyton in a montane stream affected by acid mine drainage: Limnology and Oceanography.
Nordstrom, D.K., and Ball, J.W., 1986, The geochemical behavior of aluminum in acidified surface water: Science, v. 232, p. 54-56.
Robbins, E.I., Anderson, J.E., Cravotta, C.A., Bilger, M.D., Desmond, G.B., Earle, J.I., Flohr, M.J.K., Jordan, B.M., Krishnaswamy, Rama, Nord, G.L, Jr., Seal, R.R., II, and Snyder, C.D., 1997, AMD flocculates and precipitates--Potential for habitat destruction by sediment of a different color: U.S. Geological Survey Sediment Workshop, Harpers Ferry, W.Va., 12 p.
Smith, K.S., Ranville, J.F., and Macalady, D.L., 1991, Predictive modeling of copper, cadmium, and zinc partitioning between streamwater and bed sediment from a stream receiving acid mine drainage, Saint Kevin Gulch, Colorado, *in* Mallard, G.E., and Aronson, D.A., eds., U.S. Geological Survey Toxic Substances Hydrology Program--Proceedings of the technical meeting, Monterey, Calif., March 11-15, 1991: U.S. Geological Survey Water-Resources Investigations Report 91-4034, p. 380-386.
Sode, A., 1983, Effect of ferric hydroxide on algae and oxygen consumption by sediment in a Danish stream: Archives fur Hydrobiologia Supplement, v. 65, p. 134-162.
Tate, C.M., Broshears, R.E., and McKnight, D.M., 1995, Phosphate dynamics in an acidic mountain stream--Interactions involving algal uptake, sorption by iron oxide, and photoreduction: Limnology and Oceanography, v. 40, p. 938-945.
Webster, J.G., Swedlund, P.J., and Webster, K.S., 1998, Trace metal adsorption onto an acid mine drainage iron(III) oxy hydroxy sulfate: Environmental Science and Technology, v. 32, no. 10, p. 1361-1368.

AUTHOR INFORMATION

Dev K. Niyogi, U.S. Geological Survey, Denver, Colorado, and University of Colorado, Boulder, Colorado (niyogi@colorado.edu)

Diane M. McKnight and William M. Lewis, Jr., University of Colorado, Boulder, Colorado

Briant A. Kimball, U.S. Geological Survey, Salt Lake City, Utah

Considerations of Observational Scale when Evaluating the Effect of, and Remediation Strategies for, a Fluvial Tailings Deposit in the Upper Arkansas River Basin, Colorado

By Kathleen S. Smith, Katherine Walton-Day, and James F. Ranville

ABSTRACT

We examined the water-quality effects of a fluvial tailings deposit along the flood plain of the upper Arkansas River south of Leadville, Colorado. Fluvial tailings deposits are a possible diffuse source of acid and metal contamination to surface and ground water. We used four different scales of observation to evaluate the potential effect of fluvial tailings on water quality. First, we collected surficial material and subjected it to batch water-leaching tests. Second, we excavated an intact 8-inch-diameter (60 centimeters in length) core, leached it under unsaturated conditions for 23 days, and collected the effluent. Third, we examined the water quality of the shallow ground water beneath the fluvial tailings deposit; and fourth, we monitored water quality along a 5-kilometer reach of the adjacent Arkansas River. Our results illustrate the importance of observational scale in the interpretation of the effect of the fluvial tailings deposit on water quality. Leaching of surficial samples indicates that there is a large reservoir of readily water-soluble material yielding elevated metal concentrations and high acidity that could degrade water quality. However, the river-water-quality data indicate that there is no measurable effect from the fluvial tailings deposit. It is important to note that this data set does not include any stormwater sampling. Natural attenuation processes (including dilution) appear to contribute to our different findings at different observational scales. Attention to the importance of observational scale can lead to informed remediation decisions.

INTRODUCTION

The flood plain of the upper Arkansas River south of Leadville, Colorado, contains numerous deposits of tailings from historical mining operations in the Leadville area (URS Operating Services, 1997). These deposits are a possible source of acid and metal contamination to surface and ground water. Our study site is at one of these fluvial tailings deposits, approximately 13 kilometers south of Leadville (fig. 1). The size of the site is about 0.1 square kilometer (km^2), and it is virtually devoid of living vegetation.

The fluvial tailings deposits are generally fine-grained overbank and pointbar deposits containing mixtures of tailings and other sediment. Cored material from the deposits is usually extremely heterogeneous. At our study site, the top of the fluvial tailings deposit commonly consists of a fine-grained pyrite-rich layer, the middle portion of the deposit is clay-rich with sand and silt lenses, and the bottom contains an organic-rich layer underlain by a sand and gravel shallow aquifer. The dominant minerals are quartz, feldspar, and mica.

We used four different approaches and observational scales to study and evaluate the effects of fluvial tailings on water quality at the study site. First, we collected surface and near-surface material from the fluvial tailings deposit and subjected it to batch water-leaching tests. Second, we excavated an intact 8-inch-diameter core from the deposit and determined its leaching behavior under unsaturated conditions. Third, we installed shallow ground-water wells at the site and collected ground-water-quality samples. Finally, we collected water-quality samples along a 5-kilometer reach of the adjacent Arkansas

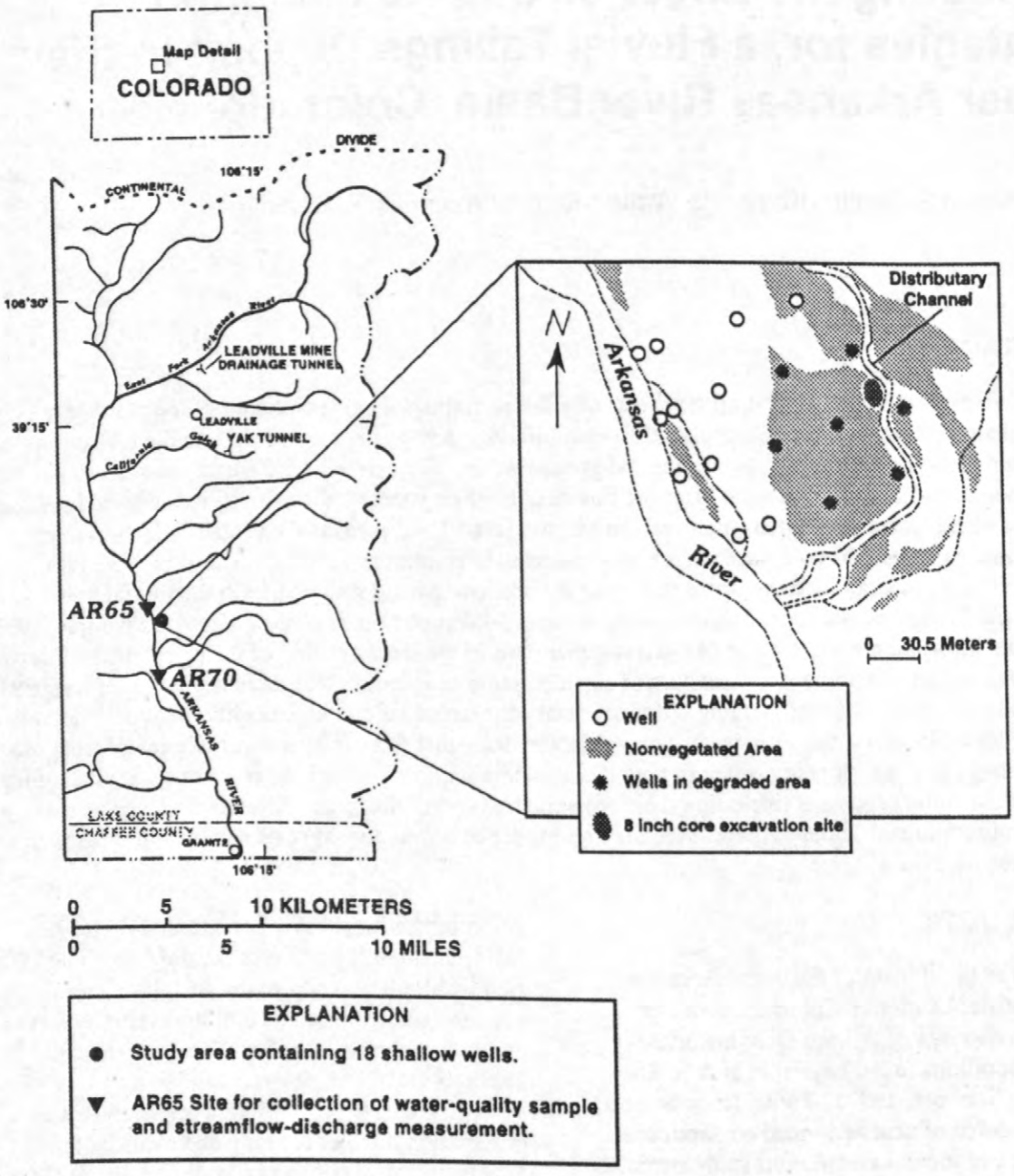

Figure 1. Schematic of the study site showing the main study area where shallow ground water wells were installed and surficial materials collected. Also shown are the excavation site of the 8-inch-diameter core, and the upstream and downstream sampling sites along the Arkansas River.

River. These four approaches represent different scales of observation of the potential effect of the fluvial tailings on water quality. In this paper, we compare results and interpretations among these different scales of observation. Related work at this study site is reported by Walton-Day and others (1996), Jerz (1998), and Smith and others (1998b, 1999).

METHODS

Collection and Leaching of Surficial Fluvial Tailings-Deposit Material

We used a one-inch stainless steel soil corer with plastic liners to collect five cores at the site. After air drying the cores, we separated the cored material into visually distinct stratigraphic segments on the basis of color and textural differences. Data for the top segments are given in this paper (top segments ranged from 5 to 15 centimeters [cm] in length). Batch water leaches of core segments were performed by combining 2 grams of sample with 40 grams of deionized water and shaking the mixture for 3 hours. After shaking, pH measurements were made and the leach suspension filtered through 0.45-µm (micrometer) filters. Filtered leachates were acidified with nitric acid and analyzed by inductively coupled argon plasma - mass spectroscopy (ICP-MS). A more detailed description of the collection and leaching methods is contained in Smith and others (1998b).

Collection and Leaching of an Intact 8-Inch-Diameter Core

An 8-inch-diameter core was excavated intact from the bank of a distributary channel that cuts through the fluvial tailings deposit (fig. 1). A clear polymethylmethacrylate tube was placed on top of the bank. The fluvial tailings around the tube were slowly excavated and the tube pushed down to encase the remaining material. The process was repeated until the shallow aquifer material was reached (approximately 60 cm of overlying material). The bottom of the tube was fitted with a polyvinylchloride (PVC) cap and the joint sealed with silicone cement. The cap contains sampling ports designed to separate water draining along the interface between the cored material and the inner edge of the tube from water draining through the center part of the core (center port). Deionized water was applied to the top of the core at a rate of 2 mL/min (milliliters per minute) by using a peristaltic pump. The deionized water was allowed to drain by gravity through the core. Effluent was collected from the center port at the bottom of the core at various times. Forty sequential effluent samples were collected under unsaturated conditions over a 23-day period. Specific conductance and pH measurements were made on the effluents, and a portion of the unfiltered effluents was acidified with nitric acid and analyzed by ICP-MS. A more detailed description of the core leaching method is in Smith and others (1999).

Installation and Sampling of Shallow Ground-Water Wells

Eighteen shallow ground-water wells were installed in a grid throughout the study area (see fig. 1). The 3.8-cm-diameter wells were designed to contain a screened interval within the zone of shallow water-table fluctuation. The annulus of each well was filled with sand to a depth approximately 15 cm above the screened interval. The annular fill of each well was completed with a bentonite seal topped by concrete containing a 7.5-cm-diameter PVC collar. The wells were developed by repeated surging and pumping until the well water was visibly clear. Prior to water-quality sampling, the wells were pumped until at least three well volumes of water had been pumped and pH and specific conductance remained steady. Values of pH and specific conductance were determined using a Hydrolab multiparameter sampling probe installed in a flow-through cell downstream from the peristaltic pump. Unfiltered samples were collected and acidified with concentrated nitric acid to pH less than 2.0 and analyzed by inductively coupled argon plasma - atomic emission spectroscopy (ICP-AES). All equipment that contacted sample water was cleaned using the procedure described by Horowitz and others (1994).

River Sampling

Water-quality samples were collected and streamflow discharge measurements made at two sites along the upper Arkansas River that were upstream and downstream from the study site. Sampling at each site was conducted from a bridge so that a composite water-quality sample could be obtained across the entire stream width and depth using the equal-width increment sampling technique (Shelton, 1994). Standard USGS (U.S. Geological Survey) techniques were used to collect water-quality samples and to conduct streamflow-discharge measurements (Rantz and others, 1982a, 1982b; Shelton, 1994). Field parameters, such as pH and specific conductance, were measured using a Hydrolab multiparameter sampling probe. Unfiltered samples were acidified with concentrated nitric acid to pH less than 2.0 and analyzed by ICP-AES. All equipment that contacted sample water was cleaned using the procedure described by Horowitz and others (1994). Instantaneous mass loads were computed for several elements and compared along the river reach. An instantaneous load for a particular element is the product of concentration and streamflow discharge and is expressed in units of mass per unit of time.

WATER-QUALITY RESULTS AT DIFFERENT OBSERVATIONAL SCALES

Average values for water-quality constituents and properties are presented in table 1 for the different scales of observation. Results for unfiltered samples are reported for core effluent, shallow ground water, and river water. Unfiltered samples represent the total amount of metal present in a given medium. More detailed results can be found in Smith and others (1998b, 1999) and Walton-Day and others (1996). A brief discussion of the interpretation for each observational scale follows.

Leachates of Surficial Fluvial Tailings-Deposit Material

Leaching of the surficial fluvial tailings-deposit material produces elevated metal concentrations and a median pH value of 2.3 (table 1). These results indicate that waters draining from the fluvial tailings deposit should degrade the quality of receiving waters. Maximum degradation would likely be from surface runoff and subsurface flow following snowmelt and periodic rainfall.

Effluents from Cored Fluvial Tailings-Deposit Material Under Unsaturated Conditions

Effluents obtained by leaching an 8-inch-diameter core with deionized water contained elevated metal concentrations and pH values ranging from 2.8 to 3.5. Results presented in table 1 represent average metal concentrations of 40 samples collected under unsaturated leaching conditions of the core over a period of approximately 23 days. Most metals exhibit a large spike in concentration early in the leaching process followed by a gradual decrease in concentration (Smith and others, 1999). The elevated metal concentrations and acidity released from the core indicate that uncontaminated shallow ground water should be degraded by infiltration of water through the tailings. Average iron and lead concentrations are higher in the most degraded shallow ground-water wells than in the core effluent (table 1).

Shallow Ground Water

The quality of shallow ground water beneath the fluvial tailings deposit is clearly degraded by the overlying tailings, as exhibited by depressed pH values (pH less than 3.0 in as many as four wells) and elevated specific conductance and unfiltered metal concentrations in some wells. Shallow ground-water quality shows some seasonal variability that affects the number of wells exhibiting degradation of water quality. Degradation of most water-quality constituents and properties is geographically restricted to wells located directly beneath tailings deposits (seven wells). Table 1 presents results for these wells and for all 18 wells. Zinc contamination is most pervasive and is present in almost all wells. At this scale of observation, degraded water quality is demonstrated in the shallow ground water, but no conclusions can be drawn about the adjacent river water.

Table 1. Average values and ranges of various constituents and properties in 20:1 water leachates of surficial material, core effluent, shallow ground water for 7 wells in the most degraded area, shallow ground water for all 18 wells, and adjacent river water [pH values are median values; n, number of measurements; ND, not determined; µS/cm, microsiemens per centimeter; µg/L, micrograms per liter; mg/L, milligrams per liter; <, less than].

Constituents and properties	Surficial leachate	Core effluent	Ground water (7 wells)	Ground water (18 wells)	River water
pH					
n	5	40	34	85	58
range	2.1 - 2.9	2.8 - 3.5	2.3 - 6.1	2.3 - 8.1	7.2 - 8.2
median value	2.3	2.9	3.3	6.0	7.8
Specific conductance (µS/cm)					
n	ND	40	34	85	57
range	ND	1,560 - 3,480	210 - 2,760	90 - 2,760	79 - 230
average value	ND	2,530	850	500	150
Cadmium (µg/L)					
n	5	40	39	97	4
range	22 - 280	250 - 4,000	< 5 - 410	< 5 - 410	< 5 - 6
average value	95	1,520	55*	32*	< 5
Copper (µg/L)					
n	5	40	39	97	60
range	120 - 1,400	240 - 1,860	< 50 - 1,150	< 50 - 1,150	< 50
average value	570	940	120#	65#	< 50
Iron (mg/L)					
n	5	40	39	97	60
range	3.6 - 490	0.89 - 35	0.050 - 112	< 0.02 - 110	0.27 - 4.0
average value	180	16	24	10+	1.0
Lead (µg/L)					
n	5	40	39	97	38
range	140 - 3,500	40 - 96	< 5 - 2,100	< 5 - 2,100	6.0 - 120
average value	1,660	68	170*	74*	25
Manganese (mg/L)					
n	5	40	39	97	60
range	0.23 - 4.1	0.23 - 8.7	0.011 - 7.0	< 0.005 - 12	0.076 - 0.97
average value	1.2	2.3	1.6	1.6*	0.27
Zinc (mg/L)					
n	5	40	39	97	60
range	2.1 - 34	6.2 - 170	0.016 - 29	0.016 - 29	0.085 - 0.99
average value	11	62	4.8	3.4	0.31

* Detection limit = 5 µg/L; substituted 2.5 µg/L for all samples < 5 µg/L.
\+ Detection limit = 0.020 mg/L; substituted 0.010 mg/L for all samples < 0.020 mg/L.
\# Detection limit = 50 µg/L; substituted 25 µg/L for all samples < 50 µg/L.

River Water

With the possible exception of iron on one sampling date, there is no statistical difference between instantaneous loads for unfiltered metals upstream and downstream from the study site in the upper Arkansas River Basin. In addition, pH values are circumneutral, indicating minimal to no effect from the low-pH waters. This result indicates that there is no measurable evidence that the fluvial tailings deposits are degrading water quality along this river reach. It is likely that some metals from the study site reach the Arkansas River during certain times of the year, but these metals appear to be undetectable when conventional mass-loading techniques are used. The variation in these mass-loading techniques can be as high as 20 percent. Therefore, load changes of less than 20 percent probably will not be detected. It is important to note that this data set does not include any stormwater or snowmelt sampling, so we are not able to evaluate degradation of water quality during storm events. At this scale of observation, there is no apparent effect on water quality from the fluvial tailings deposit.

REMEDIATION IMPLICATIONS AT DIFFERENT OBSERVATIONAL SCALES

High concentrations of soluble metals at tailings-deposit surfaces have been explained by precipitation of hydrated metal sulfates resulting from soil moisture that is drawn to the surface and evaporated during warm, dry periods (Nimick and Moore, 1991; Bayless and Olyphant, 1993). We collected hydrated metal sulfate salts from the surface of the fluvial tailings deposit at the study site and dissolved them in deionized water (1:20 ratio). Iron concentrations were in the 1,000's mg/L (milligrams per liter), zinc in the 10's mg/L, manganese, copper, and lead in the 1,000's µg/L (micrograms per liter), and cadmium in the 100's µg/L. Dissolution of these salts probably is the source of most of the dissolved metals and acidity in leachates of tailings material from the site. These salts may degrade water quality during storm events. Water-quality data from shallow ground-water wells indicate localized areas of elevated metal concentrations and acidity, but there does not appear to be a measurable effect on the quality of the adjacent river water. Geochemical processes in the sediment column might attenuate metals as they migrate through the fluvial tailings deposit. Some possible attenuation processes include dilution, precipitation of saturated mineral phases, sorption onto hydrated metal-oxide minerals (Smith and others, 1998a) or organic material, and precipitation of sulfide phases in the organic-rich layer.

When studies such as ours are done, observational scale affects the results and interpretation at scientific, remediation strategy, and regulatory levels. The integration of the four scales of observation indicates that natural attenuation processes, including dilution, may decrease concentrations of some metals as the scale of observation goes from surficial samples to river-water monitoring. However, looking at any of these observational scales individually would not reveal any attenuation processes.

Remediation decisions depend on observational scale and on the remediation objectives. For example, if remediation objectives and the accompanying sampling plan only encompass water quality in the Arkansas River, our results indicate that the effects of the fluvial tailings are minimal to nonexistent, and no remediation may be necessary. However, if remediation objectives include the riparian ecosystem, it is clear that the effects of the tailings material on the sediment and riverbank are extreme and that remediation is necessary to improve sediment and vegetation quality. Since we did not evaluate storm events in our study, we do not know their short-term effects on water quality.

From a regulatory point of view, it appears that water-quality effects from the fluvial tailings would not be detected by monitoring water quality in the Arkansas River (unless perhaps storm events are monitored). However, if cleanup decisions were made on the basis of evaluation of the surficial tailings-deposit material, the material may be determined to be a hazardous waste. For example, the regulatory level that determines a hazardous waste under the Resource Conservation and Recovery Act (RCRA) Toxicity Characteristic Leaching Procedure (TCLP) is 5 mg/L for lead (U.S. Environmental Protection Agency, 1986). Some of the surficial leachates approached this level in

our simple deionized water leach, and it is likely that some of these samples would exceed the regulatory level for lead in a TCLP test.

Our study illustrates that it is important to consider observational scale and remediation objectives when evaluating the effect of fluvial tailings on an ecosystem. Natural attenuation processes, including dilution, may play a role in metal transport from one observational scale to another. With an awareness of the importance of observational scale, land managers may take remediation actions that make use of the potential benefits of natural attenuation processes.

ACKNOWLEDGMENTS

We would like to acknowledge the landowner who has graciously allowed us to work on his property. Analytical chemistry was performed in the U.S. Geological Survey Mineral Resources Program Analytical Laboratories in Denver, Colorado, and at the Colorado School of Mines in Golden, Colorado. We acknowledge Monique Adams, Linda Gerner, Paul Lamothe, Allen Meier, and Frederick Rossi for their analytical assistance; Jon Evans, Philip Hageman, Eric Sampson, Michael Singleton, and Craig Walker for their field assistance; and Jeanette Jerz and Donald Macalady for their help with laboratory experiments. Stan Church and Rob Runkel provided helpful reviews of this manuscript. This work was funded through the U.S. Geological Survey Toxic Substances Hydrology Program and the U.S. Environmental Protection Agency Rocky Mountain Headwaters Mining Waste Initiative.

REFERENCES CITED

Bayless, E.R., and Olyphant, G.A., 1993, Acid-generating salts and their relationship to the chemistry of groundwater and storm runoff at an abandoned mine site in southwestern Indiana, U.S.A.: Journal of Contaminant Hydrology, v. 12, p. 313-328.

Horowitz, A.J., Demas, C.R., Fitzgerald, K.K., Miller, T.L., and Rickert, D.A., 1994, U.S. Geological Survey protocol for the collection and processing of surface-water samples for the subsequent determination of inorganic constituents in filtered water: U.S. Geological Survey Open-File Report 94-539, 57 p.

Jerz, J.K., 1998, Mechanisms of acid and metal release from a fluvial tailings deposit: Golden, Colorado School of Mines, Master's thesis.

Nimick, D.A., and Moore, J.N., 1991, Prediction of water-soluble metal concentrations in fluvially deposited tailings sediments, Upper Clark Fork Valley, Montana, U.S.A.: Applied Geochemistry, v. 6, p. 635-646.

Rantz, S.E., and others, 1982a, Measurement and computation of streamflow--v. 1, Measurement of stage and discharge: U.S. Geological Survey Water-Supply Paper 2175, p. 1-284.

Rantz, S.E., and others, 1982b, Measurement and computation of streamflow--v. 2, Computation of discharge: U.S. Geological Survey Water-Supply Paper 2175, p. 285-631.

Shelton, L.R., 1994, Field guide for collecting and processing stream-water samples for the National Water Quality-Assessment Program: U.S. Geological Survey Open-File Report 94-455, 42 p.

Smith, K.S., Ranville, J.F., Plumlee, G.S., and Macalady, D.L., 1998a, Predictive double-layer modeling of metal sorption in mine-drainage systems, *in* E.A. Jenne, ed., Adsorption of metals by geomedia: San Diego, Academic Press, p. 521-547.

Smith, K.S., Sutley, S.J., Briggs, P.H., Meier, A.L., Walton-Day, Katherine, Ranville, J.F., and Jerz, J.K., 1998b, Trends in water-leachable lead from a fluvial tailings deposit along the upper Arkansas River, Colorado: Proceedings of the Fifth International Conference on Tailings and Mine Waste '98, Fort Collins, Colorado, January 26-29, 1998, Rotterdam, A.A. Balkema, p. 763-768.

Smith, K.S., Ranville, J.F., Lamothe, P.J., Meier, A.L., and Walton-Day, Katherine, 1999, Metal leaching through a fluvial tailings deposit along the upper Arkansas River, Colorado: Proceedings of the Sixth International Conference on Tailings and Mine Waste '99, Fort Collins, Colorado, January 24-27, 1999, Rotterdam, A.A. Balkema, p. 627-632.

URS Operating Services, 1997, Sampling activities report, upper Arkansas River Fluvial Tailings, Leadville, Colorado: URS Operating Services, 73 p. plus plates.

U.S. Environmental Protection Agency, 1986, Test methods for evaluating solid waste, vol. 1 and 2 (SW-846), 3rd edition, November, 1986: U.S. Environmental Protection Agency (updates are available through Revision 2B, published April 4, 1995).

Walton-Day, Katherine, Jerz, J.K., Ranville, J.F., Evans, J.B., and Smith, K.S., 1996, Effects of fluvial tailings deposits on the quality of surface and ground water at a site in the upper Arkansas River basin, Colorado: Abstracts with Programs, Geological Society of America Annual Meeting, Denver, Colorado, October 28-31, 1996, p. A-466.

AUTHOR INFORMATION

Kathleen S. Smith and Katherine Walton-Day, U.S. Geological Survey, Denver, Colorado (ksmith@usgs.gov; kwaltond@usgs.gov)

James F. Ranville, Department of Chemistry and Geochemistry, Colorado School of Mines, Golden, Colorado (jranvill@mines.edu)

Research on Hard-Rock Mining in Arid Southwest Alluvial Basins

Hard-rock mining for copper, gold, silver, and other minerals has been an important part of the economy of the southwestern United States for more than a century. Unfortunately, historical mining practices have contaminated ground water and surface water at many abandoned and active mine sites. Leakage and runoff from unlined wastewater ponds, heap-leach areas, tailings, and other contaminant sources can migrate from areas of hard-rock mining into regional alluvial aquifers that provide the sole source of drinking water to many local communities. Contaminants may also discharge to limited surface-water supplies, either by direct runoff or by ground-water discharge to streams. The Globe-Miami Mining District in Arizona has been a major copper-producing area since the late 19th century. Past mining practices there have contaminated the regional alluvial aquifer and a perennial stream in the area with acidic, metal-laden mine wastes. The U.S. Geological Survey (USGS), in collaboration with researchers at the University of Arizona and Arizona State University, is studying this contamination with the overall objective of increasing scientific understanding of the controls on transport of metals and other inorganic contaminants. This knowledge, and new methods and models developed as part of these investigations should have considerable transfer value to other similarly contaminated sites.

Since 1984, the USGS has monitored the distribution of contaminants in the Globe area by sampling and analyzing ground water, surface water, aquifer materials, and streambed sediments. The chemical and physical processes that control contaminant movement and fate are being examined using laboratory experiments, ground-water flow models, inverse- and forward- geochemical models, stream-tracer experiments, and stream-transport modeling.

A plume of acidic, contaminated ground water is moving northward through the alluvium beneath the major stream in the basin, Pinal Creek. Acidic ground water is neutralized mainly through the dissolution of carbonate minerals. As the pH of ground water increases, the dissolved concentrations of trace metals, such as copper, cobalt, nickel, and zinc, decrease through the pH-dependent sorption to iron hydroxide (Stollenwerk, 1994). The oxidation and precipitation of iron hydroxide in the aquifer are coupled, at least in part, to the reductive dissolution of manganese oxide. Recharge to the basin is quite low in most years. Intense rainfall and (or) snowmelt in some years do result in significant recharge that contributes to substantial dilution of contaminants. Other factors that contributed to remediation of contamination was the removal in the early 1980's of the wastewater pond that was a significant source of contamination, and pumping of contaminated ground water that began in the mid 1980's. All of those factors contributed to a significant decrease in the concentrations of many of the metals; however, the pH in the acidic part of the plume remains near 4. Contaminated ground water is not in a state of geochemical equilibrium with selected solid phases in the aquifer (Stollenwerk, 1994; Brown and others, 1998). Because of this, knowledge of reaction rates is necessary to better understand the movement and fate of contaminants in the basin. One goal of laboratory and field activities is to determine appropriate site-specific rates for carbonate and manganese-oxide dissolution reactions. Preliminary results indicate that field dissolution rates of calcite were considerably lower than rates measured in laboratory experiments by other investigators. A three-dimensional ground-water flow model of the aquifer system is being developed to better understand ground-water flow patterns and interaction of ground water and surface water. The use of chlorofluorocarbon-derived ground-water ages to constrain simulated travel times and velocities should increase the accuracy and reliability of model parameter estimates. Sampling for a variety of other isotopes and dissolved gases should help to better define recharge areas and mixing of contaminated and uncontaminated ground water.

Slug tests and field investigations of ground-water and surface-water interactions should provide information on the hydraulic characteristics of discrete layers of stream alluvium and further improve the estimates of model parameters.

In the northern part of the basin, contaminated ground water discharges to Pinal Creek in the 6-km perennial reach near the downstream end of the basin (where the aquifer is truncated by impermeable rock formations). Carbon dioxide degassing to the atmosphere in the perennial reach causes the pH of surface water to rise from about 6 near the beginning of the perennial flow to about 8 near the basin outlet (Choi and others, 1998). Movement of stream water into shallow ground water beneath the channel (hyporheic zone) increases the pH and dissolved oxygen in shallow ground water, resulting in the enhancement of the precipitation of manganese oxide coatings onto streambed gravels. Enhanced precipitation of manganese oxides in the hyporheic zone cumulatively removes approximately 20 percent of the load of dissolved manganese in the stream (Harvey and Fuller, 1998). Trace metals such as nickel, cobalt, and zinc are also removed in the hyporheic zone by co-precipitation or sorption onto manganese oxides. Laboratory experiments confirmed that precipitation of manganese oxides in the hyporheic zone is microbially mediated, that microbial activity increases with increasing pH, and that higher amounts of pre-existing manganese-oxide solids increase the rate of manganese precipitation.

One goal of ongoing research is to improve the design of stream-tracer experiments to increase the reliability of those experiments as a tool to characterize rates of metal removal at various sites (Wagner and Harvey, 1997). Another goal is to use our detailed understanding of processes at Pinal Creek to develop and test improved models of surface- and ground-water interactions and chemical transport that are transferable to other areas with different physical and chemical characteristics.

References

Brown, J.G., Bassett, R.L., and Glynn, P.D., 1998. Analysis and simulation of reactive transport of metal contaminants in ground water in Pinal Creek Basin, Arizona, in Steefel, C.I., and Van Cappellen, P., Eds., Reactive Transport Modeling of Natural Systems: New York, Elsevier, Journal of Hydrology, v. 209, nos. 1-4, August 1998, p. 225-250.

Choi, J., Hulseapple, S.M., Conklin, M.H., and Harvey, J.W., 1998. Modeling CO2 degassing and pH in a stream-aquifer system, in Steefel, C.I., and Van Cappellen, P., Eds., Reactive Transport Modeling of Natural Systems: New York, Elsevier, Journal of Hydrology, v. 209, nos. 1-4, August 1998, p. 297-310.

Harvey, J.W., and Fuller, C.C., 1998. Effect of enhanced manganese oxidation in the hyporheic zone on basin-scale geochemical mass balance: Water Resources Research, v. 34, no. 4, p. 623-636.

Stollenwerk, K.G., 1994. Geochemical interactions between constituents in acidic groundwater and alluvium in an aquifer near Globe, Arizona: Applied Geochemistry, v. 9, no. 4, p. 353-369.

Wagner, B.J., and Harvey, J.W., 1997. Experimental design for estimating parameters of rate-limited mass transfer: Analysis of stream tracer studies: Water Resources Research, v. 33, no. 7, p. 1731-1741.

For additional information contact:

James G. Brown, USGS, Tucson,
Arizona (email: jgbrown@usgs.gov), or

Judson W. Harvey, USGS, Reston,
Virginia (email: jwharvey@usgs.gov)

Geochemistry and Reactive Transport of Metal Contaminants in Ground Water, Pinal Creek Basin, Arizona

James G. Brown, Pierre D. Glynn, and R.L. Bassett

ABSTRACT

Activities related to more than a century of large-scale copper mining in the Pinal Creek Basin in central Arizona have contaminated the regional alluvial aquifer and perennial streamflow with acidity and metals. Water-chemistry and solid-phase analyses and computer-aided geochemical modeling were used to understand the evolution of the ground-water plume between 1984 and 1998. The ground-water plume consists of three hydrochemical zones: (1) an acidic zone, which contains large concentrations of metals and has a pH that ranges from 3.6 to about 5; (2) a transition zone where carbonate-mineral dissolution causes pH to increase to above 5, which results in the precipitation of iron hydroxide and the adsorption of trace metals such as nickel and zinc; and (3) a neutralized zone, which contains large concentrations of manganese, calcium, and sulfate, and has a pH of about 6 to 7. Inverse geochemical modeling using NETPATH revealed that, in addition to calcite dissolution, silicate dissolution was required to account for the mass transfers of calcium and magnesium across the transition zone. Analysis of the measured changes in plume geochemistry was aided by PHREEQC reactive-transport modeling, which helped determine that oxidation-reduction reactions were significant in the acidic zone of the plume through the late 1980's. The local equilibrium assumption required by reactive-transport modeling probably was invalid for oxidation-reduction reactions that involved manganese and, to a lesser extent, neutralization reactions that involved calcite. Sensitivity analyses indicated that the rate of advance of the pH front was highly sensitive to the initial calcite concentration, and that ground water along a flow path near the base of the alluvium was in partial or indirect contact with the atmosphere, possibly through mixing with shallower water.

INTRODUCTION

Activities related to more than a century of large-scale copper mining in the Pinal Creek Basin in central Arizona (fig. 1) have contaminated the regional aquifer and perennial streamflow. Potential contaminant sources include mine tailings, unlined surface-water impoundments of mine-process water, heap-leach areas, and occasional spills of contaminated water into streambeds. Acidic ground-water contamination has a pH of about 3.6 to 5, and neutralized-contaminated water has a pH that ranges from about 6 in the aquifer to 8 in perennial streamflow. Contaminants that occur in large concentrations are iron (Fe), sulfate (SO_4), manganese (Mn), copper (Cu), cobalt (Co), nickel (Ni), zinc (Zn), and other metals. Investigations by the U.S. Geological Survey (USGS) at the site have been ongoing since 1984 and are a collaborative effort among USGS scientists and investigators at several universities.

The purpose of this paper is to give an overview of recent and ongoing ground-water investigations at the site with a focus on the results of inverse modeling and reactive-transport geochemical modeling that were used to help understand the important processes that control the movement and distribution of contaminants in ground water. Information gained from these investigations should provide insight into processes that occur at other sites similarly contaminated.

The regional aquifer includes two distinct lithologic units. The older of the two is semiconsolidated to consolidated basin fill that is Tertiary in age. The unit has a maximum thickness of more than 1,000 meters (m) and consists of conglomerates, sand, silt, and fine-grained lakebed sediments. Incised into the basin fill in the major drainages is an unconsolidated alluvium that is less than 50 m

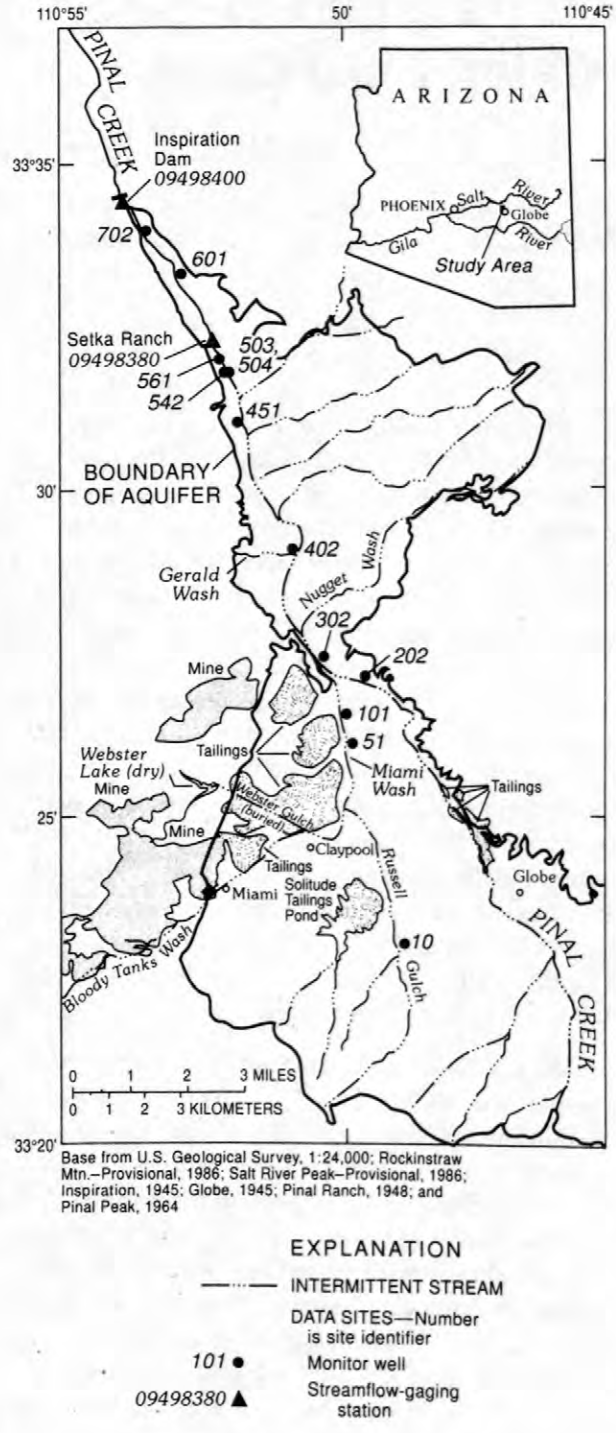

Figure 1., Pinal Creek Basin, Arizona

thick and contains more than 90 percent sand and gravel. Detailed discussions of the geology and hydrogeology of the basin have been published in Peterson (1962), Brown and Eychaner (1996), and Neaville and Brown (1994).

METHODS

From 1984 to 1996, 37 monitor wells and 6 test holes were drilled into the alluvium and shallow basin fill at 12 locations in or near contaminated areas. Aquifer materials collected at the time of drilling were analyzed by particle-size analysis, macroscopic- and microscopic-mineralogical identification (Eychaner and others, 1989), x-ray diffraction (Lind and Stollenwerk, 1996), sequential extractions (Ficklin and others, 1991a, b), column and batch experiments (Stollenwerk, 1994, 1996), and other methods. Water samples were collected from most monitor wells one or two times a year and analyzed for major ions and trace elements to characterize the distribution and movement of contaminants. Less frequently, ground water from selected wells was analyzed for stable isotopes, tritium, chlorofluorocarbons, and dissolved gases. Ongoing investigations include the examination of changes in aquifer materials that have been exposed to contaminated water in wells for periods ranging from 6 to18 months. The purpose of these investigations is to examine changes in mineralogy and the rates of selected geochemical reactions in acidic and neutralized ground water.

Several computer geochemical models have been used in the analysis of contaminant movement at the site. Stollenwerk (1994) used PHREEQE (Parkhurst and others, 1980) and MINTQA2 (Allison and others, 1980) to analyze the important reactions that controlled the evolution of the plume through the mid-1980's using laboratory batch and column experiments, and geochemical modeling. Glynn and Brown (1996) used NETPATH (Plummer and others, 1991) and PHREEQC (Parkhurst, 1995) to refine Stollenwerk's findings and examine the possible effects of reactions not considered by Stollenwerk. Brown and others (1998) used PHREEQC's transport capabilities to help examine the changes observed in the ground-water plume from 1984–94. This paper provides an overview of the analysis of Glynn and Brown (1996), extends the model of Brown and others (1998) through 1998, and summarizes the major findings.

DISTRIBUTION OF HYDROCHEMICAL ZONES IN THE AQUIFER

The ground-water plume in the Pinal Creek Basin can be separated into three major zones

(fig. 2) on the basis of aqueous and solid-phase geochemistry. An acidic zone in which the pH of the ground water was between 4 and 5 in 1998 extends from Miami Wash to well 561.

The acidic zone contains large concentrations of dissolved metals and other contaminants. In 1984, concentrations of dissolved Fe, Mn, and aluminum (Al) at well 51 were 57, 1.3, and 11.1 mmol/L, respectively (table 1). Metals, such as Cu, Co, Ni, and Zn, occurred in the acidic zone at concentrations that ranged from 0.02 to more than 2 mmol/L.

Downgradient from the acidic zone is a transition zone characterized by steep pH and redox gradients and the precipitation and adsorption of metals. In 1984, this zone was about 1.5 km south of the future location of well 451. In this zone, calcite ($CaCO_3$) and, to a lesser extent, dolomite ($CaMg(CO_3)_2$), react with and partially neutralize acidic ground water according to the reactions:

$$CaCO_3 + H^+ = Ca^{2+} + HCO_3^-,$$

and

$$CaMg(CO_3)_2 + 2H^+ = Ca^{2+} + Mg^{2+} + 2HCO_3^-.$$

Oxidation and reduction reactions are important as well. The reductive dissolution of Mn oxide is coupled to the oxidation and precipitation of Fe hydroxide (Stollenwerk, 1994). The overall reaction can be written as:

$$MnO_{2(s)} + 2Fe^{2+} + 4H_2O \rightarrow 2Fe(OH)_{3(a)} + 2H^+ + Mn^{2+}.$$

Although this last reaction produces protons, the net result of reactions in the transition zone was to raise the pH from about 5 to about 6. Metals, such as Cu, Co, Ni, and Zn, are adsorbed to Fe hydroxide and possibly other surfaces in the transition zone because of the increase in pH (Stollenwerk, 1994).

Advective flow moves through the alluvium at an average velocity of 5 meters per day (m/d), which is about 7 times the rate of movement of the acidic front (Eychaner, 1991). As a result, contaminants that remain in solution as the pH increases move beyond the transition zone into the neutralized zone (fig. 2), and eventually surface in the perennial reach of Pinal Creek. Neutralized water generally contains large concentrations of calcium (Ca), Mn, and SO_4; other contaminants, including Fe, Cu, Co, Ni, and Zn, occur at concentrations less than 1 mmol/L (table 1).

Mineral species and other solid phases in the regional aquifer were characterized by the examination and analysis of drill cores and cuttings. Calcite and Mn oxide are present in uncontaminated alluvium, the basin fill, and the neutralized zone of the plume. Sequential extractions of aquifer material and the measured water chemistry indicate that in the acidic zone of the plume most if not all the Mn oxide and carbonate minerals have been dissolved by reaction with the acidic ground-water plume. Minerals present throughout the aquifer include Fe hydroxide and the silicate minerals orthoclase and plagioclase feldspar, muscovite, biotite, and tremolite. The degree to which each reacts with contaminated ground water varies.

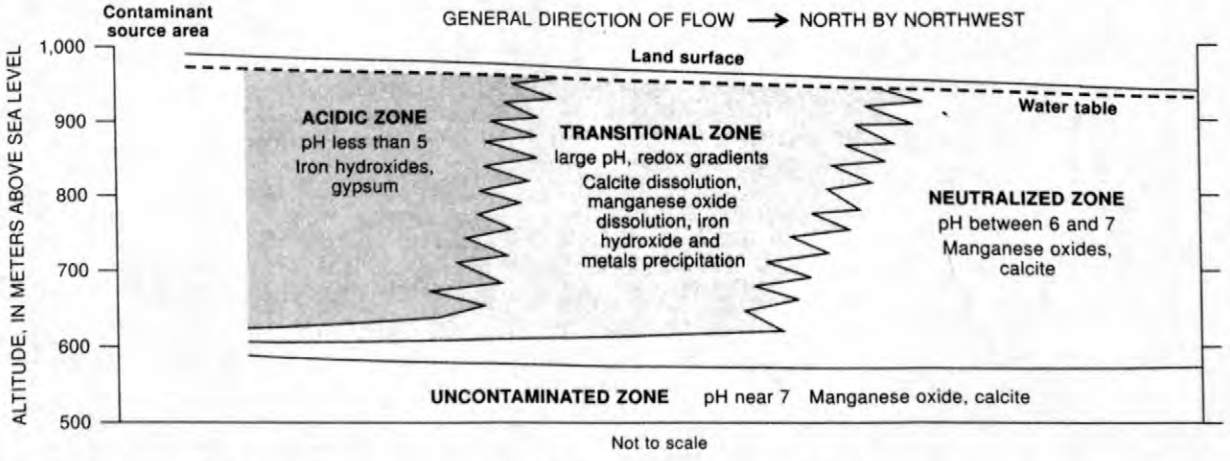

Figure 2. Generalized longitudinal section indicating hydrochemical zones in aquifer.

Table 1. Measured water chemistry and related data for water in selected wells and in streamflow, Pinal Creek Basin, 1984–97

[Values are in millimoles per liter (mmol/L) except for pH. At most locations, earliest available analysis is shown. Dashes indicate no data; km, kilometer; m, meter; <, less than; PCID, Pinal Creek at Inspiration Dam; Depth, depth of well below land surface]

Well number	Distance along flow path (km)	Date of sample	Well depth (m)	pH	Dissolved oxygen (DO as O)	Calcium (Ca)	Magnesium (Mg)	Sodium (Na)	Potassium (K)	Alkalinity	Total inorganic carbon (TIC)	Sulfate (SO_4)
51	0	11–84	33.4	3.6	<0.02	12	16	10	0.24	---	---	100
101	.7	11–84	36.1	3.6	<.02	12	12	8.3	.25	---	---	74
202[1]	---	03–85	12.3	7.2	.46	1.2	.37	.96	.036	2.3	---	.7
302	2.1	11–84	35.8	3.5	---	17	12	7.0	.21	---	---	72
402	5.8	11–84	20.9	4.2	<.02	13	5.8	3.5	.19	---	---	27
451	10.1	03–89	24.4	4.9	<.006	15	5.5	3.6	.28	---	4.7	25
503	11.4	07–86	25.3	6.2	.01	15	5.8	3.4	.11	2.0	---	21
542	11.4	05–97	19.8	4.3	.01	7.7	3.3	2.4	.16	---	1.3	14
561	11.8	05–97	15.3	5.0	.01	7.6	3.1	2.5	.17	---	1.7	13
601	14.2	11–92	8.6	6.4	.04	13	4.5	3.3	.11	2.9	---	18
702	16.3	05–90	7.3	7.0	.006	14	5.1	3.0	.16	3.5	---	18
PCID[1]	---	01–93	---	7.7	.64	1.4	.31	.33	.087	.93	---	1.5

Well number	Distance along flow path (km)	Chloride (Cl)	Fluoride (F)	Silica (Si)	Iron (Fe)	Manganese (Mn)	Aluminum (Al)	Copper (Cu)	Cobalt (Co)	Nickel (Ni)	Strontium (Sr)	Zinc (Zn)
51	0	11	---	1.7	57	1.3	11.1	2.4	0.18	0.065	0.017	0.29
101	.7	10	---	1.6	39	1.0	8.54	1.7	.14	.054	.018	.18
202[1]	---	.48	---	.36	.00072	<.0006	<.003	.00016	<.00034	<.0085	.0023	<.00023
302	2.1	8.7	---	1.8	32	1.1	6.69	1.5	.12	.051	.034	.14
402	5.8	4.0	---	1.4	6.3	.91	.409	.30	.030	.019	.020	.046
451	10.1	5.1	.53	1.1	2.5	1.9	1.53	.18	.031	.020	.018	.53
503	11.4	3.7	.021	1.0	.0032	.82	.0007	.0005	<.0007	.007	.240	.0029
542	11.4	1.3	.19	1.1	1.1	.81	.213	.075	---	.005	.013	.037
561	11.8	1.3	.25	1.1	.00016	1.0	.13	.076	.020	.012	.013	.039
601	14.2	2.4	.01	.72	.00072	.031	<.0004	<.0005	<.0002	<.0005	.024	.00038
702	16.3	2.3	.013	.46	.019	.052	.186	<.002	<.003	<.008	.027	.00026
PCID[1]	---	.11	.02	---	.0001	.00098	---	.00047	---	---	---	<.00005

[1]Not on simulated flow path.

INVERSE GEOCHEMICAL MODELING

Inverse geochemical modeling has been used at Pinal Creek to help identify and understand the important chemical reactions and physical processes that controlled the evolution of the contaminant plume. Glynn and Brown (1996) used the geochemical codes NETPATH and PHREEQC to examine some plausible reaction models that might have been responsible for the changes in ground-water chemistry that have been measured across the transition zone.

Inverse modeling uses a mass-balance approach to determine the reactions responsible for observed changes in water chemistry between two wells along a flow path. Inverse modeling requires that the system be in a chemically steady-state condition if the wells are sampled at the same time. Because contaminated ground water at the study site was not at steady state, Glynn and Brown (1998) considered the chemical changes between wells that occurred over a period of time equal to the estimated ground-water travel time between the two wells. The inverse-modeling approach also assumes that all potentially important reactions were considered and that the important existing and potential solid phases in the aquifer were known. The assumption of a steady-state flow field also is required. The computer codes do not require that the postulated reactions be thermodynamically feasible, although the thermodynamics of any postulated reaction should be considered when evaluating potential models.

Required input for inverse modeling includes chemical analyses for the selected wells, the chemical composition of solid phases (minerals or amorphous solids) and dissolved gases in the aquifer, and some knowledge about which minerals and gases have the potential to react with the ground water. NETPATH and PHREEQC allow for the initial water to be mixed with one or more waters along the flow path to produce the final water.

Glynn and Brown (1996) examined dozens of models using different combinations of plausible and not so plausible solid- and gas-phase reactants and different assumptions concerning the degree to which the flow path was in contact with gases in the unsaturated zone. Space limitations here preclude a detailed discussion of particular models. Instead, this paper focuses on the common characteristics shared by the more plausible models and will summarize major conclusions.

The analysis of Glynn and Brown (1996) considered a flow path across the transition zone from well 402 (sampled on January 12, 1989) to well 503 (sampled on November 22, 1991). Mixing with uncontaminated water along the flow path was represented by water from well 504 (sampled on November 22, 1991), which is perforated in uncontaminated basin fill. The chemical composition of water from these wells during 1989–91 was similar to that during 1984–89 (table 1); although contaminant concentrations generally decreased from 1984–89. Three minerals were required to be included in all models: calcite, geothite (FeOOH), and gypsum ($CaSO_4$).

For most models, the system was considered closed to atmospheric oxygen because the flow path across the transition zone was more than 7 m below the water table during 1989–91. Dissolved-oxygen concentrations of water from shallow wells at both sites indicated that essentially all the oxygen moving downward from the unsaturated zone into the plume was consumed near the water table. Although the well openings were not in contact with the unsaturated zone, the degassing of carbon dioxide (CO_2) was allowed in some models because CO_2 had the potential of leaving the flow path through diffusion or mixing processes.

The NETPATH models considered to be most plausible shared several characteristics—the dissolution of calcite and dolomite ($CaMg(CO_3)_2$), and the precipitation of rhodochrosite ($MnCO_3$) and gypsum. The results of the PHREEQC simulations were similar, except that accounting for analytical uncertainty (a feature unavailable in NETPATH) resulted in some significantly different results. When a 5-percent relative uncertainty was assumed for SO_4, the precipitation of gypsum was not necessary. This was because SO_4 occurred at concentrations more than 5 times that of Ca, and the uncertainties in the SO_4 concentrations were large in relation to the measured mass transfer of Ca between wells 402 and 503.

A significant conclusion from the NETPATH and PHREEQC inverse modeling was that in order to satisfy the mass-balance constraints on Ca and Mg, the dissolution of Ca-Mg silicates was required. The measured increase in dissolved strontium (Sr) along the flow path was additional evi-

dence of silicate dissolution along the flow path (Glynn, 1991). Solid-phase mass transfers of rhodochrosite and Al were significant particularly in models that allowed no CO_2 exsolution.

GROUND-WATER REACTIVE TRANSPORT, 1984–98

From 1984 to 1998, the concentrations of most contaminants in the acidic zone decreased primarily because of the drainage of an unlined surface-water impoundment that contained acidic mine-process water, other source control measures, remedial pumping that began in the mid-1980's, and recharge of uncontaminated ground water from record high streamflow in 1993. This paper focuses on the most contaminated well at each monitor well group. At each site, this generally was the well perforated closest to the contact with the alluvium and the underlying basin fill. The wells were located along, or reasonably close to, an assumed flow path near the base of the alluvium. Lithologic evidence of a boulder zone near the base of the alluvium was additional evidence that the zone near the base of the alluvium was a preferred pathway for contaminants.

A one-dimensional reactive-transport model was developed using PHREEQC (Parkhurst, 1995) to help characterize the reactions and processes that were responsible for the measured changes in plume geochemistry from 1984 to 1994 (Brown and others, 1998). Equilibrium reactive-transport modeling requires some of the same assumptions as inverse modeling. One such assumption was that the wells in the model were located along a flow path; another was that all important reactions were accounted for. Unlike inverse modeling, equilibrium reactive-transport modeling assumes that water along the flow path reacts to a local equilibrium with selected solid phases in the aquifer. As a result, some of the reactions considered for inverse modeling (silicate dissolution, for example) were not included in the reactive-transport model because these reactions were known to be slow in relation to the travel time of water through contaminated alluvium.

PHREEQC uses a mixing-cell approach (Appelo and Postma, 1993) to simulate contaminant transport. In this approach, a series of mixing cells is set up in which geochemical reactions are calculated. In this simulation, these reactions involve water, minerals, and surfaces to which selected constituents may adsorb or desorb. Before each transport step, the aqueous and solid-phase equilibrium condition is calculated. Water is then shifted to the next adjacent cell where equilibrium is then re-established through the precipitation or dissolution (if the solid phase is present) of the required solid phases. For this analysis, dispersion was simulated using the mixing option. A dispersivity of 30 m was used for this analysis on the basis of a review of field estimates of dispersivities made by Gelhar and others (1992). Glynn and Brown (1996) found that varying the dispersivity from 0 to 10 percent of the length of the flow path had little effect on movement of the acidic front except where the initial calcite concentration was <0.03 mol/kg H_2O. This concentration was less than half the initial calcite concentration used in the neutralized zone of the present model.

For this report, the reactive-transport model of Brown and others (1998) was extended to June 1998. Water from well 51, the monitor well closest to upgradient contaminant sources, was used as inflow to the model. The flow path from well 51 to well 702 (fig. 1) was divided into 82 cells, which were each 200 m long. The earliest available water-chemistry analysis for each well (table 1) along the flow path was used to define the initial conditions for the model. Simulated input for missing constituents were estimated from the earliest available analysis. For example, total inorganic carbon (TIC) was first measured in 1987 and was used to represent 1984 conditions in the model. Between wells, initial water chemistry in each cell consisted of water from a nearby well, or a mixture of water from the nearest upgradient and downgradient wells, as appropriate. The minerals included in the model (table 2) in each cell were determined on the basis of solid-phase analyses. Gypsum and Fe hydroxide were assumed to be initially present along the entire flow path. Adsorption along the flow path was assumed to occur on the Fe hydroxide that is present throughout the aquifer (Stollenwerk, 1994). Calcite was assumed to be initially present in the neutralized zone and absent in the acidic zone where calcite would have been substantially depleted or completely consumed by acidic ground water. Sequential extractions by Ficklin and others (1991a, b) indicated that extractable Mn was present at much lower concentrations

Table 2. Mineral reactions and solubility-product constants used in simulation of reactive transport

[*logKsp*, log of the solubility- product constant]

Mineral	Reaction	*LogKsp*
Calcite	$CaCO_{3(c)} = Ca^{2+} + CO_3^{2-}$	-8.48
Gypsum	$CaSO_{4(c)} * 2H_2O = Ca^{2+} + SO_4^{2-} + 2H_2O$	-4.58
Iron hydroxide	$Fe(OH)_{3(a)} + 3H^+ = Fe^{3+} + 3H_2O$	4.89
Manganese oxide	$MnO_{2(c)} + 4H^+ + e^- = Mn^{2+} + 2H_2O$	41.38
Aluminum-mineral equilibria: $Al(OH)_{3(a)}$	$Al(OH)_{3(a)} + 3H^+ = Al^{3+} + 3H_2O$	10.8
$AlOHSO_4$	$AlOHSO_{4(s)} + H^+ = Al^{3+} + SO_4^{2-} + H_2O$	-3.23
Rhodochrosite	$MnCO_{3(c)} = Mn^{2+} + CO_3^{2-}$	-11.13

in the acidic zone than in the neutralized zone. Because of this, most if not all of the reactive Mn oxide in aquifer material was assumed to be reductively dissolved with the passage of the transition zone, and the simulated concentration of Mn oxide in the acidic zone was set to 0 in the model. Under these conditions, simulated Fe behaved as a conservative constituent in the acidic zone and reacted with Mn only in cells where Mn oxide was present.

Conservative Transport

Chloride (Cl) is a conservative constituent at Pinal Creek (Stollenwerk, 1994) and was used to measure the degree to which contaminated water was diluted by uncontaminated water along the flow path. Uncontaminated ground water from the underlying basin fill and tributary alluvium was represented in the model by water from well 202, which is in Pinal Creek alluvium about 1 km upstream from the mouth of Miami Wash. Dilution from flood-related recharge was represented in the model by a sample of water from Pinal Creek at Inspiration Dam obtained during a flood in January 1993. Both sources of uncontaminated inflow were mixed with contaminated ground water in each cell in amounts necessary to match measured Cl concentrations in wells along the flow path.

In 1984, the Cl concentration of water decreased from 11.0 mmol/L at km 0 to 3.95 mmol/L at km 5.8 (fig. 3). From km 5.8 to the end of the flow path (km 16.3), Cl decreased only slightly to 2.34 mmol/L in 1990. Because of contaminant-source removal, remedial pumping, and significant ground-water recharge in the early 1990's, Cl concentrations decreased along the entire flow path from 1984 to 1998. By 1998, the trend observed in 1984 had disappeared, and Cl concentrations were about equal along the flow path. Distribution of Cl simulated with PHREEQC matched measured concentrations reasonably well using mixing fractions that ranged from 0.06 at the upstream end of the model to 0.01 at the downstream end. (Water resulting from a mixing fraction of 0.06 consisted of 94-percent contaminated water and 6-percent uncontaminated water.) For 1993, the fraction of water mixed with contaminated water in each cell was increased slightly from km 3 to 11.4 to account for recharge of uncontaminated water from the 1993 flood.

Acidity and Related Equilibria

Unlike Cl, pH and other species, including Al, Ca, inorganic carbon, SO_4, Mn, and Fe, were affected by chemical reactions with solids in the aquifer or gases in the unsaturated zone. The pH along the flow path defined the acidic, transition, and neutralized zones in the aquifer. In 1984, the pH in the acidic zone was about 3.8, and by 1998, the pH had risen slightly to about 4 (fig. 4). Stollenwerk (1994) attributed the persistence of low pH in the aquifer to the gradual desorption of protons from Fe hydroxide surfaces in the aquifer. Several reactions acting in combination controlled the pH in the plume. The dissolution of calcite and mixing of contaminated ground water with uncontaminated ground water increased the pH. The

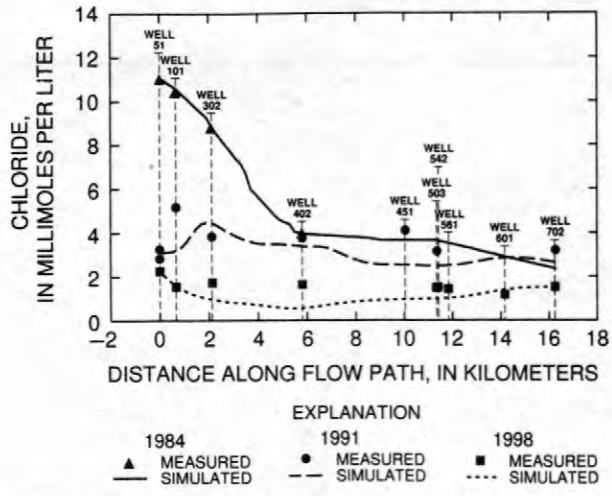

Figure 3. Measured and simulated concentrations of chloride along the flow path in the aquifer, 1984, 1991, and 1998, and locations of wells.

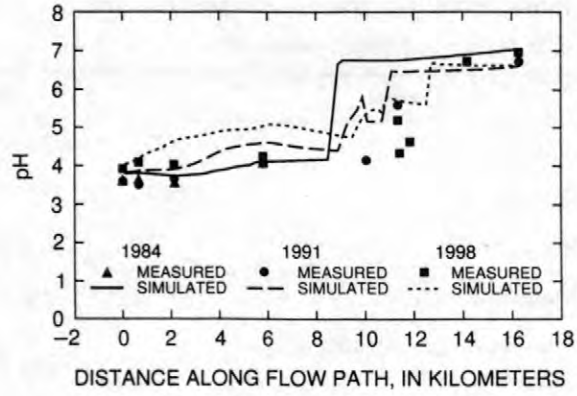

Figure 4. Measured and simulated ph along the flow path in the aquifer, 1984, 1991, and 1998.

reductive dissolution of Mn oxide and the consequent oxidation and precipitation of Fe hydroxide decreased the pH, as did the gradual desorption of protons from Fe hydroxide surfaces.

Concentrations of Ca in the aquifer were controlled by equilibrium with calcite and gypsum, and by mixing of contaminated ground water with uncontaminated ground water. Calculations using PHREEQC indicated that water in the acidic part of the flow path was slightly supersaturated or in equilibrium with gypsum from 1984 until 1991 and was increasingly undersaturated from 1992 to 1998 (fig. 5). Gypsum equilibria can be expressed by the following reaction:

$$Ca^{2+} + SO_4^{2-} + 2H_2O = CaSO_4 \cdot 2H_2O.$$

Although this reaction does not directly affect the pH, the increase in dissolved Ca that results from the redissolution of precipitated gypsum increases the calcite saturation index and indirectly plays a role in acidity equilibria.

Concentrations of Ca in water at km 0 decreased slightly from 12 mmol/L in 1984 to 11 mmol/L in 1992 and then decreased abruptly to 3.9 mmol/L in 1994 after the aquifer received recharge from flooding in 1993. Ca increased to 7.8 mmol/L by 1998 (fig. 6). During the same period, Cl decreased by a factor of 3.6, which indicates that dissolution of gypsum was responsible for the small decreases in measured Ca concentrations relative to Cl concentrations.

As previously mentioned, carbonate mineral dissolution in the transition zone increased the pH from about 4 to greater than 6. Calcite saturation indices were between –0.2 and –1.0 at km 14.2 in the neutralized zone (fig. 7), which indicated that calcite dissolution in the transition zone was not sufficient to bring partially neutralized water into equilibrium with calcite. Ground water was undersaturated with calcite at km 14.2, and equilibrium with calcite was established by km 16.3. The saturation indices indicate that calcite dissolution in the neutralized zone was responsible for the measured increase in Ca along the flow path from km 10 to km 16 through 1998.

From 1984 to 1998, simulated concentrations of Ca generally were larger than measured concentrations (fig. 6). The measured decreases in Ca from 1991 to 1998 were not reflected in the model, probably because simulated gypsum dissolution was greater than that in the aquifer. Beginning in 1991 (figs. 5 and 6), acidic water became undersaturated with respect to gypsum; however, the model maintained equilibrium through dissolu-

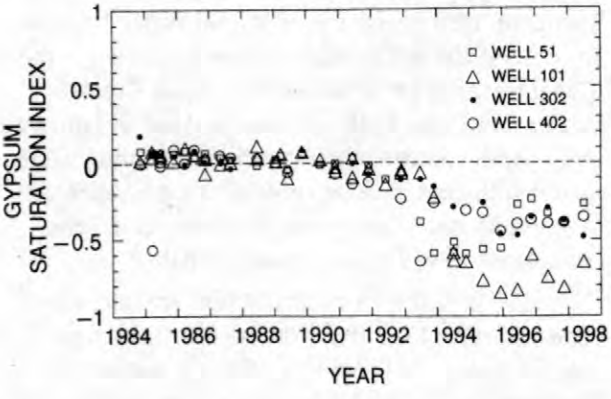

Figure 5. Saturation indices for gypsum in water from wells in the acidic part of the flow path, 1984–1998.

tion with gypsum. The simulated concentration of gypsum initially in the acidic part of the aquifer estimated from sequential extractions done by Ficklin (1991a, b) probably was unreasonably large.

Iron, Manganese, and Oxidation-Reduction Reactions

As previously mentioned, concentrations of Fe and Mn were controlled in part by oxidation-reduction reactions in the transition zone and mixing of contaminated ground water with uncontaminated ground water along the flow path. Mn also may sorb to Fe hydroxide surfaces under certain conditions. In 1984, concentrations of dissolved Fe decreased from 57 mmol/L at km 0 to less than 10 mmol/L at km 5.8 (fig. 8), which is a factor of about 6. Over the same interval, Cl decreased by a factor of 3 (fig. 3) and Mn decreased by less than half, from 1.3 mmol/L to 0.9 mmol/L (fig. 9). These differences suggest that oxidation-reduction reactions in part controlled the concentrations of Fe and Mn more than 2 km upgradient from the transition zone. In addition, the simulated and measured concentrations of dissolved Fe and Mn at km 6 differed significantly in the late 1980's. In 1987 at km 5.8, the simulated concentration of Fe was greater than the measured concentration, and the simulated concentration of Mn was less than the measured concentration. Because the initial modeled concentration of Mn oxide was 0 in the acidic zone, simulated Fe moved conservatively through the acidic zone to the transition zone where reaction with Mn oxides occurred. The differences between measured and simulated concentrations of Mn and Fe at km 5.8 provided additional evidence for the continued reductive dissolution of Mn oxides and oxidation and precipitation of Fe in the acidic zone.

In the transition zone, simulated Mn concentrations were unreasonably large (fig. 9) probably because the reductive dissolution of Mn is kinetically controlled. The simulated attainment of equilibrium with each transport step caused excessive Mn dissolution in the transition zone. Although Stollenwerk (1994) observed a peak of similar magnitude in a column experiment using acidic ground water and alluvium from the site, such a peak has not been observed in the field. The slight

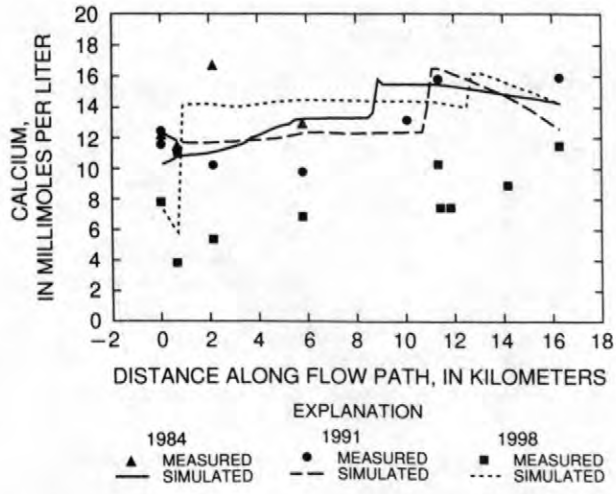

Figure 6. Measured and simulated concentrations of dissolved calcium along the flow path in the aquifer, 1984, 1991, and 1998.

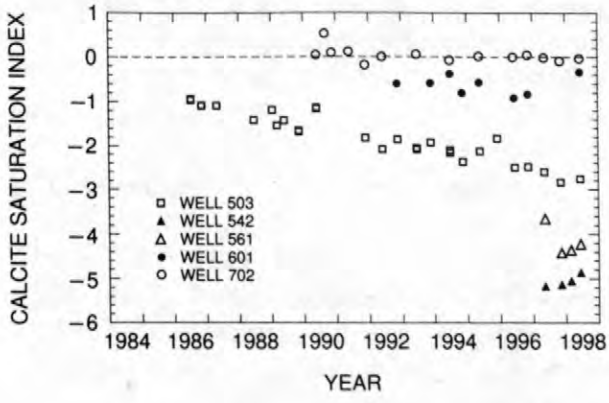

Figure 7. Saturation indices for calcite in the transition and neutralized zones of the plume, 1984–98.

decrease in concentrations of dissolved Mn between km 12.1 and km 16.2 was attributed to rhodochrosite precipitation on the basis of measured saturation indices near 0 at km 16.2 (Brown and others, 1998).

Aluminum Equilibria

Inverse modeling indicated that the measured attenuation of Al across the transition zone was in part controlled by mineral reactions. The determination of the solubility controls on dissolved Al over the range in pH measured in the plume, however, remains problematic. Stollenwerk (1994) used amorphous aluminum hydroxide ($Al(OH)_{3(a)}$; table 2) as the solubility control above

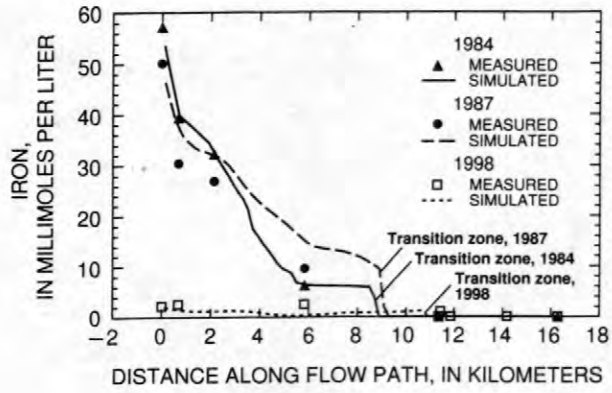

Figure 8. Measured and simulated concentrations of dissolved iron along the flow path in the aquifer, 1984, 1987, and 1998.

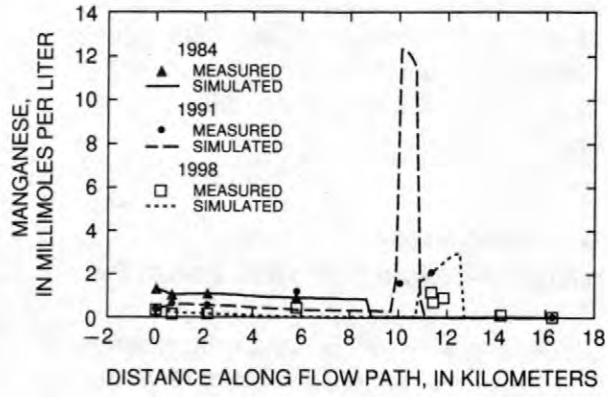

Figure 9. Measured and simulated concentrations of dissolved manganese along the flow path in the aquifer, 1984, 1991, and 1998.

a pH of 4.5, and a mineral with the formula $AlOHSO_4$ below a pH of 4.5, but changed the equilibrium constant by more than an order of magnitude to obtain a reasonable fit between his simulation and measured concentrations of dissolved Al.

Because the precipitation of each mineral releases protons to solution, Al mineral reactions could have a significant effect on pH in the plume. Because of the uncertainties related to the control on dissolved Al concentrations below a pH of 4.5, however, no controls were placed on Al solubility in the present simulation.

SENSITIVITY ANALYSES

As is the case with many field studies, the physical and chemical characteristics of the ground-water flow system in the Pinal Creek Basin were determined on the basis of sparse or incomplete data. Similarly, the reactions that control the movement and transformation of the plume have not been determined with absolute certainty. Sensitivity analyses are useful, therefore, to examine the effects of uncertainty on reactive transport in the plume. Uncertainties considered below are the calcite content, the nature of reactions with gases in the unsaturated zone, and Al-mineral equilibria. Not discussed here because of space limitations are the uncertainties in initial solid-phase concentrations, other than calcite, and slow reactions that may nonetheless be significant.

Calcite Content

The calcite content of 0.075 mol/kg H_2O used to simulate transport from 1984 to 1998 was estimated on the basis of a mass balance of Ca done on Stollenwerk's (1994) column experiment. At this concentration, the movement of the simulated pH front had a retardation factor of 7. A calcite concentration of 0.038 mmol/kg H_2O was used as the lower limit in this sensitivity analysis. Other measurements have yielded larger concentrations. Stollenwerk (1994) measured 0.17 mol/kg H_2O of calcite in the uncontaminated alluvium used in his experiment. Buffer-capacity measurements done by Hydro Geo Chem, Inc. (1989) yielded carbonate content estimates that ranged from 0.125 mol/kg H_2O in sand and gravel to 0.76 mol/kg H_2O in calcareous clay. Adjusting these values for the average particle size of sediments at monitor well group 500 yielded a value of 0.29 mol/kg H_2O, which was used as the upper limit in this sensitivity analysis.

Increasing the calcite content in the neutralized zone from 0.075 to 0.29 mol/kg H_2O reduced the rate of movement of the acidic front from by a factor of 9 (fig. 10). Decreasing the calcite content to 0.038 mol/kg H_2O increased the rate of movement by a factor of 1.7 and created a zone from km 11 to km 12 where Mn oxide dissolution occurred in the absence of calcite dissolution. Such a zone (and pH's associated with those conditions) has not been observed in the field. Glynn and Brown (1996) noted a similar zone when the initial

carbonate-mineral to Mn oxide ratio was greater than 3:2.

Carbon Dioxide Exchange

The simulation of the plume at Pinal Creek was made with the assumption that the plume was closed to the in-gassing of oxygen from the unsaturated zone and the out-gassing of CO_2 to the unsaturated zone. Field values of dissolved oxygen suggest that the system is closed, but the extent to which CO_2 does or does not decrease along the flow path through mixing or diffusion cannot be known with complete certainty. Opening the system to CO_2 at a constant pCO_2 of $10^{-1.33}$ atmospheres (calculated from measured concentrations of total inorganic carbon, TIC) decreased by less than 0.25 km the distance traveled by the pH front from 1984 to 1998. For both simulations, the 1993 decrease in simulated TIC marked the point at which carbonate dissolution was complete upgradient from km 11.4). The simulations indicate that when carbonate dissolution is ongoing, keeping the system closed allowed for unreasonable buildup of TIC in the neutralized zone (fig. 11). After all the simulated calcite had dissolved, the closed system simulated that the TIC concentrations were in good agreement. These results indicate that the water along the flow path was in partial or indirect contact with the atmosphere possibly through mixing with shallower water that is in direct contact with the unsaturated zone. More realistic simulation of this (and other gas-exchange processes) will require the use of a two-dimensional model.

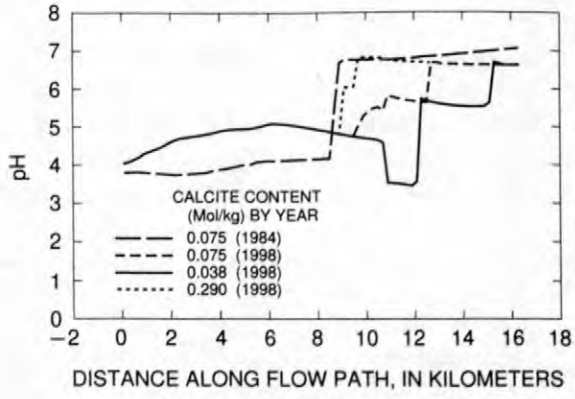

Figure 10. Simulated pH for selected concentrations of calcite in aquifer material, 1984 and 1998.

Aluminum Equilibria

Because of the uncertainty regarding the solid-phase controls on Al solubility, no controls were placed on dissolved Al in the model. The effects of Al solid phases on the movement of the pH front were explored by a sensitivity analysis that allowed for the control of dissolved Al concentrations by $Al(OH)_{3(a)}$ and $AlOHSO_4$. Initial concentrations of these minerals were set to 0. By allowing for the precipitation and redissolution of these minerals, the simulated pH from km 0 to km 10 was as much as one unit less in 1998. Between km 9 and km 10, the pH decreased by as much as one unit. These changes had little effect on the rate of movement of the simulated acidic front of the plume. Glynn and Brown (1996) simulated flow between wells 402 and 503 and found that allowing $AlOHSO_4$ to precipitate rather than $Al(OH)_{3(a)}$ increased the retardation factors of the rhodochrosite and Al solid-phase dissolution fronts, which are associated with the breakthrough of the low pH front.

CONCLUSIONS

From 1984 to 1998, concentrations of contaminants in the alluvial aquifer in Pinal Creek Basin, Arizona, decreased as a result of mixing, recharge, source removal, remedial pumping, and chemical reactions. Inverse and reactive-transport geochemical modeling were used to help understand the important reactions and processes that controlled the measured changes in chemistry. The major conclusions of this analysis are as follows.

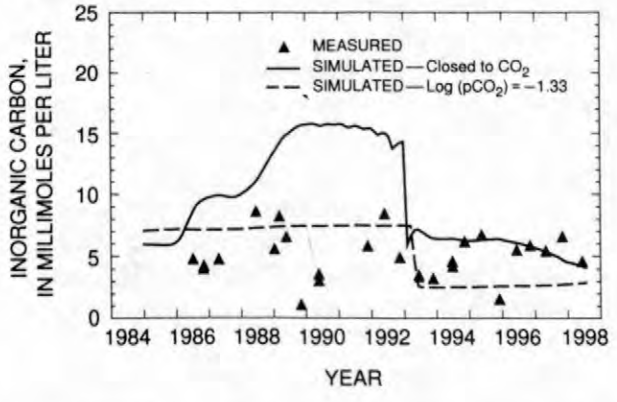

Figure 11. Measured and simulated concentrations of total inorganic carbon in water at km 11.4, 1984–98.

NETPATH and PHREEQC inverse modeling indicated that in order to satisfy the mass-balance constraints on Ca and Mg, the dissolution of Ca-Mg silicates were required. Rhodochrosite and Al solid-phase mass transfers were significant, particularly in models that allowed no CO_2 exsolution.

Simulated and measured concentrations of Fe, Mn, and Ca differed mainly because water along the flow path appeared not to be in a state of local equilibrium. The lack of equilibrium is related at least in part to slow reaction kinetics, but an apparent lack of equilibrium also could result from diffusion processes that limit the interaction of solid-phase surfaces with solutes in the aquifer. Distinguishing reaction kinetics from diffusion limitations in the subsurface is difficult if not impossible at the present time.

Because of the apparent lack of equilibrium, the primary usefulness of the model was as a means of comparing the system at Pinal Creek with a system in local equilibrium. Although the equilibrium approach provided insight as to which processes at the site were kinetically controlled and which were not, future work will require a kinetic modeling approach to more thoroughly characterize selected reactions between the plume and aquifer materials and will require the use of a two- or three-dimensional reactive-transport model.

From 1984 to 1990, water along the flow path was supersaturated or in equilibrium with gypsum, and gypsum equilibria controlled dissolved concentrations of Ca and SO_4. Beginning in 1991, water in the acidic part of the plume became increasingly undersaturated with gypsum indicating that the gypsum available for dissolution in the aquifer became limited beginning in about 1991.

Rhodochrosite precipitation probably was responsible for the measured attenuation in dissolved Mn in the neutralized zone. For reactions involving gypsum and rhodochrosite, the assumption of a local geochemical equilibrium generally was valid.

For oxidation-reduction reactions, the local equilibrium assumption generally was not valid. Reaction kinetics appear to control the measured concentrations of dissolved Fe and Mn in the acidic and transition zones.

For reactions involving calcite, the local equilibrium assumption did not appear valid. Although dissolution of calcite in the transition zone was not sufficient to establish equilibrium, calcite undersaturation decreased along the flow path in the neutralized zone, and equilibrium was reached by the end of the flow path.

Sensitivity analysis indicated that the rate of advance of the pH front was highly sensitive to the initial calcite concentration. Increasing the calcite content from 0.075 to 0.29 mol/kg H_2O reduced the calculated rate of advance of the pH front by a factor of 9. Decreasing the calcite content to 0.038 mol/kg H_2O increased the rate of the pH front advance by a factor of 1.7.

Opening the system to CO_2 at a constant pCO_2 of $10^{-1.33}$ atmospheres produced a better agreement between measured and simulated concentrations of dissolved TIC when calcite dissolution was occurring. After simulated calcite was completely consumed, better agreement between measured and simulated concentrations of dissolved TIC was achieved when the exsolution of CO_2 was not allowed. The simulations indicate that when calcite dissolution is ongoing, keeping the system closed allowed for unreasonable buildup of dissolved carbon in the neutralized zone. After all the simulated calcite had dissolved, the simulated carbon concentrations in the closed system were in good agreement. Water along the flow path was in partial or indirect contact with the atmosphere possibly through mixing with shallower water that is in direct contact with the unsaturated zone. More realistic simulation of this (and other gas-exchange processes) will require the use of a two-dimensional model.

REFERENCES CITED

Allison, J.D., Brown, D.S., and Novo-Gradac, K.J., 1991, MINTEQA2/PRODEFA2, A geochemical assessment model for environmental systems—Version 3.0 user's manual: U.S. Environmental Protection Agency Report 600/3–91/021, 105 p.

Appelo, C.A.J., and Postma, D., 1993, Geochemistry, groundwater and pollution: Rotterdam, A.A. Balkema, 536 p.

Brown, J.G., Bassett, R.L., and Glynn, P.D., 1998, Analysis and simulation of reactive transport of metal contaminants in ground water in Pinal Creek Basin, Arizona, *in* Steefel, C.I., and Van Cappellen, P., eds., Special Issue: Reactive Transport Modeling of Natural Systems: New York, Elsevier, Journal of Hydrology, v. 209, nos. 1–4, August 1998, p. 225–250.

Brown, J.G., and Eychaner, J.H., 1996, Research of acidic contamination of ground water and surface water, Pinal Creek Basin, Arizona, *in* Brown, J.G., and Favor, Barbara, eds., Hydrology and geochemistry of aquifer and stream contamination related to acidic water in Pinal Creek Basin near Globe, Arizona: U.S. Geological Survey Water-Supply Paper 2466, chap A, p. 1–20.

Eychaner, J.H., 1991, Dissolved-metal transport in Pinal Creek streamflow, *in* Mallard, G.E., and Aronson, D.A., eds., U.S. Geological Survey Toxic Substances Hydrology Program—Proceedings of the Technical Meeting, Monterey, California, March 11–15, 1991: U.S. Geological Survey Water-Resources Investigations Report 91–4034, p. 439–447.

Eychaner, J.H., Rehmann, M.R., and Brown, J.G., 1989, Chemical, geologic, and hydrologic data from the study of acidic contamination in the Miami Wash-Pinal Creek area, Arizona, water years 1984–87: U.S. Geological Survey Open-File Report 89–410, 105 p.

Ficklin, W.H., Love, A.H., and Briggs, P.K., 1991a, Analytical results for total and partial metal extractions in aquifer material, Pinal Creek, Globe, Arizona: U.S. Geological Survey Open-File Report 91–111, 33 p.

Ficklin, W.H., Love, A.H., and Papp, C.S.E., 1991b, Solid-phase variations in an aquifer as the aqueous solution changes, Globe, Arizona, *in* Mallard, G.E., and Aronson, D.A., eds., U.S. Geological Survey Toxic Substances Hydrology Program—Proceedings of the Technical Meeting, Monterey, California, March 11–15, 1991: U.S. Geological Survey Water-Resources Investigations Report 91–4034, p. 475–480.

Gelhar, L.W., Welty, C., and Rehfeldt, K.R., 1992, A critical review of data on field-scale dispersion in aquifers: American Geophysical Union, Water Resources Research, v. 28, no. 7, p. 1955–1974.

Glynn, P.D., 1991, Effect of trace impurities in gypsum on contaminant transport at Pinal Creek, Arizona, *in* Mallard, G.E., and Aronson, D.A., eds., U.S. Geological Survey Toxic Substances Hydrology Program—Proceedings of the Technical Meeting, Monterey, California, March 11–15, 1991: U.S. Geological Survey Water-Resources Investigations Report 91–4034, p. 466–474.

Glynn, P.D., and Brown, J.G., 1996, Reactive-transport modeling of acidic metal-contaminated ground water at a site with sparse spatial information, *in* Lichtner, P.C., Steefel, C.I., and Oelkers, E.H., eds., Reactive Transport in Porous Media: Washington, D.C., Mineralogical Society of America, Reviews in Mineralogy, v. 34, p. 377–438.

Hydro Geo Chem, Inc., 1989, Investigation of acid water contamination along Miami Wash and Pinal Creek, Gila County, Arizona: Claypool, Arizona, Cyprus Miami Mining Corp., 1,140 p.

Lind, C.J., and Stollenwerk, K.G., 1996, Alteration of alluvium by acidic ground water resulting from copper mining at Pinal Creek, Arizona, *in* Morganwalp, D.W., and Aronson, D.A., eds., U.S. Geological Survey Toxic Substances Hydrology Program—Proceedings of the Technical Meeting, Colorado Springs, Colorado, September 20–24, 1993: U.S. Geological Survey Water-Resources Investigations Report 94–4015, v. 2, p. 1089–1094.

Neaville, C.C., and Brown, J.G., 1994, Hydrogeology and hydrologic system of Pinal Creek Basin, Gila County, Arizona: U.S. Geological Survey Water-Resources Investigations Report 93–4212, 32 p.

Parkhurst, D.L., 1995, Users guide to PHREEQC—A computer model for speciation, reaction-path, advective- transport, and inverse geochemical calculations: U.S. Geological Survey Water-Resources Investigations Report 95–4227, 143 p.

Parkhurst, D.L., Thorstenson, D.C., and Plummer, L.N., 1980, PHREEQE—A computer program for geochemical calculations: U.S. Geological Survey Water-Resources Investigations Report 80–96, 195 p.

Peterson, N.P., 1962, Geology and ore deposits of the Globe-Miami district, Arizona: U.S. Geological Survey Professional Paper 342, 151 p.

Plummer, L.N., Prestemon, E.C., and Parkhurst, D.L., 1991, An interactive code (NETPATH) for modeling net geochemical reactions along a flow path: U.S. Geological Survey Water-Resources Investigations Report 91–4078, 227 p.

Stollenwerk, K.G., 1994, Geochemical interactions between constituents in acidic groundwater and alluvium in an aquifer near Globe, Arizona: Applied Geochemistry, v. 9, no. 4, p. 353–369.

_____ 1996, Simulation of reactions affecting transport of constituents in the acidic plume, Pinal Creek Basin, Arizona, *in* Brown, J.G., and Favor, Barbara, eds., Hydrology and geochemistry of aquifer and stream contamination related to acidic water in Pinal Creek Basin near Globe, Arizona: U.S. Geological Survey Water-Supply Paper 2466, chap. B, p. 21–50.

Use of Chlorofluorocarbons, Dissolved Gases, and Water Isotopes to Characterize Ground-Water Recharge in an Aquifer Contaminated by Acidic, Metal-Laden Wastewater

By Pierre D. Glynn, Eurybiades Busenberg, and James G. Brown

ABSTRACT

Chemical and isotopic analyses of ground waters sampled from the Pinal Creek Basin, near Globe, Arizona, between 1991 and 1998 provide valuable information on this highly transient ground-water flow system. Improved knowledge of the flow system and of the recharge processes affecting it is essential in predicting the chemical evolution and migration of the extensively contaminated waters in the basin. Data for dissolved nitrogen and argon indicate that most of the ground-water recharge occurs very rapidly during floods in the winter and early spring. Ground-water samples collected in 1991 have chlorofluorocarbon ages that generally increase with depth and distance downgradient in the metal- and acid-contaminated ground waters. The ground-water ages calculated from chlorofluorocarbon-11 concentrations are reasonable—3 to 15 years for acidic ground waters and 20 to 30 years for neutralized, contaminated ground waters. Ground waters sampled in 1993 have chlorofluorocarbon ages as much as 8 years younger than the waters sampled in 1991. Ground waters sampled in 1996 and in 1998 show that the age of waters in the acidic zone of the system increased by as much as 7 years. Deuterium and oxygen-18 isotope contents measured in the ground waters and their correlation with the specific conductance of the sampled ground waters support the hypothesis that Webster Lake was a major source of metal and acid contamination of ground water in the Pinal Creek Basin. The ground-water ages presented here, however, cannot be used to determine the age of the ground-water solutes introduced by the copper mining and refining operations because the introduced solutes are affected by water-rock reactions and because of remaining uncertainties concerning the application of the chlorofluorocarbon dating technique in this extensively contaminated and highly transient ground-water system.

INTRODUCTION

Acidic, metal-laden water has contaminated shallow ground waters in the Pinal Creek Basin near Globe, Arizona (figs. 1 and 2). Chemical and isotopic ground-water data have been collected in an effort to describe and understand the movement and origin of ground waters in the unconsolidated alluvium and in the underlying consolidated basin fill, which together form the regional aquifer in the basin. The objectives of the project are (1) to determine the ages of the ground waters in the basin, (2) to determine the provenance of these ground waters, (3) to understand the recharge processes affecting ground-water flow in the basin, and (4) to understand how reactions have affected the chemical and isotopic evolution of the contaminated waters. Although the technique of using chlofluorocarbon concentrations to date young ground waters is well established, the application of the technique to such an extensively contaminated ground-water system is novel. This paper presents chemical and isotopic data for ground water sampled between 1991 and 1998 in Pinal Creek Basin, and some preliminary conclusions that may be drawn from those data.

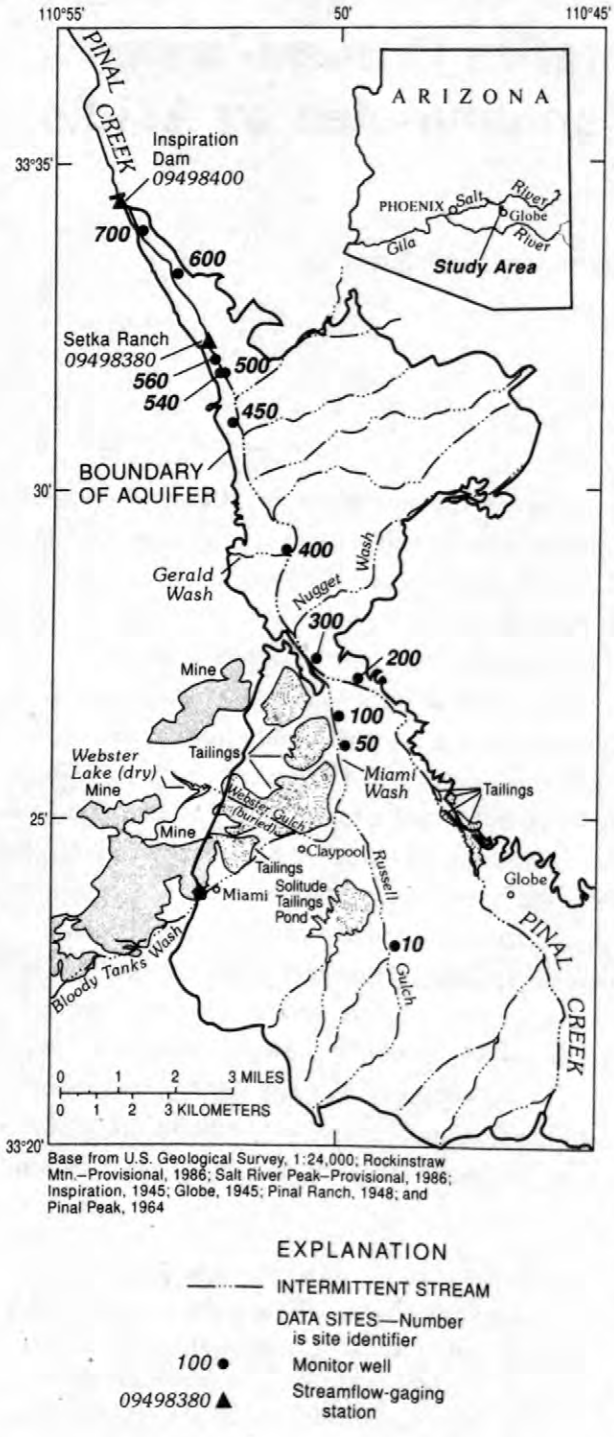

Figure 1. Pinal Creek Basin, Arizona

SUMMARY DISCUSSION

To augment routine sampling for major ions and dissolved metals, project monitoring wells were analyzed for concentrations of chlorofluorocarbon-12 (CFC-12) and chlorofluorocarbon-11 (CFC-11), dissolved gases, and stable isotopes of water in 1991, 1993, 1996, and 1998. Concentrations of dissolved nitrogen and dissolved argon in the ground waters are used to estimate recharge temperatures and the amounts of excess air trapped during recharge. The average recharge temperature calculated from the 1991 data was about 12°C±2°C—6 to 7°C colder than the average ground-water temperatures. Excess-air concentrations in 1993 were as high as 18 ml/L, indicating very rapid recharge during floods in the winter and early spring. Local precipitation records, air-temperature records and a 10°C temperature recorded in Pinal Creek during a large recharge event in February 1993 support the recharge-temperature estimates and the hypothesis of fast recharge provided by measurements of dissolved gas. Nitrogen production by denitrification is not considered a significant source of dissolved nitrogen. Indeed, concentrations of dissolved oxygen are high in all uncontaminated ground waters because of low organic-carbon contents in the water and in the aquifer materials. High partial pressures of carbon dioxide (pCO_2) were measured in the acidic ground waters and in the neutralized, contaminated ground waters. The high pCO_2 values are caused by the dissolution of carbonate minerals by the acidic ground waters.

Concentrations of CFC-11 and CFC-12 are used to calculate the dates when the sampled ground waters last equilibrated with atmospheric CFC concentrations, that is, at the time of ground-water recharge. The ground-water ages calculated from CFC-11 and CFC-12 concentrations depend on the estimated recharge temperature, recharge elevation, and excess-air concentration (Busenberg and Plummer, 1992). Concentrations of CFC-12 in ground water of Pinal Creek are abnormally high in many instances and are thought to be a consequence of a local atmospheric anomaly and of the high concentrations of excess air trapped during recharge rather than the result of point-source contamination. Ground-water ages calculated from concentrations of CFC-11 are insensitive (relative to CFC-12 ages) to excess air, and differed by no more than 1 year from age estimates that did not account for excess air.

Ground waters in the Pinal Creek Basin were first sampled for CFC analysis in 1991, following a

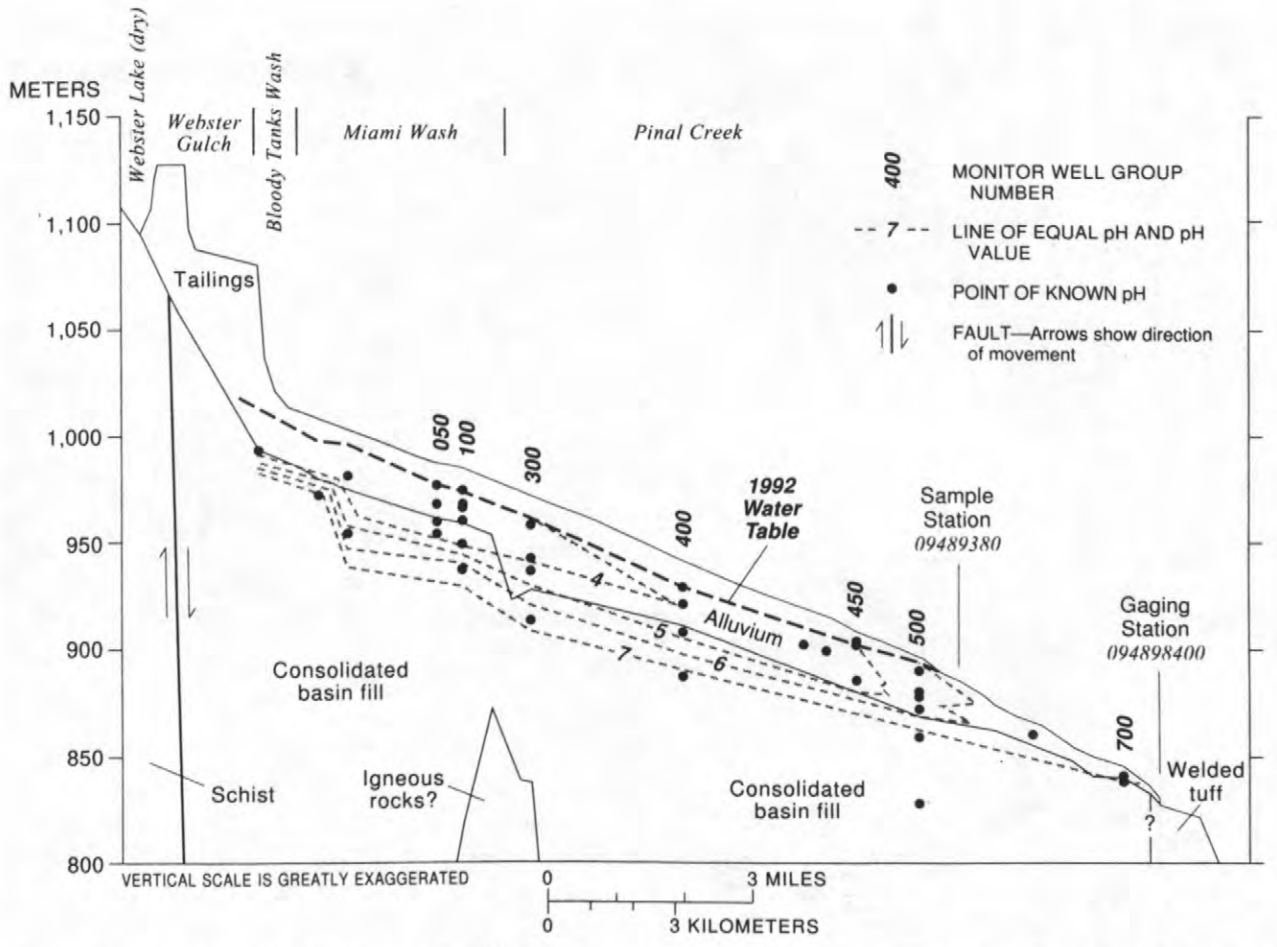

Figure 2. Distribution of pH in the aquifer in 1992. Line of section approximates the principal ground-water-flow line from Webster Lake to Inspiration Dam along the channels of Webster Gulch, Bloody Tanks Wash, Miami Wash, and Pinal Creek (Brown and Harvey, 1996).

period of steadily declining ground-water levels that began in about 1987. The ground waters were resampled in 1993, several months after a large winter flood recharged large amounts of water to the aquifer and caused the water table to rise by as much as 15 m in the southern part of the basin. Ground-water levels have again steadily declined since late 1993. In anticipation of increased remedial pumping and of the installation of a subsurface, impermeable barrier in the alluvium about 6 km upstream from Inspiration Dam, ground-water samples were collected and analyzed for CFC concentrations in 1998.

Samples collected in 1991 generally increase in age with depth and distance downgradient in the metal- and acid-contaminated ground waters (fig. 3). Ground-water ages calculated from CFC-11 concentrations are reasonable—3 to 15 years for acidic ground waters and 20 to 30 years for neutralized, contaminated ground waters. Deep uncontaminated ground waters have little or no measurable CFC-11 or CFC-12, which indicates that they are more than 50 years old. This observation also is supported by the low tritium contents (<0.1 TU) measured in those waters, which indicates that the deep waters were recharged before atmospheric nuclear testing started in the 1950's.

Ground-water recharge in winter and spring of 1993 significantly altered the ages calculated on the basis of CFC-11 and CFC-12 concentrations. Ground-water ages were as much as 8 years younger in samples collected in 1993 than in those collected in 1991, probably because recharge in the late winter and early spring of 1993 resulted in the mixing of ground water of different ages (fig. 4). Ground-water ages in water from the deepest wells at well group 400 and well group 500 were not affected by the recharge event; the ages of waters

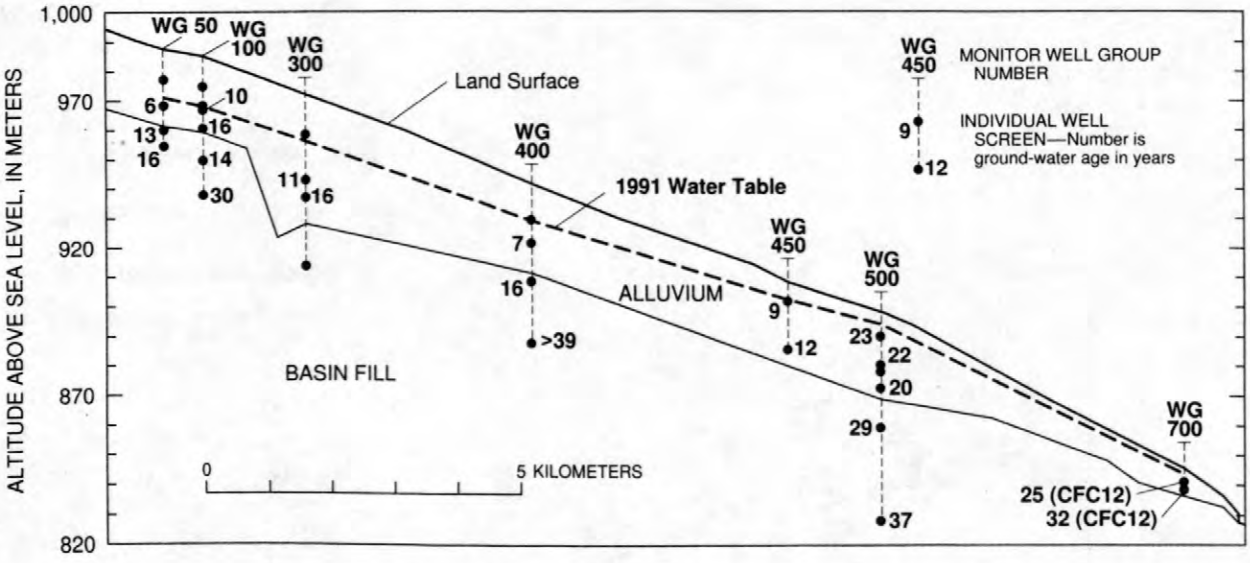

Figure 3. Hydrogeologic section showing ground-water ages based on chlorofluorocarbon 11 [and some chlorofluorocarbon 12(CFC12)] concentrations in Pinal Creek Basin, 1991.

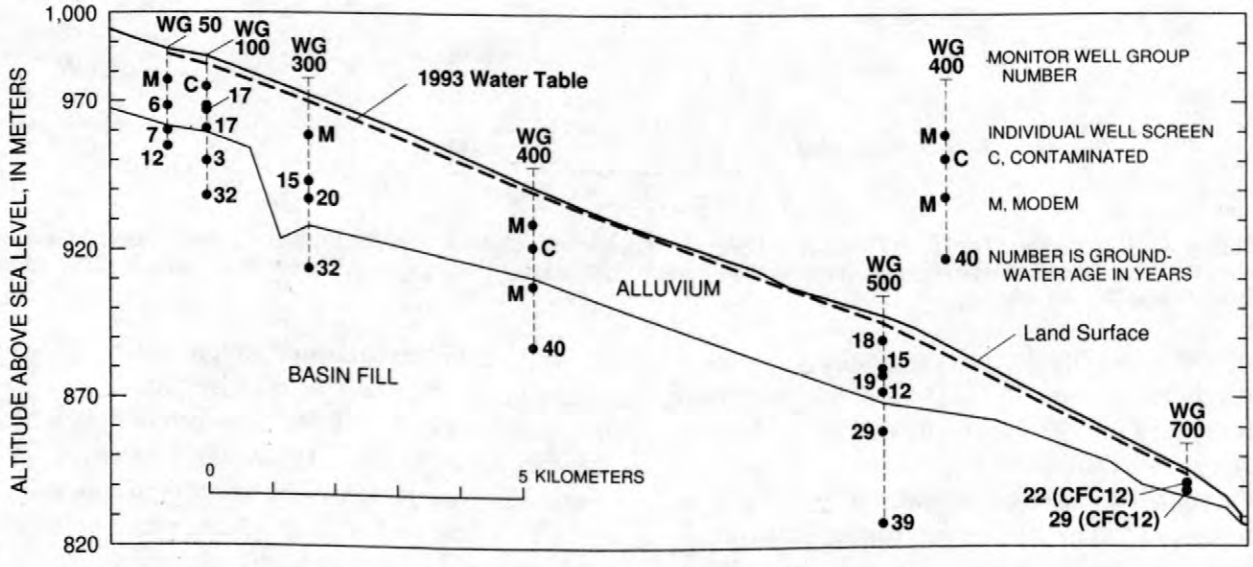

Figure 4. Hydrogeologic section showing ground-water ages based on chlorofluorocarbon 11 [and some chlorofluorocarbon 12(CFC12)] concentrations in Pinal Creek Basin, 1993.

sampled from those wells were the oldest of all the samples collected from the Pinal Creek Basin in 1993. Ground waters sampled in 1993 from wells that were dry in 1991 gave CFC ages that were either "modern" or "contaminated." Waters with "modern" CFC ages are defined here as those in which CFC concentrations were near equilibrium with the standard atmospheric concentrations at the time of sampling (after correction for excess air). Waters with "contaminated" CFC ages had CFC concentrations that were above equilibrium with the standard atmospheric concentrations at the time of sampling (after correction for excess air). By 1996, CFC concentrations in these same wells produced ages that ranged from 9 to 33 years as a result of the continued mixing of ground water of different ages (fig. 5). By 1998, ground-water

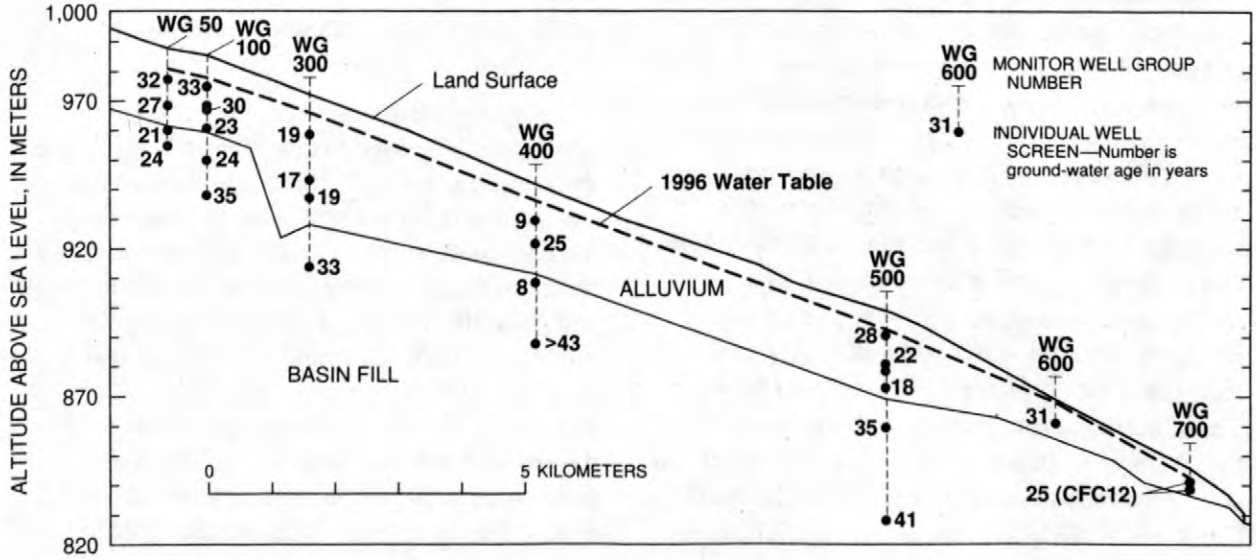

Figure 5. Hydrogeologic section showing ground-water ages based on chlorofluorocarbon 11 [and some chlorofluorocarbon 12(CFC12)] concentrations in Pinal Creek Basin, 1996.

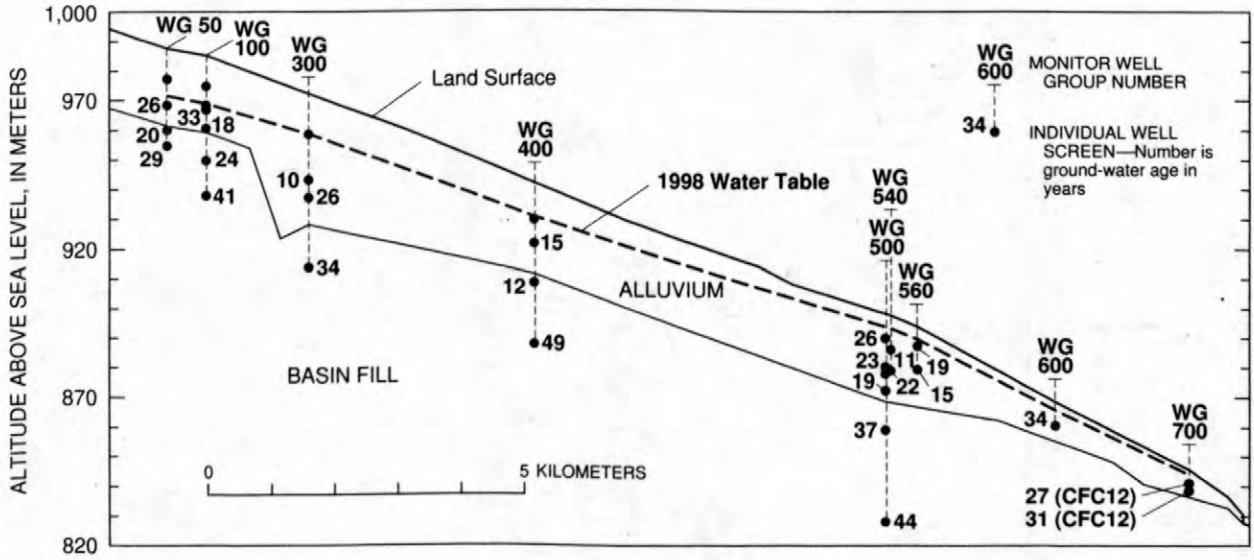

Figure 6. Hydrogeologic section showing ground-water ages based on chlorofluorocarbon 11 [and some chlorofluorocarbon 12(CFC12)] concentrations in Pinal Creek Basin, 1998.

levels had declined below the well screens of the shallowest wells in the acidic zone (fig. 6).

From 1996 to 1998, ground-water ages in the acidic ground water changed by as much as 7 years. In some wells, ground-water ages increased; in others, ground-water ages decreased. In neutralized ground waters, ages changed 3 years or less in most cases. The lack of an apparent trend is an indication of the complexity inherent in a transient-flow system that is affected by occasional large recharge events, by pumping for water supply and remediation, and by the removal of recharge sources (contaminated and uncontaminated) to the aquifer.

The recharge ages determined on the basis of of CFC-11 concentrations are consistent with available tritium, deuterium, oxygen-18, and dissolved-gas data, as well as with travel times

calculated using observed ground- water levels and estimated aquifer characteristics. Deuterium and oxygen-18 values in water do not plot on the global meteoric water line (GMWL), but instead plot on a line with a slope of 5 (instead of 8 for the GMWL; fig. 7). These results imply that the ground waters are mixtures of deep, uncontaminated waters recharged at high elevations and cold temperatures and shallow contaminated waters that have undergone extensive evaporation. The specific conductance of the waters is highly correlated with their deuterium (or oxygen-18) content (fig. 8). This correlation is consistent with the hypothesis that Webster Lake was a major source of metal and acid contamination of ground water in the Pinal Creek Basin. Webster Lake was an artificial lake used between 1940 and 1988 for the storage of acidic, metal-laden, process water from the copper-refining industry.

The ground-water ages presented in this paper cannot be used to determine the age of the various ground-water solutes introduced by copper mining and refining operations. Indeed, many of the introduced solutes are affected by water-rock reactions (sorption, precipitation and dissolution) and generally will be retarded with respect to movement of the water and CFC molecules. Eychaner (1991), Stollenwerk (1994), Glynn and Brown (1996) and Brown and others (1998) discuss in detail the chemical and physical processes controlling the chemical evolutions of ground waters in Pinal Creek. Additionally, many

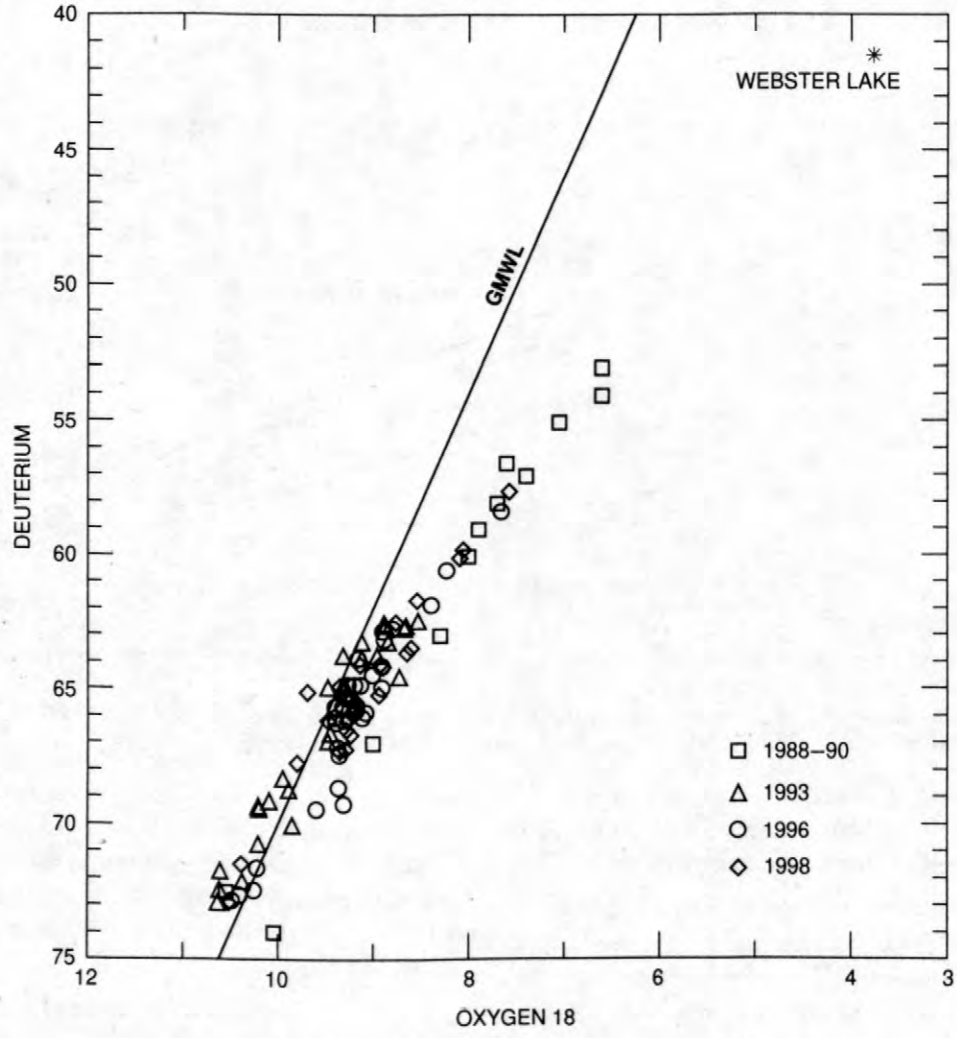

Figure 7. Oxygen 18 and deuterium concentrations in ground water and lake water, 1988–98.

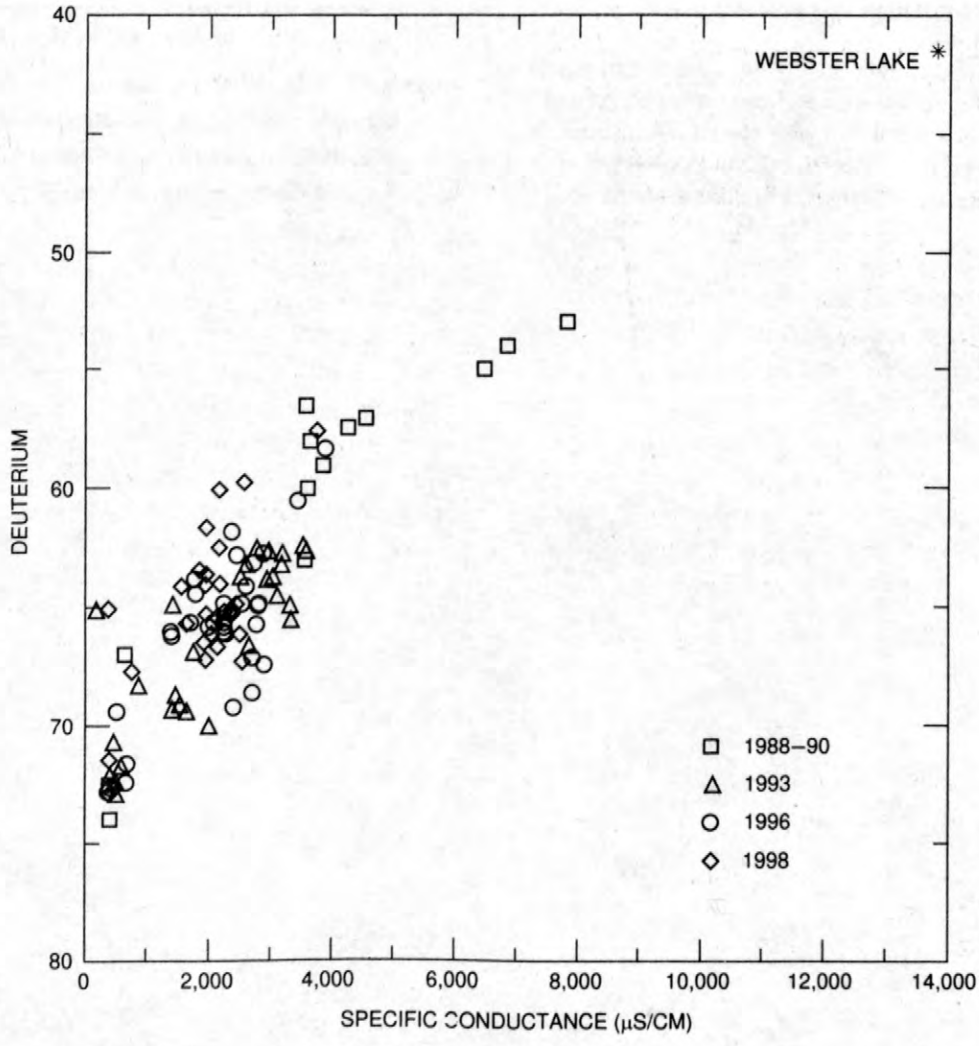

Figure 8. Specific conductance and deuterium concentrations in ground water and lake water, 1988–98.

uncertainties remain concerning the application of the CFC dating technique in this extensively contaminated and highly transient ground-water system.

REFERENCES

Brown, J.G., and Harvey, J.W., 1996, Hydrologic and geochemical factors affecting metal contaminant transport in Pinal Creek Basin near Globe, Arizona, *in* Morganwalp, D.W., and Aronson, D.A., eds., U.S. Geological Survey Toxic Substances Hydrology Program - Proceedings of the technical meeting, Colorado Springs, Colorado, September 20–24, 1993: U.S. Geological Survey Water Resources Investigation Report 94–4015, p. 1035–1042.

Brown, J.G., Bassett, R.L., and Glynn, P.D., 1998, Analysis and simulation of reactive transport of metal contaminants in ground water in Pinal Creek Basin, Arizona: Journal of Hydrology, v. 209, p. 225–250.

Busenberg, E., and Plummer, L.N., 1992, The use of chlorofluorocarbons (CCL_3F and CCL_2F_2) as hydrologic tracer and age-dating tools—The alluvium and terrace system of central Oklahoma: American Geophysical Union, Water Resources Research, v. 28, no. 9, p. 2257–2283.

Eychaner, J.H., 1991, Dissolved-metal transport in Pinal Creek streamflow, *in:* Mallard, G.E., and D.A., Aronson, eds., U.S. Geological Survey Toxic Substances Hydrology Program - Proceedings of the technical meeting, Monterey, California, March 11-15, 1991: U.S.Geological Survey

Water Resources Investigation Report 91–4034, p. 439–447.

Glynn, P.D., and Brown, J.G., 1996, Reactive transport modeling of acidic metal-contaminated ground water at a site with sparse spatial information, *in* Lichtner, P.C., Steefel, C.I., and Oelkers, E.H., eds., Reactive Transport in Porous Media, Reviews in Mineralogy: Washington, D.C., Mineralogical Society of America, v. 34, p. 377–438.

Stollenwerk, K.G., 1994, Geochemical interactions between constituents in acidic groundwater and alluvium in an aquifer near Globe, Arizona: Applied Geochemistry, v. 9, no. 4, p. 353–369.

The Effect of Trace-Metal Reactive Uptake in the Hyporheic Zone on Reach-Scale Metal Transport in Pinal Creek, Arizona

By Christopher C. Fuller and Judson W. Harvey

ABSTRACT

The extent of hydrologic exchange between surface water and the streambed and the rate of trace metal uptake by hyporheic sediments was evaluated in Pinal Creek, Arizona. Trace metal uptake was quantified by measuring a conservative tracer injected into the stream and metal concentrations in the hyporheic zone. Fractional reactive uptake of metals entering the hyporheic zone averaged 55, 27 and 39 percent for cobalt (Co), nickel (Ni), and zinc (Zn), respectively, at 29 sites. Manganese (Mn) uptake averaged 24 percent at the same sites. First-order rate constants (λ_h) of metal uptake in the hyporheic zone were determined at seven sites. Reaction-time constants ($1/\lambda_h$) averaged 0.41, 0.84, and 0.38 hours for Co, Ni, and Zn, respectively, and 1.3 hours for Mn. Overall a trend of increased metal uptake with increasing Mn uptake was observed. Laboratory metal uptake experiments with streambed sediments indicate that metal removal increased with pre-existing Mn oxide concentration, suggesting that the enhanced Mn oxidation in the hyporheic zone contributed to trace metal uptake. Surface-water metal concentrations were simulated over a 2.8-km reach using the average λ_h coupled with hydrologic parameters derived from modeling in-stream tracer experiments. Simulations of Mn and Ni using the average λ_h indicated that reactive uptake in the hyporheic zone could account for the net uptake of Mn and Ni downstream over this reach. Simulations of Co and Zn indicated that the extent of uptake in the hyporheic zone could not be accurately distinguished from conservative transport. Uncertainties in defining metal inflows, however, limited the accuracy of reach-scale simulations for Co and Zn.

INTRODUCTION

Understanding the fate of mining-related metal contaminants in surface water systems requires assessing the ability of the system to attenuate contaminant loads naturally. The extent of this intrinsic remediation for a stream is dependent on the accessibility of reactive solutes to zones favorable to chemical reactions. Flow of surface water through the streambed can enhance metal attenuation by transporting metals into zones where removal processes are more favorable (Kimball and others, 1994; Benner and others, 1995; Bencala and others, 1984). The portion of a streambed containing surface-water flow paths is termed hyporheic zone and is defined as having a component of at least 10 percent surface water (Triska et al, 1993). Exchange of surface water with the hyporheic zone increases the effective reactive site density per volume of surface water by providing contact of dissolved metals with potential sorption sites within the streambed. Our previous investigation at Pinal Creek determined that enhanced oxidation of dissolved Mn in the hyporheic zone resulted in a net decrease of 20 percent in the Mn load flowing out of the drainage basin (Harvey and Fuller, 1998).

The focus of this study is to evaluate the role of the hyporheic zone for uptake of dissolved cobalt (Co), nickel (Ni), and zinc (Zn) and to determine the significance of the hyporheic zone on trace-metal transport. Because enhanced oxidation of Mn in the hyporheic zone results in ongoing formation of Mn oxides (Harvey and Fuller, 1998), we hypothesize that the manganese oxidation results in continuous formation of sorption sites that should enhance removal of trace metals. This hypothesis is based on the

affinity of metals for sorption by Mn oxides (Catts and Langmuir, 1986; Balistrieri and Murray, 1986; McKenzie, 1980). In this paper we present a summary of the amount and rate of metal uptake in the hyporheic zone determined from streambed dissolved metal profiles. In-stream conservative tracer injections were used as a means to introduce a solute tracer into the hyporheic zone to quantify surface-water exchange with the hyporheic zone, and determine the rate of metal uptake. Laboratory measurements of metal adsorption by streambed sediments were conducted to determine if Mn oxides enhanced Co, Ni, and Zn uptake.

SITE DESCRIPTION

Pinal Creek is a sand and gravel bed stream with a 1-percent average slope (Harvey and Fuller, 1998). Perennial flow results from constriction of an alluvial aquifer by underlying bedrock in the Pinal Creek basin. Mining operations upgradient have generated a plume of acidic ground-water. Reaction of acidic ground water with aquifer sediments has formed a plume of neutralized, contaminated ground water with elevated dissolved Mn, Co, Ni and Zn (Stollenwerk, 1994). Surface water chemistry of Pinal Creek in the upper 4-kilometer (km) of perennial flow is dominated by discharge of the neutralized, contaminated ground water. Contaminated groundwater contributes about 50 percent of the base-flow discharge at Inspiration Dam (Eychaner, 1991), where Pinal Creek exits the alluvial basin (fig. 1). Stream-water chemistry is characterized by high dissolved solids (sulfate 2,200 milligrams per liter (mg/L); calcium 500 mg/L) and a downstream pH increase from about 6 near the head of perennial flow to about 7.8 7-km downstream at Inspiration Dam resulting from CO_2 outgassing (Choi and other, 1998). Mn, Co, Ni and Zn are elevated in the perennial stream. Dissolved Mn and Ni in Pinal Creek have increased between 1984 and 1990 with little subsequent change (Brown and Harvey, 1996). Co and Zn concentrations in shallow ground water recharging the stream have increased by more than a factor of 15 since 1990. Most input of dissolved metals to the stream occurs with ground-water inflow in the first 3 to 4 kilometers (km).

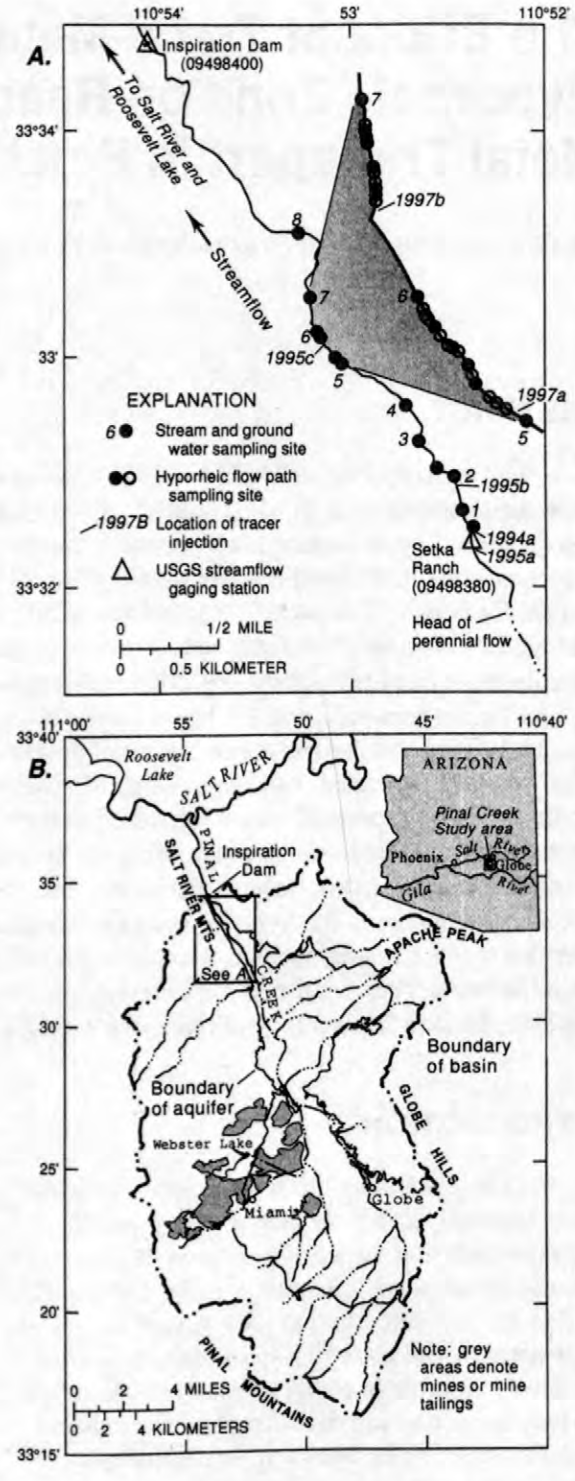

Figure 1. Site map showing location of (A) the 2.8-km study reach with hyporheic zone sampling sites and (B) perennial stream flow.

METHODS

Vertical profiles of dissolved metals in the streambed were measured at two sites in June 1994, three sites in June 1995, and 24 sites in May 1997 (fig. 1). The data presented here expands on Mn hyporheic zone profiles presented in Harvey and Fuller (1998) by including the 24 sites sampled in 1997. The 1997 sites are located along a 0.5-km reach in the lower end of the 2.8-km study reach downstream of all significant ground-water metal inputs, where stream water pH ranged from 7.0 to 7.2. Streambed dissolved metal and tracer samples were collected at close intervals (2.5-cm) over a 10 or 15-cm depth using the mini-drivepoint (MINIPOINT) sampler array (Duff and others, 1998). This device consists of six 1/8-inch-diameter stainless steel piezometers in a circular array installed within an hour of sampling. All depths were sampled simultaneously by multi-head peristaltic pump at 4 milliliters (mL) per minute. This rate did not disturb the vertical profile of a conservative tracer that had reached plateau concentration (Duff and others, 1998). Samples for dissolved metal and field water quality parameters (pH, DO, and alkalinity) were collected after tracer samples.

Surface-water and shallow ground-water samples also were collected and processed (fig. 1) as described by Harvey and Fuller (1998). Surface-water samples were collected by dipping into the stream. Shallow ground-water samples, used to define inflow concentrations, were collected from 3/8-inch-diameter stainless steel drive point piezometers inserted 30 to 200 centimeters (cm) into the streambed.

All dissolved metal samples were filtered through 0.45-micron (μm) pore-size filters that are effective because colloidal metals are not significant at this site (Harvey and Fuller, 1996). Release of metals from stainless steel piezometers or sorption by sampling devices was negligible in laboratory tests.

Dissolved metal concentrations were determined by ICP-OES (inductively coupled plasma-optical emission spectroscopy). Method detection limits (method of Glaser and others, 1981) were 0.4, 1.1, 1.6, and 0.3 micromoles per liter (μM) for Co, Mn, Ni and Zn, respectively. Coefficient of variation of metal analyses averaged 3.2, 1.9, 3.4, and 2.4 percent for Co, Mn, Ni, and Zn, respectively.

The fraction of surface water in the hyporheic zone was determined from the tracer concentration at each depth relative to surface-water tracer concentration at that site. The in-stream conservative tracer injections are described in Harvey and Fuller (1998). Dissolved bromide (Br) was injected at a constant rate for between 4 and 28 hours to attain a stream-water Br of about 5 mg/L. Travel time for tracer arrival in hyporheic zone was measured at all sites in 1994 and 1995 and at six sites in 1997 by continuously sampling a MINIPOINT sampler for three hours after commencement of tracer injection. After the stream water Br concentration reached plateau (2 to 3 hours), tracer and metal samples were collected. Bromide concentrations were measured by ion chromatography with a detection limit of 0.02 mg/L and coefficient of variation of 2.5 percent.

Streambed cores of up to 30-cm depth were collected at each site where Br travel time was measured. Cores were sectioned at 3- or 4-cm intervals, air dried and sieved to remove the greater than 1-millimeter-diameter (>1 mm) size fraction. Sediment metal concentrations were determined by partial extraction with 0.1 moles per liter (M) hydroxylamine hydrochloride (HH) in 0.05-M nitric acid for 1 hour. HH extracts were analyzed by ICP-OES.

Metal uptake by streambed sediments was determined in laboratory batch experiments following methods described in Harvey and Fuller (1998) for Mn-uptake. Briefly, sediments were collected at four sites along the perennial reach from the upper 2 cm of the streambed. Particles >1 mm were removed by wet sieving. Wet sediments were suspended in an artificial ground water of similar major ion composition to Pinal Creek in polycarbonate centrifuge tubes. The pH was controlled at 7±.1 units by imposing a 1% CO_2 in air mixture for the gas phase. At each time point, supernatant from a pair of tubes was sampled after centrifugation. Metal uptake was calculated from the change in dissolved metal concentration determined by ICP-OES.

RESULTS

Stream-water dissolved metal concentrations decreased 30 percent or more in the 2.8-km study reach (fig. 2). Co and Zn were

about five times higher in 1995 than in 1994 because of increasing inputs from ground water upstream of the study reach. Little difference in Ni or Mn concentrations were observed between the two sampling periods. Surface-water pH increased from about 6.5 to 7.5 downstream over the study reach because of CO_2 outgassing (Choi and other, 1998). Ground-water Mn and Ni were equal to or greater than surface water over the first 0.6 km of the study reach. Mn in ground water decreased to background by 1.2 km; Ni decreased to below detection limit by 1 km. Co and Zn in ground water were detectable only at the upstream sampling site. Calculations using the chemical equilibrium program HYDRAQL (Papelis and others, 1988) indicated both surface-water and shallow ground-water dissolved Co, Ni, and Zn at all sites were below saturation with respect to solid phases such as carbonate or hydroxides. Free ion and sulfate complexes were the dominant dissolved metal species.

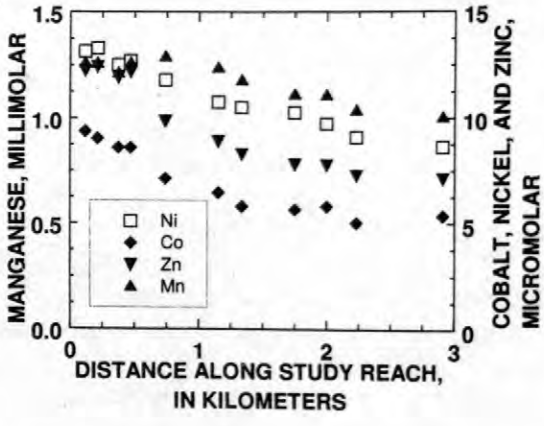

Figure 2. Surface-water dissolved metal concentrations in June 1995 over the 2.8-km study reach.

The penetration of Br tracer into the subsurface ranged from less than 2.5 cm to over 15 cm among the 29 sites sampled. Twenty-six of these sites had greater than 10 percent surface water to depths of 2.5 cm or deeper and are therefore considered as hyporheic zone sites (Triska and others, 1993). Travel time was defined as the elapsed time for Br to reach 50 percent of plateau at any depth relative to the next shallower depth. Tracer arrival in the subsurface ranged from 2 to 80 minutes.

Dissolved Mn, Co, Ni, and Zn in the hyporheic zone typically decreased in concentration with depth below surface water (fig. 3), except in the upstream end of the reach where elevated Mn and Ni are present in shallow groundwater. To calculate if metal uptake or release occurred, measured metal concentrations were compared to concentrations expected based on conservative mixing between adjacent sampled depths in the hyporheic zone. Reactive uptake of dissolved metal by sediment (sorption) is inferred if the calculated non-reactive metal concentration is significantly greater than the measured concentration. The mixing of water within the hyporheic zone is determined by the Br concentration corrected for background. A steady-state transport equation that considered the extent and rate of mixing of surface and ground water in the hyporheic zone was rewritten in finite difference form and rearranged to predict metal concentrations at successive depths in the hyporheic zone (after Harvey and Fuller, 1998):

$$ {}^{*}C_h^{i+1} = C_h^i + \beta^{i+1/2}(C_L - C_h^i) - \lambda_h^{i+1/2}\tau_h^{i+1/2}(C_h^i + C_h^{i+1})/2 \qquad (1) $$

where,

$^{*}C_h$	predicted metal concentration (M)
C_h	metal concentration in hyporheic zone (M)
C_L	metal concentration in ground water (M)
τ_h	travel time of tracer (minutes)
β	fraction of ground water in a depth increment
λ_h	hyporheic zone first-order rate constant for metal uptake (min^{-1}).

The superscript i refers to a specific sampling depth, i+1 refers to the next deeper depth, and i+1/2 to the average value for the interval. The fraction of groundwater input at any depth, $\beta^{i+1/2}$, was determined from measurements of the Br tracer after concentrations had plateaued at all depths:

$$ \beta^{i+1/2} = \frac{Br_h^{i+1} - Br_h^i}{Br_L - Br_h^i} \qquad (2) $$

where Br is the tracer concentration for the depths denoted by subscripts and superscripts used in equation 1. $\beta^{i+1/2}$ was assumed to equal 1 at depths where Br concentrations was equal to or less than Br background. The uncertainty in $\beta^{i+1/2}$, σ_β, was estimated from the average coefficient of

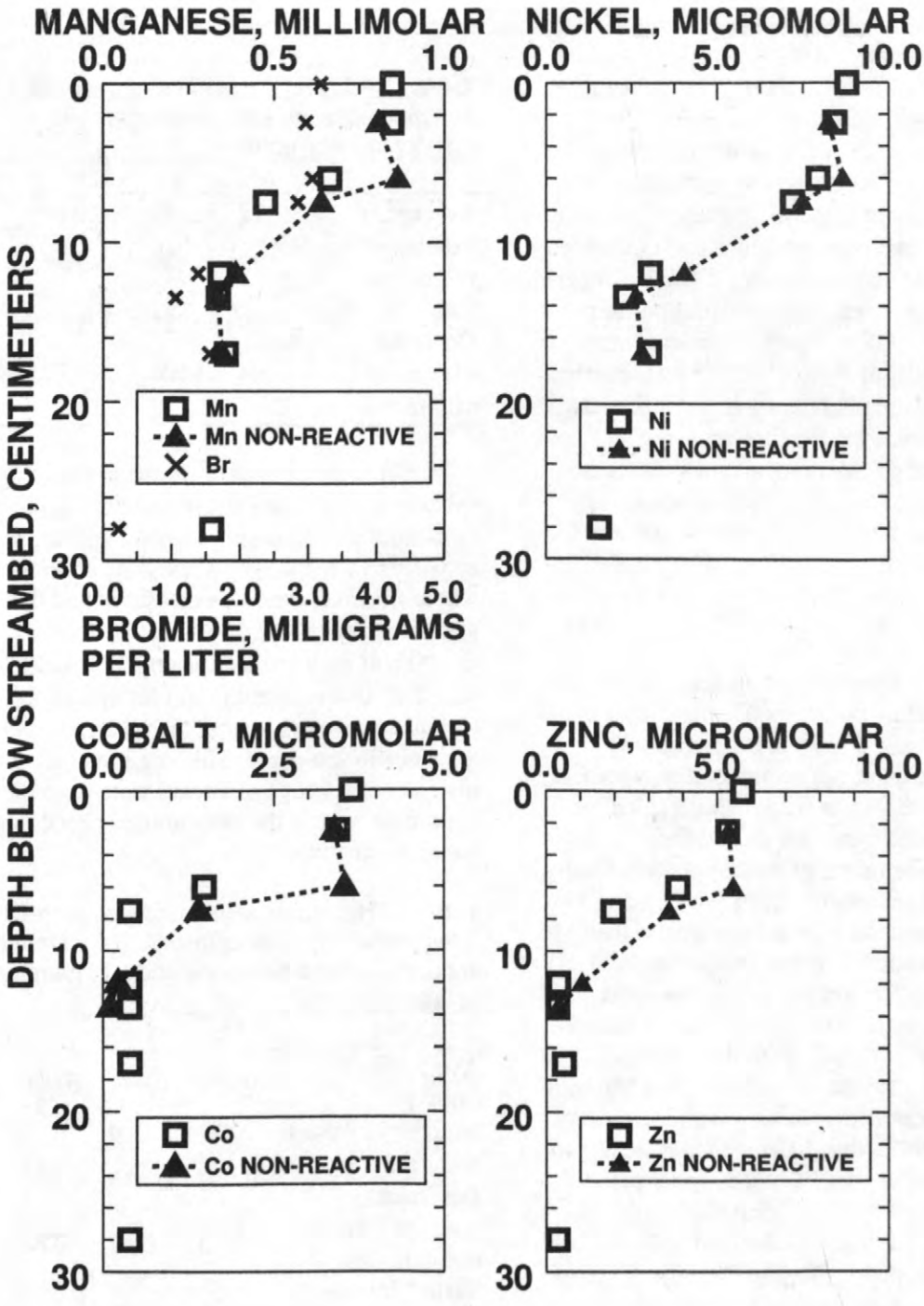

Figure 3. Streambed dissolved metal and Br profiles at a site with a hyporheic zone of over 17-cm depth. Calculated non-reactive metal concentrations also are plotted. Values at 28-cm represent average concentration in ground water. Significant uptake was calculated at 6 and 7.5-cm for all metals and at 12 cm for Mn, Ni, and Zn.

variation of Br measurements propagated through equation 2. The metal concentration in the absence of reaction was determined by setting $\lambda_h = 0$ in equation 1 and solving for ${}^*C_h^{i+1}$. In cases where C_L or C_h^{i+1} was below detection limit, the detection limit was used for calculation. The difference between C_h^{i+1} and ${}^*C_h^{i+1}$ was assumed to represent metal uptake by sediments if ${}^*C_h^{i+1}$ was greater than C_h^{i+1}, or release if C_h^{i+1} was greater than ${}^*C_h^{i+1}$. Uncertainty in ${}^*C_h^{i+1}$, σ_{C^*}, was estimated by propagating the coefficients of variation for metal concentrations and σ_β through equation 1. The uncertainty in C_h^{i+1} was estimated from the average coefficient of variation for metal analyses by ICP-OES. Uptake or release was termed insignificant if $({}^*C^{i+1} - C_h^{i+1})$ was less than sum of σ_{C^*} and the uncertainty in C_h^{i+1}. Depths with an insignificant difference were not considered further. Metal uptake was expressed as a percentage of the difference between calculated concentration without reaction and the measured concentration:

$$f_M = \frac{C_h^{i+1} - {}^*C_h^{i+1}}{{}^*C_h^{i+1}} \times 100 \qquad (3)$$

where f_M is the percent metal uptake.

Depending on the metal, significant metal uptake was observed at 75 to 96 percent of hyporheic zone sites. An example of a hyporheic zone profile is shown in figure 3 with calculated, non-reactive concentrations plotted for comparison. The extent of metal uptake typically decreased with increasing depth. The Co and Zn average percent uptake were both greater than Mn with Ni uptake similar to Mn uptake (table 1). The average f_{Mn} for this expanded data set is significantly greater than average f_{Mn} estimated by Harvey and Fuller (1998) from the 1994 and 1995 data alone. Because the oxidation rate of Mn by Pinal Creek sediments increases with increasing pH (Marble, 1998), this difference may be due to the greater number of sites in the higher pH subreach sampled in 1997. Most sites with significant Co, Ni or Zn uptake also had significant Mn uptake. Despite the wide range of f_M, trace metal uptake typically increased with increasing Mn uptake although trace metal and Mn uptake are not correlated. For all metals, about half of the hyporheic zone sites had no significant difference between measured and non-reactive concentrations at the 2.5-cm depth, but most of these sites had measurable uptake at the deeper depths. The lack of significant metal uptake at the 2.5-cm depth of these sites may represent a zone where metals are at sorptive equilibrium because ongoing absorbent phase formation is not occurring.

Table 1. Fractional percent metal uptake, f_m, for all hyporheic zone sites and depths with significant metal uptake.

	Mn	Co	Ni	Zn
Average	22	52	27	36
Number of values	39	39	32	41
Standard Deviation	19	25	19	24
Maximum	94	100	74	92
Minimum	5	8	7	7

The rate constant for metal uptake was calculated by solving equation 1 for λ_h, the overall first-order rate constant for metal uptake. Rate constants varied widely among the seven sites where Br travel time was measured and that had significant metal uptake (table 2). However, λ_h for Co, Ni and Zn were always greater than λ_h for Mn. The time constant ($1/\lambda_h$) for uptake for all metals was always greater than the Br travel time for that site and depth. This suggests that uptake instead of exchange of stream water into the hyporheic zone is the rate-limiting process in metal attenuation.

Table 2. Hyporheic zone metal uptake reaction rate constant, λ_h, and uptake time constant ($1/\lambda_h$) in hours for hyporheic zone and for laboratory uptake experiments.

	Mn	Co	Ni	Zn
Average λ_h (min^{-1})	0.013	0.041	0.020	0.058
Number of values	11	9	5	9
Standard Deviation	0.014	0.035	0.022	0.037
Average time constant (hours)	1.3	0.41	0.84	0.38
Scaled, laboratory uptake time constant range (hours)	2-4	0.2-0.9	0.5-1.6	0.2-0.6

Concentrations of Co, Ni, Zn, and Mn in bed sediments determined by HH extraction were

elevated by factor of two or more to depths of up to 10-cm compared to deeper sediments (data not shown). The depth range of elevated sediment metal concentrations coincides with the zone of calculated reactive metal uptake. The presence of elevated sediment metal concentrations in the hyporheic zone is consistent with metal uptake occurring in the streambed.

Laboratory Metal Uptake Experiments

Uptake of Co, Ni, and Zn by streambed sediments in batch experiments increased with increasing concentration of pre-existing Mn oxides defined by HH extraction (fig. 4). Because metal uptake was measured under identical experimental conditions (pH, sediment to water ratio, and initial metal concentration), the observed increase in metal uptake with Mn oxide concentration indicates that Mn oxides are an important sorbent phase in Pinal Creek sediments. Addition of poison to inhibit microbial Mn oxidation (Harvey and Fuller, 1998) had little effect on trace-metal sorption, probably because pre-existing Mn oxide content greatly exceeded Mn precipitation during the course of these experiments.

Uptake of Co, Ni, and Zn by streambed sediments occurs rapidly over the first 10 hours followed by a slower approach to equilibrium through four days. Apparent first order rate constants for the uptake over the first 10 hours were calculated. Rate constants were scaled linearly to account for the higher sediment concentration (g/L) in the streambed assuming a porosity of 0.3, sediment density of 2.7 g/cm^3, and assuming uptake occurs primarily on the <1 mm fraction, which is about 40 percent of sediment mass (Harvey and Fuller, 1998). These scaled time constants for metal uptake (table 2) have a similar range to the time constants for metal uptake calculated from hyporheic zone profiles.

DISCUSSION

The observed uptake of trace metals in the hyporheic zone is postulated to result from surface complexation by Mn oxide surfaces concurrently forming on streambed sediments. The dependence of metal uptake on sediment Mn oxide concentration in laboratory experiments indicates

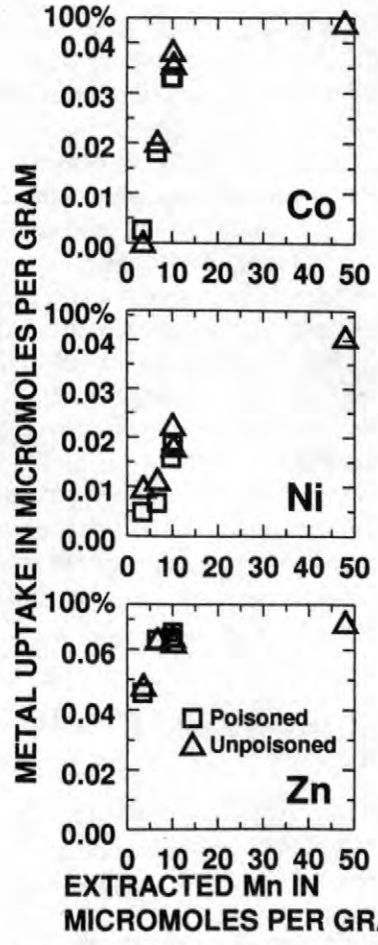

Figure 4. Co, Ni, and Zn uptake by streambed sediments versus pre-existing, extracted sediment Mn concentration. Experiments were conducted using a sediment concentration of 160 grams per liter, and initial dissolved Co, Ni, and Zn of 7.2, 7.5, and 9.2 μmoles/L, respectively.

that Mn oxide is an important absorbent for trace metals in Pinal Creek sediments. The role of Mn oxides as a metal absorbent is further evident from an X-ray absorption spectroscopic data of metal-contaminated sediments from Pinal Creek that suggests Zn is likely coordinated by Mn(III) and Mn(IV) octahedra (O'Day and others, 1998). These data are consistent with adsorption of Zn as a surface complex by Mn oxides and with substitution of Zn into Mn oxide phase. The trend of increased trace-metal uptake with increased Mn uptake in the hyporheic zone, and the elevated metal concentrations in hyporheic zone sediments support the hypothesis that ongoing Mn oxide formation enhances metal uptake.

Because surface complexation or adsorption is a reversible process (Davis and

Kent, 1990), a steady state or sorption equilibrium should develop between dissolved metals and pre-existing surface adsorption sites within the hyporheic zone provided that stream-water metal concentrations are constant over time. At sorption equilibrium, no net metal uptake should occur (${}^{*}C_h^{i+1} = C_h^{i+1}$). Equilibrium with pre-existing sorption sites at Pinal Creek is likely since stream-water metal concentrations typically do not vary more than 10 percent during base flow conditions (Konieccski and Angeroth, 1997). In addition, there was no measurable change in Mn, Co, Ni, or Zn concentration in five samples collected over a two-day period at one site in 1994 during this study. Assuming the pre-existing sorption sites are at equilibrium, metal uptake must occur by sorption to new Mn oxides as they are precipitated in the hyporheic zone, in order to account for the metal uptake calculated at most sites.

Effect of Hyporheic Zone Metal Uptake on Transport

Previously, we determined that enhanced Mn oxidation in the hyporheic zone accounts for the net uptake of 20 percent of Mn over the perennial reach to Inspiration Dam (Harvey and Fuller, 1998). The present study also demonstrates that net uptake of trace metals. Mass balance calculations support those conclusions, indicating net metal losses of 17, 12, 68, and 45 percent for Mn, Co, Ni and Zn, respectively, in 1994, and 26, 22, 37, and 38 percent in 1995. Loss percentages were calculated by subtracting the metal load at Inspiration Dam from the sum of the load at the upstream end of the 2.8-km reach and the averaged metal inflows over the 2.8-km reach, and dividing by the sum of the upstream and ground-water inputs.

Reach-scale simulations were used to determine if the observed reactive hyporheic-zone uptake affected stream-water metal concentrations over the 2.8-km study reach. The 1994 and 1995 stream-water trace-metal concentrations were simulated using OTIS, a one-dimensional transport model that accounts for inflow and storage (Runkel and Broshears, 1991). The simulations used the hydrologic and storage zone parameters derived by Harvey and Fuller (1998) from modeling the Br tracer injections in the 2.8-km study reach. Average metal concentrations from shallow ground water (< 2m) within each model subreach were used to define metal inflows. Dissolved metal concentrations in surface water were calculated over the 2.8-km reach using the average λ_h for each metal (table 2) for reactive uptake rate in the storage zone, λ_s. For comparison, metal concentration in the absence of hyporheic zone uptake ($\lambda_s = 0$) also were simulated.

The model successfully simulated surface-water Mn and Ni over the 2.8-km study reach using the average λ_h for storage-zone uptake (fig. 5). Model fits for Mn were of similar quality to simulations by Harvey and Fuller (1998), which optimized λ_s. However, the simulations of Co and Zn with reactive uptake predicted lower metal concentrations than the measured concentration (for example Zn, fig. 5). The simulation of Co with no reactive uptake provided a better fit to the measured Co concentrations than did the simulation with reactive uptake. Poor fits of reactive uptake are likely the result of uncertainties in model parameters. Because Mn and Ni can be simulated using the reach scale parameters, the inability to accurately simulate surface-water Co and Zn concentrations over a 2.8-km reach may result from greater uncertainty in defining inflow concentrations for these metals. Co and Zn inflows are limited to the most upstream model subreach and are based on a small data set that has a large variability.

Based on the calculated metal uptake in the hyporheic zone and the elevated sediment metal concentrations, we are confident that metal attenuation occurred over the study reach. The wide range in measured λ_h values, however, limits our conclusions from reach-scale simulations about the extent of reactive uptake in the hyporheic zone. Harvey and others (this volume) came to a similar conclusion having shown that the large standard deviation of the average λ_h for Mn results in simulations that overlap both the measured data and non-reactive simulation. The measured reaction rates in the hyporheic zone, therefore, can not be used alone to reliably demonstrate that metal removal occurs over the 2.8-km reach, but must be coupled with reach scale parameter estimation. We conclude that enhanced Mn oxidation and subsequent metal sorption in the hyporheic zone result in the decreases in metal load over the 7-km reach. However, Co, Ni and Zn attenuation can not be accurately simulated over the 2.8-km study reach

because of the measured range of λ_h and the uncertainty in defining metal inflows.

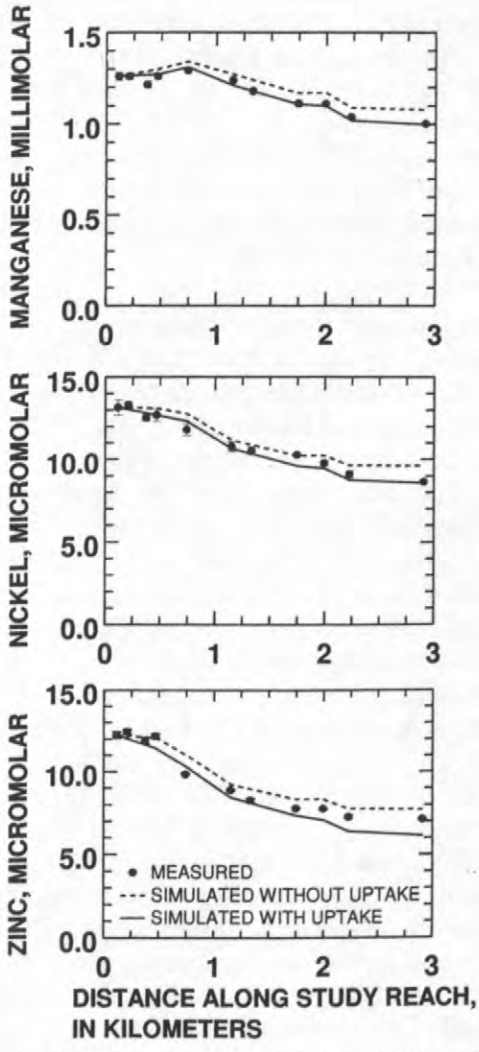

Figure 5. Simulations of surface-water Mn, Ni and Zn concentrations for June 1995 with and without reactive uptake in the hyporheic zone.

SUMMARY

Metal uptake by streambed sediments was observed at most hyporheic-zone sites. In laboratory experiments, Co, Ni and Zn uptake increased with increasing Mn oxide concentration of sediments. These findings suggest that Mn oxidation in the hyporheic zone enhanced trace-metal uptake. The calculated decreases in metal loads over the 7-km reach are attributed, in part, to Mn oxidation and subsequent metal uptake in the hyporheic zone. Trace-metal concentrations could not be accurately simulated over the 2.8-km study reach because of uncertainties in average measured hyporheic zone rate constants.

REFERENCES

Bencala, K.E., Kennedy, V.C., Zellweger, G.W., Jackman, A.P, and Avanzino, R.J., 1984, Interactions of solutes and streambed sediments, 1. An experimental analysis of cation and anion transport in a mountain stream: Water Resources Research, v. 20 p. 1797-1803.

Benner, S.G., Smart, E.W., and Moore, J.N., 1995, Metal behavior during surface-groundwater interactions, Silverbow Creek, Montana: Environmental Science and Technology, v. 29 p. 1789-1795.

Balistrieri, L.S., and Murray, J.W., 1986, The surface chemistry of sediments from the Panama Basin: The influence of Mn oxides on metal adsorption: Geochimica et Cosmochimica Acta, v. 50 p. 2235-2243.

Brown, J.G., and Harvey, J.W., 1996, Hydrologic and geochemical factors affecting metal contaminant transport in Pinal Creek Basin near Globe, Arizona, in Morganwalp, D.W., and Aronson, D.A. (eds.), U.S. Geological Survey Toxic Substances Hydrology Program--Proceedings of the technical meeting, Colorado Springs, CO., September 20-24, 1993: U.S. Geological Survey Water-Resources Investigations Report 94-4014 p. 1035-1042.

Catts, J.G., and Langmuir, D.L., 1986, Adsorption of Cu, Pb and Zn by δMnO_2: applicability of the site binding-surface complexation model: Applied Geochemistry, v. 1, p. 255-264.

Choi, J., Hulseapple, S., Conklin, M.H., and Harvey, J.W., 1998, Modeling CO2 degassing and pH in a stream-aquifer system:, Journal of Hydrology, v. 209 p. 297-310.

Davis, J. A. and Kent, D. B., 1990, Surface complexation modeling in aqueous geochemistry, Hochella, M. F., and White A. F. eds, Mineral-Water Interface Geochemistry: Mineralogical Society of America, Washington D.C., pp. 177-260.

Duff, J.H., Murphy, F., Fuller, C.C., Triska, F.J., Harvey, J.W., and Jackman, A.P., 1998, A mini-drivepoint sampler for measuring porewater solute concentrations in the

hyporheic zone of sand-bottom streams: Limnology and Oceanography, v. 43 p. 1378-1383.

Eychaner, J.H., 1991, Solute transport in perennial stream flow at Pinal Creek, Arizona, in Mallard, G.E., and Aronson, D.A. (eds.), U.S. Geological Survey Toxic Substances Hydrology Program--Proceedings of the technical meeting, Monterey, California, March 11-15, 1991: U.S. Geological Survey Water Resources Investigation Report 91-4034, p. 481-485.

Glaser, J.A., Foerst, D.L., McKee, G.D., Quave, S.A., and Budde, W.L., 1981, Trace analyses for wastewaters: Environmental Science and Technology, v. 15 p. 1426-1435.

Harvey, J.W. and Fuller, C.C., 1996, Association of metal contaminants with colloidal and suspended material in shallow groundwater and surface water at Pinal Creek, Arizona, in Morganwalp, D.W., and Aronson, D.A. (eds.), U.S. Geological Survey Toxic Substances Hydrology Program--Proceedings of the technical meeting, Colorado Springs, CO., September 20-24, 1993: U.S. Geological Survey Water-Resources Investigations Report 94-4014 p. 1073-1080.

Harvey, J.W. and Fuller, C.C., 1998, Effect of enhanced manganese oxidation in the hyporheic zone on basin-scale water quality:. Water Resources Research, v. 34 p. 623-636.

Harvey, J.W., Fuller, C.C., and Conklin, M.H., Enhanced removal of dissolved manganese in hyporheic zones: centimeter-scale causes and kilometer-scale consequences, in Morganwalp, D.W. and Buxton, H.T., eds., U.S. Geological Survey Toxic Substances Hydrology Program—Proceedings of the Technical Meeting, Charleston, South Carolina, March 8-12, 1999: U.S. Geological Survey Water-Resources Investigations Report 99-4018A, this volume

Kimball, B.A., Broshears, R.E., Bencala, K.E., and McKnight, D.M., 1994, Coupling of hydrologic transport and chemical reactions in a stream affected by acid mine drainage: Environmental Science and Technology, v. 28 p. 2065-2073.

Koniecski, A.D., and Angeroth, C.E., 1997, Hydrologic data from the study of acidic contamination in the Miami Wash-Pinal Creek area, Arizona, water years 1994-96: U.S. Geological Survey Open-File Report 97-247.

Marble, J.C., 1998, Biotic contribution of Mn(II) removal at Pinal Creek, Arizona: Tucson, University of Arizona, Department of Hydrology and water Resources, unpublished M.S. thesis, 191 p.

McKenzie, R.M., 1980, The adsorption of lead and other heavy metals on oxides of manganese and iron, Australian Journal of Soil Research, v. 18 p. 61-73.

O'Day, P.A., Geiger, K.E., and Fuller, C.C., 1998. Molecular scale characterization of manganese oxides and trace metals in stream sediments from a mining-contaminated site, in Arehart, G.B. and Hulston, J.R., eds., Water Rock Interaction--Proceedings of the 9th International Symposium--WRI-9 Taupo, New Zealand, April 1998, p. 993-996.

Papelis, C., Hayes, K.F., and Leckie, J.O., 1988. HYDRAQL: A program for the computation of chemical equilibrium composition of aqueous batch systems including surface complexation modeling of ion adsorption at the oxide/solution interface. Tech. Rep. 306, Dept. Civil Eng., Stanford Univ. 130 pp.

Runkel, R.L., and Broshears, R.E., 1991, One-dimensional transport with inflow and storage (OTIS): A solute transport model for small streams, Boulder, University of Colorado, Center for Advanced Decisions Support in Water and Environmental Science, Technical Report 91-01, 85 p.

Stollenwerk, K.G., 1994, Geochemical interactions between constituents in acidic groundwater and alluvium in an aquifer near Globe, Arizona: Applied Geochemistry v. 9 p. 353-369.

Triska, F.J., Duff, J.H., and Avanzino, R.J., 1993, The role of water exchange between a stream-channel and its hyporheic zone in nitrogen cycling at the terrestrial-aquatic interface,: Hydrobiologia, v. 251 p. 167-184.

AUTHOR INFORMATION

Christopher C. Fuller, U.S. Geological Survey, Menlo Park, California

Judson W. Harvey, U.S. Geological Survey, Reston, Virginia

Environmental Factors Affecting Oxidation of Manganese in Pinal Creek, Arizona

By Justin C. Marble, Timothy L. Corley, Martha H. Conklin, and Christopher C. Fuller

ABSTRACT

The objectives of the laboratory work reported here were to quantify the net rates of removal of manganese [Mn(II)] by streambed sediments collected from a metals contaminated, perennial stream system (Pinal Creek near Globe AZ) and to determine the key variable(s) responsible for the limited removal of Mn(II) observed at this field site. Pinal Creek is characterized by significant spatial gradients in pH, alkalinity, and Mn(II) along its length and by spatial gradients in pH, dissolved oxygen, and Mn(II) across hyporheic zones of varying thickness. These gradients are established by mixing of surface water and entering shallow ground water in the sediments. The mixing of waters in the hyporheic zones define the local chemical environments in which Mn(II) is removed by incorporation into pre-existing and newly formed mineral surfaces through abiotic and biotic processes. As a consequence of the site characteristics, particularly the spatial gradients in the hyporheic zone, the primary chemical parameters included in the test matrix were pH, initial Mn(II) concentration, and dissolved oxygen. Streambed sediments collected from the site were used in laboratory batch investigations of the rate of Mn(II) removal. Results of these studies indicate that removal of Mn(II) within the hyporheic zone primarily occurs via biotic oxidation processes, is approximately first-order with respect to the Mn(II) concentration and inversely proportional to $[H^+]$, and independent of dissolved oxygen concentration except at very low levels.

INTRODUCTION

Quantifying the interdependence of biogeochemical factors that affect natural remediative processes of dissolved metals in mine-drainage-contaminated stream systems provides a basis for interpretation of field observations and, potentially, identification of inherent factors that limit the ability of a system to remediate itself. In small streams gradients in pH, dissolved oxygen (O_2), metals concentrations, and other chemical parameters in stream-bed sediments are established by mixing of surface and entering contaminated ground water in the hyporheic zone. The distinct character and the importance of hyporheic zone to microbial communities within the sediments and the fluxes of dissolved O_2 (DO) and nutrients (e.g., particulate and dissolved organic carbon and nitrate) within a stream system are well documented and accepted as a key aspect of stream ecosystems [Grimm and Fisher, 1984; Findlay and others, 1993; Triska and others,1993; Jones and others, 1995a, 1995b; Valett and others, 1996]. The significance of hyporheic exchange in the biogeochemistry of metal contaminants in coupled surface water/ground water systems has also received attention but a quantitative understanding of its role is still being developed [Cerling and others, 1990; Bourg and Bertin, 1993; Kimball and others, 1994; Benner and others, 1995; Broshears and others, 1996; Harvey and Fuller, 1998].

The work reported herein focuses on biogeochemical processes occurring in a small, perennial stream, Pinal Creek near Globe, Arizona. Overall removal rates of Mn(II) from Pinal Creek have been determined by Harvey and

Fuller (1998), however, the dependence on key parameters has not been quantified. The specific aims of this work were to quantify the net rates of removal of Mn(II) under different conditions using sediments collected from the perennial reach of Pinal Creek and to identify the key variable(s) responsible for the limited removal of Mn(II) observed at the field site. Because pH and Mn(II) values change along the perennial reach and spatial gradients across the hyporheic zone are observed for pH, Mn(II), and O_2, it was hypothesized that one or more of these chemical parameters controlled removal of Mn(II) from the system. To test this, a set of laboratory experiments was conducted to establish the dependence of the rate of removal of Mn(II) on these chemical parameters.

SITE DESCRIPTION

Pinal Creek is the outlet of the Pinal Creek basin (a typical alluvial basin of the Southwest) and the perennial stream reach (approximately 13 km (kilometer) length from head of flow to the confluence with the Salt River) is fed by groundwater from the alluvial aquifer that has been contaminated by copper-mining activities in the area [e.g., Eychaner, 1989]. Surface water chemistry in the upper 4-km length of the perennial reach is dominated by discharge of partially neutralized, metals-contaminated groundwater (pH 5.5 – 6). Manganese is the primary metal contaminant in the perennial reach and its concentration in surface waters near the head of flow has remained approximately constant at about 1.2 mM (millimolar) from 1990 to 1996 [Gellenbeck and Hunter, 1994; Konieczki and Angeroth, 1997, Marble, 1998]. Other dissolved metals present in the upper length of the perennial reach include Ni (10 μM, micromolar), Zn (15 μM), Co (10 μM), and Cu (1 μM) (Marble and Corley, unpublished data). Since October, 1998, these concentrations have changed due to remediation activities (unpublished data). This paper reflects the situation prior to that date.

Manganese entering the perennial reach is oxidized to produce a mixture of Mn(III,IV)-oxyhydroxide precipitates (Mn oxides) of various textures from fine flocculent materials to layered concretions within the stream sediments resembling asphalt at some locations [Lind, 1991; Hulseapple, 1995; Flinchbaugh, 1996; Harvey and Fuller, 1998; Marble, 1998]. The biogeochemical processes responsible occur predominantly in the hyporheic zone at Pinal Creek and result in an overall reactive loss of about 20% of dissolved Mn(II) along the upper 4-km length of the perennial reach [Harvey and Fuller, 1998]. The hyporheic zone varies in depth along the perennial reach from less than 2 cm (centimeter) below the sediment-surface water interface to greater than 20 cm [Harvey and Fuller, 1998], and is typical of the depths expected for perennial systems [White, 1993]. DO concentrations in the hyporheic zone at Pinal Creek typically decrease with depth from about 60 μM at the interface with surface water to the merging groundwater value of about 3 μM. Spatial and depth gradients across this zone are also observed for pH (6 to 7.8 for surface water to 5.5 to 6 for emerging ground water) and for the different metal contaminants (e.g., shallow groundwater Mn(II) concentrations range from 1.2 mM to 0.1 mM, depending on the location along the reach, Corley and Marble, unpublished data). In addition, over the 4-km length of the perennial reach the pH of surface water increases from 6 to 7.8. and Mn(II) in surface water decreases from 1.2 mM to about 0.9 mM.

MATERIALS AND METHODS

A series of batch experiments were conducted to determine the net rates of Mn(II) removal from aqueous solution in the presence of streambed sediments. Sediments collected from different sites along the perennial reach of Pinal Creek were used: 1) sediments from site 4 to investigate Mn(II) and pH dependence; 2) sediments from sites 2 and 3 to determine the dependence on DO; and, 3) sediments from site 1 and at Inspiration Dam (about 2.2 km downstream of site 4) were used in an initial set of experiments (see Figure 1). At each site, the top 2.5 cm layer of sediments was pushed aside and the sample was taken from the sediments immediately below in order to minimize or eliminate the introduction of algae into the batch bottles. The sediments were wet-sieved to collect the < 250 μm (micrometer) or the < 2 mm

(millimeter) size fraction depending on the experiment. Approximately 15 g (gram) of sediments were added to each batch bottle containing 100 mL (milliliter) of artificial stream water. The batch bottles were placed on shaker tables and agitated during the different experiments.

An artificial stream water (ASW) based on the measured major ion composition of Pinal Creek was used in these experiments after tests confirmed that identical results were obtained whether filtered (0.45 μm, mixed cellulose acetate

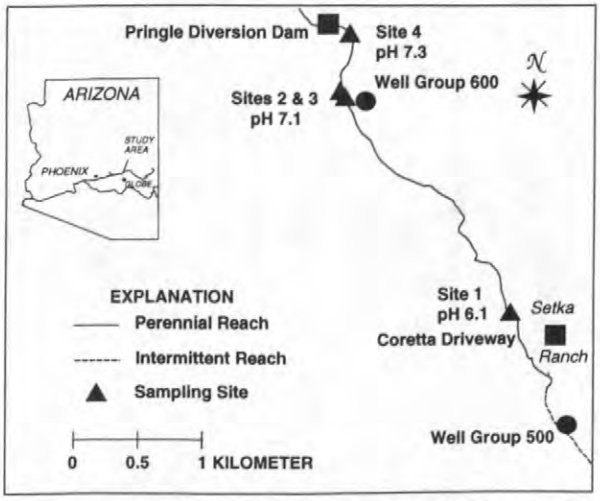

Figure 1. Field site and sampling locations in the upper perennial reach.

and nitrate) surface water or ASW was used. The use of ASW allowed experiments with the same sediments to be conducted at different pH values and at different Mn(II) concentrations.

The test matrix for these experiments included: 1) fixed pH (7.1 or 7.3), atmospheric O_2 concentration, and different initial Mn(II) concentrations (0.2 to 1.5 mM); 2) fixed initial Mn(II) concentration (0.82 mM), atmospheric O_2 concentration, and different pH values (6 to 7.8); and, 3) fixed initial Mn(II) concentration (0.82 mM) and pH (7.1), and different DO concentrations (0.015 mM to 0.45 mM).

DO concentrations were varied by mixing gas streams of nitrogen (N_2), air, and O_2 in a simple manifold system and introducing the resulting gas mixture into the headspace of the batch bottles. Mass flow controllers were used to maintain accurate control of the individual gas flows and therefore the mixture composition. The O_2 concentration in the headspace and DO were measured periodically with a minielectrode to make sure that conditions did not change during the course of specific experiments. The lids to the bottles for DO independent studies were left loosely attached during experiments conducted at atmospheric O_2 levels to prevent production of anaerobic conditions.

Different buffers (HEPES, MES and PIPES) were used to minimize or eliminate any changes in pH. Although a recent paper (Yu and others, 1997) indicates that HEPES may complex metals, particularly copper, no evidence of such an interference was observed in our studies as the use of different buffers for the same pH value gave the same results. The initial pH values for each batch bottle were achieved by adding HCl or NaOH until the target value had been reached.

Since it was anticipated that the biogeochemical processes responsible for Mn(II) removal in Pinal Creek would involve a strong biotic component, the batch experiments were conducted under "poisoned" and "unpoisoned" conditions. Of the choice of biological poisons that have been used in studies of Mn(II) oxidation by bacteria [Kepkay, 1985; Adams and Ghiorse, 1987; Moffet, 1994], sodium azide (NaN_3) was selected for use in these studies. The key factor in choosing NaN_3 was the fact that it has been shown not to interfere with manganese chemistry. Batch bottles with NaN_3 added were designated abiotic and those without NaN_3 were designated biotic. Although it is recognized that both biotic and abiotic mechanisms participate in experiments without NaN_3, the unpoisoned batch studies are designated biotic only. Controls were conducted without sediments present.

Aliquots (0.25 mL or less) of the solution were removed at specific times after the start of the experiments and analyzed for Mn(II) via flame atomic absorption spectroscopy (FAAS) after appropriate dilutions to reach the linear region of the instrument's response. Partial dissolution of the sediments with acidified hydroxylamine hydrochloride [Chao, 1972] was used to determine total Mn in the sediment coatings via FAAS of the supernatant.

The net rates of removal of Mn(II) were determined from slopes of the linear sections of

semi-logarithmic plots of the measured Mn(II) concentrations versus time. The slope represents a pseudo first-order rate constant and the rate was calculated by multiplying by the Mn(II) concentration. The resulting value of the net rate of Mn(II) removal is the sum of all processes releasing Mn(II) into solution minus the sum of all processes removing Mn(II) from solution. As a result, the observed net rate of Mn(II) removal may be positive, negative, or zero.

RESULTS AND DISCUSSION

An initial set of experiments used sediments and filtered surface water collected from sites 1 and 4 and at Inspiration Dam to determine the relative rates of Mn(II) removal by sediments from the perennial reach. These locations were characterized by different surface water pH values (6.1, 7.3, and 7.8, respectively), different surface water Mn(II) concentrations (1.25 mM, 0.90 mM, and 0.82 mM, respectively), and different densities of aquatic vegetation and algae.

No measurable removal of Mn(II) occurred using sediments and filtered surface water collected from the pH 6.1 site during the 34 days that these experiments were run. The initial and final concentrations of Mn(II) were identical for abiotic and biotic conditions and for the controls run without sediments. As no net release of Mn(II) was observed, the results of these experiments indicate that dissolution of the Mn oxides did not occur on the timescale of these experiments.

At the higher pH values, significant Mn(II) concentration changes were observed over time and identical results were obtained using either filtered surface water or ASW. Representative results are shown in Figures 2 and 3 for the sediments and filtered surface water collected at Inspiration Dam (pH 7.8 and initial Mn(II) ~ 0.93 mM) and for the sediments collected at site 4 using ASW (pH 7.3 and initial Mn(II) ~ 0.80 mM), respectively. It is apparent from these plots that the addition of NaN_3 suppresses the rate at which Mn(II) is removed from solution as well as the fraction removed. The concentration versus time data at pH 7.8 yield an apparent first-order rate constant for Mn(II) removal under abiotic conditions of $(8.2 \pm 0.4) \times 10^{-7}$ s^{-1} (per second) and a value of $(1.7 \pm 0.3) \times 10^{-5}$ s^{-1} under biotic conditions, i.e., the biotic net rate of removal is approximately a factor of 20 times that of the abiotic rate. The results in Figure 3 yield an apparent first-order rate for Mn(II) removal of $(0.44 \pm 0.18) \times 10^{-5}$ s^{-1} for abiotic conditions versus $(1.7 \pm 0.05) \times 10^{-5}$ s^{-1} in the absence of NaN_3, a factor of 4 difference.

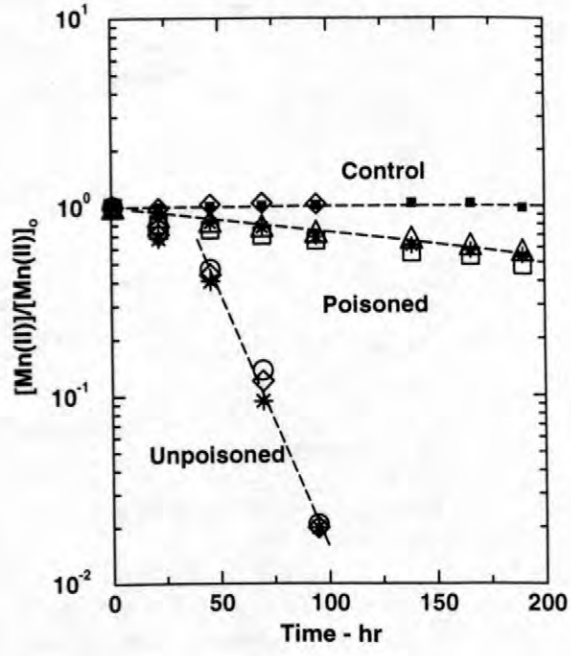

Figure 2. Removal of Mn(II) using sediments and filtered surface water from Inspiration Dam (pH 7.8). Dashed lines are for visual aid.

The normalized concentration versus time plots in Figures 2 and 3 also illustrate a feature of the batch experiments that was dependent on the length of time between collection of sediments and the start of the experiment. A "lag time" was observed at early times in a subset of the experiments in which the decrease in Mn(II) concentration with time was essentially the same for both abiotic and biotic conditions. In Figures 2 and 3 the divergence between the abiotic and biotic Mn(II) profiles began after 24 and 10

hours, respectively. This lag time increased with the interval between collection of sediments and the start of an experiment but disappeared completely if the sediments were used within 2-3 days of collection. It should also be noted that the differences in Figures 2 and 3 between the Mn(II) concentration profiles for abiotic and biotic conditions were still obtained with sediments that had been stored at < 10 °C for up to 6 months.

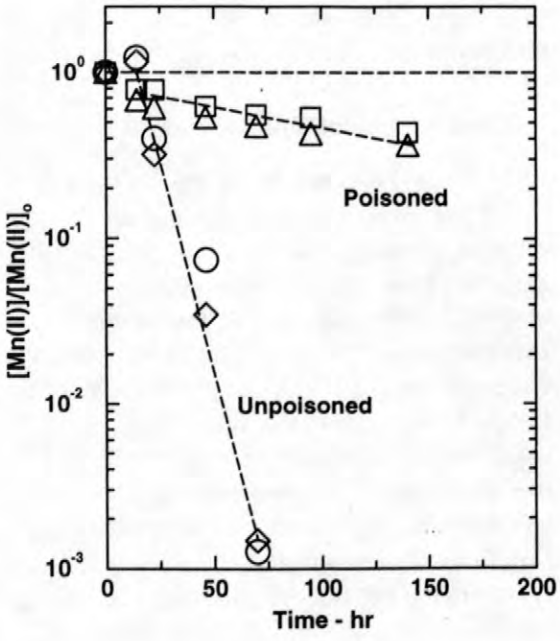

Figure 3. Removal of Mn(II) using sediments from site 4 and ASW (pH 7.3). Dashed lines are for visual aid.

The sediments collected from Inspiration Dam (surface water pH 7.8) had a total Mn concentration of (2230 ± 250) mg kg^{-1} dry sediment (milligram per kilogram dry sediment). The sediments from site 4 (surface water pH 7.3) had a total Mn concentration of (2920 ± 615) mg kg^{-1} dry sediment. These values refer specifically to the sediments used for batch studies in presented in Figures 2 and 3.

Mn(II) Dependence

The dependence of the net rate of removal of Mn(II) on Mn(II) concentration is shown in Figure 4. All of these batch experiments were conducted with ASW and at a fixed pH of 7.3 using natural sediments from site 4. The results obtained under both biotic and abiotic conditions suggest that between 0.2 and 1.25 mM Mn(II) the net rate of removal is directly proportional to Mn(II) and that a simple first-order dependence on Mn(II) is a reasonable assumption. However, it is apparent from Figure 4 that the net rates of Mn(II) removal for these natural sediments do not extrapolate to a zero intercept at zero Mn(II) concentration.

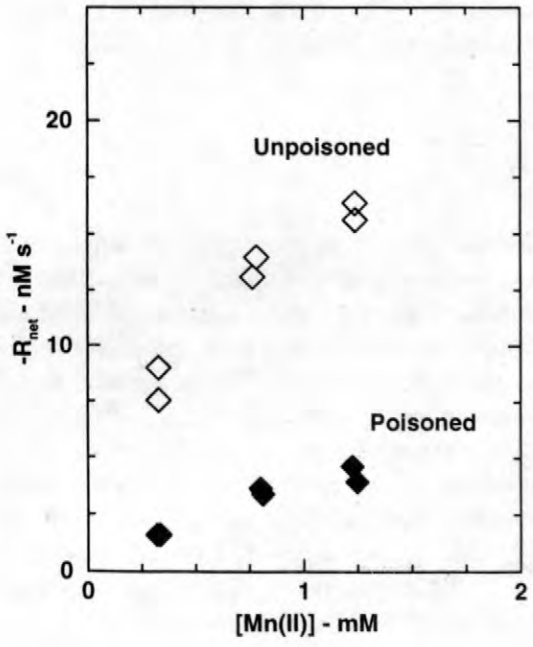

Figure 4. The net rate of Mn(II) removal increases with Mn(II) concentration.

In other studies of Mn(II) removal (oxidation) in microbially active media without sediments present (pure and enriched cultures and unfiltered water samples) it has been demonstrated that the rate of Mn(II) removal is consistent with a Michaelis-Menten-type of rate expression [e.g., Tebo and Emerson, 1985; Tebo and others,1997],

$$\frac{-d[Mn(II)]}{dt} = V_m \frac{[Mn(II)]}{[Mn(II)] + K_m},$$

where V_m is the maximum rate (e.g., nM s^{-1}, nanomolar per second) and K_m is the Michaelis constant (e.g., mM). If this equation held for the current studies then an apparent linear dependence of net removal on Mn(II) would be expected over some range of initial concentrations with a distinct curvature over a wider concentration range and an asymptotic plateau value for the net rate at high Mn(II) concentrations. Although the derived rates of Mn(II) removal can be fitted to the Michaelis-Menten functional form (r^2 values ≥ 0.96), a more rigorous test is obtained by considering the integrated form for Michaelis-Menten kinetics and plotting the data in transformed coordinates [Levenspiel, 1996];

$$\frac{\ln \frac{C_0}{C}}{(C_0 - C)} = -\frac{1}{K_m} + \frac{V_m}{K_m} \frac{t}{(C_0 - C)}.$$

Results of this test show that our data are inconsistent with a simple Michaelis-Menten-type mechanism, or extensions to a mechanism with simple competitive and noncompetitive inhibition or substrate inhibition. This suggests that the reaction mechanism responsible for a net removal of Mn(II) in our experiments is more complicated, or may reflect indirect oxidation mechanisms associated with microorganisms [Wehrli and others, 1995; Tebo and others, 1997].

An alternative explanation of our results may be inferred from the results of abiotic experiments conducted with Mn-oxide coatings removed from sand filter materials used in water treatment facilities in Europe to remove Mn(II) from ground water [Graveland and Heertjes, 1975]. The coatings collected from these "biologically ripened sands" were a mixture of Mn(II,III,IV)-oxyhydroxides (MnO_x, x ~ 1.33) and were sterilized by drying at 70 C under a N_2 atmosphere. Based on the results of their sorption and oxidation experiments, these researchers concluded that a single site, or Rideal reaction mechanism, in which Mn^{2+} in solution reacts with O_2 sorbed at the surface, provided a consistent explanation of the linear dependence for abiotic uptake. Since the Mn-oxide coatings on the sediments collected from Pinal Creek were also formed predominantly through biological processes involving Mn-oxidizing bacteria they may be similar to the coatings used by Graveland and Heertjes [1975] and a similar reaction mechanism may be applicable in part. However, the exact mechanism may not be critical in terms of the overall objective of these experiments, since the concentration range over which a linear dependence of net removal on Mn(II) was observed corresponds approximately to the range of Mn(II) concentration values observed at Pinal Creek (0.2 to 1.25 mM). Our rate data and rate coefficients can definitely be used to interpret field data within this common range of Mn(II) concentrations.

pH Dependence of Mn(II) Removal

The pH dependence of the net rates of Mn(II) removal is presented in Figure 5 on a semi-logarithmic scale. For natural sediments collected from site 4, a linear correlation was observed for both biotic and abiotic conditions. However, a net release of Mn(II) was observed under abiotic conditions for pH less than or equal to 6.5. This suggests that under these experimental conditions Mn(II) reversibly bound to surface sites or to other binding sites (e.g., extracellular polysaccharides) is released at a faster rate than adsorbtion and oxidation. Linear regression of the $\log_{10}[-R_{net}]$ versus pH data yielded a slope of 0.80 ± 0.12 for unpoisoned sediments and 0.75 ± 0.14 for poisoned sediments, i.e., statistically indistinguishable slopes that are statistically different from unity at the 95% confidence level.

The pH dependence of the net rate of Mn(II) removal indicates that the rate is approximately inversely proportional to H^+, or proportional to OH^-. An increase of Mn(II) removal and oxidation with an increase pH has been reported for abiotic conditions with different metal oxide substrates [Brewer, 1975; Davies and Morgan, 1989] and Mn-oxide coatings from sand filter materials [Graveland and Heertjes, 1975], and for biotic conditions with soils [Gerretsen, 1937; Sparrow and Uren, 1987].

The experiments conducted by Graveland and Heertjes [1975] may again be most relevant to the current sets of batch experiments with streambed sediments removed from Pinal Creek.

Results from these earlier abiotic experiments indicated that the rate of Mn(II) removal was directly proportional to [OH^-], as observed in the current studies, and decreased to zero at pH 7, a slightly higher value than in our batch studies (pH ~ 6.5). The differences in the pH "cut-off" may be due to different Mn oxides or coverage on the sediment surfaces, to other adsorption phases, or to micro-environments created by micro-organisms that are not poisoned by NaN_3. Our results for abiotic conditions may be consistent with the arguments proposed by Graveland and Heertjes [1975] who inferred that overall mass transfer of Mn^{2+} from solution to active sites at the surface decreased as pH decreased because of competition with H^+.

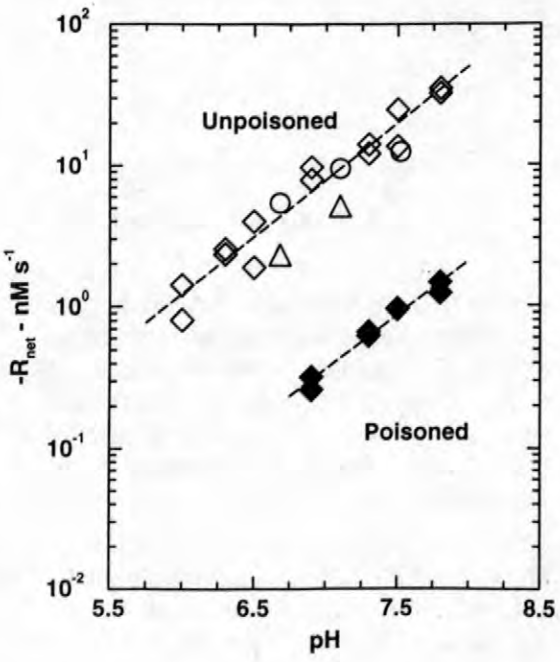

Figure 5. The net rate of Mn(II) removal increases with pH. Different symbols represent different experiments. Dashed lines represents results of linear regression.

The similarities that we observed between the pH dependence of the rate of Mn(II) removal under biotic and abiotic conditions suggest that an autocatalytic mechanism also participates in the removal of Mn(II) under biotic conditions. The increased rate of Mn(II) removal under biotic conditions can be explained if bacteria, or other microorganisms, continually produce fresh Mn oxides via direct or indirect processes. This is an important point as it has been shown that the autocatalytic activity of Mn(III,IV)-oxyhydroxide coatings decreases as the coatings age and become more oxidized and crystalline [Graveland and Heertjes, 1975].

Dissolved-O_2 Dependence

The DO dependence of the observed net rate of removal is presented in Figure 6. Natural sediments from site 3 (pH 7.1) were used in these experiments but the samples were collected at two different times of the year. Above about 30% of saturation, the data for the sediments collected in June 1998 exhibit no significant dependence on DO concentration. Below this value the net rate of Mn(II) removal was approximately first-order with respect to DO concentration, as shown by the log-log plot of the data. The data for the sediments collected in August 1998 suggest that these sediments were not dependent on dissolved-O_2 concentration until a value less than about 10-30% of saturation was reached. A marked change in rates of Mn(II) removal occurring at 5 to 15% air saturation has been previously reported in experiments with Mn-oxidizing bacteria present in marine waters [Tebo and Emerson, 1985; Tebo and others, 1991].

The lack of dependence of the rate of Mn(II) removal on DO above some "critical" O_2 level has also been observed in abiotic studies with Mn oxides that were biotically produced [Graveland and Heertjes, 1975]. These researchers reported no dependence of the rate of Mn(II) removal on DO above concentrations of about 1 mg L^{-1} (milligram per liter) (~ 12% air saturation, or 0.03 mM) and an approximate linear dependence at lower DO values. Our data may reflect relative populations of macro- and micro-aerophilic Mn-oxidizers in Pinal Creek, a decrease in biotic activity at lower DO levels that results in lower production of a key chemical from microorganisms present on the sediments, and/or a decrease in surface adsorbed O_2.

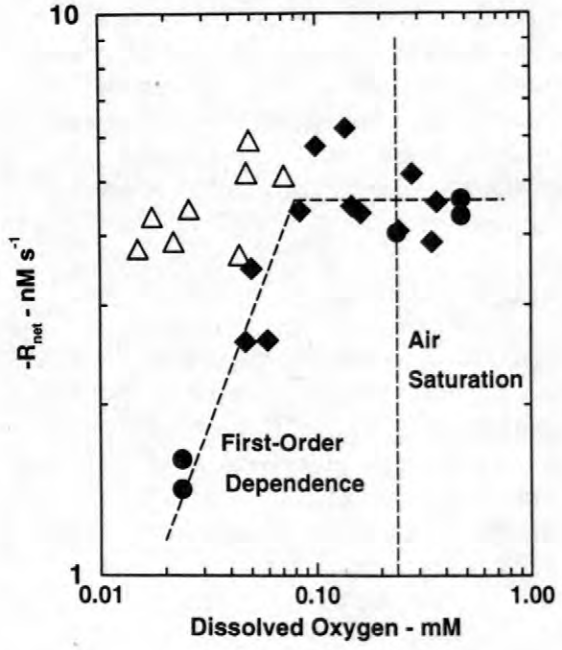

Figure 6. The net rate of Mn(II) removal is independent of DO above 30% air saturation (filled symbols from June, 1998; open symbols from August, 1998). Dashed lines are for visual aid.

Pre-existing Mn Oxides

The results of our batch experiments have identified the dependences of the net rate of removal of Mn(II) on initial Mn(II) concentration, pH, and DO. However, it is apparent from the data presented in Figures 2-6 that, depending on the date and the site at which the samples were collected the absolute values of the net rates of removal are different. The different rates may be due to differing amounts of active surface sites and/or different microbial populations. As we do not have a direct measure of active surface sites, the correlation of rate versus concentration of pre-existing Mn oxides was considered. This was done by scaling the rates obtained under different experimental conditions (initial Mn(II), pH), but at air-saturated O_2 levels, to a reference set of values for pH and Mn(II) using the functional dependences that have been determined in these studies. Different sediment samples with two size ranges (< 250 μm and < 2 mm) were used. Figure 7 shows the results of such calculations (reference pH = 7.1 and reference Mn(II) = 1 mM) for sediments collected at different sites and on different dates plotted against Mn-loading of the solids. There is no

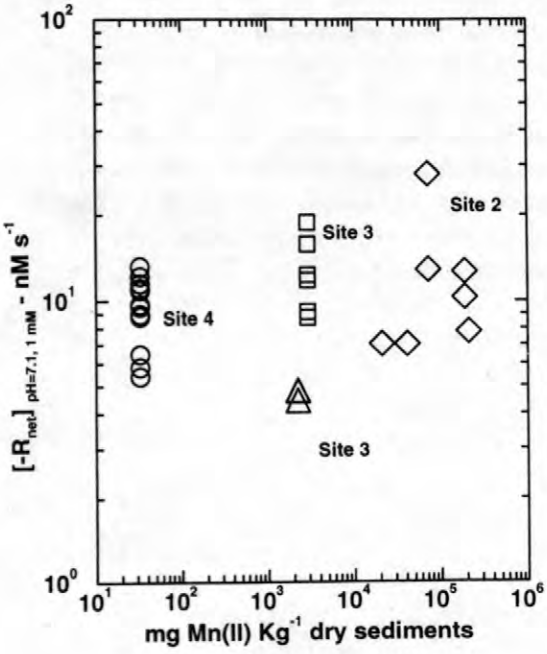

Figure 7. The net rate of Mn(II) removal on unpoisoned sediments is not affected by pre-existing Mn coatings. Different symbols refer to different experiments. Site refers to the site of sediment collection. The diamonds represent experiments done with < 250 mm sediments; the other experiments used < 2mm sediments.

apparent (at least no strong) correlation between the total Mn-loading of the sediments and the rates after differences in pH and initial Mn(II) concentration have been taken into consideration, and there is no size fraction dependence. This finding does not preclude a key role for a specific form of Mn in the sediment coatings but it does indicate that total Mn-loading is not necessarily a good indicator of the potential Mn-oxidation rate. This inference is in contrast to the findings of Harvey and Fuller [1998] who reported an increase in the observed Mn-oxidation rate with an increase in pre-existing Mn-oxide concentration. The explanation for this difference is not obvious. The second possibility considered

here, microbial populations and/or activity, cannot be addressed with our current database, but it is a testable hypothesis that can be addressed in future work.

CONCLUSIONS

The findings of this study clearly indicate that biotic processes are key factors in determining the net removal of Mn(II) and the net rates of Mn(II) removal at Pinal Creek. The rate is approximately first-order with respect to Mn(II) concentration and inversely proportional to H^+ (directly proportional to OH^-), and independent of DO above about 0.05 – 0.07 mM. Comparisons between the results using poisoned and unpoisoned sediments strongly suggest that the microbial processes for Mn(II) removal in Pinal creek include both indirect and direct mechanisms. Finally, there is no signficant evidence from our studies that pre-existing Mn-oxide concentrations influence the Mn-oxidation rate.

Acknowledgements. This publication was made possible by grant number EAR-9523881 from the National Science Foundation and grant number P42 ESO4940 from the National Institute of Environmental Health Sciences, NIH with funding provided by EPA. Its contents are solely the responsibility of the authors and do not necessarily represent the official views of the NIEHS, NIH or EPA. We appreciate the assistance on the DO experiments by R. Koelsch and Mn batch studies by E. Parker. We thank J. Villinski and J. Harvey for their helpful review comments.

REFERENCES

Adams, L.F., Ghiorse, W.C., 1987, Characterization of Extracellular Mn^{2+}-Oxidizing Activity and Isolation of Mn^{2+}-Oxidizing Protein from Leptothrix discophora SS-1, Journal of Bacteriology, 169, 1279-1285.

Benner, S.G., Smart, E.W., Moore, J.N., 1995, Metal behavior during surface-groundwater interaction, Silver Bow Creek, Montana, Environmental Science and Technology, 29, 1789-1795.

Bourg, A. C. M. and Bertin, C., 1993, Biogeochemical processes during the inflitration of river water into an alluvial aquifer, Environmental Science and Technology 27, 661-666.

Brewer, P.G., 1975, Minor Elements in Sea Water, Riley, J.P. and G.Skirrow (Eds.), Chemical Oceanography, Academic Press, New York, 415-496.

Broshears, R. E., Runkel, R. L., Kimball, B. A., Mcknight, D. M., and Bencala, K. E., 1996, Reactive solute transport in an acidic stream: Experimental pH increase and simulation of controls on pH, aluminum, and iron, Environmental Science & Technology, 30(10), 3016.

Cerling, T.E., Morrison, S.J., Sobcinski, R.W., 1990, Sediment-water interaction in a small stream: adsorption of ^{137}Cs by bed load sediments, Water Resources Research, 26, 1165-1176.

Chao, T.T., 1972, Selective dissolution of manganese oxides from soils and sediments with acidified hydroxylamine hydrochloride, Proceedings – Soil Science Society of America, 36, 764-768.

Davies, S.H.R., Morgan, J.J., 1989, Manganese(II) oxidation kinetics on metal oxide surfaces, Journal of Colloid and Interface Science, 129, 63-77.

Eychaner, J.H., 1989, Movement of inorganic contaminants in acidic water near Globe, Arizona. Technical Report, U.S. Geological Survey, Water Resources Investigation Report 88-4220, Reston, VA, p. 567.

Findlay, S., Strayer, D., Goumbala, C., Gould, K., 1993, Metabolism of streamwater dissolved organic carbon in the shallow hyporheic zone. Limnology and Oceanography, 38, 1493-1499.

Flinchbaugh, H., 1996, Biotic and abiotic processes contributing to the removal of Mn(II), Co(II) and Cd(II) from Pinal Creek, Globe, Arizona, unpublished M.S. Thesis, University of Arizona, Tucson, AZ, Department of Hydrology and Water Resources.

Gellenbeck, D. J. and Y.R. Hunter, 1994, Hydrological data from the study of acidic contamination in the Miami Wash-Pinal Creek Area, Arizona, water years 1992-93. 94-508, U.S. Geological Survey Open-file Report.

Gerretsen, F.C., 1937, Manganese Deficiency of Oats and its Relation to Soil Bacteria, Annals of Botany, 1, 207-230.

Graveland, A., Heertjes, P.M., 1975, Removal of manganese from ground water by heterogeneous autocatalytic oxidation, Transactions of the Institution of Chemical Engineers, 53, 154-164.

Grimm, N.B., Fisher, S.G., 1984, Exchange between interstitial and surface water: Implications of stream metabolism and nutrient cycling, Hydrobiologia, 111, 219-228.

Harvey, J.W., Fuller, C.C., 1998, Effect of enhanced manganese oxidation in the hyporheic zone on basin-scale geochemical mass balance, Water Resoures Research, 34, 623-636.

Hulseapple, S. M., 1995, A Field Study of Reaeration and Solute Transport at Pinal Creek, Globe, Arizona, unpublished M.S. Thesis, University of Arizona, Department of Hydrology and Water Resources.

Jones, J.B.Jr., Holmes, R.M., Fisher, S.G., Grimm, N.B., Greene, D.M., 1995a, Methanogenesis in Arizona, USA dryland streams, Biogeochemistry, 31, 155-173.

Jones, J.B.Jr., Fisher, S.G., Grimm, N.B., 1995b, Vertical hydrologic exchange and exosystem metabolism in a Sonoran desert stream, Ecology, 76, 942-952.

Kepkay, P.E., 1985, Kinetics of microbial manganese oxidation and trace metal binding in sediments: Results from an in situ dialysis technique, Limnology and Oceanography, 30, 713-726.

Kimball, B.A., Broshears, R.E., Bencala, K.E., Mcknight, D.M., 1994, Coupling of hydrologic transport and chemical reactions in a stream affected by acid mine drainage, Environmental Science and Technology, 28, 2065-2073.

Konieczki, A. D. and Angeroth, C. E., 1997, Hydrologic data from the study of acidic contamination in the Miami Wash-Pinal Creek area, water year 1994-96. 97-247, Tucson, Arizona, U.S. Geological Survey. U.S. Geological Survey Open-file Report.

Levenspiel, O., 1996, The Chemical Reactor Omnibook. Corvallis, Oregon, OSU Book Stores.

Lind, C., 1991, Manganese minerals and associated fine particulates in the Pinal Creek stream bed. In: Mallard, G.E., ed., U.S. Geological Survey Toxic Substances Hydrology Program -- Proceedings of the Technical Meeting, Monterey, California, March 11-15, 1991, Water-Resources Investigations Report 91-4034, Reston VA, U.S. Geological Survey, , p. 486.

Marble, J. , 1998, Biotic contribution of Mn(II) removal at Pinal Creek, Globe, Arizona, unpublished M.S. Thesis, University of Arizona, Department of Hydrology and Water Resources.

Moffett, J.W., 1994, The relationship between cerium and manganese oxidation in the marine environment. Limnology and Oceanography, 39, 1309-1318.

Sparrow, L.A., and N.C. Uren, 1987, Oxidation and Reduction of Mn in Acidic Soils: Effect of Temperature and Soil pH, Soil Biology and Biochemistry, 19(2), 143-148.

Tebo, B.M., Emerson, S., 1985, Effect of oxygen tension, Mn(II) concentration, and temperature on the microbially catalyzed Mn(II) oxidation rate in a marine fjord, Applied and Environmental Microbiology. 50(5), 1268-1273.

Tebo, B.M., Ghiorse, W.C., van Waasbergen, L.G., Siering, P.L., Caspi, R., 1997, Bacterially-mediated mineral formation: Insights into manganese(II) oxidation from molecular genetic and biochemical studies, Reviews in Mineralogy,. 35, 225-266.

Tebo, B.M., Rosson, R.A., Nealson, K.H., 1991, Potential for manganese(II) oxidation and manganese(IV) reduction to co-occur in the suboxic zone of the black sea, : Izdar, E. and J.W. Murray (Eds.), Black Sea Oceanography, Kluwer Academic Publishers, Netherlands. N.A., 173-185.

Triska, F.J., Duff, J.H., and Avanzino, R.J., 1993, The role of water exchange between a stream

channel and its hyporheic zone in nitrogen cycling at the terrestrial-aquatic interface, Hydrobiologia, 251, 167-184.

Valett, H.M., Morrice, J.A., Dahm, C.N., Campana, M.E., 1996, Parent lithology, surface-groundwater exchange and nitrate retention in headwater streams, Limnology and Oceanography, 41, 333.

Wehrli, B., G. Friedl, and Manceau, A., 1995, Reaction Rates and Products of Manganese Oxidation at the Sediment-Water Interface, Huang, C.P., C.R. O'Melia and J.J. Morgan (Eds.), Aquatic Chemistry: Interfacial and Interspecies Processes, Advances in Chemistry Series 244, p.111-134, American Chemical Society, Washington, D.C.

White, D.S., 1993, Perspectives on defining and delineating hyporheic zones, Journal of the North American Benthological Society, 21(1), 61-69.

Yu, Q., Kandegedara, A., Xu, Y., Rorabacher, D.B., 1997, Avoiding interferences from Good's Buffers: A continguous series of noncomplexing tertiary amine buffers covering the entire range of pH 3-11, Analytical Biochemistry. 253, 50-56.

AUTHOR INFORMATION

Justin C. Marble, Timothy L. Corley, and Martha H. Conklin, University of Arizona, Department of Hydrology & Water Resources, Tucson Arizona.

Christopher C. Fuller, U.S. Geological Survey, Menlo Park, California.

Use of Multi-Parameter Sensitivity Analysis to Determine Relative Importance of Factors Influencing Natural Attenuation of Mining Contaminants

By Jungyill Y. Choi, Judson W. Harvey, and Martha H. Conklin

ABSTRACT

Combining multi-Parametric Sensitivity Analysis (MPSA) with stream transport modeling is proposed to determine the relative importance of physical and biogeochemical processes controlling natural attenuation of contaminants. The MPSA is based on a large number of Monte-Carlo simulations to identify the sensitive parameters over a broad range of each parameter. This combined approach is applied to the transport of a mining contaminant, dissolved manganese in Pinal Creek basin, Arizona. The MPSA results show that transport of dissolved Mn(II) in Pinal Creek is controlled mainly by ground-water inflow, resulting spatial variation of pH in stream water, and the effect of pH on microbially mediated Mn(II) oxidation in the hyporheic zone.

INTRODUCTION

The fate and transport of contaminants in streams and rivers are controlled by a variety of physical and biogeochemical processes. The physical processes play an important role in determining the fate of solutes in surface-water environments. These physical processes include advection, dispersion, hyporheic exchange, and ground-water interaction. In many situations, however, the transport of contaminants are also greatly affected by biogeochemical processes, such as sorption/desorption, oxidation/reduction, volatilization, hydrolysis, biodegradation, and other biochemical reactions. Therefore, transport of contaminants in natural streams and rivers is best described by considering all of the relevant physical and biogeochemical processes simultaneously (fig. 1).

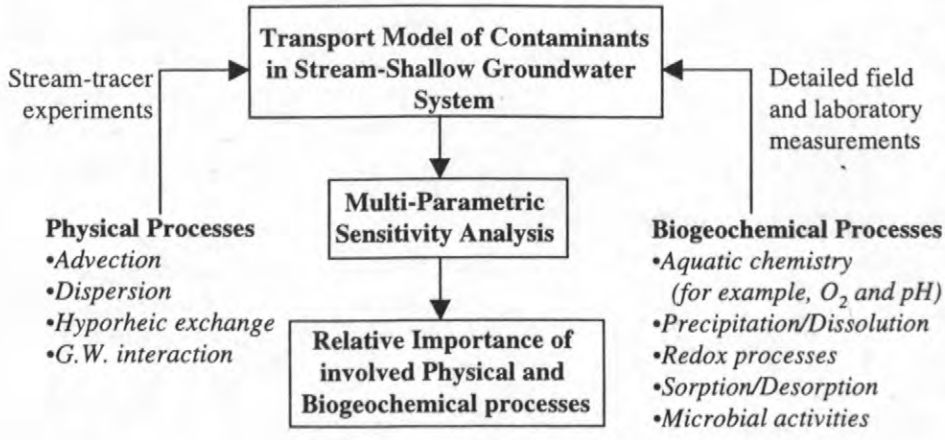

Figure 1. Coupling MPSA with transport model to identify the relative importance of physical and biogeochemical processes.

To answer the question about relative importance of factors, the sensitivity of a numerical transport model needs to be tested for the physical and biogeochemical parameters (processes) that are involved in the forward transport model. However, traditional parameter-sensitivity analysis pertains to a particular point (localized) in the parameter space, which is defined by all possible combinations of parameter values. Also, in the localized sensitivity analysis, the importance or sensitivity of a selected parameter can be affected greatly by the values of other parameters, because the significance of one selected process is usually dependent on other processes. Typically, the importance of biogeochemical processes are highly dependent on the physical processes, whereas the physical processes are not affected by the biogeochemical processes. For example, the biogeochemical reactions of solutes in the hyporheic sediments are enhanced by the prolonged retention time of solutes in these sediments. Therefore, to account for parameter interactions, the relative importance of the physical and biogeochemical processes of the transport model can be evaluated more accurately by a generalized (multi)-parameter sensitivity analysis, which encompasses the entire parameter space (fig. 1).

This paper presents the concepts and procedures of multi-parameter sensitivity analysis (MPSA) that is used to determine the relative importance of transport processes. In addition, a case study shows how the MPSA can be applied to the transport of metal contaminants in a drainage basin affected by acidic mine drainage.

MULTI-PARAMETRIC SENSITIVITY ANALYSIS

A numerical transport model may include detailed field measurements as well as ill-defined parameters that cannot be measured with a high degree of accuracy in the field or in the laboratory. These ill-defined parameters will severely limit the accuracy of any single simulation and increase the difficulty of assessing the relative importance. In an attempt to overcome this difficulty and to recognize the relative significance of parameters involved in the model, the sensitivities of simulations results to input parameters need to be evaluated by assigning either a range of variation or a degree of uncertainty to each parameter and implementing a generalized sensitivity analysis (Hornberger and Spear, 1980; Chang and Delleur, 1992; Choi et al., 1998; Choi, 1998). This multi-parametric sensitivity analysis (MPSA) followed the procedure proposed by Chang and Delleur (1992) and Choi et al. (1998). The procedure includes the following steps:

1. Select the parameters to be tested.
2. Set the range of each parameter to include the variations experienced in the field and laboratory measurement.
3. For each selected parameter, generate a series of, for example, 500 independent random numbers with a uniform distribution within the design range.
4. Run the model using selected 500 parameter sets and calculate the objective function values.
5. Determine whether the 500 parameter sets are 'acceptable' or 'unacceptable' by comparing the objective function values to a given criterion (R).
6. Statistically evaluate parametric sensitivity. For each parameter, compare the distributions of the parameter values associated with the acceptable and unacceptable results. If the two distributions are not statistically different, the parameter is classified as insensitive; otherwise, the parameter is classified as sensitive. Relative importance can be evaluated statistically if desired.

The objective function values of the sensitivity analysis usually are calculated from the sum of squared errors between observed and modeled values:

$$f = \sum_{i=1}^{n} [x_0(i) - x_c(i)]^2 \qquad (1)$$

where f is the objective function value and $x_c(i)$ and $x_o(i)$ are calculated and observed values, respectively. Observed values often are obtained from simulations that used the mid-points of the characteristic range for each parameters. The ranges for each parameter are determined from minimum to maximum values that are obtained from parameter estimations and field measurements through the study reaches. If the objectve function value obtained from the simulation is less than a subjective criterion then the result is classified as acceptable, otherwise the result is classified as unacceptable. Three different objective function values often are tested for a subjective criterion. Those values typically define the 33, 50 and 66% divisions of 500 sorted objective functions.

The basic concept of MPSA is illustrated by using a hypothetical model with only two parameters (fig. 2). In addition, the modleing procedure of MPSA described above is summarized using a flowchart (fig. 3).

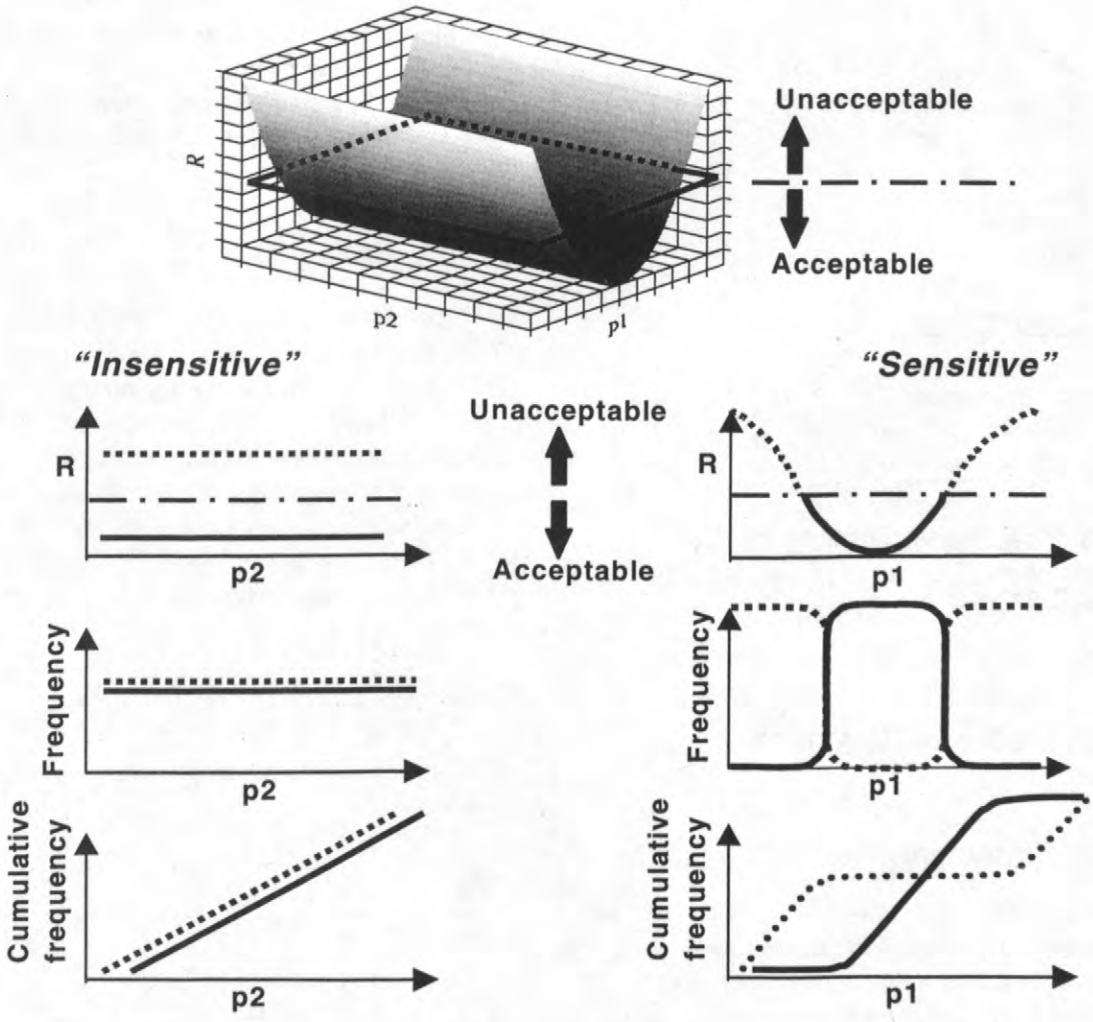

Figure 2. Basic concept of multi-parametric sensitivity analysis (MPSA) using a hypothetical model with only two parameters.

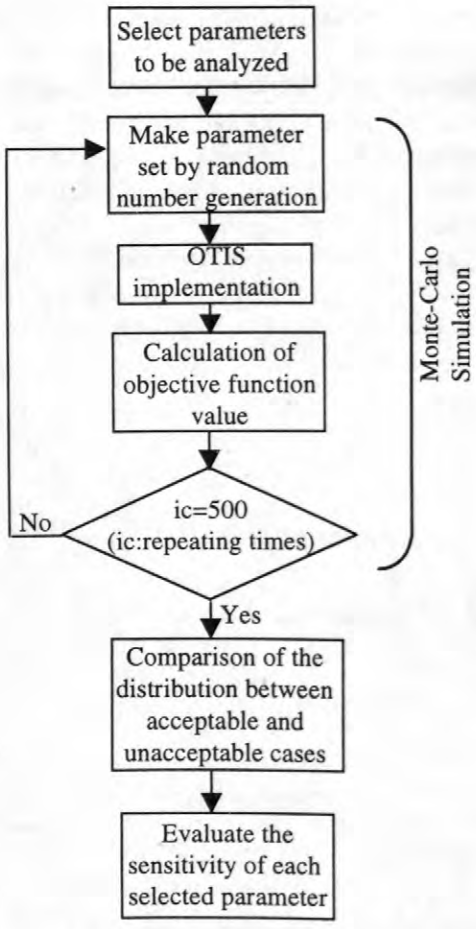

Figure 3. Flow chart illustrating the procedure of multi-parameteric sensitivity analysis (MPSA)

EXAMPLE OF APPLICATION

Problem Statement

Surface-water chemistry of Pinal Creek is dominated by discharge of the neutralized, contaminated ground water in the upper 4-Km of perennial flow. The neutralized contaminated groundwater is characterized by high dissolved solids (sulfate 2200 mg/L; Ca 500 mg/L) with pH of 5.5 to 6 and elevated pCO_2 resulting from neutralization of the acid plume by carbonate minerals, and elevated concentrations of dissolved Mn, Co, Ni and Zn. Beginning at the head of perennial stream flow in Pinal Creek, pH in the stream increases from approximately 6.0 to 7.8, and dissolved manganese, Mn(II) decreases from approximately 70 to 50 mg/L.

Although manganese is a toxic substance, it is not usually one of the more toxic metals present in acidic mine drainage. Manganese is of particular interest at acidic mine drainage sites, however, because precipitation of manganese oxide has a high potential to reduce downstream transport of other dissolved metals (including nickel, cobalt, and zinc at the Pinal Creek basin site). Harvey and Fuller (1998) showed that oxidation of Mn(II) to form manganese precipitates is enhanced by microbial activities in the hyporheic zone of Pinal Creek. Furthermore, the microbial activities in the hyporheic zone are highly dependent on the pH of stream water (Marble, 1998).

Modeling Analysis

The one-dimensional solute transport model (OTIS; Runkel and Broshears, 1991, Runkel, 1998), developed to describe the transport processes in streams and rivers, was used in our study. This transport model was extended to include a pH-dependence of the microbially-mediated uptake processes of manganese (Choi, 1998). The governing equations of the extended pH-dependent transport model are,

$$\frac{\partial C}{\partial t} = -\frac{Q}{A}\frac{\partial C}{\partial x} + \frac{1}{A}\frac{\partial}{\partial x}\left(AD\frac{\partial C}{\partial x}\right) + \frac{q_L^{in}}{A}\left(C_L - C\right) + \alpha\left(C_s - C\right) - \lambda(pH)C \quad (2)$$

$$\frac{\partial C_s}{\partial t} = \alpha\frac{A}{A_s}\left(C - C_s\right) - \lambda_s(pH)C_s \quad (3)$$

where

- A main channel cross-sectional area [L^2],
- A_s storage zone cross-sectional area [L^2],
- C main channel solute concentration [ML^{-3}],
- C_L lateral inflow solute concentration [ML^{-3}],

C_s storage zone solute concentration [ML^{-3}],
D dispersion coefficient [L^2T^{-1}],
Q volumetric flow rate [L^3T^{-1}],
q^{in}_L lateral inflow rate [$L^3T^{-1}L^{-1}$],
t time [T],
x distance [L],
α storage zone exchange coefficient [T^{-1}],
λ main channel first-order decay coefficient [T^{-1}], and
λ_S storage zone first-order decay coefficient [T^{-1}].

The parameters involved in the model were obtained from field measurements and inverse estimation using tracer dilution data (Harvey and Fuller, 1998). The rate constants for microbial uptake of dissolved Mn(II) were specified on the basis of experimentally-determined net rates of removal of Mn(II) from laboratory experiments (Marble, 1998). On the basis of two different data sets (June, 1994 and June, 1995) from Pinal Creek, the extended pH-dependent model was executed to simulate the transport of dissolved manganese in the stream system. The simulation results are presented on figure 4. As we can see from figure 4, the spatial distributions of dissolved manganese along the Pinal Creek were well simulated by the extended pH-dependent transport model.

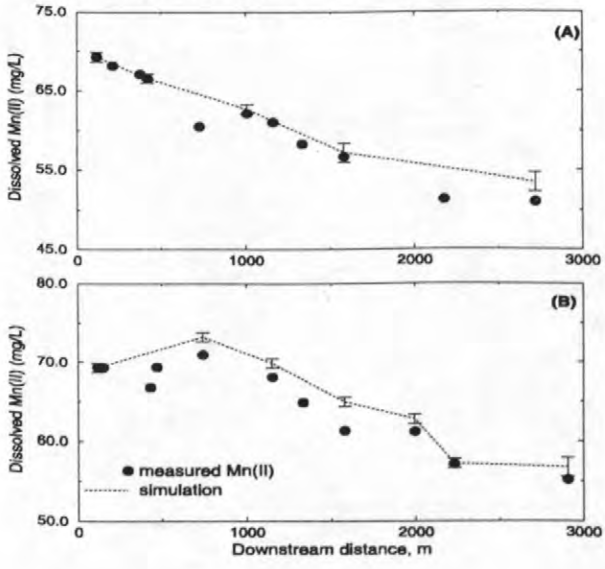

Figure 4. Simulation results from forward modeling approach. (June, 1994 (A) and June, 1995 (B)).

Even though there were good agreements bewteen observations and simulation results from predictive forward modeling approach (fig. 4), it is not possible to identify the relative importance of each physical and biogeochemical processes from the graph alone.

Application of MPSA

As one example of the application of the proposed sensitivity analysis, MPSA was applied to the transport of dissolved manganese in Pinal Creek. Using MPSA, the physical and biogeochemical processes involved in the extended pH-dependent transport model were evaluated for their relative importance.

MPSA was performed for selected physical parameters of ground-water inflow/outflow, cross-sectional area of main channel and storage zone, exchange rate with storage zone and dispersion coefficient, and chemical parameters of Mn(II) concentration of ground-water inflow and pH of stream water. The ranges for each parameter determined from parameter estimation and field/laboratory measurements are shown in table 1. The objective functions are calculated by the departure of the modeling results (Mn(II) concentration of streamwater at downstream) from a standard result, which is obtained by using the midpoint values from selected parameter ranges.

Table 1. Ranges of parameters used in multi-parametric sensitivity analysis

parameters	test range
cross-sectional area of main channel (A)	0.1 - 0.5 [m^2]
Dispersion coefficient (D)	0.5 - 8.0 [m^2s^{-1}]
cross-sectional area of storage zone (A_s)	0.02 - 0.15 [m^2]
exchange rate (α)	4.0×10^{-4} - 2.0×10^{-3} [s^{-1}]
pH	5.5 - 8.0
Groundwater (GW) inflow rate (q_L^{in})	0.0 - 1.5×10^{-4} [$m^3s^{-1}m^{-1}$]
GW outflow rate (q_L^{out})	0.0 - 4.0×10^{-5} [$m^3s^{-1}m^{-1}$]
Mn(II) concentration of GW inflow (C_L)	0.3 - 55.0 [mgL^{-1}]

The resulting cumulative frequency distributions of acceptable and unacceptable cases, which are divided by comparing subjective criteria and objective function values are shown in figure 5. If the two distributions are not statistically different, the parameter is classified as insensitive; otherwise, the parameter is classified as sensitive. The objective function values were compared with 3 different subjective criteria, which define the 33-, 50-, and 66-percent divisions of 500 sorted objective function values. In this example, however, the MPSA results were not affected by the choice of the subjective criterion. Therefore, the 50 percent criterion was used to obtain the resulting cumulative frequency distributions of acceptable and unacceptable cases in Figure 5.

The multi-parametric sensitivity analysis identified the ground-water inflow rate (q_L^{in}), Mn(II) concentration in ground-water inflow (C_L), and resulting pH variation in the system as the most important parameters (fig. 5). This indicates that the transport of dissolved manganese in this small stream system is mainly controlled by ground-water inputs with low-Mn(II) and high alkalinity, and the resulting spatial variation of pH through influencing the rate of Mn(II) oxidation. The moderate sensitivity of Mn(II) transport to cross-sectional area (A_s) and exchange rate (α) of storage zone (fig. 5) can be explained by the fact that A_s and α control the retention time and influence the amount of uptake of dissolved manganese in the hyporheic zone. On the basis of these results, it can be inferred that the difference between observation and simulation (fig. 4) may have resulted from the uncertainties in estimating the parameters, such as ground-water inflow rate (q_L^{in}), hyporheic parameters (A_s and α), or pH measurement.

In conclusion, the combined efforts of forward modeling approach and generalized sensitivity analysis can provide an integrated view of contaminant transport processes in natural stream systems. The multi- parametric sensitivity analysis especially helps identify the relative importance of physical and

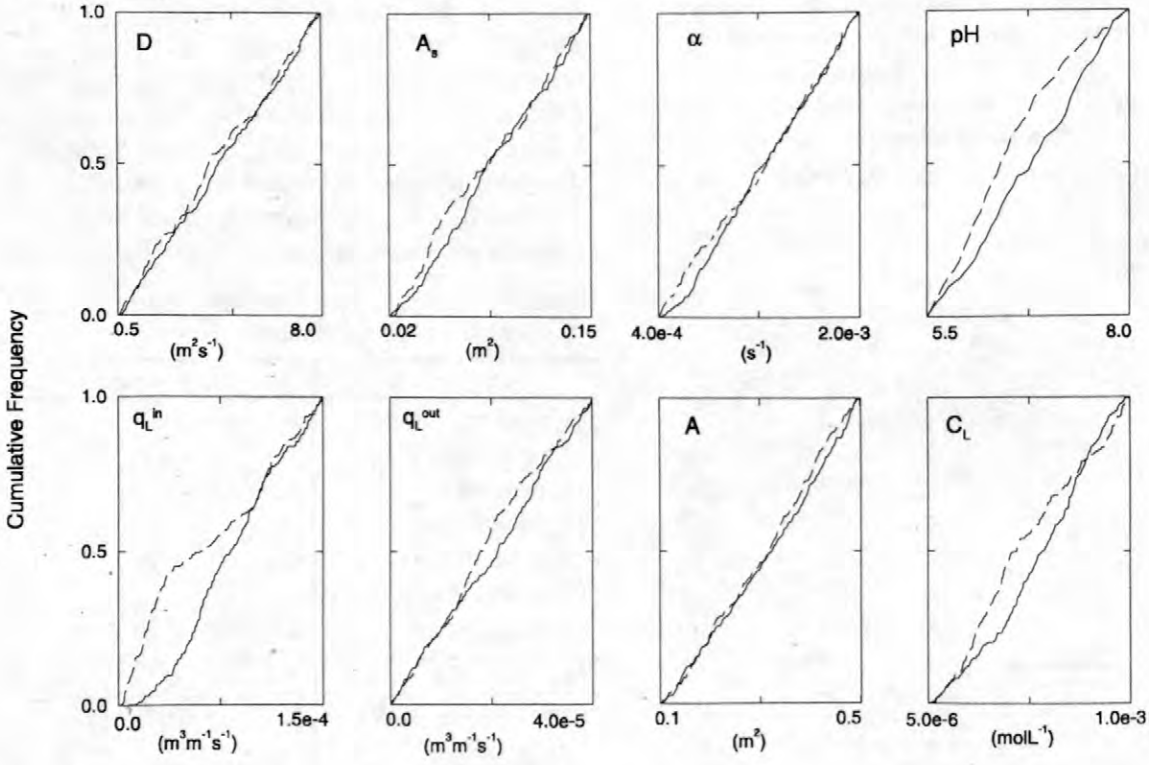

Figure 5. Results of MPSA for transport of dissolved Mn(II) in Pinal Creek, AZ. Solid and dashed lines indicate acceptable and unacceptable cases, respectively. Extent of separation between two cases represents degree of sensitivity of each parameter.

biogeochemical processes controlling the transport of contaminants. Furthermore, this methodology can provide a guide for future data-collection efforts and to order research priorities.

ACKNOWLEDGMENTS

This project was made possible by grant number EAR-9523881 from the National Science Foundation and grant number P42 ES04949 from the National Institute of Environmental Health Science, NIH with funding provided by USGS Toxic Substances Hydrology Program and EPA. Its contents are solely the responsibility of the authors and do not necessarily represent the official view of the NIEHS, NIH or EPA. We thank Tim Corley for his helpful manuscript review.

REFERENCES

Chang, F., and Delleur, J.W., 1992, Systematic parameter estimation of watershed acidification model; Hydrological Processes, v. 6, p. 29-44.

Choi, J, 1998, Transport modeling of metal contaminants in a stream-aquifer system; University of Arizona, Department of Hydrology and Water Resources, unpublished Ph.D. thesis, 225p.

Choi, J.Y., Hulseapple, S.M., Conklin, M.H., Harvey, J.W., 1998, Modeling CO_2 degassing and pH in a stream-aquifer system; Journal of Hydrology, v. 209, p. 297-310.

Harvey, J.W, and Fuller, C.C., 1998, Effect of enhanced manganese oxidation in the hyporheic zone on basin-scale geochemical mass balance, Water Resources Research, v. 34, no. 4, p. 623-636.

Hornberger, G.M., and Spear, R.C., 1980, An approach to the preliminary analysis of environmental system; Journal of Environmental Management, v. 12, p. 7-18.

Marble, J.C., 1998, Biotic contribution of Mn(II) removal at Pinal Creek, Globe, Arizona: University of Arizona, Department of Hydrology and Water Resources, unpublished M.S. thesis.

Runkel, R.L., and Broshears, R.E., 1991, One-dimensional transport with inflow and storage (OTIS): A solute transport model for small streams; Technical Report 91-01, Cent. For Adv. Dec. Support for Water and Environ. Sys., Univ. of Colo., Boulder.

Runkel, R.L., 1998, One-dimensional transport with inflow and storage (OTIS): A solute transport model for small streams; U.S. Geological Survey, Water-Resources Investigations Report 98-4018, 73p.

AUTHOR INFORMATION

Jungyill Choi, U.S. Geological Survey, Reston, Virginia (jchoi@usgs.gov)

Judson W. Harvey, U.S. Geological Survey, Reston, Virginia

Martha H. Conklin, University of Arizona, Department of Hydrology and Water Resources, Tucson, Arizona

Enhanced Removal of Dissolved Manganese in Hyporheic Zones: Centimeter-Scale Causes and Kilometer-Scale Consequences

By Judson W. Harvey, Christopher C. Fuller, and Martha H. Conklin

ABSTRACT

Characterizing both the causes and consequences of enhanced oxidation of dissolved manganese (Mn) in the hyporheic zone required measurements with spatial resolution varying across five orders of magnitude. Our measurements at Pinal Creek basin, AZ ranged in scale from that of the fundamental interactions between surface and ground water (centimeters) to the scale of the perennial stream that receives ground-water discharge from the entire drainage basin (kilometers). Mean rate constants for the removal of dissolved manganese agreed closely between three scales of resolution in the field, ranging from centimeter-scale field measurements acquired *in situ* in hyporheic zones to kilometer-scale estimates determined using stream tracers. The laboratory estimate of the Mn removal-rate constant was approximately 30% lower than field estimates. *In situ* and laboratory rate constants had relatively large coefficients of variation (107% and 84%, respectively), which may be too large to be used reliably in transport simulations. Stream-tracer experiments provided estimates of the rate constant with lower uncertainties; 56% when averaged at the reach-scale (approximately 500 meters) and 26% when averaged at the basin-scale (3 kilometers). Because of the lower uncertainties the stream-tracer approach appeared to provide the most reliable basin-scale simulation of the effects of enhanced Mn-removal in hyporheic zones. The stream-tracer characterization alone, however, could not determine that removal of manganese was pH-dependent, or even that the reaction occurred in hyporheic zones (as opposed to slow-moving zones in surface water). Laboratory and *in situ* measurements within hyporheic zones provided the crucial evidence to support interpretations about the causal processes. Our experience at Pinal Creek basin leads us to conclude that a multi-scale approach is a necessity for characterizing enhanced biogeochemical reactions in hyporheic zones.

INTRODUCTION

Hydrologic exchange of streamwater and ground water back and forth across channel beds of rivers and streams enhances chemical transformations in shallow groundwater beneath the streambed (hyporheic zone). The hyporheic zone is defined hydrologically by flow paths that route streamwater temporarily through the subsurface and chemically by subsurface water that can be shown to receive greater than 10% of its water from the surface (Triska and others, 1993). Steep chemical gradients in dissolved oxygen, dissolved organic carbon, and pH in hyporheic zones enhance biogeochemically mediated transformations of solutes, such as nitrification and denitrification (Grimm and Fisher, 1984; Triska and others, 1993), oxidation of metals (Benner and others, 1995), and biodegradation of volatile organic compounds (Heekyung and others, 1995). Hyporheic flow paths are typically small in their spatial dimensions, but if chemical reaction rates are fast enough, and if enough exchange occurs between flowing water and sediment, then the effects can accumulate downstream and affect water quality (Harvey and Fuller, 1998).

This paper considers three types of measurements at different spatial scales of resolution. Our previous comparisons across spatial scales (Harvey and Fuller, 1998) are updated here with new findings by Marble and others (this volume) and Fuller and Harvey (this volume). The purpose was twofold: (1) to verify

previous conclusions that were based on a limited data set, and (2) to assess the relative merits of the three modes of investigation in informing us about causes and consequences of enhanced chemical reactions in hypohreic zones. The three measurement types are:
(1) laboratory-batch experiments that quantify solute-sediment interactions at the millimeter-scale, i.e. the scale of individual sediment grains, (2) *in-situ* measurements in hyporheic flow paths at the scale of centimeters beneath the streambed, and (3) stream-tracer experiments that quantify removal rates at the scale of experimental subreaches in the perennial stream (approximately 500 meters) or at the scale of the perennial stream that receives ground-water discharge from the entire drainage basin (3 kilometers).

A number of physical and chemical measurements of the hyporheic zone have been made as part of our investigations, including the hyporheic-zone depth, hydrologic residence time in the hyporheic zone, net removal-rate constant for dissolved manganese (Mn), and percent removal of Mn in hyporheic flow paths. Previously, we found good agreement across scales of measurement based on a relatively limited data set (Harvey and Fuller, 1998). In this paper, we update with new data the means and standard deviations for manganese removal-rate constants and compare them among the three measurement types. Field methods, analyses, and modeling calculations for reach-scale and in-situ measurements are presented in Harvey and Fuller (1998) and Fuller and Harvey (this volume). Laboratory methods and analyses are given by Marble and others (this volume) and Harvey and Fuller (1998).

COMPARISON OF REMOVAL-RATE CONSTANTS ACROSS SCALES

All available data from field work in 1994, 1995, and 1997 were used to compute a mean and standard deviation for *in situ* rate constants (cm-scale). The summary statistics shown in Figure 1 were determined for sub-reaches (500-m scale) by averaging results from 9 experimental sub-reaches from stream-tracer injections in 1994 and 1995. The basin-scale estimates were computed by averaging the mean rate constant from the four subreaches in 1994 with the mean for the five subreaches in 1995. The laboratory estimates were computed using data from the subset of experiments conducted between pH 6 and 6.9, which matches the range of pH's that were measured *in situ*.

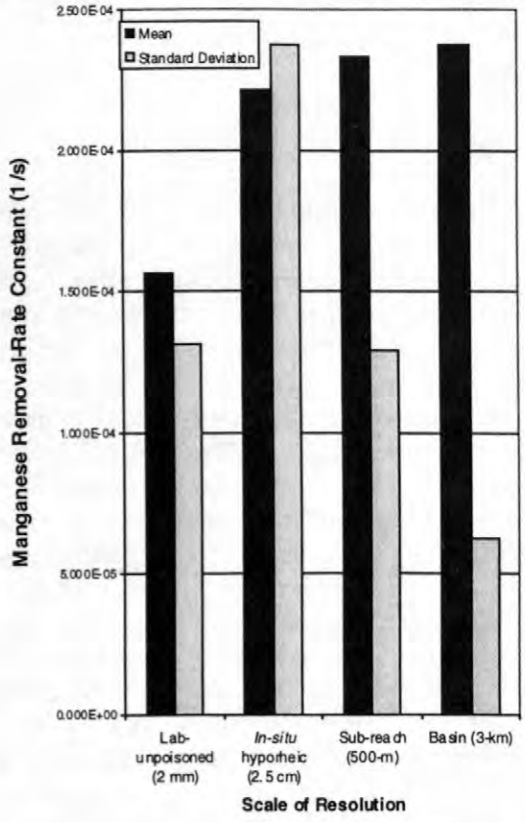

Figure 1. Means and standard deviations for Mn removal-rate constants estimated at different spatial scales. Summary statistics are based on sample sizes of 8, 11, 9, and 2 for laboratory, *in-situ*, sub-reach, and basin-scale estimates, respectively.

The mean rate constants for field estimates (e.g. *in situ*, sub-reach, and basin-scale) varied little (4% coefficient of variation), however the estimate from the laboratory was approximately 30% lower. Standard deviations varied widely across all scales over approximately a factor of four. We chose the coefficient of variation (standard deviation divided by the mean) as a measure of uncertainty. The *in situ* estimate of the removal-rate constant was most uncertain with a coefficient of variation of 107%. Estimates made at the kilometer-scale

based using the stream-tracer approach were least uncertain, with a coefficient of variation equal to 26%. The coefficient of variation for laboratory and sub-reaches had intermediate values of 84% and 56%, respectively.

CAUSES OF ENHANCED OXIDATION OF DISSOLVED MANGANESE IN HYPORHEIC FLOW PATHS

Evidence for the influence of microbial activity and pH is illustrated in Figure 2, which summarizes all of the data from Marble (1998), Marble and others (this volume), Fuller and Harvey (this volume), and Harvey and Fuller (1998). Laboratory experiments were controlled for the effects of microbial activity and pH demonstrated that manganese oxidation rates are highly sensitive to the presence of an active microbial colony and to pH.

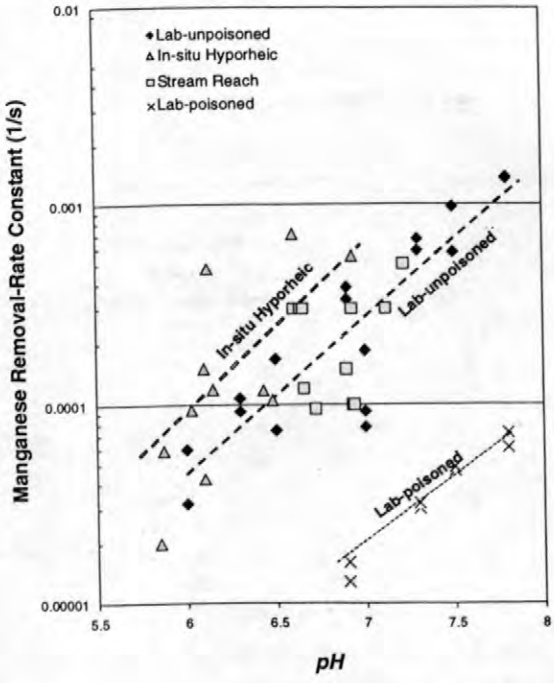

Figure 2. Laboratory measurements and *in-situ* estimates of rate constants indicate a positive relationship with pH, but reach-scale estimates do not.

Figure 2 shows that for a given pH, the rate constants are approximately an order of magnitude lower in samples that were poisoned to reduce or eliminate microbial activity. A statistically significant positive correlation ($p = 10^{-6}$) between unpoisoned laboratory rate constants and pH was also apparent. A similar positive correlation with pH was apparent for the removal-rate constants determined within hyporheic flow paths, although that relation was only barely significant at $p = 0.05$ (using a typical statistical criterion for significance that p is less than or equal to 0.05). No correlation with pH was apparent for removal-rate constants determined by stream-tracer experiments. The lack of a pH relation for reach-scale removal rates stems at least in part from using stream pH as a proxy for a reach-averaged pH in the hyporheic zone.

CONSEQUENCES FOR REACH-SCALE WATER QUALITY

The data requirements for characterizing spatially-variable processes in hyporheic zones using small-scale sampling are massive. As a result, *in-situ* field sampling and laboratory measurements of Mn removal-rate constants might not be reliable to determine cumulative effects in the drainage basin. Stream-tracer experiments offer a possible means to average over small-scale spatial variability to estimate cumulative effects (Kimball and others, 1994). The principal advantage of the stream-tracer approach is that average characteristics of mass transport and chemical reactions are determined at spatial scales that are appropriate for water-quality modeling (hundreds of meters to tens of kilometers). A major disadvantage of the stream-tracer approach, however, is the empirical nature of the parameters. For example, the 'storage-exchange' parameters of the stream-tracer approach describe a zone of temporary retention of stream water on the basis of fitted-parameter values that best match in-stream bromide tracer experiments.

To justify an interpretation that storage zones inferred by tracer methods represent hyporheic zones, it is necessary to directly compare stream-tracer results with *in situ* measurements within hyporheic zones. Figure 3 compares measured depths of the hyporheic zone with inferred depths from modeling.

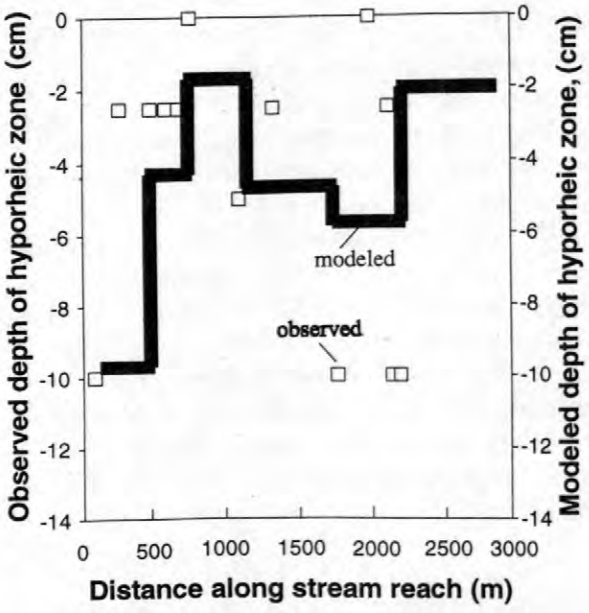

Figure 3. Comparison of *in-situ* measurements of the depth of the hyporheic zone with depths inferred by modeling transport of a stream tracer.

Although site-specific measurements of the depth of the hyporheic zone were much more variable than modeled stream-tracer results, there was a general correspondence between the central tendencies and the downstream trends in the two data sets. These results supported our interpretation that the stream-tracer experiments at Pinal Creek were in fact sensitive to hydrologic exchange with hyporheic zones, rather than stagnant or recirculating areas in surface water.

The use of *in-situ* and basin-scale estimates of rate constants to simulate the cumulative effects of manganese removal in Pinal Creek basin are compared in Figure 4.

Transport of Mn in a 3-km reach of Pinal Creek (about half the length of the perennial stream in the basin) in 1994 is used as the basis for comparison with field data. The model allows for removal of dissolved manganese only in storage (hyporheic) zones for which the physical dimension and hydrologic residence time were determined by modeling bromide injections in the stream. The analysis equations and supporting information are presented in Harvey and Fuller (1998). The 'non-reactive' simulation only indicates the effects of dilution by inflow of groundwater with lower Mn concentration. For 'reactive' simulations, mean removal-rate constants were determined either by averaging all of the available *in-situ* rate-constant estimates (Figure 4A), or by averaging rate-constants determined by stream-tracer methods in five sub-reaches in 1995 (Figure 4B). The dashed simulations and shaded represent uncertainties of plus or minus one standard deviation around simulations that used the mean removal-rate constant.

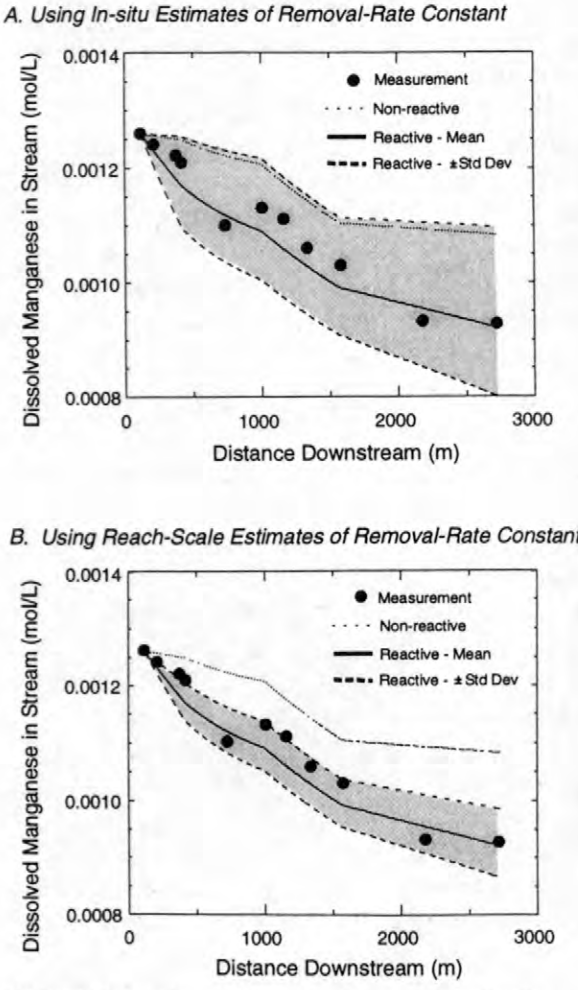

Figure 4. In-situ estimates of the removal-rate constant are too variable to reliably simulate basin-scale consequences. Reach-scale estimates of the rate constant reliably simulate the basin-scale effect of enhanced manganese oxidation in the hyporheic zone.

In both panels of Figure 4, measured Mn and simulated Mn were lower in concentration than indicated by the non-reactive simulation, suggesting that removal of dissolved manganese

occurs in hyporheic zones. Uncertainty of the simulation using the *in-situ* rate constant, however, overwhelmed our ability to characterize cumulative effects in the drainage basin. This is apparent in Figure 4A by the large envelope of uncertainty that overlaps the measured data as well as the simulation for non-reactive transport. If judged alone, the modeling result in Figure 4A would cast doubt as to whether a significant loss of mass of manganese even occurs at Pinal Creek. In contrast, the simulation in Figure 4B had a smaller error envelope that only encompassed the measured data. Simulated concentrations in Figure 4B were well below those predicted by the non-reactive transport simulation, suggesting greater confidence that substantial removal of Mn occurred in hyporheic zones. Comparison of simulated non-reactive and reactive Mn concentrations indicated that approximately 14% of the manganese in the 3-km reach was removed by enhanced oxidation in hyporheic zones.

DISCUSSION

Rate constants for removal of manganese differed little between laboratory experiments, *in-situ* field measurements, and measurements based on stream-tracer experimentation. The advantage of laboratory experiments was the isolation of the effects of microbial colonies and pH. Marble and others (this volume) discuss pH and other factors affecting Mn-oxidation reactions. One problem of the batch-laboratory experiments is extrapolating results to sediment-water ratios that more accurately approximate field conditions. Following Harvey and Fuller (1998), we scaled laboratory-rate constants by multiplying them times the ratio between the average sediment concentration (grams/liter) in the streambed at Pinal Creek and the sediment concentration used in laboratory experiments. That adjustment assumes that grain-size variations, which are likely to affect sediment-surface area available for oxidation of manganese, are the same in laboratory experiments and in the streambed. Another possible problem of the laboratory experiments is controlling for variation in activity levels of microbial colonies. For example, Marble and others (this volume) report a significant time lag before removal in Mn begins in sediment samples that were stored before usage in experiments. Either of those possible problems might explain the lower Mn removal-rate constant compared with in-situ and stream-tracer estimates.

In-situ sampling within hyporheic flow paths addresses the problem of realistic field conditions by quantifying rates of removal without disturbing the sediments or natural hydrologic fluxes. But this method has practical limitations, however. *In-situ* sampling has the disadvantage that the measurements are difficult and time consuming to make in the field, which limits sample sizes. In addition there is also the problem that ancillary physical and chemical factors cannot be varied except though careful site selection. The principal advantage of *in-situ* field measurements is that interactions between flow and biogeochemical processes are preserved, which potentially could reveal findings that would be difficult to detect in a laboratory setting.

Stream-tracer experiments provided the the most reliable reach-averaged rate constants for modeling the basin-scale consequences of enhanced chemical reactions in hyporheic zones. Nevertheless, there remains a major disadvantage of the stream-tracer approach for quantifying hyporheic-zone processes. On the basis of stream-tracer experiments alone, we cannot be sure that the removal of reactive solutes actually occurs in hyporheic-zones, or on the leaves of aquatic vegetation in slowly-moving surface water at channel margins or behind channel obstructions. Another problem with stream-tracer methods is that the detection sensitivity for hyporheic zones is not equal across the multiple types of hyporheic zones that may be present in a given system (Harvey and others, 1996). Only direct sampling of hyporheic zones using *in-situ* methods can provide the independent confirmation needed to support physical interpretations at larger spatial scales.

CONCLUSIONS

We compared rates of microbially-enhanced oxidation of manganese in hyporheic zones at Pinal Creek basin in Arizona across spatial scales ranging from that of individual sediment grains in laboratory investigations to the

scale of a 3-km reach of the perennial stream. Marble and others (this volume) illustrated how Laboratory measurements illustrated the biogeochemical factors that influence reaction rates, with pH-dependent activity of manganese-oxidizing bacteria being a primary factor (Marble and others (this volume). *In-situ* measurements in the field were much more difficult to make and results were more variable than in the laboratory. Consequently, the positive relation of removal-rate constants with pH that was easily detected in the laboratory data was only marginally significant for field data. *In-situ* studies, however, had the advantage of investigating chemical and physical factors and their interactions simultaneously, and the agreement with laboratory rate constants thus lent support to interpretations. At the largest spatial scale, stream-tracer investigations provided reliable estimates of overall removal of manganese in the reach, but interpretations about where reactions occur or what factors control them could not be defended without supporting information from *in-situ* measurements in hyporheic zones. Our experience leads us to conclude that, due to the disparity in scales between the fundamental processes and their consequences, a multi-scale approach is essential to investigating enhanced chemical reactions in hyporheic zones.

REFERENCES

Benner, S.G., Smart, E.W., and Moore, J.N., 1995, Metal behavior during surface-groundwater interaction, Silver Bow Creek, Montana, Environmental Science and Technology, 29, 1789-1795.

Fuller, C.C., and Harvey, J.W., The effect of trace-metal reactive uptake in the hyporheic zone on reach-scale metal transport in Pinal Creek, Arizona, in Morganwalp, D.W. and Buxton, H.T., eds., U.S. Geological Survey Toxic Substances Hydrology Program—Proceedings of the Technical Meeting, Charleston, South Carolina, March 8-12, 1999—Volume 1—Contamination from Hard Rock Mining: U.S. Geological Survey Water-Resources Investigations Report 99-4018A, this volume

Grimm, N.B., and Fisher, S.G., 1984, Exchange between interstitial and surface water: implications for stream metabolism and nutrient cycling. Hydrobiologia 111:219-228.

Harvey, J.W., and Fuller, C.C., 1998, Effect of enhanced manganese oxidation in the hyporheic zone on basin-scale geochemical mass balance, Water Resources Research, 34, 623-636.

Harvey, J.W., Wagner, B.J., and Bencala, K.E., 1996, Evaluating the reliability of the stream-tracer approach to characterize stream-subsurface water exchange, Water Resources Research, 32(8), 2441-2451.

Heekyung, K., Hemond, H.F., Krumholz, L.R., and Cohen, B.A., 1995, In-situ biodegradation of toluene in a contaminated stream, 1, Field Studies, Environmental Sciences and Technology, 29, 108-116.

Kimball, B.A., Broshears, R.E., Bencala, K.E., and McKnight, D.M., 1994, Coupling of hydrologic transport and chemical reactions in a stream affected by acid mine drainage, Environmental Science and Technology, 28, 2065-2073.

Marble, J.C., Corley, T.L., Conklin, M.H., and Fuller, C.C., , Environmental factors affecting oxidation of manganese in Pinal Creek, Arizona., in Morganwalp, D.W. and Buxton, H.T., eds., U.S. Geological Survey Toxic Substances Hydrology Program—Proceedings of the Technical Meeting, Charleston, South Carolina, March 8-12, 1999—Volume 1—Contamination from Hard Rock Mining: U.S. Geological Survey Water-Resources Investigations Report 99-4018A, this volume

Marble, J.C., 1998, Biotic contribution of Mn(II) removal at Pinal Creek, Globe, Arizona, unpublished M.S. thesis, University of Arizona, Department of Hydrology and Water Resources, Tucson. 91 p.

Triska, F.J., Duff, J.H., and Avanzino, R.J., 1993, The role of water exchange between a stream channel and its hyporheic zone on nitrogen cycling at the terrestrial-aquatic interface, Hydrobiologia, 251, 167-184.

AUTHOR INFORMATION

Judson W. Harvey, U.S. Geological Survey,
Reston, Virginia (jwharvey@usgs.gov)

Christopher C. Fuller, U.S. Geological Survey,
Menlo Park, California

Martha H. Conklin, The University of Arizona,
Tucson, Arizona

Evaluating the Ability of Tracer Tests to Quantify Reactive Solute Transport in Stream-Aquifer Systems

By Brian J. Wagner and Judson W. Harvey

ABSTRACT

Tracer experiments are valuable tools for characterizing the fate and transport of solutes carried in stream waters; however, the results can have high uncertainty when the technique is not properly implemented. The goal of this study was to identify the limitations that apply when we couple conservative-tracer injection with reactive solute sampling to identify the transport and reaction processes active in a stream. The conservative-tracer injection is used to characterize the physical transport processes of advection, dispersion, ground-water inflow, and stream-storage exchange (the movement of stream water and solute between the active stream channel and storage zones in the channel margins and in the subsurface). The reactive-solute sampling is used to characterize the removal of reactive solute due to geochemical/biotic processes occurring in the storage zones. We apply the methodology of Wagner and Harvey (1997) to evaluate the tracer approach for the wide range of transport and reaction conditions likely encountered in high-gradient streams. The methodology couples solute transport simulation with parameter uncertainty analysis in a Monte Carlo framework to identify those combinations of stream transport and reaction properties that pose limitations to the tracer approach. Our results show that the uncertainty associated with determining the reaction rate constant is strongly related to the reactive loss factor, which is a dimensionless combination of the reaction rate constant, the average solute residence time in the storage zone, the experimental reach length, and the average distance travelled by a stream solute before entering a storage zone. As the reactive loss factor increases, the effect of reactive loss in the storage zones along the study reach increases and the uncertainty in the reaction rate estimate decreases.

INTRODUCTION

There are a wide range of processes that affect solute transport, physical retention, and reactive uptake in stream and shallow ground-water systems. Numerous studies have shown that exchange between stream and storage zones, coupled with solute reactions, can play an important role in determining the quality of stream waters (e.g. Bencala, 1984; Grimm and Fisher, 1984; D'Angelo and others, 1993; Runkel and others, 1996; Harvey and Fuller, 1998). The stream-storage exchange process — the movement of stream water between the active channel and storage zones in the channel margins or in subsurface hyporheic flow paths — serves to increase solute retention time. The increased contact of stream-water solutes with sediment, in turn, stimulates biotic and geochemical processes that affect solute reaction during downstream transport.

Stream-tracer studies are one of the primary tools used to characterize transport and reaction processes. In a stream tracer study, a tracer-labelled solution is injected into the stream. As the tracer body moves downstream, it is affected by the various processes active in the stream system. At some point(s) downstream of the tracer injection site, water samples are collected, providing a record of the tracer's transport and evolution. The tracer data are then analyzed to describe (in a quantitative fashion) the transport and reaction processes. The approach commonly used is to combine the tracer data with a solute transport simulation model to estimate solute transport parameters for the stream. Conservative-tracer injection studies are commonly used to estimate the physical process parameters

that characterize stream-solute dynamics (see Stream Solute Workshop, 1990). Investigators have also injected reactive solutes to characterize reactive solute transport (e.g. Bencala and others, 1984, Triska and others, 1993). However, because of the elevated concentrations of the reactive constituent that result from the reactive-tracer injection, the results from such studies may not be representative of the naturally-occurring reactions.

An alternative to reactive-tracer injection is to use a tracer approach that does not alter the natural levels of the reactive constituents, such as the approach used by Kimball and others (1994), Heekyung and others (1995), and Harvey and Fuller (1998). In this approach, a conservative-tracer injection experiment is coupled with synoptic sampling of the reactive constituent. The conservative-tracer data are combined with a transient solute-transport simulation model to characterize the physical processes active in the study reach. The reactive-constituent data are combined with a steady-state simulation model to determine the reaction rate(s) describing the net loss of the reactive constituent along the study reach. The result is a set of models and parameters that can be used to analyze solute transport and reactive loss.

Here we extend the work of Wagner and Harvey (1997) to analyze tracer test design for the combined conservative/reactive tracer approach described above. Wagner and Harvey evaluated the ability of the conservative-tracer injection study to characterize the physical transport processes of advection, dispersion, dilution from ground-water inflow, and stream-storage exchange. They evaluated a variety of different tracer test designs for a broad range of stream transport characteristics and found that the success of a tracer study is limited by its ability to quantify the stream-storage exchange process. The goal of this study was to identify any additional limitations that might apply when we attempt to use the conservative/reactive tracer approach to identify both the transport and the reaction processes.

METHODOLOGY

The approach used in this study follows that developed by Wagner and Harvey (1997). The methodology is based on the concept of global parameter uncertainty analysis, which combines

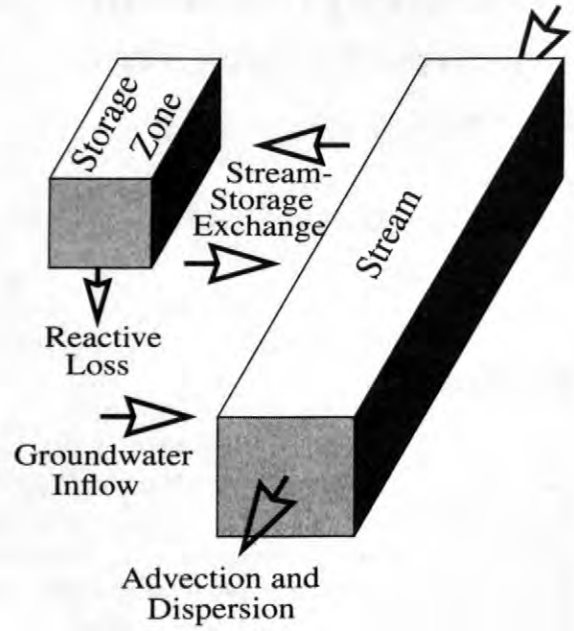

Figure 1. Schematic representing stream-solute transport and reaction system: advection and dispersion, stream-storage exchange, groundwater inflow, and reactive loss in storage zones.

solute transport simulation with parameter uncertainty analysis in a monte carlo framework. Simply stated, the methodology considers the wide range of transport conditions likely to be encountered in the field and identifies the conditions under which tracer experiments will be successful, that is, the conditions under which solute transport processes can be reliably identified.

Modeling Stream Solute Transport

In the conceptualization of stream-solute transport used in this study, the hydrologic regime is divided into two coupled systems; a system of flowing water in the main stream channel (where advection, dispersion, and groundwater inflow processes are active) and a system of storage zones at the margins of the stream channel or in the subsurface (fig. 1). The two systems are coupled by a mass transfer mechanism that exchanges solutes between the main channel and the storage zones. It is only in the storage zones that reactive loss occurs. The assumption that reactive loss occurs only in the storage zones is based on the fact that biological and geochemical reactions are expected to take place much faster in contact with sediment, due to

geochemical coatings and microbes on sediments that catalyze the reactions (for example, Harvey and Fuller, 1998). It should be noted that although this study is limited to the conditions described above, the methodology is flexible and can be adapted to handle any solute transport and reaction scenario for which a mathematical model can be developed.

The mathematical model for one-dimensional advective-dispersive transport with inflow and storage-zone exchange is

$$\frac{\partial C}{\partial t} = -\frac{Q}{A}\frac{\partial C}{\partial x} + \frac{1}{A}\frac{\partial}{\partial x}\left(AD\frac{\partial C}{\partial x}\right) + \frac{q_L}{A}(C_L - C) + \alpha(C_s - C) \quad (1)$$

$$\frac{\partial C_s}{\partial t} = -\alpha\frac{A}{A_s}(C_s - C) \quad (2)$$

where

- C solute concentration in the stream (mg L^{-1}),
- Q volumetric flow rate (m^3 s^{-1}),
- A cross-sectional area of stream channel (m^2),
- D dispersion coefficient (m^2 s^{-1}),
- q_L lateral volumetric ground-water inflow rate (per length) (m^3 s^{-1} m^{-1}),
- C_L solute concentration in the lateral inflow (mg L^{-1}),
- C_s solute concentration in the storage zone (mg L^{-1}),
- A_s cross-sectional area of the storage zone (m^2),
- α stream-storage exchange coefficient (s^{-1}),
- t time (s),
- x distance (m).

To simulate solute transport using (1) and (2) the process parameters must be specified. Since direct measurement of these parameters is difficult or impossible, they must be determined by fitting the model described by equations (1) and (2) to the data collected as part of the tracer study. We advocate using techniques of optimization and statistics to estimate the parameters that best reproduce the tracer data and to determine the reliability of the parameter estimates (for example, Wagner and Gorelick, 1986; Wagner and Harvey, 1996).

The above equations are used to analyze the data from a conservative-tracer injection. Measurements of a reactive solute can be combined with this physical transport analysis to determine a rate constant describing the removal of the reactive solute in the storage zones. The following steady-state form of (1) and (2) is used

$$0 = -\frac{Q}{A}\frac{\partial C_r}{\partial x} + \frac{1}{A}\frac{\partial}{\partial x}\left(AD\frac{\partial C_r}{\partial x}\right) + \frac{q_L}{A}(C_{rL} - C_r) + \alpha(C_{rs} - C_r) \quad (3)$$

$$0 = -\alpha\frac{A}{A_s}(C_{rs} - C_r) - \lambda_s C_{rs} \quad (4)$$

where all parameters remain the same as in (1) and (2) with the following exceptions

- C_r concentration of the reactive solute in the stream (mg L^{-1}),
- C_{rL} concentration of the reactive solute in the lateral inflow (mg L^{-1}),
- C_{rs} concentration of the reactive solute in the storage zone (mg L^{-1}),
- λ_s first-order reaction rate constant describing solute removal in the storage zone (s^{-1})

Because the physical transport parameters are determined from modeling the conservative-tracer injection, only the rate constant, λ_s, remains to be determined. This is done by modeling the reactive solute data using (3) and (4) with the physical transport parameters determined from the conservative-tracer data. Again, we advocate the use of formal inverse methods for this task.

Evaluating Parameter Reliability

The complexity of stream-solute transport can make it difficult to reliably determine the solute transport and reaction parameters. Parameter uncertainty analysis provides a quantitative measure of the reliability of parameters estimated from tracer data and forms the basis of the methodology for evaluating and comparing alternative tracer experi-

ment designs. The underlying assumption here is that a tracer experiment is successful if the solute transport and reaction parameters can be reliably determined. Here we calculate parameter reliability using the first-order approximation to the parameter estimate covariance matrix, V_p

$$V_p = (J^t V_c^{-1} J)^{-1} \quad (5)$$

where

V_p covariance matrix that defines the uncertainty in the parameter estimates, an nxn matrix where n is the number of parameters,

V_c covariance matrix that defines the uncertainty in the concentration data, an mxm matrix where m is the number of concentration data,

J jacobian, the matrix of sensitivities of modeled concentrations with respect to changes in the model parameters, an mxn matrix.

The parameter estimate covariance matrix can be used to identify the parameters that are well (or poorly) estimated. In this study we use the coefficient of variation as the ultimate measure of a parameter's reliability

$$cov(p_i) = \frac{sd(p_i)}{p_i} \quad (6)$$

where

p_i process parameter i,

$cov(p_i)$ coefficient of variation for process i,

$sd(p_i)$ standard deviation of p_i, which is defined as the square root of the i^{th} diagonal element of V_p.

The coefficient of variation is a unitless measure that defines the standard deviation as a fraction of the parameter value. We use this measure in our analyses because it allows us to compare results across all parameter types, regardless of the magnitudes or dimensions of the parameters.

Monte Carlo Analysis of Stream Tracer Test Design

The methodology applied here uses Monte Carlo analysis to account for the wide range of transport characteristics that can be encountered in the field. In brief, the methodology proceeds as follows. On the basis of prior information, we generate many realizations of the solute transport and reaction parameters needed to define (1) - (4), with each realization representing a possible "model" of the true stream solute transport and reaction system. We then define a tracer-test design (that is, a combination of a conservative-tracer injection and sampling strategy and a reactive-solute sampling strategy). Next, a Monte Carlo parameter uncertainty analysis is performed to analyze parameter reliability for each parameter realization for the tracer-test design considered. The result is a suite of parameter uncertainties that are used to analyze the capabilities and limitations of the tracer approach over the spectrum of possible transport and reaction conditions. A detailed description of the methodology can be found in Wagner and Harvey (1997).

Prior Parameter Information

As outlined above, the first step in the analysis is to define the prior parameter information. Here we analyzed the ability of the tracer approach to identify transport and reaction processes for the range of conditions representative of high-gradient streams. These streams have widely varying physical transport properties. Stream discharge and velocity, ground-water inflow, dispersion, and stream-storage exchange properties can vary by orders of magnitude from one system to another. In addition, the reaction properties of the system can vary significantly depending on the biological and geochemical characteristics of the stream-storage system and the solute, and on the amount of interaction between the solute and the subsurface hyporheic flow paths. Here we define the ranges of transport and reaction parameters on the basis of parameter values that have been reported in the literature. The parameter ranges are listed in Table 1. Note that the ranges for the physical transport parameters are identical to those used in Wagner and Harvey (1997).

Once the parameter ranges have been defined, the next step is to generate many realiza-

tions of the stream transport and reaction parameters. For the analyses presented here we generated 1,000 sets of transport and reaction parameters. The parameters were generated using the same approach as Wagner and Harvey (1997). In brief, the parameters were randomly selected assuming they varied uniformly and independently between their lower and upper levels. The only exceptions were stream discharge and cross-sectional area which were constrained to be consistent with the physics of open-channel flow.

Table 1. Solute transport and reaction parameter ranges for high-gradient stream analysis.

Parameter	Range
Q (m^3/s)	0.005 - 0.2
q_L (m^3/s m)	0.0 - 0.0001
A (m^2)	0.02 - 0.6
D (m^2/s)	0.025 - 0.8
A_s (m^2)	0.01 - 2.0
α (1/s)	0.000005 - 0.001
λ_s (1/s)	0.00001 - 0.01
C_L (mg/L)	1.0

The Basic Tracer Test

There are many variables that must be considered when designing a tracer study, such as the length of the reach over which the study is performed, the duration of the conservative-tracer injection, the frequency of sampling of the conservative tracer, and the sampling plan for the reactive constituent in the stream. In order to compare results across the wide range of transport and reaction conditions considered, we have adopted the standardized design variables used by Wagner and Harvey (1997). For every case analyzed, the experiment was assumed to take place over a 150-m reach of stream. For the conservative-tracer injection, we assume a continuous injection with sampling of the tracer rise, plateau, and fall. It was further assumed that the conservative-tracer injection would give a plateau concentration at the sampling site that was 25 times the background concentration, and that stream water would be sampled in 30-second intervals. For the reactive constituent, it was assumed that 15 samples would be collected at evenly spaced intervals along the stream reach. It also was assumed that the reactive-constituent concentration entering the study reach was 10 times the background concentration in ground-water inflow. Finally, for both conservative and reactive constituents, it was assumed that the concentration data errors, which define V_c in (5), have standard deviations equal to 15 percent of the true concentration values. In later sections we will investigate the sensitivity of the results to changes in study reach length, which we found to be the most important design variable.

Using the design variables described above, we assessed the ability of the tracer study approach to estimate solute transport and reaction parameters. For each of the 1,000 transport and reaction scenarios described in Table 1, the parameter covariance (5) was calculated. The suite of 1,000 covariance matrices provides the basis for assessing the capabilities and limitations of the tracer approach.

RESULTS

Identifying The Physical Transport Parameters

As noted earlier, there are six unknown parameters in (1) - (4) that must be estimated based on tracer data: the physical transport parameters (A, D, q_L, A_s, and α) and the reactive-loss rate parameter (λ_s). Previous work by Wagner and Harvey (1997) provides a comprehensive analysis of the ability of conservative-tracer injection studies to estimate the physical transport parameters. That study showed that the success of a tracer test is limited by our ability to estimate the stream-storage exchange parameters (A_s and α), and that the limitations can be defined using the experimental Damkohler number

$$DaI = \frac{\alpha(1 + A/A_s)L}{v} \qquad (7)$$

where A, A_s, and α are as defined earlier and

v average stream water velocity (m/s),

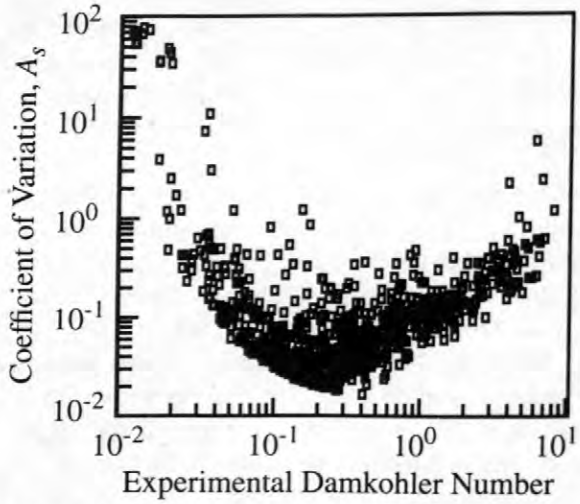

Figure 2. Plot of coefficient of variation vs. experimental Damkohler number for storage-zone cross sectional area, A_s.

L length of the study reach (m).

The results of this study mirror those of Wagner and Harvey (1997). In general, uncertainty associated with A_s and α reaches a minimum when *DaI* is on the order of 0.1-1.0, and uncertainty increases when *DaI* decreases below or increases above this value. This relationship is shown in Figure 2, which plots the experimental Damkohler number *DaI* versus the coefficient of variation for the storage-zone cross-sectional area A_s (a similar relationship is found for α). This relationship can be explained based on the degree of interaction between the solute and storage zones. When *DaI* is small (due to high v, small α and A/A_s, and(or) small L) parameter uncertainties are high because only a small amount of tracer interacts with the storage zones along the study reach. In this case, the effect of stream-storage exchange is small and cannot be identified. When *DaI* is large, solute exchange rates are high relative to advective movement, and tracer dispersion caused by stream-storage exchange reaches an equilibrium condition. In this case, uncertainty is high because the effect of exchange cannot be separated from that of dispersion.

Identifying The Reactive Loss Parameter

The experimental Damkohler number is useful for assessing the limitations of the stream tracer approach. We would like to identify a similarly useful expression for determining the limitations on estimating the reaction rate constant, λ_s. Here we test the dimensionless parameter grouping suggested by Harvey and Fuller (1998) that we call the reactive loss factor (*RLF*)

$$RLF = \frac{\lambda_s t_s L}{L_s} \tag{8}$$

where λ_s and L are as defined earlier and

t_s $= A_s/\alpha A$, average residence time of water in storage zones,

L_s $= v/\alpha$, average distance travelled by a parcel of water before entering a storage zone.

The reactive loss factor (8) is a measure of the effect of the reactive loss process along the study reach. When *RLF* is small, there is little loss of the reactive constituent within the experimental reach. This occurs when the reaction rate, λ_s, is small, the residence time in the storage zones, t_s, is small, and(or) the turnover length, L_s, is large relative to the experimental reach length, L. As *RLF* increases (due to increasing λ_s, increasing t_s, or decreasing L_s) the effect of reactive loss becomes more pronounced.

Figure 3 is a plot of *RLF* versus the coefficient of variation for λ_s. This plot highlights two important characteristics of the conservative/reactive tracer approach. First, for the conditions analyzed here, the tracer approach is consistently unable to reliably determine the reaction rate constant λ_s. Across the entire range of transport and reaction conditions analyzed, the coefficient of variation of λ_s reaches a minimum of approximately 1, which we consider to be an unacceptably high level of uncertainty. (Although somewhat arbitrary, we believe a parameter is reliably estimated only if its coefficient of variation is considerably less than 1. This choice is based on the concept of a 95 percent confidence interval for a normally distributed random variable. For example, a parameter with a coefficient of variation equal to 0.1 will have a 95 percent confidence interval that is approximately plus or minus 20 percent of the parameter value.) We will show later how the design variables used in this base case can be changed to improve parameter estimate reliability.

The second characteristic highlighted in Figure 3 is the relationship between the reactive loss

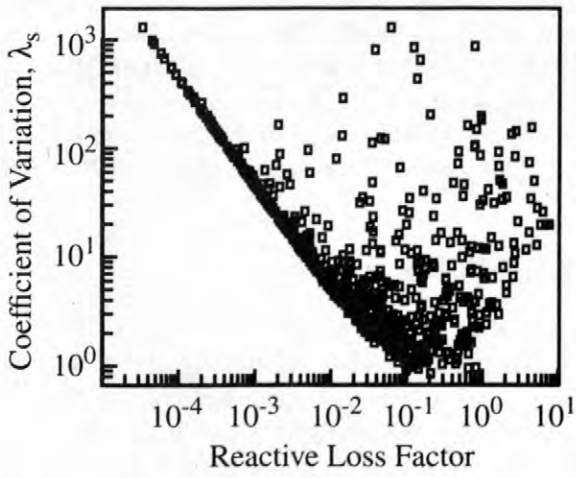

Figure 3. Plot of coefficient of variation vs. reactive loss factor for reaction rate constant λ_s.

factor and the coefficient of variation of λ_s. For the lower-range values of *RLF*, there appears to be a strong relationship between increasing *RLF* and decreasing uncertainty in λ_s. For the upper-range values, however, this relationship disappears. We believe this can be explained by the linkage between the physical and reaction transport processes and the need to identify the physical transport processes (specifically the stream-storage exchange process) before the reaction rate constant can be determined. Recall that the conceptual model (fig. 1) used here assumes that reactive loss occurs only in the storage zones. Further, the amount of reactive loss — that is, the imprint of the reactive loss process — along the study reach is dependent on both the degree of interaction between the solute and the storage zones and the magnitude of the reaction rate constant. Although the reactive loss factor *RLF* accounts for both, it does not account for the fact that the stream-storage exchange process is not always reliably determined. It appears that when the exchange parameters' uncertainty is very high, the reaction rate constant cannot be reliably determined, even when the *RLF* is large.

IMPROVING THE TRACER TEST DESIGN

The above analysis focused on the ability of the tracer approach to characterize reactive loss in the storage zones. The results show that, for the basic tracer test design used in our analyses, it is not possible to obtain a reliable estimate of the reaction rate constant λ_s. However, we know that there is a strong tendency for decreasing uncertainty in λ_s with increasing reactive loss factor, and that this relationship holds only when the storage-exchange parameters are reliably estimated. We also know that in order to reliably characterize stream-storage exchange, the experimental Damkohler number should be on the order of 0.1-1.0. The obvious question to ask is: Can we alter the tracer test design to improve the reliability with which λ_s is estimated?.

The one defining property of *DaI* and *RLF* that we can control when designing a stream tracer study is the experimental reach length *L*. This suggests that the choice of the experimental reach length could be an important factor in determining whether the reaction rate constant can be reliably estimated. To investigate the influence of the reach length on λ_s uncertainty, we selected a single parameter realization and performed a series of parameter uncertainty analyses, with reach length varied from 150 m (the base case) to 1,000 m. Furthermore, in order to normalize the results, we assumed that the same number (15) of reactive-constituent measurements would be collected in each analysis. The results of this sensitivity analysis are presented in Figure 4.

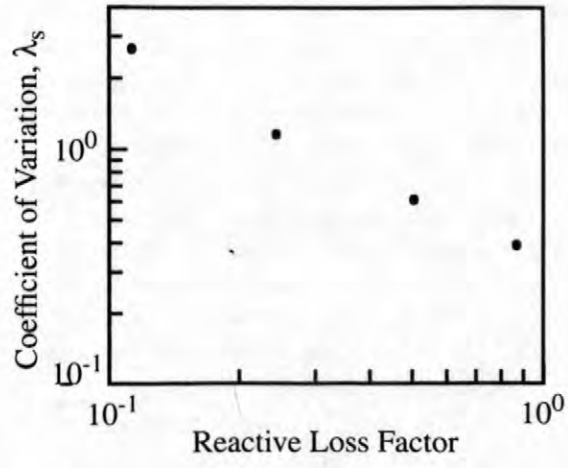

Figure 4. Plot of λ_s coefficient of variation vs. reactive loss factor. The data correspond to reach lengths of 150 m, 300 m, 600 m, and 1000 m.

The data plotted in Figure 4 show a strong dependency between the uncertainty associated with λ_s and the *RLF* value. It is important to note that in these analyses, the only factor changed was the experimental reach length. As *RLF* increases (due to the increase in the reach length *L*), the coefficient of variation of λ_s decreases. This suggests that the *RLF* may be useful for designing tracer studies by providing guidance for selecting the appropriate experimental reach length. However, because the data in Figure 4 are based on a single parameter realization, additional research is required to determine if these results can be transferred for use in stream systems with different transport and reaction properties. Moreover, we know that the reliable estimation of the reaction rate constant is dependent on reliably estimating the stream-storage exchange parameters, which in turn is dependent on having the appropriate *DaI* value. We also know that the only means we have of varying *DaI* when designing a stream tracer study is by varying the experimental reach length, just as we did to get the data plotted in Figure 4. Therefore it will be very important when designing a stream tracer study to consider the effects of varying experimental reach length on both *DaI* and *RLF*.

SUMMARY

We analyzed the capabilities and limitations of the stream tracer approach that combines conservative-tracer injection with measurement of a reactive constituent in a stream. The methodology used Monte Carlo parameter uncertainty analysis to evaluate and compare tracer test efficiencies over the spectrum of transport and reaction scenarios that are likely to be encountered in the field. Our analyses found that determining the reaction rate constant is dependent on two factors: (1) the reactive loss factor, *RLF*, is sufficiently large; and (2) the experimental Damkohler number, *DaI*, is in the range that provides reliable estimates of the stream-storage exchange parameters.

We demonstrated how the reaction rate constant can be reliably estimated by increasing the experimental reach length, which increases the reactive loss factor, *RLF*. However, this analysis was limited to a single realization of the solute transport and reaction parameters. Research is ongoing to determine how(if) the reactive loss factor might be used to select the reach length that provides a reliable estimate of the reactive loss parameter, and to better understand the trade-offs encountered when designing the conservative-tracer injection (based on *DaI*) and the synoptic sampling of the reactive solute (based on *RLF*).

REFERENCES

Bencala, K.E., Kennedy, V. C., Zellweger, G. W., Jackman, A.P., and Avanzino, R.J., 1984, Interactions of solutes and streambed sediments, 1, An experimental analysis of cation and anion transport in a mountain stream, Wat. Resour. Res., v. 20, p. 1797.

Bencala, K.E., 1984, Interactions of solutes and streambed sediment 2. A dynamic analysis of coupled hydrologic and chemical processes that determine solute transport: Wat. Resour. Res., v. 19, no. 3, p. 718-724.

D'Angelo, Webster, J.R., Gregory, S. V., and Meyer, J. L, 1993, Transient storage in Appalachian and Cascade mountain streams as related to hydraulic characteristics: Jour. N. Am. Benthol. Soc., v. 12, p. 223-235.

Grimm, N. B., and Fisher, S. G., 1984, Exchange between interstitial and surface water: Implications for stream metabolism and nutrient cycling: Hydrobiologia, v. 111, p. 219-228.

Harvey, J.W., Wagner, B.J., and Bencala, K.E., 1996, Evaluating the reliability of the stream tracer approach to characterize stream-subsurface water exchange: Wat. Resour. Res., v. 32, no. 8, p. 2441-2452.

Harvey, J.W., and Fuller, C. F., 1998, Effect of enhanced manganese oxidation in the hyporheic zone on basin-scale geochemical mass balance: Wat. Resour. Res., v., p.

Heekyung, K., Hemond, H. F., Krumholz, L. R., and Cohen, B. A., 1995, In-situ biodegradation of toluene in a contaminated stream, 1. Field studies: Environ. Sci. Technol., v. 29, p. 108-116.

Kim, B. K. A., Jackman, A. P., and Triska, F. J., 1992, Modeling biotic uptake by periphyton and transient hyporheic storage of nitrate in a natural stream: Wat. Resour. Res., v. 28, no.10, p. 2743-2752.

Runkel, R. L., McKnight, D., Bencala, K. E., and Chapra, S. C., 1996, Reactive solute transport

in streams, 2, Simulation of a pH modification experiment: Wat. Resour. Res., v. 32, no. 2, p. 419-430.

Stream Solute Workshop, 1990, Concepts and methods for assessing solute dynamics in stream ecosystems: Jour. N. Am. Benthol. Soc., v. 9, no. 2, p. 95-119.

Triska, F. J., Duff, J. H., and Avanzino, R. J., 1993, The role of water exchange between a stream channel and its hyporheic zone in nitrogen cycling at the terrestrial-aquatic interface: Hydrobiologia, v. 251, p. 167.

Wagner, B.J, and Gorelick, S. M., 1986, A statistical methodology for estimating transport parameters: Theory and applications to one-dimensional advective-dispersive systems: Wat. Resour. Res., v. 22, no. 8, p. 1303-1315.

Wagner, B.J, and Harvey, J. W., 1996, Solute transport parameter estimation for an injection experiment at Pinal Creek, Arizona: in Morganwalp, D.W., and Aronson, D.A., eds., U.S. Geological Survey Toxic Substances Hydrology Program -- Proceedings of the Technical Meeting, Colorado Springs, Colorado, September 20 - 24, 1993: U.S. Geological Survey Water-Resources Investigations Report 94-4015.

AUTHOR INFORMATION

Brian J. Wagner, U.S. Geological Survey, Menlo Park, California (bjwagner@usgs.gov)

Judson W. Harvey, U.S. Geological Survey, Reston, Virginia (jwharvey@usgs.gov)

Preliminary Model Development of the Ground- and Surface-Water System in Pinal Creek Basin, Arizona

By Cory E. Angeroth, S. A. Leake, and Brian J. Wagner

ABSTRACT

Ongoing studies of surface water and ground water contaminated by acidic-mine wastes in the Pinal Creek Basin near Globe, Arizona, include the development of a ground-water flow model. The flow system is being simulated with the U.S. Geological Survey's updated three-dimensional, finite-difference, ground-water flow model, MODFLOW-96. The model has been vertically discretized into five layers and horizontally discretized into 62.5-meter by 125-meter cells. Simulation of the hydrologic processes in the basin will provide information on the effects of streamflow infiltration, ground-water discharge to a perennial stream reach, ground-water pumping, and an unlined surface-water impoundment. The model also will be used to test the value of various types of data for calibrating ground-water flow models. The aquifer is bounded by impermeable crystalline rocks and is composed of a thick conglomerate and, near major drainages, unconsolidated alluvium where the bulk of the contamination is present.

INTRODUCTION

A plume of acidic-mine wastes have contaminated ground and surface waters in the Pinal Creek Basin near Globe, Arizona. A number of studies are underway at the U.S. Geological Survey (USGS) Pinal Creek Toxic-Substances Hydrology Research site to identify the processes that control the migration and transformation of contaminants in ground water and surface water. The major source of contamination is mine-process water that was stored in an unlined surface-water impoundment, referred to as Webster Lake, for 43 years. In 1986, the lake was ordered drained by the U.S. Environmental Protection Agency (USEPA), and by May 1988, the lake was dry. Because of the complex patterns and dynamics of ground-water flow, a model capable of simulating these effects is needed. One of the uses of the model is to test the value of alternative forms of data in estimation of model parameters. MODFLOW-96 will be used to simulate the aquifer and flows in Pinal Creek and its tributaries. This paper describes the preliminary design of a ground-water and surface-water flow model that will be used for these studies.

GEOHYDROLOGIC SETTING

Pinal Creek Basin is a broad alluvial valley bounded by mountain ranges that were formed by block faulting. The mountain ranges are composed of igneous, metamorphic, and sedimentary rocks. The geology and structure of the Pinal Creek Basin has been documented in several publications and will be summarized here.

Basin Structure

Pinal Creek Basin has been divided into two structural compartments—the southern and northern blocks, which are connected by a structurally complicated area termed the "bottleneck" (fig. 1) by Neaville and Brown (1993). The southern block is bounded on the west by the Miami Fault and is bounded on the south by the Pinal Mountains (fig. 1). Miami Fault is a northeastward-trending normal fault that has a dip that ranges from 35° to vertical and a vertical displacement of more than 500 m (Neaville and Brown, 1993, p. 7). The eastern boundary of the block is the Pinal Creek fault zone that is covered

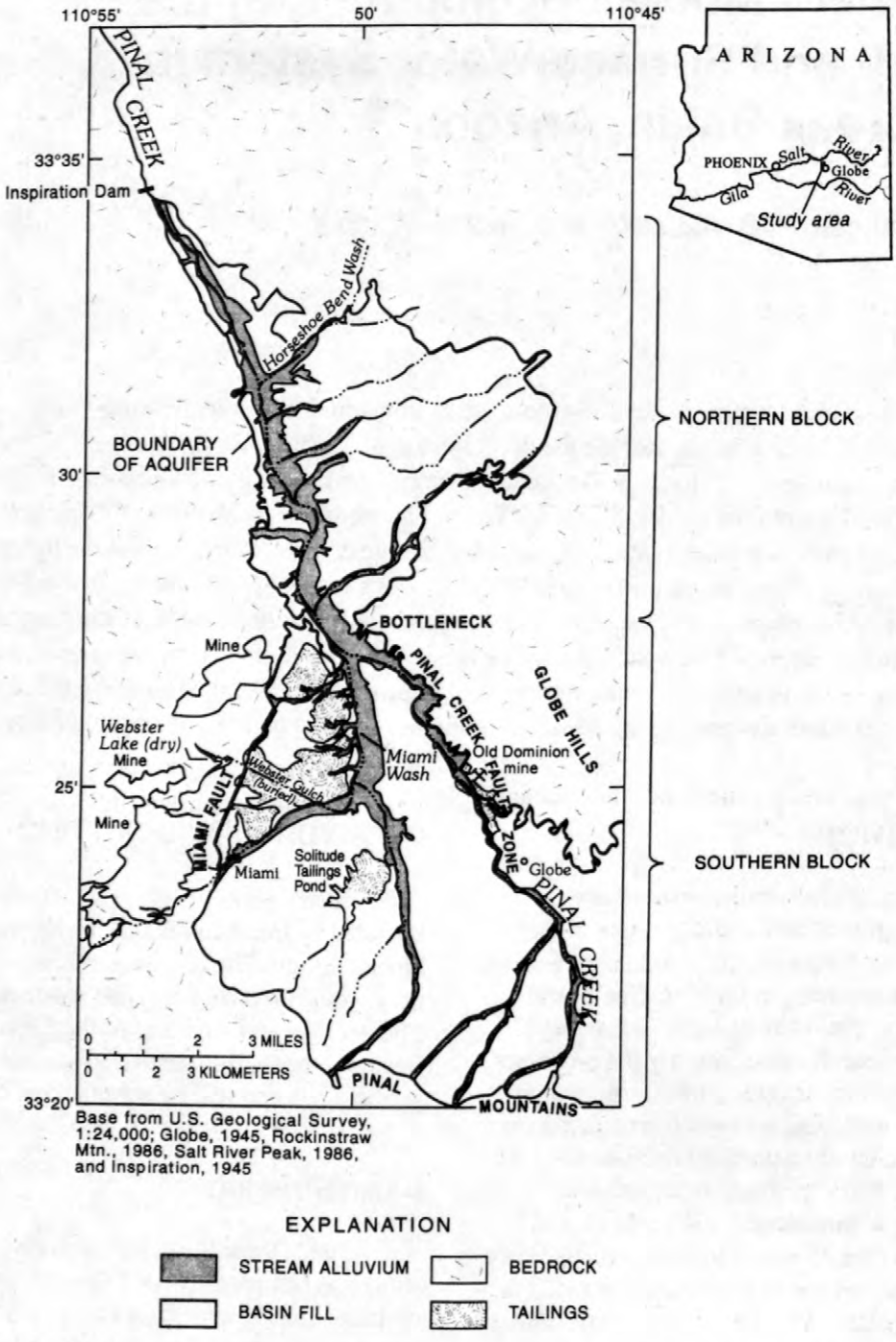

Figure 1. Geologic setting and tributary streams, Pinal Creek Basin, Arizona.

on the surface in most places by a detritus mantle but is more than 1.5 km wide in the underground workings of the Old Dominion mine. The fault zone has a vertical displacement that is probably less than 200 m and consists of a series of southwestward-dipping step faults (Peterson, 1962, p. 46). The Miami Fault and the Pinal Creek fault zone intersect at the bottleneck to form the northern boundary of the southern block.

The northern block is subdivided into two areas. The northern area is north of Horseshoe Bend Wash (fig. 1). Alluvial material in this area thins to the north and overlies igneous rock. The southern area is south of Horseshoe Bend Wash

and is bounded by steep-angled normal faults along which the basin block has been down-dropped (D.R. Pool, hydrologist, USGS, written commun., 1984). Drillers' logs of wells in the area indicate a vertical displacement of about 300 m. The southern boundary of the northern block is the intersection of the Miami Fault and the Pinal Creek fault zone at the bottleneck.

Hydrogeologic Units

Ransome (1903) and Peterson (1962) mapped the geology of most of the basin. On the basis of their hydrologic properties, the geologic units in the basin are grouped into three major categories—bedrock, basin fill, and unconsolidated stream alluvium. A Precambrian-age basement complex of schist that has been intruded by large bodies of igneous rocks makes up most of the bedrock group (Neaville and Brown, 1993, p. 8). The bedrock group is much older than the basin fill that uncomformably overlies it. Bedrock also makes up the mountains and basement complex that bound the study area. This group has low permeability, and most ground-water flow occurs through fractures and faults.

The basin fill is alluvial material of Pliocene and Pleistocene ages that filled structural troughs. This unit is faulted in areas because of mild volcanic activity (Peterson, 1962, p. 8). The hydraulic-conductivity values of this unit range from 0.1 to 0.2 m/d (Neaville and Brown, 1993, p. 11). The degree of cementation plays a large role in determining the hydraulic properties of this unit. Thickness of this unit varies from as much as 1,000 m in the southern part of the basin to 0 at the lateral bedrock boundary.

Unconsolidated stream alluvium is Quaternary to recent in age and is incised in the basin fill along the active channels in the basin (fig. 1). The unit can be divided into two distinct zones, a basal boulder zone and an overlying sandy zone. The boulder zone is only a couple of meters thick, and the hydraulic conductivity for the zone is greater than 400 m/d. The remainder of the unit is the sandy zone, and the hydraulic conductivity ranges from about 50 to 150 m/d. Most of the unit consists of gravel; however, material size ranges from clay to boulders (Neaville and Brown, 1993, p. 12). The unit is about 50 m thick near the confluence of Miami Wash and Pinal Creek and thins to 0 along the upper reaches of the drainage basin and at Inspiration Dam. This unit is hydraulically connected to the basin fill, which bounds the stream alluvium laterally and at depth.

OCCURRENCE AND MOVEMENT OF SURFACE WATER

Most of the stream channels within the study area are dry during most of the year. Perennial flow exists only in the lower 6 km of Pinal Creek and at a few springs in the Pinal Mountains, Globe Hills, and the hills north of Miami (Neaville and Brown, 1993, p. 13). Streamflow losses in the Pinal Mountains have been measured by Hazen and Turner (1946), Neaville and Brown (1993), and in the spring of 1998, as a part of this study. The measurements allow a characterization of the distribution of infiltration in the southern part of the basin. Streamflow lost through infiltration has the potential to recharge ground water in the stream alluvium and basin fill.

Pinal Creek upstream from Inspiration Dam is perennial because the shallow bedrock forces ground water toward the land surface. The head of flow of the perennial reach moves upstream and downstream depending on ground-water levels in the unconsolidated deposits (stream alluvium and basin fill).

The ground-water system also is recharged by surface water stored in unlined impoundments. Webster Lake was the largest unlined impoundment in the basin and was used to store mine-process water. The surface elevation of the lake varied and, on several occasions, the lake overflowed into Webster Gulch. The maximum capacity of the lake, estimated from topographic maps, was 7,150,000 m^3 (Neaville and Brown, 1993, p. 14). Seepage of lake water into the aquifer may have contributed large amounts of contaminants to the ground-water system before the lake was drained in 1988. The lake may partially fill after large rainstorms but any standing water is expeditiously removed.

OCCURRENCE AND MOVEMENT OF GROUND WATER

Ground water occurs almost exclusively within the basin fill and stream alluvium. Flow in the bedrock units probably is restricted to intensely fractured or faulted areas, and flow is considered insignificant compared with flow in the unconsolidated deposits (Neaville and Brown, 1993, p. 15). Most ground-water recharge originates as infiltration into the streambed in the headwaters of Pinal Creek and tributaries and flows northward in the same direction as Pinal Creek.

In the area near the confluence of Pinal Creek and Miami Wash, the alluvial aquifer is constricted, horizontally and vertically, by bedrock. This constriction forces ground water toward the land surface, and at times, flow in the creek can result if the water table is above land surface. This surface-water flow, however, usually is short lived as the water infiltrates the channel of Pinal Creek and recharges the aquifer in the northern block. As the ground water flows northward, the aquifer again thins and narrows until it is truncated by bedrock near Inspiration Dam. This truncation causes all ground-water flow to discharge to the surface at Inspiration Dam. Surface-water measurements from above and below the dam confirm that all flow goes over the dam.

MODEL DESIGN

MODFLOW-96 (Harbaugh and McDonald, 1996) will be used to simulate steady-state and transient surface-water and ground-water flow in the basin. The model is an update of the modular three-dimensional finite-difference ground-water flow model of McDonald and Harbaugh (1988). The model will include a modified stream package that allows ground-water recharge to the uppermost active layer. A steady-state simulation will be done using average annual conditions that are based on estimated inflows and outflows. Transient flow will be modeled using stress periods that will allow for simulation of major hydrologic events in the basin after September 1984.

The model will simulate ground-water flow in the basin fill and stream alluvium, which are bounded by relatively impermeable bedrock. The contact between the basin fill and bedrock will form the boundary of the active-flow area (fig. 1). The model grid has been rotated 20° west of north. This orientation places the model columns nearly parallel to the long axis of the stream alluvium. The aquifer has been uniformly discretized horizontally into cells that are 125 m wide along the 231 rows and 62.5 m wide along the 242 columns. These grid dimensions were selected to allow adequate representation of the thin stream alluvium in the upper reaches of the streams. The aquifer has been discretized vertically into five layers (fig. 2). The uppermost layer will represent stream alluvium and will vary in thickness from 0 at the periphery of the model to a maximum of 100 m in the central part. The second layer will represent the boulder zone at the base of the stream alluvium. This layer is a couple of meters thick and will have a higher hydraulic conductivity than the upper layer of the model. Layers 3 through 5 will represent basin fill. Layer 3 will be used to simulate the shallow basin fill and will be 100 m thick except in the far northern part of the basin where the aquifer thins and is truncated by bedrock. The fourth layer will simulate the basin fill to an intermediate depth, and north of the bottleneck, will extend to the bedrock contact. South of the bottleneck, the bottom of the fourth layer has been assigned a constant elevation of 640 m, and the layer is underlain by a fifth layer that extends to the bedrock contact at depth.

The bedrock and basin-fill contact is represented as a no-flow boundary, and all model cells outside this contact are inactive. A no-flow boundary also will be used to simulate the ground-water divide that corresponds to the surface-water divide in the southeastern part of the model area. The stream package will be modified to allow for recharge to the uppermost active layer. This modification will be standard in the new version of the stream package that is currently being developed (David E. Prudic, hydrologist, USGS, oral commun., 1998). Allowing recharge to the uppermost active layer provides for a better simulation of the system because the water level in the stream alluvium rises and declines in response to changes in amounts of precipitation. The draining of Webster Lake in the 1980's will be simulated using the general-head boundary package.

The model will be run in the steady-state and transient modes. Head data from the

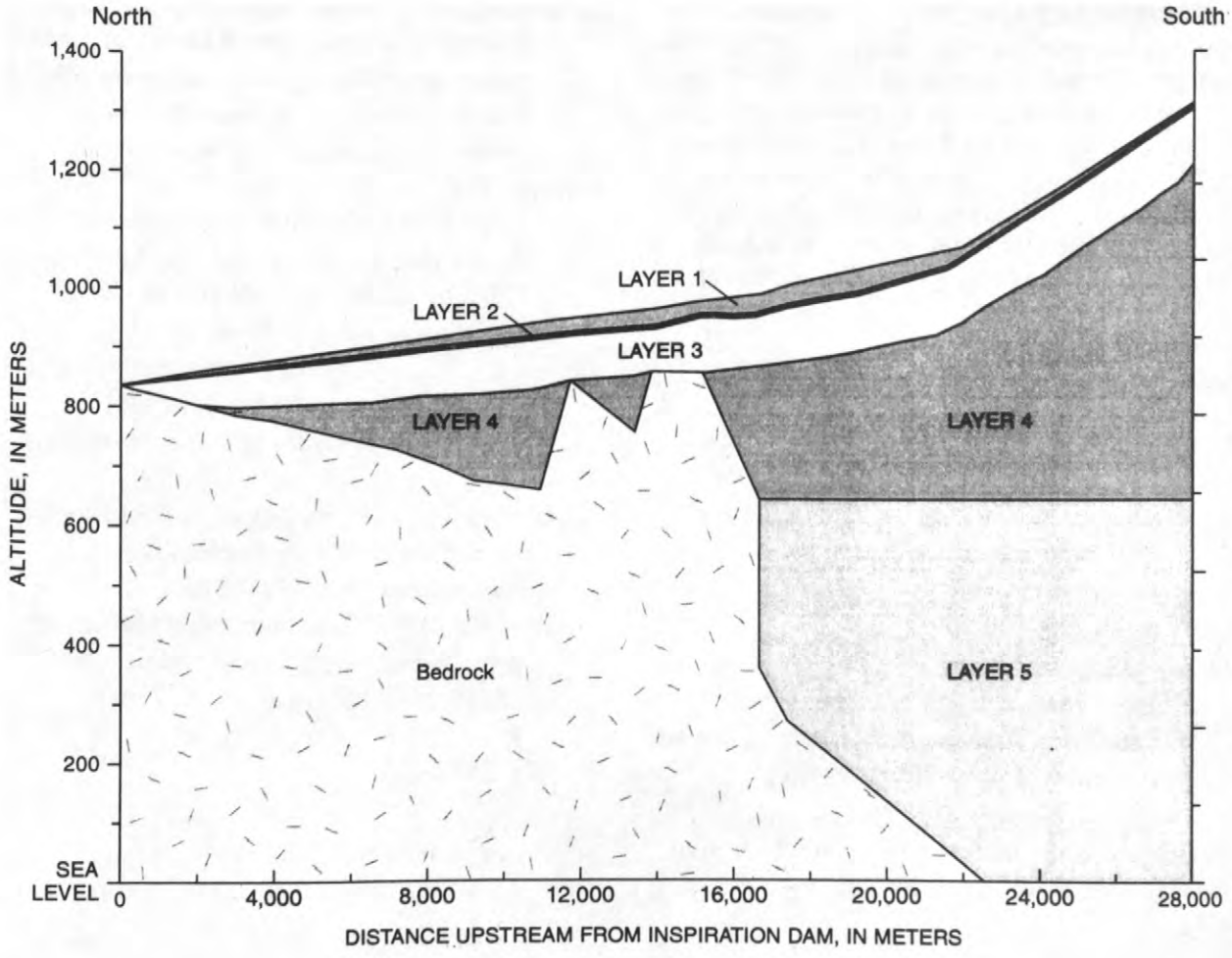

Figure 2. Generalized vertical discretization for ground-water flow model.

steady-state simulation will be used as the starting head for the transient simulation. The steady-state model will be calibrated using water levels measured before large-scale remedial pumping began in the late 1980's, before Webster Lake was drained in the late 1980's, and using discharge data for Pinal Creek at Inspiration Dam that have been collected since July 1980. Transient simulations will be calibrated using water levels and discharge data from Inspiration Dam and the location of the head of flow in Pinal Creek.

The model will be used to test the value of alternative forms of data in estimation of model parameters. In particular, the suitability of using available time-of-travel data in the model-calibration process will be tested. Results of chemical-tracer tests also will be incorporated into the calibration process. Another use of the model will be to apply the monitoring-network-design model developed by Wagner (1995) to evaluate the information and cost tradeoff between ground-water head and age data.

SUMMARY

Ground water and surface water in Pinal Creek Basin near Globe, Arizona, have been contaminated by acidic-mine wastes. The USGS is using the model package, MODFLOW-96, with a modified stream package to simulate the ground water in the aquifer in order to study the movement of contaminants in the aquifer system. Information provided by the model will be used to better understand the hydrologic processes in the aquifer. The aquifer has been vertically discretized into five layers and horizontally discretized into

cells that are 62.5 m by 125 m. Pinal Creek Basin presents a unique opportunity to analyze the value of using alternative types of data for calibrating ground-water flow models. The model will incorporate age data (and chemical-tracer data in general) and also will be used in conjunction with another model to evaluate the information and cost tradeoff between the use of ground-water head and age data.

REFERENCES CITED

Harbaugh, A.W., and McDonald, M.G., 1996, User's documentation for MODFLOW-96, an update to the U.S. Geological Survey modular finite-difference ground-water flow model: U.S. Geological Survey Open-File Report 96–485, 56 p.

Hazen, G.E., and Turner, S.F., 1946, Geology and ground-water resources of the upper Pinal Creek area, Arizona: U.S. Geological Survey unnumbered open-file report, 55 p.

McDonald, M.G., and Harbaugh, A.W., 1988, A modular three-dimensional finite-difference ground-water flow model: U.S. Geological Survey Techniques of Water-Resources Investigations, book 6, chap. A1, 586 p.

Neaville, C.C., and Brown, J.G., 1993, Hydrogeology and hydrologic system of Pinal Creek Basin, Gila County, Arizona: U.S. Geological Survey Water-Resources Investigations Report 93–4212, 32 p.

Peterson, N.P., 1962, Geology and ore deposits of the Globe-Miami District, Arizona: U.S. Geological Survey Professional Paper 342, 151 p.

Ransome, L.F., 1903, Geology of the Globe copper district, Arizona: U.S. Geological Survey Professional Paper 12, 168 p.

Wagner, B.J., 1995, Sampling design methods for groundwater modeling under uncertainty: American Geophysical Union, Water Resources Research, v. 31, no. 10, p. 2581–2591.

A Flow-Through Cell for *In Situ*, Real Time X-ray Absorption Spectroscopy Studies of Geochemical Reactions

By John E. Villinski, Peggy A. O'Day, Tim L. Corley, and Martha H. Conklin

ABSTRACT

The contact of acid mine waste with mineral surfaces can result in a series of complex geochemical reactions, including mineral precipitation and dissolution, which are often kinetically controlled proceses. One problem in formulating rate expressions for dissolution/precipitation reactions is that intermediate species are often formed. Identification of these species can lead to more accurate models, and hence, better predictions of the fate of the various chemical species. The use of spectroscopic probes to directly identify chemical species often requires high vacuum, which can induce modifications in surfaces and surface species. Synchrotron X-ray absorption spectroscopy is an element-specific method which can be used to probe samples in an aqueous environment. We developed a flow-through reaction cell for use at the Stanford Synchrotron Radiation Laboratory (SSRL), Stanford CA, that allowed for spectroscopic probing of minerals undergoing precipitation or dissolution reactions. This cell, coupled with X-ray absorption near-edge structure (XANES) spectroscopy, allowed us to detect the changes in elemental speciation of manganese during the reductive dissolution of MnO_2 by Fe(II). The use of this flow-through reaction cell will allow for the coupling of spectroscopic measurements of elemental oxidation states with conventional rate measurements.

INTRODUCTION

The Pinal Creek Basin, near Globe, AZ, has been impacted by an acidic, suboxic plume originating from wastes produced by the copper mining industry. The plume is characterized by high concentrations of ferrous iron and sulfate, as well as elevated concentrations of other heavy metals. The Fe(II) reductively dissolves the manganese (hydr)oxide coatings from the alluvial aquifer material, releasing Mn(II) to the aqueous phase, and precipitating a ferric iron phase. The acid in the plume is retarded due to 0.34 percent carbonate by weight in the alluvial material (Eychaner and Stollenwerk, 1989). For a more complete description of the site, the reader is referred to Eychaner (1991).

Stollenwerk (1994) conducted column experiments using natural sediments with uncontaminated and contaminated groundwater. The effluent profile of Mn(II) was a sharp spike followed by a very slow tail towards influent conditions. In addition, the total release of Mn(II) over an experiment lasting 30 pore volumes was only 46% of the amount that would be predicted by the amount of Fe precipitated and the stoichiometry of the following reaction:

$$MnO_2 + 2Fe^{2+} + 4H_2O = Mn^{2+} + 2Fe(OH)_3 + 2H^+. \quad (1)$$

Stollenwerk, (1994) found that the transport of Mn(II) through the basin could not be modeled adequately using equilibrium principles.

Results from batch experiments performed at the University of Arizona with MnO_2-coated quartz and artificial acid mine drainage (AAMD) were similar to those from column experiments done by Stollenwerk (1994) in that there was an initial fast release of Mn(II), followed by a drastically slower release as the week-long experiment continued. In addition, the

proportion of Fe(II) consumed to Mn(II) released increased as the experiment progressed.

Stollenwerk (1994) proposed that the discrepancy between the amount of Mn released and the amount predicted to be released was due to Mn remaining associated with the solid phase, either coprecipitated with Fe or that the Mn(IV) was incompletely reduced. No known Mn phase was identified in the reacted sediments using X-ray diffraction (XRD) (Lind and Stollenwerk, 1995).

Other researchers have proposed the existence of an intermediate phase in the reduction of Mn(IV) (hydr)oxides (Jardine and Taylor, 1995; Kozawa and Yeagar, 1965; Perez-Benito and others, 1996). Few studies have actually detected the presence of Mn(III). Giovanoli and others, (1971) detected the presence of manganite in samples of birnessite reduced by cinnamyl alcohol using electron microscopy. Crowther and others, (1983) detected Mn(III) at the surface of birnessite reacted with Co(II) using X-ray photoelectron spectroscopy (XPS). Likewise, the presence of Mn(III) was detected on the surface of birnessite reduced in the presence of As(III) using XPS (Nesbitt and others, 1998).

One problem with the use of these high vacuum techniques (XPS, SEM) is the fact that the mineral surface is removed from the environmental state as it is dried prior to analysis. Synchrotron X-ray absorption spectroscopy (XAS), on the other hand, allows for spectral analysis of elements in a complex matrix and in the presence of an aqueous solution.

XAS is an element-specific probe that has the advantages over other spectroscopic techniques including low detection limits (as low as 10-100 ppm depending on the element and the matrix), and the ability to probe samples of varying phases (crystalline or amorphous solids, gases and liquids) (Brown and others, 1988). XAS also provides a unique spectral signal for each local environment of the element of interest (Brown and others, 1988). For a more complete review of XAS the reader is referred to Brown and others (1988).

The focus of this paper is on the design of a flow cell for XAS that can be used in a fluoresence detector at the Stanford Synchrotron Radiation Laboratory (SSRL). XAS is generally separated into two parts, the extended X-ray absorption fine structre (EXAFS) and the X-ray absorption near-edge structure (XANES). In this study we used the XANES portion of the spectra to shorten the acquisition time for data acquisition in order to monitor changes in the oxidation state during the dissolution reaction.

The system we chose to study was the geochemical reactions that occur in the alluvial aquifer at Pinal Creek. The system was simplified significantly from the natural state. This was done to focus on the Mn/Fe redox couple, rather than other possible competing reactions. Thus synthetic materials were used which allow for better pH control and a more complete description of the mineral surfaces. Likewise, other trace metals were excluded from the solution to minimize other surface reactions (sorption, precipitation) that might compete with the Mn/Fe redox reactions.

EXPERIMENTAL PROCEDURES

Materials

All chemicals used were reagent grade. The solid materials used for the flow experiments conducted at the SSRL was a MnO_2-coated silica gel. The silica gel was SiLCRON G-604 (SCM Corporation) with a nominal grain size of 13.5 μm, a specific surface area of 320 $m^2 g^{-1}$, a specific gravity of 2.1 g cm^{-3}, and a dry bulk of 0.18 g cm^{-3} (SCM Corp. technical data sheet). Fine particles (< 1 μm) were removed by suspending the material in purified water (Milli-RO 6 plus/Milli-Q plus reagent water system Millipore Corp., USA, with a resistivity of 10^{18} MΩ cm, referred to herein as Milli-Q) in a 0.4 m high cylinder, and allowing it to settle for 24 hours. This process was continued until the supernatant was free of fine particles.

A rigorous cleaning process was used to remove surface contaminants from the silica gel. Following a wash with Milli-Q, the silica gel was refluxed with 2 M HNO_3 (trace metal grade, Fisher Scientific) for two hours. This was followed by rinsing with Milli-Q until the

conductivity of the effluent was equal to that of the influent, and finally, the silica gel was dried at 105°C.

The silica gel was then coated with a Mn(IV) oxide using a modification of a dry oxidation procedure of $Mn(NO_3)_2$ (J. T. Baker, Inc.) (Stahl and James, 1991; Covington and others, 1962). A measured mass of silica gel was placed in a teflon vessel. $Mn(NO_3)_2$ was added to the vessel in an amount that would yield a desired MnO_2 concentration, and then Milli-Q was added to allow the $Mn(NO_3)_2$ to be mixed evenly through the solid. The vessel was then placed in an oven at 105°C and allowed to dry. During the initial drying process, the solid/liquid mixture was stirred every 10-15 minutes to prevent the salts from wicking. After 24 hours, the dried solids were baked at 160°C for 72 hours.

After cooling, the Mn(IV)-coated silica was placed in 250 ml polyethylene bottles and filled with Milli-Q. The bottles were placed on their sides, and placed on a shaker table over night. The supernatant was decanted, and the procedure was repeated until the supernatant was free of visual Mn(IV) oxides (referred to herein as MnO_2). This allowed for the removal of easily "sloughed-off" MnO_2. The average valence of the Mn in the MnO_2-coated silica was determined to be 4.01±0.02 by the oxalate method (Hem, 1980). The MnO_2 concentration of the MnO_2- coated silica gel was 14.4 mg MnO_2 g^{-1} total, or 0.91% Mn by weight.

All solutions were made with Milli-Q water that had less than 10 µg/l dissolved oxygen (DO), measured using an Hach DR100 spectrophotometer with low-range DO AccuVac vials (detection limit: 10 µg/l, Hach Co.). To accomplish this, Milli-Q water was boiled for at least five minutes, cooled under a constant stream of N_2 gas, and then placed in a glove box (Coy Laboratory Products), and exposed to a 97% N_2-3% H_2 atmosphere for at least five days. The $FeSO_4 7H_2O$ (Aldrich Chemical Co., Inc.) was stored in the N_2-H_2 atmosphere to prevent oxidation of the Fe(II). The composition of the solutions are listed in Table 1. The pH of the solutions were adjusted with either HNO_3 or NaOH (Fisher Scientific) solutions standardized against known quantities of potassium hydrogen phthalate (MCB Manufacturing Chemists, Inc.).

Table 1. Chemical composition of contaminated groundwater from Pinal Creek and solutions used in flow-through experiments. All values in mmol expect for pH (standard units) and temperature (°C).

Constituent	Cont. GW*	Inert elect.**	Reactive solution
pH	3.30	3.00	3.00
Temperature	17	25	25
Dissolved O_2	<0.006	<0.0004	<0.0004
Ca	11.6	6.3	6.3
Mg	15.8	93.7	82.7
Na	9.4	9.5	9.5
K	0.2	0	0
Fe	52.4	0	11.0
Mn	1.34	0	0
Al	10.5	0	0
Cu	2.4	0	0
Co	0.20	0	0
Ni	0.06	0	0
Zn	0.33	0	0
SO_4^{2-}	100	102	102
Cl	9.5	9.5	9.5
Ionic Strength	232	220	220

*Contaminated groundwater, values from Stollenwerk (1994)
**Inert electrolyte

Flow Cell Design

The incoming X-ray beam at the SSRL has a horizontal profile that is 20 mm wide and is usually slit down to 1-2 mm high. The design of the cell was made with this in mind (Figure 1). The flow cell was constructed of polycarbonate. The bed support was made from a porous sheet of ultra-high molecular weight (UHMW) polypropylene with pore size ranging from 10-20 µm (X-4920, Porex Technologies). The bed support was treated with concentrated H_2SO_4 to make the surfaces hydrophilic. The windows consisted of Kapton tape with an acrylic adhesive. The tubing connections to the cell were made by

threading 1/16" O.D. PEEK tubing with a 1-72 die, and tapping the cell inlet, outlet and ports.

Experimental Design

The experimental set-up is shown in Figure 2. All tubing other than the PEEK tubing that was directly connected to the cell was either Teflon (0.020" I.D.) or Tygon (0.030" I.D.). The solution was delivered with a Ismatec IPN peristalic pump (Ismatec SA) at flow rates from 50-125 µl min^{-1}.

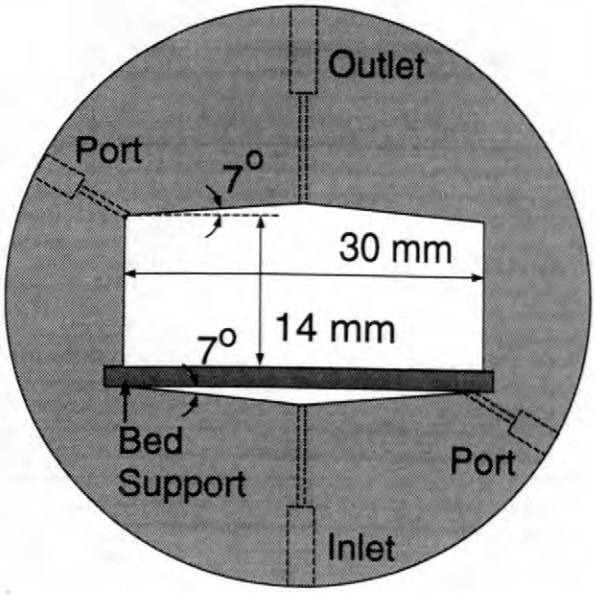

Figure 1. Plan view of the flow cell used at SSRL. The cell was constructed of 3 mm thick polycarbonate. The bed support was constructed from a porous sheet of 1/16" thick UHMW polypropylene. The inlet, outlet and side ports were all tapped to accept a 1-72 thread size. Dashed lines indicate elements that are internal to the cell.

Micro pH and reference electrodes with 3 µl dead volumes were used to monitor effluent pH (Microelectrodes, Inc.). The effluent was then collected in set fraction sizes using a Frac100 fraction collector (Pharmacia). The fractions were then analyzed for Mn(II) and total Fe (Fe_T) by flame AA.

The cell was packed with the MnO_2-coated silica gel, which was kept wet at all times, The cell was packed wet by attaching a syringe filled with MnO_2-coated silica gel and Milli-Q to the outlet port of the cell, and allowing gravity to pack the cell.

In order to prevent oxygen entering into solution during the experiment, the solutions as well as the sample chamber of the fluoresence detector were purged continually with ultra-high purity He gas.

Experiments with this cell differ from those of a normal column experiment. Firstly, the cell is not rigid due to the fact that Kapton windows can stretch. Thus the dimensions of the cell can change due to pressure changes within the cell. Because of this, the experiments have been run as a fluidized bed-reactor with no filter constraining the top of the bed. With a filter on top of the packed bed, pressure can build up within the cell, causing the windows to stretch outward. At this point, channeling can occur within the bed.

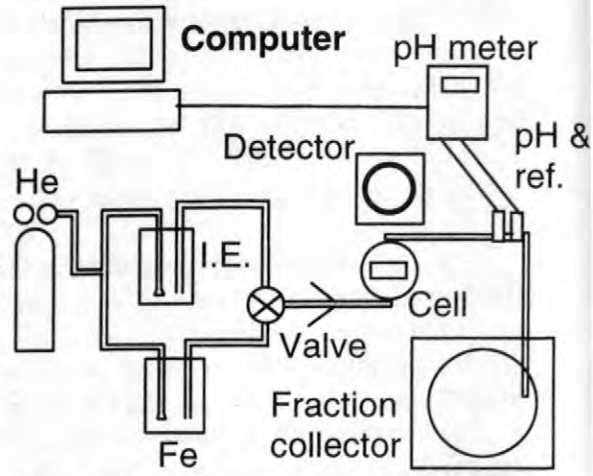

Figure 2. Experimental design. Ultra high purity He was used to sparge the solutions to prevent O_2 from entering the cell. **I.E.** stands for inert electrolyte, and **Fe** is the 11 mM Fe(II) solution. **pH and ref.** refers to the in-line pH and reference electrodes.

Conversely, with no confining filter on top of the bed, other problems can occur such as loss of bed material from the cell from changes in solution composition or increases in flow rate, or a siphoning action which can occur when moving

the cell in and out of the detector chamber (thus changing the head in the system). Keeping all parts of the system from the cell to the fraction collector at the same elevation helped to mitigate siphoning.

Secondly, the dead volume of the cell is large compared to the pore volume due to the size of the X-ray hutches at SSRL, and the placement of the ion and fluoresence detectors. The estimated pore volume of a normal experiment was on the order of 350 µl. The dead volume was estimated to be 1760 µl, which is a factor of five greater than the pore volume and therefore the majority of the dispersion could occur in the dead volume as opposed to the bed.

Therefore the determination of the dispersive properties of the system are not as straight forward as with a conventional column experiment. The performance and dispersive properties of the system were characterized in the laboratory prior to experiments at SSRL. A tracer test was conducted with the packed cell by changing the ionic strength of the influent inert electrolyte solution from 5 mM to 10 mM $CaSO_4$ and monitoring the conductivity with an Altech 320 conductivity detector (Altech Associates, Inc.).

XAS Data collection

All spectra were collected at the SSRL (Stanford, CA) on wiggler beam lines IV-1 and IV-3. Beam current ranged from 30-90 mA at 3 GeV and the magnetic field of the wiggler was 18 kG. Either Si(111) or Si(220) monochromators were used with an unfocused beam. The monochromators were detuned such that the incoming beam flux was reduced by 30-50% to reject higher-order harmonic reflections. Energy was calibrated by assigning the first inflection of the absorption edge of Mn metallic foil to 6539 eV.

Fluoresence spectra were collected with the sample at a 45° angle to the incident beam using a Stern-Heald-type detector (Lytle and others, 1984) with Soller slits and a Cr filter to reduce background scattering and fluoresence. Transmission spectra of the reference compounds were collected using two gas-filled ion chambers.

After beam alignment and energy calibration, the sample in the flow cell was placed in the path of the beam with an inert electrolyte solution flowing at a predetermined flow rate. A background spectrum was then recorded. Next the flow was switched to the reactive Fe(II) solution and spectra were collected for two hours as the reaction progressed. The pH was recorded and the effluent was collected in fractions.

All the XANES spectra were treated in the same manner. The background was subtracted from the spectrum using a low-order polynomial fit over the pre-absorption edge region of 6520-6533 eV using the computer program EXAFSPAK (George, 1995).

RESULTS AND DISCUSSION

Cell Characteristics

Results of the aqueous phase data are shown in figure 3. The salt tracer break-through curve (BTC) is asymmetric, with significant tailing as the normalized concentration approaches a value of one. This type of behavior is often attributed to diffusion-limited mass transfer to immobile regions of the pore volume (van Genuchten and Wierenga, 1976). This is expected as the silica gel has a significant internal porosity. The porosity of the MnO_2-coated silica gel under static conditions was determined to be 74%. Assuming a 42% external porosity (representative porosity for clay-sized particles, Todd, 1980), then 43% of the pore volume would be internal pores, or immobile.

The pH BTC shows an initial increase in pH indicating that the MnO_2 coating is being reductively dissolved by the Fe(II). The subsequent precipitation of the resulting Fe(III) can be noted to occur fairly rapidly, as the pH starts to decrease at approximately 16 minutes. The pH continues to decrease until approximately 80 minutes into the experiment and then slowly increases back above the starting pH. This drift in the pH was probably due to some solid accumulating on the porous frit of the pH electrode. After cleaning the pH electrode returned to normal operation.

The Mn(II) BTC indicates that, initially, the reaction is not kinetically limited. However, as time progresses, the tailing present in the down-sloping portion of the Mn_T BTC suggests a kinetically limited reaction. The deviation of the Mn(II) BTC from the tracer BTC as the tracer BTC aproaches a normalized concentration of one could also be due to kinetic limitations.

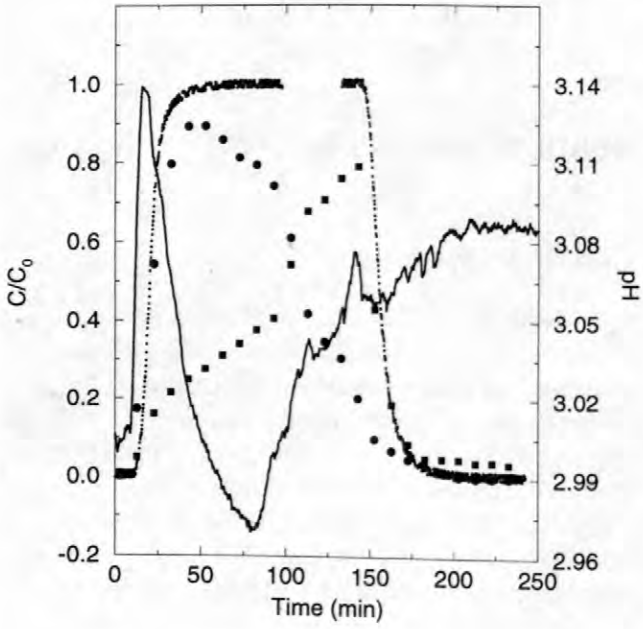

Figure 3. Breakthrough curves for flow-through reaction conducted at SSRL and tracer experiment conducted in the laboratory. The dots are the tracer data, the circles are the Mn(II) data, the squares are Fe_T data and the continuous line is the pH data. The Fe_T data was normalized to the influent Fe(II) concentration of 11 mM, and the Mn(II) data was normalized to a concentration of 5.5 mM as the stoichiometry of the reaction requires two Fe(II) to reduce one Mn(IV). The tracer was normalized to a conductivity of one.

The apparent early release of Mn(II) as compared to the tracer at 12 mins, as well as the early change in pH, was probably due to the siphoning action mentioned earlier. The effect of the siphoning would have decreased the pressure within the cell. This would lead to a smaller cell volume as the Kapton windows were drawn inward. This would decrease the total dead volume, and therefore the travel time from the control valve to the fraction collector would decrease. A decrease in the cell volume of 0.35 ml could explain the early release of Mn(II) and the early rise in pH. This would translate to a 25% decrease in the cell volume, not an unreasonable amount given the degree to which the Kapton tape can stretch.

The Fe(II)/Fe(III) in the effluent starts to increase slowly, and this increase coincides with both the deviation of the Mn(II) BTC from the tracer BTC and the start of the Fe(III) precipitation as noted by the decreasing pH. The overall Fe_T BTC mirrors that of the Mn(II) BTC, which is expected. The desorption portion of the Fe_T BTC, like the sorption portion of the Mn(II) BTC, occurs before the tracer BTC, and could be due to reduced cell volume. Significant tailing is noted after 160 minutes, and this is probably due to the desorption of Fe(II) and/or Fe(II) from the newly formed ferric precipitates. Fe(III) is slightly soluble at pH 3.

XANES Data

Figure 4 shows the series of spectra collected on the same cell described above. For visual comparison, the spectra have been normalized to a value of one for the absorption edge height. The absorption edge height, which is related to the overall Mn concentration, actually decreased from 2.52 to 0.30 absorption units (abritrary units) over the two hours the spectra were collected. This corresponds approximately to an one-order-of-magnitude decrease in total Mn concentration.

From figure 4, two trends can be noted. First is that the shoulder at 6554 eV increases as the experiment progresses. This is consistent with the release Mn(II) into the aqueous phase and the corresponding absorption maximum for an $MnSO_4$ solution at 6554 eV. The release of Mn(II) to the aqueous phase is known from the solution data.

The second notable feature in figure 4 is the shift in the position of maximum absorption to a lower energy as the reaction progresses. This would not be expected if the spectra were

composed only of our two known spectra, the starting Mn mineral (MnO_2), and the Mn(II) solution.

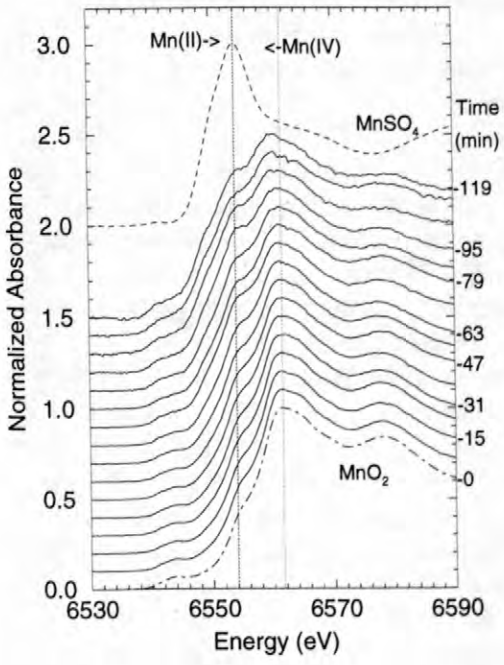

Figure 4. XANES spectra collected during the reductive dissolution of MnO_2 by Fe(II). The dot-dash line is the spectra of the original MnO_2 and the dashed line is the spectra of an $MnSO_4$ solution. For visual clarity, the spectra have all beenn normalized to an edge height of one, and the individual spectra have been shifted upward indicating a progression in time.

This suggests the presence of another Mn phase. An argument can be made that this phase could contain Mn(III). The shape of the XANES spectra is dependent on the valence of the element as well as on the short- and long-range order around the Mn atoms. Studies of XANES data indicate that the absorption edge (1st inflection point) and the 1s - 4p peak (energy of maximum absorption) of the transition metals shifts to a lower energy as the valence decreases (Wong and others, 1985; Qi-wu and Wong, 1984).

While the manganese minerals that we have studied exhibit a general decrease in absorption maxumum with lower oxidation state, the range of absorption maximum for a particular oxidation state is fairly wide. The ranges of absorption maximum for the the II, III and IV oxidation states overlap each other. The range of maximum absorption for Mn(III) and Mn(IV) oxides we have studied are 6557.7-6561.2 and 6560.2-6562.3 eV, respectively.

The absorption maxima shifted from 6561.6 to 6560.3 during the course of the experiment. This shift in the energy of maximum absorption could be due to either the formation of Mn(III) or the rearrangement of the Mn(IV) oxide structure. Fitting the reaction spectra with spectra of reference compounds (e.g., well-characterized Mn minerals) indicate the presence of an hausmannite-like phase is present during the reaction (Villinski and others, 1999)

CONCLUSIONS

We have demonstrated that the flow-through reaction cell constructed for use at SSRL is a valuable tool for studying complex geochemical reactions at the molecular level. This configuration not only allows for the identification of reaction intermediates, but also provides kinetic information of the formation and destruction of these reaction intermediates through the specstroscopic probing of the system *in situ* and in real time.

The one minor drawback of the system as designed is the fact that the cell is not rigid due to the use of Kapton tape for the window materials. This allows for the cell volume to change and thus the interpretation of effluent data is qualitative rather than quantitative. The use of a very thin window made of a low molecular weight material is necessary in order to maintain the low detection limit of the instrument due to absorption of the X-ray beam and the fluoresence signal by the window.

Various changes could be made to the cell design that would overcome this limitation. The windows of the cell could be made with either a thicker Kapton window (0.005") that was actually glued in place or with beryllium. The thicker Kapton window would decrease the incoming X-ray flux by approximately 15 % (from 96% transmission to 82 %), but would increase the rigidity of the window. A beryllium window

would obviate this loss of flux, with 96% transmission for a thickness of 0.005", similar to that of a Kapton window of 0.001" thickness, albeit with a higher cost.

This experimental approach yields information about complex geochemical systems that are not available from conventional bench-scale laboratory experiments. The coupling of information from these *in situ* real-time XAS experiments with conventional batch experiments can provide the improved formulation of reaction rate equations and lead to better predictions of the fate and transport of trace metals in aqueous environments.

ACKNOWLEDEMENTS

Funding for this research was provided by the National Institute of Environmental Health Sciences (grant ES04949) and the National Science Foundation (grant NSF-EAR-962-9276 to P.A. O'Day). Work done (partially) at SSRL which is operated by the Department of Energy, Office of Basic Energy Sciences. The SSRL Biotechnology Program is supported by the National Institutes of Health, National Center for Research Resources, Biomedical Technology Program, and by the Department of Energy, Office of Biological and Environmental Research.

Thanks is also given to Porex Technology for the donation of the porous UHMW polypropylene sheet that was used to make the bed supports for the flow cells.

REFERENCES

Brown, G.E. Jr., Calas, G., Waychunas, G.A., and Petiau, J. 1988, X-ray absorption spectroscopy and its applications in mineralogy and geochemistry, *in* Hawthorne, F.C., ed., Spectroscopic Methods in Mineralogy and Geology, Reviews in Mineralogy, v.18, p. 431-512.

Covington, A.K., Cressey, T., Lever, B.G., and Thirsk, H.R., 1962, Standard potential of the β-manganese dioxide electrode, Transactions of the Faraday Society, v. 50, p. 1975-1988.

Crowther, D.L., Dillard, J.G., and Murray, J.W., 1983, The mechanism of Co(II) oxidation on synthetic birnessite, Geochimica et Cosmochimica Acta, v. 47, p. 1399-1403.

Eychaner, J.H. and Stollenwerk, K.G., 1985, Neutralization of acidic ground water near Globe, Arizona, *in* Schmidt, K.D., ed., Groundwater Contamination and Reclamation, Proceedings of a symposium, Tucson, Arizona, 1985: Bethseda, MD, American Water Resources Association, p. 141-148.

Eychaner, J.H. 1991, The Globe, Arizona, research site -- Contaminants related to copper mining in a hydrologically integrated environment, *in* Mallard, G.E. and Aronson, D.A., eds., U.S. Geological Survey Toxic Substances Hydrology Program-- Proceedings of the technical meeting, Monterey, California, 1991, Water-Resources Investigations Report 91-4034, U.S. Geological Survey, Reston, VI, p. 439-447.

George, G., 1995, EXAFSPAK: A suite of computer programs for analysis of X-ray absorption spectra, SSRL, p. 63.

Giovanoli, R., Feitknecht, W. and Fischer, F., 1971, Reduktion von mangan(III)-manganat(IV) mit zimtalkohol, Helvetica Chimica Acta, v. 54, p. 1112-1124.

Hem, J., 1980, Redox coprecipitation mechanisms of manganese oxides, *in* Kavanaugh, M.C., and Leckie, J.O., Particulates in Water, Advances in Chemistry Series, American Chemical Society, Washington, D.C., v. 189, p. 45-72.

Jardine, P.M. and Taylor, D.L., 1995, Kinetics and mechanisms of Co-EDTA oxidation by pyrolusite, Geochimica et Cosmochimica Acta, v. 59, no. 20, p. 4193-4203.

Kozawa, A. and Yeager, J.F., 1965, The cathodic reduction mechanism of electrolytic manganese dioxide in alkaline electrolyte, Journal of the Electrochemical society, v. 112, no. 10, p.959-963.

Lind, C.J., and Stollenwerk, K.G., 1995, Alteration of alluvium of Pinal Creek, Arizona, by acidic ground water resulting from copper mining, *in* Morganwalp, D.W. and Aronson, D.A., eds., U.S. Geological Survey Toxic Substances Hydrology Program – Proceedings of the Technical Meeting, Colorado Springs, Colorado, September 20-

24, 1993. U.S. Geological Survey Water-Resources Investigations Report, 94-4015.

Lytle, F.W., Sandstrom, D.R., Marques, E.C., Wong, J., Spiro, C.L., Huffman, G.P., and Huggins, F.E., 1984, Measurement of soft x-ray absorption spectra with a fluorescent ion chamber detector, Nuclear Intruments and Methods in Phisics Research, v. 226, p. 542-548.

Nesbitt, H.W., Canning, G.W., and Bancroft, G.M., 1998, XPS study of reductive dissolution of 7 A-birnessite by H_3AsO_3, with constraints on reaction mechanism, Geochimica et Cosmochimica Acta, v. 62, no. 12, p. 2097-2110.

Perez-Benito, J.F., Arias, C. and Amat, E., 1996, A kinetic study of the reduction of colloidal manganese dioxide by oxalic acid, Journal of Colloid and Interface Science, v. 177, p. 288-297.

Qi-wu, W., and Wong, J., 1984, Mn valence and Mn-O bond length in $La_{0.7}A_{0.3}MnO_3$ perovskite catalysts (A = Ca, Sr, Ba, and Pb), *in* Hodgson, K.O., Hedman, B. and Penner-Hahn, J.E., eds., EXAFS and Near Edge Structure III: Proceedings of an international Conference, Stanford, CA, July 16-20, 1984, Springer Velag, New York, p. 202-205.

Stahl, R.S., and James, B.R., 1991, Zinc sorption by manganese-oxide-coated sand as a function of pH, Soil Science Society of America Journal, v. 55, p. 1291-1294.

Stollenwerk, K.G., 1994, Geochemical interactions between constituents in acidic groundwater and alluvium in an aquifer near Globe, Arizona, Applied Geochemistry, v. 9, p. 353-359.

Todd, K.T., 1980, Groundwater Hydrology, second edition, John Wiley and Sons, New York, p. 28.

Van Genuchten, M.Th. and Wierenga, P. J., 1976, Mass transfer studies in sorbing porous media, I, Analytical solutions, Journal of the Soil Science Society of America, v. 40, p. 473-480.

Villinski, J.E., O'Day, P.A. and Conklin, M.H., 2000, Evidence for step-wise reduction of MnO_2 by Fe(II): Results from an *in situ* real-time X-ray absorption spectroscopy experiment, in preparation.

Wong, J., Koch, E.F., Henja, C.I., and Garbauskas, M.F., 1985, Atomic and microstructural characterizations metal impurities in synthetic diamonds, Journal of Applied Physics, v. 58, p. 3388-3393.

AUTHOR INFORMATION

John E. Villinski (john@hwr.arizona.edu), Timothy L. Corely and Martha H. Conklin, The Department of Hydrology and Water Resources, The University of Arizona, Tucson, AZ, USA, 85721-0011.

Peggy A. O'Day, Geology Department, Arizona State University, Tempe, AZ, USA 85287-1404.

Partitioning of Trace Metals Between Contaminated Stream Waters and Manganese Oxide Minerals, Pinal Creek, Arizona

By Jill E. Best, Katherine E. Geiger, and Peggy A. O'Day

ABSTRACT

Copper mining activities near a perennial stream in central Arizona have produced high trace metal concentrations in addition to cobalt, copper, nickel, and zinc, in solution and ubiquitous precipitation of manganese oxide minerals as coatings on stream sediments. Analyses of coating samples at two sites along the stream indicate bulk manganese concentrations of 7.2 to 29.4 wt. %. At the upstream site (R2b), manganese minerals (identified by XRD) are primarily birnessite and rancieite with minor amounts of rhodochrosite, pyrolusite, cryptomelane, and franklinite. At a site ≈5 kilometers downstream (9272a), the manganese mineral assemblage is dominantly pyrolusite with smaller amounts of todorokite, birnessite, rhodochrosite, and kutnahorite. Maps of elemental distributions in coatings from site R2b (using SIMS and LA-ICP-MS) show strong correlations of cobalt to manganese and correlation of copper to both manganese and iron. Samples from site 9272a show that trace metal concentrations relative to total manganese are lower than at site R2b and that calcium and iron are associated with manganese. Trace metal distributions in samples from R2b and 9272a are attributed to cation substitutions in birnessite, rancieite, and todorokite. Activities of dissolved metals decrease downstream as pH increases and metals are removed by precipitation. Thermodynamic equilibrium between stream waters and end-member manganese oxides predicts mineralogical conversion from metastable birnessite and todorokite to stable pyrolusite, consistent with observations of the stream sediments. Manganese phases may persist metastably by substitution of trace metals into the mineral structure. Conversion to thermodynamically stable manganese oxide minerals may exclude trace metals and potentially remobilized them.

INTRODUCTION

Pinal Creek, located near Globe, Arizona, is a perennial stream which discharges into the Salt River, a major municipal Phoenix water source. It has suffered contamination from acid releases and copper mining activities over the past ~100 years (Figure 1). Waters from past waste disposal and acid leaching have seeped into the alluvial aquifer upgradient of Pinal Creek, creating a low-pH subsurface plume. Reaction of acidic waters with alluvial minerals results in acid neutralization, mineral dissolution, and release of metals to solution, primarily cobalt, copper, iron, manganese, nickel, and zinc. When the neutralized groundwater is discharged into the headwaters of Pinal Creek, manganese oxide minerals precipitate on detrital stream sediments. Previous studies have demonstrated that precipitation of manganese oxides and, to a lesser extent, iron oxide minerals control trace metal uptake and mobility (Hem and Lind, 1993; Lind and Hem, 1996; Lind and Stollenwerk, 1996).

This study compares the distribution and chemistry of manganese oxide minerals to the chemistry of the overlying stream water at two sites along the stream channel (Figure 1). The upstream site (R2b) is ≈2 km from the head of perennial stream flow. The second site is ≈5 km downstream from R2b just below Inspiration Dam, a small abandoned dam. At the time of sample collection at site R2b, recent floods had removed old crust and sediment material, and the manganese oxides present in the stream were thought to be relatively young (T. Corley, personal communication). In contrast, the sample collected at site 9272a appeared to be older, more cemented channel. Mineralogy, total chemical composition, and spatial distributions of elements within crust and coating particles were character-

ized for in sediment samples and separated manganese coatings. Due to the complex mineralogy and poor crystallinity of manganese oxide minerals in the sample, characterization using only bulk methods is difficult. In this study, we combine bulk and spatially-resolved analytical techniques to describe the mineralogy and chemistry of manganese oxide coatings. Changes in the aqueous composition of the contaminated stream waters between the two sampling sites are compared with changes in manganese oxide mineralogy and trace element concentrations. From these comparisons, we evaluate the thermodynamic stability of end-member manganese oxides and the partitioning of trace metal cations from aqueous solution into manganese mineral solid solutions.

METHODS

Sediment Samples

Analytical techniques used to characterize Pinal Creek sediment samples are summarized in Table 1. Bulk analyses were performed on the sediments and separated coatings to determine their mineral and chemical compositions. Powder X-ray diffraction (XRD), optical microscopy, and scanning electron microscopy with energy dispersive spectrometry (SEM-EDS) were used to determine the detrital mineralogy of stream sediments. X-ray diffraction of the clay size fraction (<2 mm) was used to identify the manganese minerals that coat and cement the stream sediments, although positive identification was complicated in some cases by significant interferences in the XRD patterns. Discrimination between peaks and background was set to 0.12, a value slightly greater than the 1/5 peak width at half its maximum intensity step size (0.02) (Moore and Reynolds, 1997). SEM maps for qualitative comparisons were collected with pixel resolutions of 2-6 mm and dwell times of 200 to 400 ms.

Elemental concentrations of bulk sediment, crust samples (<2 mm), and grain coatings separated by sonification (approximately <60 μm) were measured by inductively coupled plasma-atomic emission spectrometry (ICP-AES, performed by CHEMEX Labs in Sparks, NV). Man-

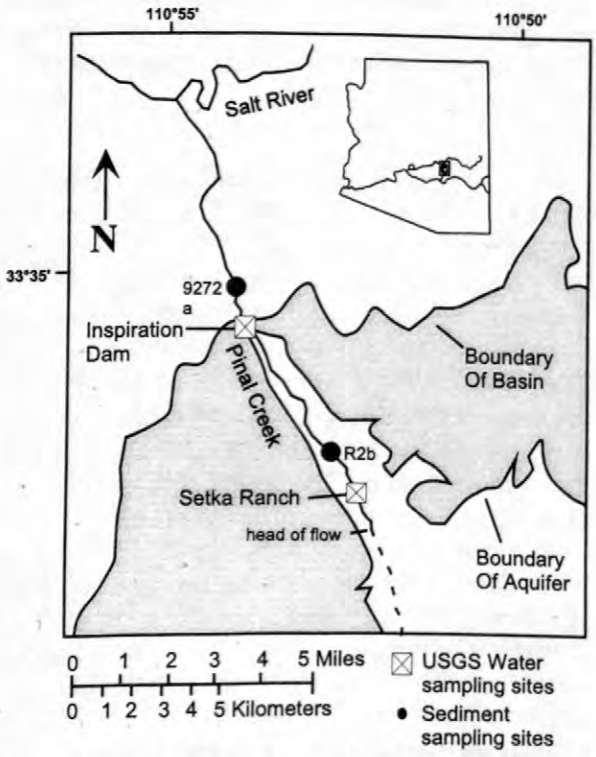

Figure 1. Location map of sediment and surface water sampling sites, Pinal Creek basin, Arizona.

Table 1. Description of sample analyses

Sample[1] Analyzed	Grain Size (μm to mm)	Analytical Method	Determination
R2b	bulk, <60, <2mm	XRD	mineral identification
9272a	125-250, <2mm		
R2b	bulk	SEM-EDS	distributions of elements Mn, Fe, Ca, Si, Al, and K
9272a	250-500		
R2b	bulk	SIMS[2]	trace element distribution in thick sections
9272a	250-500		
R2b	bulk	LA-ICP-MS[3]	trace element concentrations in Mn or Fe coatings (semi-quantitative)
9272a	250-500		
R2b	<1 mm, coating	ICP-AES	bulk elemental analysis (quantitative)
9272a	<2 mm, coating		

[1] Both samples were collected from the stream channel. R2b is unconsolidated sediment, and 9272a is a cemented manganese crust.

[2] trace elements: ^{55}Mn, ^{56}Fe, ^{40}Ca or ^{42}Ca, ^{28}Si, ^{59}Co, ^{60}Ni, ^{63}Cu, and ^{64}Zn

[3] trace elements: ^{55}Mn, ^{56}Fe, ^{44}Ca, ^{59}Co, ^{60}Ni, ^{63}Cu, and ^{66}Zn

ganese concentrations of coating samples exceeded the maximum detection limits of 5 wt. % for R2b and 10 wt. % for 9272a. Values of 7.2 wt. % for R2b and 29.4 wt. % manganese for 9272a were estimates from the measured concentrations of transition metals (excluding iron) to manganese in the <1 mm and <2 mm size fractions. Precision for ICP-AES analysis was ±5% of the mean value at a concentration 400 times the detection limit.

Spatial analyses by elemental mapping and point analyses of grain and coating cross-sections were used to correlate metal distributions to minerals identified by bulk XRD. Secondary ion mass spectrometry (SIMS) scanning ion imaging was used to map spatial distributions of the trace metals (cobalt, copper, nickel, and zinc) and major elements (manganese, iron, and calcium) within sediment coatings and manganese crust particles. Detection limits were parts per million or parts per billion and spatial resolution was approximately 10-20 μm. Count statistics for trace metals were typically one to five counts per pixel. These maps provided qualitative information on trace metal spatial distribution and relative concentration. Quantification of data was limited by the presence of complex mineral matrices, which prohibited the use of standards.

The same samples were analyzed by laser ablation-inductively coupled plasma-mass spectrometry (LA-ICP-MS) to determine the relative concentrations of trace metals. This technique used a focused UV laser with a spatial resolution of 10-50 μm to ablate selected areas of the manganese oxide coatings and crust particles. Ablated material is carried by argon gas to an electromagnetic sector mass spectrometer and quantitatively analyzed.

Because trace metal concentrations were near or below the detection limits of electron microprobe (typically < 0.1 wt. %), LA-ICP-MS was used instead for semi-quantitative analyses. However, the application of LA-ICP-MS to thin oxide coatings is subject to some limitations. For instance, the inability to use compositional standards that matched the sample complicated quantification and error analysis. For each spot ablated, three averaged mass spectra were collected. The resulting isotope counts were corrected for the background composition of the carrier gas. Counts were then converted to total elemental counts based on known isotopic abundances. Results were ratioed to the concentrations of manganese and iron. Comparisons of results for each ablation gave an average precision of ±25%. Spatial distributions of elements by SIMS and factor analysis of the LA-ICP-MS data (Reyment and others, 1993), were used to correlate trace metals to iron and/or manganese.

Water samples

Water samples from Setka Ranch and Inspiration Dam were collected and analyzed by the U.S. Geological Survey. Setka Ranch is 1.7 km upstream of R2b and Inspiration Dam is 0.5 km upstream of 9272a (Figure 1). Water sample analyses of 5/23/97 for R2b and 9/26/96 for 9272a

Table 2. Sample bulk mineralogy and Mn oxide mineralogy[1]

Sample	Major Minerals[2]	Minor Minerals	Manganese Mineral	Formula
R2b	Feldspar[3]	Illite	Birnessite	$(Ca,Na,K)(Mn^{4+},Mn^{3+})_2O_4 \cdot nH_2O$
	Quartz	Mica	Rancieite	$(Ca,Mn^{2+})_{2x}Mn^{4+}{}_{1-x}O_2 \cdot nH_2O$
		Chlorite	Rhodochrosite	$MnCO_3$
		Magnetite	Pyrolusite	βMnO_2
		Ilmenite	Cryptomelane	$K(Mn_8O_{16}) \cdot nH_2O$
9272a	Feldspar	Illite	Pyrolusite	βMnO_2
	Quartz	Mica	Todorokite	$Ca_x(Mn^{4+}{}_{1-x},Mn^{2+}{}_x)_6O_{12} \cdot nH_2O$
		Chlorite	Birnessite	$(Ca,Na,K)(Mn^{4+},Mn^{3+})_2O_4 \cdot nH_2O$
		Magnetite	Rhodochrosite	$MnCO_3$
		Hematite	Kutnahorite	$Ca,Mn^{2+}(CO_3)_2$
		Ilmenite		

[1] Minerals are listed in decreasing order of relative concentration.

[2] Major minerals are greater than 25% of the sample, minor minerals are less than 25%, and manganese minerals are likely less than 1%.

[3] Feldspar includes mostly plagioclase and lesser amounts of alkali-feldspar.

Table 3. Chemical analyses of samples R2b and 9272a.

Sample		Major Elements (wt. %)			Trace Elements (ppm)							
		Mn	Fe	Al	Mg	Ca	K	Co	Cu	Na	Zn	Ni
R2b	Coatings[1]	7.2[2]	3.67	2.38	9600	8600	4600	1300	990	700	660	310
	< 1 mm	0.5	7.21	1.03	4200	6300	2400	90	115	1100	110	35

Sample		Major Elements (wt. %)				Trace Elements (ppm)						
		Mn	Fe	Al	Ca	K	Mg	Co	Na	Cu	Zn	Ni
9272a	Coatings	29.4[2]	1.5	2.2	1.85	7000	5500	2500	2000	580	2300	1710
	< 2 mm	1.35	8.15	0.91	0.56	2400	3800	120	1300	115	165	75

[1] Coatings samples are fine-grained black material separated from bulk sediments by sonification.
[2] Manganese concentrations of coating samples exceeded maximum detection limits of 5-10 wt. %. Values reported are estimated from measured concentrations in the <1 mm and <2 mm size fractions.

were taken from Konieczki and Angeroth (1997) and Angeroth (personal communication, unpublished data, 1998) and correspond to dates of bulk sediment sample collection. Water samples were analyzed by methods reported in Konieczki and Angeroth (1997). Colloidal particles, which comprise most of the aqueous iron and very little manganese (Harvey and Fuller, 1998), were filtered out of the samples before chemical analyses. Measured aqueous concentrations were used in the geochemical modeling program EQ3 version 8.0 (Wolery, 1992, and Wolery, personal communication) to calculate activities of aqueous species. Ion activity coefficients were calculated with the Davies equation, which was chosen because the ionic strength is less than 0.5 molal (Nordstrom and Munoz, 1994).

RESULTS

Bulk sediments

Bulk sediments at both sites are composed mainly of plagioclase, and quartz grains, with minor amounts of potassium feldspar, mica, clays, and iron oxides (Table 2). Table 2 also shows the manganese minerals identified at each site and their stoichiometric formulas (Chukhrov, 1981; Kim, 1991; Waychunas, 1991; Gaines and others, 1997; Klein and Hurlbut, 1997). The <2 mm fraction of R2b contains approximately 50% silicates (quartz, feldspars, clay, and mica) and 50% oxides (approximately 80% birnessite + rancieite, 10% rhodochrosite, 8% pyrolusite + cryptomelane, and 2% franklinite). Mineralogy of 9272a bulk sediment <2 mm fraction is approximately 85% silicates (quartz, feldspars, clay, and mica) and 15% oxides (approximately 40% pyrolusite, 23% todorokite, 13% birnessite, 8% each rhodochrosite, kutnahorite, and hematite). These are observational percentages based on peak intensities of XRD patterns.

Concentrations of metals in bulk sediments (<1 and <2 mm fraction) compared to those in separated coatings (<60 μm fraction) showed that the coatings are enriched in transition metals by factors of 2.0 to 21.0 ±0.5 (Table 3). However, iron is not enriched in the <2 mm fraction of the bulk sample due to the presence of iron-bearing detrital minerals.

Spatially resolved images

In grains from sample R2b analyzed by SIMS imaging and LA-ICP-MS analysis, Manganese coatings show a distinct enrichment in cobalt (Figure 2). Iron is restricted to discrete layers within or beneath the thicker manganese coatings near grain boundaries. Copper, nickel, and zinc concentrations are elevated in the iron-rich layer. Spot analyses with LA-ICP-MS show association of cobalt with manganese in this sample, while copper shows a correlation to both manganese and iron (Tables 4 and 5). In contrast, nickel and zinc were not detected in manganese coatings with SIMS or LA-ICP-MS, and were lower in bulk concentrations in the coating fraction compared to cobalt and copper (Table 3).

The spatial and bulk analyses of sample 9272a coatings and crust particles show evidence for higher calcium and lower iron concentrations than in sample R2b. In 9272a, both calcium and iron are typically associated with manganese. However, localized areas of iron in EDS and

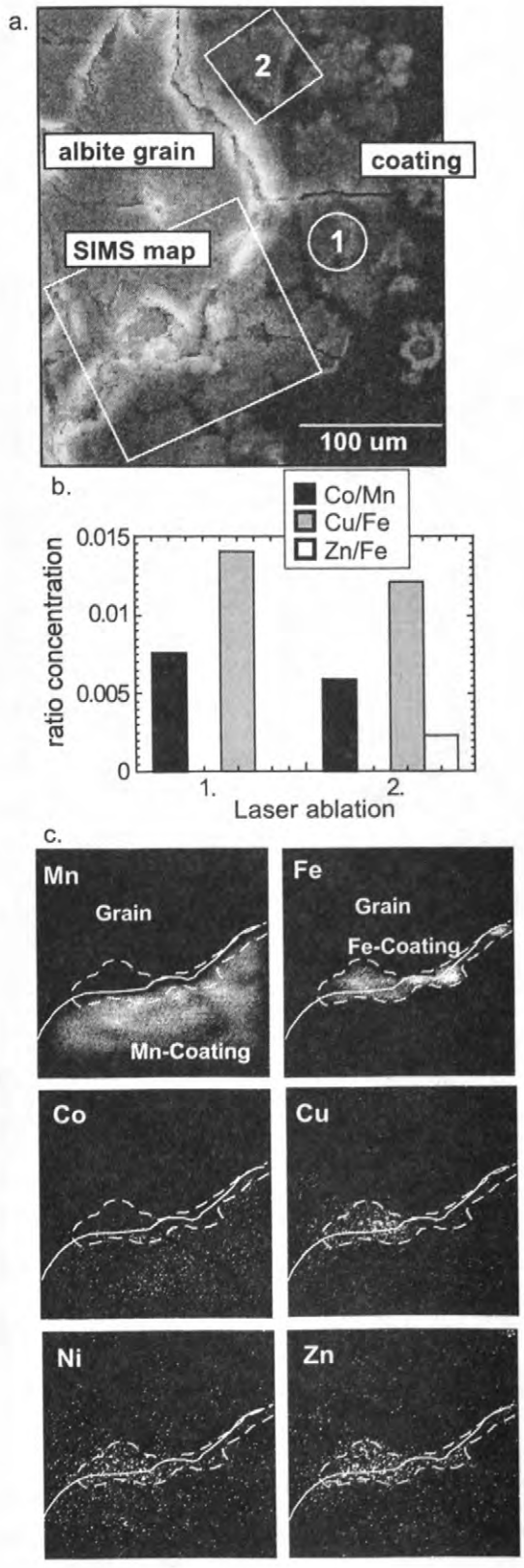

Figure 2. Spatial analysis of R2b sample coating. a. SEM secondary electron image of albite grain and coating cross-section. b. LA-ICP-MS relative concentrations. c. SIMS elemental maps.

SIMS dot maps did not correlate to manganese coatings or crusts, but to small (<20 μm) iron-bearing detrital silicate grains that were identified in SEM images. In comparison to sample R2b, SIMS maps and bulk analyses of 9272a coating samples showed higher metal concentrations in general, including more nickel and zinc. All trace metals, including iron, were fairly well associated to each other and to manganese, with some variability measured in zinc concentrations.

Results from XRD analyses of the <2 mm fraction and observations from SIMS and LA-ICP-MS suggest that at site R2b, birnessite is the primary manganese mineral that incorporates trace metals. At 9272a, trace metal substitution in todorokite appears to be important. Site-specific stoichiometric formulas were calculated for these two manganese minerals (Table 5) using ratios of metals to manganese measured by LA-ICP-MS. In order to minimize formula errors, laser ablation analyses were chosen that had low mean deviations (<±25%) and Fe/Mn ratios less than 0.5 to avoid measurements from iron oxides. These formulas provide a general representation of the amount of trace element substitution observed in these two minerals.

Aqueous chemistry

Significantly elevated concentrations of dissolved metals are discharged into the stream waters of Pinal Creek from the alluvial aquifer. In the upper reaches of the stream, dilution from non-

Table 4. SIMS imaging results. Trace metals are tabulated according to their associations with Mn and/or Fe.

Sample	Host Grain	SIMS Associations		
		Mn	Fe	Mn + Fe
R2b	albite[1]	Co	Cu, Zn, Ni	
	biotite	Co, Cu		
	plag[2]			Co, Cu
9272a[3]	plag/mica			Co, Ni, Zn, Ca
	plag[4]	Ca, Co, Ni, Zn		
	crust particle	Zn		Co, Ni, Ca

[1] Shown in Figure 2.
[2] Plag = plagioclase for this and the following table
[3] Copper was not measured with SIMS for this sample.
[4] Iron was below detection.

Table 5. Results of trace element correlations to manganese and iron by LA-ICP-MS analysis.

Sample	Host Grain	LA-ICP-MS[1]		Empirical Formula
		Mn	Fe	birnessite
R2b[2]	albite and biotite plag	Co, Cu Cu Ca	Cu	$Ca^{2+}_{0.078}((Mn^{4+}_{1.853}Mn^{3+}_{0.129})Co^{3+}_{0.014}Cu^{2+}_{0.004})O_4 \cdot nH_2O$
				todorokite[4]
9272a[3]	plag /mica and plag crust particle	Co, Cu, Zn Cu, Zn Cu, Zn	Zn Cu, Zn, Co, Ca	$Ca^{2+}_{0.13}(Mn^{4+}_{5.871}Fe^{2+}_{0.092}Co^{2+}_{0.029}Cu^{2+}_{0.005}Zn^{2+}_{0.002})O_{12} \cdot nH_2O$

[1] Nickel was excluded because of instrumental interferences.

[2] Cobalt was correlated to copper, relative to manganese.

[3] Cobalt was correlated to zinc, relative to manganese and iron.

[4] Formula based on LA-ICP-MS measurement of the plag/mica coating. The crust particle had a similar formula, but with slightly lower trace metals and calcium substitution.

Table 6. Aqueous concentrations, activities, and activity ratios of dissolved metal ions (sites R2b and 9272a).

Site[1]	Metal Ion	Aqueous Concentration[2] (mg/L)	$(aMe^{2+})^3$ $(x10^{-6})$	$(aMe^{2+})/(aMn^{2+})$
R2b		Setka Ranch		
	Mn2+	60.3	330	1
	Co2+	0.675	0.796	0.0024
	Ni2+	0.856	5.11	0.0154
	Cu2+	0.199	0.902	0.0027
	Zn2+	1.14	5.43	0.0164
	Ca2+	360	3170	9.6060
9272a		Inspiration Dam		
	Mn2+	42	218	1
	Co2+	0.2	0.00064	2.94E-06
	Ni2+	0.48	2.79	0.0128
	Cu2+	0.01	0.0053	2.43E-05
	Zn2+	0.31	1.36	0.00624
	Ca2+	410	3500	16.055

1. Sample collected and analyzed by USGS, 5/23/97 for R2b and 9/26/96 for 9272a.
2. Taken from Konieczki and Angeroth (1997) and Angeroth (personal communication, unpublished data, 1998).
3. Activities calculated with EQ3.

contaminated groundwater is minimal (Harvey and Fuller, 1998). As shown in Table 6, metal concentrations decrease downstream from site R2b to site 9272a, with the exception of nickel. This is consistent with precipitation of manganese minerals and removal of trace metals from solution (measured dissolved iron concentrations were generally near or below instrumental detection limits and not considered here). Calculated aqueous divalent ion activities are lower than measured total concentrations due to significant complexing in solution with sulfate. For example, the manganese sulfate aqueous complex ($MnSO_4(aq)$) has a higher activity than the free $Mn^{2+}(aq)$ ion.

In a general way, metal partitioning between aqueous and solid phases can be examined by comparing the activity ratios of metal ions ($aMe^{2+}(aq)$) and manganese ($aMn^{2+}(aq)$) in solution to bulk element ratios measured in the solid sediment coatings. In Figure 3, aqueous $(aMe^{2+})/(aMn^{2+})$ are compared to metal concentrations in coatings divided by either manganese

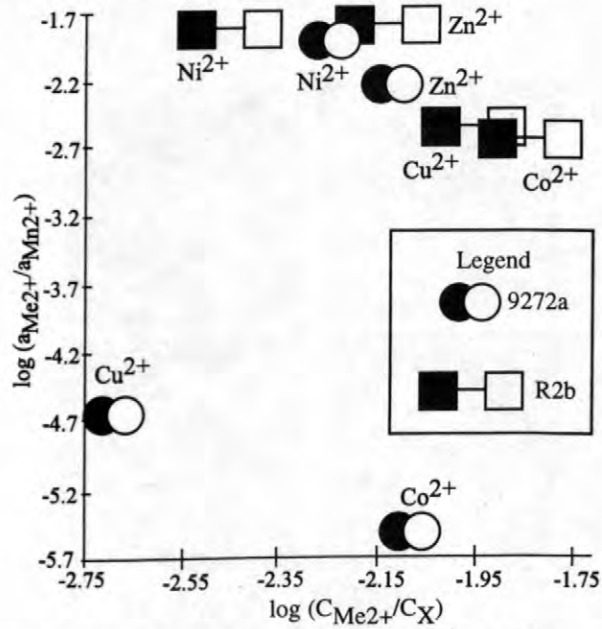

Figure 3. Log activity ratios of aqueous metal species ($a_{Me2+}(aq)$) to manganese ($a_{Mn2+}(aq)$) compared to log ratios of measured element concentrations ($c_{Me}(ppm)$) to concentration X [manganese ($c_{Mn}(ppm)$) or manganese + iron ($c_{Mn+cFe}(ppm)$)] in bulk coatings from sites R2b and 9272a (values from Table 6). Solid bar or circle: log $(c_{Me}/(c_{Mn+cFe}))$; open bar or circle: $(c_{Me})/(c_{Mn})$.

concentration or the manganese + iron concentration (Table 5). This comparison provides an approximate measure of whether or not iron minerals in the sediments are related to the partitioning of trace metals from solution compared to manganese minerals. In sample R2b, trace metal ratios shift to lower values when iron is included, compared to the shift for sample 9272a, indicating lower trace metal association with iron for R2b. Although all trace metal aqueous activities decrease downstream at site 9272a, Figure 3 shows significantly more depletion of Co^{2+} and Cu^{2+} compared to Ni^{2+} and Zn^{2+} when all metals are ratioed to aqueous manganese activity. For cobalt and copper, corresponding decreases in total metal concentrations are observed in the solid-phase manganese oxide coatings for 9272a.

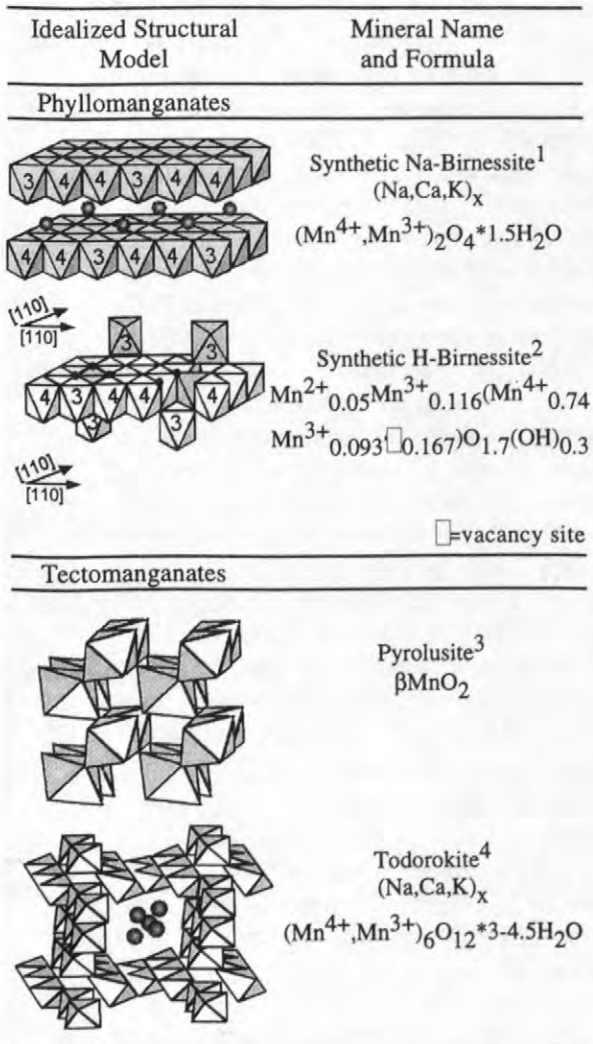

Figure 4. Crystal structures of birnessite, todorokite, and pyrolusite 1. Post and Bish, 1988. 2. Manceau and others, 1997. 3. Post and Veblen, 1990. 4. Baur, 1976.

DISCUSSION

Manganese oxide phases

From XRD, sample R2b manganese coatings are primarily composed of the 7Å-phyllomanganates birnessite and rancieite, which are efficient sinks for cobalt and copper. The major structural difference between these two oxides is that divalent calcium and manganese are the major cations in rancieite (Ca/Σ cations = 0.4-0.8), whereas these cations plus sodium, potassium, magnesium, and transition metals all occur in birnessite (Ca/Σ cations = 0.02-0.25) (Chukhrov and others, 1981). Higher concentrations of calcium (Ca^{2+} = 1.00 Å) in rancieite increase the lattice spacings relative to birnessite (Chukhrov and others, 1980).

Birnessite has a layered structure of MnO_6 octahedra with structural water and cations located in between the layers (Figure 6). Cobalt and copper substitute initially in the interlayers above and below octahedral vacancy sites (Burns and Burns, 1979; Manceau and others, 1997; Silvester and others, 1997). Copper remains sorbed to the interlayer while Co^{2+} interacts with Mn^{3+}, oxidizes to a more stable Co^{3+}, and then is incorporated into the vacant site (Manceau and others, 1997). Assuming birnessite is primarily responsible for trace metal uptake in sample R2b, its formula, based on LA-ICP-MS data and formulas from Drits and others (1998), is $Ca^{2+}_{0.078}\ Mn^{4+}_{1.853}\ Mn^{3+}_{0.129}\ Co^{3+}_{0.014}\ Cu^{2+}_{0.004}\ O_4 \bullet nH_2O$.

Sample 9272a manganese coatings contain mostly the tectomanganates pyrolusite and todorokite according to XRD data. The formula for todorokite calculated from LA-ICP-MS analyses of a crust particle is $Ca^{2+}_{0.13}\ (Mn^{4+}_{5.871}\ Fe^{2+}_{0.092}\ Co^{2+}_{0.029}\ Cu^{2+}_{0.005}\ Zn^{2+}_{0.002})\ O_{12} \bullet nH_2O$. This formula accounts for coupled substitution of calcium and trace metals, where molar calcium (based on charge balance) is within 1% of the measured concentrations. Pyrolusite, the major manganese oxide mineral in 9272a bulk sediments, is made up of single chains of MnO_6 edge-sharing octahedra (Burns and Burns, 1979). These octahedra have no vacancies or distortions and thus, direct

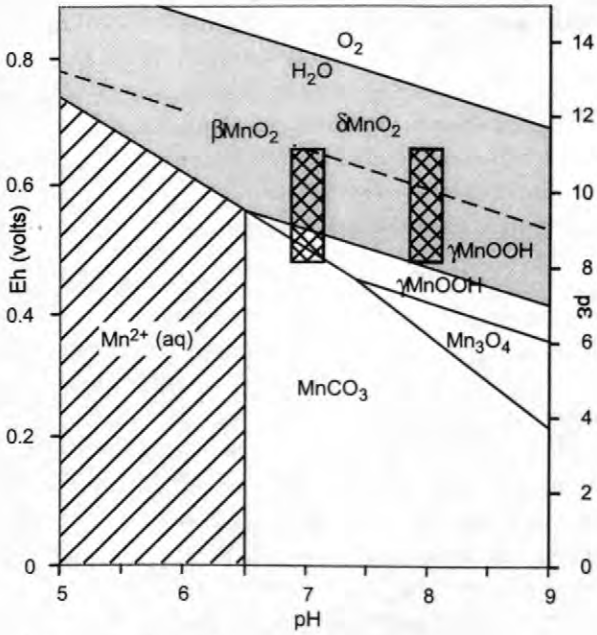

Figure 5. Eh-pH diagram of the Mn-C-H_2O system for 25°C, 1 atmosphere, log aMn^{2+}=-3.5 and log $aHCO_3^-$=-3.3. Stability fields are shown for dissolved Mn2+ and the ideal manganese end-member minerals, pyrolusite (βMnO_2-entire shaded field), manganite (γMnOOH), hausmannite (Mn_3O_4), and rhodochrosite ($MnCO_3$), and the metastable boundary of birnessite (δMnO_2)-manganite (dashed line).

substitution for tetravalent manganese is the only means of incorporating trace metals. In contrast, todorokite is a tunnel-structure manganese oxide, with 3x3 chains of MnO_6 octahedra (Post and Veblen, 1990). Substitution of divalent cations such as Co^{2+} and Cu^{2+} in Mn^{4+} octahedral sites requires stoichiometric charge balance by Ca^{2+} or other cations in the tunnel site. Element mapping by SIMS and LA-ICP-MS support the correlation of cobalt, copper, and calcium to manganese in 9272a sediments. Therefore, the conversion from the metastable oxides birnessite and todorokite, which tend to incorporate trace metals, to the thermodynamically stable phase pyrolusite, which tends to exclude substituting ions, may potentially release trace metals back to solution.

Aqueous chemistry

Equilibrium between stream waters and ideal manganese oxide minerals can be evaluated using the Eh-pH diagram shown in Figure 5. The stability fields for minerals were calculated using total manganese and bicarbonate activities from stream water measurements and thermodynamic data (Bricker, 1965; Wagman and others, 1982; Robie and Hemmingway, 1985). The ranges of pH and Eh for stream waters were constrained by surface water pH measured in the field (Konieczki and Angeroth, 1997) and by an estimation of Eh. Assuming that surface water is in equilibrium with atmospheric oxygen at 1 bar pressure overestimates the Eh, placing it above the stability limit for liquid water (Langmuir, 1997). A typical Eh range for mine waters and streams in contact with the atmosphere is approximately 0.45 to 0.70 volts (Krauskopf and Bird, 1995; Langmuir, 1997).

Using this range of Eh and a pH near 7 for site R2b (Fuller, personal communication, 1999), Pinal Creek water plots across several phase boundaries among rhodochrosite, metastable birnessite, and pyrolusite. The aqueous composition is consistent with metastable equilibrium between stream waters and the major manganese minerals identified by XRD in the sample coatings. On the other hand, at site 9272a with a pH near 8, the estimated range of aqueous Eh and pH falls primarily in the pyrolusite field. Pyrolusite was identified by XRD as the dominant manganese mineral at site 9272a and the Eh-pH diagram is consistent with the observed mineralogy. Hausmannite may exhibit some solid solution through the uptake of dissolved trace metals, making the placement of its stability lines more variable. Todorokite, which was also identified in sample 9272a, is poorly constrained thermodynamically because of its extensive solid solution and does not appear on Figure 5, but it is believed to be stabilized by cationic substitutions (Burns and Burns, 1979). Water samples are probably not completely in equilibrium with atmospheric carbon dioxide. If they were, then the stability field of $MnCO_3$ would expand in Eh and the predicted equilibrium mineral assemblage would be mostly rhodochrosite. Overall, the observed change in pH from site R2b to site 9272a is thermodynamically consistent with the observed conversion in mineralogy from metastable birnessite to stable pyrolusite, with the persistence of other metastable manganese phases such as todorokite and rhodochrosite.

Other correlations regarding the aqueous chemistry and bulk sediments can be made by comparing bulk sediment concentrations of metals (c_{Me}(ppm)) to manganese (c_{Mn}(ppm)) or manga-

nese + iron ($c_{Mn}+c_{Fe}$(ppm)) against the ionic radii (Shannon and Prewitt, 1969) of the metals (Me^{2+}/Mn^{4+}) (Figure 6). As the ionic size increases relative to Mn^{4+}, less substitution of divalent metals into vacant manganese sites in manganese oxide minerals is expected. At site R2b, this trend is observed with the exception of nickel, which shows depletion in the sediments. At site 9272a, sediment concentration ratios decrease linearly as the ionic ratio increases for cobalt, nickel, and copper, with zinc as the exception increasing in concentration. Valence electrons for zinc occupy a completely filled d^{10} orbital while cobalt, nickel, and copper are only partially filled. Because the d^{10} orbital is completely filled, the zinc radius decreases slightly (Hund's rule; e.g., Brown and others, 1997) and makes it more compatible substituting ion. The total manganese concentration is significantly higher in sample 9272a than in R2b (Table 3), but the ratio of trace metals to manganese is higher at R2b (Figure 6). This reflects the higher proportion of birnessite observed at R2b, which preferentially incorporates cobalt and copper, and the higher proportion of pyrolusite at 9272a with less trace metal substitution. The association of trace metals with both manganese and iron at 9272a noted in SIMS mapping is shown on a bulk scale in Figure 6 by the small variation in concentration ratios of elements relative to manganese or manganese + iron.

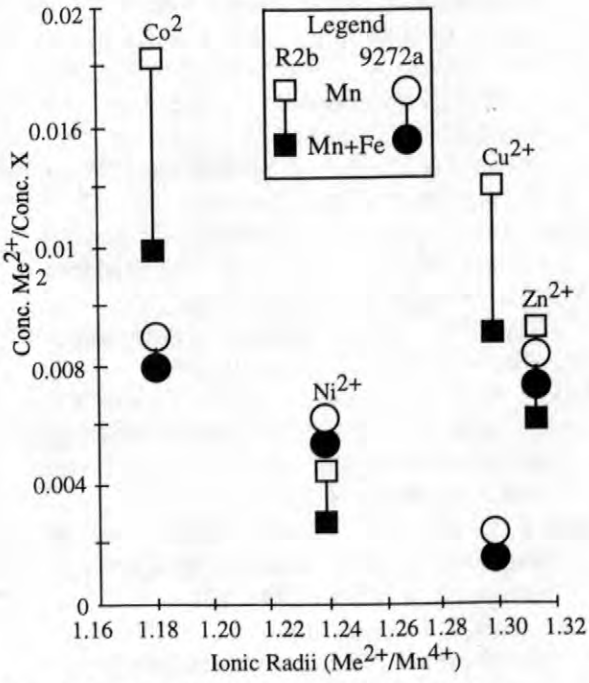

Figure 6. Measured element concentrations (c_{Me}(ppm)) relative to concentration X [manganese (c_{Mn}(ppm)) or manganese + iron ($c_{Mn}+c_{Fe}$(ppm))] in bulk coatings from sites R2b and 9272a compared to ionic radii ratios (Me^{2+}/Mn^{4+}) (values from Tables 3 and 6). Solid bar or circle: $(c_{Me}/(c_{Mn}+c_{Fe}))$; open bar or circle: $(c_{Me})/(c_{Mn})$.

CONCLUSIONS

In this study, we identified the primary manganese oxide mineral assemblages and evaluated trace metal distribution in sediments and sediment coatings at two sites along contaminated Pinal Creek (AZ). The manganese oxide mineralogy at site R2b is dominated by birnessite and rancieite, with minor amounts of rhodochrosite, pyrolusite, cryptomelane, and franklinite. Consideration of heterogeneous equilibrium between stream waters and manganese oxides indicates that this assemblage is metastable under the Eh-pH conditions of the sample. Elevated concentrations of the trace metals cobalt and copper are correlated to birnessite. At site 9272a, the mineral assemblage is dominated by pyrolusite, with lesser amounts of todorokite and birnessite, and carbonate minerals rhodochrosite and kutnahorite. Owing to the dominance of pyrolusite, structural trace metal substitution is more limited and substitution in todorokite is the primary means of incorporating trace metals. At this downstream site, higher pH and some association of trace metals with iron may suggest uptake of metals by both manganese and iron oxides, either by structural substitution or surface sorption. At both sites, the complex mixture of manganese oxides and trace metal substitutes presents a challenge for thermodynamic analysis using solid solutions of pure oxide end-members. However, this study points out the importance in natural systems of the slow conversion of metastable to stable phases in controlling the partitioning and distribution of trace metal contaminants. Although the initial precipitation of manganese oxides at Pinal Creek is known to be bacterially mediated (Harvey and Fuller, 1998), it is unclear whether or not the mineralogical aging is strictly abiotic. Metastable manganese phases may persist by the oxidation and/or subsequent incorporation of trace metals into vacant octahedral sites. Quantification of the maximum concentrations of metal substitution and knowledge of the rates of mineral conversion would aid in predicting the long term stability of

these phases. If it is not possible to stabilize a trace metal in a metastable mineral structure, then the trace element may be remobilized.

REFERENCES

Baur W. H., 1976, Rutile-type compounds. V. Refinement of MnO_2 and MgF_2 Acta Crystallographica, v. B32, p. 2200-2204.

Bricker, O.P., 1965, Some stability relations in the system Mn-O_2-H_2O at 25°C and one atmosphere total pressure: American Mineralogist, v. 50, p. 1296-1354.

Brown, T.L., LeMay, Jr., H.E., and Burnsten, B.E., 1997, Chemistry: The Central Science, 7th edition, New York, Prentice Hall, pp. 195-234.

Burns, R.G., and Burns, V.M., 1979, Manganese Oxides: Reviews in Mineralogy, v. 6, Mineralogical Society of America, Washington, p. 1-46.

Chukhrov, F.V., Gorshkov, A.I., Rudnitskaya, E.S., Beresovkskaya, V.V., and Sivtsov, A.V., 1980, Manganese Minerals in Clays: A Review: Clays and Clay Mineralogy, v. 28, no. 5, p. 346-354.

Chukhrov, F.V., Gorshkov, A.I., Svitsov, A.V., Berezovskaya, V.V., and Rudnitskaya, Ye.S., 1981, The nature of rancieite: International Geology Review, v. 23, no. 1, p. 115-124.

Drits, V.A., Lanson, B., Gorshkov, A.I., and Manceau, A., 1998, Substructure and superstructure of four-layer Ca-exchanged birnessite: American Mineralogist, v. 83, p. 97-118.

Gaines, R.V., Catherius, H., Skinner, W., Foord, E.E., Mauson, B., Kosenweig, A., 1997, Dana's New Mineralogy, 8th edition, New York, John Wiley & Sons, Inc.

Harvey, J.W., and Fuller, C.C., 1998, Effect of enhanced manganese oxidation in the hyporheic zone on basin-scale geochemical mass balance. Water Resour. Res. v. 34, p. 623-637.

Hem, J.D., and Lind, C.J., 1993, Manganese minerals and associated fine particulates in the streambed of Pinal Creek, Arizona, U.S.A.: a mining-related acid drainage problem, Applied Geochemistry, Vol. 8, p. 67-80.

Kim, S.J., 1991, New characterization of takanelite: American Mineralogist, v. 76, p. 1426-1430.

Klein, C., and Hurlbut, C.S., 1997, Manual of Mineralogy, 20th edition, Canada, John Wiley and Sons, Inc., p.596.

Konieczki, A.D., and Angeroth, C.E., 1997, Hydrologic data from the study of acidic contamination in the Miami Wash-Pinal Creek Area, Arizona, Water Years 1994-96: Tucson, U.S. Geological Survey , U.S. Geological Survey Open-File Report .

Krauskopf, K.B. and Bird, D.K., Introduction to Geochemistry, New York, McGraw-Hill, Inc., 1995, pp. 647.

Langmuir, D., 1997, Aqueous Environmental Geochemistry, New York, Prentise Hall, pp. 408-415.

Lind, C.J., and Hem, J.D., 1996, Manganese and iron oxide deposits and trace-metal associations in stream sediments, Pinal Creek Basin, Arizona, In J. G. Brown and B. Favor, eds., Hydrology and geochemistry of aquifer and stream contamination related to acidic water in Pinal Creek basin near Globe, Arizona, U.S. Geol. Surv. Water-Supply Paper, p. 81-103.

Lind C. J. and Stollenwerk K. G., 1996, Alteration of alluvium by acidic ground water resulting from copper mining at Pinal Creek, Arizona, U.S. Geological Survey Toxic Substances Hydrology Program--Proc. Tech. Meet., Colorado Springs, Colorado, September 20 1993-September 24 1993, U.S. Geol. Surv. Water Resour. Invest. Rept. 94-4015.

Manceau, A., Drits, V.A., Silvester, E., Bartoli, C., and Lanson, B., 1997, Structural Mechanism of Co(II) Oxidation by the Phyllomanganate, Na-buserite: American Mineralogist, v. 82, p. 1150-1175.

Moore, D.M. and Reynolds, Jr, R.C., 1997, X-Ray diffraction and the identification and analysis of clay minerals, 2nd ed., New York, Oxford University Press, p. 278.

Mucci, A., 1991, The solubility and free energy of formation of natural kutnahorite: Canadian Mineralogist, v. 29, p. 113-121.

Nordstrom, D.K., and Munoz, J.L., 1994, Geochemical Thermodynamics, Boston, Blackwell Publications, p. 493.

Post J. E. and Bish D. L., 1988, Rietveld refinement of the todorokite structure: American Mineralogist, v. 73, p. 861-869

Post, J.E., and Veblen, D.R., 1990, Crystal structure determinations of synthetic sodium, magnesium, and potassium birnessite using

TEM and the Rietveld method: American Mineralogist, v. 75, p. 477-489.

Reyment, R.A., Jöreskog, K.H., and Marcus, L.F., 1993, Applied factor analysis in the natural sciences, 2nd ed., New York, Cambridge University Press, p. 371.

Robie, R.A., and Hemmingway, B.S., 1985, Low temperature molar heat capacitites and entropies of MnO_2 (pyrolusite), Mn_3O_4 (hausmannite), and Mn_2O_3 (bixbyite), Journal of Chemical Thermodynamics, v. 17, p. 165-181.

Silvester, E., Manceau, A., and Drits, V.A., 1997, Structure of synthetic monoclinic Na-rich birnessite and hexagonal birnessite: II. Results from chemical studies and EXAFS spectroscopy. American Mineralogist, v. 82, p. 961-978.

Shannon, R., and Prewitt, C.T., 1969, Acta Crystallographica, v. B25, p. 925.

Wagman, D.D., Evans, W.H., Parker, V.B., Schumm, R.H., Halow, I., Bailey, S.M., Churney, K.L., and Nutall, R.L., 1982, The NBS tables of chemical thermodynamic properties, Journal of Physical Chemistry Reference Data, v. 11, Supplement 2.

Waychunas, G., 1991, Reviews in Mineralogy: Oxide Minerals, vol. 25, MSA, pp.11-61.

Wolery, T.J., 1992, EQ3NR, A computer program for geochemical aqueous speciation-solubility calculations: theoretical manual and user's guide, Lawrence Livermore National Lab, p. 246.

Representative Plant and Algal Uptake of Metals near Globe, Arizona

By Justin C. Marble, Timothy L. Corley, and Martha H. Conklin

ABSTRACT

Past acid-mining activities in the Globe-Miami, Arizona area have resulted in the release of metal contaminants into the perennial reach of Pinal Creek. Dissolved manganese (Mn(II)) is the dominant metal with lower concentrations of dissolved zinc (Zn(II)), nickel (Ni(II)), copper (Cu(II)), iron (Fe(II,III)), and cobalt (Co(II)). In this study, uptake of metals by plants along the perennial reach of Pinal Creek was measured. Specifically, water speedwell (Veronica anagallis-aquatica), rabbitfoot grass (Polypogon monspeliensis (L.) Desf.), duckweed (Lemna minor), and algae (Microcystis, Vaucheria, and Oocystis) and moss were collected, digested, and analyzed for total Mn, Zn, Ni, Cu, Fe, and Co to determine the extent of bioaccumulation. Results indicate that bioaccumulation of these metals is occurring along the perennial reach of Pinal Creek with bioconcentration factors of 100 to over 10,000 depending upon the plant and the location along the reach. Comparisons with data from Pinto Creek, a nearby perennial creek with significantly lower metal concentrations, indicate that the bioconcentration factors are similar, but the mass of metals present in the aquatic plants at Pinal Creek is significantly higher.

INTRODUCTION

Dissolved Mn is an essential element for higher plant systems and is involved in photosynthesis (the Hill reaction) and activation of different enzyme systems (e.g., superoxide dismutase production) (Mukhopadhyay and Sharma, 1991). Critical deficiency levels of Mn(II) range between 0.01-0.02 microgram Mn per gram (μg Mn(II) g^{-1}) dry weight in dry mature leaves but vary tremendously between plants (Mukhopadhyay and Sharma, 1991). Vascular plants and algae also require certain amounts of other trace metals for normal plant growth (Zn, Ni, Cu, Fe, Co, Ca, and Mg).

Although Mn(II) supplements can increase growth yields of plants, large amounts of Mn(II) can interfere with the uptake of other trace metals (Mukhopadhyay and Sharma, 1991). In addition, excess concentrations of Zn, Ni, Cu, Fe, and Co can trigger an inherent defense mechanism that plants have developed that involves production of phytochelatins—polypeptides that bind metals (Ahner and others, 1995). Phytochelatin production in response to high metal levels has been identified in land plants, vascular aquatic plants, fungi, and marine and freshwater algae. This mechanism results in an accumulation of the excess metals within the plants with the final metal concentration often being significantly higher than found in water supplied to the plants.

The work reported in this paper focuses on bioaccumulation of metals by aquatic plants, algae, and moss in Pinal Creek, an Arizona State Superfund site, near Globe, Arizona, that has been contaminated by acid-mining activities in the area. The primary purposes of this study were to determine the extent to which metals were taken up by the diverse plant community at Pinal Creek and to determine which plants were particularly effective at bioaccumulation of metals. To further aid in our assessment of the potential role of plants as a sink for metal contaminants in Pinal

Creek, comparisons of metals uptake were made with other measurements reported for similar plants in Pinto Creek, also near Globe, Arizona.

SITE DESCRIPTIONS

Pinal Creek

The Pinal Creek Basin is a 504 km^2 drainage area with general surface flow direction to the north from the Pinal Mountains towards the Salt River (Figure 1) (Neaville and Brown, 1993).

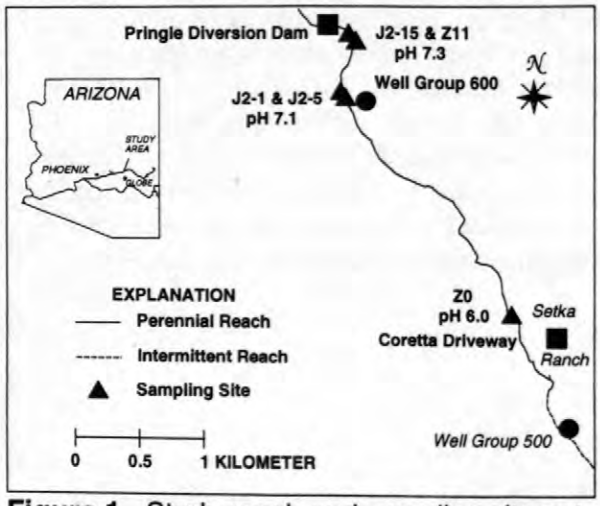

Figure 1. Study reach and sampling sites at Pinal Creek. Median pH values are shown for the study period.

Most of Pinal Creek is ephemeral during the year with flows occurring during snow runoff (December and January) or summer thunderstorms (June, July, and August) (Neaville and Brown, 1993). However, a northern portion of the Pinal Creek Basin is perennial and extends approximately 13 kilometers (km) from the head of flow to its confluence with the Salt River. The upper 3-km length of the reach from the Coretta Driveway to Pringle Diversion Dam is the section of the reach included in our studies (see Figure 1).

Past mining in the Globe-Miami area created large piles of tailings and waste rock that eventually formed a barrier across Webster Gulch. Webster Lake, which has been drained, was formed from the liquid waste from the mining operations (Brown and Favor, 1996). Contaminated, acidic water originating from several sources including the former Webster Lake now travels through the alluvial material into the perennial reach of Pinal Creek Basin. Dissolved Mn levels in Pinal Creek have reached as high as 100 milligram per liter (mg L^{-1}) near the head of flow, but during the period of this study Mn(II) concentrations in the surface water ranged from 70 to 40 mg L^{-1} over the length of the study reach. Table 1 lists water quality data at the beginning of our study reach, values which essentially remained constant over the course of the work (November, 1996 through June, 1997).

The spatial variation in Mn(II) along the study reach is a function of groundwater inflow and mixing with surface water in the hyporheic zone, of microbial removal processes occurring within the streambed sediments at local values of pH and dissolved oxygen (O_2) (Harvey and Fuller, 1998; Marble and others, 1999), and of plant uptake. Although natural attenuation of Mn(II) and other trace metals due to microbial processes has been the subject of other research, the role of plants in attenuation of metal contaminants in Pinal Creek has not been previously considered.

Table 1. Physical and Chemical Values for Pinal Creek (Z0 on January 25, 1995) and Pinto Creek (near Miami, Arizona, on June 18, 1997, USGS). (mg L^{-1} except for pH which is in standard pH units).

	Pinal	Pinto
Parameter	Value	Value
pH	6.4	7.8
Oxygen	6.9	9.0
Alkalinity[1]	51	180
TDS	2,640	531
Co(II)	0.410	0.003
Cu(II)	0.050	0.010
Fe(II)	<0.130	0.0053
Mn(II)	72.0	0.0038
Ni(II)	0.790	0.010
Zn(II)	0.500	0.0060

[1] As $CaCO_3$.

Pinto Creek

Pinto Creek is a northerly flowing stream starting in the Pinal Mountains and is dependent upon runoff from snow, rain, and small springs. It is a 48 to 56 km long stream and is made up of ephemeral, intermittent, and perennial stretches

(Lewis and Burraychak, 1979). Pinto Creek has two stream gages maintained by the U. S. Geological Survey, one near Haunted Canyon and the other near Miami; flows at these two stations are typically different Pinto Creek was also contaminated by mining activities in the area (Lewis and Burraychak, 1979), but remediation efforts were successful and returned this system to its current state of low metals concentrations. Table 1 also lists chemical and physical parameters for a perennial section of Pinto Creek. As is apparent, the metals concentrations are significantly lower than those reported for Pinal Creek, but values of other physical and chemical parameters fall within the ranges reported for Pinal Creek. Pinto Creek also has a wide variety of aquatic vegetation including cattail, water speedwell, water cress, pondweed, rush, monkey flower, various algae (Microcystis, Vaucheria, and Oocystis)(Lewis and Burraychak, 1979), similar to plant types and algae found in Pinal Creek.

METHODOLOGY

Plant grab samples were collected from several locations and rinsed with creek water to remove insects and loosely attached sediment material. At Pinal Creek, plant samples were collected from sites Z0, J^2-1, J^2-5, J^2-15, and Z11 (Figure 1). At Pinto Creek, grab samples were collected from USGS stream gaging sites 09498501 (below Haunted Canyon near Miami, Arizona) and 09498502 (Pinto Creek near Miami, Arizona).

After rinsing with creek water, the plant samples were placed in plastic bags and put into a cooler. Upon arrival at the laboratory, samples were dried at 60°C for 24 hours. Dried samples were ground and sieved, then digested with nitric acid (HNO_3). Digested plant samples were analyzed by flame or graphite atomic absorption spectroscopy (FAAS or GFAAS) for different metal concentrations. Results are reported as concentration ratios and bioaccumulation. Plant bioaccumulation is reported as mg of metal per kg of dried plant material (mg kg^{-1}) and the concentration ratio is the ratio of metal found in the plant material (mg kg^{-1}) to the metal concentration found in the creek water (mg L^{-1}). The values reported represent the average of 2 subsamples with the maximum and minimum values measured being within ±2 percent of the average value.

RESULTS

The aquatic plant species found at Pinal Creek varied in type and density depending upon the time of year and the location. Before plant sampling started in 1996, water speedwell and rabbitfoot grass dominated the upstream portion of Pinal Creek (J^2-1) and algae dominated in the downstream section (J^2-15). However, over the study period (November, 1996 through June, 1997), water speedwell, rabbitfoot grass, and algae were found along the entire study reach. Duckweed was less widely distributed and was typically only found in slow moving or stagnant water near the banks of the creek.

Water speedwell from Pinal Creek was collected from several field locations (Z0, J^2-1, and J^2-15) over a period of 8 months and analyzed for Mn(II) (Table 2). Site J^2-1 consistently had lower bioaccumulation than the downstream site J^2-15; approximately 30 percent that of J^2-15 in November, 1997, and increasing to 63 percent that of J^2-15 in April, 1998. There is no obvious correlation between sampling date and bioaccumulation of Mn at either site.

Mn(II) concentrations in Pinal Creek were lower at the downstream site (Table 2) due to dilution and natural attenuation caused by biogeochemical reactions and plant uptake (an overall loss of 10-20 percent of the entering Mn(II) has been attributed to non-dilution processes, Harvey and Fuller, 1998). Bioaccumulation values for water speedwell were greater downstream compared to upstream sites (Table 2). Since tracer studies were not conducted when the plant samples were collected, nothing definitive can be said regarding the temporal changes in Mn(II) levels determined at both sites.

A subset of the water speedwell samples from sites J^2-1 and J^2-15 were analyzed for other trace metals (Table 3). No trend with location was observed for concentrations of Fe, but Zn and Ni were higher at J^2-15 than at J^2-1 and Cu was higher at J^2-1 than at J^2-15 . Bioaccumulation of

Mn and Co exhibited consistently higher bioaccumulation at J²-15 compared to J²-1, about a factor of 2 difference.

Rabbitfoot grass samples from J²-1 and J²-15 were also analyzed for Mn, Zn, Ni, Co, and Fe (Table 4). Both upstream and downstream sampling sites had similar bioaccumulation values for Zn and Ni, but Mn, Cu, Co, and Fe values were larger at site J²-1 than J²-15. A factor of about 2 between values at J²-1 and J²-15was observed for Mn, Co, and Cu, and a factor of about 10 for Fe. Bioaccumulation of Mn at both sites was also greater than the other metals.

Table 2. Bioaccumulation by water speedwell and surface water concentrations of Mn in Pinal Creek (units are mg kg^{-1} for plant uptake and mg L^{-1} for surface water).

	Plant Concentration			Surface Water	
Date	Z0	J²-1	J²-15	J²-1	J²-15
11/15/96	6380	6610	23000	50.3	40.5
12/13/96		6450	18600	52.7	45.0
1/31/97		7990	16400	49.1	42.3
3/14/97		4600	8570	55.5	49.9
4/25/97		6190	9760	50.8	45.1
6/25/97		3870		52.0	
Average	6380	5950	15300	51.7	44.6
Standard deviation		1490	6070	2.24	3.56

Table 3. Water speedwell bioaccumulation from Pinal Creek collected on December 1996 and January 1997 for Mn, Zn, Ni, Cu, Co, and Fe (units are mg kg^{-1}).

Metal	Date	J²-1	J²-15
Mn	12/13/96	6450	18600
Mn	1/31/97	7990	16400
Fe	12/13/96	4400	1880
Fe	1/31/97	2520	2670
Ni	12/13/96	109	151
Ni	1/31/97	148	182
Cu	12/13/96	901	824
Cu	1/31/97	1750	1130
Co	12/13/96	80.5	158
Co	1/31/97	134	279
Zn	12/13/96	516	665
Zn	1/31/97	772	801

Duckweed was found in Pinal Creek during the summer months and the early fall at sites with zones of slow moving or stagnant water. A sample was collected from site J²-5 on June 25, 1997 (surface water pH 7.1; Mn(II) concentration, 47.0 mg L^{-1}). The bioaccumulation value was 10760 mg kg^{-1} and the concentration ratio was 229 (mg kg^{-1})/(mg L^{-1}).

Algae is prolific at both Pinal Creek and Pinto Creek and grab samples included the species Microcystis, Vaucheria, and Oocystis. Samples were collected from both creeks to compare bioaccumulation and the concentration ratio for Mn (Table 5). Although Pinal Creek samples had more bioaccumulation, Pinto Creek samples had larger concentration ratios.

Table 4. Rabbitfoot grass bioaccumulation in samples from Pinal Creek collected on January 31, 1997 (units are mg kg^{-1}).

Metal	J²-1	J²-15
Mn	13600	5240
Fe	6890	691
Cu	1640	828
Ni	163	161
Co	237	130
Zn	581	534

Table 5. Algae samples from Pinal Creek and Pinto Creek : bioaccumulation and concentration ratio for Mn (mg kg^{-1} for bioaccumulation and (mg kg^{-1})/(mg L^{-1}) for concentration ratio).

Site	Date	Mn	Concentration ratio
Pinal, Z11	7/17/96	49700	996
Pinal, Z11	11/15/96	90200	1810
Pinal, J²-15	12/12/96	5550	1110
Pinal, J²-15	1/31/97	79300	1590
Pinto, Miami	6/18/97	240	29800
Pinto, Miami	6/18/97	1460	181000

Water speedwell collected from Pinto Creek also had larger concentration ratios for Mn than samples collected from Pinal Creek (Table 6). However, the bioaccumulation of Mn was again greater in Pinal Creek samples: 3870 mg

kg^{-1} for the Pinal Creek sample; 47, 97, and 505 mg kg^{-1} for the Pinto Creek samples.

Table 6. Water speedwell concentration ratio ((mg kg^{-1})/(mg L^{-1})) comparison between Pinal Creek and Pinto Creek.

Site	Date	Concentration Ratio
Pinal, J^2-1	6/25/97	74.5
Pinto, Haunted	6/18/97	133000
Canyon	6/18/97	25400
Pinto, Miami	6/18/97	12400

DISCUSSION

All of the plants analyzed exhibited bioaccumulation of metals, whether the samples were collected from Pinal or Pinto Creek. Water speedwell from Pinal Creek and Pinto Creek had high levels of Mn, as well as significant concentrations of the other metals considered in this study. Mn bioaccumulation and Mn(II) stream concentrations were basically the same over the sampling period at both the upstream (J^2-1) and downstream (J^2-15) sites (Tables 2). These bioaccumulation levels for Mn are similar to those measured for another type of water speedwell (Veronica americana) (Muztar and others, 1978) and to measurements reported for other aquatic plants (Kadukin and others, 1982; Albers and Camardese, 1993). Bioaccumulation by water speedwell of the other metals also occurred but to a slightly lesser degree than for Mn (Table 3).

Rabbitfoot grass had similar bioaccumulation levels of metals as measured for water speedwell. Bioaccumulation of Mn by duckweed was of the same order-of-magnitude as observed for water speedwell and rabbitfoot grass, but bioaccumulation of Mn by algae was an order-of-magnitude greater than any of the plants analyzed. These differences in metals uptake may reflect different uptake mechanisms and/or be due to the age of a plant or algal community and the length of time it has been exposed to metals contaminated water.

Duckweed collected from site J^2-5 at Pinal Creek had a significantly larger concentration ratio for Mn than reported by Frick (1985) for duckweed at a similar Mn(II) level (see Table 7). In addition, the bioaccumulation values measured by Frick were significantly lower than at Pinal Creek: 3.9, 129, 192, and 220 mg kg^{-1} for the lowest to highest Mn(II) values used by Frick versus 10760 mg kg^{-1} at Pinal Creek. The differences between the values for bioaccumulation and the concentration ratio at approximately the same concentration (47 mg L^{-1} in Pinal Creek versus 55 in Frick's work) suggests that concentration of Mn(II) is not the only variable that determines uptake by aquatic plants at Pinal Creek. Nutrients and other dissolved species (e.g., Mg^{+} and Ca^{2+}) present in Pinal Creek at different levels than in the laboratory experiments may explain part of this difference in bioaccumulation. However, a more likely explanation is that one, or more, of the other dissolved metals present in Pinal Creek (Zn(II), Ni(II), Cu(II), Co(II), and Fe(II,III)) has a synergistic effect that results in a greater bioaccumulation of Mn(II) by duckweed in the field situation than observed by Frick (1985).

Table 7. Comparison data for duckweed concentration ratios at Pinal Creek (mg L^{-1} for surface water and (mg kg^{-1})/(mg L^{-1}) for concentration ratio).

Source/Site	Mn(II))	Concentration Ratio
Frick, 1985	54.9	4.02
Frick, 1985	27.5	6.98
Frick, 1985	13.7	9.93
Frick, 1985	0.0560	69.6
J^2-5, 6/25/97	47.0	229

Mn uptake by water speedwell has been reported by Muztar and others (1978), although the species they used was Veronica americana and not Veronica anagallis-aquatica, the species identified in Pinal Creek. The concentration ratios for the Pinal Creek water speedwell samples were lower than determined by these researchers (Table 8), but the bioaccumulation was an order-of-magnitude greater in the Pinal Creek plants (3870 and 4040 mg kg^{-1} for Pinal Creek versus 315 to 370 mg kg^{-1}). Since the Mn(II) concentration in Muztar's studies was 3 orders-of-magnitude lower than the Mn(II) concentration in Pinal Creek (Table 8), the lower concentration ratio for Pinal Creek may be an

indication of a capacity limitation and/or a toxic affect at the higher Mn(II) concentrations in Pinal Creek.

Table 8. Comparison data for water speedwell (Veronica anagallis-aquatica) from J^2-1 to Veronica americana concentration ratios (mg L^{-1} for surface water and (mg kg^{-1})/(mg L^{-1}) for concentration ratio).

Source	Mn(II)	Concentration Ratio
Muztar and others, 1978, washed	0.043	7330
Muztar and others, 1978, unwashed	0.043	8600
J^2-1, 6/25/97, rinsed	52.0	74.5
J^2-1, 6/25/97, not rinsed	52.0	77.7

Data from Pinto and Pinal Creek show that both sites have algal bioaccumulation of Mn. For algae, the concentration ratio at Pinal Creek is lower than Pinto Creek although Mn(II) creek concentrations are greater at Pinal Creek (Table 5). These differences in concentration ratios again suggest that at Pinal Creek the plant capacity for metal uptake may have been reached and/or that a toxicity effect is responsible for the differences between the algal samples from these two creeks. The same trend is also exhibited by water speedwell (Table 6).

CONCLUSIONS

These studies indicate that water speedwell, rabbitfoot grass, and algae bioaccumulate Mn. Zinc, Ni, Co, Cu, and Fe were shown to also bioaccumulate in water speedwell and rabbitfoot grass. Water speedwell and other aquatic plants are prolific in Pinal Creek and could play a significant role in determining the fate of metal contaminants entering the stream. Additional data concerning the total biomass in the system, and the potential release of metals as plants die and decay, are required to assess the potential and actual contribution of plants to total metals removal in this system.

Acknowledgements. This publication was made possible by grant number P42 ESO4940 from the National Institute of Environmental Health Science with funding provided by EPA and by grant number EAR-95-23881 from the NSF. Its contents are solely the responsibility of the authors and do not necessarily represent the official views of the NIEHS, NIH, or EPA, or NSF.

REFERENCES

Ahner, B. A., Kong, S., and Morel, F. M. M., 1995. Phytochelatin production in marine algae. 1. An interspecies comparison, Limnology and Oceanography. 40: 649-657.

Albers, P. H. and Camardese, M. B., 1993. Effects of Acidification on Metal Accumulation by Aquatic Plants and Invertebrates. 1. Constructed Wetlands, Environmental Toxicology and Chemistry. 12: 959-967.

Brown, J. G. and Favor B., 1996. Hydrology and Geochemistry of Aquifer and Stream Contamination Related to Acidic Water in Pinal Creek Basin Near Globe, Arizona, Water-Supply Paper 2466, U. S. Geological Survey.

Frick, H., 1985. Micronutrient Tolerance and Accumulation in the Duckweed, Lemna, Journal of Plant Nutrition. 8: 1131-1145.

Harvey, J.W., Fuller, C.C., 1998, Effect of enhanced manganese oxidation in the hyporheic zone on basin-scale geochemical mass balance: Water Resources Research, v. 34, p. 623-636.

Kadukin, A. I., Krasintseva, V. V., Romanova, G. I., and Tarasenko, L. V., 1982. Concentration of Iron, Manganese, Zinc, Copper and Chromium in Some Aquatic Plants, Hydrobiological Journal. 18: 64-67.

Konieczki, A. D. and Angeroth, C. E., 1997. Hydrologic Data from the Study of Acidic Contamination in the Miami Wash—Pinal Creek Area, Arizona, Water Years 1994-96, Open-File Report 97—247, U.S. Geological Survey.

Lewis, M. A. and Burraychak, R., 1979. Impact of Copper Mining on a Desert Intermittent Stream in Central Arizona: A Summary, Journal of the Arizona-Nevada Academy of Science. 14:22-29.

Marble, J. C., 1998. Biotic Contributions of Mn(II) Removal at Pinal Creek, Globe, Arizona: The University of Arizona, Department of Hydrology and Water Resources, unpublished M.S. thesis, 191p.

Marble, J.C., Corley, T.L., Conklin, M.H., and Fuller, C.C., 1999, Environmental Factors Affecting Oxidation of Manganese in Pinal Creek, Morganwalp, D.W., and Buxton, H.T., U.S. Geological Survey Toxic Substances Hydrology Program—Proceedings of the Technical Meeting, Charleston, South Carolina, March 8-12, 1999—Volume 2—Contamination of Hydrologic Systems and Related Ecosystems: U.S. Geological Survey Water-Resources Investigations Report 99-4018B, this volume.

Mukhopadhyay, M. J. and Sharma, A., 1991. Manganese in Cell Metabolism of Higher Plants, The Botanical Review. 57: 117-149.

Muztar, A. J., Slinger, S. J., and Burton, J. H., 1978. Chemical Composition of Aquatic Macrophytes. III. Mineral Composition of Freshwater Macrophytes and Their Potential for Mineral Nutrient Removal from Lake Water, Canadian Journal of Plant Science. 58: 851-862.

Neaville, C. C. and Brown, J. G., 1993. Hydrogeology and Hydrologic System of Pinal Creek Basin, Gila County, Arizona, Water-resources Investigation Report 93-4212, U. S. Geological Survey.

U.S. Geological Survey, unpublished data of chemical and physical parameters from Pinto Creek near Miami, AZ, Station Number 09498502, Lab ID 1830173, 6/18/97.

AUTHOR INFORMATION

Justin C. Marble, Timothy L. Corley, and Martha H. Conklin, The University of Arizona, Department of Hydrology & Water Resources, Tucson, Arizona.

Manganese Removal by the Epilithic Microbial Consortium at Pinal Creek near Globe, Arizona

By Eleanora I. Robbins, Timothy L. Corley, and Martha H. Conklin

ABSTRACT

Interaction of an acidic mine drainage plume with subsurface material in an alluvial aquifer has released dissolved manganese [(Mn(II)] into the perennial reach of Pinal Creek near Globe, Arizona. A combination of hydrologic and biogeochemical processes is responsible for precipitation of a fraction of the Mn(II) which precipitates as Mn-oxyhydroxides on surficial sediments, within the streambed sediments, beneath algal mats formed on surficial sediments, and among mosses and emergent aquatic plants. This study focuses on the variety and seasonality of biological processes associated with Mn-oxyhydroxide precipitates formed on glass substrates placed in surface waters characterized by different flows and vegetation. The glass slides were emplaced monthly at a single subreach of Pinal Creek to assess epilithic attachment and Mn oxidation; epiphytic oxidation was assessed periodically also. Oxidized Mn was associated with almost every organism in the consortium at Pinal Creek, from the microscopic to the macroscopic. Epilithic bacteria, fungi, algae, and protozoans were coated with oxidized Mn; every macrophyte examined had patches of oxidized Mn. The dominant epilithic precipitation forms were around holdfasts and within secreted substances. The black holdfasts of the iron bacterium, Leptothrix discophora, and the green alga, Ulothrix sp., were doughnut-shaped forms. Expansive patches of black extracellular polysaccharides were secreted primarily by bacterial filaments and fungal hyphae. The dominant macrophytic precipitation form was clumps of oxidized Mn on mosses, green algae, and cyanobacteria. These clumps are consistent with Mn precipitation by elevated pH during photosynthesis. More Mn-oxide precipitates were found in the spring and summer months than the fall and winter, consistent with biological and chemical activity models, and more formed in swifter water than in slower moving water, consistent with oxygen elevation models. These findings provide a better understanding of the biological factors that influence natural attenuation of Mn at Pinal Creek and identify some of the complex interactions between biota, hydrologic processes, and water chemistry that need to be considered to fully assess the affects of acidic mine drainage on stream systems.

INTRODUCTION

Manganese (Mn) is typically released from the rock strata and enters surface and ground water during mining. Mn is dissolved in anoxic and acid water. Homogeneous precipitation of Mn(II) as an oxide phase does not occur below pH 8, but Mn(II) oxidation does occur in the presence of different mineral surfaces and/or via bacterial processes between pH 6 and 8 (Diem and Stumm, 1984). It is also known that bacterially mediated oxidation of dissolved manganese [Mn(II)] is an important component of metals redox chemistry in soils, and marine and fresh water environments (Ehrlich, 1996). Among the microorganisms capable of oxidizing Mn(II) are bacteria, algae, yeast, and fungi (Ehrlich, 1996). Because aqueous environments are dynamic, and water chemistry, aquatic plants, and algal communities can change with time, even when Mn(II) precipitates as stable oxide

phases, these precipitates can be resolubilized if new reducing environments form.

Release of Mn(II) is a major problem for the mining industry. Federal regulations require that Mn(II) released from active mines not exceed 4 mg L^{-1} (U.S. Code of Federal Regulations, 1996), a value that is typically far exceeded in practice. Mn(II) is not generally considered a health risk and the main interest has been on the formation of Mn-oxyhydroxide precipitates because other metals (e.g., Zn, Ni, and Co) can be removed from solution by these precipitates (Hem and others, 1989; Tamura and Furuichi, 1997).

Remediation efforts are underway around the world to utilize chemical, hydrologic, and biological processes to precipitate Mn(II) from acidic mine drainage (AMD). Both active and passive treatments are being explored. Active, and expensive, treatment typically utilizes CaO and NaOH to raise the pH in treatment ponds (Robbins and others, 1997). Municipal water treatment plants in the United States rely on oxidants such as chlorine, while biologically active sand filters are used in Europe (Vandenabeele and others, 1992). Passive treatments involve the establishment of oxidizing zones in wetlands and limestone beds (Hedin and others, 1996; Watzlaf, 1997). Localities where oxidized Mn is naturally precipitating are being studied intensively (Usui and Mita, 1995) to learn about processes that might be used or modified to apply to AMD contaminated systems and lower treatment costs (Phillips and others, 1995).

Three biological processes are particularly effective in precipitating Mn oxyhydroxides. The neutralophilic iron bacteria are the major microbial group that catalyzes the oxidation of Mn(II) (Nealson, 1982), a process that produces energy for some bacteria, but not all (Ehrlich, 1996). Cyanobacteria and algae have been found to cause precipitation of oxidized Mn as a result of pH elevation to values greater than 8 due to photosynthesis (Richardson and other, 1988). Enzymatic reactions involving extracellular polysaccharides may also oxidize Mn (Tebo and others, 1997).

Pinal Creek, near Globe, Arizona, is a locality where oxidized Mn precipitates naturally after partially neutralized, contaminated ground water enters the perennial reach. Geochemical, hydrologic, and biological processes have been invoked to explain both dissolution and precipitation of Mn oxyhydroxides in Pinal Creek. Geochemical mechanisms (Lind, 1991) and hydrologic mixing of surface and ground water in hyporheic zones, coupled with biogeochemical processes within these microbially active zones have been proposed to explain field observations that 20 % of the Mn(II) entering the perennial reach is precipitated over the upper 4 km of the reach (Harvey and Fuller, 1998; Marble and others, 1999a).

This paper focuses on biological processes that occur in the water column above the streambed sediments and outside of the hyporheic zone. Specifically, we investigated the wide variety and seasonal changes of biotic processes that are associated directly, or indirectly, with Mn-oxyhydroxide precipitation on surficial sediments and among vegetation present in the perennial reach of Pinal Creek.

STUDY SITE

Pinal Creek is the outlet of the Pinal Creek Basin, a typical alluvial basin of the southwest United States. The perennial stream reach, which is approximately 13 km in length from head of flow to its confluence with the Salt River, is fed by ground water from the alluvial aquifer that has contaminated by copper-mining activities in the area (Eychaner, 1989; Brown and Favor, 1996). This riparian system has been designated as a State of Arizona Superfund site and a USGS Toxic Substances Hydrology Program site. The USGS has been studying the hydrology, geology, and contaminant plume since 1984. Surface water chemistry in the upper 4-km length is dominated by discharge of partially neutralized, metals-contaminated ground water with pH increasing from 5.5-6 at the head of flow to about 8 at the confluence with the Salt River. Manganese is the primary metal contaminant in the system with lower levels of Zn and Ni (Eychaner, 1989; Gellenbeck and Hunter, 1994; Konieczki and Angeroth, 1997). Mn(II) at the head of flow has been as high as 99 mg L^{-1} (1.8 mM) but has remained constant at about 66 mg L^{-1} (1.2 mM) since 1990 (Gellenbeck and Hunter,

1994; Konieczki and Angeroth, 1997; Marble and others, 1999a, 1999b).

Vascular aquatic plants include water speedwell (Veronica anagallis-aquatica) and grasses such as rabbit foot (Polypogon monspeliensis) (Marble and others, 1999b). Spindler and Sommerfeld (1996) found 62 kinds of algae including cyanobacteria, greens, euglenids, cryptomonads, and golden brown algae including diatoms. Bioconcentration of Mn by algae and vascular aquatic plants has been shown to occur (Marble and others, 1999b).

Mixtures of Mn oxyhydroxides of various textures from fine, flocculent materials to layered concretions resembling asphalt within the streambed sediments at some locations are found along the entire reach (Lind, 1991). These precipitates form on top of the sediment bed, within the hyporheic zone (2-20 cm typical thickness, Harvey and Fuller, 1998), among mosses and the root structures of aquatic plants, and beneath algal mats present on sediments and sandbars. The precipitates range from particulates that are < 75 μm to visible coatings on medium sand and on larger grains.

A subreach that is actively precipitating oxidized Mn in Pinal Creek was chosen for a year-long study between October 1997 and October 1998 (Figure 1) (GPS location 33° 33' 10.41" N lat., 110° 53' 13.67" W long.) at an elevation of 850 m. We conducted experiments about 20-25 m upstream of a site named J2-5 that is sampled on a regular basis by researchers at the University of Arizona; it is a known source of biotically active surficial and subsurface sediments that oxidize Mn(II). Analyses of Mn oxyhydroxide-coated sediments collected at this location indicate Mn loadings of 1,000 to 350,000 mg Mn per kg of dry sediment, i.e, 0.1% to 35% Mn by weight (Marble and others, 1999a).

Two locations near opposite banks of the creek were selected because the flow regimes were representative of the extremes found at J2-5. Analyses of tracer data indicated a main channel flow of approximately 0.18 $m^3 s^{-1}$ which yields a mean velocity of 20-25 cm s^{-1}. Due to the presence of small sandbars (15 cm to 1 m separation) on the left-hand side (LHS) of the creek, the water velocity ranges from the main channel value to about one-half of this value. As a result of vegetation and fine sediments trapped by this vegetation, the RHS velocity ranges from about 1 cm s^{-1} to about one- half of the main

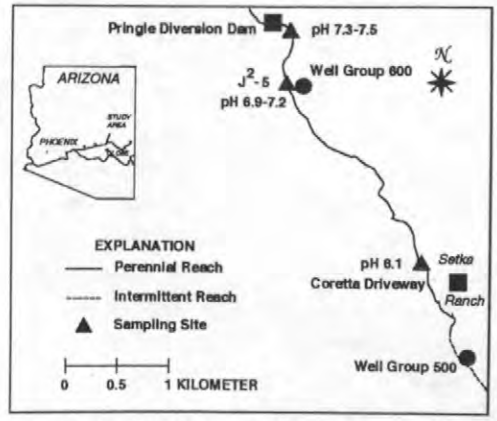

Figure 1. Field site and location in the upper perennial reach.

channel value. Flowrates also change seasonally and episodically due to precipitation at the site or elsewhere in the Pinal Creek Basin. The total braided channel width is 13.2 m, the main channel is 2.2 m in width; and the maximum depth of the channel is 45 cm.

MATERIALS AND METHODS

The experiment was designed to learn about biological processes associated with precipitation of oxidized Mn on surfaces in the oxic water column, above the sediment-surface water interface, and on surfaces next to small sandbars and vegetation zones. The primary objective was to analyze epilithic attachment, the process by which organisms colonize and cause precipitation on surfaces. A few samples were analyzed for epiphytic attachment (the process by which organisms colonize and cause precipitation on macrophytes), specifically, on moss, algae, and water speedwell. Analysis consisted of detailed microscopic studies of dry slides and moist macrophytes.

Glass microscope slide sets (artificial substrates) were tied to wooden dowels and placed into the creek at 2 sites (2 sets on the LHS, 3 sets on the RHS) and during the next year were replaced monthly to view changes in precipitation of oxidized Mn. When retrieved, slides were rinsed with deionized water to prevent salt crystal

growth and allowed to air-dry at the site before returning to the laboratory for analysis. The drying step is important because of prolific growth of an unidentified fungus/actinomycete on the Mn-bearing glass substrates. The presence of oxidized Mn was tested with orthotoluidine (Morgan and Stumm, 1965).

The LHS slide sets were in a narrow channel approximately 1 m from the left bank defined by two small, water speedwell-covered sandbars. The chemical values for surface water in this small channel were essentially those of the main channel. The RHS slide sets were in a vegetation zone characterized in the initial months of this study by slower flows than are found in the main channel or the LHS sites. This location had a relatively high vegetation density of water speedwell and grasses, with fine silts and sands around the submerged plant structures and a substrate of organic-rich material that produced local reducing zones.

Water chemistry [Mn(II), pH, dissolved oxygen (O_2), and alkalinity], temperature, and flow characteristics were measured as part of other research projects at Pinal Creek.

RESULTS AND DISCUSSION

Evolution of Site Over Study Year

As the sampling year progressed, changes occurred in the main channel, as well as the LHS and RHS of Pinal Creek. These changes included increased consolidation of the sediment bed (the depth of sediments that could be easily penetrated decreased from 70 cm to between 5 and 20 cm), fill-in due to sediment transport from upstream during rainfall events, fill-in due to plant succession, and changes in vegetation densities and distributions across the channel. Increases in the density and distribution of water speedwell were observed across the entire channel. The vegetation zone along the RHS increased from 45 cm to between 1 and 1.5 m in width. Algal mats were established on the sediment bed in the main channel and on the sides of the small sandbars. Although normal and episodic rainfall events did not entirely scour out the vegetation (a typical occurrence in the past), fine silt-size sediments were swept into the area periodically and caused the death of a significant fraction of mature water speedwell. Filamentous algae then appeared in the main channel and in smaller channels between sandbars, and served as anchoring sites for new water speedwell to take root. A layered structure of dead plants and sediments coated with oxidized Mn, and new plant growth on top of this material was observed and reflected this succession of plant types and density. In addition, the reducing zones on the RHS observed in the fall of 1997 (an odor from sulfur-containing species was released when this organic-matter-rich material was disturbed) decreased in size and disappeared over the course of this study. These changes undoubtedly affected the results of our study.

Although the initial positions of the slides were controlled upon submersion in the system, flow conditions over the period of submersion in LHS often moved both sets of slides into contact with the left bank of the sandbar. In addition, one or both sets of slides were frequently found underneath algal mats that had formed in a one-month period and/or within the root structures of water speedwell which was not present on the submersion dates. Movement of the slide sets on the RHS were also observed.

During this study year, surface water chemistry values in the main channel were pH (6.9-7.2), dissolved O_2 (0.25-0.15 mM), temperature (8-37 °C), alkalinity (40-65 mg L^{-1}), and Mn(II) (47 ± 3 mg L^{-1}, or 0.85 ± 0.055 mM). Mn(II) values peaked in midsummer at 54 mg L^{-1} (Tables 1 and 2). The ranges listed are due to seasonal and diel changes. Shallow ground water beneath the main channel was sampled once at 70 cm below the sediment-surface water interface with a standard drivepoint sampler that was 1.2 m in length. Chemical values in the ground water were pH (6.6), dissolved O_2 (0.033 mM), temperature (15 °C), alkalinity (127 mg L^{-1}), and Mn(II) (6 mg L^{-1} or 0.11 mM). These values for surface and ground water are typical of the water chemistry at J2-5 before active remediation of the contaminated ground water plume began in the first part of October, 1998.

Biological Interactions with Manganese in the Zone of Oxidation

Almost every organism at the J2-5 study site, from microscopic to macroscopic, was associated with precipitates of oxidized Mn. Oxidized Mn coated bacteria, fungi, protozoans, and algae in the epilithic consortium (Table 1). Every macrophyte examined (Table 2) had patches of oxidized Mn, suggesting that precipitation of oxidized Mn was a mediated process.

Many iron bacteria are known to co-precipitate Mn (Nealson, 1982), and several of these were sampled as epiliths at Pinal Creek. Oxidized Mn precipitates on epilithic bacteria were predominantly attached to Mn-coated holdfasts anchoring the iron bacterium, Leptothrix discophora, to surfaces, a finding consistent with other research (Robbins and others, 1992; Robbins, 1998). This bacterium was present year round (Table 1) at both the LHS and RHS sites, but oxidized Mn coated bacteria were found in greater numbers in the spring and summer months at the LHS locality (Tables 1a and 1b). This may be due to increased bacterial populations during this period and/or an increased rate of Mn oxidation at more optimal temperatures for biological activity (Tipping, 1984).

Other bacterial morphotypes found with precipitated oxidized Mn on individual cells were cocci, rods, filaments, and a rosette form that is usually called Metallogenium (Maki and others, 1987). The Metallogenium-type rosettes at the LHS locality were present only periodically and never abundant (Table 1b) in freely flowing water. The brown rods were present throughout the year and common at the LHS site but rarer at the RHS site.

A mixed population was found in contact with vegetation (Tables 1a and 1c) and in the fine sediments associated with the water speedwell root structure at RHS (Table 1e). This includes Leptothrix discophora filaments, an unnamed Leptothrix that has cells that stay inside the sheaths ("L. inside"), Metallogenium, and Siderocystis. Biofilms of various colors, including the brown color of oxidized Mn, coated microscope slides; biofilms are typically formed by the rods and cocci attached to them (Brown and others, 1994).

Because fungi and actinomycetes are known to precipitate Mn (the American Type Culture Collection, 1996, lists 4 species), it was not unexpected that some evidence of this process would also be found at Pinal Creek. Oxidized Mn was only found on fungal hyphae but not on spores (Table 1). This type of precipitation occurred on all slide sets at both emplacement sites, but mainly at LHS. Oxidized Mn took two forms: smooth patches along some hyphae, and loose, rather lumpy accumulations on other hyphae. At present, the dominant fungus has not been identified, but it has elongated, segmented colorless hyphae that colonize entire surfaces of the slides; its colorless spores resemble those of actinomycetes. Its sporangia are also colorless. This unidentified fungus became so heavily coated that a thick, black sooty oxidized Mn powder formed on LHS-V1 (#101) and RHS-V1 (#65) slides.

On certain slides as much as 50 % of the Mn precipitates were associated with epilithic algae. The dominant type was coated holdfasts of the filamentous green alga, Ulothrix. Spindler and Sommerfeld (1996) identified 2 species of Ulothrix in Pinal Creek, both present at the current study site and both forming holdfasts. The Mn-coated holdfasts were primarily found at the LHS site and were most abundant in August at the LHS-V1 slow flow site; they were abundant during many months at the LHS-V2 moderate flow site. Smooth accumulations of precipitated oxidized Mn were noted on filaments of Ulothrix, Spirogyra, and an unidentified filamentous green alga. Lumpy accumulations built up as patches on intertwined filaments. This lumpy type is similar to that ascribed to localized photosynthetic elevation of pH (Richardson and others (1988).

Other algae and cyanobacteria not yet identified are most probably involved in the precipitation of oxidized Mn, because mixed colonies have been found to be extremely efficient (Phillips and others, 1995; Stuetz and others, 1996). In addition, changes in populations and age will influence the role of these microorganisms because it has been shown that cyanobacteria and algae must attain a certain size

before Mn is oxidized on the cells (Richardson and Stolzenback,1995).

In some instances, epilithic diatoms were coated brown from oxidized Mn. Hunt and Smith (1980) recognized that diatoms precipitated Mn but were unsure of the mechanism. If photosynthesis alone were sufficient to explain the association of oxidized Mn precipitates with diatoms, then every diatom in the Pinal Creek data set should have been coated brown, which is not the case.

Oxidized Mn was most commonly observed on extracellular polysaccharide (EPS) at Pinal Creek. EPS and Mn were concentrated on the external cell walls and holdfasts of bacteria, hyphae of fungi, and on the filaments of algae, and decreased with distance away from these structures. EPS around these structures was present at all sampling localities, but more abundant at the LHS site. The moderate flow site at LHS had abundant EPS in the spring months, but even the slow flow and no flow sites at RHS had significant accumulation by EPS in the summer months.

This visual inspection suggests that EPS secreted by cells, holdfasts, hyphae, and filaments plays a key role (direct and/or indirect) in oxidation of Mn(II) at Pinal Creek. This inference receives support from studies that indicate that Mn oxidation by bacteria takes place within a complex matrix of excreted heteropolysaccharides (Tebo and others, 1997). Additional support comes from work reported by Fortin and others (1997), who proposed an indirect, non-enzymatic mechanism for Mn oxidation in which EPS simply serves as sorption and nucleation sites.

Epilithic protozoan cells and tests were patchily coated by oxidized Mn. In most instances, bacteria had colonized the cells and tests and precipitated the Mn, but in some cases it appeared that the Mn precipitated directly on the protozoan cells and tests.

Macrophytes were also found with oxidized Mn precipitates (Table 2). Much of the Mn was attached to holdfasts of Leptothrix discophora and Ulothrix that colonized the mosses and speedwell, but clumps that are similar to those ascribed to pH elevation during photosynthesis were noted on mosses, speedwell, and cyanobacteria.

Biological Interactions with Manganese in the Zone of Weak Oxidation/Reduction

There is a distinct difference between the numbers and types of organisms found on the glass substrates emplaced in the moderate and slow flow of LHS versus the highly vegetated RHS site having very slow, or no perceptible, flow. The RHS sets, like the LHS site, had epilithic bacteria, fungi, algae such as Ulothrix and diatoms, and protozoans. However, filamentous bacteria at RHS were more diverse than from the LHS site, and the RHS sets had either significantly less or no oxidized Mn.

The glass substrates were pushed into the vegetation and fine sediments and/or organic-rich substrate at RHS to sample the zone of reduction and the redox zone. In only one instance was the redox zone unequivocally captured. At RHS-V1 between September to October, slides #105 and 106 had a distinct red/orange line that identified the location of the iron redox zone at the sediment-water interface. The biofilm above this zone was brown in color and tested positive for oxidized Mn. This biofilm contained reddish brown bacterial filaments and sheaths, numerous diatoms, and reddish brown-coated short and medium rods. Below this, biofilm was lacking and the attached bacteria were all colorless.

CONCLUSIONS

Organisms appear to have played a major role in precipitating oxidized Mn on artificial substrates emplaced at the Pinal Creek study site. Oxidized Mn was found on bacteria, cyanobacteria, algae, fungi/actinomycetes, protozoans, and macrophytes. The macroscopic appearance of the precipitates often resembled that of the specific organism. Most of the oxidized Mn was observed on holdfasts and EPS. Holdfasts with oxidized Mn include those of the green alga, Ulothrix, and the iron bacterium, Leptothrix discophora. EPS and oxidized Mn were found around bacterial cells and holdfasts, fungal hyphae, and algal holdfasts and filaments.

Our study indicates that there is a seasonal component to the precipitation of oxidized Mn, because the glass substrates were more heavily

coated with oxidized Mn during the spring and summer months. Whether this is due to a dependence of biological activity on temperature (population types, numbers and density), or a temperature dependence of an underlying chemical mechanism, cannot be answered with the current data, but it is a question that can be addressed in future research.

The observation that more Mn precipitated onto the glass substrates where water flow was fastest may reflect a dependence on velocity of mass transfer of key chemical species from the bulk surface water to the local chemical environments associated with the biofilm communities responsible for precipitates of oxidized Mn. Transport of nutrients, dissolved O_2, and Mn(II) to active sites would certainly be expected to depend on water velocity, but confirmation of this inference would require measurements at the microscale.

There are indications that some of the oxidized Mn precipitates may be easily reduced or mobilized in response to stream water chemistry changes. For example, the sooty form of oxidized Mn on the unidentified fungus/actinomycete appears to be very loosely bound to surfaces; physical detachment of the anchoring structures may be a facile process occurring in response to relatively small changes in pH and/or major ions. This could be readily tested in the laboratory. The stability of different oxidized Mn precipitates could be tested in the field by placing colonized glass substrates into reducing zones to learn which form of biologically precipitated oxidized Mn lasts the longer.

Results of this year-long study indicate that a consortium of microorganisms at Pinal Creek acts in concert to remove Mn(II) from circumneutral surface water. Both bacteria (e.g., Leptothrix discophora) and algae (e.g., Ulothrix sp.) are associated with this overall process, with EPS having some general, but not yet defined, role. The positive roles of temperature and water velocity in increasing Mn(II) removal by microorganisms is suggested by our data and Ulothrix sp. has been identified as a particularly effective organism for removal of Mn(II). However, quantitative studies must be undertaken (field and laboratory) to define the contribution of the epilithic communities to overall Mn(II) removal and the environmental conditions that optimize this overall process. It may then be possible to suggest constructive ways in which to use these natural attenuation mechanisms in remediation efforts at different contaminated sites.

ACKNOWLEDGMENTS

This publication was made possible by grant number P42 ESO4940 from the National Institute of Environmental Health Science with funding provided by EPA and by grant number EAR-95-23881 from the NSF. Its contents are solely the responsibility of the authors and do not necessarily represent the official views of the NIEHS, NIH, EPA, NSF, or USGS.

REFERENCES

American Type Culture Collection, 1996, Catalogue of Filamentous Fungi at the ATCC, 19th edition: American Type Culture Collection, p. 572.

Boogerd, R. C. and de Vrind, J.P.M., 1987, Manganese oxidation by Leptothrix discophora: Journal of Bacteriology, v. 169, p. 489-494.

Brown, D.A., Kamineni, D.C., Sawicki, J.A., and Beveridge, T.J., 1994, Minerals associated with biofilms occurring on exposed rock in a granitic underground research laboratory: Applied and Environmental Microbiology, v. 60, p. 3182-3191.

Diem, D., and W. Stumm, 1984, Is dissolved Mn^{2+} being oxidized by O_2 in absence of Mn-bacteria or surface catalysts: Geochimica et Cosmochimica Acta, v. 48, p. 1571-73.

Ehrlich. H. L., 1996, Geomicrobiology: New York, Marcel Dekker, 719 p.

Eychaner, J.H., and Stollenwerk, K.G., 1985, Neutralization of acidic ground water near Globe, Arizona, in Schmidt, K.D., ed., Proceedings of Symposium on Groundwater Contamination and Reclamation: American Water Resources Association, Tucson, Arizona, August 14-15, 1985, p. 141-148.

Fortin, D., Ferris, F.G., and Beveridge, T.J., 1997, Surface-mediated mineral development by bacteria, in Banfield, J.F., and Nealson, K.H., eds., Geomicrobiology: Interactions Between Microbes and Minerals: Reviews in Mineralogy, v. 35, p.161-180.

Gellenbeck, D.J. and Hunter, Y.R., 1994, Hydrological data from the study of acidic contamination in the Miami Wash-Pinal Creek Area, Arizona, water years 1992-93: U.S. Geological Survey Open-File Report 94-508, 103 p.

Ghiorse, W.C., and Ehrlich, H.L., 1992, Microbial biomineralization of iron and manganese, in, H. C. W. Skinner, H.C.W., and Fitzpatrick, R.W., eds., Biomineralization Processes, Iron and Manganese: Catena Supplement, v. 21, p. 75-99.

Harvey, J.W., Fuller, C.C., 1998, Effect of enhanced manganese oxidation in the hyporheic zone on basin-scale geochemical mass balance: Water Resources Research, v. 34, p. 623-636.

Hedin, R.S., Watzlaf, G.R., and Nairn, R.W., 1996, Passive treatment of acid mine drainage with limestone: Jour. Environmental Quality, v. 23, p. 1338-1345.

Hem, J.D., Lind, C.J., Roberson, C.E., 1989, Coprecipitation and redox reactions of manganese oxides with copper and nickel: Geochimica et Cosmochimica Acta, v. 53, p. 2811-2822.

Hunt, C.D., and Smith, D.L., 1980, Conversion of dissolved manganese to particulate manganese during a diatom bloom: Effects on the manganese cycle in the MERL microcosms, in Glesy, J.P., ed. Microcosms in Ecological Research: U.S. Tech. Information Center, U.S. DOE Symposium Series 52, p. 850-868.

Konieczki, A.D., and Angeroth, C.E., 1997, Hydrologic data from the study of acidic contamination in the Miami Wash-Pinal Creek area, water year 1994-96: U.S. Geological Survey Open-file Report 97-247, 94 p.

Lind, C.J., 1991, Manganese minerals and associated fine particulates in the Pinal Creek stream bed: U.S. Geological Survey Water-Resources Investigations Report 91-4034, p. 486-491.

Maki, J.S., Tebo, B.M., Palmer, F.E., Nealson, K.H., and Staley, J.T., 1987, The abundance and biological activity of manganese-oxidizing bacteria and Metallogenium-like morphotypes in Lake Washington, USA: FEMS Microbiology Letters, v. 45, p. 21-29.

Marble, J.C., Corley, T.L., Conklin, M.H., and Fuller, C.C., 1999a, Environmental factors affecting oxidation of manganese in Pinal Creek, in Morganwalp, D.W., and Buxton, H.T., eds., U.S. Geological Survey Toxic Substances Hydrology Program—Proceedings of the Technical Meeting, Charleston, South Carolina, March 8-12, 1999—Volume 2—Contamination of Hydrologic Systems and Related Ecosystems: U.S. Geological Survey Water-Resources Investigations Report 99-4018B, this volume.

Marble, J.C., Corley, T.L., and Conklin, M.H., 1999b, Representative plant and algal uptake of metals near Globe, Arizona, in Morganwalp, D.W., and Buxton, H.T., eds., U.S. Geological Survey Toxic Substances Hydrology Program—Proceedings of the Technical Meeting, Charleston, South Carolina, March 8-12, 1999—Volume 2—Contamination of Hydrologic Systems and Related Ecosystems: U.S. Geological Survey Water-Resources Investigations Report 99-4018B, this volume.

Morgan, J.J., and Stumm, Werner, 1965, Analytical chemistry of aqueous manganese: Journal of the American Water Works Association, v. 57, p. 107-119.

Nealson, K.H., 1982, The microbial manganese cycle, Chapter 7, in Krumbein, W.E., ed., Microbial Geochemistry: Boston, Blackwell Scientific, p. 191-221.

Phillips, P., Bender, J., Simms, R., Rodriquez-Eaton, S., and Britt, C., 1995, Manganese removal from acid coal-mine drainage by a pond containing green algae and microbial mat: Water Science and Technology, v. 31, p. 161-170.

Richardson, L.L., Aguilar, C., and Nealson, K.H., 1988, Manganese oxidation in pH and O_2 microenvironments produced by

phytoplankton: Limnology and Oceanography, v. 33, p. 352-363.
Richardson, L.L., and Stolzenbach, K.D., 1995, Phytoplankton cell size and the development of microenvironments: FEMS Microbiology Ecology, v. 16, p. 185-192.
Robbins, E.I., 1998, New roles for an old resource, Ferromanganese nodules assist mine cleanup: Geotimes, v. 43, p. 14-17.
Robbins, E.I., D'Agostino, J.P., Ostwald, J., Fanning, D.S., Carter, Virginia, and Van Hoven, R., 1992, Manganese nodules and microbial oxidation of manganese in the Huntley Meadows wetland, Virginia, USA: Catena Supplement, v. 21, p. 172-202.
Robbins, E.I., Maggard, R.R., Kirk, E.J., Belkin, H.E., and Evans, H.T., Jr., 1997, Manganese removal by chemical and microbial oxidation and the effect on benthic macroinvertebrates at a coal mine in Wayne County, western West Virginia: Proceedings, West Virginia Surface Mine Task Force Symposium, Morgantown, WV, p. 110-124.
Schmidt, J.M., Sharp, W.P., and Starr, M.P., 1982, Metallic-oxide encrustations of the nonprosthecate stalks of naturally occurring populations of Planctomyces bekefi: Current Microbiology, v. 7, p. 389-394.
Spindler, P.H., and Sommerfeld, M.R., 1996, Distribution of algae in Pinal Creek, Gila County, Arizona: Journal of the Arizona-Nevada Academy of Science, Issue 2, p. 108-117.
Stuetz, R.M., A.C. Greene, and J.C. Madgwick, 1996, Microalgal-facilitated bacterial oxidation of manganese: Journal of Industrial Microbiology, v. 16, p. 267-273.
Tamura, H, and R. Furuichi, 1997, Adsorption affinity of divalent heavy metal ions for metal oxides evaluated by modeling with the Frumkin isotherm: Journal of Colloid and Interface Science, v. 195, p. 241-249.
Tebo, B.M., Ghiorse, W.C., van Waasbergen, L.G., Siering, P.L., and Caspi, R., 1997, Bacterially-mediated mineral formation: Insights into manganese(II) oxidation from molecular genetic and biochemical studies, in Banfield, J.F., and Nealson, K.H., eds., Geomicrobiology: Interactions Between Microbes and Minerals: Reviews in Mineralogy, v. 35, p. 225-266.
Tipping, E., 1984, Temperature dependence of Mn(II) oxidation in lakewaters: a test of biological involvement: Geochimica et Cosmochimica Acta, v. 48, p.1353-1356.
Usui, Akira, and Mita, Naoki, 1995, Geochemistry and mineralogy of a modern buserite deposit from a hot spring in Hokkaido, Japan: Clays and Clay Minerals, v. 43, p. 116-127.
U.S. Code of Federal Regulations, 1996, Title 40—Protection of Environment. Chapter 1—Environmental Protection Agency; Part 434--Coal mining point source categories, Subpart C—Acid or ferruginous mine drainage: Washington, DC, p. 222-223.
Vandenabeele, J., de Beer, D., Germonpre, R., and Verstraete, W., 1992, Manganese oxidation by microbial consortia from sand filter: Microbial Ecology, v. 24, p. 91-108.
Watzlaf, G.R., 1997, Passive treatment of acid mine drainage in down-flow limestone systems: American Society for Surface Mining and Reclamation, 14th Annual Meeting, Austin, TX, p. 611-622.

AUTHOR INFORMATION

Eleanora I. Robbins, U.S. Geological Survey, Reston, VA

Timothy L. Corley and Martha H. Conklin, University of Arizona, Department of Hydrology & Water Resources,Tucson, AZ

Table 1a. Chemical and microscopic biological data at site LHS-V1 [slides in contact with vegetation]
(Symbols and abbreviations: +++++, >5 every field; ++++, >2 every field; ++, 1 every field; +, <1 every field; ---, not present or no data; c, curved; co, cocci; l, long; m, medium; r, rod; s, short; vi,vibrio)

No.	Submersion dates	Temperature (°C) and season at retrieval date	pH at retrieval date	DO (mg/L) at retrieval date	Mn(II) (mg/L)	Brown cocci (co) or rods (r) (l,long s,short)	Brown coated bacterial filaments	Iron bacteria	Brown holdfasts of Leptothrix discophora (or other)	Colored biofilms	Brown exo-polysac-charide	Brown coated fungal hyphae	Brown algal holdfasts (and filaments)	Diatoms (*brown coated) (no. of species)
1-2	10/6/97-11/17/97	14.3 Fall	7.06	---	46	---	---	---	+++	---	+	---	+	+* (4)
11-12	11/17/97-12/17/97	--- Winter	---	---	45	+ (sr)	+	---	+ (+ other)	---	+	+	+	+ (7)
19-20	12/17/97-1/20/98	13.8 Winter	6.94	---	45	---	---	Siderocystis	+	---	---	---	+	+ (6)
33-34	2/20/98-3/19/98	18.4 Winter	---	---	47	---	---	---	+ (+ other)	brown (sr)	+	---	+	+ (4)
43-44	3/19/98-4/17/98	18.5 Spring	7.08	---	43	---	---	L. discophora	+++++	---	---	---	++	+ (4)
51-52	4/17/98-5/18/98	20.2 Spring	---	---	44	+	---	---	++++ (+ other)	---	+++	+	+	+ (5)
61-62	5/18/98-6/24/98	--- Summer	---	---	---	---	+	L. discophora	++++ (+ other)	orange	+	---	+	+ (7)
71-72	6/24/98-7/22/98	22.7 Summer	7.41	---	54	++ (sr,cr)	++	---	+	brown (sr)	+++	+	++	+* (7)
81-82	7/22/98-8/21/98	25.6 Summer	7.10	7.3	50	+ (sr,co)	+	+Metallogenium?	+++++	---	+++	+	+++++	+* (8)
91-92	8/21/98-9/29/98	--- Summer	---	---	47	+ (sr,vi)	+	+ Metallogenium	+	beige (sr)	+	---	+	++ (5)
101-102	9/25/98-10/30/98	16.6 Fall	6.76	8.4	36	+ (sr, lr)	+	++Metallogenium	+	yellow, orange (sr)	+	+	+ +filaments	++* (11)

Table 1b. Chemical and microscopic biological data at site LHS-V2 [slides freely floating in water moving 20-25 cm s^{-1}]
(See Table 1a for symbols and abbreviations)

No.	Submersion dates	Temperanure (°C) and season at retrieval date	pH at retrieval date	Mn(II) (estimated) mg/L	Brown cocci (co) or rods (r) (l,long s,short)	Brown coated bacterial filaments	Iron bacteria	Brown holdfasts of Leptothrix discophora (or other)	Colored biofilms	Brown exo-polysac-charide	Brown coated fungal hyphae	Brown algal holdfasts (and filaments)	Diatoms (*brown coated) (no. of species)	Brown-coated proto-zoans
5-6	10/6/97-11/17/97	--- Fall	---	46	---	+	---	+++++	brown (co)	+	---	+++++	+ (5)	+
13-14	11/17/97-12/17/97	--- Winter	---	45	---	---	+ Metallogenium	++	---	+	---	++ (+filaments)	+* (6)	---
21-22	12/17/97-1/20/98	--- Winter	---	45	---	+	---	+ (+ other)	---	+	+	++	+ (5)	---
27-28	1/20/98-2/20/98	--- Winter	---	---	+ (r)	+	---	+	brown (sr)	---	+	++	+ (3)	+
35-36	2/20/98-3/19/98	--- Winter	---	47	---	---	---	+	orange (sr)	---	---	---	+ (6)	---
45-46	3/19/98-4/17/98	--- Spring	---	43	+++++ (r)	+	---	+++++	---	++++ +	+	+++++ (+filaments)	+ (3)	---
53-54	4/17/98-5/18/98	--- Spring	---	44	---	+	---	+++++	very dark brown	+++	---	++++ (+filaments)	+* (6)	+
63-64	5/18/98-6/24/98	--- Summer	---	---	+ (mr)	---	---	+++++	brown (sr)	++++ +	+	+++++	++ (6)	---
73-74	6/24/98-7/22/98	22.7 Summer	7.43	54	+ (sr)	+	---	+++ (+ other)	brown (sr)	+++	+	+++ (+filaments)	+++++ (8)	---
83-84	7/22/98-8/21/98	--- Summer	---	50	+ (sr)	+	+ Metallogenium	+	brown (co)	++++	+	---	++++* (5)	---
93-94	8/21/98-9/29/98	--- Summer	---	47	+ (sr)	---	---	+	light brown (sr)	---	---	+	+ (6)	---
103-104	9/25/98-10/30/98	--- Fall	---	36	+(sr,co,lr)	+	+ Metallogenium	+++	---	+++	+	+++ (+filaments)	++++* (9)	---

Table 1c. *Chemical and microscopic biological data at site RHS-V1 [slides in contact with grasses, flow ≈cm s^{-1}]*
(See Table 1a for symbols and abbreviations)

No.	Submersion dates	Temperature (°C) and season at retrieval date	pH at retrieval date	DO at retrieval date (mg/L)	Mn(II) (estimated) mg/L	Brown cocci (co) or rods (r) (l,long s,short)	Brown coated bacterial filaments	Iron bacteria	Brown holdfasts of Leptothrix discophora (or other)	Colored biofilms	Brown exo-polysac-charide	Brown coated fungal hyphae	Brown algal holdfasts	Diatoms (*brown coated) (no. of species)	Brown-coated proto-zoans
3-4	10/6/97-11/17/97	--- Fall	---	---	38	+ (lr)	+	L. inside	+	brown (sr)	+	+	+	+* (5)	+
15-16	11/17/97-12/17/97	--- Winter	---	---	38	---	---	L. discophora	+	---	---	---	+	+ (4)	+
23-24	12/17/97-1/20/98	--- Winter	---	---	38	---	---	---	+	---	---	+	---	+ (2)	---
37-38	2/20/98-3/19/98	--- Winter	---	---	39	---	---	---	+	beige (sr)	---	---	++	+* (7)	---
47-48	3/19/98-4/17/98	--- Winter	---	---	36	---	+	---	---	---	---	---	++	+ (2)	---
55	4/17/98-5/18/98	--- Spring	---	---	37	---	---	---	+ (+ other)	light brown (sr)	---	---	+	+ (3)	---
65	5/18/98-6/24/98	21 Summer	6.7	6.5	---	+ (r)	+	Metallogenium	+	---	++	+	+	+* (10)	---
75-76	6/24/98-7/22/98	23.6 Summer	7.24	---	45	+ (sr)	+	L. discophora, Siderocystis	+	brown (mr,cr)	+++	+	+	+ (4)	---
86	7/22/98-8/21/98	21.6 Summer	6.69	6.5	42	---	---	---	+	---	---	+	---	+ (4)	---
95-96	8/21/98-9/29/98	--- Summer	---	---	39	---	---	L. inside	+	brown (sr, mr)	---	---	+	+ (7)	---
105-106	9/25/98-10/30/98	--- Fall	---	---	30	---	+	L. discophora?	---	yellow, brown (mr)	---	+	+	++ (5)	---

Table 1d. Chemical and microscopic biological data for site RHS-V2 [slides partly in fine sediment; 10 cm downstream from RHS-V1]
(See Table 1a for symbols and abbreviations)

No.	Submersion dates	Season at retrieval date	Mn(II) (estimated) mg/L	Brown holdfasts of Leptothrix discophora (or other)	Brown cocci (co) or rods (r) (l,long s,short)	Brown coated bacterial filaments	Iron bacteria	Brown holdfasts of Leptothrix discophora (or other)	Colored biofilms	Brown exo-polysac-charide	Brown coated fungal hyphae	Brown algal holdfasts	Diatoms (* brown coated) (no. of species)	Brown-coated proto-zoans
7-8	10/6/97-11/17/97	Fall	38	+ (+ other)	+ (sr)	+	---	+ (+ other)	light brown (sr)	---	---	+	+ (5)	+
17-18	11/17/97-12/17/97	Winter	38	+	---	+	L. discophora	+	light brown (sr)	---	+	+	++ (8)	---
25-26	12/17/97-1/20/98	Winter	38	---	+ (sr)	---	---	---	orange	---	---	---	+ (10)	---
29-30	1/20/98-2/20/98	Winter	---	+ (+ other)	+ (sr)	+	---	+ (+ other)	brown (sr)	---	---	---	+* (8)	+
39-40	2/20/98-3/19/98	Winter	39	(+ other)	---	---	---	(+ other)	brown (sr)	+	---	++	+ (2)	---
49-50	3/19/98-4/17/98	Spring	36	+	---	+	---	+	brown (mr)	---	---	---	---	---
57-58	4/17/98-5/18/98	Spring	37	+	---	+	L. discophora?	+	brown, red	---	---	+	+ (6)	---
67-68	5/18/98-6/24/98	Summer	---	+	---	---	---	+	---	++	+	+	+++ (6)	---
77-78	6/24/98-7/22/98	Summer	45	+	---	---	---	+	light brown (sr, cr)	---	---	+	+ (2)	---
87-88	7/22/98-8/21/98	Summer	42	+	+ (co)	+	---	+	---	+	+	+	+ (8)	---
97-98	8/21/98-9/29/98	Summer	39	---	---	---	---	---	orange brown (sr)	---	---	---	+ (6)	---
107-108	9/25/98-10/30/98	Fall	30	+	+ (sr)	+	L. discophora	+	brown (sr)	---	---	+	+ (7)	---

Table 1e. Chemical and microscopic biological data for site RHS-V3 [slides pushed entirely into sediments] (See Table 1a for symbols and abbreviations)

No.	Submersion dates	Season at retrieval date	Mn(II) (estimated) mg/L	Brown coated bacterial filaments	Iron bacteria	Brown holdfasts of Leptothrix discophora (or other)	Colored biofilms	Brown exo-polysac-charide	Brown coated fungal hyphae	Brown algal holdfasts (and filaments)	Diatoms (number of species)	Brown-coated proto-zoans
9-10	10/6/97-11/17/97	Fall	38	+	Siderocystis	+	light brown (co, sr)	---	---	---	+ (8)	+
31-32	1/20/98-2/20/98	Winter	---	---	L. discophora, L. inside	+ (+ other)	---	---	---	---	+ (6)	+
41-42	2/20/98-3/19/98	Winter	39	---	L. inside, L. discophora	---	orange (mr,lr)	---	---	---	---	---
59-60	4/17/98-5/18/98	Spring	37	---	L. inside	+	yellow	+	+	---	+ (2)	---
69-70	5/18/98-6/24/98	Summer	---	+	---	++	brown (sr)	---	---	++++	++++ (4)	---
79-80	6/24/98-7/22/98	Summer	45	---	L. discophora?	(+ other)	brown (mr)	---	---	---	+ (4)	---
89-90	7/22/98-8/21/98	Summer	42	+	---	+	light & dark brown (co)	+++	+	+++++ (+filaments)	---	---
99-100	8/21/98-9/29/98	Summer	39	---	---	+	light brown (sr)	---	---	+	+ (3)	---
109-110	9/25/98-10/30/98	Fall	30	+	---	+	yellow, light brown (sr)	---	---	+ (+filaments)	+ (5)	---

Table 2. Physical, chemical, and biological data for macrophytes at LHS (See Table 1a for symbols and abbreviations)

No.	Material	Date	Temperature (°C) and season	pH	DO (mg/L)	Mn(II) (mg/L)	Attached brown Leptothrix discophora holdfasts	Brown clumps
A	Moss	3/19/98	18.4 Winter	---	---	47	+	+
B	Speedwell (Veronica) roots	3/19/98	18.4 Winter	---	---	47	+	+
C	Spirogyra	7/22/98	22.7 Summer	7.4	---	54	+	+
D	Mixed mat of moss and Spirogyra	7/22/98	22.7 Summer	7.4	---	54	+	+
E	Mixture of moss, filamentous green, and Spirogyra	9/25/98	--- Summer	---	---	47	+	+
F	Ulothrix dominantly	10/30/98	16.6 Fall	6.8	8.4	36	+	+
G	Ulothrix and filamentous cyanobacteria	10/30/98	16.6 Fall	6.8	8.4	36	+	+

Additional Research on Contamination from Mining-Related Activities

A significant amount of mining-related research is conducted within the U.S. Geological Survey (USGS) in addition to that conducted through the Toxic Substances Hydrology Program. The Program emphasis has been on environmental issues related to hard-rock mining. The research has been focused on four principal field sites: 1) upper Arkansas River, Colorado; 2) Pinal Creek, Arizona; 3) upper Animas River, Colorado; and 4) Boulder River, Montana. The papers in this section provide a sampling of the additional USGS research activities on mining-related contamination issues from across the country.

Much of the additional mining-related research by the USGS is conducted in cooperation with other federal agencies, and state and local agencies. Federal partners include the Bureau of Land Management (U.S. Department of the Interior), the Forest Service (U.S. Department of Agriculture), the U.S. Environmental Protection Agency (EPA. Some of these efforts include testing and application of field and laboratory methods developed through Program activities, such as the papers by Ball and others and the paper by Nordstrom and others. The paper by Naftz and others describes an effort, supported by EPA, to demonstrate the field application of reactive barrier technology applied to uranium contamination in ground water.

Numerous ongoing USGS investigations address the environmental effects of coal mining, particularly acid mine drainage and its treatment or mitigation. Some of the USGS work on coal-mine drainage is being conducted in District (state) Offices of the USGS, throughout the coal mining regions of the Nation, such as the paper by Cravotta and others. Other coal-related investigations are being conducted by the USGS Energy Resources Program. Other investigations on hard-rock mining, environment issues are being conducted by the USGS Mineral Resources.

The addition of the Biological Resources Division (BRD) to the USGS has facilitated significant collaboration between biologists and scientists from other disciplines in existing Programs. The interdisciplinary teams of the USGS Abandoned Mine Lands Initiative are an example. At the same time, there are significant additional mining-related research activities ongoing within the BRD. The presentation at this meeting of the papers by Fairchild and others and by Wildhaber and others are examples of the continued efforts of BRD scientists to establish interdisciplinary partnerships within USGS.

Additional information on USGS mining-environment research is available through the USGS Mine Drainage Interest Group, on the World Wide Web at: **http://mine-drainage.usgs.gov/mine/.** This web site has links to on-line information on all related USGS programs.

For additional information contact:

Herbert T. Buxton, USGS, W. Trenton,
New Jersey (email: hbuxton@usgs.gov), or

Charles N. Alpers, USGS, Sacramento,
California (email: cnalpers@usgs.gov)

Evaluation of the Recovery of Fish and Invertebrate Communities Following Reclamation of a Watershed Impacted by an Abandoned Coal Surface Mine

By James F. Fairchild, Barry C. Poulton, Thomas W. May, and Stuart M. Miller

ABSTRACT

A 5-yr study was conducted to measure the rates of recovery of fish and invertebrate communities following reclamation of a watershed impacted by an abandoned coal surface mine in Southwest Missouri. Quarterly monitoring of water quality parameters (pH, conductivity, and alkalinity) was conducted at 10 sites. Annual monitoring of biological (benthic invertebrate and fish community structure), physical (substrate grain size), and chemical (metals, pH, conductivity, and alkalinity) variables was conducted at 5 of the 10 sites. Prior to the reclamation effort the stream was nearly devoid of aquatic life above Hwy 2 for a distance of approximately 2 miles due to extremely low pH (<3) and elevated levels of calcium, magnesium, iron, zinc, aluminum, copper, strontium, boron, and cobalt. State water quality standards for zinc, copper, and cadmium were exceeded. Fish were present at reference sites (largemouth bass, white crappie, bluegill, minnows, and darters) but were absent at sites impacted by acid mine drainage within the project boundaries. Benthic invertebrates were similarly impacted. Reclamation activities were initiated late in 1991 and continued through 1995. Significant recovery of water quality, fish, and invertebrate communities was observed following the reclamation. Both chemical and biological approaches were useful in monitoring the recovery of the aquatic system following the watershed reclamation.

INTRODUCTION

The Clean Water Act (originally the Federal Water Pollution Control Act of1972; amended in 1977 and 1987) is the primary regulatory authority used in the United States to protect aquatic life from contaminant exposures associated with industry and mining (Hurdiburgh 1995). Water quality criteria, developed using single species laboratory toxicity data, establish maximum levels of individual toxic substances which are believed to be protective of aquatic life.

However, this water quality based approach is not always protective of aquatic life in natural ecosystems (LaPoint et al. 1989). In many cases, organisms are exposed to mixtures of contaminants which are not considered in water quality criteria (Kimball and Levin 1985). Further, the chemical form or ionized state of chemicals are frequently altered by the environment; such fluctuations are not always revealed in a water-quality based monitoring program (Chapman et al. 1992). In addition, secondary biological effects can occur due to alteration in competition, predation, or grazing (Giesy et al. 1979). These effects are difficult to predict using laboratory toxicity data or chemistry analysis alone.

Thus, biological assessment approaches are frequently used to measure the direct impacts of industrial and mining wastes on aquatic ecosystems (EPA 1994). Direct measures of population and community structure of invertebrate and fish communities can provide an in-situ, integrated assessment of the effects of multiple chemicals on the environment. These measures provide direct assessments of the resources which we seek to protect, and thus can be more direct, interpretable, and cost-effective.

In 1977 the Surface Mining Control and Reclamation Act (SMCRA) was established to permit recovery of abandoned coal mines in the United States (Starnes 1996; U.S. Office of Surface Mining 1996). Acid drainage from abandoned coal mines represents a significant threat to aquatic resources due to the effects of low pH and increased metals such as copper, cadmium, silver, manganese, and zinc.

The West Branch of the Middle Fork of Tebo Creek, located in Southwest Missouri, drains approximately 1200 acres of abandoned coal surface mine properties located on private lands approximately 12 miles northeast of Clinton, MO. This tributary is a major hydrologic input to Truman Reservoir which is recognized as one of the most significant sport fisheries and recreational areas of the Midwest. Historically, leachates from the mining site have resulted in numerous fish kills in the stream. In addition, several acidic impoundments existed which represented additional sources of pollution to Truman Reservoir.

Thus, the Abandoned Mine Lands Section, Land Reclamation Program, Missouri Department of Natural Resources (DNR), initiated the Tebo Creek Reclamation Project in 1991 to minimize current and future impacts of the site. This reclamation project involved recovery of 331 acres of acid-forming spoils, 92 acres of coal refuse, and 13 acres of acid impoundments. In addition, approximately 30 acres of wetlands were constructed to improve water quality. This paper describes a cooperative research project conducted between the Land Reclamation Division of the DNR and the Columbia Environmental Research Center (CERC), Biological Resources Division, USGS, Columbia, MO, USA. The project was conducted to measure the success of the watershed reclamation effort and to compare the relative utility of using chemical versus biological approaches as indicators of stream recovery.

MATERIALS AND METHODS

Site descriptions

Sampling stations for the Tebo Reclamation Project are illustrated in Figure 1 and described in Table 1. Site 1 was immediately north of County Road NE 880, and served as an upstream reference station. Station 2 was immediately south of Road NE 880, and represented a major source of surface-mine runoff. Stations 2, 3, and 4 were located within the immediate area of the reclamation. Station 5 was located at Hwy 2, which represents the lower end of the physical reclamation effort. Stations 6, 7, 8, and 9 were located downstream of the reclamation site and represented the stream recovery zone (Figure 1; Table 1). Site 11, located approximately 5 miles southwest of the reclamation area on Sand Creek (County Road NE 301) served as the reference location for estimating undisturbed conditions.

Quarterly water quality assessments

A total of 10 sites were monitored for baseline water quality (Table 1; Figure 1). Dissolved oxygen, temperature, pH, conductivity, and alkalinity were monitored.

Annual biological assessments

On an annual basis intensive biological, physical, and chemical measures were performed at 5 of the 10 water quality sites following procedures outlined in EPA (1994). Measures included benthic invertebrate community structure, fish community structure, substrate grain size, pH, alkalinity, conductivity, and metals.

At each site 5 replicate invertebrate samples were taken from a pool habitat. A stovepipe sampler (30-cm diameter) was driven into the substrate to a depth of approximately 10 cm. Substrates, organic matter, and invertebrates were removed using a fine net and transferred to a WILDCO benthic sieve bucket (535 um mesh) and washed to retain invertebrates. All invertebrate samples were preserved in 90% ethanol until identification in the laboratory. At each site 5 replicate substrate samples were taken using a 15-cm diameter stovepipe sampler. Materials were wet-sieved to 5 size classes (<0.063 mm, 0.063-0.500 mm, 0.50-2.00 mm, 2.00-6.3 mm, 6.3-25.4 mm, and >25.4 mm) and then weighed to determine relative contribution of each fraction. Weights were determined to the nearest g.

At each benthic community assessment site a fish community assessment was also conducted. A standard pool area at each site (approximately 400 m^2 area) was seined (3 mm mesh) one time. Fish were identified to species, enumerated, and returned to the stream. Water quality was determined at each benthic/fish collection site as described above for the quarterly water quality monitoring. Additionally, aqueous metals were determined. Samples were filtered using Nucleopore Polycarbonate Membranes (0.4 um pore size) and a polysulfone filtration apparatus. Samples were then acidified to pH<2 using ultra-pure HNO_3 and refrigerated until analysis by ICAP analysis.

Table 1. Description of sampling sites used in the study. For additional spatial orientation refer to Figure 1.

Site	Sample type[1]	Sample Zone
1	B/F/WQ	reference
2	WQ	impact
3	WQ	impact
4	WQ	impact
5	B/F/WQ	impact
6	WQ	recovery
7	B/F/WQ	recovery
8	B/F/WQ	recovery
9	WQ	recovery
11	B/F/WQ	reference

[1] Benthic (B), fish (F), and water quality (WQ) samples, respectively.

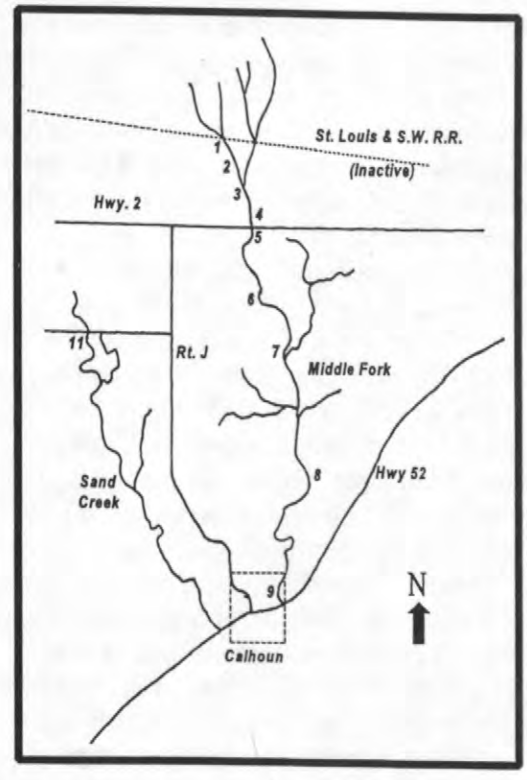

Figure 1. Map showing spatial distribution of sites rom table 1.

RESULTS AND DISCUSSION

Prior to the restoration effort the stream was nearly devoid of aquatic life north of Highway 2 (site 5) due to high levels of acidity and dissolved metals. Fish were absent, and the invertebrate community was dominated by only a few extremely tolerant species of Chironomidae. Water quality conditions were extremely degraded from station 1 downstream to station 6 (1 mile N of County Road NE 1130; approximately 2 miles south of Hwy 2).

In August 1991, at the onset of the reclamation project, pH levels at sites 2, 3, 4, 5, and 6 were less than pH 3.6, which is well below levels supportive of fish and invertebrates (Figure 3; Table 2). The pH at sites 1 and 11 (reference sites) and sites 7, 8, and 9 (downstream recovery zone) exceeded pH of 6.5 which is typical of normal, ambient conditions for the area. Sites 2 and 5, at the upper and lowermost portions of the reclamation area (Figure 1) exhibited low alkalinity and high levels of calcium, magnesium, iron, zinc, aluminum, copper, strontium, boron, and cobalt; Missouri state water quality standards for zinc, copper, and cadmium were exceeded (Table 2). Impacted sites typically contained high levels of iron precipitates, which imparted an orange, rust-colored hue to bottom sediments. Metal levels at downstream sites (7 and 8) and Sands Creek (site 11) were much lower. Fish were absent at sites 2, 3, 4, and 5 at this time. In contrast, many fish species, including largemouth bass, white crappie, bluegill, minnows, and darters were found at sites 7,8, 9, and the Sands Creek site (reference site 11) (Figure 1). Reclamation activities were initiated late in 1991 and continued through 1995. The relative success and rate of progression of the reclamation is illustrated by the temporal pH data from site 5, which is located at the extreme southern edge of the reclamation site (Figure 2). The pH of site 5 remained less than 4 until January of 1993.

At this point, significant progress in the reclamation effort had been made,

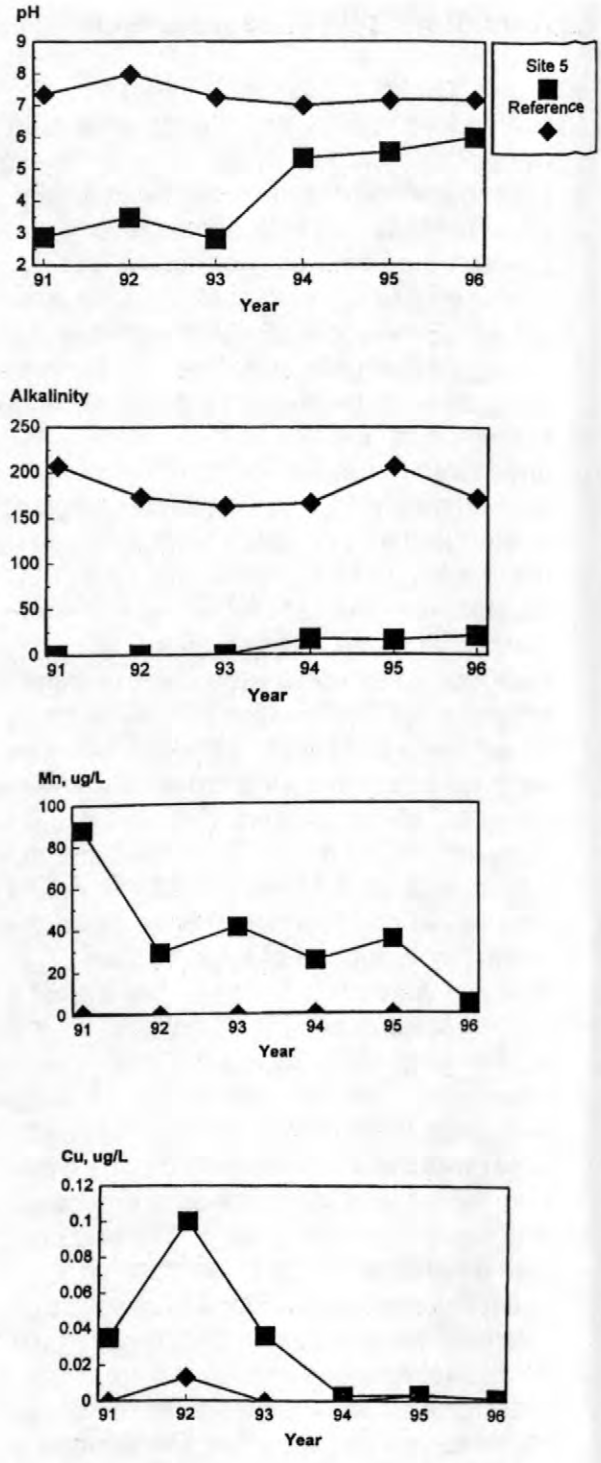

Figure 2. Trends in water quality at site 5 compared to the reference site.

Table 2. Changes in water quality parameters at 4 sites over the 5-yr Tebo Creek Study.

Site	Year	pH	alkalinity (mg/L)	Zn (ug/L)	Cd (ug/L)	Cu (ug/L)
5 (lower end site)	1991	2.87	0	510	34	34
7 (4 miles downstream)		6.87	90	0	0	0
8 (6 miles downstream)		7.21	117	0	0	0
reference		7.35	206	0	0	0
5 (lower end site)	1992	3.50	0	1,300	15	100
7 (4 miles downstream)		7.05	83	0	0	110
8 (6 miles downstream)		6.91	31	0	0	80
reference		7.98	173	0	0	10
5 (lower end site)	1993	2.82	0	6,600	50	40
7 (4 miles downstream)		7.12	111	100	0	0
8 (6 miles downstream)		7.25	98	0	0	0
reference		7.25	163	0	0	0
5 (lower end site)	1994	5.33	17	1,000	5	3
7 (4 miles downstream)		6.58	98	0	1	0
8 (6 miles downstream)		6.69	61	0	1	0
reference		6.99	166	0	1	0
5 (lower end site)	1995	5.53	17	1,600	8	4
7 (4 miles downstream)		6.96	91	0	0	6
8 (6 miles downstream)		6.93	83	0	0	2
reference		7.16	208	0	0	3
metals criteria				100	12	20

which was reflected in a dramatic increase in the pH of water. However, in 1993 many large floods occurred from May through August which produced excessive erosional runoff. Significant damage was received at the site, including damaged gabions, side-cutting of channels, and surface erosion. At site 5 pH levels again declined until remediation efforts were completed at the end of 1994. Since October 1994, pH levels at site 5 have remained at pH 5 or higher. Levels of dissolved metals, including manganese and copper are also decreasing following the restoration (Figure 2; Table 2).

Most recent chemical and biological sampling was conducted in October 1995. Significant recovery of water quality, fish, and invertebrate populations was observed. Although the pH at site 5 was only 5.5, fish (green sunfish) were observed for the first time in over 5 years. The pH at site 5 was actually lower in October 1995 than previous samples in January, March, June, and August which probably is due to a combination of extremely low water conditions late in 1995 and a continuing seep located above Hwy 2. This problem is continuing to be investigated.

Data from 1991 to 1995 were combined in Figure 3 to demonstrate the relationship between biological communities and pH. The data indicate that fish cannot tolerate pH levels below pH=6.5. As seen in Figure 3, the number of fish and invertebrate species increases dramatically at pH 6.5. However, in some cases species richness is still low such as at site 1 where fish recolonization is restricted. The highest diversity of both fish and invertebrates was observed at the Sands Creek reference site (site 11). However, as the restoration progresses, additional fish and invertebrate species are expected to move into the downstream sites below the reclaimed watershed.

Bivariate correlations were used to compare the relationship between various biological and chemical variables (Table 3). High negative correlations were observed between pH and cadmium (r=-0.82) and copper r=-85) due to the increased solubility of these metals at low pH. Fish and invertebrate species richness were positively correlated with pH (r=0.54 and 0.59, respectively) and negatively correlated with Cd (r=-0.48 and -0.47, respectively) and Cu (r=-0.45 and -0.38) (Table 3).

Canonical correlation was also used to discriminate between the various sites by comparing a multivariate dataset of 4 biological variables (fish total numbers, fish species richness, invertebrate total numbers, invertebrate species richness)

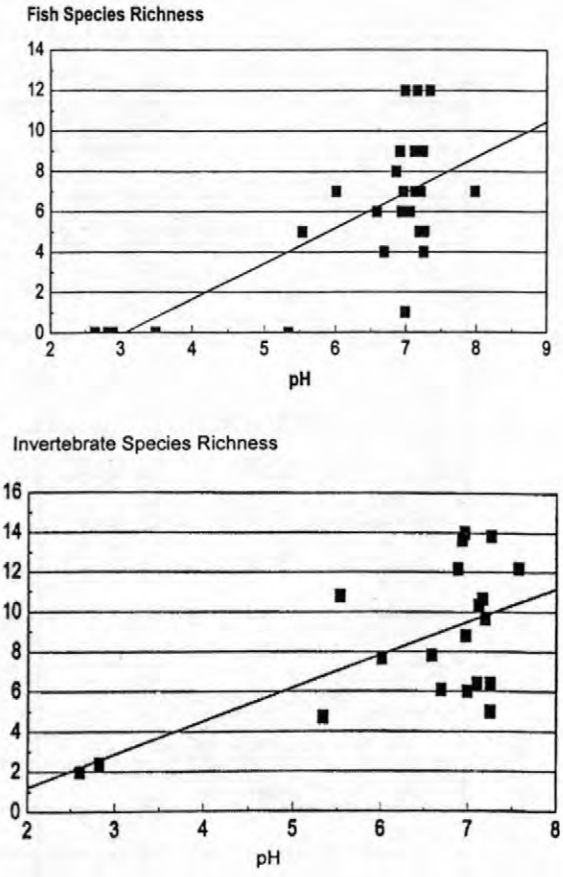

Figure 3. Relationships between fish and invertebrate species richness and pH over the 5 - yr study duration.

and fourteen chemical measures (pH, dissolved oxygen, conductivity, hardness, alkalinity, Al, Cd, Cr, Cu, Fe, Mg, Mn, Mo, and Pb) (e.g. total 18 variables) combined across the entire study period (Figure 4). This multivariate approach clearly distinguished between site 5 (highly impacted) and the other sites. Sites 7 and 8, located in the lower impact zone, grouped together but were distinct from the two reference sites (site 1 and Sands Creek) due to the intermediate effects of ow pH and metals. As recovery progresses, the sites should converge as chemical and biological conditions continue to improve.

Neither chemical nor biological approaches were clearly superior in this study. At extremely impacted sites, the biological variables could not distinguish between sites due to the total absence of species. In this case pH alone was effective in monitoring restoration success. As pH increased, however, both chemical and biological assessment were useful. Chemical assessments must continue to be relied upon because they are clearly tied to regulatory limits. However, analysis of metals is expensive and can take several months to complete. Biological measures, however, can be done rapidly in the field if taxonomy is held to a basic level. Increased resolution can be achieved by archiving samples for later identification to a higher level of taxonomic resolution. However, increased taxonomic resolution can come at a higher monetary and time cost that approaches that of metals analysis. However, when water quality conditions improve, greater resolution of both chemical and biological approaches are necessary to determine if remaining impacts are caused by continued mining impacts or other factors such as temperature, dissolved oxygen, physical habitat, or hydrologic limitations. For example, a few remaining acid seeps and over-razing near the Tebo Creek Reclamation Site is known to be contributing to additional water quality impacts to the project site. Multi-disciplinary chemical, biological, and hydrologic assessments can be used to isolate and identify multiple sources of impacts and are necessary to insure that reclaimed aquatic resources meet their optimum potential.

Table 3. Bivariate correlations between selected biological and chemical variables combined over the 5-yr study.

	Fish #sp	inv #sp	pH	alk	Cd	Cu
fish#sp	---					
inv.#sp	.19	---				
pH	.54	.59	---			
alk	.32	.13	.75	---		
Cd	-.48	-.47	-.82	-.49	---	
Cu	-.45	-.38	-.85	-.08	.88	---

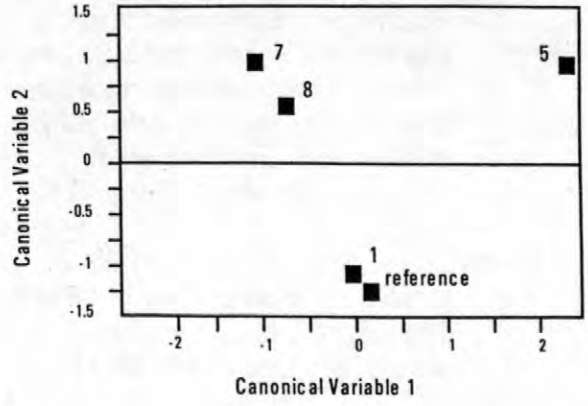

Figure 4. Canonical correlation of eighteen variables used to discriminte between sites at the Tebo Creek Project. Data are combined over the 5-yr study.

SUMMARY

The Tebo Creek Reclamation Project has resulted in significant improvement in water quality and fish populations in the West Fork of Tebo Creek. In 1995 fish populations were observed within portions of the reclamation occurred within one year of pH stabilization. Some small seeps continue to contribute acid to the stream. However, the restoration effort has solved the major problems impacting the stream. Both chemical and biological approaches were useful in monitoring the recovery of stream resources; the relative value of each approach, however, depended on the severity of impact and the stage and needs of the assessment.

ACKNOWLEDGMENTS

The authors thank Robin Calfee, Doug Hardesty, Phil Lovely, Linda Sappington, and David Whites for their assistance in this study.

REFERENCES

Chapman, P.M., E.A. Power, and G.A. Burton, Jr. 1992. Integrative assessments in aquatic ecosystems. Pp. 313-340 in G.A. Burton, ed., Sediment Toxicity Assessment, Lewis Publishers, Chelsea, MI.

Giesey, J.P. Jr., H.J. Kania, J.W. Bowing, R.L. Knight, S. Mashburn, and S. Clarkin. 1979. Fate and biological effects of cadmium introduced into channel microcosms. EPA 6002/3-79-039, U.S. Environmental Protection Agency, Athens, GA.

Kimball, K.D., and S.A. Levin. 1985. Limitations of laboratory bioassays: The need for ecosystem-level testing. Bioscience 35:165-171.

Hudiburgh, G.W. Jr. 1995. The Clean Water Act. Pp. 717-734, in G.M. Rand, ed., Fundamentals of Aquatic Toxicology: Effects, Environmental Fate, and Risk Assessment. Taylor and Francis Publishers, Washington, DC. 1125 pp.

LaPoint, T.W., J.F. Fairchild, E.E. Little, and S.E. Finger. 1989. Laboratory and field techniques in ecotoxicological research: strengths and weaknesses. Pp. 239-255, in A. Boudou and F. Ribeyre, eds. Aquatic Ecotoxicology: Fundamentals Concepts and Methodologies, Vol. II. CRC Press, Boca Roton, FL.

Starnes, L.B. and D.C. Gasper. 1996. Effects of surface mining on aquatic resources in North America. Fisheries 21(5): 24-26.

U.S. Environmental Protection Agency. 1994. Rapid Bioassessment Protocols for Use in Streams and Rivers: Benthic Macroinvertebrates and Fish. EPA 444/4-89-001.

U.S. Office of Surface Mining. 1996. 1996 Annual Evaluation Report on the Missouri Regulatory and Abandoned Mine Reclamation Programs: January 1, 1996 through September 30, 1996. Public Affairs Office, Office of Surface Mining, U.S. Dept. of the Interior, Washington, DC. 19 pp.

Author information: James F. Fairchild, Barry C. Poulton, and Thomas E. May are located at the Columbia Environmental Research Center, Biological Resources Division, USGS, 4200 New Haven Rd., Columbia, MO, 65201. Stuart Miller is located at the Missouri Dept. of Natural Resources, Abandoned Mine Lands Program, Division of Environmental Quality, P.O. Box 176, Jefferson City, MO, 65102.

Factors Explaining the Distribution and Site Densities of the Neosho Madtom (*Noturus placidus*) in the Spring River, Missouri

By Mark L. Wildhaber, Christopher J. Schmitt, and Ann L. Allert

ABSTRACT

The Neosho madtom, a Federally-listed threatened species endemic to the Arkansas River system, is presently restricted to selected mainstem reaches of the Neosho, Cottonwood, and Spring rivers in Missouri, Kansas, and Oklahoma. These rivers are affected by anthropogenic factors such as municipal waste discharges and agricultural runoff. The Spring River also drains the Tri-State Mining District, where zinc-lead mining occurred in the past. Our objective was to assess effects of water quality degradation, due mainly to mining-related contaminants, on aquatic communities of the Spring River by comparison with those of the Neosho-Cottonwood system. We found higher densities of *N. placidus*, finer-textured riffle substrate, and lower concentrations of cadmium and lead in benthic macro-invertebrates in the Neosho-Cottonwood system than in the Spring River. In the Spring River, we found no substrate differences between sites with and without *N. placidus*; however, taxonomic richness of the benthic macro-invertebrate and fish communities were greater, densities of *N. placidus* and other fishes were higher, and concentrations of zinc and cadmium in benthic macro-invertebrates were lower at sites with *N. placidus*. Pore waters from three sites in the Spring River system were toxic to *Ceriodaphnia dubia*; mortality was greater than 80%, and there was no reproduction. Concentrations of zinc and cadmium in pore waters and sediment were high at these sites relative to non-toxic sites, and had SEM/AVS ratios considered potentially toxic. Toxicity tests, concentrations of metals in benthic macro-invertebrates, toxic unit (U_T) modeling of pore waters, and an empirical habitat model support a hypothesis of contaminant involvement in the distribution of *N. placidus*.

INTRODUCTION

The Federally-listed (threatened) Neosho madtom (*Noturus placidus*) is a small ictalurid (generally <75 mm total length) endemic to parts of the Arkansas River system. *N. placidus* is currently found in the mainstems of the Neosho, Cottonwood, and Spring rivers in Kansas, Missouri, and Oklahoma, where it inhabits reaches with slow to moderate flow, moderate depths, and unconsolidated pebble and gravel substrate (Moss 1983). The Spring River and its tributaries drain the Tri-State Mining District, where abandoned zinc (Zn)-lead (Pb) mines and the weathering of tailings has caused elevated concentrations of cadmium (Cd), Pb, and Zn in water, sediment, and biota; some tributaries (Short, Turkey, Center, Willow, and parts of Shoal Creeks) are heavily contaminated (Barks 1977; Schmitt et al. 1993; Wildhaber et al. in press a). *N. placidus* population densities are much greater in the Neosho-Cottonwood system than in the Spring River (Wilkinson et al. 1996; Wildhaber et al. in press b). The reaches inhabited by most Spring River Neosho madtoms are upstream of most current sources of mining-derived pollution in the watershed (Barks 1977; Wilkinson et al. 1996).

METHODS OF STUDY

Our overall objective was to assess the natural and anthropogenic factors that may be limiting populations of riffle-dwelling benthic fishes in the Spring River, especially the Neosho madtom. Our basic approach was to quantitatively

characterize the riffle environment inhabited by and aquatic communities found with *N. placidus* in the Neosho-Cottonwood system, where no mining has occurred; and to use this information as a baseline against which to compare the mining-affected Spring River system.

We developed an empirical model based on 1991 physical habitat, water chemistry, and nutrient measurements from the Neosho-Cottonwood system to predict 1994 *N. placidus* densities in the Neosho, Cottonwood, and Spring rivers (Wildhaber et al. in press b). By comparing 1991 and 1994 data; 1994 predicted vs. observed densities; and the results of toxicity tests and other measurements, we assessed the extent to which basic environmental quality, metals contamination, or both limited *N. placidus* in the Spring River. Along with *N. placidus* densities, our measurements included: aquatic community (i.e., riffle-dwelling fishes and benthic macro-invertebrates); physical habitat; water chemistry (including nutrients); metals in surface waters, pore waters, sediments, and invertebrates; and porewater toxicity tests conducted with *Ceriodaphnia dubia*. Here we present an overview of our investigations; details of methods and results are presented elsewhere (Wilkinson et al. 1996; May et al. 1997; Schmitt et al. 1997; Allert et al. 1997; Wildhaber et al. 1997, in press a; in press b).

Field and Laboratory Procedures

Study sites were located on the Neosho and Cottonwood rivers, and on the Spring River and several of its tributaries. Measurements of aquatic community, water quality (including contaminants and nutrients), and habitat were made at 33 sites spanning both river systems during late summer and early fall, 1994. In 1995, 12 sites in the Spring River system were re-sampled, and porewater sampling and toxicity testing were conducted (Figure 1). Sediment and pore water from a reference site in another watershed (Tavern Creek, Site 13) were also evaluated.

At each fish collection site, 3-5 transects were established to sample all potential *N. placidus* habitat (i.e., the total length of gravel bars to a maximum water depth of 1.25 m). On each transect, 3-5 stations spaced equally across the stream were sampled for fish, benthic macro-invertebrates, and substrate. Fish collected by kick-seining an area of 3.0-m × 1.5-m using a 3-mm (square) mesh. Fishes were identified in the field and released. Benthic macro-invertebrates were collected with a Hess sampler (0.1-m^2 area, 0.3-mm mesh collection bag). Benthic macro-invertebrate samples were preserved and returned to the laboratory for sorting and identification to the lowest taxonomic level possible without mounting individual specimens (generally genus, except for the Chironomidae). Substrate was collected with a cylindrical grab sampler and sieved and weighed in the field; fines (<2 mm) were returned to the laboratory for further textural analysis. Current velocity and water depth were also measured at each station.

Dissolved oxygen, pH, conductivity, and temperature were measured and a surface grab sample for nutrient and elemental analyses was collected at the center transect of each site. Additional non-quantitative samples of benthic macro-invertebrates were collected for analyses of elemental contaminants. Sediment was collected from depositional areas for chemical analysis and porewater extraction. Most metals were analyzed by inductively coupled argon plasma (ICAP) emission spectroscopy; Pb and Cd in some samples were analyzed by atomic absorption spectroscopy (AAS).

Pore water was extracted under pressure (N_2) by the method of Carr and Chapman (1995). Porewater samples were serially diluted and tested for toxicity with *Ceriodaphnia dubia*; tests ran for 7 d (U.S. EPA 1989). Aliquots of the composited sediments were collected for elemental analyses by ICAP and for acid volatile sulfide (AVS) and simultaneously extracted metals (SEM). Pore water was also analyzed by ICAP-ES, AAS (Pb and Cd), and ICAP-mass spectrometry.

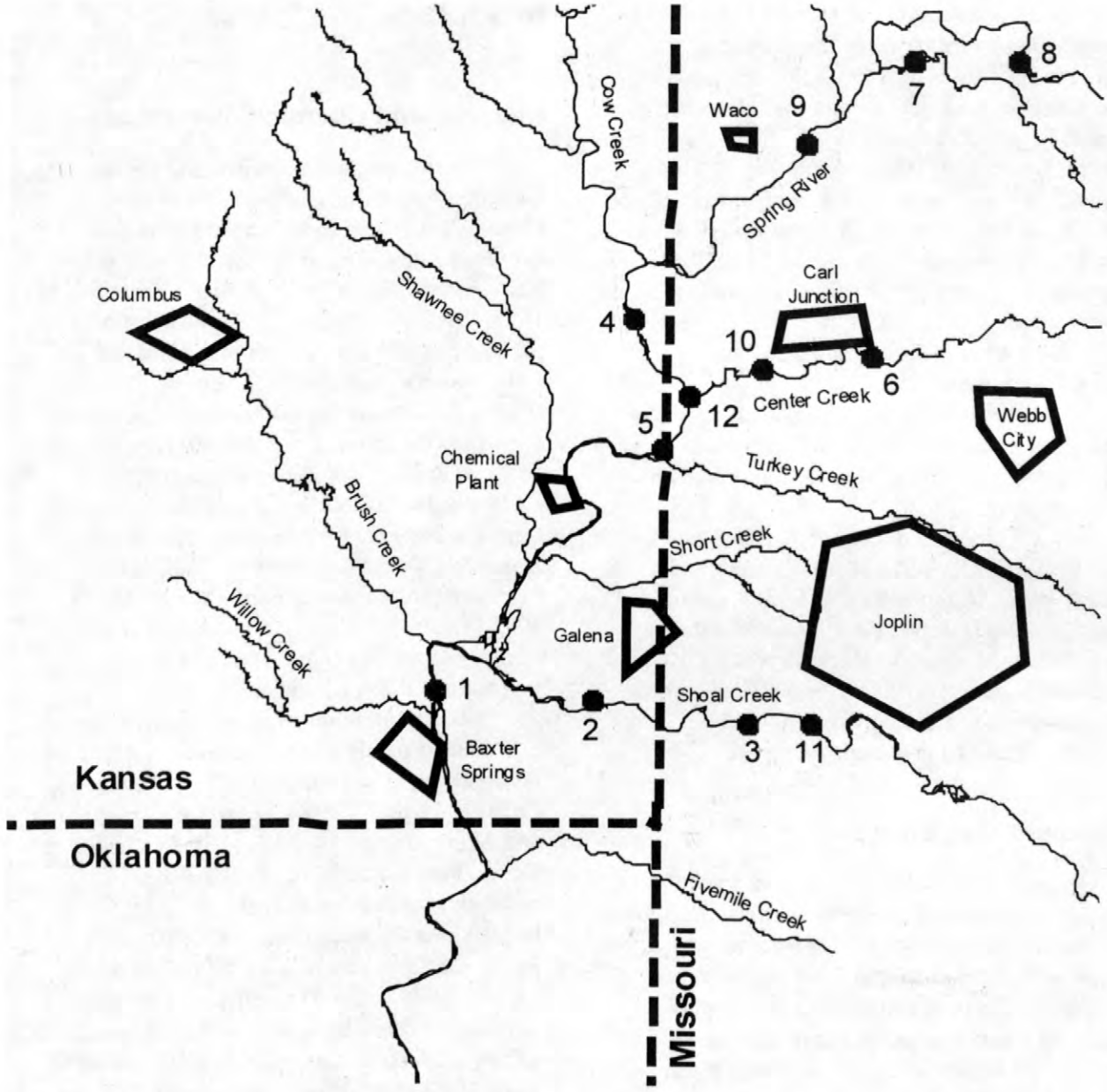

Figure 1. Spring River sites sampled in 1995.

Toxic Units and AVS Modeling

Relative ecological risks from sediment metals were evaluated using the toxic unit model of Wildhaber and Schmitt (1996). A toxic unit (U_T) is defined as the ratio of the estimated concentration of a contaminant in the pore water of a test sediment (C_{wp}) to the estimated chronic aquatic toxicity of that contaminant (C_{wps}):

$$U_T = C_{wp} / C_{wps}$$

The U_T for all measured contaminants (here, just metals) are summed to obtain a total toxicity estimate for that sediment.

The AVS model is based on the assumption that under the reducing conditions present in sediment pore waters, sulfides control the concentrations and hence bioavailability of divalent metals. Because the sulfide salts of metals are extremely insoluble; their formation renders the metals biologically unavailable. AVS modeling of porewater concentrations therefore adjusts the

maximum potential porewater concentrations of metals downward based on the amount of AVS present (DiToro et al. 1990). We allocated AVS to metals in weak acid extracts based on the solubility product constants, K_{sp}, of their sulfide salts (Weast et al. 1988). Accordingly, AVS was allocated to metals in the following order: Copper (Cu), Cd, Pb, Zn, nickel (Ni), and iron (Fe); i.e., FeS is the most soluble sulfide and CuS the least. An equimolar amount of sulfide was allotted to each metal, in the order of their K_{sp}, until either all AVS was accounted for or all SEM were considered sulfide-bound.

The following relative potential toxicity values (i.e., one toxic unit) were obtained or computed from chronic toxicity information for each element, as follows: Cu (5.6 µg/L, U.S. EPA 1980), Cd (computed, U.S. EPA 1984a), Pb (computed, U.S. EPA 1984b), Zn (computed, U.S. EPA 1987), Ni (computed, U.S. EPA 1986), and Fe (1000 µg/L, U.S. EPA 1976). Because the computed values are hardness-dependent, we used hardness values typical of the Neosho-Cottonwood and Spring River systems (i.e., 150 mg/L as $CaCO_3$) in our computations.

Statistical Analysis

We analyzed the data at the level of site averages to assess differences between the Neosho-Cottonwood and Spring River systems, and among Spring River sites with and without Neosho madtoms. We calculated site densities of *N. placidus* and, as a group, the riffle-dwelling fishes that could be considered benthic competitors of *N. placidus*, by dividing the total number of Neosho madtoms or benthic fish competitors collected at a site by the total area sampled with the kick seine. Determination of benthic fish competitors was based on known habitat preferences and feeding habitats of each species as described by Pflieger (1975). We also computed fish species rarefaction (Hurlbert 1971) for each site. Statistical methods included analysis of variance, correlation analysis, multivariate analysis of variance, principal componants analysis, and discriminant analysis.

RESULTS

Physical and Chemical Variables

Substrate, water quality, and contaminant concentrations differed between the Neosho-Cottonwood system and the Spring River and between Spring River sites with and without Neosho madtoms (Allert et al. 1997; Schmitt et al. 1997; Wildhaber in press b). Mean substrate particle diameter was smaller in the Neosho-Cottonwood system than in the Spring River (Figure 2). Among the mining-derived metals of concern in the Spring River system, only Zn occurred at ICAP-detectable concentrations in surface waters and Zn concentrations was generally higher in the tributaries than in the mainstem. Detectable levels of Zn, Cd, Pb, Cu, Fe, and Ni were found in pore waters at all sites in 1995 (Table 1). Concentrations of all elements were higher in the tributaries except for Ni, which was highest at Sites 1 and 4.

Concentrations of mining-derived elements in sediments paralleled those found in surface and pore waters. Concentrations of Pb (2120 µg/L), Zn (13800 µg/L), Cd (84.1 µg/L), Cu (51.2 µg/L), and Al (16000 µg/L) were 3- to 10-fold higher at Site 12 than any other site by ICAP-ES. Sediments collected at sites above Center Creek had the lowest concentrations of Cd (0 - 2.88 µg/L), Cu (5.74 - 16.7 µg/L), Pb (6.77 - 34.4 µg/L), and Zn (103 - 615 µg/L). Concentrations of Ni in sediments from Sites 1, 4, 5, 7, and 12 were similar (21.8 - 29.1 µg/L). AVS and SEM results for sediments were consistent with ICAP results (Table 2). Total toxic units (mostly attributable to Pb and Zn) were greatest at Sites 5 and 12 (Table 3), at the mouths of Turkey and Center creeks, respectively (Figure 1).

Concentrations of Cd, Mn, Ni, and Pb were higher in benthic macro-invertebrates from the Spring River than the Neosho-Cottonwood system; however, Mg and Sr concentrations were higher in the Neosho-Cottonwood system (Figure 3). Concentrations of Ba in benthic macro-invertebrates were significantly lower and concentrations of Cd and Zn were significantly higher at sites without *N. placidus* than at sites with.

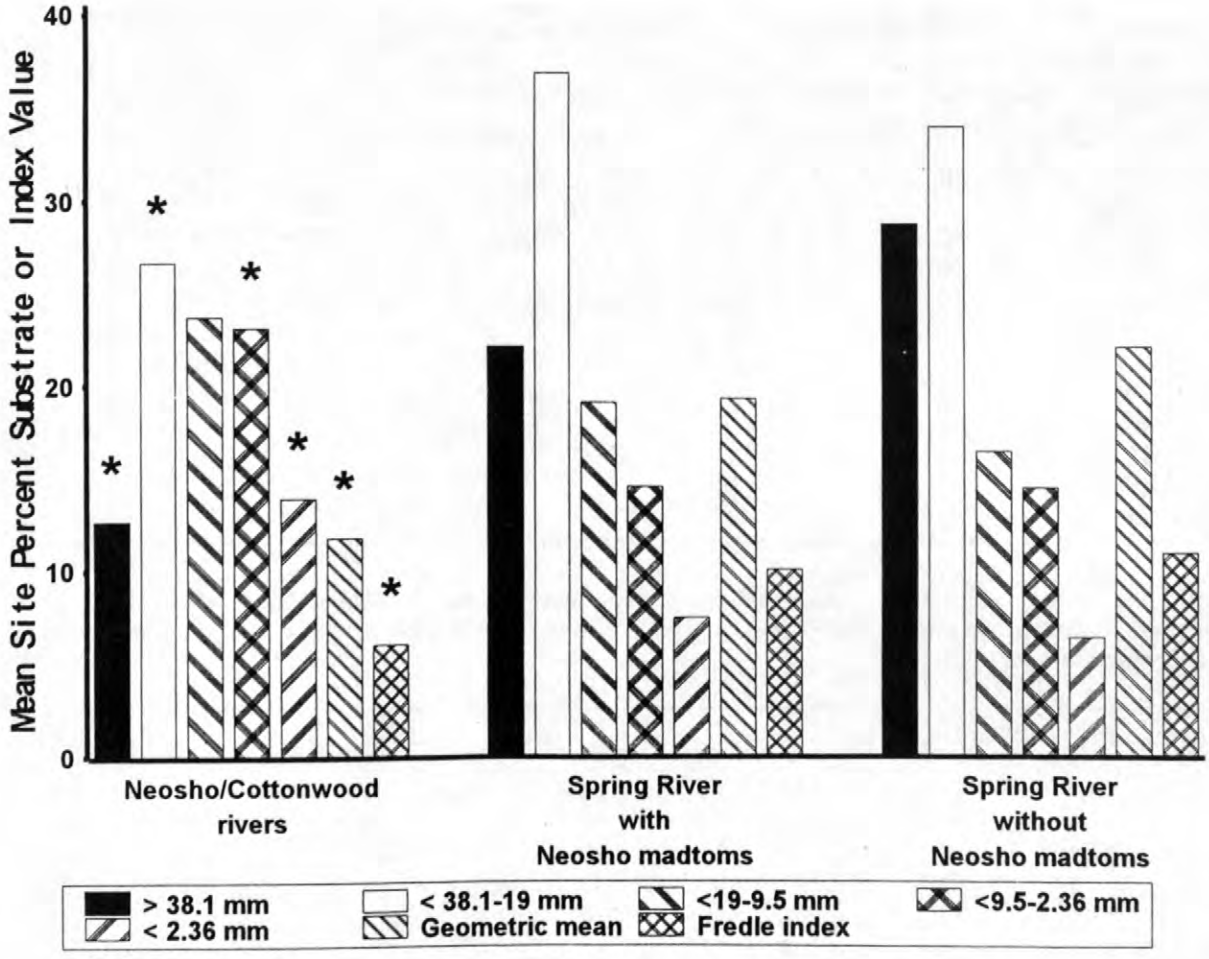

Figure 2. Mean proportion by weight of substrate in each of five size categories, and geometric mean, and fredle index (McMahon et al. 1996) for combined size categories. None of the substrate measures showed a significant ($P > 0.05$) difference between Spring River sites with and without Neosho madtoms based on analysis of variance (ANOVA). '*' represents significant ANOVA differences in substrate measures between the Neosho-Cottonwood system and the Spring River.

Biological Variables

Neosho madtoms were found at many Neosho-Cottonwood sites and at 8 of the 10 uppermost Spring River sites sampled in 1994 (Wildhaber et al. in press a, in press b). No Neosho madtoms were found in any Spring River tributaries. Results of 1995 fish sampling in the Spring River were similar--Neosho madtoms were present at the 4 mainstem sites sampled (all four had yielded Neosho madtoms in 1994), and none were found in tributaries (Allert et al. 1997). In benthic macro-invertebrate samples, the uppermost Spring River sites also supported the greatest numbers of Ephemeroptera, Plecoptera, and Trichoptera (the EPT taxa) (Wildhaber et al. in press b). The lowest numbers of EPT taxa were found at contaminated sites on Spring River tributaries, the benthic macro-invertebrate faunas of which were dominated by chironomids and oligochaetes. The reduced representation of EPT taxa and the dominance of Chironomidae and Oligochaeta at these sites suggest that water or habitat quality is degraded.

There were both similarities and differences in fish species densities and fish community composition between the Neosho-Cottonwood and Spring River systems. Fish rarefaction was significantly lower in the Neosho-Cottonwood system than in the Spring River system, and

Table 1. Dissolved concentrations (µg/L) of 8 elements in porewaters as measured by ICAP-MS ([a]) and Zeeman atomic absorption ([b]) Porewaters were collected from depositional areas at each site. TC represents Tavern Creek.

Site	Ca	Cd[a]	Cd[b]	Cu[a]	Cu[b]	Fe	Mg	Ni	Pb[a]	Pb[b]	Zn
1	171500	3.2	2.9	1.8	2.1	7760	24500	15.0	2.0	1.8	467.0
2	44500	1.4	1.2	2.5	2.6	75.0	3370	5.6	0.69	0.70	87.0
3	43700	1.0	0.97	13.0	9.5	15.0	3290	7.2	1.3	1.2	77.0
4	60300	0.44	0.38	1.6	1.9	38.0	8250	9.0	0.48	0.61	19.0
5	57500	0.70	0.71	1.6	1.3	32.0	7650	6.3	0.90	1.3	28.0
6	43100	0.16	0.24	0.8	0.62	2240	2660	4.9	0.75	0.69	197.0
7	43000	0.39	0.33	1.2	1.6	77.0	3050	2.4	0.62	1.0	20.0
8	104700	0.35	0.27	2.6	2.2	14600	7840	6.8	0.70	0.58	19.0
9	39000	0.32	0.23	1.2	1.3	73.0	3070	3.0	0.51	0.43	8.1
10	49500	0.13	0.12	0.88	0.77	49.0	3120	3.6	0.75	0.90	68.0
11	40400	0.27	0.24	1.2	1.1	22.0	2850	2.2	0.9	1.0	36.0
12	46600	2.6	2.3	2.0	2.0	1170	3010	5.7	3.1	2.4	1681
TC	34200	0.68	0.61	1.6	1.4	2780	24200	2.7	0.98	1.0	18.0

Table 2. Percent moisture, loss on ignition (LOI), concentrations of acid volatile sulfide (AVS) and simultaneoulsy extracted metals (SEM) in sediment. AVS are µmol/g dry weight and SEM concentrations are expressed in µg/g dry weight.

Site	% Moisture	LOI	AVS	Cd	Cu	Fe	Ni	Pb	Zn
1	28.06	1.5	2.10	3.60	2.30	1490	9.0	78.0	573
2	30.72	1.2	0.85	6.20	5.10	2640	4.9	94.0	756
3	36.05	0.8	0.06	2.50	1.40	797	4.2	71.0	777
4	21.89	2.3	0.16	0.39	1.40	1570	4.4	5.6	75.0
5	19.75	1.2	0.53	2.00	1.60	2430	4.8	42.0	355
6	41.04	1.5	6.00	21.0	13.0	3170	6.8	821	3570
7	26.94	1.8	0.50	0.57	1.80	1960	2.4	10.0	60.0
8	24.97	0.7	0.68	0.65	0.75	2940	1.1	4.4	46.0
9	23.48	1.2	0.31	0.18	0.79	1050	1.3	3.3	22.0
10	26.57	0.9	4.80	4.60	1.80	2130	3.0	127	997
11	23.34	0.9	0.04	1.40	1.10	777	4.1	44.0	270
12	40.13	3.2	1.20	108	45.0	13300	20.4	3410	14500
Tavern Creek	21.26	0.8	1.00	0.03	1.10	684	1.0	2.7	4.8

Table 3. Toxic units (U_T).attributable to the indicated element and total toxic units (ΣU_T) at each site in 1995 (see Figure 1).

Site	Cd	Pb	Zn	Ni	Fe	ΣU_T
1	<0.1	<0.1	7.20	0.94	3.7	11.0
2	<0.1	<0.1	11.3	0.05	6.0	17.3
3	<0.1	23.7	9.50	0.03	1.4	34.7
4	<0.1	<0.1	1.40	0.06	5.6	7.02
5	<0.1	<0.1	104	0.09	9.9	114
6	<0.1	<0.1	37.4	0.05	4.6	42.0
7	<0.1	<0.1	0.53	0.03	5.3	5.90
8	<0.1	<0.1	0.08	0.01	8.8	8.90
9	<0.1	<0.1	0.25	0.02	3.4	3.70
10	<0.1	<0.1	12.0	0.03	5.9	17.9
11	<0.1	25.2	5.90	0.06	2.5	33.7
12	43.9	773	584	5.50	19.8	1426
Tavern Creek	<0.1	<0.1	<0.1	<0.1	2.4	2.40

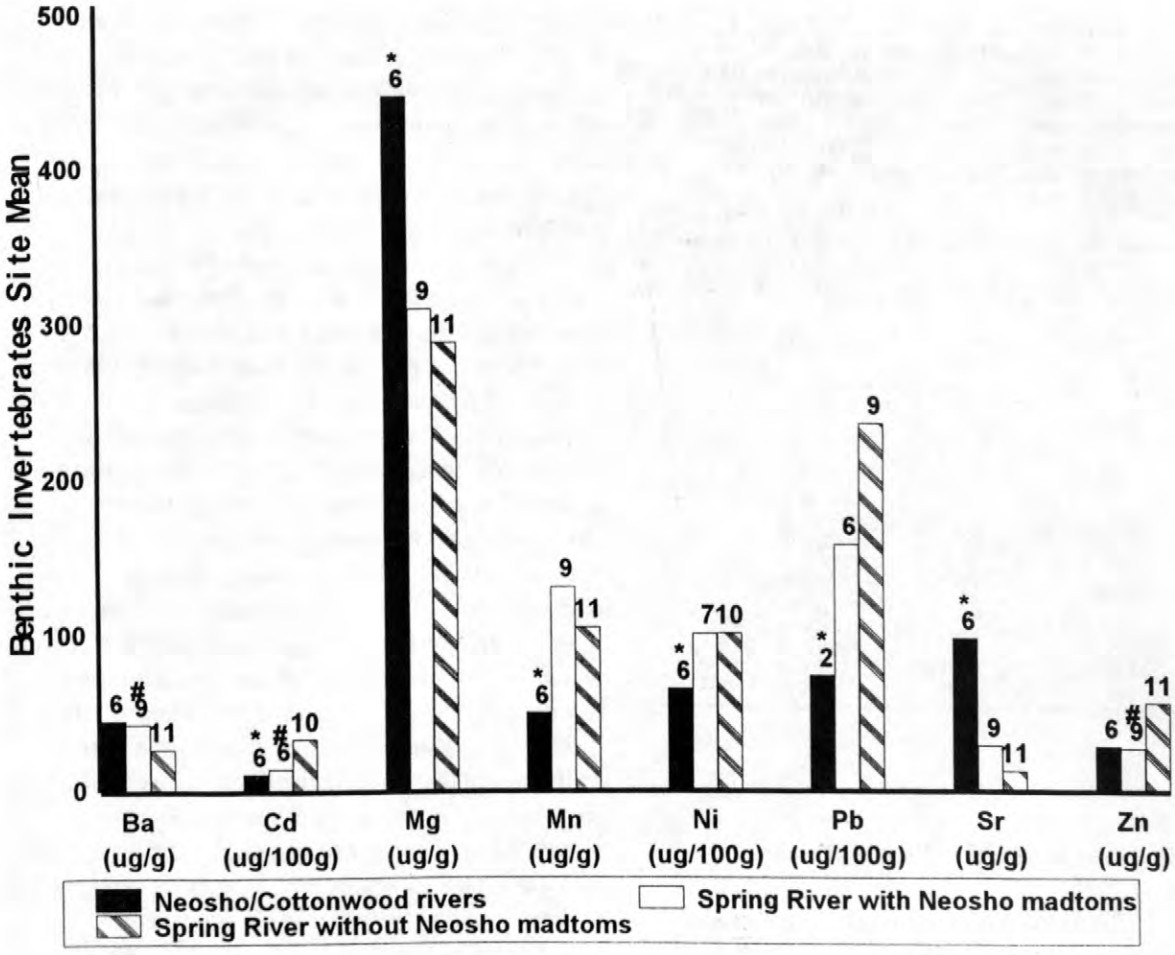

Figure 3. Mean benthic invertebrate tissue elemental concentrations that showed a significant difference ($P < 0.05$ analysis of variance--ANOVA) between the Neosho-Cottonwood system and the Spring River and/or Spring River sites with and without Neosho madtoms. Numbers over bars represent number of sites where the element was found at detectable levels (number of values used to calculate the bar value). Significant differences between Spring River sites with and without Neosho madtoms are represented by '#'. Significant differences between the Neosho-Cottonwood system and the Spring River are represented by '*'.

richness indices for fish species, macroinvertebrates, and the EPT index were significantly greater at Spring River sites with *N. placidus* than at sites without (Wildhaber et al. in press a, b). Pore water from three contaminated Spring River sites (Sites 1, 6, and 12) were toxic to *C. dubia*; survival of adults was >80% at all other sites (Table 4).

Relationships Among Variables

Principal component analysis (PCA) using all variables from both watersheds resulted in the selection of percentages of substrate fines, turbidity, alkalinity, hardness, NH_3, SO_4, Ba, Cu, Mn, Ti, NO_2/NO_3, porewater oxidation-reduction potential, and concentrations of Mg, Sr, Cd, Mn, and invertebrate Ni, which collectively accounted for 59% of the variability in data separating sites in the Neosho-Cottonwood system from those in the Spring River system (Figure 4). Restricting PCA to Spring River sites resulted in the selection of porewater alkalinity, NH_3, turbidity; EPT, and invertebrate Ba and Zn concentrations, which accounted for 81% of the variability in the data

Table 4. Summary of acute toxicity tests (*Ceriodaphnia dubia*) using site waters. Reproduction was calculated according to EPA guidelines. Site 1 - Site 7 and Tavern Creek (TC) were included in Test 1. Site 8 - Site 12 were included in Test 2. W1 and W2 represent well water for Tests 1 and 2, respectively. [a] = 50% dilution water.

Site	Number of replicates	% Survival	Average reproduction
1[a]	10	0	0
2[a]	10	90	29.0
3	10	90	25.6
4	10	100	28.4
5	10	90	22.9
6	9	22.2	0
7	9	100	27.1
8	10	90	19.5
9	10	80	20.4
10	9	100	28.1
11	10	100	25.0
12	10	0	0
TC	10	100	23.9
W1	10	100	24.6
W2	10	100	24.6

separating sites with and without *N. placidus* (Figure 4).

In the Neosho-Cottonwood system and in the Spring River above Center Creek, *N. placidus* densities predicted by the empirical model (see Wildhaber et al. in press b) on the basis of physical habitat attributes, water quality, and elemental analyses did not differ significantly from observed densities. At Spring River sites below Center Creek, however, observed densities were significantly lower than predicted values (Wildhaber et al. in press b; Figure 5).

CONCLUSIONS

Concentrations of mining-derived metals (i.e., Pb, Cd, Zn) were elevated in sediments and pore waters at sites on Shoal and Center Creeks, and at Spring River sites below the confluences of these tributaries. Toxic unit values indicated that some metals were bioavailable in Center and Shoal Creeks, and at sites in the Spring River below Center Creek. Toxicity test results indicated that populations of *N. placidus* could be affected in Center Creek and in the Spring River below Center Creek. Results obtained in 1995 (Allert et al. 1997) corroborated those of the 1994 studies (Schmitt et al. 1997; Wildhaber et al. 1997), which found lower than expected densities of *N. placidus* in the Spring River where contaminants (i.e., Pb, Cd, Zn) were elevated in sediments, pore waters, and benthic invertebrates.

Collectively, our findings of higher *N. placidus* densities, smaller substrate, and lower concentrations of Cd and Pb in benthic invertebrates in the Neosho-Cottonwood system than in the Spring River system suggest that differences in Neosho madtom densities are due both to differences in habitat and to contaminants. In the Spring River, both anthropogenic and natural factors may limit populations of *N. placidus*. Where levels of mining-derived contamination are low, *N. placidus* densities seem to be limited primarily by physical habitat and water quality. Where significant contamination has occurred, metals may limit *N. placidus* either directly (i.e., through food or waterborne toxicity) or indirectly (by limiting the benthic invertebrate food base). Our studies demonstrate that an integrated approach, which includes the assessment of natural and anthropogenic factors, is necessary to determine the factors that may limit fish populations.

Acknowledgments

This study was jointly funded and undertaken by the U.S. Environmental Protection Agency, Region VII; the U.S. Department of the Interior (USDI)-National Biological Service (now the Biological Resources Division of the USGS), through its Midwest Science Center (now the Columbia Environmental Research Center); and the USDI-Fish and Wildlife Service, through its Ecological Services Field Offices in Manhattan, KS and Columbia, MO.

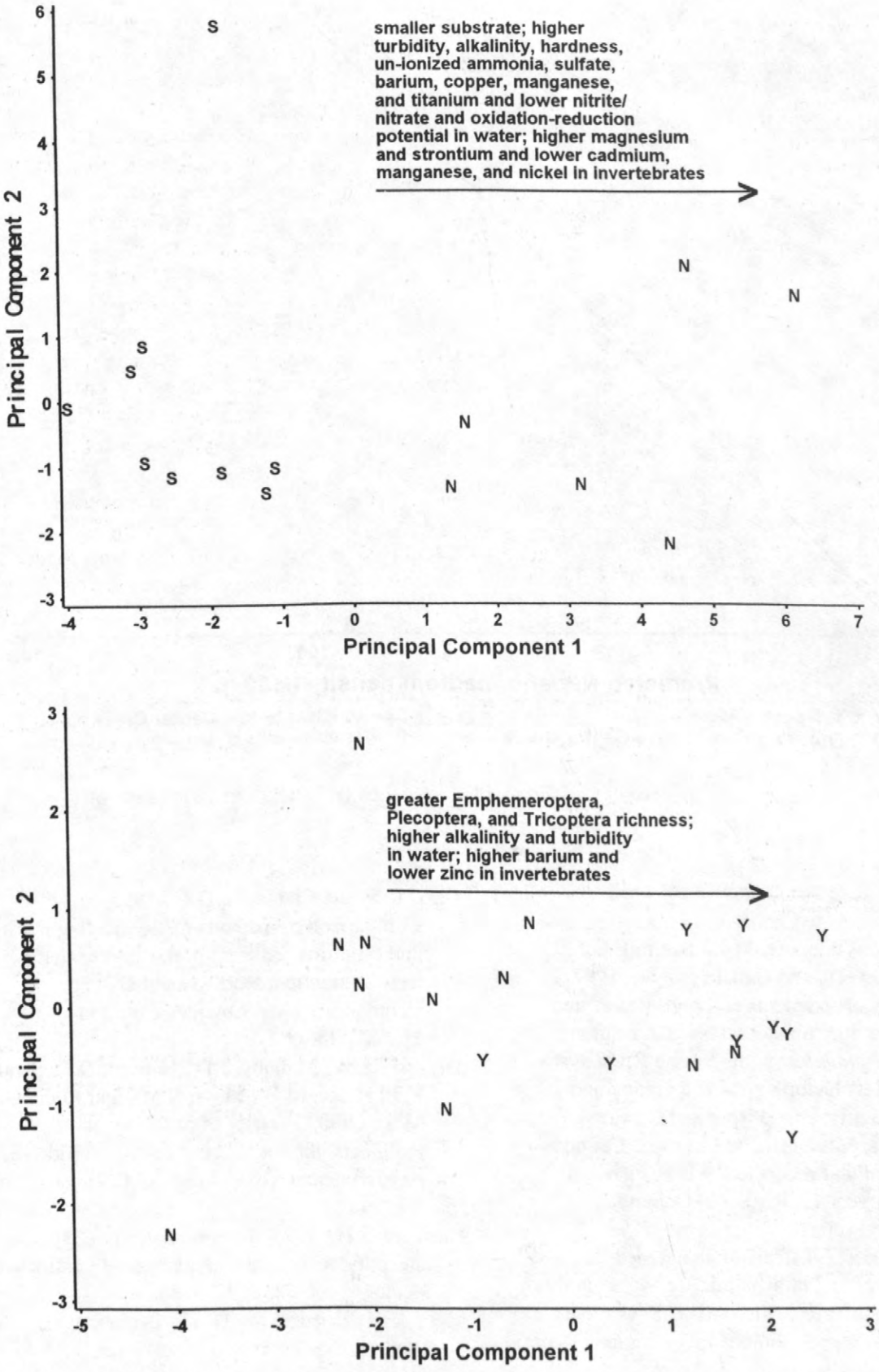

Figure 4. Principle components analyses differentiating Neosho-Cottonwood (N) from Spring River (S) sites (upper panel); and Spring River sites with (Y) and without (N) Neosho madtoms (lower panel).

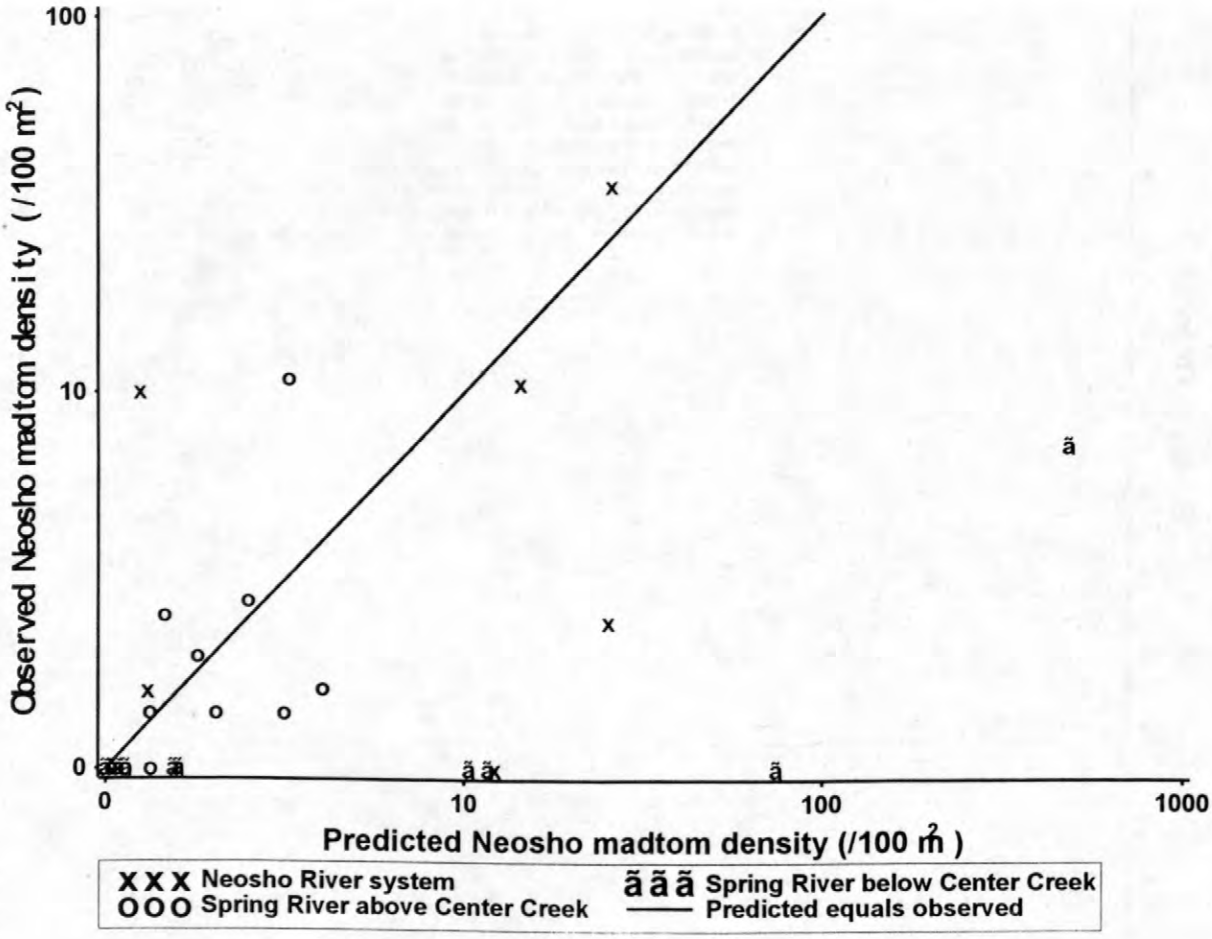

Figure 5. Predicted vs. observed Neosho madtom densites (Wildhaber et al. in press b).

References

Allert, A.L., Wildhaber, M.L., Schmitt, C.J., Chapman, D., and Callahan, E.V., 1997, Toxicity of sediments and pore-waters and their potential impact on Neosho madtom, *Noturus placidus*, in the Spring River system affected by historic zinc-lead mining and related activities in Jasper and Newton Counties, Missouri; and Cherokee County, Kansas: Final report to the U.S. Fish and Wildlife Service, Region 3, Columbia, Missouri, 100 p.

Barks, J.H., 1977, Effects of abandoned lead and zinc mines and tailings piles on water quality in the Joplin area, Missouri: U.S. Geological Survey Water-Resources Investigations Report 77-75, p. 1-49.

Carr, R.S. and Chapman, D.C., 1995, Comparison of methods for conducting marine and estuarine sediment pore-water toxicity tests -extraction, storage and handling techniques. *Arch. Environ. Contamin. Toxicol.* 28:69-77.

DiToro, D.M., Mahony, J.D., Hansen, D.J., Scott, K.J., Hicks, M.B., Mayr, S.M., and Redmond, M.S., 1990, Toxicity of cadmium in sediments: the role of acid volatile sulfide: Environmental Toxicology and Chemistry, vol. 9, p.1487-1502.

Hurlbert, S.H., 1971, The non-concept of species diversity: a critique and alternative parameters: Ecology, vol. 52, p. 577-586.

May, T.W., Wiedemeyer, R.H., Brumbaugh, W.G., and Schmitt, C.J., 1997, The determination of metals in sediment pore-waters and in 1N HCl-extracted sediments by

ICP-MS: Atomic Spectroscopy, vol.18, p. 133-139.

McMahon, T. E., Zale, A.V., and Orth, D.J., 1996, Aquatic habitat measurements Murphey B.R., and Willis D.W., eds., Fisheries Techniques, Second Edition: Bethesda, Maryland, American Fisheries Society, p. 83-120.

Moss, R.E., 1983, Microhabitat selection in Neosho River riffles: Lawrence, University of Kansas, unpublished Ph.D. thesis, p. 294.

Pflieger, W. L., 1975, The Fishes of Missouri. Second edition: Missouri, Department of Conservation.

Schmitt, C.J., Wildhaber, M.L., Allert, A.L., and Poulton, B.C., 1997, The effects of historic zinc-lead mining and related activities in the Tri-State Mining District on aquatic ecosystems supporting the Neosho madtom, *Noturus placidus*, in Jasper County, Missouri; Ottawa County, Oklahoma; and Cherokee County, Kansas: Final Report to the U.S. Environmental Protection Agency, Region VII, Kansas City, Kansas, 88 p.

———, Wildhaber, M.L., Hunn, J.B., Nash, T., Tieger, M.N., and Steadman, B.L., 1993, Biomonitoring of lead-contaminated Missouri streams with and assay for erythrocyte - aminolevulinic acid dehydratase (ALA-D) activity in fish blood: Archives of Environmental Contaminants and Toxicology, vol. 25, p. 464-475.

U.S. Environmental Protection Agency. 1976. Quality Criteria for water: Washington, D.C., EPA 440/9-76-023.

———. 1980. Ambient water quality criteria for : copper: Washington, D.C., EPA 440/5-80-036.

———. 1984a. Ambient water quality criteria for: cadmium: Washington, D.C., EPA 440/5-84-032.

———. 1984b. Ambient water quality criteria for : lead: Washington, D.C., EPA 440/5-84-027.

———. 1986. Ambient water quality criteria for : nickel: Washington, D.C., EPA 440/5-86-006.

———. 1987. Ambient water quality criteria for : zinc: Washington, D.C., EPA 440/5-87-003.

———, 1989, Short-term methods for estimating the chronic toxicity of effluents and receiving waters to freshwater organisms: Washington, D.C., EPA 660/4- 89/001.

Weast, R.C., Astle, M.J., and Beyer, W.H., 1988, CRC Handbook of Chemistry and Physics: Boca Raton, Florida, CRC Press, Inc.

Wildhaber, M.L., Allert, A.L., and Schmitt, C.J., In press a, Potential effects of interspecific competition on Neosho madtom (*Noturus placidus*) populations. Journal of Freshwater Ecology.

———, Allert, A.L., Schmitt , C.J., Tabor, V.M., Mulhern, D., Powell, K.L., and Sowa, S.P., In press b, Natural and anthropogenic factors and the benthic community of a midwestern stream: emphasis on the threatened Neosho madtom: Transactions of the American Fisheries Society.

———, and Schmitt, C.J., 1996, Estimating aquatic toxicity as determined through laboratory tests of Great Lakes sediments containing complex mixtures of environmental contaminants: Environmental Monitoring and Assessment, vol., 41, p. 255-289.

———, Allert, A.L., and Schmitt, C.J. 1997, Elemental concentrations in benthic invertebrates from the Neosho, Cottonwood, and Spring river systems of Missouri, Kansas, and Oklahoma: Project completion report to the U.S. Fish and Wildlife Service, Region 6, Manhattan, Kansas, 17 p.

Wilkinson, C., Edds, D.R., Dorlac, J., Wildhaber, M.L., Schmitt, C.J., and Allert, A., 1996, Neosho madtom distribution and abundance in the Spring River: The Southwestern Naturalist, vol. 41, p. 78-81.

AUTHOR INFORMATION

Mark L. Wildhaber, Christopher J. Schmitt, and Ann L. Allert, U.S. Geological Survey, Columbia, Missouri.

Field Demonstration of Permeable Reactive Barriers to Control Radionuclide and Trace-Element Contamination in Ground Water from Abandoned Mine Lands

By D.L. Naftz, J.A. Davis, C.C. Fuller, S.J. Morrison, G.W. Freethey, E.M. Feltcorn, R.G. Wilhelm, M.J. Piana, J. Joye, and R.C. Rowland

ABSTRACT

Pump-and-treat methods are costly and often ineffective in meeting long-term protection standards for contaminated ground water. Permeable reactive barriers (PRBs) may offer a cost-effective alternative to other ground-water remediation methods. A PRB functions as a passive in-situ treatment zone that degrades or immobilizes contaminants. A demonstration project is currently (1999) underway at an abandoned uranium upgrader operation site in southeastern Utah to evaluate the removal of uranium from ground water by using six different PRBs. Two methods of PRB deployment, the funnel and gate design and non-pumping well design, were installed to passively treat uranium-contaminated ground water. The six different PRBs have removed uranium from the ground water with various levels of efficiency. With respect to the PRBs installed using the funnel and gate design, the barrier containing zero-valent iron has consistently removed more than 99.9 percent of the input uranium concentration during the first year of operation. The percentage of uranium removed in the bone char phosphate and amorphous ferric oxyhyroxide PRBs was slightly less, averaging 94.0 and 88.1 percent, respectively. The three barrier deployment tubes in the non-pumping wells containing mixtures of bone-char phosphate and iron-oxide pellets removed less uranium than the PRBs deployed using the funnel and gate design. Numerous geochemical and hydrological factors that affect uranium removal efficiencies and processes in each of the PRBs are currently (1999) being evaluated.

INTRODUCTION

Potable ground-water supplies worldwide are contaminated or threatened by advancing plumes containing radionuclides and metals. Pump-and-treat methods are costly and often ineffective in meeting long-term protection standards (Travis and Doty, 1990; Gillham and Burris, 1992; National Research Council, 1994). Alternative, cost effective approaches to pump-and-treat methods could have widespread applicability to abandoned and active mine sites throughout the United States and other parts of the world.

Permeable reactive barriers (PRBs) are potentially cost-effective alternative technology to pump-and-treat methods. A PRB is a permanent, semi-permanent, or replaceable unit that is installed across the flow path of a contaminant plume (RTDF Permeable Reactive Barriers Action Team, 1998). A PRB contains a zone of reactive material that acts as a passive in-situ treatment zone. This in-situ treatment zone degrades or immobilizes contaminants, such as radionuclides and other trace elements, as ground water flows through it (fig. 1). Operational and maintenance costs are lower because water flow across the PRBs is driven by the natural gradient and the treatment system does not require operational maintenance. Reactions within the

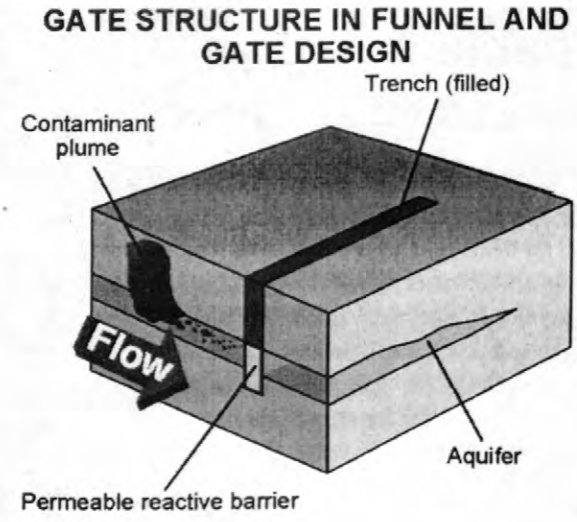

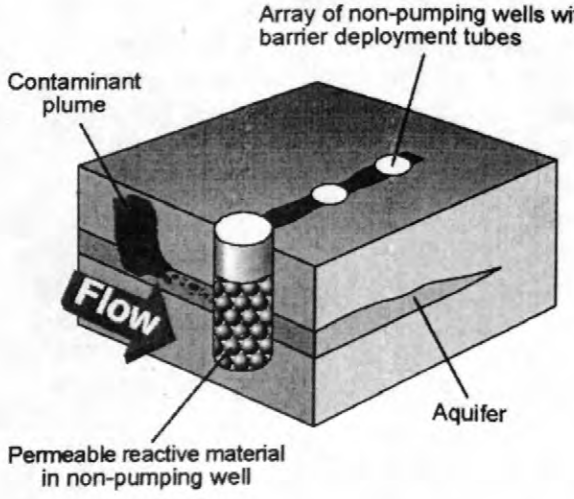

Figure 1. Schematic diagrams of permeable reactive barriers currently being demonstrated at Fry Canyon, Utah.

PRB material either degrade contaminants to non-toxic forms or transfer the contaminants to an immobile phase. Potential limitations to PRBs include re-release of contaminants after aging of reactive material, removal and disposal of the reactive material after breakthrough, and deleterious effects of barrier material on downgradient water quality.

The project is currently (1999) testing six different PRBs and two different deployment techniques at the Fry Canyon demonstration site

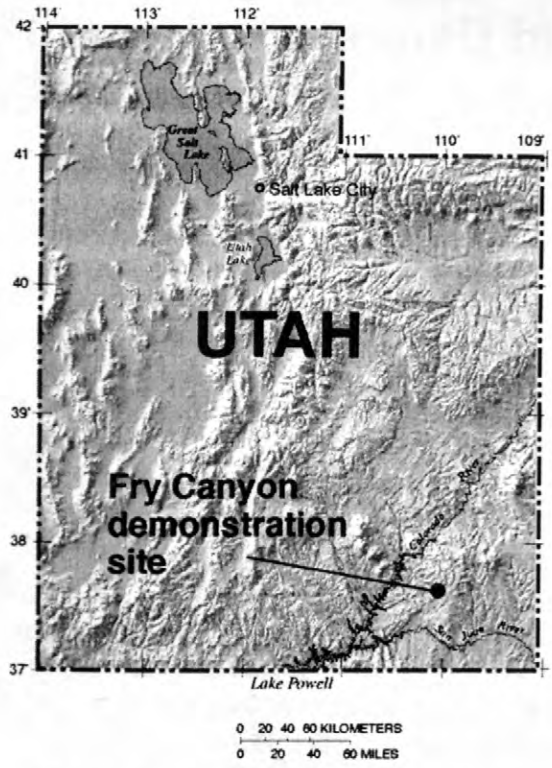

Figure 2. Location of the Fry Canyon demonstration site in southeastern Utah.

in southeastern Utah (fig. 2). This site is an abandoned uranium upgrader operation on Federal land managed by the Bureau of Land Management (BLM). The shallow ground water in the colluvial aquifer is contaminated with elevated concentrations of uranium that can exceed 20,000 micrograms per liter (µg/L). Objectives of this paper are to describe the techniques used for installation and monitoring of PRBs and present the initial results of PRB performance during the first year of field demonstration. The U.S. Environmental Protection Agency (USEPA)/Superfund and Office of Radiation and Indoor Air and the U.S. Geological Survey Technology Enterprise Office provided funding for this ongoing project.

INSTALLATION AND OPERATION

Funnel and gate PRBs

A funnel and gate design was chosen to demonstrate three of the six PRBs installed at the site (fig. 1). Funding for this installation was provided by the U.S. Environmental Protection Agency (USEPA)/Superfund and Office of Radiation and Indoor Air. This design consisted of three "permeable windows" or gates where each of the PRBs were placed, separated by impermeable walls between the gate structures and impermeable wing walls on each end to channel the ground-water flow into the PRBs. Dimensions of each gate structure are 7 feet long by 3 feet wide by about 4 feet deep. The three PRBs and no-flow walls were keyed into the bedrock (Cedar Mesa Sandstone) underlying the colluvial aquifer. A 1.5-foot-wide layer of pea gravel was placed on the upgradient side of the PRBs to facilitate uniform flow of contaminated ground water into each gate structure. The three barriers consist of (1) bone char phosphate (PO_4); (2) zero valent iron (ZVI) pellets; and (3) amorphous ferric oxyhyroxide (AFO).

The mechanism of uranium removal in each of the PRBs is a function of the type of barrier material. The PO_4 barrier material consists of pelletized bone charcoal used as phosphate source to facilitate formation of insoluble uranyl phosphate compounds. The ZVI barrier material consists of pelletized iron designed to remove uranium by reduction of uranium (VI) to the less soluble uranium (IV). The AFO barrier material consists of pea gravel coated with amorphous ferric oxyhydroxide that removes uranium by adsorption to the ferric oxide surface. Materials were pelletized or used as a coating on gravel to increase the permeability of the gate structure relative to the permeability of the native aquifer material.

Heavy equipment consisting of a track-mounted backhoe and a bulldozer was used to install the PRBs (fig. 3). This design-and-installation technique was used for the following reasons: (1) amenable for multiple PRBs placed side by side; (2) low construction cost; (3) conducive to a shallow ground-water system; and (4) transferability to other remote, abandoned mine sites with shallow contaminated ground water.

Figure 3. Placement of reactive material into the gate structure of the bone-char phosphate barrier at Fry Canyon, Utah, during September 1997.

Each PRB is instrumented so its performance can be assessed and compared during the demonstration period (fig. 4). Four transducers and a water-quality minimonitor (measuring temperature, pH, specific conductance, oxidation reduction potential, and dissolved oxygen) are deployed in each barrier. Water-level and water-quality data from the instruments are recorded hourly. Flow direction and velocity are measured in each PRB using a flow sensor during site visits at monthly to quarterly intervals. Each PRB has a total of 20 monitoring points for the collection of water-quality samples. Seven monitoring points are located downgradient of the barriers in the colluvial aquifer.

Barrier deployment tubes in non-pumping wells

An array of 6-inch-diameter wells, installed using a cable tool drilling rig, was used to deploy three additional PRBs at the Fry Canyon site (fig. 1). Funding for this installation was provided by the U.S. Geological Survey Technology Enterprise Office. Barrier deployment tubes containing different proportions of bone char phosphate and foamed iron oxide pellets were placed in the large-diameter wells. Use of arrays of unpumped wells has been proposed by Wilson

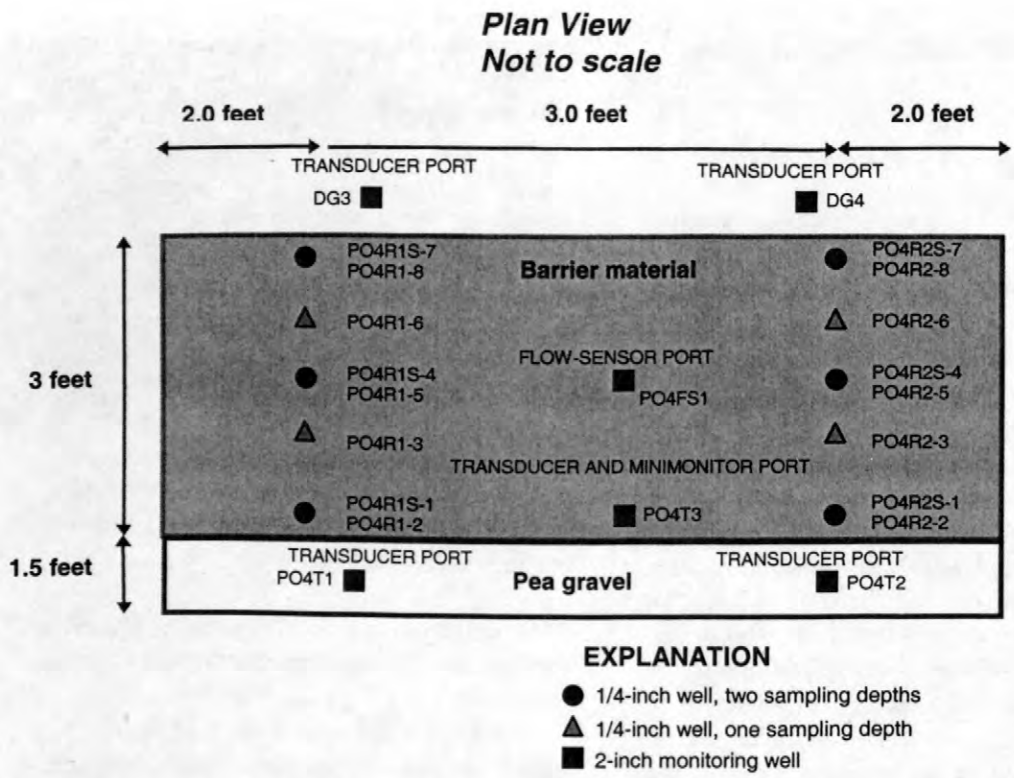

Figure 4. Schematic diagram showing monitoring well placement in the bone char phosphate permeable reactive barrier. The monitoring design in the zero valent iron and amorphous ferric oxide barriers is the same.

and Mackay (1997) as a method to remediate contaminant plumes when the installation of treatment walls is not possible because of technical or financial constraints. This type of deployment technology is useful for treatment of deeper contaminant plumes. Use of barrier deployment tubes allows for cost-effective retrieval and replacement of reactive material, which would not be possible with other deployment technologies.

Under natural flow conditions at Fry Canyon, ground water converges to the non-pumping well array and the associated barrier deployment tubes in response to the difference in hydraulic conductivity between the well and aquifer (fig. 5). Numerical simulations of ground-water movement through the non-pumping well array indicate that each well intercepts ground water in a portion of the upgradient aquifer approximately twice the inside diameter of the well (fig. 5).

Three of the barrier deployment tubes were installed on site in October 1998 (fig. 6). Different proportions of bone char phosphate and iron oxide pellets were used to facilitate increased uranium removal from ground water. The iron oxide pellets strongly adsorb the phosphate released from the phosphate pellets. The adsorbed phosphate can then react with the uranium in the ground water to facilitate formation of insoluble uranyl phosphate compounds. The following proportions of bone char phosphate:iron oxide pellets (volume ratio) were used: (1) 25:75 (intermixed), well BZ2; (2) 50:50 (intermixed), well BZ1; and (3) 50:50 (layered verttically), well BZ3. Each barrier package has five monitoring points for the collection of water samples (fig. 6).

RESULTS

Funnel and gate PRBs

One year of uranium-concentration data has been collected from the three PRBs installed using funnel and gate designs (fig. 7). The input uranium concentrations are significantly different

for each PRB, ranging from less than 1,000 µg/L in the PO_4 PRB to more than 20,000 µg/L in the amorphous ferric oxyhydroxide (AFO) PRB. The input uranium concentrations to each of the PRBs also vary seasonally by approximately 4,000 to 7,000 µg/L.

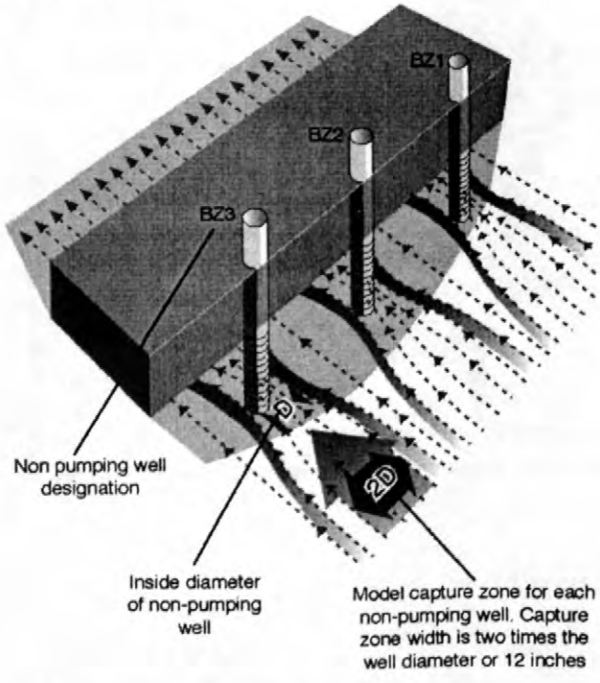

Figure 5. Schematic diagram showing the array of non-pumping wells and modeled ground-water flow paths and capture zones, Fry Canyon, Utah.

During the first year of operation, the PRBs removed most of the incoming uranium (fig. 7); however, the percentage of uranium removal varies with time and barrier material (table 1). Percent uranium removal was calculated using the following formula:

$$U_{removed} = 100 - (U_{barr}/U_{input}) \quad (1)$$

Where

$U_{removed}$ is the percent of uranium removed

U_{barr} is the concentration of uranium in ground water 1.5 feet from the pea gravel/PRB interface

U_{input} is the concentration of uranium in ground water prior to entering the PRB

The zero valent iron (ZVI) PRB has consistently removed more than 99.9 percent of the input uranium concentration in flow-path 1 (table 1). The percentage of uranium removed in the PO_4 and AFO PRBs is slightly less than the ZVI PRB. Except for two monitoring periods, more than 90 percent of the input uranium concentration was removed in the PO_4 barrier. The AFO PRB removed more than 90 percent of the input uranium concentration through November 1997. From January 1998 through September 1998 the uranium removal percentage was reduced to less than 90 percent.

Table 1. Percentage of input uranium concentration removed after traveling 1.5 feet into each of the permeable reactive barriers that were constructed using the funnel and gate design, Fry Canyon, Utah.

Date	PO4 barrier	ZVI barrier	AFO barrier
SEP 1997	99.7	> 99.9	95.3
OCT 1997	94.8	> 99.9	94.9
NOV 1997	89.4	> 99.9	93.6
JAN 1998	79.2	> 99.9	85.9
APR 1998	96.7	> 99.9	77.8
JUN 1998	98.3	> 99.9	81.9
SEP 1998	> 99.9	> 99.9	87.4

Numerous geochemical and hydrological factors that affect uranium removal efficiencies and processes in each of the PRBs are currently (1999) being evaluated. These factors include changes in the amount and velocity of water flowing through the PRBs, type and quantities of minerals forming within the PRBs, leakage between no-flow boundaries between the PRBs, small-scale ground-water flow paths through the PRBs, and effects of PRBs on downgradient water quality. Downgradient effects from the ZVI PRB may include increased iron concentrations in ground water.

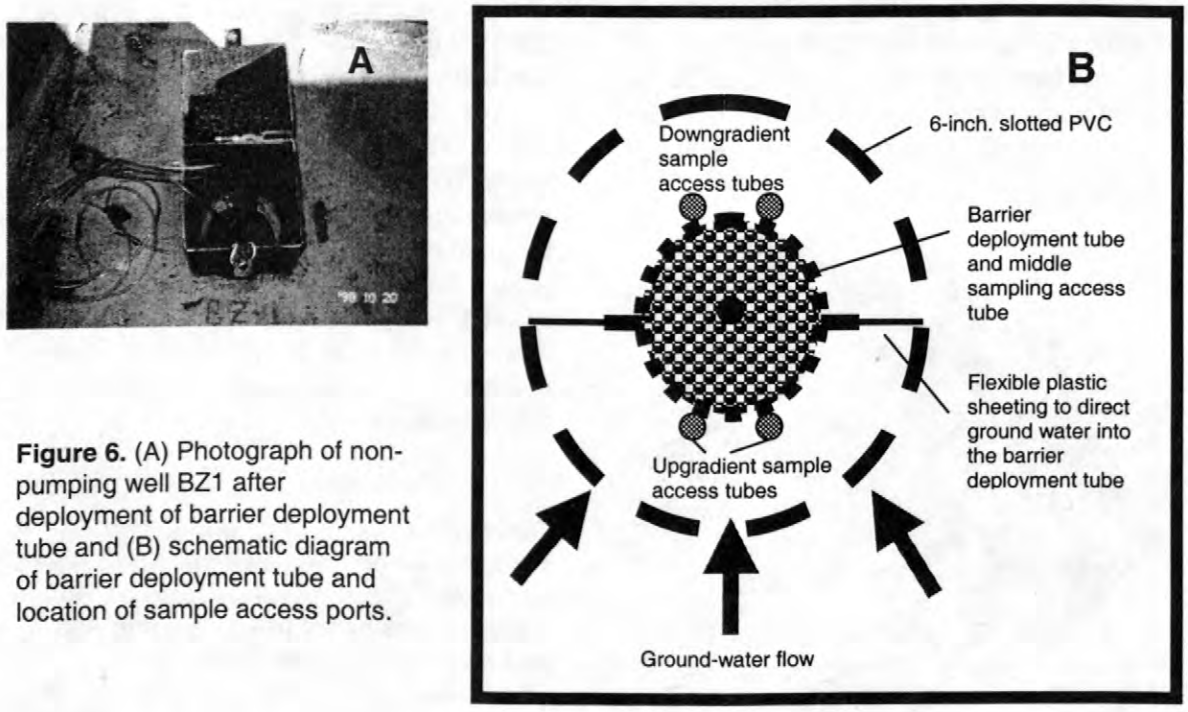

Figure 6. (A) Photograph of non-pumping well BZ1 after deployment of barrier deployment tube and (B) schematic diagram of barrier deployment tube and location of sample access ports.

Barrier packages in non-pumping wells

Three months of uranium-concentration data have been collected from the three barrier deployment tubes (fig. 8) that were installed in the non-pumping well array. During this initial operation, the barrier deployment tubes were removing less uranium than the PRBs deployed using the funnel and gate design. For example, during the first year of operation the PO_4 PRB removed an average of 94 percent of the input uranium after traveling 1.5 feet into the barrier material. In October 1998, the average percent removal of uranium from the three barrier deployment tubes was 67 percent. This removal percentage was calculated using equation 1. Possible explanations for the lower removal efficiencies in the barrier deployment tubes could include mixing of bone char phosphate material with the foamed iron source, reduced flow-path lengths, shorter reaction times, uncertainty in small-scale ground-water-flow directions, and artificial gradients introduced during sampling.

SUMMARY

During the initial period of operation, the six different PRBs removed uranium in the ground water with various levels of efficiency. With respect to the PRBs installed using the funnel and gate design, the ZVI barrier consistently removed greater than 99.9 percent of the input uranium concentration during the first year of operation. The percentage of uranium removed in the PO_4 and AFO barriers was slightly less during the same operation period. The three barrier deployment tubes removed less uranium than the PRBs deployed using the funnel and gate design. During October 1998 the average removal of uranium from the three barrier deployment tubes was 67 percent. Numerous geochemical and hydrological factors that affect uranium removal efficiencies and processes in each of the PRBs are currently (1999) being evaluated.

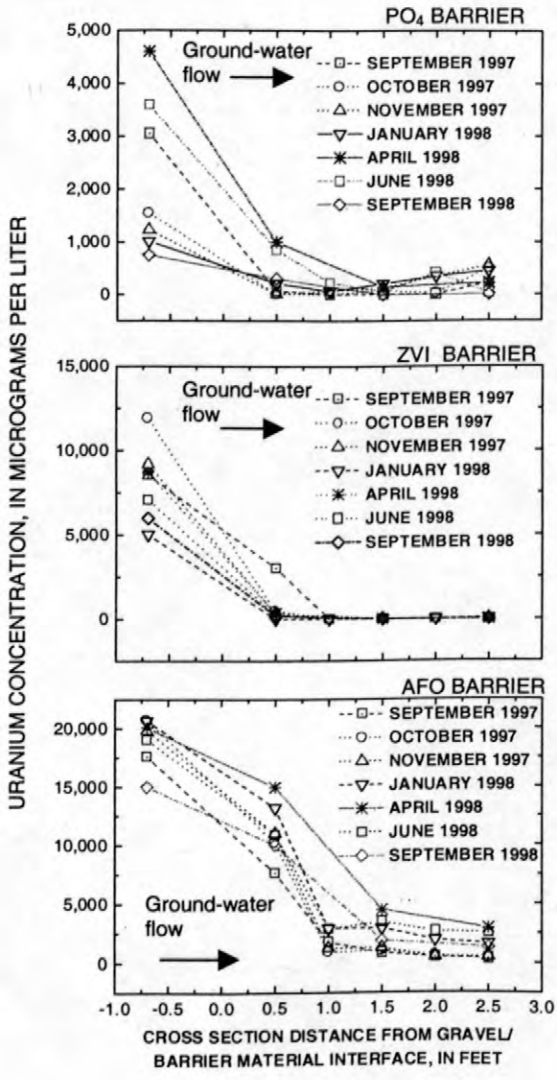

Figure 7. Changes in dissolved uranium concentrations in the three permeable reactive barriers installed using the funnel and gate design, Fry Canyon, Utah.

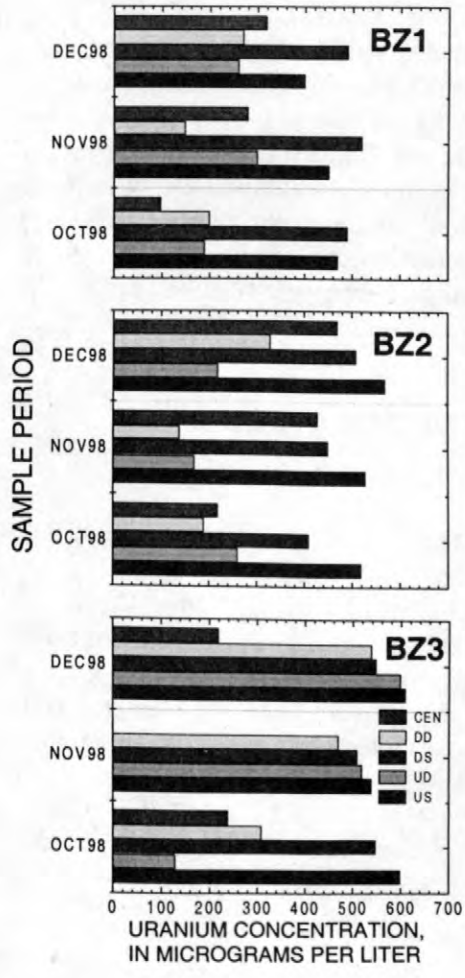

Figure 8. October, November, and December 1998 uranium concentrations in water samples taken along the perimeter and center parts of the barrier deployment tubes, Fry Canyon, Utah. Preinstallation uranium concentration in October 1998 was 635 micrograms per liter. The CEN, DD, DS, UD, and US designations refer to individual sample tubes on each of the barrier deployment tubes.

REFERENCES

Gillham, R.W., and Burris, D.R., 1992, Recent developments in permeable in situ treatment walls for remediation of contaminated groundwater: Proceedings, Subsurface Restoration Conference, June 21-24, Dallas, Texas.

National Research Council, 1994, Alternatives for ground water cleanup, National Academy Press, Washington, D.C., 315 p.

RTDF Permeable Reactive Barriers Action Team, 1998, Permeable reactive barrier installation profile, accessed September 3, 1998, at URL http://www.rtdf.org/barrdocs.htm

Travis, C.C., and Doty, C.B., 1990, Can contaminated aquifers at Superfund sites be remediated?: Environmental Science and Technology, vol. 24, p. 1464-1466.

Wilson, R.D., and Mackay, D.M., 1997, Arrays of unpumped wells: An alternative to permeable walls for in situ treatment: International Contaminant Technology Conference Proceedings, February 9-12, 1997, St. Petersburg, Flor., p. 888-894.

AUTHOR INFORMATION

D.L. Naftz, G.W. Freethey, R.C. Rowland, U.S. Geological Survey, Salt Lake City, Utah; J.A. Davis, C.C. Fuller, M.J. Piana, J. Joye, U.S. Geological Survey, Menlo Park, California; S.J. Morrison, Weston, Inc., Grand Junction, Colorado; E.M. Feltcorn and R. G. Wilhelm, U.S. Environmental Protection Agency, Washington, DC

Geochemistry, Toxicity, and Sorption Properties of Contaminated Sediments and Pore Waters from Two Reservoirs Receiving Acid Mine Drainage

By D. Kirk Nordstrom, Charles N. Alpers, Jennifer A Coston, Howard E. Taylor, R. Blaine McCleskey, James W. Ball, Scott Ogle, Jeffrey S. Cotsifas, and James A. Davis

ABSTRACT

Acid mine waters from the Iron Mountain Superfund Site, Shasta County, California, flow through Spring Creek Reservoir and into Keswick Reservoir on the Sacramento River. In Keswick Reservoir, the acid mine waters have neutralized on mixing with neutral-pH lake water, producing fine-grained, metal-rich sediments. Sediment cores were collected during 1997 from both reservoirs for characterization and pore waters were extracted under anoxic conditions. Chemical composition, mineralogical identification, redox chemistry, sorption properties, and toxicity were determined on several samples. Metal concentrations in sediment ranged from 4 to 47 % for Fe, 200 to 4,800 mg/kg (milligrams per kilogram) for Cu, and 85 to 6,600 mg/kg for Zn. Pore waters ranged in pH from 4.7 to 6.7 and their Fe(II) concentration range was 10 to 2,000 mg/L (milligrams per liter). Although pore-water Zn concentrations ranged from 0.1 to 9 mg/L, Cu concentrations were less than 0.01 mg/L. Considerable reductive iron dissolution has occurred in the Keswick Reservoir sediments, but there is little or no indication of sulfate reduction. Adsorption and desorption experiments for Cu, Zn, and Cd on composite sediment samples demonstrated typical sorption behavior for metal ions on iron oxides, except that the adsorption edge is moved about one pH unit lower than expected compared to a hydrous ferric oxide substrate, but similar to that for a schwertmannite (ferric oxyhydroxysulfate) substrate. Schwertmannite was identified in the sediments by x-ray diffraction and Mössbauer spectroscopy. Toxicity tests, using dilutions of Keswick sediment pore waters and *Ceriodaphnia dubia* as a test animal, demonstrated that iron is the causative agent for both acute and chronic toxicity with a minor contribution to toxicity from zinc.

INTRODUCTION

The Iron Mountain Superfund Site is located in Shasta County, northern California, 9 mi. (miles) northwest from the town of Redding (fig. 1). Mineral deposits of the West Shasta district are Kuroko-type massive-sulfide deposits of Devonian Age. The ore bodies are pyrite-rich and hosted in quartz-porphyry rhyolite which has minimal acid-buffering capacity. Iron Mountain is a group of mines that include Old Mine, No. 8, Confidence-Complex, Brick Flat Open Pit, Mattie, Richmond, and Hornet. Recovery for silver (Ag) and gold (Au) from surficial gossan began in the 1860s and by 1896, underground mining for copper (Cu) and Ag had begun. Some zinc (Zn) was produced during World War II and open-pit mining for pyrite to produce sulfuric acid was active during 1955–62. Iron Mountain was once the largest producer of Cu in California and now it is the largest producer of acid mine drainage in the State. Prior to Superfund remediation efforts, more than 2,500 tons of pyrite weathered every year and about 300 tons of dissolved Cu, Zn, and cadmium (Cd) drained annually into the Sacramento River via Spring Creek (fig. 2). Massive fish kills have been recorded in the Sacramento River during periods of high runoff; up to 100,000 anadromous fish have died in a major storm event (Nordstrom and

Figure 1. Map showing location of Iron Mountain, California

by the U.S. Geological Survey (USGS), including information on regulatory remedial activities, can be found in Nordstrom (1977), Nordstrom and others (1977), Alpers and others (1992), Nordstrom and Alpers (1995; unpublished data), and references therein.

Large metal-rich sediment deposits (piles) have accumulated in Keswick Reservoir, the receiving water body on the Sacramento River for acid drainage from Iron Mountain. Important questions regarding these deposits need to be addressed: How large are these piles of contaminated sediment? How much Cd, Cu, and Zn are in these piles and how mobile are these contaminants? How toxic are the sediments and are the pore waters of comparable or different toxicity? Is there an identifiable source of toxicity? Are the deposits more hazardous if left alone or removed or contained? A multi-organizational study was begun to resolve these questions. This paper describes the results from analytical, sorption, and toxicological investigations by the USGS in cooperation with the U.S. Environmental Protection Agency (EPA), its contractors (CH2M Hill and Pacific Eco-Risk Laboratories), and the Bureau of Reclamation (BOR) on the sediments and pore waters from Keswick and Spring Creek Reservoirs. Iron Mountain was placed on the National Priority List by the EPA under the Comprehensive Environmental Response, Compensation, and Liability Act (CERCLA), or Superfund, in 1983 and current studies continue under its auspices.

GENERAL SITE DESCRIPTION

Acid mine waters from Iron Mountain drain into Slickrock and Boulder Creeks, two tributaries of Spring Creek, which is the main drainage that flows into Spring Creek Reservoir and then into Keswick Reservoir (fig. 2). Spring Creek Debris Dam, an earth-fill structure, was built in 1963 to prevent debris and sediment from interfering with the tailrace to Spring Creek Power Plant and to provide control of acid mine waters so that they could be adequately diluted by outflows from Shasta Dam and Spring Creek Power Plant to mitigate risks to aquatic life. Prior to remediation at Iron Mountain, the pH of Spring Creek Reservoir was about 2.5 during low flow and sometimes more than 5 during high flows. The water level in Spring Creek Reservoir is generally kept as low as possible by the BOR, to provide temporary storage for flood events during the wet season. Unfortunately, the total storage capacity of only 5,850 acre-feet or 7.2 million m^3 (cubic meters) in Spring Creek Reservoir has been exceeded on several occasions since 1963, resulting in uncontrolled releases of acidic, metal-rich mine drainage into the Sacramento River. Keswick Reservoir has a total storage capacity of 23,800 acre-feet or 29.3 million m^3. The Spring Creek arm of the reservoir has been the repository for approximately 260,000 m^3 of chemically-precipitated sediment formed by the neutralization of acid mine water with the circum-neutral pH reservoir water. High-resolution seismic-reflection soundings (T. Bruns and others, USGS, written commun., 1999), combined with direct coring, have outlined three

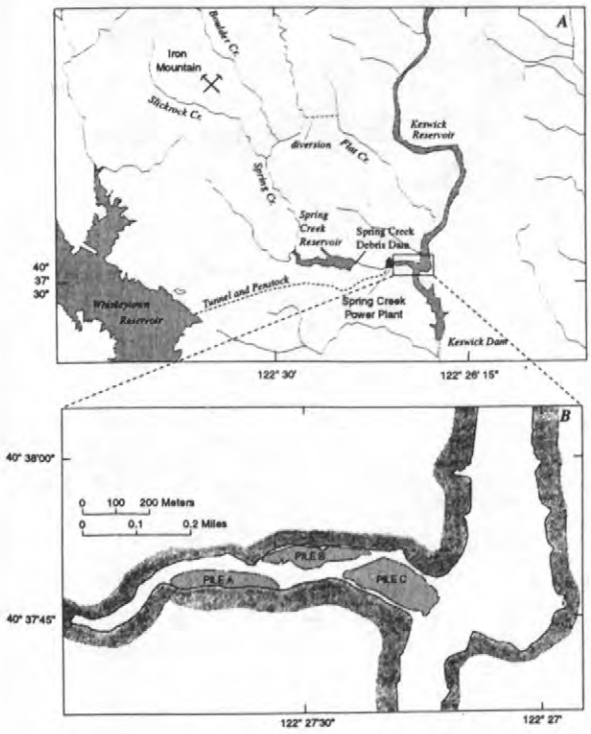

Figure 2. Maps showing location of (A) Spring Creek Reservoir and (B) sediment piles in Spring Creek arm of Keswick Reservoir, California. Pile A is up to 2 meters (m) thick, Pile B is up to 5 m thick and Pile C is up to 8 m in thickness.

contaminated sediment piles in the Spring Creek arm of Keswick Reservoir, named A, B, and C (fig. 2). The general geochemical characteristics of each pile are similar but pile C was chosen for detailed study because it is the largest, thickest, and most contaminated.

SEDIMENT CHEMISTRY

Field work was conducted at Keswick and Spring Creek Reservoirs during September, October, and November 1997. Sediment cores and extracted pore waters were obtained to determine the potential hazard that these sediments might cause if allowed to remain in place or the possible contamination that could result from resuspension or remobilization in association with proposed remediation efforts such as dredging or encapsulation. A field laboratory for sample processing and analysis was set up at the Spring Creek Power Plant with the cooperation of the BOR.

Coring and On-Site Measurements

Sediments in Spring Creek Reservoir were collected in dry areas with a hollow-stem auger or from trenches dug with a backhoe. Some sediment cores were obtained below a shallow layer of water by advancing 2-in.-diameter PVC (polyvinyl chloride) tubes. Sediments in Keswick Reservoir piles were obtained from a barge platform by advancing 2-in.-diameter PVC tubing until refusal. Samples for chemical characterization were carefully extruded, composited, and processed into centrifuge bottles in an argon gas-filled glove bag. The samples were centrifuged at a centripetal acceleration of about 27,000 times the gravitational acceleration constant to separate pore waters from the sediment. Aliquots of pore waters were taken, under argon, to a mobile lab truck where measurements of pH, Eh, specific conductance, and alkalinity were made in an argon-filled glove box. A filtered aliquot of pore water was preserved with HCl for iron (Fe) redox determinations, that were made within 1 to 3 hours after extraction, by ultraviolet-visible spectrophotmetry using FerroZine as a complexing agent for Fe.

Sediment and Pore-Water Analyses

The top portion of every sediment core contained a layer that was predominately colloidal material and about 90% water. This layer of suspended colloids has been termed the "ghost layer" and was analyzed separately from the main sediment column by EPA's contractors. However, the ghost layer could not be distinguished chemically from the remainder of the sediment column; it differed primarily by grain size and water content.

A filtered aliquot of pore water was preserved with HNO_3 and analyzed for major cations and trace metals by inductively-coupled plasma (ICP) atomic-emission spectroscopy and ICP mass spectrometry. An unacidified, filtered aliquot was used for analysis of major anions by ion chromatography. Sediments were digested

using HNO_3-HCl-HF and analyzed for total metals by ICP.

A summary of the compositional range of selected elements in both Spring Creek Reservoir and Keswick Reservoir sediments is given in Table 1.

Table 1. Summary of iron, copper, and zinc concentrations in sediment. [Piles A, B, and C are located in the Spring Creek arm of Keswick Reservoir; SCR, Spring Creek Reservoir; mg/kg, milligrams per kilogram].

Sediment Pile	Iron %	Copper mg/kg	Zinc mg/kg
A, range	5-36	250-1,700	280-3,700
A, mean	14	780	590
B, range	6-38	410-1,900	180-2,400
B, mean	15	1,000	780
C, range	4-47	200-4,800	85-6,600
C, mean	17	1,600	1,200
SCR, range	6-21	320-960	100-340
SCR, mean	11	510	170

Plots of sediment chemistry indicate that Cu correlates closely with Fe, whereas the association of Zn and Cd with Fe are less strong. This result is expected because Cu adsorbs more strongly than Zn or Cd to iron oxides and co-precipitates with Fe more readily for a given pH and ratio of sediment to water (Davis and Kent, 1990, and references therein).

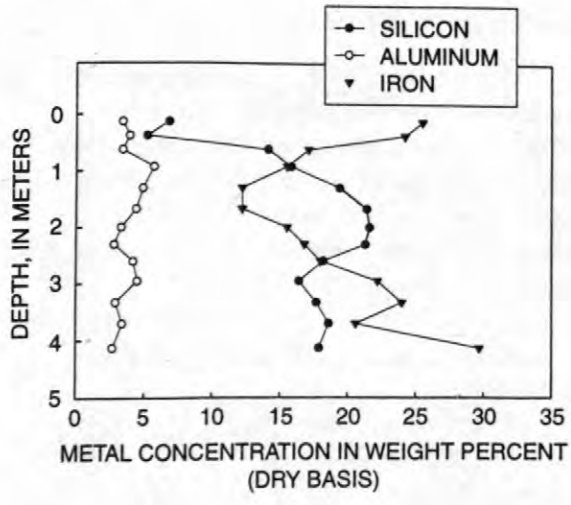

Figure 3. Concentrations of Al, Fe, and Si in sediment cores from pile C as a function of depth.

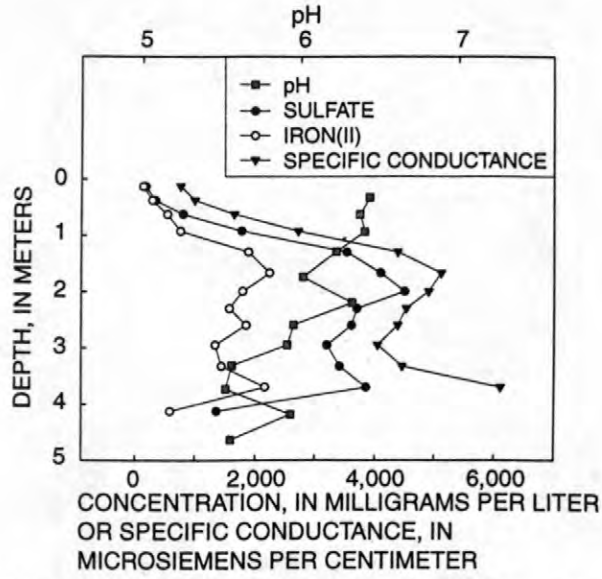

Figure 4. Concentrations of dissolved Fe(II) and SO_4 and values of specific conductance and pH in pore waters from pile C sediments as a function of depth.

One sediment core from pile C was sectioned in detail (about every 30 cm) for total metal determination and pore water extraction. Total Fe, silicon (Si), and aluminum (Al) concentrations in sediment as a function of depth are shown in Figure 3.

Combined with the data in Table 1, the enrichment in Fe is typically 3 times crustal abundance (5.4 weight percent; Krauskopf and Bird, 1995) and ranges in concentration to as high as 8 to 9 times that of the earth's crust. The tendency for Si to increase as Fe decreases suggests dilution of the mine drainage precipitates with uncontaminated silicate-rich sediment entering Keswick Reservoir.

The compositions of pore waters from the detailed core from pile C are shown as a function of depth for Fe(II), SO_4, specific conductance, and pH in Figure 4. The pore waters in the core from pile C had pH values ranging from about 5.5 to 6.5 and were dominated by Fe(II) and SO_4. Alkalinity values ranged from 1-300 mg/L (as $CaCO_3$) at the higher pH values. These Fe-SO_4 waters maintained about equimolar quantities of Fe and SO_4 and generally increased in concentration with depth.

Figure 5 shows the pore-water concentrations of Cd, Cu, Mn, and Zn with depth.

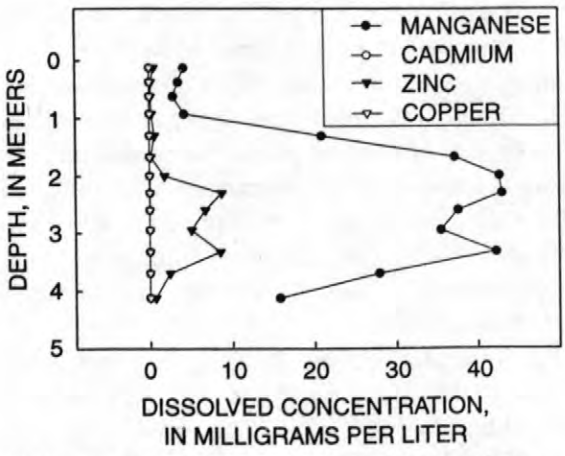

Figure 5. Concentrations of dissolved Cd, Cu, Mn, and Zn in pore waters from pile C sediments as a function of depth.

Both Cd and Cu remained very low (< 0.01 mg/L) but detectable, whereas Zn concentrations increased to a maximum of 9 mg/L and Mn concentrations increased to a maximum of 43 mg/L. The highest pore-water concentrations of Fe(II), Mn, Zn, and SO_4 occurred in the same interval, just below the midpoint of the core. The pore-water data indicate considerable reductive iron dissolution with some alkalinity production and yet little or no sulfate reduction.

Saturation Indices

Complete water analyses that gave acceptable charge balances (within 10%) were used to calculate saturation indices of phases that may have attained solubility equilibrium with pore waters in piles A, B, and C. Five minerals were frequently at or above saturation: ferrihydrite (hydrous ferric oxide), schwertmannite (hydrous ferric oxide sulfate), barite, siderite, and rhodocrosite. The reliability of the ferrihydrite and schwertmannite values is difficult to judge because of the difficulty in maintaining the samples in anoxic conditions and because of the difficulties in determining relatively low Fe(III) concentrations in the presence of very high Fe(II) concentrations. Nevertheless, saturation or supersaturation for these five minerals is reasonable given the high Fe(II), Mn, and SO_4 concentrations and relatively high pH of the pore waters. Ferrihydrite, schwertmannite, and goethite have been identified in the sediments by x-ray diffraction and Mössbauer spectroscopy, but to date no evidence of siderite or rhodocrosite has been found.

SEDIMENT SORPTION PROPERTIES

Metal adsorption and desorption studies on reservoir sediments were conducted to quantify metal partitioning between sediments and water because it is important to estimate the amounts of metals that might be released by dredging the contaminated piles. Composite sediment and water samples were taken both from SCR and from the Keswick Reservoir sediment piles. Surface areas of the sediments were measured by the Brunnauer-Emmett-Teller (BET) method, and scanning electron microscopy (SEM) was used to characterize the grain size and morphology of the colloids and fine-grained particles (fig. 6).

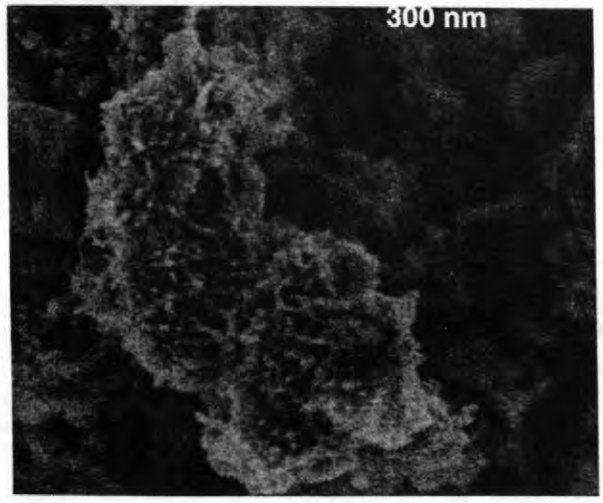

Figure 6. High resolution, cold field emission-SEM image of freeze-dried sediment from pile B. Scale bar is 300 nanometers (nm). The structure is consistent with that of synthetic schwertmannite. Major elements detected by energy dispersive spectroscopy were Fe, Al, Si, and S.

Surface areas of sediments from the three contaminated sediment piles in the Spring Creek arm of Keswick Reservoir determined by BET ranged from 19.2 to 69.6 m^2/g (square meters per gram). A weighted composite sediment sample from the Spring Creek arm had a surface area of 47.4 m^2/g. Sediment samples from Spring Creek

Reservoir were coarser grained, with BET surface areas ranging from 4.4 to 17.7 m^2/g. For reference, hypothetical spherical particles of hydrous iron oxide, 100 nanometers in diameter, would have a surface area of about 50 m^2/g.

Sorption Results

Adsorption and desorption studies were conducted with sediment composites to determine the metal partitioning with pH increases (caused by dilution with lake water on resuspension) and pH decreases (caused by iron oxidation). The adsorption and desorption curves for Cu, Zn, and Cd were found to follow normal "S"-shaped (or sigmoidal) curves typical of metal sorption isotherms (Davis and Kent, 1990). Sulfate desorption also occurred during the metal sorption experiments. Most experiments were run in 0.001 M $NaNO_3$ to maintain constant ionic strength. The sorption reaction rates approached equilibrium between 24–48 hours and sorption was found to be reversible. Comparisons between adsorption experiments (in $NaNO_3$ solutions) and whole-water mixing experiments with Spring Creek and Shasta Dam outflow or Whiskeytown Lake water gave qualitatively similar results. Sediment samples from different sites gave very similar results when normalized by surface area.

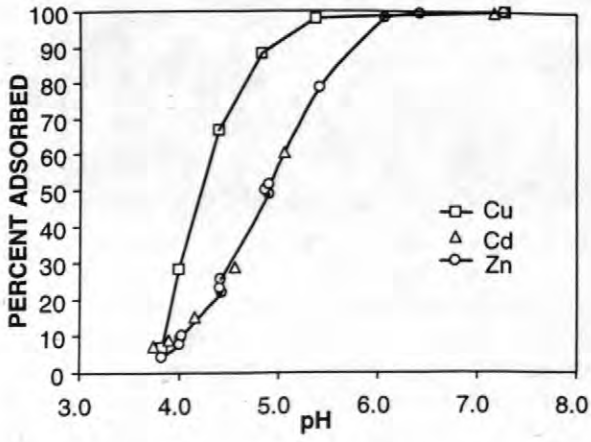

Figure 7. Cd, Cu, and Zn adsorption onto the Keswick Reservoir sediment composite in 0.001M $NaNO_3$. For a solid to liquid ratio of 11 g of sediment per liter, 50 percent of the copper is adsorbed onto the sediment at pH 4.1 and the slope of the Cu adsorption curve is steeper than the Cd or Zn slopes. Fifty percent of Cd or Zn are adsorbed between pH 4.8-4.9.

Desorption of Cu reached a minimum (with decreasing pH) at a pH of 5 and adsorption was complete (with increasing pH) at about the same pH. Although the adsorption curve shapes for Cu were typical of sorption curves for metals on hydrous ferric oxides (for example, Dzombak and Morel, 1990), the edge was displaced to a lower pH range (<4.5). This pattern is similar to adsorption of Cu onto schwertmannite (Webster and others, 1998).

Adsorption curves for Zn and Cd were similar to those for Cu but were shifted to about one pH unit higher (fig. 7). The curves were moved to a lower pH compared with adsorption onto hydrous ferric oxides, also consistent with a schwertmannite substrate. These results are entirely consistent with data from the partitioning of these metals between the sediments and their pore waters.

An interesting anomaly appeared when the Cu adsorption was measured at pH values above 7. Although maximum Cu adsorption, in terms of aqueous Cu concentration, was reached with increasing pH by values of about 5, the proportion of adsorbed Cu decreased at pH values above 7. This effect likely is caused by natural organic complexation of Cu, and has been observed in other systems (Davis, 1984). This behavior was not observed for Zn and Cd.

These results indicate that sorption is particularly effective for immobilizing the contaminant metals (especially Cu) in a resuspension scenario caused by dredging, if pH values remain above about 5. Furthermore, natural organic matter may reduce some of the effectiveness of Cu adsorption but it might also reduce aquatic toxicity if a strong Cu-organic complex is formed.

TOXICITY STUDIES

Aquatic toxicity tests were conducted on sediment pore waters and uncentrifuged sediments to determine the potential effects of sediment resuspension on aquatic life. The crustacean *Ceriodaphnia dubia* was used as a test animal. Five types of tests were completed: (1) 48-hr LC_{50} (the lethal concentration that results in 50 percent mortality of the test organisms) for the pore waters, (2) 96-hr LC_{50} for the pore waters,

(3) 48-hr LC_{50} for sediment elutriates, (4) toxicity identification and evaluation (TIE) to identify the main contaminant causing the mortalities in the pore water test solutions, and (5) a toxicity test specifically for dissolved iron. Pore waters were diluted to varying concentrations with three control waters: (1) outflow from Shasta Dam, (2) water from Spring Creek Power Plant (Whiskeytown Lake outflow), and (3) "lab" water [Evian mineral water diluted to hardness and alkalinity values similar to the other control waters (The use of trade names does not imply endorsement by the USGS.)]. Pore waters were kept anoxic and refrigerated until used in the toxicity tests. Values of pH, specific conductance, and alkalinity were monitored during the tests. The pH was maintained close to neutrality (7 ± 0.5). Samples of the test solutions were collected at regular intervals for metals determinations. The Fe(II) and Fe(total) concentrations were determined at regular intervals in the iron-specific tests.

Toxicity Results

The LC_{50} values were lower than expected. A summary of the dilution values for pile C pore waters is given in Table 2, along with the hypothetical concentrations of Fe, Cu, and Zn that would have been present if no oxidation of iron and no adsorption of Cu and Zn had occurred. The actual measured concentrations of these metals were significantly less than the hypothetical concentrations in Table 2. Nearly all the hypothetical and measured concentrations for Cu and Zn in tests at the LC_{50} dilutions were below harmful levels based on published values of LC_{50} from other studies (Fujimura and others, 1995, and references therein). The Sacramento River Basin plan for water quality limits requires Cu concentrations not to exceed 5.6 micrograms per liter (at a hardness of 40 milligrams per liter as $CaCO_3$); nearly every toxicity test indicated lower concentrations than this because of the adsorption of Cu on rapidly-precipitating iron colloids.

These results indicated that Cu and Zn concentrations were not the primary cause of toxicity. Further experiments with TIE testing indicated that dissolved iron was the primary cause of the toxicity, and that zinc may have been a secondary cause. The toxicity of Cu or Zn or both were nullified in the TIE by addition of reagents that selectively removed or complexed the individual metal, keeping the remaining experimental conditions the same. The final study using only dissolved Fe(II) with the three control waters gave results similar to the pore-water tests, demonstrating that concentrations of only a few mg/L of Fe were sufficient to cause acute and chronic toxicity in *Ceriodaphnia dubia*.

Table 2. Chemical Data for Toxicity Tests. [LC_{50}, dilution at which 50% mortality is observed; metal concentrations indicate hypothetical compositions based on dilution of starting solutions; actual metal concentrations were lower because of iron oxidation and metal coprecipitation; mg/L, milligrams per liter.]

	Pile A	Pile B	Pile C
48hr LC_{50}	1.8%	1.6%	0.6-7.1%
Fe (mg/L)	14	13	13-45
Cu (mg/L)	0.002	0.002	0.001-0.006
Zn (mg/L)	<0.006	<0.006	0.003-0.08

	Pile A	Pile B	Pile C
96hr LC_{50}	1%	0.8%	0.3-3%
Fe (mg/L)	8.2	6.7	6-15
Cu (mg/L)	0.002	0.002	0.001-0.005
Zn (mg/L)	<0.005	<0.005	0.005-0.01

The identification of iron from the pore waters of the Keswick Reservoir sediments as the primary toxicant affecting aquatic life was unexpected and has some serious implications. First, no regulatory aquatic life standard for Fe has been set by the EPA or the State of California, yet Fe appears to be the most serious threat to aquatic life in this contaminated area. Second, dissolved Fe is the most abundant cation in most, if not all, acid mine waters, yet most investigators do not employ water-quality standards for measurement of Fe in waters affected by acid mine drainage. Third, other studies of the aquatic toxicity of dissolved Fe have come to the similar conclusion: that a few mg of Fe per liter is unsafe or toxic for aquatic life in freshwaters. Fish kills are the most common environmental problem from mining activities and the causative agent of acute toxicity may be Fe or Al instead of Cd, Cu, or Zn as more commonly thought. The results of this study could have important impacts on environmental regulation of mining activities, and

restoration of watersheds impacted by historical mining.

ACKNOWLEDGMENTS

The authors wish to thank Rick Sugarek of the U.S. EPA and Kerry Rae of the BOR for supporting the USGS studies at Iron Mountain. Gerald Vogt, Michele Spence, and Rob Pexton of CH2M Hill; Bill Bluck of W.B. Enterprises, Inc.; Stuart Angerer, Sean Duffy, Janet Martin, and Diane Wisniewsky of the Bureau of Reclamation; and Karl Davidek, Michael Hunerlach, Frank Moseanko, and Cathy Munday of the USGS assisted with field work. The authors also thank Josef Friedl of the Technical University of Munich for performing the Mössbauer spectroscopy and x-ray diffraction analyses. The interpretations in this report are the responsibility of the authors and do not reflect the views of the U.S. EPA or the BOR.

REFERENCES

Alpers, C.N., Nordstrom, D.K., and Burchard, J.M., 1992, Compilation and interpretation of water-quality and discharge data for acidic mine waters at Iron Mountain, Shasta County, California, 1940–91: U.S. Geological Survey Water-Resources Investigations Report 91-4160, 173 p.

Davis, J.A., 1984, Complexation of trace metals by adsorbed natural organic matter: Geochimica et Cosmochimica Acta, v. 48, p. 679–691.

———, and Kent, D.B., 1990, Surface complexation modeling in aqueous geochemistry, in Hochella, M.F., and White, A.F. (eds.), Mineral-Water Interface Geochemistry: Washington D.C., Mineralogical Society of America, Reviews in Mineralogy, v. 23, p. 177–260.

Dzombak, D.A., and Morel, F.M.M., 1990, Surface complexation modeling- Hydrous ferric oxide: New York, John Wiley & Sons, 393 p.

Fujimura, R.W., Huang, C., and Finalyson, B., 1995, Chemical and toxicological characteristics of Keswick Reservoir sediments: Elk Grove, Calif., California Department of Fish and Game, report to the California State Water Resources Control Board, Sacramento, Calif. (I.A. 2-107-250-0), 69 p.

Krauskopf, K.B., and Bird, D.K., 1995, Introduction to Geochemistry (3rd edition): New York, McGraw Hill Book Co.

Nordstrom, D.K., 1977, Hydrogeochemistry and microbiological factors affecting the heavy metal chemistry of an acid mine drainage system: Ph.D. thesis, Stanford University, Stanford, Calif., 210 p.

———, and Alpers, C.N., 1995, Remedial investigations, decisions, and geochemcial consequences at Iron Mountain Mine, California, in Hynes, T.P., and Blanchette, M.C. (eds.), 1995, Proceedings of Sudbury '95–Mining and the Environment, Sudbury, Ontario, Canada, May 28–June 1, 1995: Ottawa, Ontario, Canada, CANMET, v. 2, p. 633–642.

———, Jenne, E.A., and Averett, R.C., 1977, Heavy metal discharges into Shasta Lake and Keswick Reservoir on the Sacramento River, California – Reconnaissance during low flow: U.S. Geological Survey Open-File Report 76-49, 25 p.

Webster, J.G., Swedlund, P.J. and Webster, K.S., 1998, Trace metal adsorption onto an acid mine drainage iron(III) oxyhydroxysulfate: Environmental Science & Technology, v. 32, no. 10, p. 1361–1368.

AUTHOR INFORMATION

D. Kirk Nordstrom (dkn@usgs.gov), Howard E. Taylor, R. Blaine McCleskey, and James W. Ball, U.S. Geological Survey, Boulder, Colorado

Charles N. Alpers, U.S. Geological Survey, Sacramento, California

Jennifer A. Coston and James A. Davis, U.S. Geological Survey, Menlo Park, California

Scott Ogle and Jeffrey S. Cotsifas, Pacific Eco-Risk Laboratories, Martinez, California

A New Method for the Direct Determination of Dissolved Fe(III) Concentration in Acid Mine Waters

By James W. Ball, D. Kirk Nordstrom, R. Blaine McCleskey, and Tanya Bangthanh To

ABSTRACT

A new method for direct determination of dissolved Fe(III) in acid mine water has been developed. In most present methods, Fe(III) is determined by computing the difference between total dissolved Fe and dissolved Fe(II). For acid mine waters, frequently Fe(II) >> Fe(III); thus, accuracy and precision are considerably improved by determining Fe(III) concentration directly. The new method utilizes two selective ligands to stabilize Fe(III) and Fe(II), thereby preventing changes in Fe reduction-oxidation distribution. Complexed Fe(II) is cleanly removed using a silica-based, reversed-phase adsorbent, yielding excellent isolation of the Fe(III) complex. Iron(III) concentration is measured colorimetrically or by graphite furnace atomic absorption spectrometry (GFAAS). The colorimetric method requires inexpensive commercial reagents and simple procedures that can be used in the field. The method detection limit is 0.002 mg/L (40 nM) using GFAAS, and 0.02 mg/L (0.4 μM) by colorimetry.

INTRODUCTION

Accurate and precise measurements of Fe reduction-oxidation (redox) species are particularly important in the study of acid mine waters because Fe is a major component in such waters. Charge balances calculated for acid mine waters depend strongly on the Fe(II)/Fe(III) ratio. Aqueous speciation is sensitive to the absolute concentrations of Fe(II) and Fe(III) as well as the Fe(II)/Fe(III) ratio. Iron(III) precipitates readily, forming hydrous ferric oxide, which adsorbs trace metals. Thus, Fe controls the mobility and toxicity of other metals. A method for determining Fe(III) concentration is needed to accurately predict the fate and mobility of metals in high-Fe aquatic environments.

Dissolved Fe(II) concentrations in waters are commonly determined by a colorimetric technique using a ferroin complexing reagent; it is also preferable to determine total dissolved Fe (Fe_T) concentrations by colorimetry. In a study comparing analytical methods for the determination of major and trace constituents in acid mine waters, Ball and Nordstrom (1993) found that colorimetric determination of Fe_T, using FerroZine®[1] as the complexing agent, was more reliable, precise, and sensitive than inductively-coupled plasma or direct-current plasma spectrometry.

Most methods for determining Fe(III) concentration are based on colorimetric determination of the Fe(II) concentration, followed by a separate determination of the Fe_T concentration after reduction of Fe(III) (Greenberg and others, 1992). The difference between the concentrations of Fe_T and Fe(II) is taken as the Fe(III) concentration. One major problem with this approach is that both accuracy and precision of the Fe(III) concentration are compromised as the proportion of Fe(II) increases, with determinations often overestimating actual Fe(III) concentrations. Acid mine waters usually contain much more Fe(II) than Fe(III), making the difference between Fe_T

[1] Registered trademark of the Hach Company, Loveland, CO. The use of trade, brand, or product names is for identification purposes only and does not constitute endorsement by the U.S. Geological Survey

and Fe(II) comparable to the error of the determination.

Prompt on-site determination of the Fe species may be important because the relative concentrations of the Fe redox states may change in the presence of oxygen, light, and biocatalysts (Nordstrom and Alpers, 1999). Portable UV-Visible spectrophotometers allow colorimetric Fe measurements to be taken immediately after sample collection.

While determination by difference of one Fe valence state is a simple matter when $0.2 \leq$ Fe(II)/Fe(III) ≤ 5, it becomes far more difficult at very large or very small ratios. In such instances, reagents are needed that are specific for the respective oxidation states. The proposed method uses selective complexing agents for both Fe(II) and Fe(III). The new method corrects for the shortcomings of many reported methods and current practices, and provides accurate and precise measurements of Fe(III) in the presence of other metals including Fe(II). Desirable features of the method include reliability, portability, and low costs.

Acetohydroxamic acid was selected as the Fe(III) chelator because it has a high selectivity for Fe(III) (Raymond and others, 1984; Hider and Hall, 1991; Purohit and others, 1994), it is commercially available, and it is inexpensive. Derivatives of this compound could be used to further enhance the molar absorptivity and sensitivity of the method.

EXPERIMENTAL

Sample Collection and Preservation

Samples collected in the field are immediately filtered through a 0.1 µm tortuous-path membrane, acidified to pH of about 1 with hydrochloric acid (2 mL 6 M HCl per 250 mL sample), and stored in acid-washed opaque plastic bottles at 4°C. Samples collected and preserved in this manner may be stored for up to 6 months without significant changes in the Fe redox distribution because microbial catalysts are removed, the pH is low enough to keep metals solubilized, and the iron oxidation rate is negligible.

Apparatus

A diode-array spectrophotometer (HP8452A) with 5cm cells, Zeeman Atomic Absorption Spectrometer (PE 4110ZL), Alltech maxi-clean C18 cartridges containing 900 mg of absorbent, and plastic syringes (10-mL and 30-mL) were used.

Reagents

Double-distilled water; 1.0 M acetohydroxamic acid ($C_2H_4NO_2$), Aldrich, 98%; 4.9×10^{-3} M FerroZine iron reagent ($C_{20}H_{13}N_4S_2O_6Na\cdot H_2O$), Hach, 95.2% pure; 6 M redistilled hydrochloric acid (HCl); methanol (CH_3OH), 99.9%, A.C.S. HPLC grade; hydroxylamine hydrochloride solution ($NH_2OH\cdot HCL$), 10% w/v; and ammonium acetate buffer solution (CH_3COONH_4), pH 7-7.5. The buffer was prepared by diluting 467 mL reagent grade (28-30%) ammonium hydroxide (NH_4OH) and 230 mL ultrapure glacial acetic acid (CH_3COOH) to 1 L. Iron(III) standard stock solution: 10.0 mg/L as ferric sulfate hexahydrate ($Fe_2(SO_4)_3\cdot 6H_2O$) in double distilled water containing 1% (v/v) 6 M redistilled HCl. The Fe in the standard was greater than 99.0% Fe(III), as determined by the FerroZine method. Iron(II) standard stock solution: 100 mg/L as ferrous ammonium sulfate hexahydrate ($Fe(NH_4)_2(SO_4)_2\cdot 6H_2O$) in double distilled water containing 1% (v/v) 6 M redistilled HCl. The Fe in the standard was greater than 99.0% Fe(II), as determined by the FerroZine method.

The following single-element standards were used for interference studies: Cu(II), 1,000 $\pm$ 3 mg/L in 2% HNO_3; Ca(II), 10,000 $\pm$ 5 mg/L in 5% HNO_3; Cr(III), 1,000 $\pm$ 3 mg/L in 5% HCl and 1% HNO_3; Al(III), 1,000 $\pm$ 5 mg/L in 5% HCl and 1% HNO_3; Co(II), 1,000 $\pm$ 3 mg/L in 2% HNO_3; Ni(II), 1,000 $\pm$ 5 mg/L in 5% HNO_3; Pb(II), 1,000 $\pm$ 3 mg/L in 2% HNO_3; Zn(II), 1,000 $\pm$ 5 mg/L in 5% HNO_3; and Cd(II), 1,000 $\pm$ 3 mg/L in 2% HNO_3.

Procedure

1. Determine dissolved Fe(II) and Fe_T using the FerroZine method as follows:

a. Pipette an adequate volume of acidified sample (up to 20 mL maximum) which will yield 0.004-1.6 mg/L Fe when diluted to volume, into a 25-mL volumetric flask.

b. Prepare appropriate blanks and standards, in 25-mL volumetric flasks.

c. If solution is a standard or blank, add 0.25 mL hydroxylamine hydrochloride solution (reduces Fe(III) to Fe(II)).

d. Add 0.5 mL FerroZine reagent and mix (the FerroZine forms a complex with Fe(II)).

e. Add 1.25 mL buffer solution (buffers the pH near neutrality), rinse down neck of flask, shake well, and allow at least 5 min for full color development.

f. If the magenta color of the FerroZine complex is masked or discolored by a brick or rust red color due to the presence of high Fe(III) concentrations, add 1.50 mL 6 M HCl, after color development. If Fe(III) interference is suspected but not noticeable to the eye, check duplicates, one with acid against one without: absorbances should be nearly identical if no interference is present.

g. Dilute to the mark and shake well.

h. Measure absorbance at 562 nm. Solutions must be measured within 1-2 hrs.

i. For Fe_T, use the same procedure with the addition of step 1.c. to all samples.

2. Transfer a maximum of 18.25 mL of sample containing no more than 14 mg/L Fe(II) and no more than 1.2 mg/L Fe(III) when diluted to volume to a 25-mL volumetric flask.

3. Add the following reagents in the order listed:

a. 5.0 mL FerroZine solution.

b. 0.5 mL acetohydroxamic acid (the acetohydroxamic acid will form a complex with Fe(III)).

c. 1.25 mL ammonium acetate buffer (buffers the pH near neutrality).

4. Dilute to volume with double-distilled water.

5. Remove the Fe(II)-FerroZine complex from the sample as follows:

a. Attach a new or regenerated C_{18} cartridge to a 10-mL plastic syringe.

b. Condition C_{18} cartridge by passing through it 5 mL methanol followed by 5 mL double-distilled water. Do not allow cartridge to dry before sample processing.

c. Remove C_{18} cartridge from syringe and attach it to a new 30-mL syringe.

d. Remove plunger, transfer sample into the syringe, then force sample through cartridge at a fast, steady drip (2-3 drops per second). Discard first 5 mL of filtrate and collect remaining 20 mL for Fe(III) determination.

6. Determine the Fe(III) concentration colorimetrically (within 5 hours) or by Zeeman-corrected graphite furnace atomic absorption spectrometry (GFAAS).

7. Regenerate C_{18} cartridge by passing 10 mL methanol through it.

RESULTS AND DISCUSSION

A typical calibration curve for Fe(III) by colorimetric analysis is shown in figure 1. The visible absorption spectrum of the Fe(III)-acetohydroxamic acid complex exhibits a single peak with maximum absorbance at 424 nm. At this wavelength, the molar absorptivity is 2,583 $cm^{-1} mol^{-1}$ and Beer's law is obeyed to approximately 16 mg/L. The Fe(III)-acetohydroxamic acid complex is stable for up to 5 hours. The redox stability of the combined Fe(II) and Fe(III) complexes was tested by time series determinations, and no change in Fe(II)/Fe(III) ratio was found for up to 3 hours.

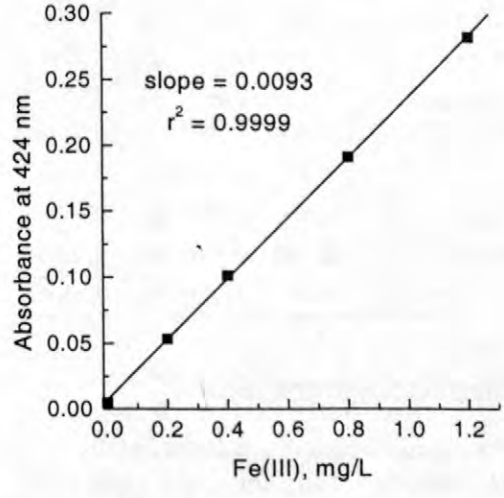

Figure 1. Standard curve for colorimetric determinations

Accuracy of Direct Fe(III) Measurements in Acid Mine Waters

The accuracy of the new method was estimated by performing spike recoveries. Two or three additions of Fe(III) standard solution were added to six different samples and treated with the described procedure. The samples were collected from three different acid mine effluents: Summitville Mine, Rio Grande County, CO; Paradise Portal in the Upper Animas Mine Drainage, San Juan County, CO; and Iron Mountain Mine, Shasta County, CA. GFAAS determinations were performed for samples found to contain less than 0.02 mg/L Fe(III) by colorimetric analysis. Recoveries were 93-101% for colorimetric determinations and 89-91% for GFAAS (fig. 2, table 1).

Table 1. Iron(III) spike recoveries using the acetohydroxamic acid method.

Sample ID	Fe(III) added mg/L	Recovered mg/L	%	Analysis
Alamosa River below	0.010	0.009	91	GFAAS
Terrace Reservoir	0.020	0.018	89	GFAAS
Spring Creek at weir	0.100	0.100	100	Color
	0.200	0.203	101	Color
	0.400	0.403	101	Color
Chandler Adit of	0.100	0.097	97	Color
Summitville Mine	0.200	0.197	98	Color
	0.400	0.400	100	Color
Paradise Portal	0.100	0.093	93	Color
	0.200	0.198	99	Color
	0.400	0.384	96	Color
Keswick Reservoir	0.100	0.097	97	Color
Pore Water	0.200	0.198	99	Color
	0.400	0.396	99	Color

Analytical Considerations

The C_{18} cartridges retain some Fe(II)-FerroZine complex. Thus, for best accuracy and precision at Fe(III) concentrations below about 0.2 mg/L, it is critical to pre-clean C_{18} cartridges by processing a blank solution through them. The C_{18} cartridges can be regenerated virtually

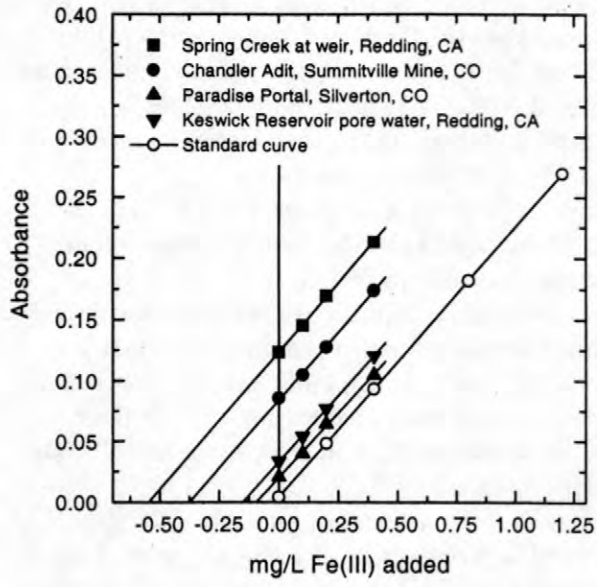

Figure 2. Method of standard additions for Fe(III) using the acetohydroxamic acid method.

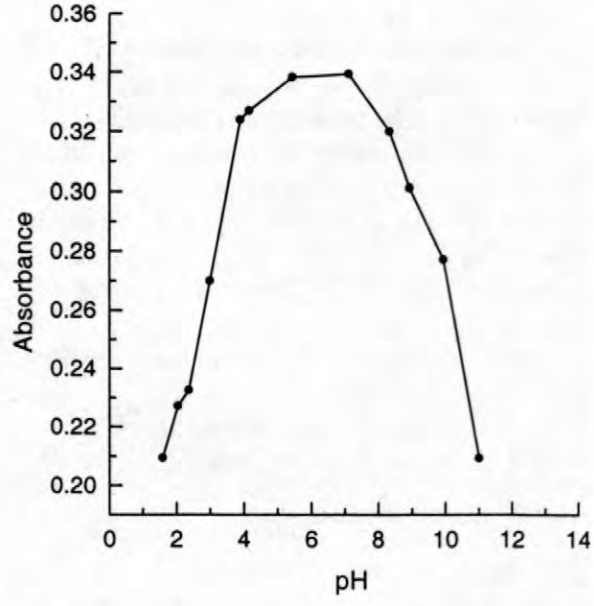

Figure 3. Effect of pH on the formation of Fe(III)-acetohydroxamic acid complex.

indefinitely when used to determine Fe(III) concentrations higher than 0.2 mg/L. The pH of the final solution should be between 4 and 7. The yellow Fe(III)-acetohydroxamic acid complex (fig. 3) and the Fe(II)-FerroZine (Stookey, 1970)

complex will form completely in aqueous solution in this pH range.

The detection limit by colorimetric analysis using a 5-cm cell is 0.02 mg/L Fe(III). Standards for colorimetric determinations were prepared in the same way as samples and contained 0, 0.2, 0.4, 0.8, and 1.2 mg/L Fe(III) when diluted to volume. The detection limit by Zeeman-corrected GFAAS is 0.002 mg/L Fe(III). The less-sensitive colorimetric analysis is preferred when Fe(III) concentrations are above its detection limit and results are needed in real time, such as during field studies.

The sample should be filtered through a 0.1 μm or smaller pore-sized membrane. In a study of filter pore-size effects on the analysis of dissolved Fe, Al, Mn, and Ti in natural water, errors of an order of magnitude or more in the measurement of the dissolved metals were found when a 0.45 μm filter was used (Kennedy and others, 1974). This was caused by fine-grained particulate material passing through the membrane. Compared with a 0.45 μm membrane, the 0.1 μm membrane reduces the passage of particulate materials without significantly increasing filtration time. More recently, investigators have demonstrated that iron colloids also can pass through a 0.1 μm membrane (Kimball and others, 1995).

Potential Interferences

The FerroZine and ammonium acetate reagents did not interfere with the Fe(III)-acetohydroxamic acid complex. Acid mine water may contain at least 31 major chemical species with concentrations that vary up to several orders of magnitude. Many of those constituents may cause interferences in the colorimetric determination of Fe(III). Ten metals found in a typical acid mine effluent that may cause interferences have been tested. Chromium(III) was selected because of its chemical similarity to Fe(III). The remaining metals were selected based on their reported binding constants with acetohydroxamic acid (Martell and Smith, 1976).

The level of interference by each metal with the quantitation of Fe(III) was determined by using the new method to measure the change in apparent Fe(III) content in the presence of each metal. Individual solutions containing zero or 0.4 mg/L Fe(III) were analyzed in triplicate with up to 40 mg/L of potential interferent, except for Ca(II) (400 mg/L), added. The change in apparent Fe(III) content in the presence of 40 mg/L Al(III), Pb(II), Zn(II), Ni(II), and Cd(II), and 400 mg/L Ca(II) was less than ±0.008 mg/L. This change is considered insignificant because it is well below the minimum difference in Fe(III) content measurable by the new method.

The apparent Fe(III) content increases by 0.052 mg/L in the presence of 40 mg/L Cu(II).

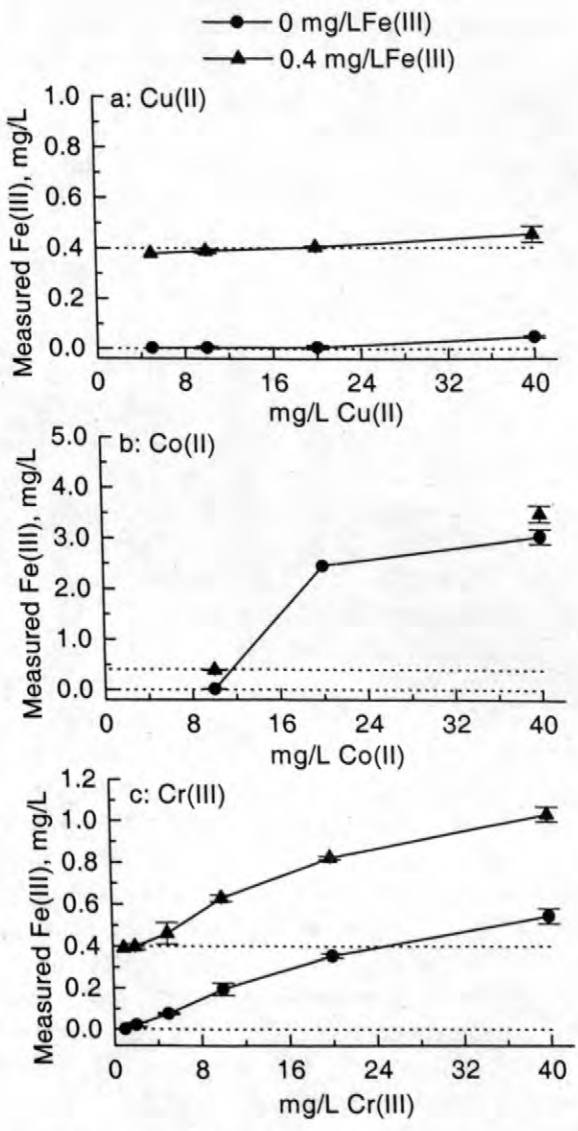

Figure 4. Apparent Fe(III) concentration in the presence of added Cu(II), Co(II) and Cr(III). [error bars represent ± 1s for triplicate determinations]

The tested Cu(II)/Fe(III) molar ratio was 88, whereas the ratio found in acid mine samples is typically less than 1. Of 25 samples taken from the Leviathan Mine drainage basin, located in California and Nevada, the average Cu(II)/Fe(III) ratio was 0.18 with 2 samples having a ratio slightly greater than 1 (Ball and Nordstrom, 1989). In the presence of 20 mg/L Cu(II), the change in apparent Fe(III) content was less than 0.008 mg/L (fig. 4a).

Co(II) forms a colored complex with FerroZine (Dawson and Lyle, 1990) which is not completely retained by the C_{18} cartridge at Co(II) > 10 mg/L and absorbs intensely at wavelengths less than 350 nm. The tail of the absorption band interferes with the 424-nm line. The highest Co(II)/Fe(III) molar ratio in the 25 Leviathan Mine drainage basin samples discussed above is 0.8. In the presence of 10 mg/L Co(II) (Co(II)/Fe(III) molar ratio of 24) the Co(II)-FerroZine complex is completely retained by the C_{18} cartridge. The change in apparent Fe(III) content was about +0.016 mg/L for a blank and about –0.008 mg/L in a 0.4 mg/L standard (fig. 4b). These deviations are not significant relative to the measured precision.

The apparent Fe(III) content increased by about 0.6 mg/L in the presence of 40 mg/L Cr(III). In the presence of 2 mg/L Cr(III) (Cr(III)/Fe(III) molar ratio of about 5), no change in the apparent content of Fe(III) in test solutions could be detected (fig. 4c). In most acid mine effluent samples the Cr(total)/Fe(III) molar ratio is usually well below 0.5. Chromium, Co, and Cu are expected to interfere only under unusual conditions.

Acetohydroxamic acid can oxidize Fe(II) to Fe(III), causing overestimation of the Fe(III) concentration. To control this source of error, it is necessary to add the FerroZine reagent before the acetohydroxamic acid so that the distribution of Fe redox species is stabilized. Separation of the two Fe complexes is necessary to prevent the strongly absorbing Fe(II)-FerroZine complex from interfering with the colorimetric determination of Fe(III). The Fe(II)-FerroZine complex exhibits a single peak with a maximum absorbance at 562 nm (Stookey, 1970). The C_{18} cartridge retains the more hydrophobic Fe(II)-FerroZine complex while allowing the more hydrophilic Fe(III)-acetohydroxamic acid complex to pass into the effluent. The 562-nm absorbance remained at the baseline for synthetic Fe samples containing 0, 0.2, and 0.8 mg/L Fe(III) and 0 to 20 mg/L Fe(II), illustrating the completeness of the separation.

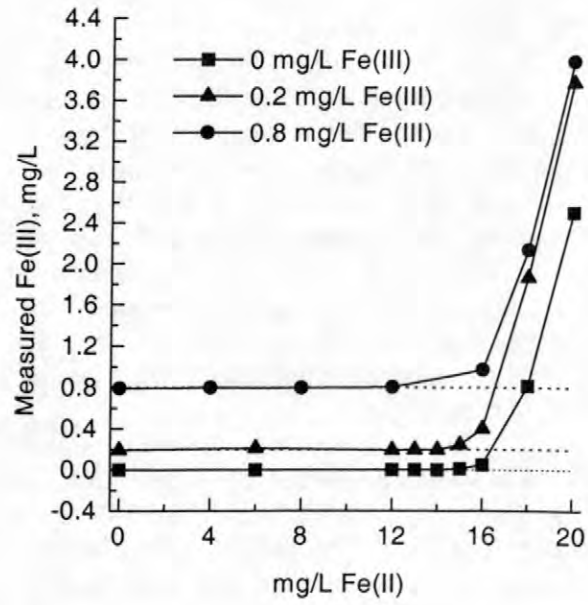

Figure 5. Iron(II) interferences and tolerance limits for direct determination of Fe(III) using the acetohydroxamic acid method.

Table 2. Lower limits of the acetohydroxamic acid method in the presence of Fe(II).

Fe(II), mg/L	Lowest Fe(III) concentration (mg/L) that can be detected by: Colorimetric	GFAAS
10,000	11.3	1.13
2,000	2.27	0.227
500	0.57	0.057
100	0.11	0.011
<20	0.02	0.002

Under the conditions stated in the procedure, Fe(II) concentrations less than14 mg/L do not interfere with the Fe(III) determination (fig. 5). The stated quantity of FerroZine has the capacity to complex a maximum of 350 µg Fe(II). More FerroZine could be used, but the capacity of the C_{18} cartridge would be exceeded. Excess Fe(II) is oxidized and forms Fe(III)-acetohydroxamic acid. Iron(III) was separated

(97-103% recovery) from synthetic iron samples containing Fe(II)/Fe(III) ratios from 0 to greater than 500. Using the stated procedure, Fe(III) can be measured colorimetrically in solution with Fe(II)/Fe(III) ratios up to 880, and by GFAAS in solutions with ratios up to 8800 (table 2).

Comparing the FerroZine Method with the New Method

The performance of the new method was compared with that of the FerroZine method for Fe(III) determinations. Four representative samples were selected for the comparison. Values of percent difference (Δ%), equation (1):

$$\Delta\% = 100 \times \frac{C_A - C_B}{(C_A + C_B) \div 2} \qquad (1)$$

were used for the comparison, where C_A is concentration determined by the FerroZine method and C_B is concentration determined by the new method with either colorimetric or GFAAS determinations. The maximum value of this function is ± 200%. A Δ% value of 0 denotes a perfect match of the analytical values, while a value approaching ± 200 means there is no similarity between values (Ball and Nordstrom, 1993). A positive Δ% value indicates that Fe(III) concentration determined by FerroZine is greater than the concentration measured by the new method. To compare the analytical results of direct Fe(III) determinations with the Fe(III) results obtained by difference using the FerroZine method, values of precision and the Δ% function were calculated. Iron(III) concentrations obtained by difference using the FerroZine method are typically greater than those obtained using the new method. The value of the Δ% function was +32% in one case. A graphical representation of results for selected samples illustrating the dramatic improvement in precision using the new method is shown in figure 6.

The power of the new method lies in its capability to determine Fe(III) concentration in samples containing very high Fe(II)/Fe(III) ratios. As the Fe(II)/Fe(III) ratio increases, the relative standard deviation of Fe(III) concentrations

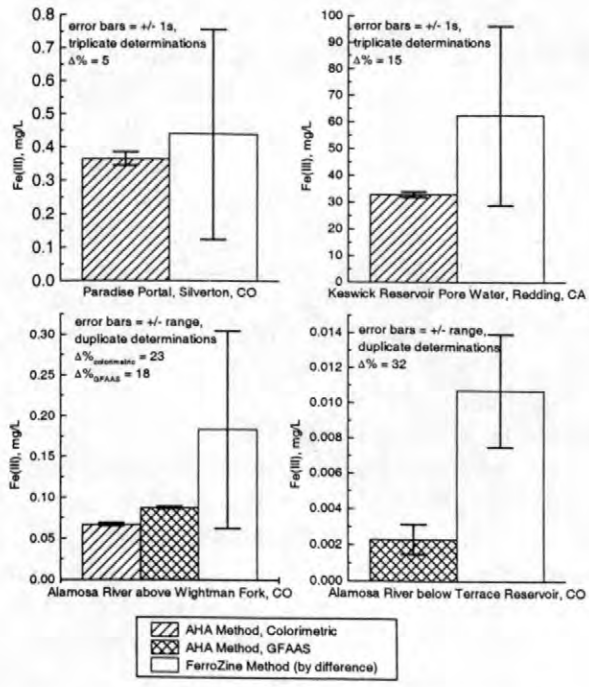

Figure 6. Comparison of Fe(III) concentrations determined directly using the acetohydroxamic acid (AHA) method with Fe(III) concentrations determined by difference using the FerroZine method.

obtained by difference generally increases. Relative standard deviations for Fe(III) determinations using the FerroZine method for 50 different samples collected from three different acid mine effluents including Summitville Mine, Rio Grande County, CO; Paradise Portal in the Upper Animas Mine Drainage, San Juan County, CO; and Iron Mountain Mine, Shasta County, CA increased to over 50 percent in samples with Fe(II)/(III) ratios of 30 or higher. This uncertainty is often too large for Fe(III) concentrations determined by difference to be meaningful. The relative standard deviations for Fe(III) concentrations determined directly using the new method are generally less than 5 percent.

A more detailed description of the method can be found in To and others (1999).

REFERENCES

Ball, J.W., and Nordstrom, D.K., 1989, Final revised analyses of major and trace elements from acid mine waters in the

Leviathan Mine drainage basin, California and Nevada--October 1981 to October 1982: USGS Water-Resources Investigations Report 89-4138: Menlo Park, CA, U.S. Geological Survey, 46 p.

———, and Nordstrom, D.K., 1994, A comparison of simultaneous plasma, atomic absorption, and iron colorimetric determinations of major and trace constituents in acid mine waters: USGS Water-Resources Investigations Report 93-4122: Boulder, CO, U.S. Geological Survey, 151 p.

Dawson, M.V., and Lyle, S.J., 1990, Spectrophotometric determination of iron and cobalt with ferrozine and dithizone: Talanta, v. 37, p. 1189-1191.

Greenberg, A.E., Clesceri, L.S., Eaton, A.D., and Franson, M.A., 1992, Standard Methods for the Examination of Water and Wastewater: Washington, D.C., American Water Works Association, Water Pollution Control Federation, p. 3-66 -- 3-68.

Hider, R.C., and Hall, A.D., 1991, Clinically useful chelators of tripositive elements: Progress in Medicinal Chemistry, v. 28, p. 41-172.

Kennedy, V.C., Zellweger, G.W., and Jones, B.F., 1974, Filter pore-size effects on the analysis of Al, Fe, Mn, and Ti in water: Water Resources Research, v. 10, p. 785-790.

Kimball, B.A., Callender, E., and Axtmann, E.V., 1995, Effects of colloids on metal transport in a river receiving acid mine drainage, upper Arkansas River, Colorado, U.S.A.: Applied Geochemistry, v. 10, p. 285-306.

Martell, A.E., and Smith, R.M., 1976, Critical Stability Constants. Volume 3: Other Organic Ligands: New York, Plenum.

Nordstrom, D.K., and Alpers, C.N., 1999, Geochemistry of acid mine waters: Reviews in Economic Geology, v. 6 (in press).

Purohit, D.N., Tyagi, M.P., Chauhan, R.S., Changani, M.K.S., and Jain, S. K. 1994, Spectrophotometric methods for determination of iron(III): Reviews in Analytical Chemistry, v. 13, p. 1-74.

Raymond, K.N., Müller, G., and Matzanke, B.F., 1984, Complexation of iron by siderophores. A review of their solution and structural chemistry and biological function: Topics in Current Chemistry, v. 123, p. 49-102.

Stookey, L.L., 1970, Ferrozine--a new spectrophotometric reagent for iron: Analytical Chemistry, v. 42, p. 779-781.

To, T.B., Nordstrom, D.K., Cunningham, K.M., Ball, J.W., and McCleskey, R.B., 1999, New method for the direct determination of dissolved Fe(III) concentration in acid mine water: Environmental Science and Technology, v. 33, (ASAP Article 10.1021/es980684z S0013-936X(98)00684-1, http://pubs.acs.org/isubscribe/journals/esthag/asap/pdf/es980684z.pdf, in press).

AUTHOR INFORMATION

James W. Ball (jwball@usgs.gov), D. Kirk Nordstrom, R. Blaine McCleskey, U.S. Geological Survey, Boulder, Colorado, and Tanya B. To, Peninsula College, Port Angeles, WA

Transport Modeling of Reactive and Non-Reactive Constituents from Summitville, Colorado: Preliminary Results from the Application of the OTIS/OTEQ Model to the Wightman Fork/Alamosa River System

By James W. Ball, Robert L. Runkel, and D. Kirk Nordstrom

ABSTRACT

Reactive-transport processes in the Wightman Fork/Alamosa River system downstream of the Summitville Mine, south-central Colorado, were simulated under low-flow conditions using the OTIS and OTEQ solute transport modeling programs. Simulation results revealed that Ca, Cu, Mg, Mn, Na, Zn, Cl, F, and SO_4 are conservative in the stream reach, whereas pH, Fe, and Al are non-conservative. Simulations that allow precipitation of $Fe(OH)_3$ and $Al(OH)_3$ match observed water quality more closely than conservative simulations. The pH could not be adequately simulated without assuming that tributary inflows had pH values of about 8 or higher and alkalinities of 50-110 milligrams per liter (mg/L). Subsequent sampling confirmed these predictions.

INTRODUCTION

The Summitville Mine is located along the upper Alamosa River in south-central Colorado (fig. 1). Gold was first discovered at Summitville in 1870 (King, 1995). Until about 1985, gold was extracted from the deposit using conventional techniques of underground mining, including the sinking of shafts, removal of the ore, and transporting it to smelters where it was refined. More recently, highly disseminated gold was recovered by the cyanide heap-leach process. The process consists of placing relatively low-grade ore on a large pad and spraying a sodium cyanide solution over its top. The leachate solution is recovered from the bottom of the pad and transported to a central area where the gold is removed from the cyanide solution. An aerial photograph of the mine workings, demonstrating the extent of removal of the mountainside, is shown in figure 2.

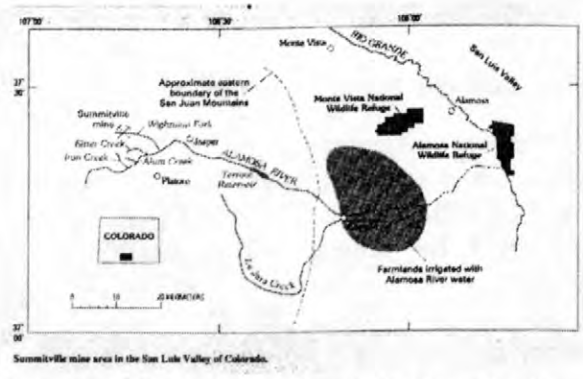

Figure 1. Schematic drawing of the Summitville Mine area (from King, 1995).

Much of the residual rock contains sulfide minerals that oxidize rapidly to form sulfuric acid solution because they have been exposed to the atmosphere during mining. This solution contains elevated concentrations of Fe, Al, Cu, Zn, Cd, Mn, and other metals that can be toxic to plants and animals living downstream.

In December 1992, the Colorado Department of Public Health and Environment (CDPHE) requested assistance from the Environmental Protection Agency (EPA) and Superfund Emergency Response was authorized. The U.S. Geological Survey (USGS) began water-quality investigations at Summitville, Terrace

Figure 2. Aerial photograph of the Summitville Mine workings, August, 1994 (from King, 1995).

Reservoir, and farther downstream in 1993 (fig. 1; King, 1995; Walton-Day and others, 1995; Balistrieri and others, 1996; Stogner and others, 1996). The USGS began routine water-quality monitoring in the upper Alamosa River (Alamosa River and tributaries above Terrace Reservoir) in 1995. The USGS began a reactive-transport modeling project in 1998 that includes preliminary modeling of 1997 data, tracer-injection studies, calibration of models, and simulations of reactive-transport under different remediation scenarios. The results of this investigation will be used by EPA and CDPHE to designate regulatory requirements and to achieve water-quality goals for the Alamosa River/Terrace Reservoir system. In mid-1998, CDPHE assumed management of the site, and began working with the USGS to characterize the upper Alamosa River system. The ultimate goal is to devise a long-term remediation strategy that will allow restoration of the Alamosa River and Wightman Fork to near pre-mining conditions. The purpose of this paper is to report on the preliminary modeling of the 1997 data.

One aspect of stream characterization is to describe the watershed in as much detail as possible. In the Alamosa River Basin, two synoptic studies, one at high flow and the other at low flow, will help quantify solute sources and sinks.

MODELING APPROACH

Conservative transport processes are modeled using the computer program OTIS (One-dimensional Transport with Inflow and Storage; Runkel, 1998). Reactive transport processes are modeled using program OTEQ (OTis with EQuilibrium calculations; Runkel and others, 1996a). OTIS models the conservative transport of solutes subject to the physical processes of advection, dispersion, transient storage, and lateral inflow. OTEQ combines the physical process description of OTIS with the chemical equilibrium capabilities of MINTEQ (Allison and others, 1991). This combination allows OTEQ to simulate pH-dependent processes such as precipitation and sorption in the context of physical transport.

Analytical results from low-flow synoptic samples collected on August 14, 1997 were selected for this study. For the preliminary modeling study, the study area was divided into 20 model reaches (fig. 3). The first reach begins at USGS sampling station 5.5 on Wightman Fork, just downstream of its confluence with Cropsy Creek (WF5.5). Cropsy Creek historically carried most of the discharge from the mine site and presently carries the effluent from the Summitville Mine treatment plant. The last reach ends about 300 meters above USGS sampling station 34.5 on the Alamosa River (AR34.5). For this simulation, the Alamosa River above its confluence with Wightman Fork (AR45.5) is considered a tributary, that is, its discharge and solute masses are represented as lateral inflow in reach 2. Other tributaries include Jasper Creek, Burnt Creek, Spring Creek, Fern Creek, Castleman Gulch, Silver Creek, Lieutenant Creek, and Ranger Creek (inflow to reaches 5, 7, 9, 11, 13, 15, 17, and 19, respectively).

Modeled Solutes

For the preliminary OTEQ calculations, only a subset of 7 components (SO_4, total excess H (H_T^+), Al, Fe(II), Fe(III), Cu, and CO_3) is considered. This approach is consistent with previous OTEQ simulations in other mine drainage streams (Broshears and others, 1996; Runkel and others, 1996b). Future simulations based on the complete component set will be used to evaluate the correctness of this assumption.

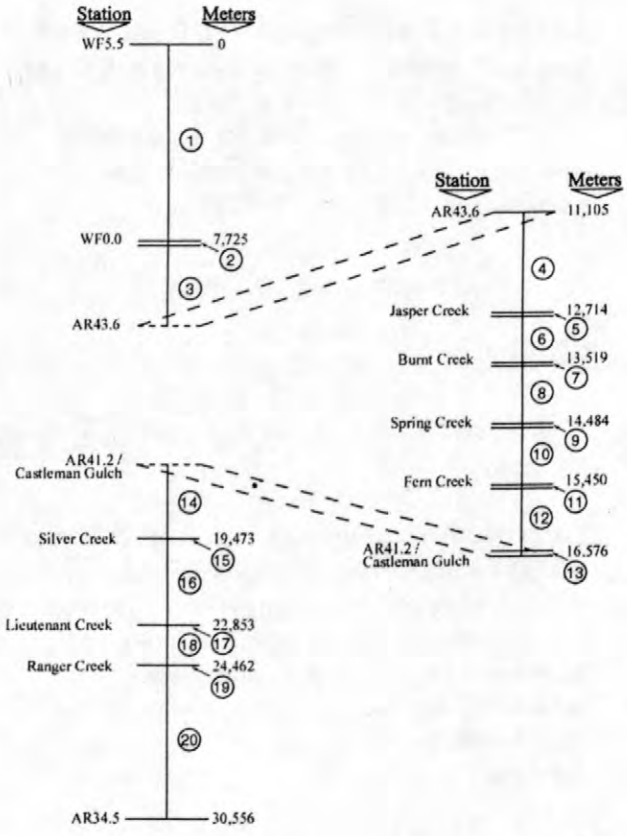

Figure 3. Schematic diagram of model reaches for the transport simulations; circled numbers are stream reach numbers; note that the present simulation does not incorporate revised distances. For this simulation, the Alamosa River above its confluence with Wightman Fork (AR45.5) is considered a tributary

Upstream Boundary Conditions

The effect of the choice of upstream boundary conditions on the model results is significant. Upstream boundary conditions were chosen using the three approaches described below.

The upstream boundary conditions for SO_4, Al, and Cu were set to the analytically determined concentrations at WF5.5 (408, 29.8, and 3.7 mg/L, respectively).

Analytical results for the modeled reach did not include Fe redox species, but total dissolved Fe = 11.3 mg/L was determined. For these preliminary simulations, Fe(II) and Fe(III) were estimated by assuming that the concentration of Fe(III) was half the total dissolved Fe concentration. Since Fe oxidation was not modeled, this approach ignores consequent effects such as production of hydronium ions. This approach may require refining for future simulations.

Values for H_T^+ and total inorganic carbon (TIC) were obtained by separate simulation using the program MINTEQA2 (Allison and others, 1991). The pH was fixed at the value of 3.6 observed at WF5.5, and equilibration with atmospheric CO_2 was allowed. The resulting H_T^+ = 3.68E-4 M and CO_3^{2-} = 3.60E-5 M values computed by MINTEQA2 were used as input to OTEQ.

Streamflow Parameters

The effect of the choice of cross-sectional areas, lateral inflow rates, and lateral inflow concentrations on the model results is frequently significant. Thus, these parameters must be defined as accurately as possible.

Cross-Sectional Areas and Lateral Inflow Rates

Values for these two components were calculated using equations (1) and (2):

$$v = d / t, \tag{1}$$

$$A = Q / v, \tag{2}$$

where

v is stream velocity,
d is distance,
t is travel time,
A is stream cross-sectional area, and
Q is stream discharge.

Measured cross-sectional areas were not available. The available distances, travel times, and discharges were used to calculate velocities (eq. 1) and cross-sectional areas (eq. 2).

Values for lateral inflow rates were calculated by dividing the difference between discharges at the ends of a reach by the length of

the reach. Thus, the units of this parameter are cubic meters per second per meter.

Lateral Inflow Concentrations

Values for lateral inflow concentrations were calculated or estimated using data available at the time of the simulation. Total excess H and TIC were determined for all inflows by running MINTEQA2 simulations with pH fixed at observed values and with dissolved carbonate species at equilibrium with atmospheric CO_2. Analytical results were available only for AR45.5 and Jasper Creek. For these two reaches (Reaches 2 and 5), Al, SO_4, and Cu concentrations were set to observed values. Iron redox species concentrations were set to observed Fe(II) and Fe(III) values for the upper Alamosa River. For Jasper Creek, all Fe was assumed to be present as Fe(II), since at pH 7.0 the concentration of dissolved Fe(III) would be too low to measure.

For the remaining tributaries, only pH and water temperature were available; thus, Al, SO_4, Fe(II), and Cu were set to the following background concentrations: 0.02, 10, 0.02, and 0.001 mg/L.

Stream discharge more than doubled along the initial reach from station WF5.5 to Wightman Fork above its confluence with the Alamosa River (WF0.0). However, no lateral inflow tributaries were monitored; thus, no flow or concentration parameters were available. Consequently, inflow Al, SO_4, Fe(II), and Cu concentrations were set to background as above. Total excess H and TIC were calculated using MINTEQA2 for Jasper Creek water chemistry and a pH fixed at 8, with inorganic carbonate species at equilibrium with atmospheric CO_2.

Of the 20 stream reaches considered, 10 were "base flow" reaches for which there existed no flow or chemistry information. For these 10 reaches, input parameters were estimated using a process analogous to that described above.

Geochemical Parameters

Temperature and ionic strength are spatially invariant within OTEQ. Therefore, since nearly all chemical reactions in the reach are nearly complete by the confluence of Wightman Fork and the Alamosa River, the temperature and ionic strength observed at stations WF0.0 and WF5.5 were used to set these two parameters to 8°C and 0.015 molal.

Defaults were retained for the solubility equilibrium constants for the precipitation reactions for $Al(OH)_3$ and $Fe(OH)_3$:

$$Al^{3+} + 3H_2O = Al(OH)_3 + 3H^+, \quad (3)$$

and

$$Fe^{3+} + 3H_2O = Fe(OH)_3 + 3H^+. \quad (4)$$

The respective default log K values of −8.77 and −4.891 for microcrystalline gibbsite and ferrihydrite solubility were used in the simulation. Uncertainties of other variables affecting Fe and Al removal from the water column were sufficiently large that sensitivity testing of variations in the log K values was not warranted at this time.

RESULTS

The OTIS simulations indicated that Fe and Al were reactive in reach 1, and that other solutes, including Ca, Cu, Mg, Mn, Na, Zn, Cl, F, and SO_4, exhibited conservative behavior.

For the reactive (OTEQ) simulations, emphasis was placed on the initial reach from WF5.5 to WF0.0. Conservative and reactive simulation results for pH, Fe, and Al are shown in figures 4-6. Figures 7 and 8 illustrate conservative simulations of SO_4 and Cu. The diamonds on the figures denote the mixture of WF0.0 and AR45.5 water, which was calculated using a discharge mass-balance relation for conservative mixing.

Using tributary inflows with pH values of about 8.2 and alkalinities derived using equilibrium with atmospheric CO_2, the reactive simulation of pH from Wightman Fork below its confluence with Cropsy Creek to above its confluence with the Alamosa River predicts the downstream pH in Wightman Fork remarkably well (fig. 4). The conservative simulation predicts the pH at the confluence calculated using the discharge mass-balance relation for conservative mixing remarkably well, as expected. However, the pH for the Alamosa River 23 km downstream

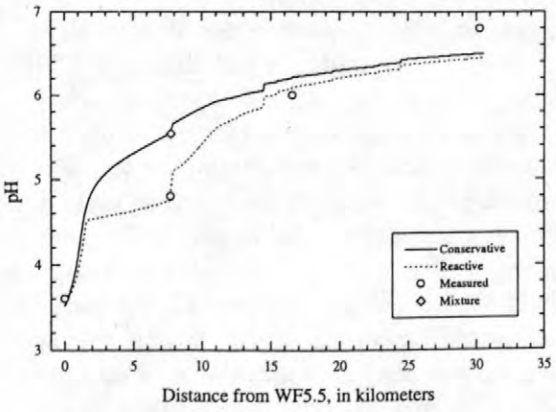

Figure 4. OTEQ simulation of pH assuming CO_2 at equilibrium with the atmosphere and ferrihydrite and gibbsite allowed to precipitate (low flow, 8/14/97).

of WF0.0 is somewhat underpredicted. This could well be due to groundwater inflows having higher pH and alkalinity than estimated.

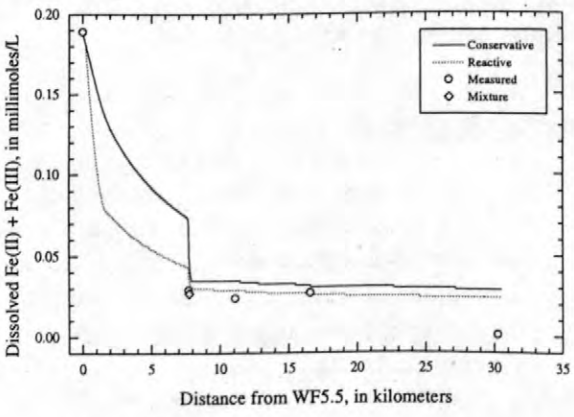

Figure 5. OTEQ simulation of dissolved Fe assuming CO_2 at equilibrium with the atmosphere and ferrihydrite and gibbsite allowed to precipitate (low flow, 8/14/97).

For the reactive Fe simulation (fig. 5), the Fe(III) concentration was set to one-half the total Fe concentration, based on the total dissolved Fe concentration measured at WF5.5. The fit of the reactive Fe simulation could be improved by increasing the proportion of Fe(III) slightly; however, a more effective approach might be to measure and use actual Fe(II) and Fe(III) concentrations.

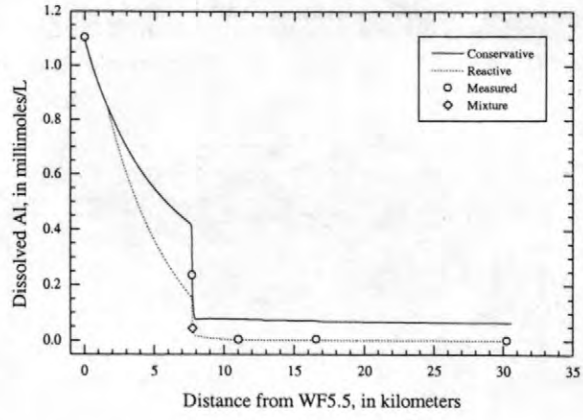

Figure 6. OTEQ simulation of dissolved Al assuming CO_2 at equilibrium with the atmosphere and ferrihydrite and gibbsite allowed to precipitate (low flow, 8/14/97).

For the reactive Al simulation (fig. 6), the model overpredicts Al precipitation in Wightman Fork. Use of an equilibrium constant for a more soluble phase such as amorphous $Al(OH)_3$ may allow for a more accurate fit to the observed data.

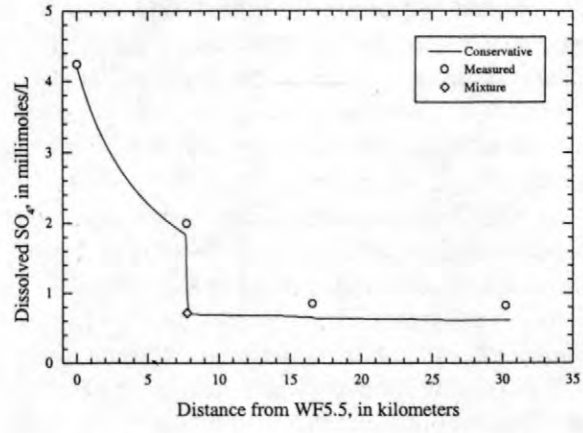

Figure 7. Conservative simulation of dissolved SO_4 (low flow, 8/14/97).

The model simulates the observed SO_4 concentrations in Wightman Fork well (fig. 7), but underpredicts them in the Alamosa River. This may be caused by use of inflow SO_4 concentration estimates that are smaller than the actual concentrations.

Although the model accurately simulates the Cu concentration calculated using the conservative

mixing equation at the confluence of Wightman Fork and the Alamosa River, the model overpredicts the Cu concentration observed at WF0.0 (fig. 8), suggesting that chemistry of this

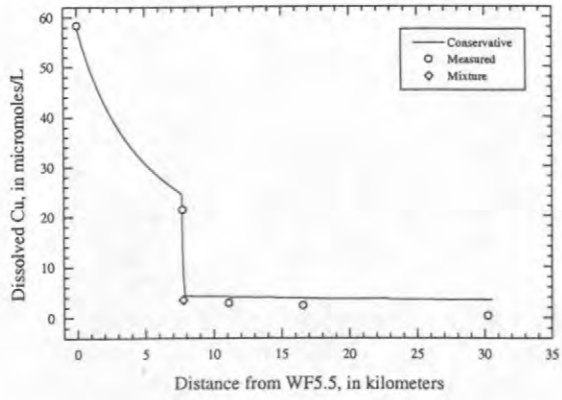

Figure 8. Conservative simulation of dissolved Cu (low flow, 8/14/97).

constituent is nonconservative. For Cu, the overprediction is small; thus the loss can be attributed to coprecipitation with or adsorption by Fe and Al oxyhydroxides. A reactive simulation (not shown) that modeled sorption of Cu to freshly precipitated hydrous ferric oxide (HFO) did not predict removal of appreciable quantities of Cu. This is most likely because the observed pH at WF0.0 is 4.8, whereas most Cu sorption occurs at pH values greater than 5 (Dzombak and Morel, 1990).

One possible explanation for the reduced Cu concentration at WF0.0, as compared with the simulated concentration, is precipitation or sorption of Cu in microenvironments where the acidic Wightman Fork water mixes with high-pH, high-alkalinity tributary water. While the pH of Wightman Fork water is not significantly changed by the relatively small-volume inflows, the precipitation or sorption may well be irreversible. Such microenvironment heterogeneity cannot be modeled at the scale of the present simulation.

During simulation runs it was necessary to assume values for pH, alkalinity, and SO_4 of many tributaries. Simulation results indicated that higher pH values and higher alkalinity and SO_4 concentrations may be present. Many of the refined pH values and alkalinity concentrations were later confirmed in field samples, providing a compelling illustration of the power of the reactive transport modeling approach as a tool to guide field investigations. Tributary inflows to Wightman Fork and parts of the Alamosa River were found to have pH ≈ 8 and alkalinity ≈ 50-110 mg/L, as predicted.

Plans for future work include completion of preliminary modeling for a high-flow scenario, correcting modeled distances based on revised estimates, and adding data which have recently become available for several tributaries along both Wightman Fork and the Alamosa River. Each of these improvements could significantly enhance the accuracy, and hence usefulness, of data to be gathered from a synoptic study planned for the spring of 1999.

ACKNOWLEDGMENTS

The authors would like to acknowledge the collaboration and support of the Colorado Department of Public Health and Environment and of the Environmental Protection Agency. The authors thank Katie Walton-Day, Rodger Ortiz, and Philip Verplanck of the USGS for many helpful comments and suggestions.

REFERENCES

Allison, J.D., Brown, D.S., and Novo-Gradac, K.J., 1991, MINTEQA2/ PRODEFA2, a geochemical assessment model for environmental systems: Version 3.0 user's manual: U.S. Environmental Protection Agency, EPA/600/3-91/021.

Balistrieri, L.S., Ortiz, R.F., Briggs, P.H., Elrick, K.A., and Edelmann, P.F., 1996, Metal fluxes across the sediment-water interface in Terrace Reservoir, Colorado: U.S. Geological Survey Open-File Report 96-040, 83 p.

Broshears, R.E., Runkel, R.L., Kimball, B.A., McKnight, D.M., and Bencala, K.E., 1996, Reactive solute transport in an acidic stream: Experimental pH increase and simulation of controls on pH, aluminum and iron: Environmental Science and Technology, v. 30, p. 3016-3024.

Dzombak, D.A., and Morel, F.M.M., 1990, Surface complexation modeling. Hydrous ferric oxide: New York, Wiley-Interscience, 393 p.

King, T.V.V., 1995, Environmental Considerations of Active and Abandoned Mine Lands – Lessons from Summitville, Colorado: U.S. Geological Survey Bulletin 2220, 38 p.

Runkel, R.L., Bencala, K.E., Broshears, R.E., and Chapra, S.C., 1996a, Reactive solute transport in streams: 1. Development of an equilibrium-based model: Water Resources Research, v. 32, p. 409-418.

Runkel, R.L., McKnight, D.M., Bencala, K.E., and Chapra, S.C., 1996b, Reactive solute transport in streams: 2. Simulation of a pH-modification experiment: Water Resources Research, v. 32, p. 419-430.

Runkel, R.L., 1998, One-dimensional transport with inflow and storage (OTIS): A solute transport model for streams and rivers: U.S. Geological Survey Water-Resources Investigations Report 98-4018, 73 p.

Stogner, R.W., Edelmann, P.F., and Walton-Day, K., 1996, Physical and chemical characteristics of Terrace Resrvoir, Conejos County, Colorado, May 1994 through May, 1995: U.S. Geological Survey Water-Resources Investigations Report 96-4150, 57 p.

Walton-Day, K., Ortiz, R.F., and von Guerard, P.B., 1995, Sources of water having low pH and elevated metal concentrations in the upper Alamosa River from the headwaters to the outlet of Terrace Reservoir, south-central Colorado, April-September, 1993, in Posey, H.H., Pendleton, J.A., and Van Zyl, D.J.A., eds., Proceedings, Summitville Forum '95: Denver, Colorado Geological Survey Special Publication 38, p. 160-170.

AUTHOR INFORMATION

James W. Ball, Robert L. Runkel, and D. Kirk Nordstrom, U.S. Geological Survey, Boulder, Colorado (jwball@usgs.gov, runkel@usgs.gov, dkn@usgs.gov)

Frequency Distribution of the pH of Coal-Mine Drainage in Pennsylvania

By Charles A. Cravotta III, Keith B.C. Brady, Arthur W. Rose, and Joseph B. Douds

ABSTRACT

The pH of coal-mine drainage in Pennsylvania has a bimodal frequency distribution, with modes at pH 2.5 to 4 (acidic) and pH 6 to 7 (near neutral). Although iron-disulfide and calcareous minerals comprise only a few percent, or less, of the coal-bearing rock, these minerals are highly reactive and are mainly responsible for the bimodal pH distribution. Field and laboratory studies and computer simulations indicate that pH will be driven toward one mode or the other depending on the relative abundance and extent of weathering of pyrite (FeS_2; acid-forming) and calcite ($CaCO_3$; acid-neutralizing). The pH values in the near-neutral mode result from carbonate buffering (HCO_3^-/H_2CO_3 and $HCO_3^-/CaCO_3$) and imply the presence of calcareous minerals; acid produced by pyrite oxidation is neutralized. The pH values in the acidic mode result from pyrite oxidation and imply a deficiency of calcareous minerals and the absence of carbonate buffering. The oxidation of only a small quantity of pyrite can acidify pure water (0.012 $g \cdot L^{-1}$ FeS_2 produces pH~4 and 20 $mg \cdot L^{-1}$ SO_4^{2-}); however, because of the log scale for pH and ion complexation (SO_4^{2-}/HSO_4^- and $Fe^{3+}/FeOH^{2+}$), orders of magnitude greater oxidation is required to produce pH < 3. Laboratory leaching experiments showed that for a specific proportion of FeS_2:$CaCO_3$, effluents produced under variably saturated hydrologic conditions, in which oxygen availability and pyrite oxidation were enhanced, had lower pH and greater dissolved solids concentrations than effluents produced under continuously saturated conditions, in which oxygen availability and pyrite oxidation were diminished.

INTRODUCTION

In the northern Appalachian Plateau of the eastern United States, drainage from abandoned coal mines affects more than 8,000 km of streams and associated ground water (Boyer and Sarnoski, 1995). Most affected streams are in Pennsylvania, where contaminated mine runoff and mine discharges impair water quality in 45 of 67 counties (Pennsylvania Department of Environmental Protection, 1998). An understanding of factors affecting the chemistry of coal-mine drainage is needed for the effective planning and implementation of future mining and remediation of abandoned mine lands. This paper evaluates geochemical and hydrological factors affecting the pH of coal-mine drainage. Data for ground-water and discharge samples and laboratory leaching experiments are presented to explain regional water-quality trends for the northern Appalachian coalfields. Geochemical simulations demonstrate the range of effects on pH from different variables, including the amount of pyrite oxidized, buffering by carbonate minerals, and the formation of secondary minerals.

Geochemistry of Coal Mine Drainage

Ground water and associated mine discharges in the coalfields of Pennsylvania range widely in quality from near-neutral, or "alkaline" (alkalinity > acidity; pH ≥ 6), to strongly acidic (Rose and Cravotta, 1998). The pH of coal-mine drainage in Pennsylvania has a bimodal frequency distribution (Brady and others, 1997, 1998); most samples are either near neutral (pH 6 to 7) or distinctly acidic (pH 2.5 to 4), with few samples having pH 4.5 to 5.5 (fig.1). The bimodal pH distribution is apparent for other regional compilations of water-quality data for coalfields in West Virginia (diPretoro, 1986), Ohio (Helsel and Hirsch, 1992, p. 61), and Germany (Klapper and Schultze, 1995). Whether near neutral or acidic, the drainage from most coal mines has elevated concentrations of dissolved solids, ranging from about 200 $mg \cdot L^{-1}$ to greater than 10,000 $mg \cdot L^{-1}$. In contrast, ground water and spring water from unmined areas typically are near neutral and are dilute compared to water from mined areas (Brady and others, 1996; Rose and Cravotta, 1998).

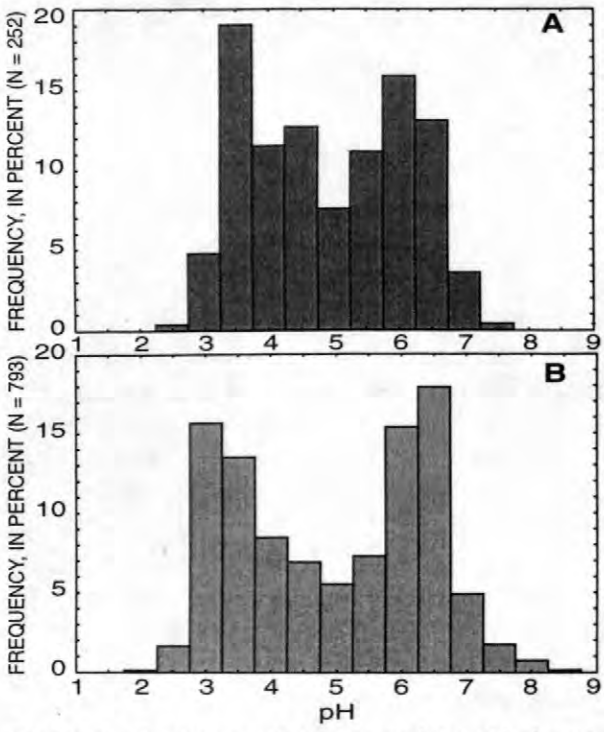

Figure 1. Frequency distribution of the pH of coal-mine discharges in Pennsylvania. *A*, Data for 252 coal-mine discharges in the anthracite coalfield (source: Growitz and others, 1985); *B*, Data for 793 surface coal-mine discharges in the bituminous coalfield (source: Hellier, 1994). Class intervals for pH ± 0.25.

Acidic mine drainage (AMD) is characterized by elevated concentrations of dissolved and particulate iron (Fe) and dissolved sulfate (SO_4^{2-}) produced by the oxidation of pyrite (FeS_2):

$$FeS_2 + 3.5\ O_2 + H_2O \rightarrow Fe^{2+} + 2\ SO_4^{2-} + 2\ H^+ \quad (1)$$

$$Fe^{2+} + 0.25\ O_2 + 2.5\ H_2O \rightarrow Fe(OH)_3(s) + 2\ H^+ \quad (2)$$

Half the acid (H^+) is produced by the oxidation of pyritic S (reaction 1), and half results from the oxidation and hydrolysis of pyritic Fe (reaction 2). Generally, mines that produce AMD feature interconnected underground "workings" (voids and rock rubble) or aboveground "spoil" (rubble and rejected coal) where pyrite has been exposed to oxygenated air and water and where the calcareous minerals, calcite ($CaCO_3$) and dolomite ($CaMg(CO_3)_2$), are absent or deficient relative to pyrite (Hornberger and others, 1990; Brady and others, 1994; Cravotta, 1994; Rose and Cravotta, 1998; Nordstrom and Alpers, 1999). Concentrations of manganese (Mn^{2+}), aluminum (Al^{3+}), and other solutes in AMD commonly are elevated due to aggressive dissolution of carbonate, oxide, and aluminosilicate minerals by acidic water.

Near-neutral mine drainage can form from rock that lacks pyrite or can originate as AMD that has been neutralized by reaction with calcareous minerals (Cravotta and others, 1994; Blowes and Ptacek, 1994). In near-neutral mine waters, bicarbonate (HCO_3^-) is a significant anion along with SO_4^{2-}; concentrations of dissolved calcium (Ca^{2+}) and magnesium (Mg^{2+}) generally are elevated relative to dissolved Fe^{3+} and Al^{3+}, which precipitate as pH increases to above 4 to 5. For example, dissolution of calcite neutralizes acid and can increase the pH and alkalinity ($[OH^-] + [HCO_3^-] + 2\ [CO_3^{2-}]$) of mine water:

$$CaCO_3(s) + 2H^+ \leftrightarrow Ca^{2+} + H_2CO_3^* \quad (3)$$

$$CaCO_3(s) + H_2CO_3^* \leftrightarrow Ca^{2+} + 2\ HCO_3^- \quad (4)$$

where $[H_2CO_3^*] = [CO_2\ (aq)] + [H_2CO_3^o]$ (Stumm and Morgan, 1996). However, because the rate of pyrite oxidation can exceed the rate of calcite dissolution, particularly where oxygen is abundant, the pH and alkalinity of mine water will not necessarily increase in the presence of calcite.

Ion complexation, principally the protolysis of anions and the hydrolysis of cations (Stumm and Morgan, 1996), also can be a significant process that stabilizes, or "buffers," the pH of mine water. For example, pH can be buffered in the near-neutral range by the protolysis reaction involving bicarbonate and carbonic acid (pK=6.35; thermodynamic data from Ball and Nordstrom, 1991):

$$HCO_3^- + H^+ \leftrightarrow H_2CO_3^* \quad (5)$$

Similarly, pH can be buffered in the acidic range by the protolysis reaction involving sulfate and bisulfate (pK=2.0)

$$SO_4^{2-} + H^+ \leftrightarrow HSO_4^-, \quad (6)$$

and by hydrolysis reactions involving ferric ions, such as the initial hydrolysis step (pK=2.2),

$$Fe^{3+} + H_2O \leftrightarrow FeOH^{2+} + H^+. \quad (7)$$

The importance of the above reactions will depend on the dissolved solute content of the water, the nature and abundance of acid-producing and neutralizing materials along flow paths, the sequence and intimacy of contact between the water and these materials, as well as the ability of the rock to transmit water and air.

Geologic and Hydrologic Framework

Bituminous coal deposits underlie western and north-central Pennsylvania, and anthracite deposits underlie east-central and northeastern Pennsylvania (fig. 2). The mineable coals, mostly of Pennsylvanian Age, are interbedded with shale, siltstone, sandstone, and occasional limestone (Brady and others, 1998). The bituminous coalfield lies within the Appalachian Plateaus Physiographic Province and is characterized by gently dipping strata; nearly horizontal coalbeds commonly crop out in the incised stream valleys. The anthracite coalfield lies within the adjacent Ridge and Valley Physiographic Province, which is characterized by complexly deformed strata. Mineable anthracite beds are present primarily in steeply folded and fractured synclinal troughs.

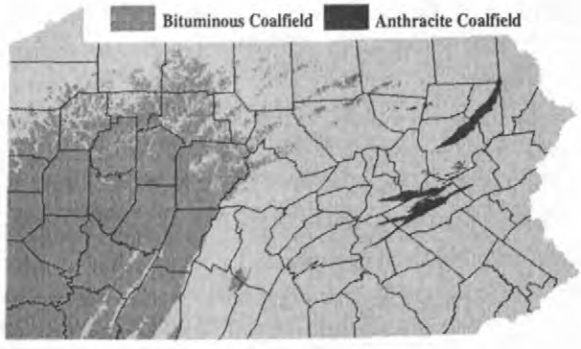

Figure 2. Locations of bituminous and anthracite coalfields in Pennsylvania (modified from Pennsylvania Geological Survey, 1964).

Coal-bearing rocks in the northern Appalachians have variable potential to produce AMD; the pyritic and calcareous contents of the rocks vary. Because weathering over many centuries has depleted reactive minerals from near-surface strata, the acid-forming and acid-neutralizing minerals generally are most abundant in rock deeper than about 10 m (Cravotta and others, 1994; Brady and others, 1996, 1998). Upon mining, however, pyrite in the deep-lying, unweathered strata is exposed to oxygenated air and water within underground workings or surface mine spoil. The spoil commonly consists of a heterogeneous mixture of rocks that are inverted stratigraphically relative to their original positions (Cravotta and others, 1994). Thus, although the relative abundance and vertical distribution of pyritic and calcareous materials at a proposed mine commonly are evaluated before mining to indicate the potential for AMD formation and to develop a materials handling plan (Brady and others, 1994), the quality and movement of water within the resultant mine spoil and backfill are difficult to predict.

Surface mines and underground mines in the bituminous coalfield generally can be categorized as "updip" or "downdip" depending on the direction that mining proceeded relative to the dip of the coal bed. In the past, most bituminous mines were mined updip so that water would drain freely and pumping costs would be minimized. Updip mines also provided greater access of oxygen to the subsurface, however, which facilitates the oxidation of pyrite and the formation of AMD (Hornberger, 1985). In contrast, downdip mines tend to fill with ground water, which requires pumping during active mining but also reduces the access of oxygen to pyritic rock. Upon mine closure, substantial parts of downdip mines can be permanently inundated thereby minimizing oxygen transport and pyrite oxidation. Hence, the downdip mines generally produce less acidic water than updip mines; however, unless calcareous strata are present, they may not produce near-neutral water.

Most anthracite mines were developed as large underground mine complexes, where shafts and tunnels connected mine workings within multiple coalbeds. Because anthracite mines commonly were developed hundreds of meters below the regional water table and because of the large size of most underground mine complexes, their discharge volumes (overflows or tunnels) tend to be substantially greater than those from surface mines. Upon closure, large volumes of the mine complexes flooded, as expected for downdip mines, producing underground "mine pools." Discharges emanated where the mine pools overflowed from topographically low points overlying the mine complex.

During active mining, the potential for catastrophic flooding of anthracite mine complexes was a major concern. Partly due to the high cost of pumping as the mines were developed to greater and greater depths, most mines had closed by 1960. At some mines, the flooding problem was solved by the construction of extensive drainage tunnels. By promoting the circulation of water and air within the mine workings, the drainage tunnels promoted the formation of AMD where pyritic strata were present. For example, the Jeddo Tunnel, the largest drainage tunnel system in the anthracite coalfield,

drains a 70-km^2 area in the Eastern Middle Anthracite Field (LeRigina, 1988). Acidic water from the Jeddo Tunnel (pH < 4; SO_4 > 400 $mg \cdot L^{-1}$) discharges at a rate of 175,000 to 270,000 $m^3 \cdot d^{-1}$ (Wood, 1996).

In addition to the mineralogical and hydrological factors described above, the age of the mine, the time elapsed since initial flooding, the origin and composition of the inflow water, the potential for stratification within the mine pool, and the location of the mine outflow can affect the mine-discharge composition. For example, water can be stratified in a mine pool, with generally older, poorer quality water at depth; overflows from the top of the pool generally will be better quality than outflows from boreholes, shafts, or tunnels tapping deeper zones (Ladwig and others, 1984). Regional data pertaining to all these factors are not generally available in digital format and, hence, their evaluation is beyond the scope of this paper.

STUDY METHODS

Available data for pH and concentrations of alkalinity, acidity, sulfate, and metals in groundwater and discharge samples from coal mines in Pennsylvania were compiled from several sources. Water-quality data for 793 bituminous surface mine discharges were obtained from the Mine Drainage Inventory data base (Hellier, 1994) maintained by the Pennsylvania Department of Environmental Protection (PaDEP). If multiple samples were reported for a discharge site, arithmetic means of concentration and discharge rate were used for that site. Data for 252 anthracite mine discharges reported by Growitz and others (1985) were obtained from the USGS National Water Information System (NWIS); the anthracite data are predominantly for underground mines. Additional water-chemistry data for selected large anthracite discharges reported by Wood (1996) and for recent USGS investigations at four surface mines in the bituminous field (Dugas and others, 1993; Cravotta and others, 1994; Cravotta, 1998) also were obtained from NWIS. Finally, data for laboratory leaching experiments were added to the compilation.

For the leaching experiments, reported in detail by Cravotta (1996), coaly shale that consisted mostly of quartz, kaolinite, and pyrite was obtained at a coal mine and taken to the laboratory to be crushed, and placed in vertical columns open to the atmosphere. The columns were leached biweekly with water simulating two different hydrologic conditions: variably saturated, aerobic (flooded for 2 days with 1.4 pore volumes, followed by 12-day drying period) or continuously saturated, stagnant (flooded continuously with 1.4 pore volumes). Powdered calcite was added on top of the shale to achieve molar ratios for $CaCO_3$:FeS_2 of 0:1, 1:1, and 2:1.

The pH data for the bituminous mines (fig. 1A) were determined in the laboratory on chilled samples. These laboratory pH values could be greater than field pH because of the exsolution of CO_2 or less than the field pH because of the oxidation and precipitation of Fe (reactions 2 and 3). Nevertheless, pH data for the anthracite mines (fig. 1B) and for the other field and laboratory data sets were determined at the time and location of sample collection. The similarity between field and laboratory pH values for the USGS mine-scale and laboratory leaching data compilations and the similarity between the pH frequency distributions for the bituminous and anthracite discharges (fig. 1) imply that the laboratory pH values are representative of field conditions. The USGS mine-scale and laboratory leaching data compilations also included values for redox potential (Eh). The Eh was determined on fresh samples using Pt and Ag/AgCl reference electrodes according to methods of Wood (1976) and Nordstrom (1977). The water-quality data were evaluated by use of computerized graphical, statistical, and geochemical routines.

The PHREEQC computer program (Parkhurst, 1995) was used to conduct "titration" simulations, where small increments of pyrite were added to a 1 L solution and oxidized. By adjusting different variables, these simulations evaluated the effects on pH, Eh, and sulfate concentrations as a function of the amount of pyrite reacted; oxygen availability; equilibrium with carbonate minerals; partial pressure of CO_2 (Pco_2); and precipitation of different hydrous iron oxide or sulfate minerals. A typical simulation involved 100 or more incremental steps with small additions of pyrite. After each of these steps, the pH, Eh, and dissolved species were calculated. The pH was plotted as a function of the total SO_4 concentration to indicate the resulting water quality for a given amount of pyrite oxidized.

RESULTS

Regional Studies

Although the bimodal frequency distribution of pH is similar for discharges from bituminous and anthracite mines (fig. 1), the relations between pH and SO_4 concentration or load differ between the two coalfields (fig. 3). The median SO_4 concentrations for bituminous discharges exceed those for anthracite discharges at each pH class interval and over the range of pH (fig. 3). Conversely, because discharge rates for most anthracite mines are significantly greater than those for the bituminous mines, the medians for SO_4 transport, or "loads," for anthracite discharges exceed those for bituminous discharges at each pH class interval (fig. 3). The anthracite mine discharges are characterized by median SO_4 concentrations of 100 to 300 $mg \cdot L^{-1}$ and loads of 20 to 400 $kg \cdot day^{-1}$ that are independent of pH. In contrast, the median concentrations and loads for bituminous discharges increase with decreasing pH, from about 500 $mg \cdot L^{-1}$ and 10 $kg \cdot day^{-1}$, respectively, for pH >5.5 to greater than 1,200 $mg \cdot L^{-1}$ and 40 $kg \cdot day^{-1}$, respectively, for pH ≤3.5 (fig. 3). The inversely correlated pH and SO_4 data (loads and concentrations) for bituminous mines imply that the extent of pyrite oxidation increases with decreasing pH, which is consistent with laboratory rate data (McKibben and Barnes, 1986; Moses and Herman, 1991; Cravotta, 1996). However, the lack of similar correlations between the pH and SO_4 data for anthracite mine discharges suggest other processes are important.

The anthracite mines generally were flooded for decades before most bituminous surface mines had been developed. Although discharges from the anthracite mines are primarily overflows from stagnant mine pools, historical data indicate that when the anthracite mines first flooded, the water chemistry was similar to that of present bituminous mine discharges, with lower pH and higher concentrations of SO_4 and Fe (Ladwig and others, 1984; Wood, 1996). Comparing data collected in 1975 and 1991 for selected anthracite discharges, pH increased from the acidic mode to the near-neutral mode while SO_4 concentrations decreased for most mines in the Southern and Western Middle Anthracite Fields (Wood, 1996). In contrast, pH data for the Eastern Middle Anthracite Field, which is largely drained by the Jeddo Tunnel, showed no

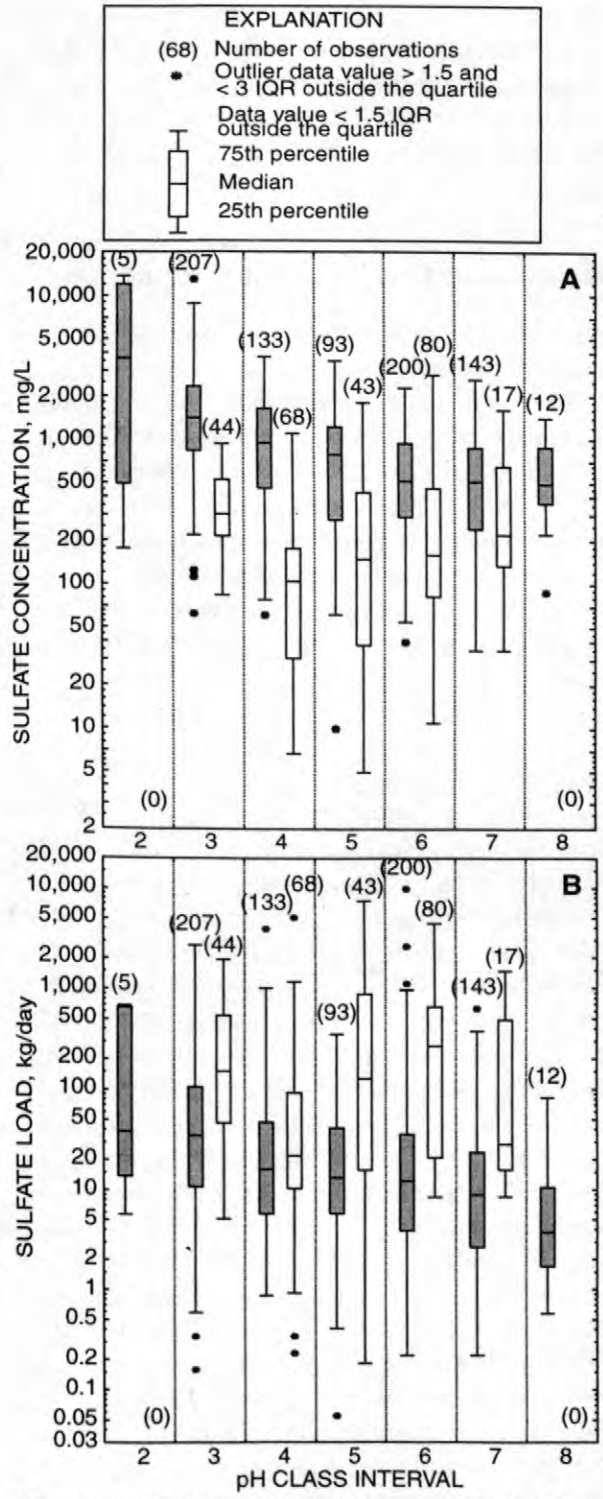

Figure 3. Boxplots showing sulfate data by pH class interval for 793 bituminous (shaded) and 252 anthracite coal-mine discharges in Pa. *A*, Sulfate concentration. *B*, Sulfate load. Class intervals for pH ± 0.5; interquartile range, IQR = 75th - 25th percentile.

change from the acidic pH mode. Hence, as pyrite and/or carbonate minerals are depleted and/or rates of reactions decrease, the pH and SO_4 frequency distributions and correlations are likely to change, but the time period for this change could span decades.

Mine-Scale and Laboratory Studies

Data for ground water and associated discharge samples from four surface mines in the bituminous coalfield, when combined so that each mine is represented equally (total frequency of 25 percent for each mine), also show a bimodal distribution of pH (fig. 4A). The pH of the ground water at each mine commonly ranges over several units, mainly caused by spatial variability or heterogeneity. Although acidic and near-neutral waters were sampled at three of the four mines, individual wells or discharges generally reflected locally acidic or near-neutral conditions. A few wells in mixed pyritic and calcareous spoil had water quality that varied temporally between acidic and alkaline (Cravotta and others, 1994; Rose and Cravotta, 1998). The effects of spoil composition and hydrology are indicated by the relations between pH and concentrations of SO_4^{2-} and Ca^{2+} (figs. 4B and 4C). Alkaline to weakly acidic water (pH $\geq$ 5) that has relatively low SO_4^{2-} is characteristic of unmined bedrock and spoil that contain calcareous minerals and have low permeability (e.g. mine 1 in fig. 4). Strongly acidic water (pH $\leq$ 4) that has high SO_4^{2-} is characteristic of high-permeability, well-drained, pyritic spoil (e.g. mines 2 and 3 in fig. 4). Moderately acidic water (pH 4 to 5) that has high SO_4^{2-} is characteristic of spoil or underlying bedrock that lacks dissolved oxygen (e.g. mines 2 and 4 in fig. 4). Although concentrations of Ca^{2+} and SO_4^{2-} are positively correlated, the linear relation between Ca^{2+} and SO_4^{2-} is evidently site specific with slopes differing among the mines. In general, calcareous strata produced water with the highest concentrations of Ca^{2+}, and noncalcareous, pyritic strata produced water with the highest concentrations of SO_4^{2-}. Lowest concentrations of Ca^{2+} and SO_4^{2-} were in water from unmined rock upgradient from the mines.

Laboratory leaching experiments demonstrate the bimodal pH distribution for water at coal mines generally results from the weathering of pyritic rocks that have a deficiency (low pH) or an abundance (near-neutral pH) of calcareous minerals necessary to buffer the pH (fig. 5A). Pyritic shale was subjected to leaching under continuously or variably saturated hydrologic conditions; calcite was added in different proportions to evaluate effects on the oxidation of pyrite and the transport of sulfate and metals (Cravotta, 1996). Without the addition of calcite, the leachate from the shale typically had pH 1.5 to 3.5 and high concentrations of sulfate and iron. However, with the addition of calcite, the leachate had pH 4.5 to 7 and lower concentrations of sulfate and iron. The dissolution of calcite not only neutralized acid but decreased pyrite oxidation rates, as indicated by higher pH and Ca^{2+} concentrations and lower SO_4^{2-} concentrations for leachate from shale with added calcite (figs. 5B and 5C). All the leachate samples were undersaturated with respect to gypsum; only leachate in continuously saturated columns with added calcite was saturated or supersaturated with respect to calcite.

The leaching tests also showed the hydrology of a mine has an important effect on pyrite oxidation. By maintaining stagnant, water-saturated conditions, which minimized the oxygen available for reactions, pyrite oxidation was minimized, as indicated by low SO_4^{2-} concentrations in leachate (figs. 5A and 5B). The leaching data can be summarized generally as follows:

- pH < 3 and SO_4 > 1,500 mg·L^{-1} for variably saturated conditions without $CaCO_3$;
- pH 3.2-3.5 and SO_4 < 1,000 mg·L^{-1} for continuously saturated conditions without $CaCO_3$;
- pH 4.5–6.5 and SO_4 < 1,000 mg·L^{-1} for variably saturated conditions with $CaCO_3$ present; and
- pH $\geq$ 6.0 and SO_4 < 1,000 mg·L^{-1} for water-saturated conditions with $CaCO_3$ present.

For each $CaCO_3$:FeS_2 molar ratio, ranging from 0:1 to 2:1, lower pH and higher SO_4^{2-} and Ca^{2+} concentrations were produced under variably saturated, oxygenated conditions than under continuously water-saturated, stagnant conditions (figs. 5B and 5C) because of greater extent and rate of pyrite oxidation and the consequent dissolution of calcite and other minerals under oxygenated, acidic conditions.

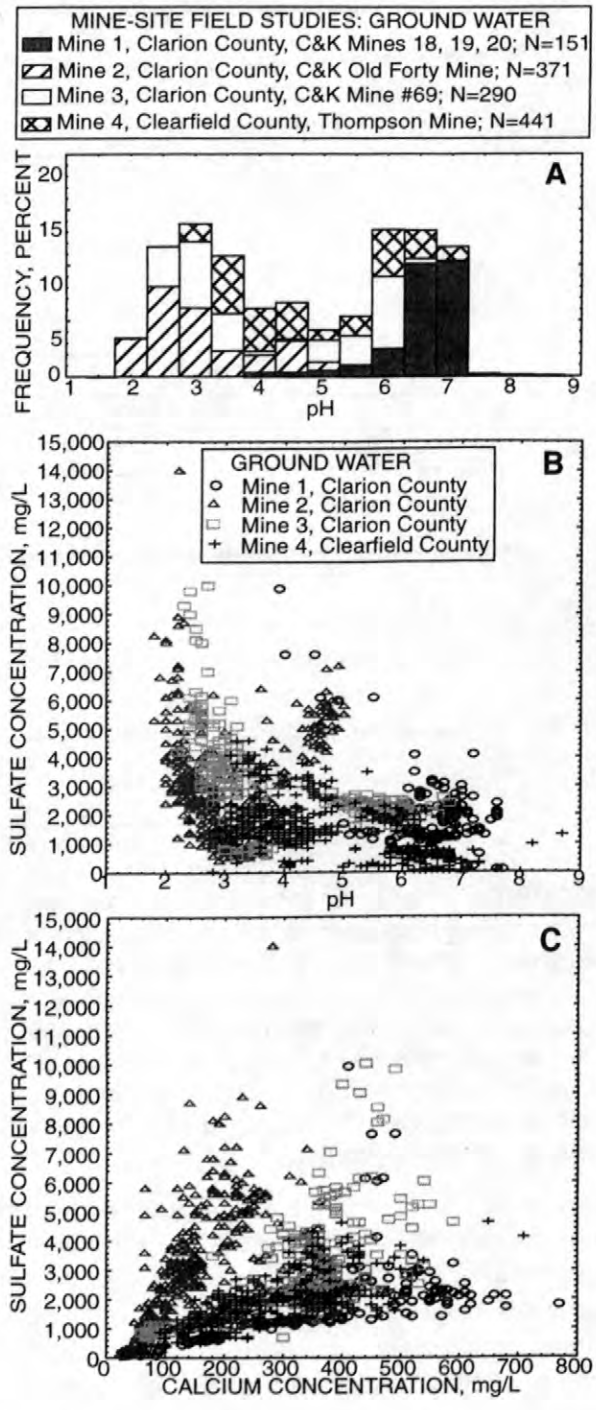

Figure 4. Chemistry data for 1,253 ground-water and discharge samples, collected monthly for 2 to 6 years, from four surface mines in the bituminous coalfield, Pa. (source: Dugas and others, 1993; Cravotta and others, 1994; Cravotta, 1996). *A,* Frequency distribution of pH; data for each mine weighted to represent 25% of the total. *B,* Relation between sulfate concentration and pH. *C,* Relation between sulfate and calcium concentrations.

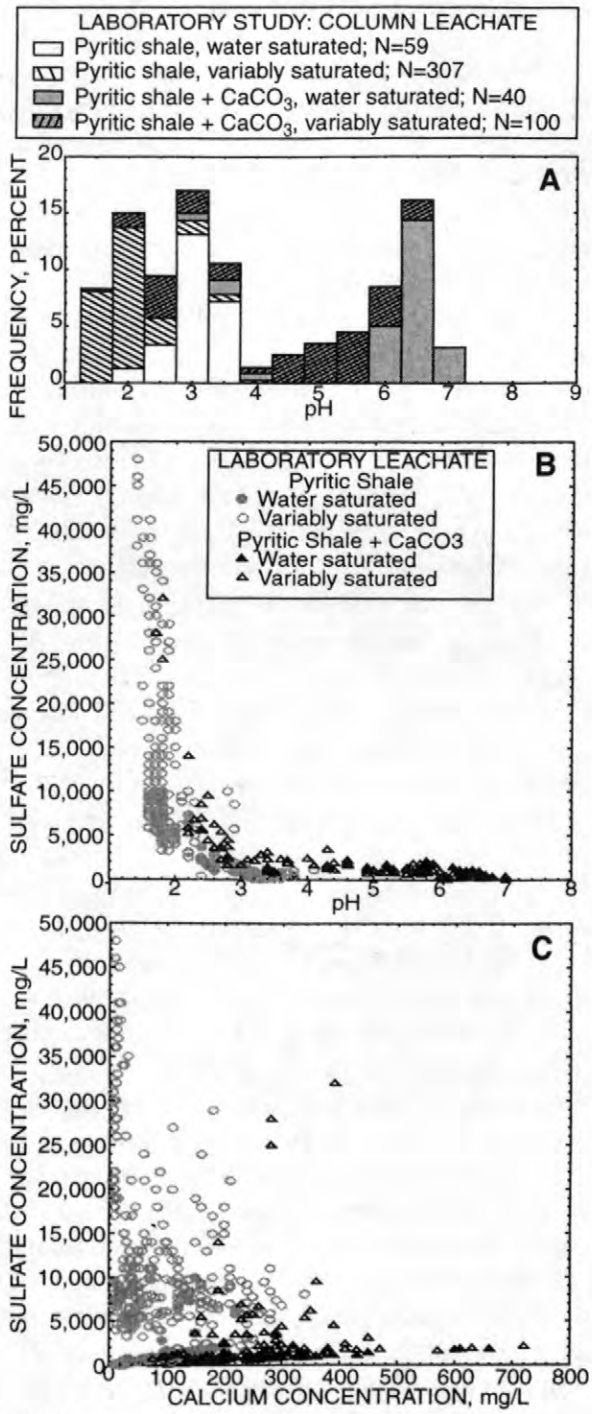

Figure 5. Chemistry data for 606 leachate samples from pyritic shale. Data for each of four leaching scenarios, collected biweekly over 3 to 9 months (source: Cravotta, 1996). *A,* Frequency distribution of pH; data for each treatment weighted to represent 25% of the total. *B,* Relation between sulfate concentration and pH. *C,* Relation between sulfate concentration and calcium concentration.

Geochemical Simulations

Geochemical simulations evaluated the effects on pH, Eh, and sulfate concentrations from pyrite oxidation over a range of conditions characteristic of the field conditions at coal mines. Although a wide range of conditions was considered, this paper evaluates only the most important variables affecting pH. A typical simulation involved 100 or more incremental steps with small additions of pyrite to 1 L solution. After each of these steps, the pH, Eh, and dissolved species were calculated. The pH was plotted as a function of the total concentration of sulfate species in solution (SO_4^{2-}, HSO_4^-, $FeHSO_4^{2+}$, etc.) which indicates the amount of pyrite oxidized (192 g SO_4 per 120 g FeS_2) if sulfate minerals do not precipitate.

Firstly, the oxidation of pyrite, in the absence of calcite, is considered for different Pco_2 and Po_2 (fig. 6A). Except for depressing the pH of initially pure water, varying Pco_2 from $10^{-3.5}$ to 10^{-1} atm has little effect on the pH after pyrite oxidation has begun. In contrast, limiting the availability of oxygen has a significant effect on the pH as simulated for an "open system" (air equilibrium, Po_2=0.2 atm, for complete oxidation of S and Fe in FeS_2 by reactions 1 and 2) or a "closed system" (3.5 mol O_2 per mol FeS_2 for oxidation of only S by reaction 1). Starting with pure water in equilibrium with ambient Pco_2, pH declines from 5.5 to 4 with the oxidation of only a small quantity of pyrite (0.012 g·L^{-1} FeS_2 produces pH~4 and 20 mg·L^{-1} SO_4^{2-}); continued pyrite oxidation decreases pH to about 3 at the point where total SO_4 concentration is 100 mg·L^{-1}. As SO_4 concentration increases from 100 to 1,200 mg·L^{-1} the pH declines asymptotically approaching 2. For an open system, where oxygen is unlimited, the oxidation of pyritic S and Fe^{2+} and the precipitation of amorphous $Fe(OH)_3$ (reactions 1 and 2) results in pH about 0.3 units *greater than* that for the closed system where oxygen is limited to only the stoichiometric amount needed to produce SO_4^{2-} (reaction 1). The pH decreases about 0.5 units if a phase such as goethite (FeOOH) precipitates instead of higher solubility amorphous $Fe(OH)_3$, resulting in pH under air equilibrium that is *less than* that under oxygen limited conditions (fig. 6A). The narrow range of pH results mainly from the logarithmic scale for pH, plus buffering by ionic complexation $Fe(OH)^{2+}/Fe^{3+}$ and SO_4^{2-}/HSO_4^-

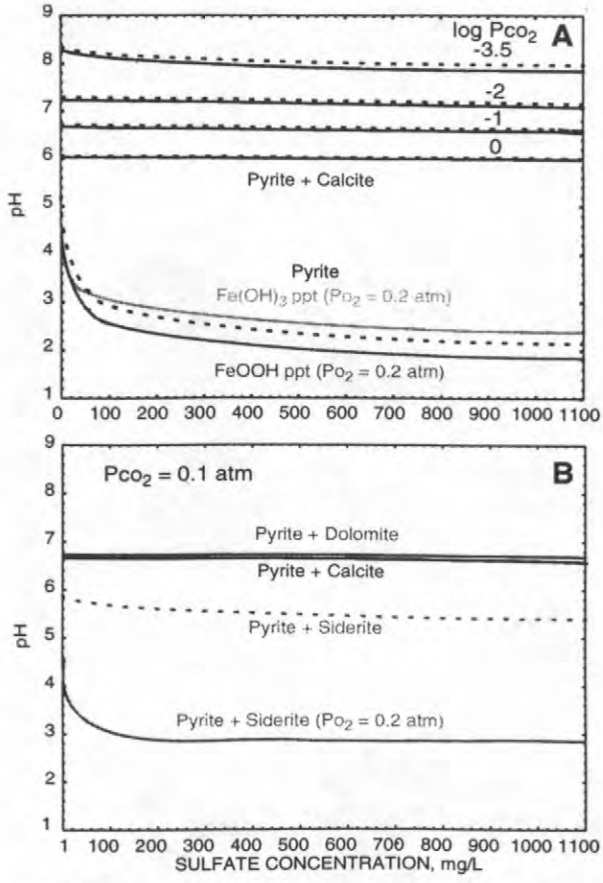

FIGURE 6. Simulated pH and sulfate concentration resulting from pyrite oxidation under different conditions (dashed line O_2 limited; solid line Po_2= 0.2 atm). Simulations conducted using PHREEQC (Parkhurst, 1995); temperature = 10°C, Pco_2 = 0.1 atm, and amorphous $Fe(OH)_3$ allowed to precipitate, unless specified. *A*, Effects of Po_2 and Pco_2 and equilibrium with calcite. *B*, Equilibrium with various carbonate minerals.

(reactions 6 and 7) and dissolution of previously formed iron minerals. The simulations illustrate that for a specific SO_4 concentration, a lower pH cannot be achieved simply from pyrite oxidation; however, most mine water samples have greater pH at a given SO_4 concentration because of neutralization reactions with other minerals that increase pH and add other solutes.

Secondly, the oxidation of pyrite in equilibrium with various carbonate minerals including calcite, dolomite, or siderite ($FeCO_3$) is considered (figs. 6A and 6B). For example, if calcite equilibrium is maintained, the pH remains relatively constant at a particular Pco_2 despite the oxidation of pyrite (fig. 6A); however, the pH can range widely as a function of Pco_2 from a relatively constant pH

value of 6 (Pco_2 = 1 atm) to pH values of 8.0 to 8.4 ($Pco_2 = 10^{-3.5}$ atm). For calcite equilibrium at Pco_2 = 0.1 atm, pH is 6.6±0.1 over the entire range of SO_4^{2-}. Little difference results if equilibrium with dolomite (pKsp = 16.5) is maintained instead of with calcite (pKsp = 8.5) (fig. 6B); for Pco_2 = 0.1 atm, these calcareous minerals buffer pH at about 6.6. However, if siderite (pKsp = 10.5) is the available carbonate mineral, the pH generally will be much lower at equilibrium. For a closed system, where oxygen is limited to only the stoichiometric amount needed to produce SO_4^{2-}, siderite buffers pH at about 5.5, because H^+ is consumed by the reaction:

$$FeCO_3 + 2\ H^+ \leftrightarrow Fe^{2+} + H_2O + CO_2(aq). \quad (8)$$

However, if oxygen is available to oxidize Fe^{2+}, siderite has little buffering effect, because all Fe is oxidized by the reaction:

$$FeCO_3 + 0.25\ O_2 + 1.5\ H_2O \rightarrow Fe(OH)_3 + CO_2(aq) \quad (9)$$

An increase in the dissolved CO_2 by reaction 9 will produce a corresponding decrease in the ratio of $HCO_3^-/H_2CO_3^*$ and hence decrease the pH (per reaction 5).

DISCUSSION AND CONCLUSIONS

The bimodal distribution of pH for coal-mine drainage, with modes at pH 2.5 to 4 (acidic) and pH 6 to 7 (near neutral), is a regional phenomenon controlled by the mineralogy and hydrology of the mines. Although iron disulfide (pyrite) and calcareous minerals (calcite and dolomite) comprise only a few percent, or less, of the coal-bearing rock, these acid-forming and acid-neutralizing minerals are highly reactive and are mainly responsible for the bimodal pH distribution. The acidic mode, classified as AMD, is produced by the oxidation of pyrite in the absence of carbonate buffering. The field and laboratory studies indicate that, where calcite and dolomite are absent, extensive pyrite oxidation can result under variably saturated conditions, producing severe AMD (pH < 3 and SO_4 > 2,000 mg·L^{-1}); these conditions can be found at some well-drained underground mines and surface mines (e.g. bituminous mines, fig. 3). The studies also indicate that, where calcareous minerals are absent or deficient, the oxidation of only small amounts of pyrite under stagnant water-saturated conditions can produce AMD (pH < 4 and SO_4 > 200 mg·L^{-1}); these conditions commonly are found at flooded underground mines (e.g. anthracite mines, fig. 3). In contrast, where calcareous minerals are abundant, the pH can be buffered to be near neutral. Some near-neutral water contains high concentrations of SO_4 (median > 200 mg·L^{-1}), suggesting an origin as AMD that had been neutralized by reactions with calcareous minerals after, or downflow from the location of, pyrite oxidation.

The geochemical simulations confirm the interpretations of the field and laboratory data. The simulations clearly illustrate the effect of pyrite oxidation on lowering pH and of calcite and dolomite dissolution on increasing pH. Specific conclusions from the simulations are as follows:

- The near-neutral pH mode results from the dissolution of calcite and dolomite and by resultant carbonate buffering ($HCO_3^-/H_2CO_3^*$; $HCO_3^-/CaCO_3$; $HCO_3^-/CaMg(CO_3)_2$). As long as carbonate equilibrium is maintained or approximated, near-neutral pH can be maintained despite continued amounts of pyrite oxidation.
- In the absence of carbonate buffering, only a small amount of pyrite oxidation produces dilute AMD (0.012 g·L^{-1} FeS_2 produces pH~4 and 20 mg·L^{-1} SO_4^{2-}). However, because of the logarithmic scale for pH and ion speciation, unit decreases in pH require greater than 1 order of magnitude increases in the amount of pyrite oxidation.
- Buffering in the acidic mode is due to ion speciation (SO_4^{2-}/HSO_4^-; $Fe(OH)^{2+}/Fe^{3+}$) and to precipitation and dissolution of $Fe(OH)_3$.
- The least frequent pH range of pH 4.5 - 5.5 indicates a poorly buffered condition and could result from limited reactions with calcareous minerals (undersaturated) or limited availability of O_2 resulting in the incomplete oxidation of Fe^{2+} from pyrite or siderite.

The results of this evaluation have several implications. Firstly, the bimodal distribution for pH and the tendency for calcareous minerals to buffer pH in the near-neutral range support the approach of using "acid-base" accounting, where only pyritic and calcareous minerals are evaluated, as a basis for predicting post-mining water quality (e.g. Brady and others, 1994). Generally, "net alkaline" mine water has pH ≥ 6 (Rose and Cravotta,

1998), and near-neutral pH is desirable to limit the mobility of iron and associated metals (Stumm and Morgan, 1996). The calcareous minerals not only neutralize acid, but their dissolution tends to slow or inhibit pyrite oxidation. Furthermore, although siderite may temporarily buffer pH in the near-neutral range, the presence of siderite should be considered as a negative factor with regard to the prediction of mine-drainage quality, because once the iron precipitates any benefits of siderite as a neutralizing agent will be negated (Skousen and others, 1997).

Secondly, the laboratory experiments indicate that addition of calcite can increase pH and reduce the transport of iron and other metals; however, equilibrium with calcite, hence buffering by the carbonate minerals, is not achieved except under conditions of water saturation. On the other hand, pyrite oxidation tends to be diminished under continuously saturated conditions, in which oxygen availability is limited, compared to variably saturated hydrologic conditions, in which oxygen availability is enhanced. Thus, for those mines where the importation and addition of alkaline materials is needed to achieve a net-neutral acid-base account, the placement of alkaline and pyritic materials in continuously wet zones would be prudent. In practice, however, a permanently wet zone in spoil generally will not be realized immediately and may be difficult to sustain (Cravotta and others, 1994).

Thirdly, recent field and laboratory work indicates iron hydroxysulfate minerals, which tend to be yellowish colored, form dominantly under acidic conditions whereas relatively pure iron hydroxide, which tends to be reddish colored, tends to form dominantly under near-neutral conditions (e.g. Bigham and others, 1996a, 1996b). Because these minerals have different coloration and related spectral properties, new approaches to characterizing mine drainage by use of remote sensing may have merit. For example, preliminary testing of aerial and ground-based spectral reflectance techniques has demonstrated the potential for differentiating between acidic and near-neutral drainages (Robbins and others, 1996). These techniques may be useful for locating and characterizing water quality where access is restricted.

REFERENCES CITED

Ball, J.W., and Nordstrom, D.K., 1991, User's manual for WATEQ4F with revised data base: U.S. Geological Survey Open-File Report 91-183, 189 p.

Bigham, J.M., Schwertmann, U., and Pfab, G., 1996a, Influence of pH on mineral speciation in a bioreactor simulating acid mine drainage: Applied Geochemistry, v. 11, p. 845-849.

Bigham, J.M., Schwertmann, U., Traina, S.J., Winland, R.L., and Wolf, M., 1996b, Schwertmannite and the chemical modeling of iron in acid sulfate waters: Geochimica et Cosmochimica Acta, v. 60, p. 2111-2121.

Blowes, D.W., and Ptacek, C.J., 1994, Acid-neutralization mechanisms in inactive mine tailings, in Jambor, J.L., and Blowes, D.W., eds., Environmental geochemistry of sulfide mine-wastes: Mineralogical Association of Canada, Short Course Handbook, vol. 22, p. 271-292.

Boyer, J., and Sarnoski, B., 1995, 1995 progress report--statement of mutual intent strategic plan for the restoration and protection of streams and watersheds polluted by acid mine drainage from abandoned coal mines: Philadelphia, Pa., U.S. Environmental Protection Agency, 33 p., appendix (http://www.epa.gov/reg3giss/libraryp.htm).

Brady, K.B.C., Hornberger, R.J., and Fleeger, G., 1998, Influence of geology on post-mining water quality-Northern Appalachian Basin, in Brady, K.B.C., Smith, M.W., and Schueck, J.H., eds., Coal Mine Drainage Prediction and Pollution Prevention in Pennsylvania: Harrisburg, Pennsylvania Department of Environmental Protection, 5600-BK-DEP2256, p. 8.1-8.92.

———, Perry, E.F., Beam, R.L., Bisko, D.C., Gardner, M.D., and Tarantino, J.M., 1994, Evaluation of acid-base accounting to predict the quality of drainage at surface coal mines in Pennsylvania, U.S.A.: U.S. Bureau of Mines Special Publication SP 06A, p. 138-147.

———, Rose, A.W., Cravotta, C.A., III, and Hellier, W.W., 1997, Bimodal distribution of pH in coal-mine drainage (abs.): Geological Society of America, GSA Abstracts with Programs, v. 29, no. 1, p. 32.

———, Rose, A.W., Hawkins, J.W., and DiMatteo, M.R., 1996, Shallow ground water flow in unmined regions of the northern Appalachian Plateau--Part 2. Geochemical characteristics, in Proceedings 13th Annual Meeting American Society for Surface Mining and Reclamation: Princeton, W.Va., American Society for Surface Mining and Reclamation, p. 52-62.

Cravotta, C.A., III, 1994, Secondary iron-sulfate minerals as sources of sulfate and acidity: The geochemical evolution of acidic ground water at a reclaimed surface coal mine in Pennsylvania, in Alpers, C.N., and Blowes, D.W., eds., Environmental geochemistry of sulfide oxidation: Washington, D.C., American Chemical Society Symposium Series 550, p. 345-364.

———1996, Municipal sludge use in coal-mine reclamation and potential effects on the formation of acidic mine drainage: University Park, Pa., Pennsylvania State University, unpublished Ph.D. thesis, 200 p.

———1998, Effect of sewage sludge on formation of acidic ground water at a reclaimed coal mine: Ground Water, v. 36, no 1, p. 9-19.

———, Dugas, D.L., Brady, K.B.C., and Kovalchuk, T.E., 1994, Effects of selective handling of pyritic, acid-forming materials on the chemistry of pore gas and ground water at a reclaimed surface coal mine in Clarion County, PA, USA: U.S. Bureau of Mines Special Publication SP 06A, p. 365-374.

diPretoro, R., 1986, Premining prediction of acid drainage potential for surface coal mines in northern West Virginia: Morgantown, W.Va., West Virginia University, unpublished M.S. thesis, 217 p.

Dugas, D.L., Cravotta, C.A. III, and Saad, D.A., 1993, Water-quality data for two surface coal mines reclaimed with alkaline waste or urban sewage sludge, Clarion County, Pennsylvania, May 1983 through November 1989: U.S. Geological Survey Open-File Report 93-115, 153 p.

Growitz, D.J., Reed, L.A., and Beard, M.M., 1985, Reconnaissance of mine drainage in the coal fields of eastern Pennsylvania: U.S. Geological Survey Water Resources Investigations Report 83-4274, 54 p.

Hellier, W.W., 1994, Best professional judgment analysis for the treatment of post-mining discharges from surface mining activities: Harrisburg, Pa., Pennsylvania Department of Environmental Resources, unpublished report, 160 p.

Helsel, D.R., and Hirsch, R.M., 1992, Statistical methods in water resources: New York, Elsevier Publishers, Inc., Studies in Environmental Science no. 49, 522 p.

Hornberger, R.J., 1985, Delineation of acid mine drainage potential of coal-bearing strata of the Pottsville and Allegheny Groups in western Pennsylvania: University Park, Pa., Pennsylvania State University, unpublished M.S. thesis, 558 p.

———, Smith, M.W., Friedrich, A.E., and Lovell, H.L., 1990, Acid mine drainage from active and abandoned coal mines in Pennsylvania, in Majumdar, S.K., Miller, E.W., and Parizek, R.R., eds., Water resources in Pennsylvania--Availability, quality, and management: Easton, Pa., The Pennsylvania Academy of Science, p. 432-451.

Klapper, H., and Schultze, M., 1995, Geologically acidified mining lakes--living conditions and possibilities of restoration: Int. Revue ges. Hydrobiol., v. 80, p. 639-653.

Ladwig, K.J., Erickson, P.M., Kleinmann, R.L.P., and Posluszny, E.T., 1984, Stratification in water quality in inundated anthracite mines, eastern Pennsylvania: U.S. Bureau of Mines Report of Investigations RI 8837, 35 p.

LeRigina, J.A., 1988, The mine drainage tunnels of the Eastern Middle Anthracite Field, in Inners, J.D., ed., Bèdrock and glacial geology of the North Branch Susquehanna lowland and Eastern Middle Anthracite Field: Harrisburg, Pa., 53rd Annual Field Conference for Pennsylvania Geologists.

McKibben, M.A., and Barnes, H.L., 1986, Oxidation of pyrite in low temperature acidic solutions--Rate laws and surface textures: Geochimica et Cosmochimica Acta, v. 50, p. 1509-1520.

Moses, C.O., and Herman, J.S., 1991, Pyrite oxidation at circumneutral pH: Geochimica et Cosmochimica Acta, v. 55, p. 471-482.

Nordstrom, D.K., 1977, Thermochemical redox equilibria of Zobell's solution: Geochimica et Cosmochimica Acta, v. 41, p. 1835-1841.

———, and Alpers, C.N., 1999, Geochemistry of acid mine waters, in Plumlee, G.S., and Logsdon, M.J., eds., The Environmental Geochemistry of Mineral Deposits--Part A. Processes, methods, and health issues: Reviews in Economic Geology, v. 6, 27 p.

Parkhurst, D.L., 1995, PHREEQC--A computer model for geochemical calculations: U.S. Geological Survey Water-Resources Investigations Report 95-4227, 143 p.

Pennsylvania Department of Environmental Protection, 1998, "Working" draft Pennsylvania's nonpoint source (NPS) management program: Harrisburg, Pa., Pennsylvania Department of Environmental Protection, 3940-BK-DEP2275, p. 14-23.

Pennsylvania Geological Survey, 1964, Distribution of Pennsylvania coals: Pennsylvania Geological Survey, Fourth Series, Map # 11.

Plummer, L.N., Parkhurst, D.L., and Wigley, M.L., 1979, Critical review of the kinetics of calcite dissolution and precipitation, in Jenne, E.A., ed., Chemical modeling in aqueous systems--Speciation, sorption, solubility, and kinetics: American Chemical Society Symposium Series 93, p. 537-573.

Robbins, E.I., Anderson, J.E., Cravotta, C.A., III, Koury, D.J., Podwysocki, M.H., Stanton, M.R., and Growitz, D.J., 1996, Development and preliminary testing of microbial and spectral reflectance techniques to distinguish neutral from acidic drainages, in Chiang, S.-H., ed., Proceedings 13th Annual International Pittsburgh Coal Conference, v. 2, p. 768-775.

Rose, A.W., and Cravotta, C.A., III, 1998, Geochemistry of coal-mine drainage, in Brady, K.B.C., Smith, M.W., and Schueck, J.H., eds., Coal Mine Drainage Prediction and Pollution Prevention in Pennsylvania: Harrisburg, Pa., Pennsylvania Department of Environmental Protection, 5600-BK-DEP2256, p. 1.1-1.22.

Skousen, J., Renton, J., Brown, H., Evans, P., Leavitt, B., Brady, K., Cohen, L., and Ziemkiewicz, P., 1997, Neutralization potential of overburden samples containing siderite: Journal of Environmental Quality, v. 26, p. 673-681.

Stumm, Werner, and Morgan, J.J., 1996, Aquatic chemistry--chemical equilibria and rates in natural waters (3rd): New York, Wiley-Interscience, 1022 p.

Wood, C.R., 1996, Water quality of large discharges from mines in the anthracite region of eastern Pennsylvania: U.S. Geological Survey Water-Resources Investigations Report 95-4243, 69 p.

Wood, W.W., 1976, Guidelines for collection and field analysis of ground-water samples for selected unstable constituents: U.S. Geological Survey Techniques of Water-Resources Investigations, book 1, chap. D2, 24 p.

AUTHOR INFORMATION

Charles A. Cravotta, III, U.S. Geological Survey, Lemoyne, Pennsylvania (cravotta@usgs.gov).

Keith B.C. Brady, Pennsylvania Department of Environmental Protection, Harrisburg, Pennsylvania (brady.keith@dep.state.pa.us).

Arthur W. Rose and Joseph B. Douds, Pennsylvania State University, University Park, Pennsylvania (rose@ems.psu.edu).